Topics in STEREOCHEMISTRY

Scott E. Denmark
EDITOR

Volume 23

ADVISORY BOARD

TOPICS IN

STEREOCHEMISTRY

EDITOR

SCOTT E. DENMARK
Department of Chemistry
University of Illinois, Urbana-Champaign
Urbana, Illinois

VOLUME 23

A JOHN WILEY & SONS, INC., PUBLICATION

This book is printed on acid-free paper.♾

Published by John Wiley & Sons, Inc., Hoboken, New Jersey.
Published simultaneously in Canada.

For ordering and customer service, call 1-800-CALL-WILEY.

Library of Congress Cataloging-in-Publication Data:

ISBN 0-471-17622-2

Printed in the United States of America

10 9 8 7 6 5 4 3 2 1

To the memory of
Andre Collet

INTRODUCTION TO THE SERIES

Since its first appearance in 1967, the *Topics in Stereochemistry* series has stood as the standard-bearer for advances in the broad field of stereochemistry. The visionaries founders of the series anticipated, with remarkable foresight, the extraordinary growth and impact that stereochemistry has had all reaches of the chemical enterprise. Fortunately, there is no cease of interest in the importance of stereochemistry as the discipline of chemistry evolves and its borders expand and diffuse into the related fields of biology, medicine, physics, materials science, chemical engineering, and environmental science.

The field of stereochemistry serves as a unifying theme for the expanded definition and diversification of chemistry. The consequences of molecular and macromolecular shape and topology are central to issues of chemical reactivity, physical properties, and biological function. With that view, the importance of stereochemistry had never been greater, and it is hoped that this series will provide a forum for documentation of significant advances in all of these subdisciplines of chemistry.

The *Topics in Stereochemistry* series has set itself apart by maintaining a remarkable balance of chapters that are both definitive, standing the test of time, and current, addressing the impact of stereochemistry at the most exciting frontiers. As a student and researcher, I have often turned to chapters in *Topics in Stereochemistry* for the foundations and the state of the art in new areas of interest. It is my hope that the series continue to enjoy that level of confidence in the chemistry community and that it retain, in this second incarnation, the esteem that the founders have worked to hard to establish.

I am fortunate in having been able to enlist the help and guidance of an international board of editorial advisors who have provided great assistance by suggesting chapter topics and suitable authors for articles both here and in future volumes. While I am grateful for the assistance of this editorial advisory board, it is the editor and the authors who are solely responsible for any shortcomings of *Topics in Stereochemistry*.

S. E. Denmark

FOREWORD

Following the publication of *Stereochemistry of Carbon Compounds* (Eliel, 1962) and *Conformational Analysis* (Eliel, Allinger, Angyal, and Morrison, 1965) N. L. Allinger and I decided in 1966 to launch a *Topics in Stereochemistry* series to keep readers informed of current and new developments in this area. The subject of stereochemistry had been in the doldrums in the first half of the twentieth century and was then just experiencing a renaissance, thanks, in no small measure, to the pioneering work of Vladimir Prelog and Derek H. R. Barton (both of whom sadly passed away earlier this year). John Wiley & Sons agreed to publish the series, which over 27 years grew into 21 volumes. Samuel H. Wilen joined the editorial team in 1982 and Lou Allinger retired as co-editor in 1986. The series was clearly buoyed by the explosive growth of stereochemistry in the 1970s and 1980s, which it may have helped along at least in a small way. In some instances the series anticipated important developments and brought them to the readers' attention at an early stage. Among the more influential articles should be mentioned an early one on determination of enantiomeric purity by nonpolarimetric means (1967), a comprehensive chapter on resolution and resolving agents (1971), a 1978 article on asymmetric synthesis, chapters on the use of carbon-13 NMR in stereochemistry (1974, 1986), an article on the stereochemistry of hydride reductions (1979), and a chapter on enzymatic resolution (1989) — one of several articles on biochemical aspects of stereochemistry. The stereochemistry of inorganic compounds was also treated in several chapters, culminating in a whole volume on this topic edited by Gregory Geoffroy in 1981.

Stereochemistry continues to be a highly viable and prolific subject. Nevertheless, in 1993 the editors reluctantly decided to retire after publication of Volume 21, in part because for some time prior they had been fully occupied with the publication of *Stereochemistry of Organic Compounds* (Wiley, 1994). Sadly, my close friend, able co-author and co-editor, and valued colleague Sam Wilen died soon thereafter. In as much as the explosive development in stereochemistry is continuing, I am delighted that Scott Denmark, who is eminently qualified for the task, has taken over editorship of the series.

I wish the new editor continued success in this "relaunch."

Ernest L. Eliel
Department of Chemistry
University of North Carolina
Chapel Hill, NC 27599-3290

PREFACE

The chapters in this second Volume of the second era of *Topics in Stereochemistry* reflect the breadth of subdisciplines for which stereochemistry is of fundamental importance. I am particularly pleased that these chapters continue the precedent set by those in Volume 22 for their scholarship, timeliness and scope.

The discovery and development of fullerenes created unprecedented opportunities in both fundamental and applied chemistry. Although the intrinsic chirality of the higher fullerene spheroids was recognized early on, the consequences of modification with chiral groups as well as substitution to create chiral structures have only been fully realized in recent years. The first chapter by Carlo Thilgen, Isabelle Gosse and François Diederich provides an insightful and thorough analysis of the origins of fullerene chirality complete with a systematic classification of structural types. Each family of chiral fullerenes is amply illustrated and discussed not only for the structural novelty but also potential applications. Now liberated from the confines of tetrahedral carbon, the fullerene molecules provide fascinating new scaffolds for chiral structures. This chapter exemplifies how the importance and consequences of chirality pervade all molecular science even as new universes of compounds are discovered.

Whereas the first chapter chronicled the leap to new and fascinating templates for chiral molecules, the second takes this progression further in the jump to chirality beyond the molecule. Chemists have long been fascinated by the field of topological stereochemistry whose members include those mysterious creatures, catenanes, rotaxanes and knots (see the cover!). To understand the stereochemical world inhabited by these intriguing species requires careful meditation and Maria-Jesús Blanco, Jean-Claude Chambron, M. Consuelo Jiménez and Jean-Pierre Sauvage provide a clear and outstanding treatment. Once tamed conceptually, however, the challenge of synthesis immediately presents itself and this chapter details both principles and practice of the use of transition metals for templated synthesis of rotaxanes.

Molecules can often surprise us in their ability to retain stereochemical information despite what appear to be stereorandomizing processes. In Chapter Three by Takeo Kawabata and Kaoru Fuji a fascinating manifestation of this phenomenon is illustrated, explained and exemplified in the chemistry of enolates derived from sterically congested ketones and α-amino acid derivatives. Although these enolates are certainly planar species, the stereochemical consequences of the ancillary substituents have, until now been unappreciated. This

thought provoking exposition invites us to formulate new systems that can display this interesting property and test the limits of competing racemization and reaction rates.

The separation of chiral compounds by crystallization is deeply rooted in the history and practice of organic chemistry. Yet, the understanding of the forces and interactions that determine the success of a given resolution is still underdeveloped and most resolutions are undertaken by empiricism. Chapter Four by Kazushi Kinbara and Kazuhikio Saigo represents the state-of-the-art in the rational design of non-natural resolving agents. From a careful analysis of the crystal packing patterns and hydrogen-bonding arrays in the X-ray crystal structures of chiral molecules with their resolving agents, these authors provide remarkable insights into the origin of discrimination and guidelines for the design of new agents.

No volume of *Topics in Stereochemistry* would be complete with out a chapter illustrating the most recent advances in the power of new methods for the stereocontrolled synthesis of chiral molecules. Nature provides us with a dazzling array of chiral molecules to challenge our mettle, but perhaps none so densely packed as carbohydrates. The natural machinery (aldolases) for the assembly of key polyol subunits has been harnessed with impressive generality and selectivity as described by Michael G. Silvestri, Grace DeSantis, Michael Mitchell and Chi-Huey Wong in Chapter Five. A large number of aldolases have been conscripted into valiant service for the synthesis of many polyhydroxylated compounds in aqueous media with out recourse to protective groups. This chapter is certain to stimulate both application of this powerful technology as well as new ideas about the design of synthetic catalysts.

It is fitting to acknowledge Darla Henderson, Senior Editor at John Wiley and Sons for her efforts in maintaining the series and for providing guidance, advice and assistance.

In the intervening four years since the appearance of Volume 22, there has both joy and sadness on the advisory board. In a wonderful recognition of the importance of stereochemistry in synthesis and catalysis, the Nobel Foundation Awarded the 2001 Nobel Prize in Chemistry to two of our board members, Ryoji Noyori and K. Barry Sharpless (along with William S. Knowles). Congratulations!

Sadly, though I must report that an esteemed Advisory Board member, Andre Collet passed away suddenly in 1999 on at the age of 54. Andre made far-reaching contributions to the understanding of resolution by crystallization methods and would have been particularly pleased by the chapter in this volume by Kinbara and Saigo. It is in his memory that Volume 23 is dedicated.

Finally, on a more positive note, I am delighted to announce that Jay S. Siegel (University of California, San Diego) will be joining *Topics in Stereochemistry* as a co-editor. Jay is a well-known and highly-respected member

of the stereochemistry community and his expertise, perspective and energy will assure the continuing success of this series.

SCOTT E. DENMARK
Urbana, Illinois
26 August 2002

CONTENTS

TOPICS IN STEREOCHEMISTRY

VOLUME 23

Chapter 1

Chirality in Fullerene Chemistry

CARLO THILGEN, ISABELLE GOSSE, AND FRANÇOIS DIEDERICH

Laboratorium für Organische Chemie, ETH-Zürich, Universitätstrasse 16, CH-8092 Zürich, Switzerland

Topics in Stereochemistry, Volume 23, Edited by Scott E. Denmark.
ISBN 0-471-17622-2

I. INTRODUCTION

Carbon is distinguished by its position in the periodic table and the resulting variety of covalent bonding patterns it can participate in. It may not therefore be totally by chance that it is the only element of which chiral molecular allotropes are known. A first chiral representative, D_2-symmetric C_{76},[1,2] was isolated and characterized only a year after a new form of elemental carbon, the fullerenes, became available in macroscopic quantities.[3] In the meantime the optical antipodes of D_2-C_{76}, which does not include stereogenic centers, could be resolved[4–6] and their absolute configurations assigned.[7] According to the structural principles of fullerenes C_n,[8–10] the number of allowed constitutional isomers increases with increasing cage size, and so does the number of chiral representatives. For $n = 78$, 80, 82, and 84, the ratio between theoretically possible chiral and achiral constitutional isomers equals 1 : 4, 2 : 5, 3 : 6, and 10 : 14, respectively.[11] A structural extreme of the fullerene concept is represented by the carbon nanotubes,[12,13] among which most members appear to be chiral. This will have significant consequences in potential technological applications as it emerges that the mechanical and electronic properties of individual tubes depend critically on the characteristics of the helical arrangement of the constituting carbon atoms.

Fullerene chirality is not limited, however, to the allotropes themselves, even if abstraction is made of the possibility to functionalize them with residues containing chiral elements. The carbon cages represent unprecedented three-dimensional building blocks allowing a great variety of spatial arrangements of chemical functions.[14–17] As opposed to the highly symmetrical arrangement of four ligands around the center of a tetrahedral structure, many less symmetrical groupings of addends around the immaterial center of a fullerene are possible. As a consequence the condition of all groups being different for a tetrahedral arrangement to be chiral is not necessary any more in the case of fullerenes. It is therefore not surprising that the abundance of fullerene derivatives synthesized during the last decade includes many chiral compounds. Furthermore macrocyclization reactions including the bridging of fullerene core atoms that do not belong to the same pentagon or hexagon on the cage surface have led to a considerable number of topologically nonplanar and even a few topologically chiral structures.[18] It is remarkable, on the other hand,

that the chirality of many molecules reported in literature has apparently passed unnoticed or was at least not addressed by the authors. Our interest in fullerene chirality originates mainly from our early work on higher fullerenes,[17] and we hope that this review will contribute to making this fascinating aspect of many fullerenes and fullerene derivatives more popular.

Regarding the plan of the chapter, we should mention that the discussion of individual molecules (generally represented in the figures by a single enantiomer) mostly follows the classification of fullerene derivatives according to different types of chirality (cf. Section II.A). For reasons of comprehension, however, we present certain chemically related compounds together even if they belong to different classes.

II. CONFIGURATIONAL DESCRIPTION OF CHIRAL FULLERENES AND FULLERENE DERIVATIVES WITH A CHIRAL FUNCTIONALIZATION PATTERN

A. Classification of Chiral Fullerenes and Chiral Fullerene Derivatives

Soon after the existence of chiral carbon spheroids and tubes had been anticipated as a result of the discovery of the structural principles of fullerenes,[8–10] the first representatives, D_2-symmetric C_{76}[1,2] and D_3-symmetric C_{78},[19–21] were isolated and characterized. Since then a number of other chiral as well as achiral higher fullerenes could be isolated and their structures elucidated (cf. Section III). Yet, chirality in fullerene chemistry is not limited to the chiral carbon cages themselves.[17,22] In 1992 the first enantiomerically pure covalent fullerene adducts, C_{60} sugar conjugates with stereogenic centers located exclusively in the addend, were prepared (cf. Section IV.C.2.c).[23] In many cases of chiral fullerene derivatives, however, the chirality is neither inherent to the parent spheroid nor related to chiral elements in the addends, but it can be attributed to the geometrical arrangement of addends[24] on the fullerene surface, a formation that we will describe by *chiral addition pattern* or more generally by *chiral functionalization pattern*.

Depending on the origin of their chirality, three classes of chiral fullerene derivatives can be distinguished (Figure 1.1):[22,25]

1. Derivatives of achiral parent fullerenes in which the functionalization creates a chiral addition pattern on the spheroid, regardless of the addends being identical or different, have an inherently chiral functionalization pattern. The derivatives of chiral parent fullerenes automatically have an inherently chiral functionalization pattern.

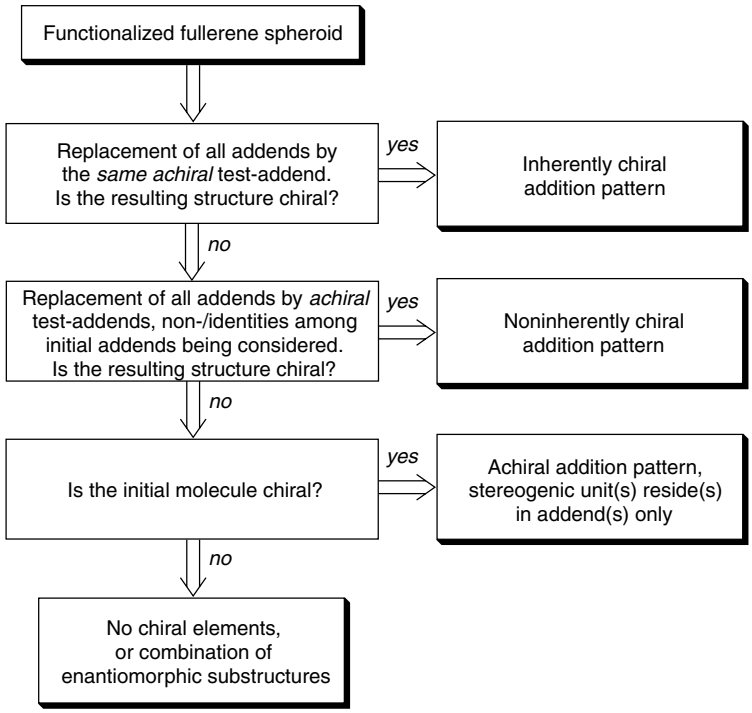

Figure 1.1. Flow diagram for the facile classification of different types of fullerene-spheroid chirality in fullerene derivatives.

2. Derivatives of achiral parent fullerenes in which the chirality of the functionalization pattern is due only to nonidentities among addends, have a noninherently chiral functionalization pattern. The analogy of this situation to that of a center of chirality should be noted.
3. Derivatives of achiral parent fullerenes in which the addition of chiral residues does not create a chiral addition pattern on the fullerene surface. Their chiral elements are located exclusively in the addends.

As the addends of derivatives belonging to classes 1 or 2 can be achiral or chiral, a superposition of different types of chiral elements in a single molecule is possible. The type of a given functionalization pattern can easily be determined by application of a simple, formal substitution test (Figure 1.1) consisting in (1) replacing *all* addends with *the same achiral* test-addend, (2) replacing *non-/identical* original addends with *non-/identical achiral* test-addends, and (3) considering the original molecule. After each step, the resulting structure of increasing degree of complexity is checked for chirality and as soon as it is found, the type of functionalization pattern is recognized.

B. Principles of the Configurational Descriptor System

With the explosive development of covalent fullerene chemistry during the last decade,[14–17,26–30] an increasing number of chiral fullerene derivatives has been published[17,22] and the need for an appropriate configurational description became imperative. Two main reasons motivated us to introduce a new configurational descriptor system for chiral fullerenes and fullerene derivatives with a chiral functionalization pattern:[25] (1) Chiral higher fullerenes do not include any stereogenic centers to be specified by the CIP (*Cahn*, *Ingold*, and *Prelog*) system,[31,32] and the consideration of other chiral elements (e.g., axes or planes) does not appear to be straightforward. (2) The configuration of fullerene derivatives with a chiral functionalization pattern could in principle be described by indicating the absolute configuration — (*R*) or (*S*) — of each stereogenic center of the molecule according to the CIP procedure.[31,32] For stereogenic centers in the spheroid moiety of fullerene derivatives, however, this operation is usually lengthy and unintuitive due to the highly branched carbon framework.[33] This may require the development of very complex hierarchic digraphs[32] of the fullerene molecule, with a difference in CIP priority becoming apparent only for high generations of connected atoms if the distance between addends is large on the surface of the spheroid.[25] For multifunctionalized fullerenes, the operation would have to be repeated for all stereogenic centers that are not equivalent by symmetry and result in a multitude of configurational descriptors accompanied by the locants of the respective atoms. Furthermore, in a specific constitutional isomer of a fullerene derivative, the configuration of individual core-resident stereogenic centers cannot be inverted, in general, independently of the others,[34] and therefore it makes sense considering their ensemble as a single chiral unit.

For these reasons we have proposed a new procedure allowing the configurational description of chiral fullerene spheroids by a single descriptor, regardless of the functionalization degree.[25,35] Even chiral parent fullerenes, or heterofullerenes, and isotopically labeled fullerenes derived from achiral parent spheroids can be assigned an absolute configuration. The system is based on the fact that in a three-dimensional model, the numbering schemes proposed for fullerenes, which can be deduced from their structure,[36,37] are chiral (helical) (cf. Figure 1.2) and thus constitute an ideal reference for differentiating between enantiomeric carbon cages.[38] Whereas two isometric, mirror-symmetric numbering schemes can be applied to an achiral parent fullerene, such as C_{60} (Figure 1.2), a unique one is associable with a specific enantiomer of an inherently chiral carbon spheroid[25,35–37] and, consequently, with all its derivatives (cf. Figure 1.3 and Section II.C.1).[25] Similarly, for a chiral derivative resulting from an inherently chiral addition pattern "laid over" an achiral parent fullerene, there is a unique numbering leading to the lowest

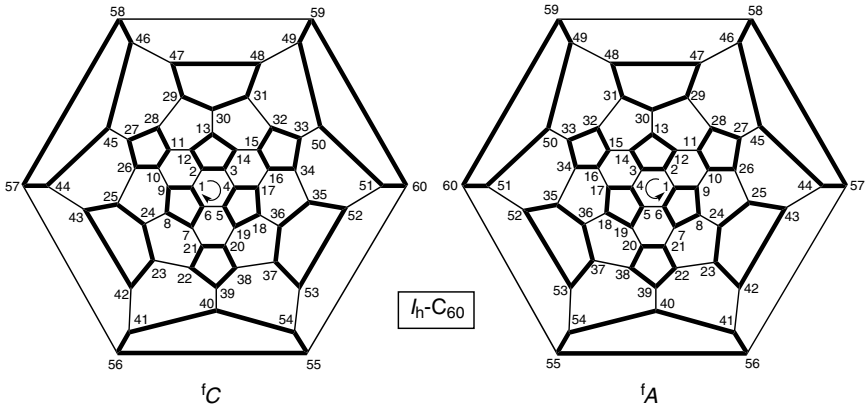

Figure 1.2. Schlegel diagrams of I_h-C_{60} with enantiomeric numbering schemes according to Godly and Taylor.[36] The arrows in the central, proximal hexagon indicate the direction of the numbering commencement.

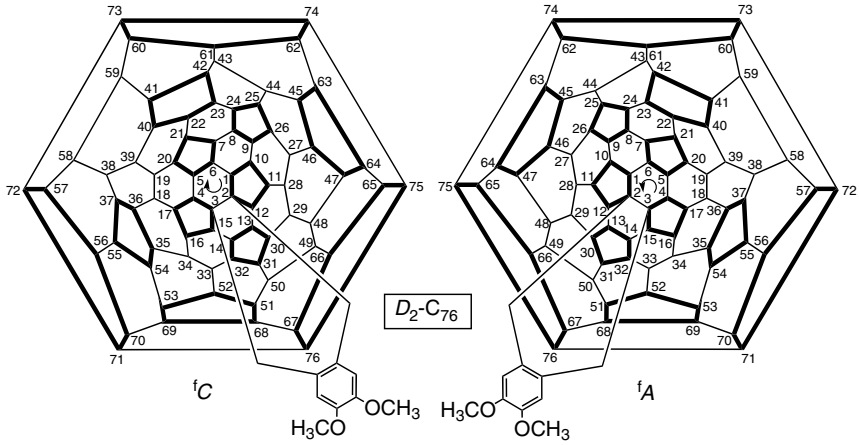

Figure 1.3. Schlegel diagrams of the enantiomers of 80,81-dimethoxy-2,3-(methano[1,2]benzenomethano)[76]fullerene.[50] In all cases of inherently chiral carbon cages, the same numbering scheme is used for a given enantiomer of the parent fullerene and its derivatives.

set of locants[39] for the addends. Depending on whether the path traced from C(1) via C(2) to C(3) of this numbering is clockwise (*C*) or anticlockwise (*A*), the descriptors are defined as ^{f}C and ^{f}A (f = fullerene), respectively.[25] In the case of a noninherently chiral functionalization pattern, CIP priorities are attributed to the addends (in the way they are to the ligands of a stereogenic

center), and the handedness of the numbering helix is chosen such that lowest locants are allocated to the addition sites bearing the addends of highest CIP priority. The configuration of chiral elements that are located exclusively in the addend(s) is described in the classical way by the descriptors (*R*) and (*S*), or (*M*) and (*P*).[31,32]

Being based on numbering, a great advantage of this descriptor system is its easy handling by computers.[40] As different numbering schemes have appeared in literature,[36,37] it should be pointed out that the principle of the descriptor system above is valid for any helical numbering. Of course, a correct interpretation of a given configurational descriptor requires knowledge of the used numbering system.

A final question to be addressed is that of the limits of the descriptor system with regard to the structures it can be applied to. In a stricter sense, it should be valid for all fullerenes and their derivatives having a cage framework that is unaltered with respect to the number of atoms and their coordination within the core. In practice, however, as various core-modified fullerenes have been synthesized,[41–49] it may appear convenient to apply it to all compounds that are relatively closely related to the carbon spheres and to which fullerene nomenclature can be easily applied.

C. Examples for the Configurational Description of the Different Classes of Chiral Fullerene Spheroids

1. Inherently Chiral Fullerenes and Their Derivatives

In the case of inherently chiral fullerenes and their derivatives, each of the two mirror-symmetric, isometric numbering schemes fits only a single parent fullerene enantiomer. Hence it is the chirality of the latter that determines the numbering scheme to be used and therefore the descriptor ^{f}C or ^{f}A specifying the absolute configuration of these carbon spheroids and of all their derivatives, regardless of the number and arrangement of addends (cf. Section IV.A.3) (Figure 1.3).

2. Derivatives of Achiral Parent Fullerenes with an Inherently Chiral Functionalization Pattern

As the parent fullerene is achiral, its C-atom numbering can in principle be achieved with either one of the two mirror-symmetric numbering schemes. For a particular enantiomer of its derivatives with an inherently chiral functionalization pattern, however, a single numbering scheme only leads to the lowest set of locants for the addends (cf. Sections IV.A.1 and IV.A.2) (Figure 1.4).

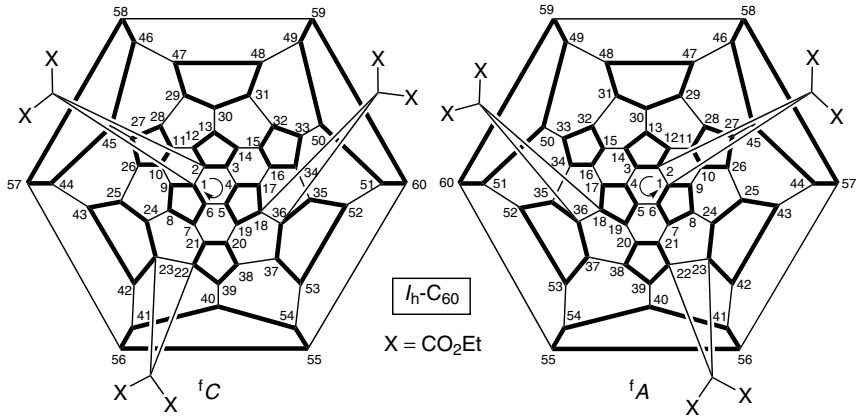

Figure 1.4. Schlegel diagrams of the enantiomers of hexaethyl 1,2:18,36:22,23-tris (methano)[60]fullerene-61,61,62,62,63,63-hexacarboxylate (*e*,*e*,*e* isomer).[51] Using the numbering scheme of opposite handedness would afford a higher set of locants for the addends (1,2:18,36:31,32) of each structure.

3. *Derivatives of Achiral Parent Fullerenes with a Noninherently Chiral Functionalization Pattern*

In the case of a noninherently chiral functionalization pattern (which is always associated with an achiral parent fullerene), no distinction between enantiomers is possible on the base of the criteria above. The same lowest set of locants is obtained with both mirror-symmetric numbering schemes, which is due to a symmetrical arrangement of the addends on the fullerene spheroid. However, the overall symmetry of the molecule is lowered by structural differences in the addends.[52] For making a discrimination between the two applicable numbering pathways, a classification of addends or of heteroatoms of the core is used. It can be achieved conveniently by use of the CIP system that allows a hierarchic ordering of ligands differing in constitution or configuration, and this has proved very useful in the configurational description of stereogenic centers, axes, and planes.[31,32] For the fullerene derivatives considered in this section, substituting heteroatoms of the cage and addends are treated alike by starting the comparison among the concerned substructures according to the CIP rules at the atom located within the fullerene core and then progressively moving outward until a priority difference becomes apparent. Of the two mirror-symmetric numbering schemes leading to the lowest set of locants, that one assigning the lower locant to an addend of higher CIP priority at the first point of difference is preferred and confers its descriptor to the enantiomer in question. Typical representatives of this class are 1,4-adducts of C_{60} with two different addends (cf. Section IV.B) (Figure 1.5).

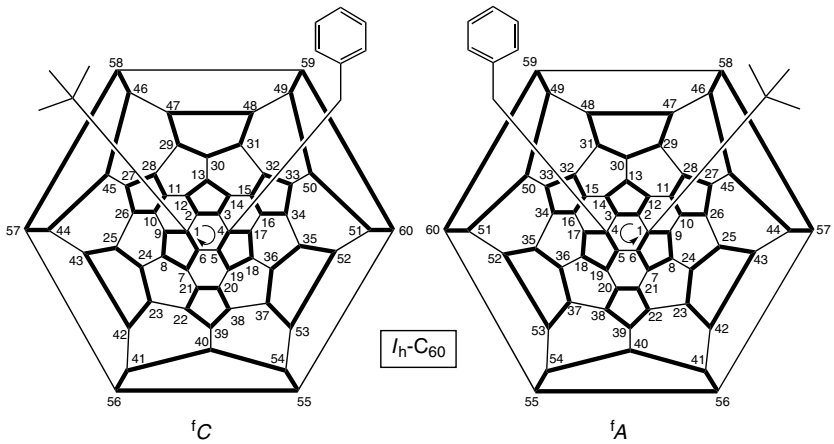

Figure 1.5. Schlegel diagrams of the enantiomers of 1-(*tert*-butyl)-4-(phenylmethyl)[60]fullerene.[53] In each structure, the lowest locant (1) is allocated to the addend of highest CIP priority (*tert*-butyl).

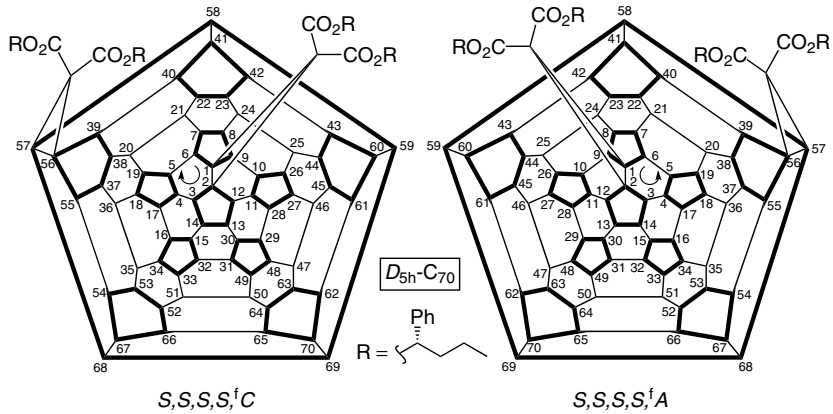

Figure 1.6. Schlegel diagrams of two stereoisomers of tetrakis[(*S*)-1-phenylbutyl] 1,2:56,57-bis(methano)[70]fullerene-71,71,72,72-tetracarboxylate.[35,54] The two types of stereogenic elements (inherently chiral addition pattern and stereogenic centers in the ester groups) are specified independently of each other. As can be seen from the descriptors (*S*,*S*,*S*,*S*,^{f}*C*) and (*S*,*S*,*S*,*S*,^{f}*A*), the depicted molecules are diastereoisomers.

4. Superposition of Chiral Elements in a Fullerene Derivative

It should be mentioned that the addition of chiral residues to an achiral fullerene does not necessarily lead to a chiral addition pattern (cf. Section IV.C and Figure 1.1). In such a case the configuration of the chiral addend(s) only

has to be determined in the usual way by application the CIP rules.[31,32] If, on the other hand, a chiral functionalization pattern is superposed to chiral addends, the configuration of both types of chiral elements has to be indicated (Figure 1.6).

III. INHERENTLY CHIRAL FULLERENES

A. The Higher Fullerenes

Even though fullerene chirality is not limited to the inherently chiral larger carbon cages, it was the isolation and characterization of the first chiral member in the series, D_2-C_{76},[2] that initiated the study of the handedness of many fullerenes and fullerene derivatives. Diederich, Whetten, and co-workers showed that the ^{13}C NMR spectrum of C_{76} consists of 19 lines of equal intensity, which confirmed the D_2-symmetric cage type fullerene structure (Figure 1.7). As a result of a computer search based on qualitative MO (molecular orbital) theory, this structure, being the only closed-shell isomer obeying the IPR (isolated pentagon rule),[55] had been predicted by Manolopoulos to be the only stable form of [76]fullerene.[8] It can be considered as a spiraling, double-helical arrangement of two identical edge-sharing strands of anellated pentagons and hexagons, tied up at the ends of the long axis of the fullerene which corresponds to one of the C_2-axes. This view emphasizes the helical distortion of the structure along this direction.[56]

Whereas the structural assignment by one-dimensional ^{13}C NMR spectroscopy is unambiguous in the case of D_2-C_{76},[2,57] Achiba and co-workers were able to determine the carbon atom connectivity by 2D ^{13}C NMR INADEQUATE (incredible natural abundance double-quantum transfer experiment) analysis performed on an isotopically enriched sample (20% ^{13}C).[58] In particular, they found that the observed chemical shifts correlate well with the curvature of the spheroid, the more strongly pyramidalized carbon atoms being shifted toward lower magnetic field.

The structure of D_2-C_{76} was further supported by X-ray crystallographic data of the van der Waals compound [(±)-D_2-C_{76}]$(S_8)_6$.[59] However, pronounced disorder in the measured crystal that contained both enantiomers of C_{76} impeded a detailed analysis, and so far, more conclusive crystallographic data are available neither for the parent fullerene nor for a C_{76} derivative. The resolution of the enantiomers of D_2-C_{76},[4–6] D_3-C_{78},[5] and D_2-C_{84}[5,60] will be described separately in Section III.C.

C_{78} can theoretically occur as five possible IPR-satisfying structures among which a single one is chiral (Figure 1.7).[9,11] This constitutional isomer, D_3-C_{78}, was indeed isolated as minor component next to achiral C_{2v}-C_{78}

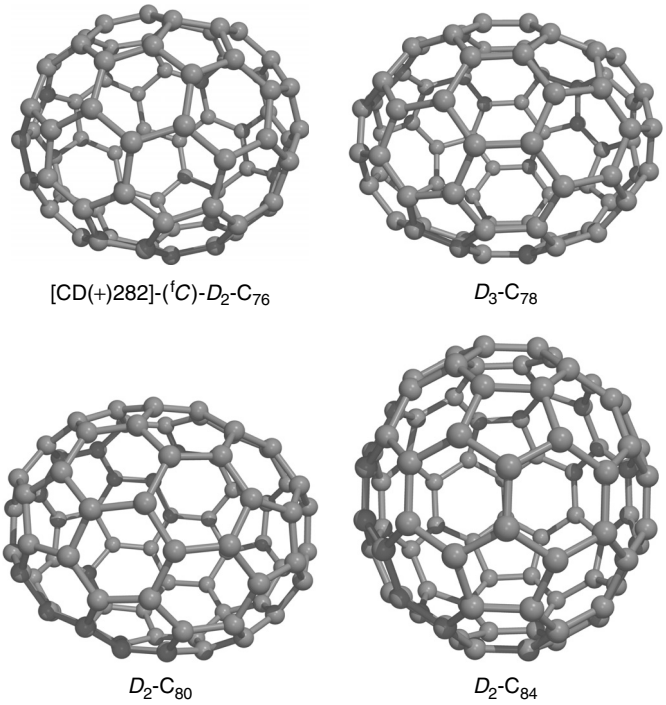

Figure 1.7. A selection of inherently chiral higher fullerenes, for which certain or confident structural assignments have been made. In the case of D_2-C_{76}, the absolute configuration as well as a characteristic CD (circular dichroism) maximum of the shown enantiomer are indicated.

when macroscopic amounts of [78]fullerene isomers were purified for the first time.[19] Depending on the conditions of the fullerene soot production, these two C_{78} isomers can be accompanied by another achiral isomer, $C_{2v'}$-C_{78}.[20,57,61] Thirteen distinct ^{13}C NMR lines of equal intensity allowed an unambiguous structural assignment of the D_3-symmetric allotrope in which the C_3-axis coincides with the long axis of the molecule, intersecting each polar cap at the central ring of a triphenylene substructure (Figure 1.7).[19–21,57]

The small amounts of D_3-C_{78} found in fullerene soot and its difficult purification have almost completely impeded the exploration of its chemistry so far.[5,62,63]

Owing to a low abundance in fullerene soot as well, and to a small near-UV extinction coefficient, it took until 1996 for the next higher fullerene, C_{80}, to be isolated and characterized by ^{13}C NMR spectroscopy.[64] The measured resonances were consistent with 20 groups of four symmetry-equivalent carbon atoms, and in combination with theoretical calculations on the structures and

energies of the seven IPR-conform isomers,[11,65] a D_2-symmetric structure was proposed for the isolated allotrope (Figure 1.7).

A chiral isomer of C_2-symmetry (41 ^{13}C NMR resonances) has been shown to be the major component in the C_{82} fraction of fullerene soot.[20,58] However, it was not possible to determine experimentally which one of the three C_2-symmetric structures among the nine IPR-satisfying C_{82} isomers[11] had been isolated.

C_{84} is certainly one of the most interesting higher fullerenes. This is due to the relatively large amounts of this carbon homologue present in fullerene soot as well as to its rich structural diversity. Early ^{13}C NMR studies revealed the presence of two major isomers of D_2- and D_{2d}-symmetry in a nearly 2 : 1 ratio.[20,56,57] In conjunction with theoretical calculations, the structures of D_2(IV)-C_{84} (Figure 1.7) and D_{2d}(II)-C_{84}[66] were confidently proposed for the major isomers. A first experimental assignment of the observed D_{2d}-C_{84} to one out of the 24 IPR-satisfying isomers,[11] was accomplished only when Balch and co-workers solved the X-ray crystal structure of $[[\eta^2\text{-}(D_{2d}\text{-}C_{84})]Ir(CO)Cl(PPh_3)_2] \cdot 4C_6H_6$, obtained by selective crystallization from a solution containing both D_2- and D_{2d}-C_{84}.[67] Four years later Shinohara and co-workers were able to separate the two major C_{84} isomers by multistage recycling HPLC (high-performance liquid chromatography) and to record the ^{13}C NMR spectrum of each allotrope.[68] Eleven carbon resonances (one of intensity 4, ten of intensity 8) allowed an unambiguous assignment of the achiral isomer as the D_{2d}(II) structure, thus confirming the crystallographic results. As to the D_2-isomer, the 21 measured resonances are in accord with all four D_2-symmetric IPR-satisfying isomers[11] and a secure assignment to the D_2(IV) structure was possible only through 2D ^{13}C NMR spectroscopy.[58] Another purification technique, involving a separation of functionalized intermediates and a reversion of the latter to the parent fullerenes, was presented shortly afterward (cf. Section III.C).[60] In this experiment Diederich and co-workers were able to isolate another, CD-silent and therefore achiral C_{84} isomer, but because of its small amounts, UV and electrochemical data only could be recorded. Moreover their strategy allowed the resolution of the optical antipodes of D_2-C_{84} (cf. Section III.C).[60] First indications for the presence of a number of further, minor isomers in the C_{84} fraction had been obtained relatively early by Taylor and co-workers.[57] This observation was corroborated by Saunders and co-workers who measured possibly up to nine ^{3}He NMR resonances for i^3HeC_{84} (C_{84} with endohedrally *incarcerated* ^{3}He, also denoted as ^{3}He@C_{84}) obtained from high-pressure helium capture by a C_{84} sample.[69] A first attempt to structurally assign minor C_{84} isomers was made by Taylor and co-workers through analysis of the ^{13}C NMR spectra of HPLC center and tail cuts of the C_{84} fraction: They identified a second D_2-symmetric isomer and obtained

indications for D_{3d}-, D_{6h}-, C_s-, and either C_s- or C_2-symmetric isomers.[70] Shinohara, Achiba and co-workers, finally, succeeded in isolating five minor C_{84} isomers from material accumulated during extensive HPLC purification of endohedral metallofullerenes.[71] Analysis by ^{13}C NMR spectroscopy showed the isolated isomers to have D_2-, D_{2d}-, C_2-, C_s-,[72] C_s-,[72] D_{2d}-, and D_2-symmetry (order of decreasing yield). Besides the isolated two major and five minor [84]fullerene allotropes, they noticed the presence of an eighth isomer that still awaits separation.

Enriched samples of fullerenes with more than 84 C-atoms were obtained as early as 1991.[1] In the meantime Achiba and co-workers have been able to purify an impressive number of these large carbon cages. Based on ^{13}C NMR data obtained for higher fullerenes such as C_{86}, C_{88}, C_{90}, C_{92}, and C_{94}, they found many chiral isomers, with C_2- and D_2-symmetry being prevalent.[58,73]

Although not a perfect fullerene spheroid, another chiral carbon allotrope, C_{119}, was isolated in the form of a ^{13}C-enriched sample from the thermolysis of $C_{120}O$.[74] On grounds of the obtained ^{13}C NMR spectra as well as molecular modeling, Krätschmer and co-workers proposed a C_2-symmetric, peanut-shaped structure consisting of two fullerene-like C_{58} units bridged by three sp^3-C-atoms, two of which are symmetry-equivalent.[74]

As a consequence of their cage structure, C_{60} and higher fullerenes can incarcerate metal ions,[75,76] noble gases,[77–79] and other nonmetal atoms such as nitrogen or phosphorus.[80] Higher fullerenes also form endohedral inclusion complexes with up to three metal ions, but difficulties in the isolation and purification, as well as a relatively low stability under ambient conditions, have hampered the elucidation of the cage structures in many cases. Although it can be assumed that a number of them are chiral, NMR studies on the isolated species i-La_2C_{80}[81] and i-Sc_2C_{84}[82] have shown the carbon spheroids to have I_h- and D_{2d}-symmetry, respectively.

Preparative amounts of helium compounds i-HeC_n ($n = 60, 70, 76, 78, 84$) could be produced by heating fullerene samples to elevated temperatures (ca. 600°C) under high He pressure (ca. 2700 atm).[78] Strong and specific magnetic shieldings were revealed by ^3He NMR spectroscopy for ^3He atoms inside the cages of different fullerenes and of their covalent derivatives, giving rise to a unique resonance for each compound measured so far.[69,83–88] Taking advantage of this sensitive probe, Saunders and co-workers concluded from ^3He NMR measurements performed on C_{78} and C_{84} samples with endohedrally trapped ^3He that these fullerenes may consist of up to five and nine isomeric cages, respectively.[69,84] Despite the possibility of small amounts of impurities being present in the samples of helium incarceranes, the number of nine C_{84} isomers is in close agreement with recent ^{13}C NMR spectroscopic investigations.[70,71]

B. Carbon Nanotubes

Next to fullerenes and their endohedral incarcerates, another form of carbon, the nanotubes, has created strong interest among physicists and chemists because of their electronic and mechanical properties which may lead to numerable materials applications.[12,13] Carbon nanotubes represent extreme cases of higher fullerenes. A perfect single-walled carbon nanotube can be considered as a cylinder made of a hexagonal graphite lattice capped at both ends by fullerene type hemispheres that include a total of 12 curvature-inducing pentagons. The closure of the cylinder has to occur in such a way that the dangling bonds at the edges match. To achieve this, the rolling of the graphite sheet does not necessarily have to occur parallel or perpendicular to opposite edges of the constituting hexagons (Figure 1.8). Any translational shift along the boundaries of the sheet leads to a different orientation of the honeycomb lattice with respect to the tube axis. Consequently the tube walls can be considered as composed of helical strands of edge-sharing hexagons, which illustrates the chirality of the resulting structure. The circumference and helicity of a nanotube can be uniquely described by pairs of integers (n, m) defining the roll-up vector **R** (Figure 1.8). The only orientations of the lattice leading to achiral tubes are represented by the **R** vectors (n, n) and $(n, 0)$. According to the appearance of their edges when broken perpendicular to the tube axis, the latter structures are called "armchair" and "zigzag" tubes, respectively.

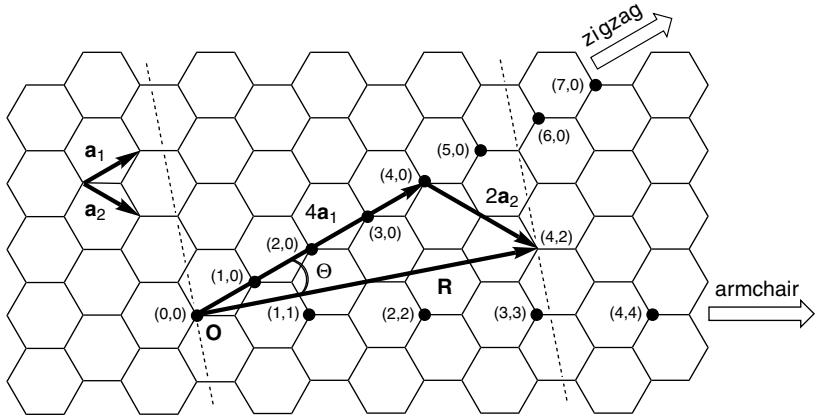

Figure 1.8. The rolling up of a graphite sheet into a nanotube cylinder can be integrally described by the vector **R** indicating the direction of the rolling and the circumference of the resulting cylinder which will be oriented parallel to the dotted lines. The helicity of the tube can be expressed by the angle Θ (chirality angle) between the primitive vector $\mathbf{a}_1$ and **R**. Achiral tubes occur only if Θ is a multiple of 30° which corresponds, for example, to a rolling of the sheet along the lattice points $(n, 0)$ (zigzag tube) or (n, n) (armchair tube).

The helicity of carbon nanotubes was among the most revealing discoveries by Ijima and co-workers in the early 1990s.[89] It was later confirmed by STM (scanning tunneling microscopy) images of single nanotube surfaces resolved at the atomic level.[90] It appears that the helicity of nanotubes is of prime importance for potential technological applications, as it is closely related to their electronic structure and properties.[13]

C. Resolution of Chiral Fullerenes and Assignment of Absolute Configurations to the Enantiomers of D_2-C_{76}

Isolation of the first chiral carbon molecule, D_2-C_{76}, as a racemic mixture[2] generated strong interest in the separation of its optical antipodes and the investigation of their chiroptical properties. In 1993 Hawkins and Meyer effectuated a small-scale kinetic resolution by asymmetric Sharpless osmylation of racemic C_{76}, using OsO_4 complexes with an enantiomerically pure ligand derived from a cinchona alkaloid[4] (Figure 1.9). Partial reaction of (±)-D_2-C_{76} with the osmium reagent afforded enantiomerically enriched unreacted C_{76} and diastereoisomerically enriched osmates. Reduction of the latter with $SnCl_2$ yielded [76]fullerene enriched in the other enantiomer. Use of a pseudoenantiomeric alkaloid-derived ligand in the osmylation afforded an enrichment of the opposite optical C_{76} antipodes in the starting material and the product, respectively (Figure 1.9). Being able thus to obtain each C_{76} enantiomer in an enriched form, Hawkins and Meyer recorded the first CD spectra of the chiral carbon molecules.[4] Repetition of the experiment with C_{78} and C_{84} afforded the respective data for the optical antipodes of D_3-C_{78} and D_2-C_{84}.[5] In these experiments it was possible to start from the isomeric mixtures (C_{2v}-C_{78} +

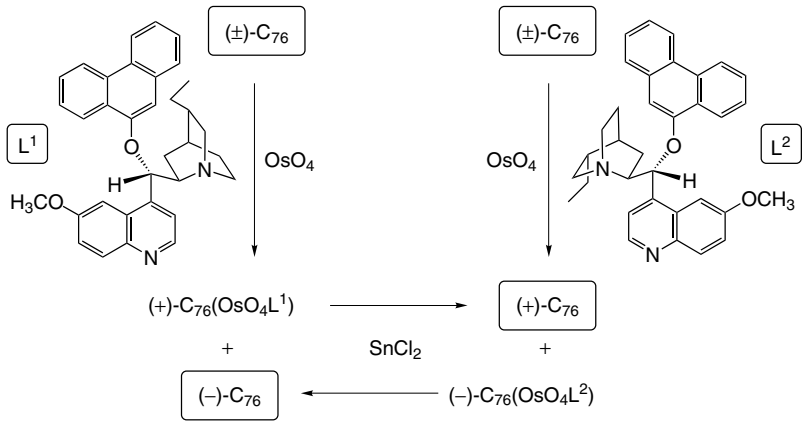

Figure 1.9. Kinetic resolution of D_2-C_{76} based on a differential reactivity of enantiomerically pure osmium complexes toward the optical antipodes of the fullerene.

D_3-C_{78}), respectively (D_2-C_{84} + D_{2d}-C_{84}), because the achiral isomers are CD inactive. The differential reactivity of the chiral reagent toward the enantiomers of D_2-C_{84} is particularly remarkable in view of the "roundness" of this fullerene when compared to the helically twisted C_{76} (*vide infra*).

As the enantiomers of D_2-C_{84} can formally be interconverted by Stone-Wales pyracylene rearrangements[91,92] via the achiral D_{2d}-C_{84}, they were ideal candidates to study the activation barrier of this transformation. However, taking into account the loss of material through decomposition, neither heating (600/700°C) nor irradiation ($\lambda = 193$ nm) led to a significant loss of optical activity in samples of enantiomerically enriched D_2-C_{84} or D_2-C_{76}. This shows that the activation barrier amounts to at least 83 kcal mol^{-1} for a potential Stone-Wales rearrangement.[5]

A comparison between the CD spectra reported by Hawkins and Meyer for the C_{76} enantiomers ($\Delta\varepsilon$-values up to 32 M^{-1} cm^{-1})[4] and those of a number of optically pure, covalent C_{76} derivatives prepared by Diederich and co-workers ($\Delta\varepsilon$-values up to 250 M^{-1} cm^{-1})[93] revealed a large difference in the magnitude of the Cotton effects. In order to reinvestigate the chiroptical properties of the enantiomerically pure allotrope, a separation based on the so-called Bingel-retro-Bingel strategy was carried out.[6] It consists of a three-step procedure starting with the functionalization of a fullerene mixture by bis(alkoxycarbonyl)methano addends (Bingel reaction).[94] Due to their enhanced polarity the derivatives are easier to separate than the unfunctionalized carbon cages, and once this is done, the Bingel addends are cleaved by exhaustive CPE (constant potential electrolysis) at a potential situated, in general, slightly below the second reduction potential of the adduct (electrochemical retro-Bingel reaction).[6,95] In brief, the method involves a reversible derivatization of fullerenes, combined with a separation of the functionalized intermediates. Following this strategy, the pure optical antipodes of [76]fullerene were obtained by application of the electrochemical retro-Bingel reaction to each of two optically pure, diastereoisomeric mono-adducts of D_2-C_{76} ((*S*,*S*,^{f}*A*)-**1** and (*S*,*S*,^{f}*C*)-**2**, Figure 1.10) that have enantiomeric carbon cores and were isolated from the Bingel reaction of (±)-D_2-C_{76} with bis[(*S*)-1-phenylbutyl]malonate (cf. Section IV.A.3.b).[93] The CD spectra of the individually generated optical antipodes of D_2-C_{76} (Figure 1.10) displayed the expected mirror image shapes with band positions in full agreement with those of Hawkins and Meyer.[4] In contrast, the Cotton effects reach up to nearly 320 M^{-1} cm^{-1} and are therefore much more in agreement with the values measured for optically pure C_{76} derivatives.[93] The lower values reported by Hawkins and co-workers may originate from a low optical purity of their samples or inaccuracies in the determination of concentrations.

In a similar experiment, derivatization of the C_{84} fraction of fullerene soot with optically pure bis[(*S*)-1-phenylbutyl]malonate afforded a series of

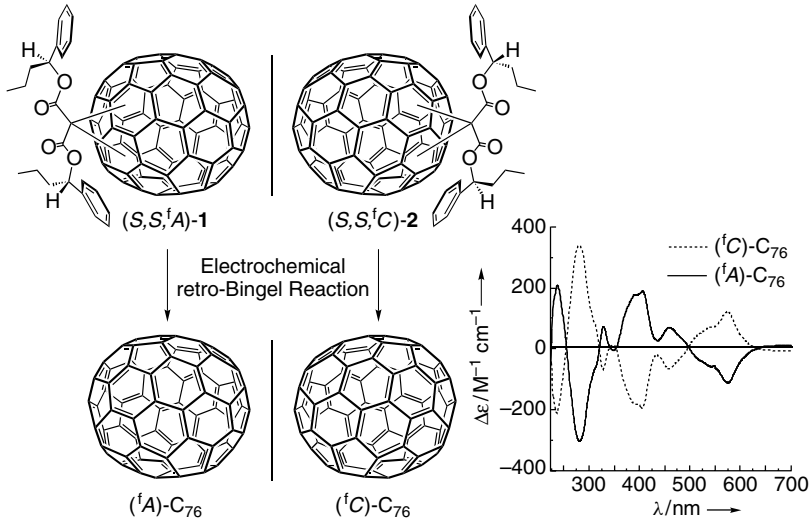

Figure 1.10. Preparation of the pure enantiomers of D_2-C_{76} by electrochemical retro-Bingel reaction of each of two optically pure, diastereoisomeric adducts with enantiomeric C_{76} cores, and circular dichroism spectra of the resolved fullerene enantiomers in CH_2Cl_2, including their configurational assignment.

mono- and bis-adducts, some of which could be separated by HPLC and their symmetries determined by ^{1}H- and ^{13}C NMR spectroscopy.[60] Among these, a pair of C_2-symmetric bis-adducts ((*S*,*S*,*S*,*S*,^{f}*C*)-**3**/(*S*,*S*,*S*,*S*,^{f}*A*)-**4**) featured mirror-image CD spectra with relatively large Cotton effects (Figure 1.11). Such spectra are characteristic of a couple of diastereoisomers, with the chiroptical contributions of the enantiomeric, inherently chiral fullerene cores, or functionalization patterns largely dominating those of the chiral addends.[17,22,35,54,96,97] The UV/Vis spectra, which differed considerably from those of D_{2d}-C_{84} derivatives, further indicated the presence of D_2-C_{84} derivatives. Controlled potential electrolysis of the separated diastereoisomers (*S*,*S*,*S*,*S*,^{f}*C*)-**3** and (*S*,*S*,*S*,*S*,^{f}*A*)-**4** gave rise to the enantiomers of D_2-C_{84}, and their mirror-image CD spectra (Figure 1.11) correspond nicely to those reported by Hawkins and co-workers for samples obtained by kinetic resolution via asymmetric osmylation (*vide supra*).[5] With $\Delta\varepsilon$-values up to 20 $M^{-1}\,cm^{-1}$, the inherently chiral D_2-C_{84} enantiomers feature much weaker Cotton effects than the optical antipodes of the smaller, inherently chiral, D_2-symmetric C_{76} ($\Delta\varepsilon$-values up to 320 $M^{-1}\,cm^{-1}$).[6] This is probably due to the fact that in D_2-C_{76}, the chirality arises from its oblong, helically twisted structure,[2,56] while D_2-C_{84} is rather "round-shaped" and only slightly distorted from achiral D_{2d}-C_{84}, into which it can formally be transformed by a single pyracylene rearrangement.

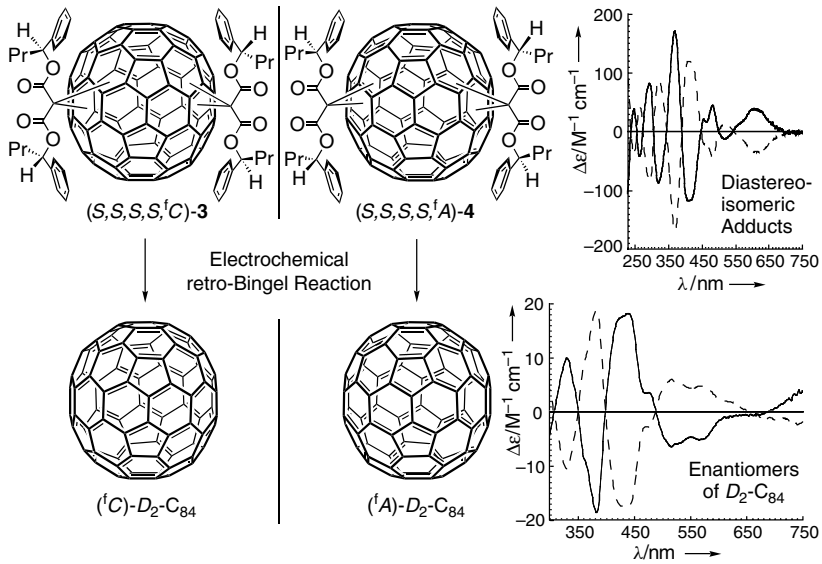

Figure 1.11. Preparation of the pure enantiomers of D_2-C_{84} by electrochemical retro-Bingel reaction of each of two optically pure, diastereoisomeric adducts with enantiomeric C_{84} cores, and circular dichroism spectra of the starting diastereoisomers as well as of the resolved fullerene enantiomers in CH_2Cl_2.

Theoretical calculation of the CD spectra of D_2-C_{76}[7,98] by the π-electron SCF-CI-DV MO (self-consistent field–configuration interaction–dipole velocity molecular orbital) method[7,99,100] and comparison with the experimental data[4,6] allowed the assignment of absolute configurations to the separated enantiomers of [76]fullerene, which can now be denominated as [CD(−)282]-(f*A*)-D_2-C_{76} and [CD(+)282]-(f*C*)-D_2-C_{76}[7] (Figures 1.7 and 1.10). A theoretical CD spectrum has also been calculated by Zerbetto and co-workers for D_2-C_{84},[101] but unlike the case of C_{76},[7,98] it does not allow an accurate determination of the absolute configuration of the isolated optical antipodes by comparison with their experimental spectra.

IV. CHIRAL FULLERENE DERIVATIVES

A. Fullerene Derivatives with an Inherently Chiral Addition Pattern

1. Derivatives of C_{60}

a. General Considerations on the Chirality of the Most Common Addition Patterns in Mono- and Bis-adducts of C_{60}. Fullerene bonds are

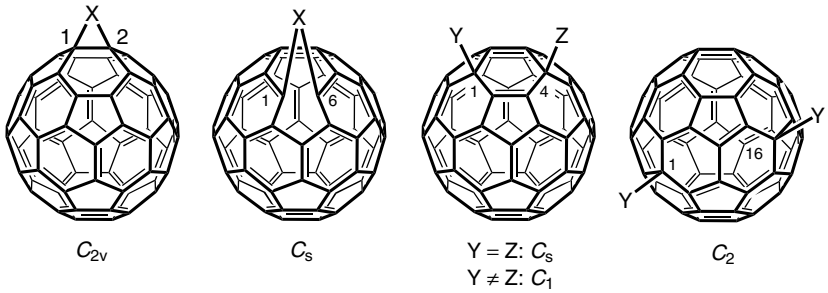

(*a*)

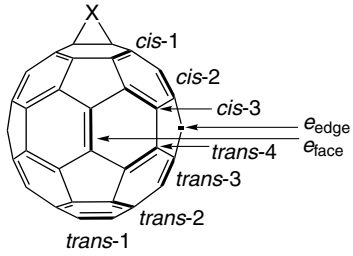

Regioisomer	Symmetry	Locants
cis-1	C_s	1,2:3,4
cis-2	C_s	1,2:7,21
cis-3	C_2	1,2:16,17
e	C_s	1,2:18,36
trans-4	C_s	1,2:34,35
trans-3	C_2	1,2:33,50
trans-2	C_2	1,2:51,52
trans-1	D_{2h}	1,2:55,60

(*b*)

Figure 1.12. (*a*) The most characteristic patterns of mono-addition to C_{60}. The symmetry indications are made under the assumption that the bridging addend *X* is C_{2v}-symmetric[102] and that *Y* and *Z* are achiral. (*b*) The possible bis-adduct regioisomers resulting from twofold addition of identical, C_{2v}-symmetric[102] addends to C_{60}.

located either between two six-membered rings (6–6 bonds) or between a six- and a five-membered ring (6–5 bonds). The most common monofunctionalization pattern of C_{60}[14–16] results from 1,2-addition across the 6–6 bond C(1)–C(2) (Figure 1.12*a*) which has the highest double-bond character. A number of primary adducts, notably fullerene-fused pyrazolines and triazolines, can rearrange to so-called homofullerenes, in which the *homo* atom is inserted into a 6–5 junction ("6–5 open" methano bridging between C(1) and C(6)) (Figure 1.12*a*; cf. also Schemes 1.2, 1.7, and 1.8; for according derivatives of C_{70}, cf. Section IV.A.2.b. and Scheme 1.9). In combination with the high symmetry of C_{60}, both addition patterns lead to achiral molecules with C_{2v}- or C_s-symmetrical addends (Figure 1.12*a*).[102] Many radical reactions, such as halogenations and a number of nucleophilic additions followed by the quenching with an electrophile, occur as intrahexagonal 1,4-additions, especially if sterically demanding groups are introduced (Figure 1.12*a*).[14–16] If the added groups in such a mono-adduct are not identical, the resulting functionalization pattern is noninherently chiral; examples of this type will be

discussed in Sections IV.B.1.a and IV.B.1.b. Very bulky groups, finally, were found to lead to a 1,6-addition mode with occupation of positions C(1) and C(16) of C_{60}, which corresponds to an inherently chiral mono-addition pattern (Figure 1.12*a*; cf. also Section IV.A.1.h).[103]

In bis-adducts of C_{60}, the situation can become much more complex. For reasons of clarity, the following general considerations will be limited to products of twofold 1,2-addition of C_{2v}-symmetric addends across 6–6 bonds.[102] According to Hirsch and co-workers, the addition patterns corresponding to the possible bis-adduct regioisomers are described as *cis*-1, *cis*-2, or *cis*-3 if both addends are located within the same hemisphere, and as *trans*-1, *trans*-2, *trans*-3, or *trans*-4 if they are located in opposite hemispheres (Figure 1.12*b*).[51] In case the second addend resides at the borderline between the hemispheres with respect to the first, the addition pattern is termed *e* (*equatorial*) (Figure 1.12*b*). If both C_{2v}-symmetric addends are identical, these eight possible relative arrangements of addends can lead to a maximum of eight regioisomers. Among the corresponding addition patterns, *cis*-3, *trans*-2, and *trans*-3 are inherently chiral and thus represent stereogenic units to be configurationally specified by the descriptors ${}^{f}C$ or ${}^{f}A$. If both C_{2v}-symmetrical addends are different, the overall symmetry of the bis-adducts is lowered to C_1 except for the *trans*-1 adduct ($D_{2h} \rightarrow C_{2v}$) and the *e* adduct which keeps its C_s-symmetry. As a consequence the formerly achiral addition patterns (*cis*-1, *cis*-2, and *trans*-4) become noninherently chiral with the exception of the *trans*-1 and the *e* pattern, the latter being distinguished by the constitutional heterotopicity of its two involved bonds. Indeed, in imagining the common case of fused rings as addends and looking from one of the functionalized *e* type bonds toward the other, one can see either the edge or the face of the cycle fused to the distal bond. Accordingly, the position of the viewer is described as e_{edge} or e_{face}, respectively, with regard to the distal *e* bond (Figure 1.12*b*).[104] As a result two achiral constitutional *e* isomers can result from addition of two different C_{2v}-symmetric addends and the total possible number of bis-adduct regioisomers rises to nine.

Before moving on to the discussion of groups of individual C_{60} derivatives with an inherently chiral functionalization pattern, it should be pointed out that the first systematic study of the regiochemistry of a bis-addition (osmylation) to C_{60} was undertaken by Hawkins and co-workers as early as 1992.[105] With the help of a 2D NMR INADEQUATE analysis of ^{13}C-enriched fullerene samples, they could isolate and identify the C_s-symmetrical *e*- and the C_2-symmetrical *trans*-3 (cf. Figure 1.12*b*) bis(osmates) and suggested also structures for the remaining three isolated isomers. Using OsO_4 in combination with ligands derived from dihydroquinine or dihydroquinidine, asymmetric bis-osmylation afforded nonracemic *trans*-3 and *trans*-2 bis-adducts (cf. Figure 1.12*b*). Subsequent ligand exchange for pyridine and purification allowed a first recording

of the CD spectra of C_{60}-bis-adducts with an inherently chiral addition pattern (Figure 1.13; the obtained compounds with unassigned absolute configurations are represented as racemates (±)-**5** and (±)-**6**) or, in other words, of inherently chiral C_{60}-derived π-chromophores.[106]

b. Methanofullerene Derivatives Resulting from Functionalization with Independent (Nontethered) Addends. Bingel type adducts, namely bis(alkoxycarbonyl)methanofullerene derivatives resulting from addition of 2-halomalonate anions across a 6–6 bond of a fullerene,[94,107] are probably the most extensively studied class of fullerene derivatives. They have thus provided the largest body of knowledge on the regio- and stereochemistry of multiple additions to C_{60} and the higher fullerenes.[14–17,22,28,42,108] In a twofold, stepwise addition of diethyl-2-bromomalonate, Hirsch and co-workers were able to isolate seven of the eight possible bis-adducts (cf. Figure 1.12*b*), and they assigned their structures based on a combination of NMR spectroscopy and the HPLC elution order which is related to their polarity.[51] Among the isolated tetraesters, three ((±)-**7** (*cis*-3), (±)-**8** (*trans*-3), and (±)-**9** (*trans*-2)) had an inherently chiral addition pattern (Figure 1.13).

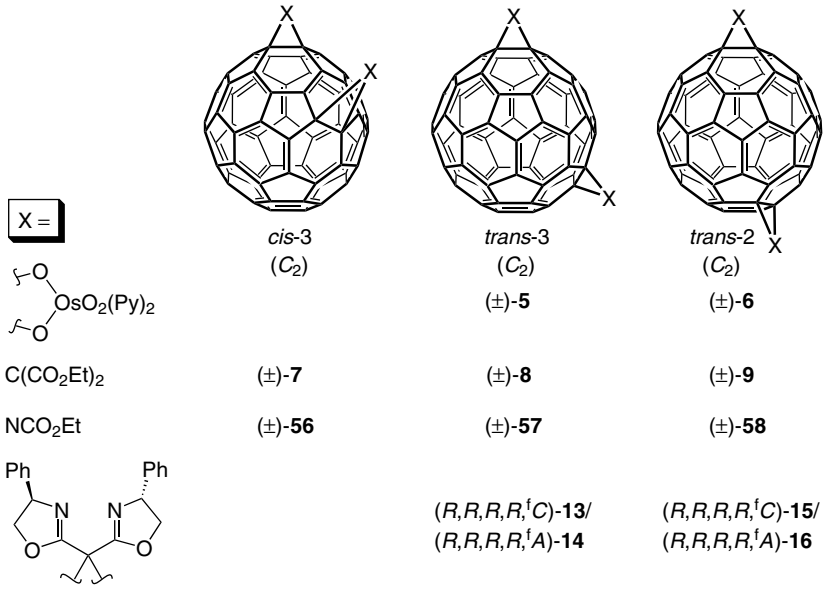

Figure 1.13. Bis-adducts of C_{60} with an inherently chiral addition pattern. Each regioisomer is represented by a single, ^{f}C-configured structure. The configuration of actually obtained products is indicated in each case by a descriptor preceding the compound number.

The preferred products were the *e* (cf. Figure 1.12b) and *trans*-3 ((±)-**8**) bis-adducts, and this regioselectivity in the kinetically controlled nucleophilic addition was explained on the basis of the enhanced coefficients of low-lying unoccupied orbitals (LUMO, LUMO+1, LUMO+2) at the respective positions in the mono-adduct.[109,110] The complete absence of the *cis*-1 adduct (cf. Figure 1.12*b*) from the product mixture was accounted for by steric hindrance of the addends. In fact a subsequent study on the formation of bis-adducts ($C_{60}[C(p\text{-}C_6H_4OCH_3)_2]_2$, $C_{60}[C(p\text{-}C_6H_4OCH_3)_2][C(CO_2Et)_2]$, and $C_{60}[C(CO_2Et)_2](NCO_2Et)$) with addends having different steric requirements showed that in the latter case, the *cis*-1 regioisomer was even formed preferentially.[111] It has a noninherently chiral addition pattern that will be discussed in Section IV.B.1.c. In summary, the observed preferences in Bingel type bis-adduct formation can be satisfactorily correlated to a combination of enhanced frontier orbital coefficients, more reactive compressed 6–6 bonds, or the formation of thermodynamically more stable products, aspects that can all be related to the characteristic cage distortion in mono-adducts of C_{60}.[111] Wilson and Lu, by using 2,6-dimethoxyanthracene as a reversible protecting and directing group for C_{60} prior to introducing two Bingel type addends, could obtain significantly increased amounts of *cis*-isomers after removal of the Diels-Alder addend.[112] An interesting and unexpected electrochemically induced regioisomerization, the so-called *walk on the sphere* rearrangement of different $C_{60}[C(CO_2Et)_2]_2$ bis-adducts by migration of the methano addends on the C_{60} surface, was observed by Echegoyen, Diederich, and co-workers in the course of nonexhaustive CPE of the tetraesters.[113]

Further cyclopropanation of *e* (cf. Figure 1.12*b*) and *trans*-3 ((±)-**8**, Figure 1.13) bis[di(ethoxycarbonyl)methano][60]fullerene leads to high yields of the tris-adducts (±)-**10** and (±)-**11**, respectively (Figure 1.14).[51,110] Whereas in C_3-symmetric (±)-**10**, all addends are located in *e*-positions relative to each other (*e*,*e*,*e* addition pattern), the arrangement is *trans*-3,*trans*-3,*trans*-3 in D_3-symmetric (±)-**11**. An exotic chiral helium compound is the incarcerane of (±)-**10** with ^{3}He, prepared in a study on the influence of the degree of functionalization and the addition pattern on the chemical shift of ^{3}He endohedrally trapped inside C_{60} derivatives.[87] Treatment of (±)-**10** with NaH, followed by acidic workup yielded the hexakis-acid (±)-**12** (Figure 1.14) as a water-soluble fullerene derivative.[114]

The enantiomers of both tris-adducts, (±)-**10** and (±)-**11**, as well as of the *cis*-3 (cf. Figure 1.12*b*) bis-adduct $C_{60}[C(p\text{-}C_6H_4OCH_3)_2]_2$ and a C_1-symmetric hexakis-adduct $C_{60}[C(CO_2Et)_2]_6$ of unknown structure have been resolved by HPLC on a chiral (*R*,*R*)-Whelk-O1 phase and their CD spectra were recorded.[115] Resolution of the *trans*-3,*trans*-3,*trans*-3 adduct (±)-**11**

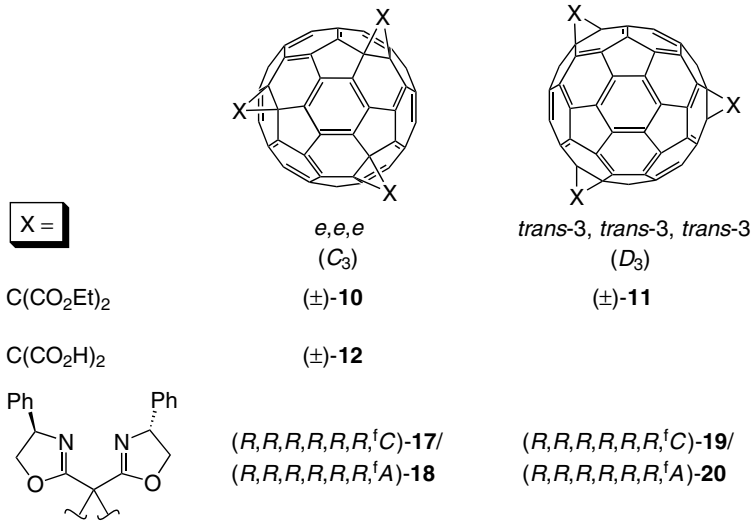

Figure 1.14. Tris-adducts of C_{60} with the inherently chiral *e*,*e*,*e* and *trans*-3,*trans*-3,*trans*-3 addition patterns. Each regioisomer is represented by a single, ^{f}C-configured structure. The configuration of actually obtained products is indicated in each case by a descriptor preceding the compound number.

(Figure 1.14) and the aforementioned C_1-symmetric hexakis-adduct was also achieved on the chiral stationary phase (R)-(−)-TAPA (2-(2,4,5,7-tetranitro-9-fluorenylidenaminoxy)propionic acid).[116]

By performing stepwise, modified Bingel reactions[117–119] with enantiomerically pure, C_2-symmetric methylene-bis(oxazolines) derived, in one enantiomeric series, from (*R*)-phenylalanine, Djojo and Hirsch obtained, among other regioisomers, bis-adducts (*R*,*R*,*R*,*R*,^{f}C)-**13**/(*R*,*R*,*R*,*R*,^{f}A)-**14**, and (*R*,*R*,*R*,^{f}C)-**15**/(*R*,*R*,*R*,^{f}A)-**16** (Figure 1.13), as well as tris-adducts (*R*,*R*,*R*,*R*,*R*,*R*,^{f}C)-**17**/(*R*,*R*,*R*,*R*,*R*,*R*,^{f}A)-**18** and (*R*,*R*,*R*,*R*,*R*,*R*,^{f}C)-**19**/(*R*,*R*,*R*,*R*,*R*,*R*,^{f}A)-**20** (Figure 1.14), each as a diastereoisomeric pair in which the (*R*,*R*)-configured side groups are combined with inherently chiral addition patterns of opposite configuration (^{f}C or ^{f}A).[96] After the separation of all isomers, they found that the formation of the bis-adducts **13**–**16** was only weakly diastereoselective (*d.e.* <10%). Furthermore the CD spectra of the diastereoisomeric pairs **13/14**, **15/16**, and **17/18** are nearly mirror-image shaped which clearly proves the opposite configuration of the addition patterns in each pair and also the predominant chiroptical contribution of the distorted residual fullerene π-chromophores in comparison to that of the addends.

This corroborates observations by Diederich and co-workers who had found analogous results for diastereoisomeric pairs of C_{70} derivatives combining a uniformly configured chiral side chain with fullerene addition patterns of opposite configuration (cf. Section IV.A.2.e).[35,54]

In an achiral *e* bis-adduct (cf. Figure 1.12) there are two possibilities for the introduction of a third addend under formation of *e*,*e*,*e* tris-adducts, the resulting addition patterns being enantiomeric. Starting from the pure regioisomers (*R*,*R*)-**21** and (*R*,*R*)-**22** (Scheme 1.1; the constitutional isomerism arises from interchange of the nonidentical addends at the constitutionally heterotopic e_{face} and e_{edge} positions), each of the two possibilities to further add a bis(ethoxycarbonyl)methano addend under formation of an *e*,*e*,*e* tris-adduct leads to a different configuration of the inherently chiral *e*,*e*,*e* addition pattern. This, in combination with the uniformly (*R*,*R*)-configured side groups, affords the diastereoisomers (*R*,*R*,^{f}C)-**23** and (*R*,*R*,^{f}A)-**24** (Scheme 1.1) which can be

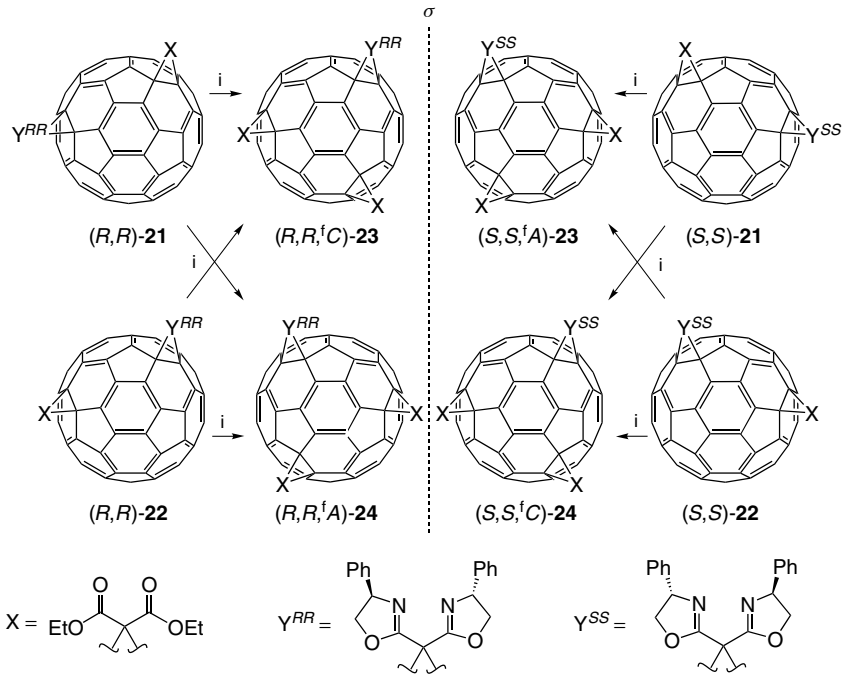

i = Diethyl 2-bromomalonate, NaH, toluene, r.t., 1 d

Scheme 1.1. Strategy for a separate preparation of the enantiomers in a set of four stereoisomeric *e*,*e*,*e* tris-adducts of C_{60} including two diastereoisomeric pairs of enantiomers, by addition of diethyl bromomalonate to an *e* bis-adduct precursor containing a chiral side chain of defined configuration.

purified by chromatography on an achiral stationary phase. Similarly, starting from the according (*S*,*S*)-configured bis-adducts (*S*,*S*)-**21** and (*S*,*S*)-**22**, the formed diastereoisomeric *e*,*e*,*e* tris-adducts (*S*,*S*,^{f}*A*)-**23** and (*S*,*S*,^{f}*C*)-**24** can each be isolated. As it is easily recognized by looking at the configurational descriptors of the four tris-adducts (Scheme 1.1), they include two diastereoisomeric pairs of enantiomers ((*R*,*R*,^{f}*C*)-**23**/(*S*,*S*,^{f}*A*)-**23** and (*R*,*R*,^{f}*A*)-**24**/(*S*,*S*,^{f}*C*)-**24**).[96] A set of C_{70} derivatives with similar configurational relationships is described in Section IV.A.2.e.[35,54]

Comparisons among the circular dichroism spectra of **13**–**20** (Figures 1.13 and 1.14), (±)-**23**, and (±)-**24** (Scheme 1.1) show that compounds having addition patterns of matching constitution and configuration give rise to (nearly) identical CD bands, regardless of the constitution or the configuration of the addends. They are (nearly) the mirror images of all the derivatives having an addition pattern of the same constitution but the opposite configuration, again independently of the constitution or the configuration of the addends. This means that the contribution of the distorted residual fullerene π-chromophore to the Cotton effects largely dominates that of the stereogenic centers in the lateral groups. Furthermore the Cotton effects of the C_2-symmetric bis-adducts (*R*,*R*,*R*,*R*,^{f}*C*)-**13**/(*R*,*R*,*R*,*R*,^{f}*A*)-**14**, and (*R*,*R*,*R*,*R*,^{f}*C*)-**15**/(*R*,*R*,*R*,*R*,^{f}*A*)-**16** (Figure 1.13) are about twice as large as those of the C_3-symmetric tris-adducts (*R*,*R*,*R*,*R*,*R*,*R*,^{f}*C*)-**17** and (*R*,*R*,*R*,*R*,*R*,*R*,^{f}*A*)-**18** (Figure 1.14) or of the D_3-symmetric tris-adducts (*R*,*R*,*R*,*R*,*R*,*R*,^{f}*C*)-**19** and (*R*,*R*,*R*,*R*,*R*,*R*,^{f}*A*)-**20** (Figure 1.14). The latter observation may be explained by the higher symmetry of the tris-adducts, which causes a less pronounced distortion of the fullerene π-chromophore.[96] This rationalization is corroborated by the large Δε values that have been observed for the helically twisted C_{76}[6] (cf. Section III.C) and some of its derivatives,[93] by a number of C_{70} derivatives with an inherently chiral addition pattern,[35,54] and also by the relatively weak Cotton effects of the rather "round-shaped" major D_2-C_{84} isomer (cf. Section III.C).[60] However, further investigations are necessary to get a clearer picture of the relationships between the structure of a chiral fullerene chromophore and the resulting Cotton effects.[97] The absolute configurations of *trans*-2 and *trans*-3 bis-adducts as well as of an *e*,*e*,*e* tris-adduct of C_{60} could be assigned by calculation of the CD spectra of the corresponding $C_{60}(CH_2)_2$ and $C_{60}(CH_2)_3$ methanofullerene isomers.[97]

Recently a series of regioisomeric tris-adducts of C_{60} with new addition patterns including *e*-, *trans*-2-, *trans*-3-, and *trans*-4 relationships among addends have been isolated and characterized.[97] In many cases correlation of the constitution and, where applicable, the configuration of the addition pattern of a product to that of the corresponding bis-adduct precursor were used as a valuable tool in their structural elucidation.[97]

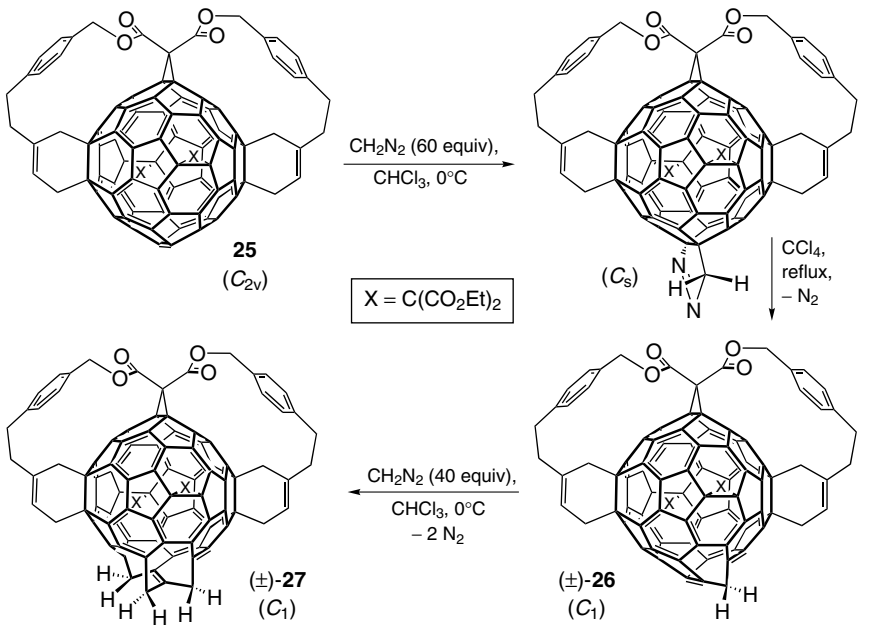

Scheme 1.2. Regioselective formation of chiral hexakis- and octakis-adducts of C_{60} by repeated addition of diazomethane to a C_{2v}-symmetric pentakis-adduct, followed by thermal dinitrogen extrusion.

Two C_1-symmetric higher adducts of C_{60} were obtained in an interesting reaction sequence involving a repeated addition of diazomethane to the C_{2v}-symmetric pentakis-adduct **25** and extrusion of dinitrogen from the pyrazoline intermediates (Scheme 1.2).[44] The starting pentakis-adduct **25**[104] has the advantage that its reactivity is limited to the 6–6 bond that will give a hexakis-adduct with a pseudo-octahedral arrangement of addends upon functionalization.[120] Kinetically controlled thermal dinitrogen extrusion from the pyrazoline intermediates was proposed to occur in an orbital-controlled [$\pi^2s + \pi^2s + \sigma^2s + \sigma^2a$] reaction[44,121] and afforded hexakis-adduct (±)-**26** and octakis-adduct (±)-**27** (Scheme 1.2). No cyclopropane substructures were produced in this rearrangement in the absence of light.[44]

c. Adducts Resulting from Tether-Directed Macrocyclizations. The tether-directed remote functionalization[122] was introduced into fullerene chemistry by Diederich and co-workers for the regioselective synthesis of multi-adducts.[123] Addition to C_{60} of bifunctional reagents including a large variety of tethers has allowed the regioselective targeting of all possible bis-addition patterns, sometimes even with a high stereoselectivity.[124] Many of

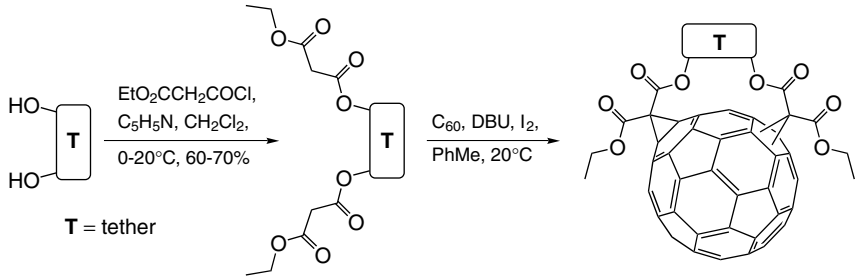

Scheme 1.3. General synthetic scheme for the regio- and stereoselective macrocyclization of C_{60} by Bingel addition of tethered bis-malonates.

these syntheses used the versatile Bingel type macrocyclization between C_{60} and a bis-malonate in a double nucleophilic cyclopropanation (Scheme 1.3).

Using a 1,10-phenanthroline-2,9-diylbis[(4-phenyl)methyl] unit as a tether in such a reaction, C_1-symmetric bis-adduct (±)-**28** is obtained as the main product, together with C_2-symmetric bis-adduct (±)-**29** (Figure 1.15).[125] In addition to the inherently chiral *trans*-3 addition pattern, both compounds include two stereogenic centers represented by the methano bridge C-atoms. Because of the steric constraints imposed by the tether, however, these centers cannot adopt all possible combinations of configurations: Depending on the relative orientation of the ethyl ester residues at the methano-C-atoms (= bridgeheads of a macropolycyclic structure including the tether as one of the bridges), one distinguishes between the *out,out* ((±)-**29**) and the *in-out* ((±)-**28**) diastereoisomers. The theoretically possible third form, the *in-in* isomer was not observed.[125] Because of the additional configurational freedom, two untethered, *e* type methano bridges with two different achiral substituents at each methano-C-atom,[126] can, on the other hand, exist as two diastereoisomeric pairs of enantiomers.

Transition to shorter tethers led to the formation of the *e* addition pattern in (±)-**30**, as well as in a similar bis-adduct containing a *p*-xylylene tether (both obtained next to the *trans*-4 adducts),[117,125] in a tethered bis-β-ketoester-adduct of C_{60},[127] and in (±)-**31** (Figure 1.15).[125] Although the *e* addition pattern itself is not chiral, (±)-**30** contains a stereogenic center in one of the two methano bridges which are constitutionally heterotopic. The stereogenic center in (±)-**30** results from the malonate addition to the e_{face} bond[104] and lowers the overall symmetry of the molecule to C_1 in comparison to the C_s-symmetry of an *e* bis-adduct with C_{2v}-symmetric addends (cf. Figure 1.12*b*).[102] The steric constraints in (±)-**30** and in similar *(vide infra)* compounds require the tether to adopt a helical conformation which adds another (conformational) chiral unit to the molecule. The helicity of the tether depends on the configuration of the stereogenic center in the methano bridge. In C_1-symmetric

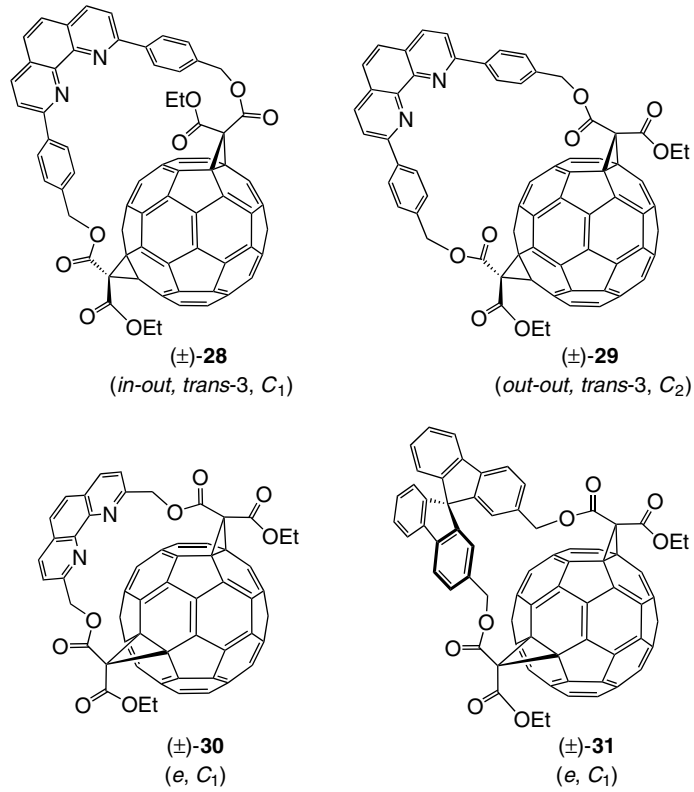

Figure 1.15. Bis-adducts of C_{60} obtained by tether-directed Bingel macrocyclization.

(±)-**31** (Figure 1.15) which has the same addition pattern as (±)-**30**, the handedness of the tether is configurationally fixed in the form of a spirobifluorene moiety.[125] It enforces a specific configuration of the methano-C-atom bridging the e_{face} bond of (±)-**31** during the second Bingel addition. When nonracemic 9,9′-spirobifluorene-2,2′-bis(methanol) was used as alcohol component in the synthesis of the tether, the *d.e.* of the resulting Bingel type bis-adduct (one enantiomer of (±)-**31**) exceeded 96%, a value that corresponds to the *e.e* of the starting diol. A comparison between the CD spectra of the enantiomers of (±)-**31** and those of the starting spirobifluorene-bis-malonate conjugate indicates a strong electronic coupling between the fullerene and spirobifluorene chromophores.[125]

An equally high diastereoselectivity (*d.e.* $\geq$96%) was observed in the generation of the inherently chiral *cis*-3 addition pattern when (R,R,^{f}A)-**32** and (S,S,^{f}C)-**32** (Scheme 1.4) were prepared (next to the corresponding *cis*-2

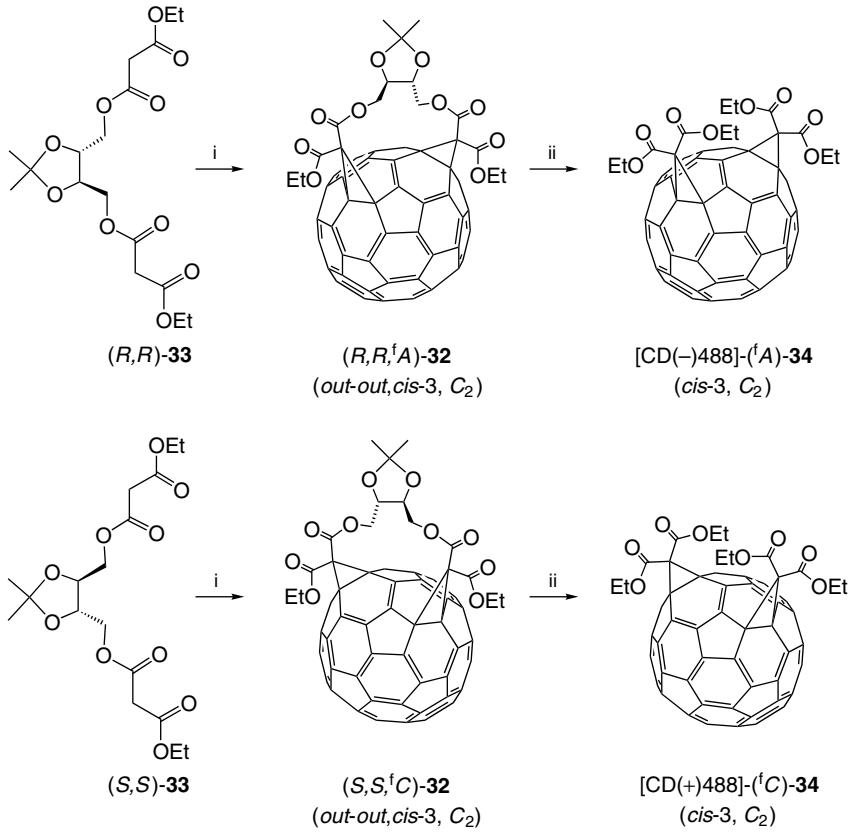

Scheme 1.4. Selective synthesis of (^{f}A)- and (^{f}C)-bis[di(ethoxycarbonyl)methano][60]fullerene by diastereoselective tether-directed bis-cyclopropanation of C_{60} and subsequent transesterification under removal of the chiral tether auxiliary.

bis-adducts having chiral elements only in the tether moiety) by Bingel addition to C_{60} of optically pure bis-malonates (*R*,*R*)-**33** and (*S*,*S*)-**33**, respectively.[117,125] Separate transesterification of (*R*,*R*,^{f}A)-**32** and (*S*,*S*,^{f}C)-**32** yielded the tetraethyl esters (^{f}A)-**34** and (^{f}C)-**34** as pure enantiomers exhibiting strong CD bands between 250 and 750 nm with $\Delta\varepsilon$ values approaching 150 $M^{-1}\,cm^{-1}$.[117,125] Comparison with spectra calculated by the π-electron SCF-CI-DV MO method[99,100,128] allowed an assignment of their absolute configurations as [CD(−)488]-(^{f}A)-**34** and [CD(+)488]-(^{f}C)-**34** (Scheme 1.4).[7] Bis-adducts derived from (*S*,*S*,^{f}C)-**32**, having the diol

moiety in the tether deprotected and bearing long araliphatic residues in the outer ester groups have been shown to form stable Langmuir films at the air-water interface.[129] Other effective tether components for the regio- and stereoselective Bingel macrocyclization include (*R*,*R*)- and (*S*,*S*)-butane-2,3-diol which afforded (*R*,*R*,^{f}*C*)- and (*S*,*S*,^{f}*A*)-configured *cis*-3 bis-adducts of C_{60} with a *d.e.* $\geq$97%.[124]

The Bingel macrocyclization is increasingly being used in the synthesis of functional supramolecular systems.[124,130] This synthetic approach allows a precise positioning of chromophores or receptor sites in close proximity to the fullerene surface, thus offering the possibility for changes in the physical properties of the carbon cage. It was exploited in macrocyclic fullerene-porphyrin dyads with the *trans*-1[131] or the inherently chiral *trans*-2[132] addition pattern. In the buckminsterfullerene-derived [2]catenane (±)-**35** · $4PF_6$ (Figure 1.16),[133] synthesized by using the self-assembly strategy of Stoddart and co-workers,[134] the handedness results from an element of planar chirality represented by the doubly *para*-bridged hydroquinone ring of the [34]crown-10 macrocycle. The combination of the C_s-symmetric *trans*-4 fullerene functionalization pattern and the C_2-symmetric planar chiral unit reduces the overall symmetry of (±)-**35** · $4PF_6$ to C_1.

Planar chirality occurs also in the cyclophane-type C_{60}-dibenzo[18]crown-6 conjugate *out-out* (±)-**36** (Figure 1.16) having a *trans*-1 addition pattern.[135] A significant perturbation of the electronic structure of the fullerene is observed by cyclic voltammetry when an alkali metal ion, in particular, K^+, is bound by the crown ether moiety which is positioned in close proximity to the fullerene surface. The chirality of C_2-symmetric (±)-**36** is due exclusively to the planar chiral element resulting from the *anti* substitution pattern of the bridged dibenzocrown ether moiety. Even at 393 K the macrocyclic bis-adduct of C_{60} does not racemize because its conformational freedom is not high enough for the crown ether to rotate and expose both faces to the fullerene. As opposed to (±)-**36**, the related crown ether conjugates, C_2-symmetric *out-out,trans*-2-(±)-**37**/(±)-**38**, and C_1-symmetric *in-out*,*trans*-3-(±)-**39** (Figure 1.16) have an inherently chiral addition pattern. In combination with the planar chirality related to the bridged and *anti* disubstituted crown ether moiety, this can lead to the appearance of two diastereoisomeric pairs of enantiomers for the *out-out*,*trans*-2 adduct, namely (*P*,*P*,^{f}*C*)-**37**/(*M*,*M*,^{f}*A*)-**37** and (*M*,*M*,^{f}*C*)-**38**/(*P*,*P*,^{f}*A*)-**38**. At 393 K the rotation of the crown ether becomes fast (in the *trans*-2 bis-adducts, its distance to the fullerene surface increases compared to (±)-**36**), which leads to fast interconversion of diastereoisomers within the pairs (*P*,*P*,^{f}*C*)-**37**/(*M*,*M*,^{f}*C*)-**38**, and (*M*,*M*,^{f}*A*)-**37**/(*P*,*P*,^{f}*A*)-**38**. In (±)-**39**, the dibenzo-crown ether moiety does not constitute a planar chiral unit because of its *syn* substitution pattern. It rotates fast around its "arms" at 333 K and shows a complex dynamic behavior below 243 K. Besides, the relative *in-out*

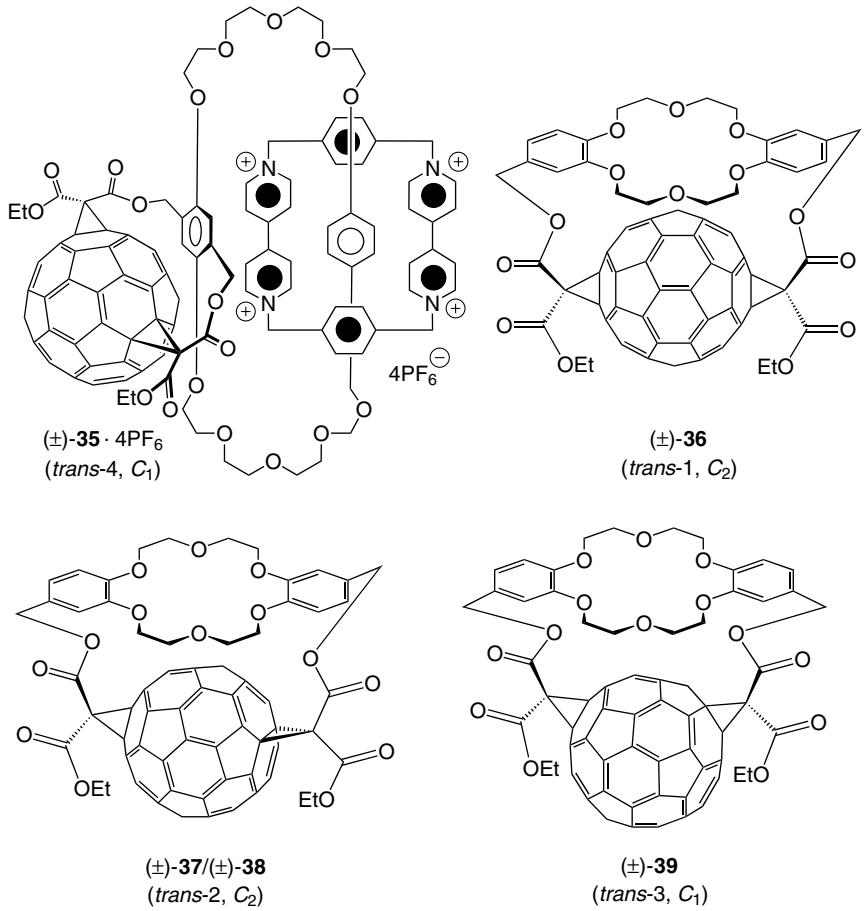

Figure 1.16. Macrocyclic bis-malonate adducts of C_{60} including planar chiral units ((±)-**35**–(±)-**38**).

configuration of the methano bridge C-atoms lowers the overall symmetry of (±)-**39** to C_1.[135]

Planar chirality was finally combined with the achiral *cis*-2 addition pattern in a tethered Bingel type bis-adduct including a *trans*-configured ethene unit as planar chiral element in the macrocyclic bridge.[118]

Even tris- and tetrakis-adducts of C_{60} were accessible in a regioselective way by sequential tether-directed macrocyclization steps. A clipping reaction starting from mono-adduct **40** with two tether-linked malonate residues thus yielded tris-adduct (±)-**41** (Scheme 1.5).[125] Under the assumption that both *m*-xylylene tethers enforce the expected *cis*-2 addition, the C_2-symmetry of

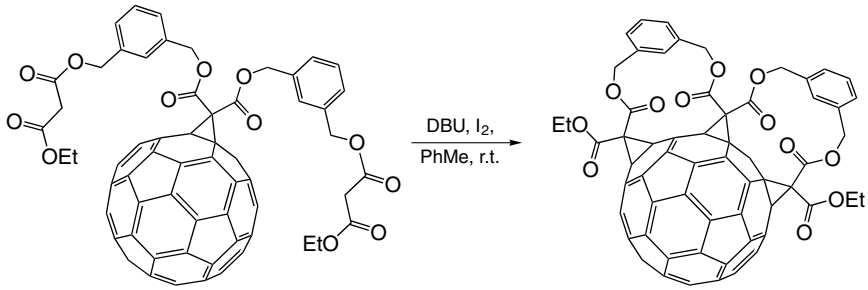

40 (C_{2v}) (±)-**41** (*cis*-2,*cis*-2,*trans*-3, C_2)

Scheme 1.5. Synthesis of a chiral tris-adduct of C_{60} by double tether-directed Bingel macrocyclization.

(±)-**41** strongly suggests the presence of an inherently chiral *cis*-2,*cis*-2,*trans*-3 addition pattern.

An interesting superposition of inherently chiral addition patterns and a conformationally chiral cyclotriveratrylene (CTV)[136] unit is realized in the C_3-symmetric *e*,*e*,*e* tris-adducts (±)-**42** or (±)-**43**, and the *trans*-3,*trans*-3,*trans*-3 adducts (±)-**44** or (±)-**45** (Figures 1.17 and 1.18).[137] The two regioisomers were obtained in a first one-step tether-directed triple Bingel addition of a racemic CTV-tris-malonate conjugate to C_{60}, a venture that was encouraged by the known favorable interactions between buckminsterfullerene and cyclotriveratrylene.[138] The triple macrocyclization proved to be highly regioselective for the *e*,*e*,*e* and the *trans*-3,*trans*-3,*trans*-3 addition patterns, and since none of the two products showed a splitting or doubling of NMR resonances, it was concluded that the addition of the CTV moiety led to both inherently chiral addition patterns with a high diastereoselectivity.[137] However, neither for the *e*,*e*,*e* nor for the *trans*-3,*trans*-3,*trans*-3 adduct has it been proved experimentally so far which one of the two diastereoisomeric pairs of enantiomers ((±)-**42** or (±)-**43**, and (±)-**44** or (±)-**45**, respectively) was formed (Figures 1.17 and 1.18). A particularly fascinating aspect of both tris-adducts (*e*,*e*,*e* and *trans*-3,*trans*-3,*trans*-3) is their topological chirality,[139] a property encountered in only a few known molecules, for example, trefoil knots,[140] and this was demonstrated for the above discussed *e*,*e*,*e* and *trans*-3,*trans*-3,*trans*-3 tris-adducts in a detailed mathematical analysis.[18] As opposed to Euclidean enantiomers, topological enantiomers cannot be interconverted by a continuous deformation in three-dimensional space without breaking a bond. In the case of the *e*,*e*,*e* regioisomer, it was shown that each of the theoretically possible four "classical" stereoisomers ((*P*, ^{f}A)-**42**, (*M*, ^{f}C)-**42**, (*M*, ^{f}A)-**43**, and (*P*, ^{f}C)-**43**) corresponds to a unique topological stereoisomer (Figure 1.17).

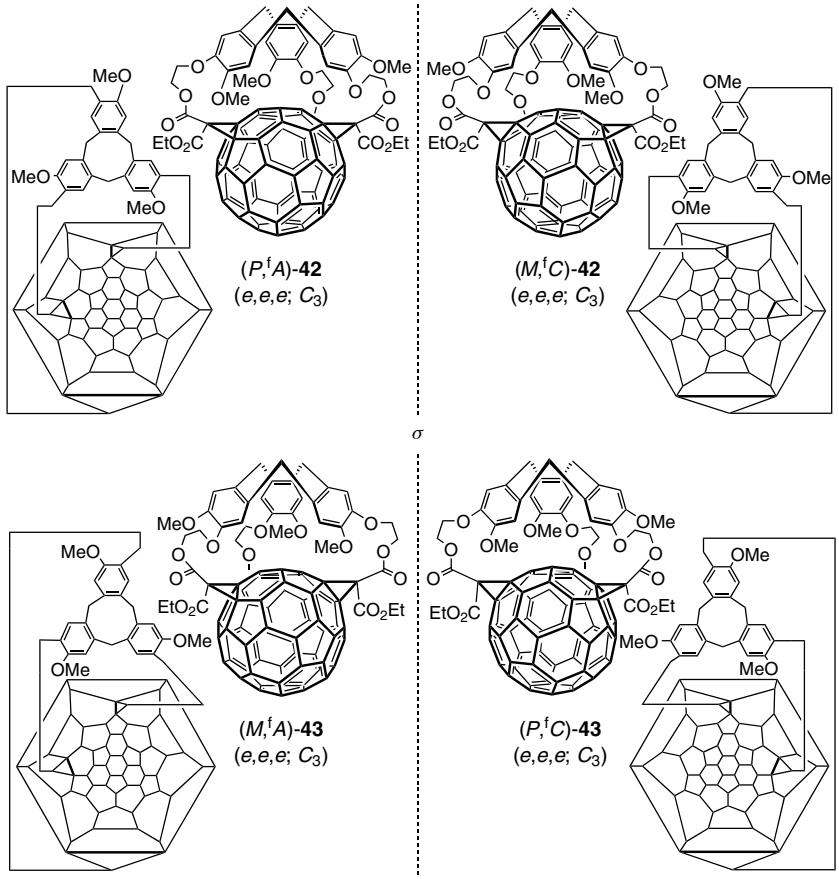

Figure 1.17. The four classical stereoisomers of a CTV-C_{60} tris-adduct conjugate with an *e*,*e*,*e* addition pattern, and their planar representations. Each structure corresponds to a unique topological stereoisomer.

On the other hand, the four stereoisomers of the *trans*-3,*trans*-3,*trans*-3 tris-adduct ((*P*, ^{f}A)-**44**, (*M*, ^{f}C)-**44**, (*M*, ^{f}A)-**45**, and (*P*, ^{f}C)-**45**) are formally interconvertible pairwise ((*P*, ^{f}A)-**44** and (*M*, ^{f}A)-**45**), and ((*M*, ^{f}C)-**44** and (*P*, ^{f}C)-**45**), respectively (Figure 1.18) by a continuous deformation making the C_{60} ball pass through the nine-membered ring of the CTV unit. In conclusion, there are four classical, but only two topological stereoisomers for the *trans*-3,*trans*-3,*trans*-3 tris-adduct.[18] This appears plausible by considering the fact that the plane including the three methano bridge C-atoms divides the fullerene spheroid into two equal halves in the *trans*-3,*trans*-3,*trans*-3 adduct, but into two different fractions in the *e*,*e*,*e* adduct.

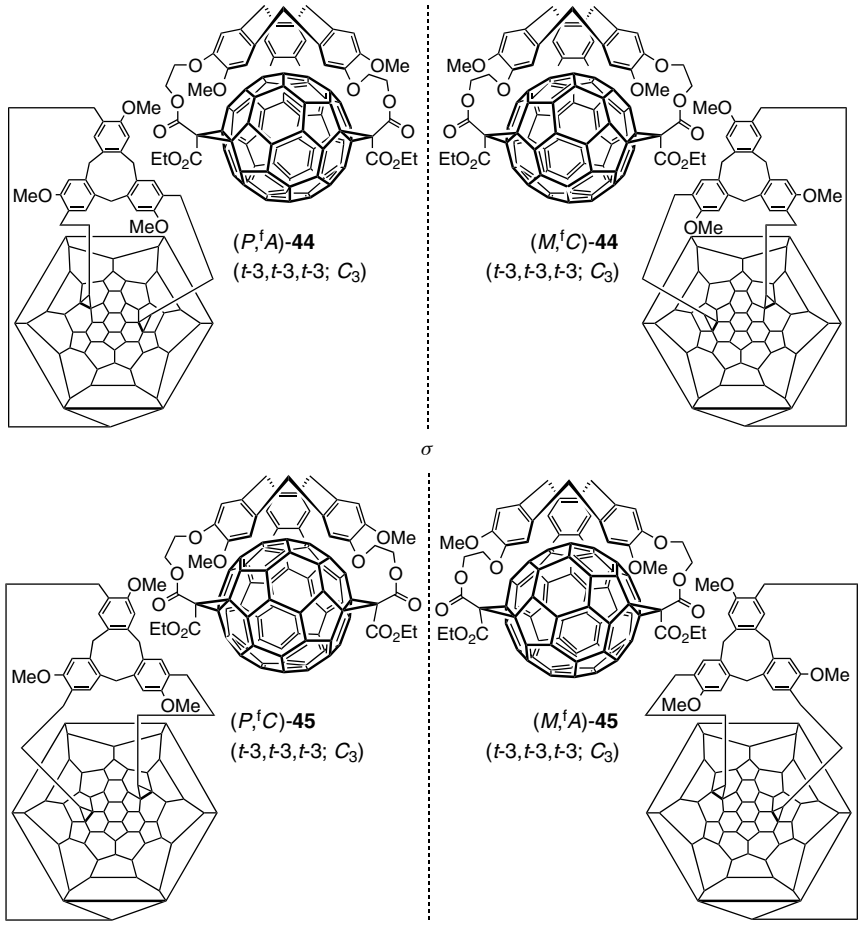

Figure 1.18. The four classical stereoisomers of a CTV-C_{60} tris-adduct conjugate with a *trans*-3, *trans*-3,*trans*-3 addition pattern, and their planar representations. Topologically, (*P*, ^{f}A)-**44** is equivalent (can be deformed without breaking any bond) to (*M*, ^{f}A)-**45**, and (*M*, ^{f}C)-**44** is equivalent to (*P*, ^{f}C)-**45**. It appears that the four classical stereoisomers can be reduced to only two different topological stereoisomers.

Some of the early work on the regio- and diastereoselective tether-directed bis-functionalization of C_{60} was reported by Nakamura and co-workers.[141,142] Their anellating reagents consisted of a methylene chain of variable length bearing cyclopropenone acetal units at both ends. Under the used reaction conditions, the latter reversibly generate minute amounts of a nucleophilic vinylcarbene which undergoes [3 + 2] cycloaddition with the fullerene. A tether chain length of six carbon atoms afforded the C_2-symmetric *cis*-3

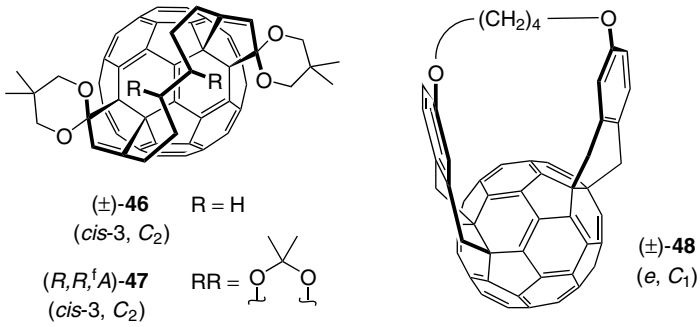

Figure 1.19. Chiral bis-adducts of C_{60} obtained by tether-directed cycloaddition reactions.

bis-adduct (±)-**46** as a single regioisomer (Figure 1.19). Use of a chiral, enantiomerically enriched (*e.e.* = 89%) tether including an acetal of an (*R*,*R*)-configured 1,2-diol unit, resulted in a diastereoisomerically pure *cis*-3 bis-adduct (**47**, Figure 1.19).[141] As the chiroptical contribution of side chains with stereogenic centers to the Cotton effects of fullerene derivatives with inherently chiral π-chromophores is almost negligible (cf. Sections IV.A.1.b and IV.A.2.e),[35,54,96,97] the absolute configuration of the *cis*-3 addition pattern of **47** could be identified as (*R*,*R*,^{f}*A*)[143] by comparison of its optical rotation $[\alpha_D] = -1875$ with the CD spectra of [CD(−)488]-(^{f}*A*)-**34** and [CD(+)488]-(^{f}*C*)-**34** (Scheme 1.4) with assigned absolute configurations.[7] Besides, reduction of the enantiomeric diones obtained by acetal cleavage in (±)-**46** and subsequent esterification of the resulting diols with (*S*)-2-methoxy-2-phenylacetic acid allowed the separation of the diastereoisomeric esters, namely of C_{60} adducts with enantiomeric addition patterns.[143]

Depending on the tether length, a regioselective Diels-Alder macrocyclization by addition to C_{60} of two *o*-quinodimethane units linked by a $(CH_2)_n$ chain afforded C_s-symmetric *cis*-2 and C_2-symmetric *cis*-3 bis-adducts ($n = 2$ or 3), or the *e* bis-adduct (±)-**48** ($n = 5$) (Figure 1.19).[144,145] Interestingly and contrarily to the tethered *e* bis-adducts (±)-**30** and (±)-**31** (Figure 1.15), the chirality of (±)-**48** cannot be associated with stereogenic centers outside the fullerene sphere but to a noninherently chiral addition pattern of the C_{60} moiety. Indeed, as the conformational average of the cyclohexene substructures corresponds to C_s-symmetric addends,[102] the ligand branches (CIP procedure)[31,32] that include a shorter path to the ether-O-atoms of the addends are allocated a higher priority, and consequently lower locants are given to the corresponding points of attachment in the fullerene core (cf. Sections II.B and II.C.3).[25] In addition and similarly to (±)-**30** (Figure 1.15), a helical conformation of the tether is enforced by this steric arrangement. The chiral *cis*-3 and *e* ((±)-**48**) adducts were successfully resolved[144] by HPLC on a chiral

stationary phase of silica gel coated with cellulose tris(3,5-dimethylphenyl carbamate).[146] Cleavage of the ether linkages in the side chain of (±)-**48** afforded the corresponding untethered chiral bis(phenols).[144]

An interesting templated bis-functionalization was reported by Shinkai and co-workers who introduced two boronic acid groups regio- and diastereoselectively into C_{60} by using saccharides or saccharide derivatives as imprinting templates.[147–149] Thus, when D-threitol was used as the template, C_2-symmetric *cis*-3 isomers ^{f}C-**49** and ^{f}A-**49**,[150] were obtained in a nearly. 72 : 28 ratio after removal of the saccharide templates (Scheme 1.6).[149] Competitive complexation studies indicated that D-threitol-imprinted boronic acid (^{f}C)-**49** and L-threitol-imprinted (^{f}A)-**49** preferentially rebind their original templates with up to 48% *d.e.*[148] Exploration of other regio- and diastereoselective double [4 + 2] cycloadditions between C_{60} and *o*-quinodimethanes

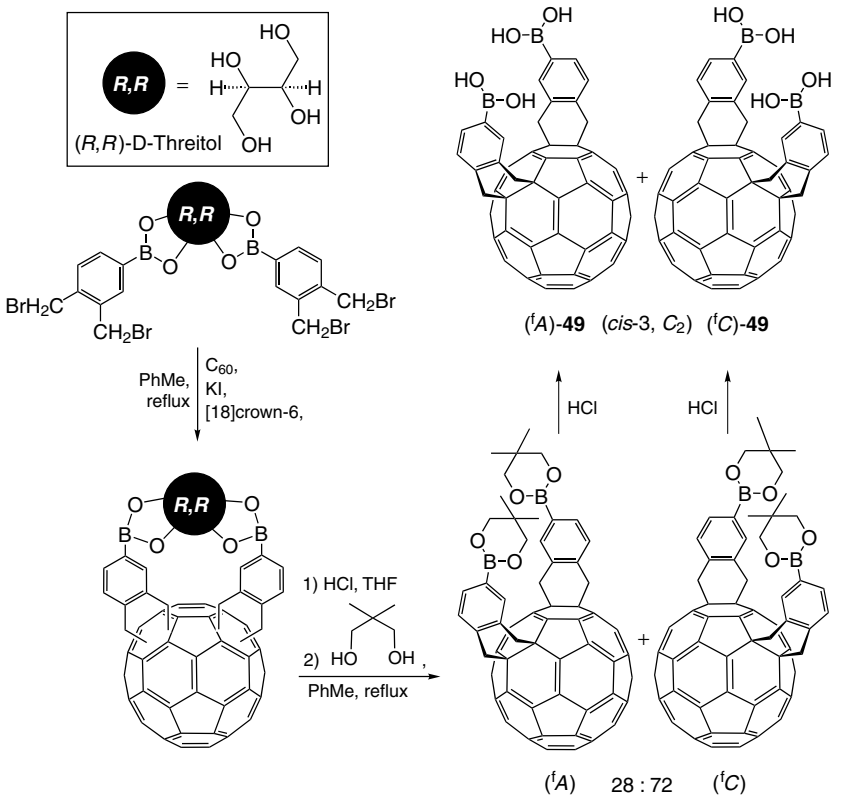

Scheme 1.6. Regio- and diastereoselective double Diels-Alder addition to C_{60} using a threitol derivative as imprinting template.

generated from bis[3,4-bis(bromomethyl)benzoates] of various steroids as well as of (2*R*,3*R*)-butane-2,3-diol showed that the magnitude of the Cotton effects induced in the fullerene π-chromophore of adducts with an achiral addition pattern reflect the size of the tether moiety and the number of stereogenic centers it contains.[151]

d. Derivatives Resulting from Initial Azide or Nitrene Addition. The addition of azides or nitrenes to fullerenes and the multitude of possible subsequent transformations engendered a rich chemistry leading to an opening of the fullerene cage and ultimately to the synthesis of azafullerenes.[46,47] When Hirsch and co-workers investigated the regioselectivity of successive additions of stabilized nitrenes or of alkyl azides to C_{60}, they found that the reaction of ethyl azidoacetate with azahomofullerene **50** selectively afforded a single bis-adduct regioisomer (±)-**51** (Scheme 1.7).[152] This core-modified derivative of C_{60} has an unusual inherently chiral functionalization pattern characterized by a formal nitrogen insertion into a 6–5 bond in addition to the fusion of a triazoline heterocycle to an adjacent 6–6 bond. The regioselective kinetic attack of the organic azide on the azahomofullerene **50** under formation of (±)-**51** is explained by the vinylamine character of **50** and the directing effect of according Mulliken charges at the bridgehead double bonds. Already at room temperature, C_1-symmetric (±)-**51** rearranges slowly to C_s-symmetric **52** as main product.[152]

In a number of groundbreaking explorations,[46] Wudl, Hummelen, and co-workers showed that photoinduced [2 + 2] cycloaddition of singlet oxygen to one of the electron-rich enamine-type double bonds of azahomo[60]fullerene derivative **53** (Scheme 1.8), followed by decomposition of the 1,2-dioxetane intermediate (not shown), led to ketolactam (±)-**54**, the first cluster-opened fullerene with a free orifice.[153] Under synthetic conditions mimicking events observed in the gas phase,[154] acid-induced loss of 2-methoxyethanol from

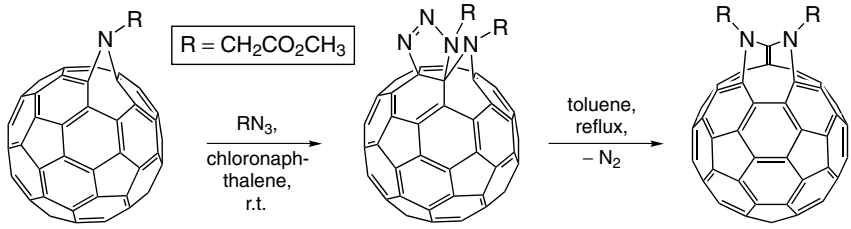

50 (C_s) (±)-**51** (C_1) **52** (C_s)

Scheme 1.7. Regioselective addition of ethyl azidoacetate to an azahomo[60]fullerene derivative followed by extrusion of dinitrogen.

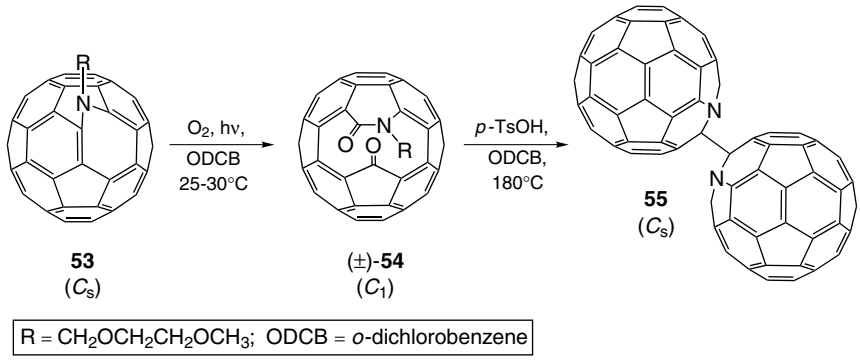

Scheme 1.8. Controlled opening of the fullerene cage by self-sensitized photooxygenation of an azahomo[60]fullerene derivative and subsequent acid-induced formation of a "dimeric" aza[60]fullerene.

(±)-**54** ultimately led to the "dimeric" C_s-symmetric 2,2′-bi-1-aza[60]fullerene **55** (Scheme 1.8).[154,155] The proposed reaction mechanism involves a rearrangement of the carbocation generated from (±)-**54** and subsequent extrusion of formaldehyde and carbon monoxide to afford the azonia[60]fullerene cation (not shown) as the crucial intermediate.[154] This was reduced to the azafullerenyl radical (not shown) which dimerized to 2,2′-bi-1-aza[60]fullerene (**55**)[154,155] or reacted further to 2*H*-1-aza[60]fullerene (not shown).[156] Many of the suggested intermediates on the way to aza[60]fullerenes have modified cores which, when structurally related to the parent C_{60}, display inherently chiral functionalization patterns. Among these, the stable C_1-symmetric "holey ball" (±)-**54** with a "chiral orifice" was isolated, characterized and resolved into the enantiomers (80 and 92% *e.e.*) by HPLC on a Pirkle type chiral stationary phase.[157] The strongest Cotton effect was found at 325 nm with $\Delta\varepsilon = 29\ M^{-1}\,cm^{-1}$. This value is relatively small for an inherently chiral fullerene chromophore and comparable to that of D_2-C_{84} (main isomer; cf. Section III.C).[60] It should be mentioned that a different synthetic route to aza[60]fullerenes was disclosed by Hirsch and co-workers. It starts from derivatives of type **52** (Scheme 1.7) with acid-labile *N*-substituents.[47,158,159]

Twofold addition of nitrenes to C_{60} by reaction of the fullerene with ethyl azidoformate under thermal conditions yielded eight regioisomeric bis-adducts.[160] Among these, seven correspond to those known from the double Bingel addition (cf. Section IV.A.1.b).[51] They include the C_2-symmetric *cis*-3 ((±)-**56**), *trans*-3 ((±)-**57**), and *trans*-2 ((±)-**58**) bis-adducts as C_{60}-derivatives with an inherently chiral addition pattern (Figure 1.13). Besides, a C_s-symmetric *cis*-1 isomer (**59**, Figure 1.37; cf. Section IV.B.1.c) was obtained as a major product thanks to the lesser steric requirement of the imino bridge

in comparison to di(alkoxycarbonyl)methano addends. The *cis*-1 bis-adduct **59** represents the first fullerene derivative with open transannular 6–6 bonds.[160]

A C_1-symmetric hexakis-adduct of C_{60} including an azahomofullerene substructure (addition pattern analogue of homo[60]fullerene derivative (±)-**26**, Scheme 1.2) was obtained as a side product upon nitrogen extrusion from a fullerene derivative bearing five Bingel type addends and a fused triazoline arranged in a pseudo-octahedral manner.[120]

e. Epoxides. Buckminsterfullerene can be oxidized with dimethyldioxirane[161] in toluene or photochemically by dioxygen in benzene[162] to give $C_{60}O$ in which an oxirane ring is fused to a 6–6 bond of the fullerene. Oxidation of C_{60} with PhIO in the presence of an efficient chemical cytochrome P450 model system additionally yielded the C_s-symmetric *cis*-1 bis-adduct (cf. Figure 1.12*b*) next to a tris-adduct fraction containing two components.[163] Based on ^{13}C NMR spectroscopy and the finding that both tris-adducts could also be obtained by epoxidation of the *cis*-1 diepoxy[60]fullerene, they were identified as C_s-symmetric *cis*-1,*cis*-1,*cis*-2 adduct (not shown) and C_2-symmetric *cis*-1,*cis*-1,*cis*-3 adduct (±)-**60** (Figure 1.20).[163] In both tris-adducts the *cis*-1 addition pattern, which is among the preferred with sterically nondemanding addends,[111] is realized twice. The above bis- and tris-adduct isomers

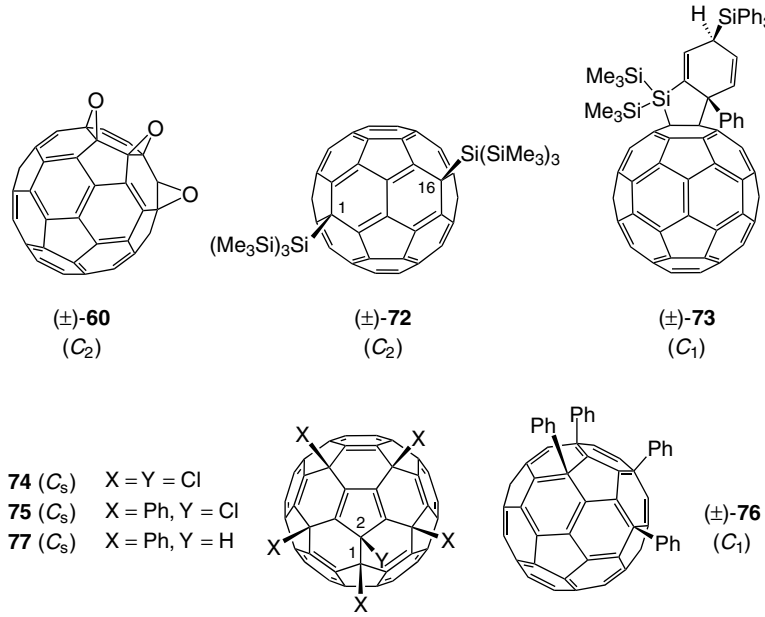

Figure 1.20. A selection of C_{60} derivatives with distinct addition patterns.

were also found in the oxidation of C_{60} with methyl(trifluoromethyl)dioxirane.[164] Additional structural proof for the *cis*-1 isomer of $C_{60}O_2$, obtained through oxidation of C_{60} with *m*-chloroperbenzoic acid, came from X-ray crystallography of its complex with $[Ir(CO)Cl(PPh_3)_2]$.[165]

f. Hydro Derivatives. In the hydrogenation of C_{60}, 1,2-addition is generally preferred over 1,4-addition despite eclipsing interactions between vicinal hydrogen atoms on the carbon spheroid.[14,166,167] Hydroboration of C_{60} and subsequent hydrolysis consequently afforded a single, C_{2v}-symmetric 1,2-dihydro[60]fullerene.[168] Six $C_{60}H_4$ regioisomers, on the other hand, were found in the reduction of $C_{60}H_2$ with $BH_3 \cdot THF$[169] or of C_{60} with anhydrous hydrazine.[170] Of these, the C_s-symmetric and thermodynamically most stable[169] *cis*-1 adduct (1,2,3,4-tetrahydro[60]fullerene; cf. Figure 1.2) could be isolated and assigned by Cahill and co-workers. Based on ^{1}H NMR spectroscopy, an unambiguous and a confident structural assignment were also possible for the C_s-symmetric *e*- and the D_{2h}-symmetric *trans*-1 adducts, respectively (cf. Figure 1.12*b*).[169] Of the remaining unassigned three tetrahydro[60]fullerenes resulting from twofold 1,2-addition, at least one must have an inherently chiral addition pattern (i.e., *cis*-3, *trans*-2, or *trans*-3); among these, the latter appears to be energetically favored based on ab initio calculations.[169]

In papers describing the isolation of several oligohydro[60]fullerene isomers together with a detailed ^{1}H- and ^{13}C NMR spectroscopic analysis, Meier and co-workers report the reaction of C_{60} with reducing metals in the presence of a proton source.[171,172] Reduction with the Zn(Cu) couple produced $C_{60}H_2$, $C_{60}H_4$, and $C_{60}H_6$ in a limited number of isomers, presumably under kinetic control.[172] Although the regioisomeric composition of the $C_{60}H_4$ fraction differed from that obtained by hydroboration (*vide supra*),[172,173] one of the two major isomers (1 : 1 ratio) was identified as the achiral *e* bis-adduct (cf. Figure 1.12*b*) characterized by Cahill and co-workers.[169] The other major $C_{60}H_4$ isomer was confidently assigned as the C_2-symmetrical *trans*-3 adduct (±)-**61** (Figure 1.21), especially in view of its probable role as an intermediate in the formation of the major $C_{60}H_6$ adduct.[172] Hexahydro[60]fullerene is formed as a 6 : 1 mixture of two regioisomers.[171,172] The cranberry-colored solution of the major isomer shows only one proton (^{1}H NMR) and 10 carbon (^{13}C NMR) resonances which, together with the 1,2-addition mode confirmed by coupling constant analysis, permits an assignment as D_3-symmetric *trans*-3,*trans*-3,*trans*-3 adduct (±)-**62** (Figure 1.21).[171,172] The ^{1}H NMR spectrum of the minor $C_{60}H_6$ isomer displays an AB pattern centered at 5.25 ppm indicating another highly symmetrical molecule and the C_3-symmetric *e*,*e*,*e* tris-adduct structure (cf. Figure 1.14) was tentatively assigned.[172] Interestingly neither the $C_{60}H_4$ nor the $C_{60}H_6$ isomers seem to interconvert under the conditions of their synthesis. Attempts to isomerize (±)-**62** with Pd/C or Pt/C resulted in dehydrogenation rather than isomerization.[172]

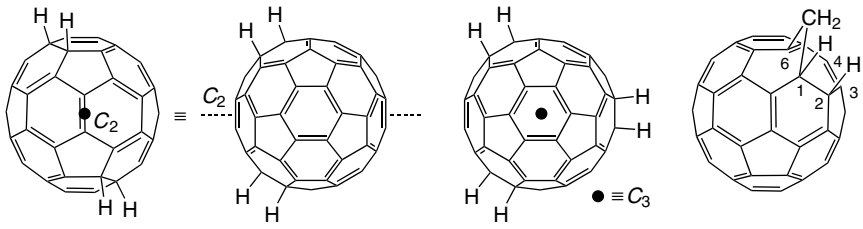

(±)-**61** (*trans*-3, C_2) (±)-**62** (*trans*-3,*trans*-3,*trans*-3; D_3) (±)-**63** (C_1)

Figure 1.21. Two major products of the reduction of C_{60} with Zn(Cu) in the presence of a proton source, and one of the two major products resulting from the according reaction with homofullerene $C_{61}H_2$.

Reduction of homo[60]fullerene, $C_{61}H_2$,[41,43] with Zn(Cu) produces two major isomers of $C_{61}H_4$ which were identified by detailed ^{1}H- and ^{13}C NMR spectroscopic analysis as C_1-symmetric 1,2-dihydro-1(6)a-homo[60]fullerene ((±)-**63**) (Figure 1.21) and C_s-symmetric 3,4-dihydro-1(6)a-homo[60]fullerene (cf. Figures 1.2 and 1.21).[174] The thermodynamic product (±)-**63** can be considered as a core-modified fullerene with an inherently chiral functionalization pattern corresponding to that observed in the addition of azides to 1(6)a-aza-1(6)a-homo[60]fullerene derivatives (cf. Scheme 1.7 and Section IV.A.1.d).[152] The high reactivity of double bonds involving a bridgehead carbon atom is attributed to the strain imposed by the π-orbital misalignment rather than the pyramidalization of the fullerene C-atoms.[174–176]

Although $C_{60}H_{18}$ and $C_{60}H_{36}$ were the first fullerene derivatives reported in literature,[177] the determination of their structures proved to be quite difficult due to facile oxidative degradation. The cognition of the parallels between hydrogenation and fluorination (cf. Section IV.A.1.g) of fullerenes provided additional means of structural elucidation.[178–180] Combining them with an analysis of the ^{1}H NMR multiplet patterns and coupling constants, Taylor and co-workers concluded on the chiral T-symmetric structure (±)-**64** (Figure 1.22, *top*) for $C_{60}H_{36}$ and on a C_{3v}-symmetric crown-shaped addition pattern, which is a substructure of the former, for $C_{60}H_{18}$.[181] A number of theoretical calculations also predict (±)-**64** to be the most stable $C_{60}H_{36}$ isomer.[182,183] The T-symmetric addition pattern of $C_{60}H_{36}$ generates four benzenoid rings on the fullerene surface thanks to which the destabilization arising from eclipsing interactions, such as in the four fully hydrogenated hexagons, is compensated by aromatic electron delocalization.[181] This structural assignment is supported by recent X-ray spectroscopic[184] and neutron diffraction[185] data. It should be mentioned that other studies, based on different experimental methods and theoretical models, led to different, though not necessarily

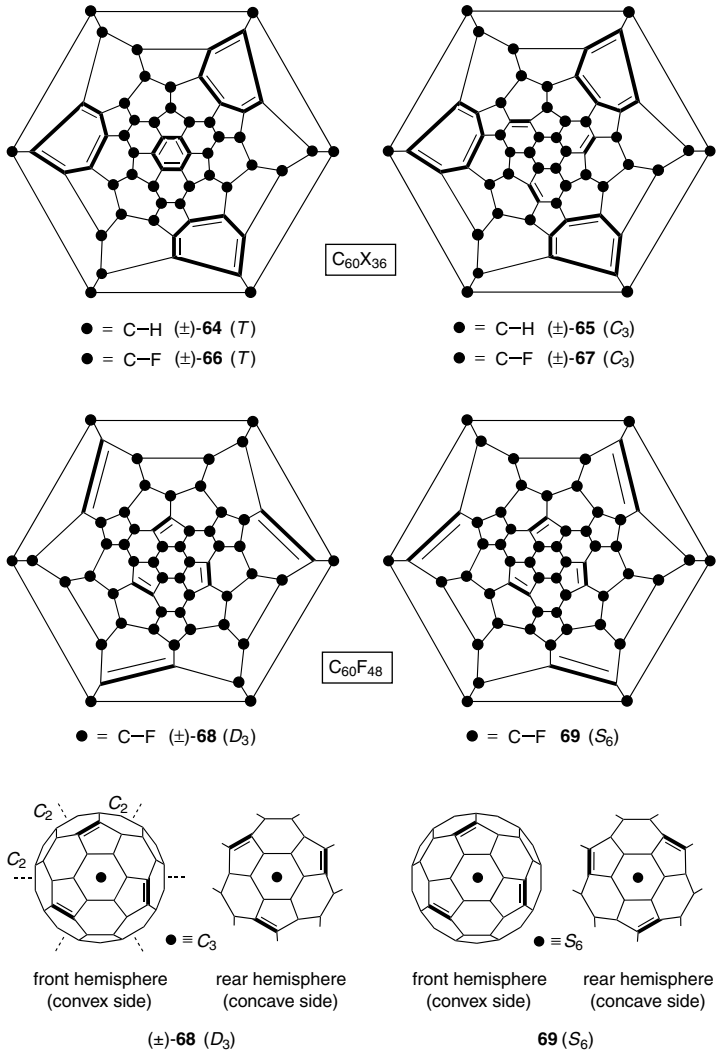

Figure 1.22. Polyhydro- and polyfluoro[60]fullerene derivatives. *Top*: Schlegel diagrams of two chiral constitutional isomers of both $C_{60}H_{36}$ and $C_{60}F_{36}$. *Center*: Schlegel diagrams of a chiral and an achiral constitutional isomer of $C_{60}F_{48}$. *Bottom*: The above two constitutional isomers of $C_{60}F_{48}$ can be considered as made up of two isoconstitutional, C_3-symmetric hemispheres; the combination of homochiral moieties leads to the D_3-symmetric constitutional $C_{60}F_{48}$ isomer and the combination of heterochiral moieties affords the S_6-symmetric constitutional isomer. It should be noted that for reasons of clarity, the F-atoms are omitted; furthermore the front hemisphere is viewed from the convex side (extra-cage view) and the rear hemisphere from the concave side (intra-cage view). The indicated symmetry elements refer to the entire functionalized carbon sphere resulting from translational superposition of the represented hemispheres (the C_3-axis is also valid for the individual hemispheres).

clear-cut conclusions.[186,187] Inspired by the observation of two close-lying ^{3}He NMR resonances measured for $i^3HeC_{36}H_{36}$[187] and by the structural elucidation of $C_{60}F_{36}$ (cf. Section IV.A.1.g), Taylor, Saunders, and co-workers proposed the presence of a second, major isomer of C_3-symmetry ((±)-**65**, Figure 1.22, *top*) for $C_{60}H_{36}$.[188]

g. Fluoro Derivatives. $C_{60}F_{18}$ was shown by 2D COSY ^{19}F NMR spectroscopy to be isostructural with the C_{3v}-symmetric $C_{60}H_{18}$.[189] The more highly fluorinated $C_{60}F_{36}$ was separated into two chiral constitutional isomers, one of C_3-symmetry and one of T-symmetry (ratio ca. 3 : 1).[180] The similarity between the ^{3}He NMR spectra of the fluoro derivatives $i^3HeC_{60}F_{18}$ and $i^3HeC_{60}F_{36}$, on one hand, and those of the corresponding polyhydro[60]fullerene-derivatives[187] (cf. Section IV.A.1.f), on the other, suggested isostructural compounds in both series.[188] Whereas the T-symmetric structure (±)-**66** (Figure 1.22, *top*) was established by a combination of ^{19}F NMR- and ^{13}C NMR spectroscopy,[180] the more subtle question of the structure of C_3-symmetric $C_{60}F_{36}$ ((±)-**67**) was answered on the grounds of a detailed 2D COSY ^{19}F NMR analysis in conjunction with calculations on the relative stabilities of different isomers, and a theoretical prediction of the ^{3}He NMR shifts of different $i^3HeC_{60}F_{36}$ isomers.[188] Considering the structures of the formed $C_{60}X_{18}$ (X = H, F) and $C_{60}X_{36}$ ((±)-**64**–(±)-**67**; Figure 1.22, *top*) isomers, a rationale was proposed for the observed addition modes in the hydrogenation and fluorination of C_{60}: Both reactions seem to proceed in a sequential manner involving a contiguous bond activation ascribed to an increased localization of double bonds adjacent to addends already in place.[188]

The first structural assignment of a highly fluorinated fullerene derivative was made for $C_{60}F_{48}$ by Gakh, Tuinman, and co-workers in 1994.[190] These early results may seem surprising in view of the 11′661′527′055 possible constitutional $C_{60}X_{48}$ isomers, out of which 11′661′270′420 are chiral,[191] but the obtained product which showed eight ^{19}F NMR resonances of equal intensity proved to have largely a single constitution.[190] 2D COSY ^{19}F NMR analysis allowed a unique structural assignment of $C_{60}F_{48}$ as energetically low-lying[192] D_3-symmetric (±)-**68** (Figure 1.22, *center*),[190] a structure that was confirmed in a later study[193] to be made up of two identical, C_3-symmetric functionalized C_{60} hemispheres (Figure 1.22, *bottom*). Careful examination of low-intensity ^{19}F NMR signals also suggested the presence of a minor, S_6-symmetric $C_{60}F_{48}$ isomer (**69**, Figure 1.22, *center* and *bottom*).[190] The structures of (±)-**68** and achiral **69** can formally be interconverted by replacing one hemisphere of the starting molecule by its mirror image (Figure 1.22, *bottom*). An analogous relationship exists also between hexakis-adduct structures (±)-**70** and **71**[194] (Figure 1.24) combining two C_{60} halves with an intrahemispheral *e*,*e*,*e* addition pattern; it is analyzed in Section IV.A.1.l.

h. Addition of Bulky Silyllithium Reagents. In the case of $C_{60}H_2$, the product of the common 1,2-addition mode was calculated to be 3.9 kcal mol^{-1} more stable than the 1,4-adduct, and even 15.5 kcal mol^{-1} more stable than the 1,16 adduct (cf. Figure 1.12*a*).[167] However, as addends become bulkier and eclipsing 1,2-interactions stronger, 1,4-addition is increasingly favored (cf. Sections IV.B.1.a and IV.B.1.b).[15,16] Upon reaction of C_{60} with certain very bulky silyllithium or germyllithium reagents, Ando and co-workers observed for the first time the rare inherently chiral 1,16-functionalization pattern (cf. Figure 1.12*a*): Whereas the addition of $(i\text{-}Pr)_2PhSiLi$, followed by quenching with EtOH, afforded the 1,2-adduct $[(i\text{-}Pr)_2PhSi]HC_{60}$, the 1,16-adduct (±)-**72** (Figure 1.20) was isolated as sole product of the addition of $(Me_3Si)_3SiLi$ under the same conditions and its C_2-symmetric structure was confirmed by X-ray crystallography.[103,195] Some of the silyllithium reagents also yielded 1,4-adducts next to the 1,16-adducts (cf. Section IV.B.1.a).[195] The latter were also obtained in the photochemical addition of disilanes to C_{60}, a reaction proceeding probably via silyl radicals.[196] In certain cases of phenyl-substituted disilanes, it led to rearranged adducts of the type (±)-**73** (Figure 1.20).[197]

i. Products Derived from $C_{60}Cl_6$. In the reaction of $C_{60}Cl_6$ (**74**, Figure 1.20)[198] with benzene and $FeCl_3$,[199] C_1-symmetric $C_{60}Ph_4$ and C_s-symmetric $C_{60}Ph_2$ were obtained as two out of several minor products besides the major product $C_{60}Ph_5Cl$ (**75**).[200] Under the assumptions that the phenyl groups are located at sites previously occupied by Cl-atoms, that phenyl groups are not located at adjacent positions on the carbon sphere (no restricted rotation observed by ^1H NMR spectroscopy), and that the number of energetically unfavorable double bonds in five-membered rings[167] is kept at a minimum, $C_{60}Ph_4$ was assigned the 1,3,11,30-adduct structure (±)-**76** which displays an inherently chiral addition pattern (Figure 1.20). Its formation was rationalized by mechanistic considerations that further indicate $C_{60}Ph_2$ to be a 1,4-adduct.[200] The products of the reaction above were also synthesized as endohedral incarceranes of ^3He. As a general trend ^3He NMR shows an increased shielding of the entrapped noble gas with increasing degree of functionalization.[201]

On exposure to air $C_{60}Ph_5H$ (**77**)[199] and $C_{60}Ph_5Cl$ (**75**)[199] are spontaneously oxidized with replacement of the hydrogen or chlorine attached to C(2) (Figure 1.20) of the carbon cage and of an *ortho*-hydrogen of the adjacent phenyl ring under formation of a benzo[*b*]furan unit fused across a 6–6 bond of the fullerene.[202,203] The observed C_1-symmetric final product (not shown) was proposed to arise from additional epoxidation of one of the double bonds in the pentagon that is surrounded by the phenyl rings (cf. Figure 1.20),[202] a structure that corresponds to a noninherently chiral addition pattern. Further oxidation and fullerene cage degradation products are $C_{60}Ph_4O_2$ and $C_{58}Ph_4$,[202] for which C_1-symmetric structures have been suggested.[204]

j. Addition of Diamines. The addition of diamines to C_{60} is particular insofar as a concomitant oxidation (dehydrogenation) affords a mono-adduct with only nitrogen atoms attached to the fullerene cage.[205] From the reaction of C_{60} with piperazine, Kampe and Egger isolated six bis-adducts of which they tentatively assigned an achiral one as either the *cis*-2 or the *trans*-4 regioisomer (cf. Figure 1.12*b*), based on ^{13}C- and ^{1}H NMR spectroscopy as well as on the retention behavior on silica gel.[206,207] Similarly, for two of the seven isolated bis-adducts resulting from addition of *N*,*N*′-dimethylethylene-1,2-diamine to C_{60}, they proposed the *trans*-3 and *e* adduct structures (cf. Figure 1.12*b*) for a C_2- and a C_s-symmetrical compound, respectively.[207] The addition of piperazine to C_{60} was reinvestigated by Balch and co-workers, who separated the mono-adduct and six bis-adducts chromatographically.[208,209] They obtained X-ray crystal structures of the mono-adduct as well as of three bis-adducts, namely the achiral *cis*-2 and *e* regioisomers (cf. Figure 1.12*b*) as well as the *trans*-2 adduct (±)-**78** (Figure 1.23). Interestingly the *cis*-2 isomer appears to have two of its nitrogen atoms well positioned for the chelation of a metal ion with a M–N bond length of 2.1 Å and a N–M–N angle of 102°.[209]

In a similar reaction, Prato and co-workers added optically pure *trans*-*N*,*N*′-dimethylcyclohexane-1,2-diamine to C_{60}.[210] Depending on the configuration of the starting diamine, they obtained enantiomerically pure (*R*,*R*)-**79** and (*S*,*S*)-**79** (Figure 1.23), having their chiral units located exclusively in the lateral group.

k. [60]Fullerene-Fused Isoxazolines. Quite a complex mixture of regioisomers can result from double additions involving C_s-symmetric instead of C_{2v}-symmetric addends.[102] Such a case is represented by the [3 + 2]

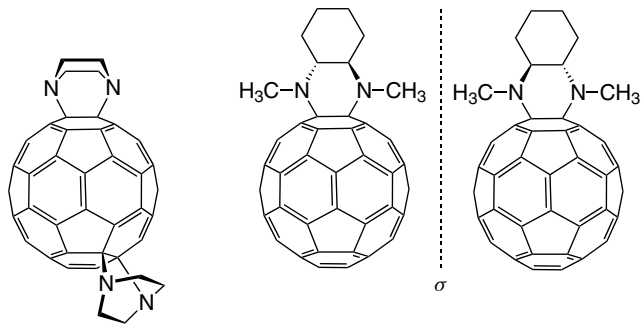

Figure 1.23. Chiral adducts resulting from the reaction of C_{60} with diamines. The mono-adducts (right side) were synthesized as pure enantiomers.

cycloaddition of 2,4,6-trimethoxybenzonitrile oxide to C_{60}, from which 22 constitutionally isomeric [60]fullerene-fused bis-isoxazolines can theoretically result.[211] Taking into account stereoisomers as well, a total of 36 product isomers is possible, and among these, 28 can be grouped into pairs of enantiomers, whose functionalization pattern is either inherently chiral (occurs with *cis*-3, *trans*-2, and *trans*-3 addition patterns; cf. Figure 1.12*b*) or noninherently chiral (can occur with *cis*-1, *cis*-2, *e*, and *trans*-4 addition patterns; cf. Figure 1.12*b*). The only bis-addition mode not generating stereoisomerism corresponds to the *trans*-1 addition pattern. ^{1}H- and ^{13}C NMR spectroscopy of different HPLC fractions isolated by Irngartinger and Fettel revealed the presence of a total of 16 constitutional isomers that could only be partially purified.[211] In a similar reaction two bis-isoxazoline fractions were obtained as isomeric mixtures from addition of (diisopropoxyphosphoryl)methanenitrile oxide to C_{60}.[212]

l. [60]Fullerene-Fused Pyrrolidines. The 1,3-dipolar cycloaddition of azomethine ylides to C_{60}, first reported by Prato and co-workers, affords fullerene-fused pyrrolidines (cf. Section IV.C.1.c, Figure 1.45, and Scheme 1.15).[213,214] Six bis-adducts were isolated by Schuster and Wilson in the reaction of *N*-methylazomethine ylide starting from the corresponding mono-adduct of C_{60}.[215] A tentative structural assignment was based on the molecular symmetry as revealed by NMR spectroscopy, a comparison of the UV/Vis spectra to those of Bingel type bis-adducts, the order of chromatographic elution, and the deshielding of the methylene and *N*-methyl protons (^{1}H NMR spectroscopy). Of the eight possible bis-adducts of C_{60}, all but *cis*-1 and *cis*-2 regioisomers (cf. Figure 1.12*b*) were found[215] and their ratio signaled a lower regioselectivity for the [3 + 2] cycloaddition of azomethine ylides as compared to the double Bingel reaction.[51] Saunders, Schuster, and co-workers investigated the differentiation among regioisomeric bis-adducts resulting from the addition of azomethine ylides or 2-halomalonates to C_{60} by ^{3}He NMR spectroscopy of the corresponding ^{3}He incarceranes.[87] Although the absolute chemical shifts differ in both adduct series, ^{3}He NMR spectroscopy revealed a significant, but not perfect, correlation between relative shifts and addition patterns. Regioisomers in which both addends are located in opposite hemispheres (*trans* adducts) tend to have their ^{3}He resonances downfield from those of *cis* adducts (cf. Figure 1.12*b*). This demonstrates that the magnetic field inside the fullerene cage, generated by ring currents in the residual π-chromophore, is very sensitive to the addition pattern on the C_{60} surface.[87] The use of transient EPR (electron paramagnetic resonance) spectroscopy of excited triplet states of fullerene bis-adducts has been proposed as another tool for the assignment of regioisomeric bis-adducts of C_{60}.[216]

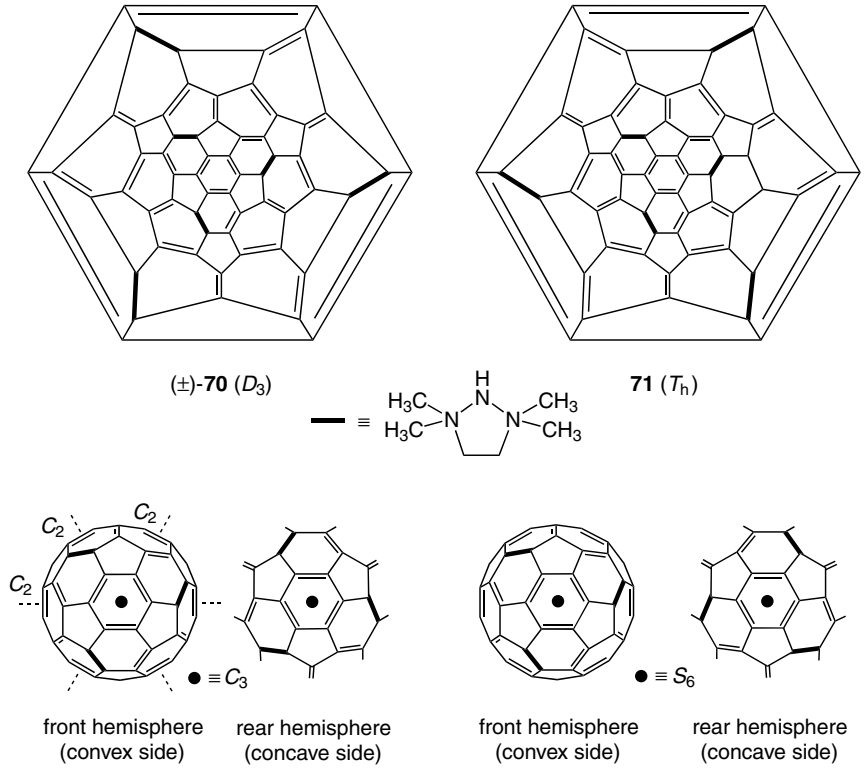

Figure 1.24. Schlegel diagrams and individual hemispheres of two constitutional isomers resulting from sixfold [3 + 2] cycloaddition of 1,1,3,3-tetramethylazomethine ylide to C_{60}. The two isomers can be considered as made up of two isoconstitutional, C_3-symmetric hemispheres; the combination of homochiral moieties leads to the D_3-symmetric regioisomer and the combination of heterochiral moieties affords the T_h-symmetric regioisomer. It should be noted that the front hemisphere is viewed from the convex side (extra-cage view) and the rear hemisphere from the concave side (intra-cage view). The indicated symmetry elements refer to the entire functionalized carbon sphere resulting from translational superposition of the represented hemispheres (the C_3-axis is also valid for the individual hemispheres).

A quite unusual, inherently chiral functionalization pattern was observed by Rubin, Garcia-Garibay, and co-workers in the sixfold addition of 1,1,3,3-tetramethylazomethine ylide to C_{60}.[194] Whereas the Bingel reaction, through an increasing selectivity for $e_{(face)}$ double bonds in every addition step, preferentially yields a T_h-symmetric hexakis-adduct with a pseudo-octahedral arrangement of addends on the fullerene sphere, the large steric bias of 1,1,3,3-tetramethylazomethine ylide appears essential in affording D_3-symmetric (±)-**70** as the major hexakis-adduct besides T_h-symmetric **71** in the [3 + 2]

cycloaddition reaction (Figure 1.24). The preferential formation of (±)-**70** over **71** must originate from the primary distribution of bis-adducts, with steric hindrance strongly affecting all subsequent additions. Both hexakis-adducts were characterized by X-ray crystallography and exhibit a strong fluorescence that is unusual for fullerenes[217] and most of their derivatives.[218] There is an interesting parallel in the relationship between the functionalization patterns of (±)-D_3-**70** and T_h-**71** (Figure 1.24), on one hand, and that of the constitutional $C_{60}F_{48}$ isomers (±)-D_3-**68** and S_6-**69** (cf. Section IV.A.1.g and Figure 1.22), on the other.[190] In both pairs the molecules are composed of isoconstitutional, C_3-symmetric chiral halves, and whereas the combination of homochiral moieties leads to the chiral, D_3-symmetric structures (±)-**70** (Figure 1.24) and (±)-**68** (Figure 1.22), that of heterochiral moieties affords the achiral molecules T_h-**71** (Figure 1.24) and S_6-**69** (Figure 1.22). The latter should, however, not be considered as *meso* forms, because they are constitutional isomers and not diastereoisomers of the chiral counterparts (±)-**70** and (±)-**68**, respectively. The constitutional isomerism arises from differences in the relative interhemispheral arrangement of addends in (±)-**70** and **71** (Figure 1.24), as well as in (±)-**68** and **69** (Figure 1.22).

2. *Derivatives of C_{70}*

a. General Considerations on the Chirality of the Most Common Addition Patterns in Mono-adducts of C_{70}. C_{60}[14–16] and the higher fullerenes[17] show a similar general behavior in addition reactions (cf. Section IV.A.1.a). However, whereas buckminsterfullerene contains only a single type of 6–6-bonds, this number increases to 4 in D_{5h}-C_{70}, to 15 in D_2-C_{76}, and to 18 and 10 in C_{2v}- and D_3-C_{78}, respectively, thus leading to a growing number of possible adduct isomers with increasing fullerene size and decreasing symmetry. If one includes the four different 6–5 bonds of C_{70}, its chemistry may appear complex in comparison to that of C_{60} which comprises only one type of each 6–6 and 6–5 bonds. Nevertheless, C_{70} and other higher fullerenes show a remarkable selectivity in the formation of mono- and multi-adducts.[17] In [70]fullerene, the first addition occurs with decreasing preference at the 6–6 bonds C(1)–C(2) and C(5)–C(6), respectively (for the numbering; cf. Figure 1.6), to a lesser extent at the 6–6 bond C(7)–C(21), and in a few instances at the 6–5 bond C(7)–C(8).[17,54,219,220] In addition and similar to C_{60}, certain primary adducts including, for example, fullerene-fused pyrazolines and triazolines (cf. Sections IV.A.2.b), can rearrange to homo[70]fullerenes with insertion of the *homo* atom into the 6–5 junction between C(2) and C(3), or C(1) and C(6) (cf. Figure 1.6 and Scheme 1.9).

For reasons of clarity, the following general considerations on chiral addition patterns of C_{70} will be limited to the most common types of mono-addition

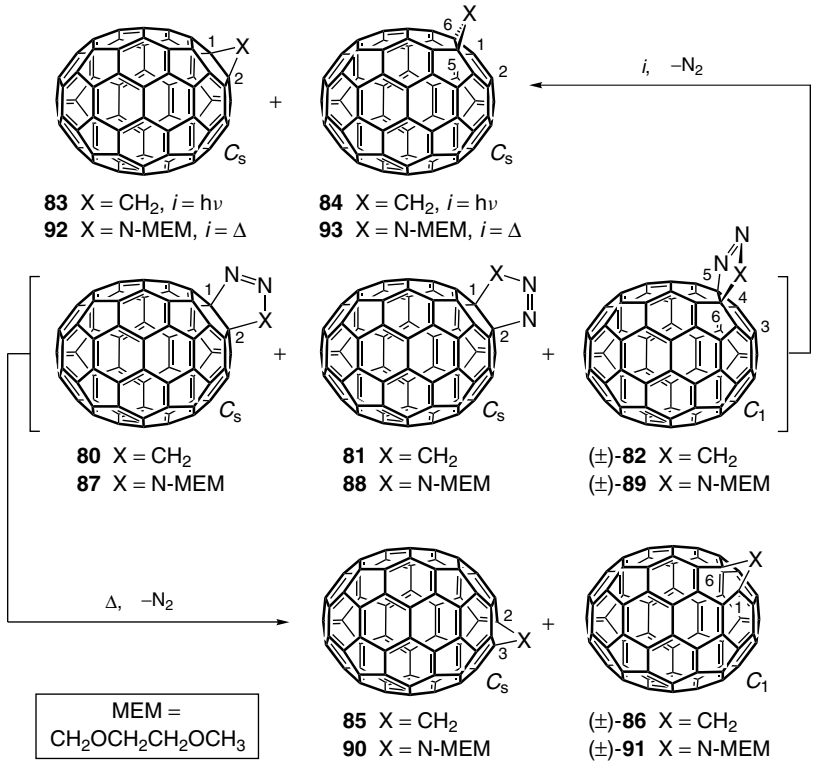

83 X = CH_2, *i* = hν
92 X = N-MEM, *i* = Δ

84 X = CH_2, *i* = hν
93 X = N-MEM, *i* = Δ

80 X = CH_2
87 X = N-MEM

81 X = CH_2
88 X = N-MEM

(±)-**82** X = CH_2
(±)-**89** X = N-MEM

85 X = CH_2
90 X = N-MEM

(±)-**86** X = CH_2
(±)-**91** X = N-MEM

Scheme 1.9. Regioisomeric adducts resulting from [3 + 2] cycloaddition of diazomethane or azide dipoles to C_{70} (central row), and subsequent extrusion of N_2 under formation of the respective "6–6 closed" (top row) or "6–5 open" (bottom row) structures.

of C_{2v}- or C_s-symmetric addends.[102] Chiral functionalization patterns of multiple adducts will be discussed in the context of particular examples. Known inherently chiral functionalization patterns of C_{70} result from addition across the C(7)–C(21) bond (cf. Figures 1.6 and 1.25) or from insertion between C(1) and C(6) (cf. Figure 1.6 and Scheme 1.9). A noninherently chiral addition pattern of C_{70} has been realized with C_s-symmetric addends[102] bridging the C(5)–C(6) bonds (cf. Figure 1.6 and Scheme 1.9). The most common C(1)–C(2) addition pattern (cf. Figure 1.6 and Scheme 1.9), on the other hand, is achiral with both types of addends, but it can give rise to constitutional isomers with C_s-symmetric addends.[102]

In this brief overview of C_{70}-addition patterns, it may also be mentioned that photochemical addition of 1,1,2,2-tetramesityl-1,2-disilirane afforded a C_2-symmetric adduct for which the unusual addition across the equatorial,

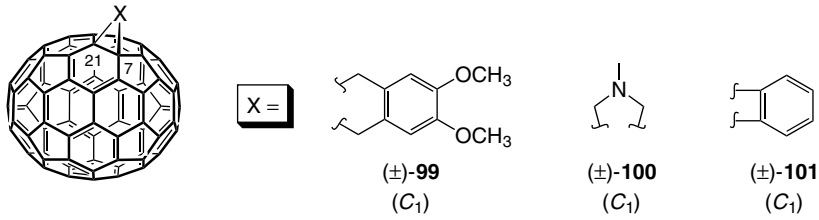

Figure 1.25. C(7)–C(21) adducts of C_{70} with an inherently chiral addition pattern.

biphenyl-like bond C(20)–C(21) (cf. Figure 1.6) was proposed.[221] This addition pattern is achiral, and the chirality was conjectured to originate from conformational effects related to the bulky mestityl substituents. An alternative structure with an inherently chiral functionalization pattern, resulting from transequatorial 1,4-addition at positions C(7) and C(23) (cf. Figure 1.6) was also suggested.[222]

Similar to the case of C_{60},[105,223] some exploratory work on the regiochemistry of single and double osmylation of C_{70} was done by Hawkins and co-workers.[224] A major and a minor mono-adduct were assigned the C_s-symmetric C(1)–C(2)- and C(5)–C(6)-adduct structures (cf. Figure 1.6), respectively. After re-submission of the mono-adducts to osmylation, a total of nine compounds was reported, but no individual structural assignments were made.[224]

b. Homo[70]fullerenes, Azahomo[70]fullerenes, and Related Compounds. An intensely investigated class of C_{70} derivatives including representatives with an inherently chiral functionalization pattern are homo-[43,85,225] and azahomo[70]fullerenes,[46,47,226–229] as well as a number of compounds resulting from further transformation of these (*vide infra*). Some of the precursors to the core-modified [70]fullerenes with a "6–5 open" bridge, on the other hand, have a noninherently chiral functionalization pattern, but for reasons of comprehensibility, they will be discussed in the context of this section.

[3 + 2] Cycloaddition of diazoalkanes to 6–6 bonds was among the first reactions tested on the carbon cages[41] and affords isolable fullerene-fused pyrazolines as primary adducts. Photochemically induced extrusion of N_2 from the latter yields 6–6-closed methanofullerenes having the functionalized bond embedded in a cyclopropane substructure, whereas the thermal process affords 6–5 open homofullerenes in which a methylene group is bridging the open junction between a six- and a five-membered ring.[15–17]

Taking into account the two possible orientations of a diazomethane dipole with respect to all nonequatorial bonds of C_{70}, two regioisomeric pyrazolines, **80** and **81** (Scheme 1.9), arise from addition at C(1)–C(2), and

a third constitutional isomer (C_1-symmetric (±)-**82**) with a noninherently chiral addition pattern results from addition across C(5)–C(6).[43,225] Irradiation of the pyrazoline mixture **80**, **81**, and (±)-**82** through Pyrex glass yielded methanofullerenes **83** and **84** besides minor amounts of a third constitutional isomer (**85**), whereas thermolysis of the same mixture gave homofullerenes **85** and C_1-symmetric (±)-**86**, the latter having an inherently chiral addition pattern (Scheme 1.9).[43,225] It should also be mentioned that ^{3}He incarceranes of the $C_{71}H_2$ isomers **83**-(±)-**86** have been prepared to study the effect of the functionalization of the C_{70} cage on the ^{3}He NMR shift.[85] (±)-i-^{3}He·**86** represents the first chiral He derivative of C_{70}.

Similarly to the reaction with diazomethane, [3 + 2] cycloaddition of alkyl azides to C_{70} affords three constitutionally isomeric adducts (**87**, **88**, and (±)-**89**).[46,226,227] Thermal elimination of N_2 from the fullerene-fused triazolines showed a preference for the formation of 6–5 open azahomofullerene structures (types **90** and (±)-**91**) as compared to the 6–6 closed aziridine isomers corresponding to **92** and **93** (Scheme 1.9).[226,227]

After the successful synthesis of the "dimeric" azafullerene $(C_{59}N)_2$ from *N*-MEM- ([2-(methoxy)ethoxy]methyl) protected azahomo[60]fullerene by Wudl and co-workers,[153,154] the proved methodology (cf. Section IV.A.1.d) was applied to azahomo[70]fullerenes **90** and (±)-**91**.[46,47,227,228] Self-sensitized photooxygenation of **90** and (±)-**91** (Scheme 1.9) with their electron-rich enamine type double bonds led to the cage-opened ketolactams (±)-**94**, and a mixture of (±)-**95** and (±)-**96**, respectively (Scheme 1.10). Treatment with acid further transformed the C_1-symmetric, inherently chiral "holey ball" (±)-**94** into isomerically pure, C_s-symmetric 1,1′-bi-2-aza[70]fullerene (**97**). Under the same conditions, ketolactam (±)-**95** gave the C_s-symmetric azafullerene "dimer" 2,2′-bi-1-aza[70]fullerene (**98**).[46,47] The two reactions proceed via the 2- and 1-azonia[70]fullerene ions (not shown), which, after reduction to the according radicals, dimerize to give **97** and **98**, respectively. As opposed to the mentioned azonia[70]fullerene intermediates, the C_1-symmetric 5-azonia[70]fullerene ion (not shown; for the numbering, cf. Scheme 1.10 and Figure 1.6), generated from ketolactam (±)-**96**, is chiral. Consequently, if racemic (±)-**96** is used as a starting material in the above sequence,[46] three possible combinations of chiral 5-aza[70]fullerene-6(6*H*)-yl radicals (not shown; for the numbering, cf. Scheme 1.10 and Figure 1.6) are expected to afford three stereoisomers of 6,6′-bi-5-aza[70]fullerene (not shown; for the numbering, cf. Scheme 1.10 and Figure 1.6), namely a C_2-symmetric *d*,*l*-pair and a C_s-symmetric *meso* form (for "dimeric" *meso* derivatives of C_{60}, cf. Section IV.B.1.b).

Hirsch and co-workers developed a different synthetic route to heterofullerenes which, in the case of $(C_{59}N)_2$, involves intermediates of type **52** (cf. Section IV.A.1.d and Scheme 1.7) bearing acid-labile *N*-substituents.[47,158,159]

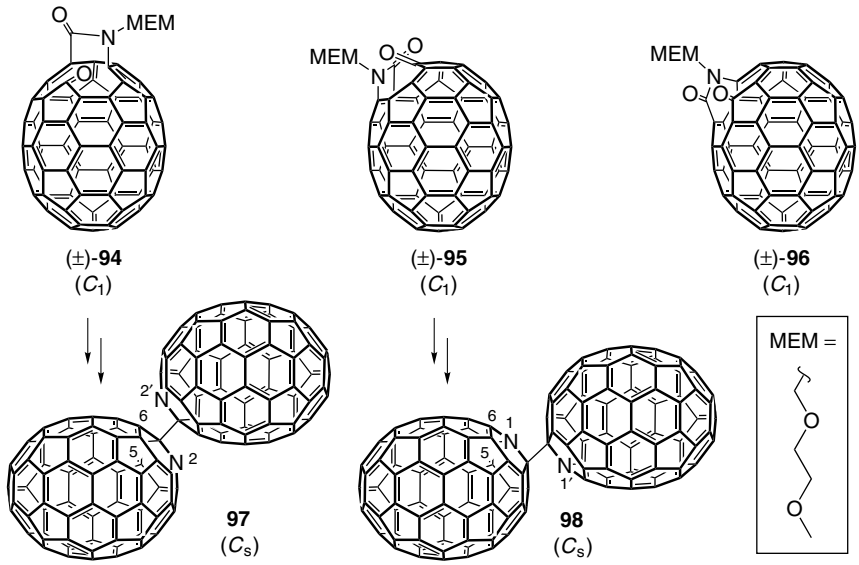

Scheme 1.10. Achiral "dimeric" aza[70]fullerenes and their chiral cage-opened ketolactam precursors. The third ketolactam (*right*) is expected to afford a mixture of *meso*- and *d*,*l*-6,6′-bi-5-aza[70]fullerene.

Its application to according derivatives of C_{70} afforded the achiral azafullerene "dimers" **97** and **98** for the first time.[47,159]

c. 7,21-Mono-adducts of C_{70}. The C_1-symmetric C(7)–C(21) adducts of C_{70} are the only 6–6-bond mono-adducts of this fullerene having an inherently chiral functionalization pattern. Only a few such adducts have been isolated, usually as minor products formed next to the achiral C(1)–C(2) and C(5)–C(6) adducts (cf. Figure 1.6). This rareness may seem surprising in view of the large number (20) of these bonds in C_{70}, but it is ascribed to the low reactivity of the C(7)–C(21) bond.[17] The first case ((±)-**99**, Figure 1.25) was detected by Diederich and co-workers in an investigation on the regioselectivity of the Diels-Alder addition of 4,5-dimethoxy-*o*-quinodimethane to C_{70} and C_{76}.[50] Another C(7)–C(21) adduct, (±)-**100** (Figure 1.25), was isolated as a minor product of the [3 + 2] cycloaddition of *N*-methylazomethine ylide to C_{70}.[215,230] The isomeric assignment was based on ^{1}H NMR spectroscopy showing the presence of two different methylene groups, each carrying two nonequivalent H-atoms. The inherently chiral C(7)–C(21) addition pattern was finally observed in one ((±)-**101**, Figure 1.25) of the minor mono-adduct isomers resulting from [2 + 2] cycloaddition of benzyne to C_{70}.[219,222] It was

accompanied by the common C(1)–C(2) and C(5)–C(6) adducts as well as by the unusual C(7)–C(8) isomer (cf. Figure 1.6).[219]

d. Mono-addition of Radicals. With five different types of C-atoms, C_{70} can give rise to a maximum of five isomeric radical mono-adducts, two of which are chiral. The latter result from attack at positions C(5) or C(7) of the fullerene (cf. Figure 1.6). By means of ESR spectroscopy, three regioisomers were detected in the addition of alkyl, Cl_3C,[231,232] methylsulfanyl,[233] or $(MeO)_2OP$,[231] up to four for H, aryl, F_3CF_2C,[232,234–236] and all five for H_3CO[233] and F_3C radicals.[235] Whereas the chiral adducts may be recognized spectroscopically by their symmetry (C_1), exact structural assignments are difficult in general.

e. Bingel Type Multi-adducts. Due to the high selectivity of the mild Bingel addition,[94] this reaction appeared perfectly suited for the investigation of the regiochemistry of multiple additions to C_{70}. In the mono-functionalization, it shows a high preference for the C(1)–C(2) bond,[35,94] and a second Bingel addition to C_{70}[35,54,107] takes place at one of the five bonds C(41)–C(58), C(56)–C(57), C(59)–C(60), C(67)–C(68), or C(69)–C(70) radiating from the polar pentagon of the unfunctionalized hemisphere (for the numbering, cf. Figure 1.6).

In the case of achiral, C_{2v}-symmetric malonate addends, three constitutionally isomeric bis(methano)fullerenes are formed,[35,54,107] an achiral one (C_{2v}-symmetric **102**), and two chiral representatives (C_2-symmetric (±)-**103** and (±)-**104**) which are obtained as pairs of enantiomers with an inherently chiral addition pattern (Figure 1.26).[35,54]

Twofold addition of optically pure bis[(*S*)-1-phenylbutyl] 2-bromomalonate to C_{70} leads to a superposition of the chirality of the addend and, in the occurrence, that of the core functionalization pattern, thus affording a total of five optically active isomers, namely C_2-symmetric (*S*,*S*,*S*,*S*)-**105**, and two additional constitutional isomers occurring as pairs of C_2-symmetric diastereoisomers ((*S*,*S*,*S*,*S*,^{f}A)-**106**/(*S*,*S*,*S*,*S*,^{f}C)-**107**) and ((*S*,*S*,*S*,*S*,^{f}A)-**108**/(*S*,*S*,*S*,*S*,^{f}C)-**109**) (Figure 1.26).[35] As the mixture of these five chiral C_{70} derivatives does not include any enantiomeric pair, they could all be separated by HPLC on silica gel, and the same was true for the five products (*R*,*R*,*R*,*R*)-**105**, (*R*,*R*,*R*,*R*,^{f}C)-**106**/(*R*,*R*,*R*,*R*,^{f}A)-**107**, and (*R*,*R*,*R*,*R*,^{f}C)-**108**/(*R*,*R*,*R*,*R*,^{f}A)-**109** (Figure 1.26), resulting from addition of the respective (*R*,*R*)-configured esters to C_{70}.[54] As a consequence 10 pure, optically active tetrakis(1-phenylbutyl) esters were obtained (Figure 1.26) which comprise five pairs of enantiomers: two with stereogenic centers in the addends only ((±)-**105**) and four with both an inherently chiral fullerene functionalization pattern and chiral side chains ((±)-**106**–(±)-**109**).

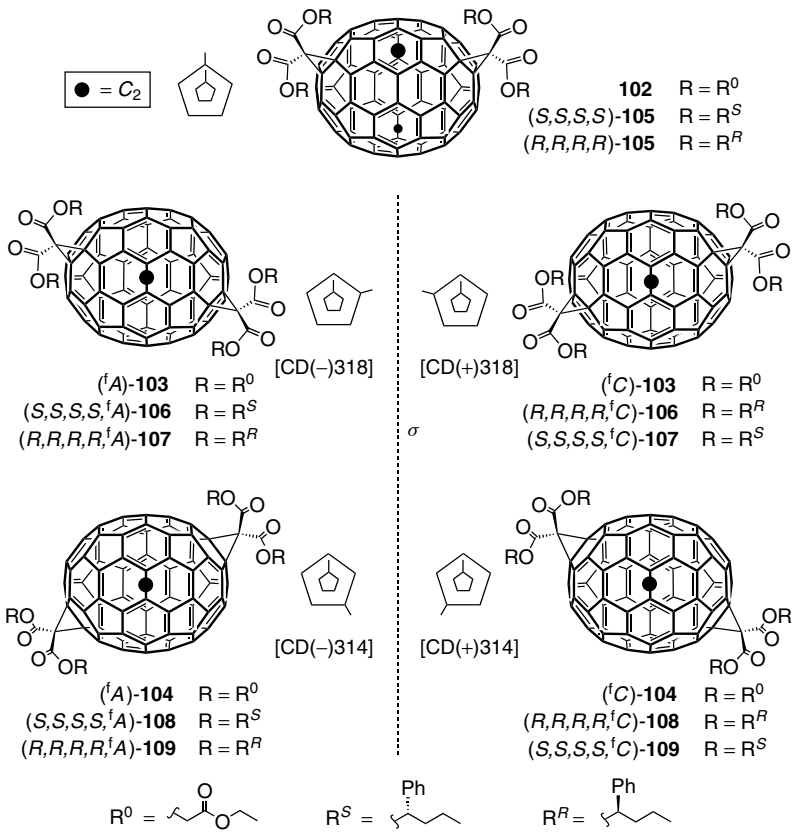

Figure 1.26. Double Bingel addition to C_{70} leads to an achiral (*top*) and two inherently chiral (*center* and *bottom*) addition patterns. Combination of each of the latter with chiral ester moieties affords two diastereoisomeric pairs of enantiomers. The enantiomers of each pair were prepared separately by addition of either (*R*,*R*)- or (*S*,*S*)-configured malonates to C_{70}, and all stereoisomers were isolated in pure state. The black dots mark intersections of the C_2-symmetry axis with the [70]fullerene spheroid. Next to the three-dimensional representations, constitution and configuration of the addition patterns are shown schematically in a *Newman* type projection along the C_5-axis of C_{70}. Of the two concentric five-membered rings, the inner one corresponds to the polar pentagon closest to the viewer, and the attached vertical line represents the bond C(1)–C(2) where the first addition occurred. The functionalized bonds at the distal pole depart radially from the outer pentagon.

Inherently chiral addition patterns give rise to chiral π-chromophores manifesting themselves by substantial[60,157] (cf. Figure 1.11) to very strong Cotton effects (Figure 1.27*b–d*; cf. also Figure 1.10) in the circular dichroism (CD) spectra (cf. Section IV.A.1.b),[4–7,22,35,54,93,96,97,106,115–117,125,149] generally in contrast to sole perturbation of achiral fullerene chromophores by chiral

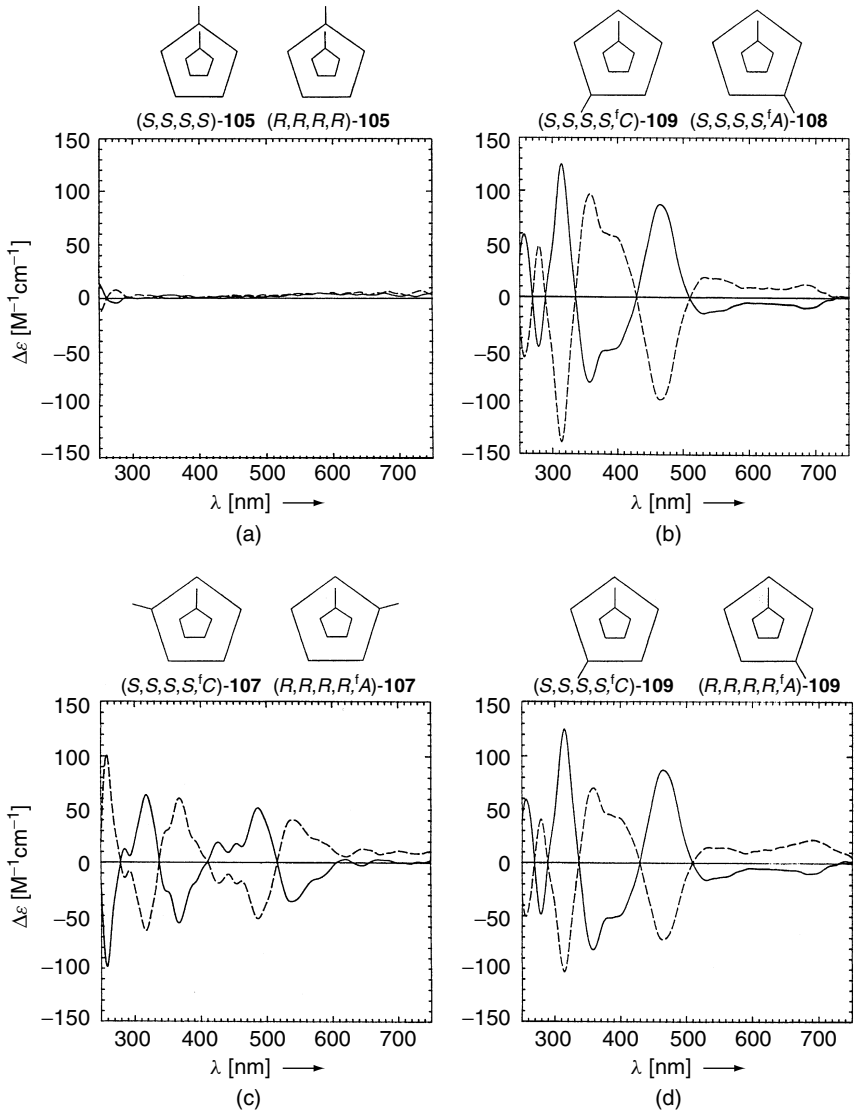

Figure 1.27. CD spectra of (*a*) the pair (*S*,*S*,*S*,*S*)-**105**/(*R*,*R*,*R*,*R*)-**105** (cf. Figure 1.26) with chiral side chains but an achiral addition pattern; (*b*) the pair (*S*,*S*,*S*,*S*,^{f}*A*)-**108**/(*S*,*S*,*S*,*S*,^{f}*C*)-**109** of diastereoisomers with enantiomeric, inherently chiral addition patterns; (*c*) and (*d*) the pairs (*S*,*S*,*S*,*S*,^{f}*C*)-**107**/(*R*,*R*,*R*,*R*,^{f}*A*)-**107**, and (*S*,*S*,*S*,*S*,^{f}*C*)-**109**/(*R*,*R*,*R*,*R*,^{f}*A*)-**109**, of enantiomers with oppositely configured addition patterns and side chains.

addends (Figure 1.27*a*; cf. also Section IV.C).[22,23,35,54,210,237–252] Furthermore, and similar to the ^{13}C NMR and UV/Vis spectra, matching core functionalization patterns lead to (nearly) identical CD curves, irrespective of the side chain configuration, a fact that is well illustrated in Figure 1.27 by selected representatives of the series (±)-**105**–(±)-**109**.[35,54] Calculation of the CD spectrum of the dimethyl ester corresponding to (*S*,*S*,*S*,*S*,^{f}*C*)-**107** (Figure 1.26) by the π-electron SCF-CI-DV MO method[99,100,128] and comparison with the experimental data allowed an assignment of the absolute configurations as [CD(−)317]-(*S*,*S*,*S*,*S*,^{f}*A*)-**106** and [CD(+)318]-(*S*,*S*,*S*,*S*,^{f}*C*)-**107** (Figures 1.26 and 1.27). Due to the negligible contribution of the stereogenic centers of the side chains to the Cotton effects (cf. Figure 1.27), [CD(−)318]-(*R*,*R*,*R*,*R*,^{f}*A*)-**107** and [CD(+)319]-(*R*,*R*,*R*,*R*,^{f}*C*)-**106** could be assigned as well. On the basis of the close analogy of both positions and signs of the CD bands over the measured λ range (Figure 1.27), we also confidently assigned the following absolute configurations (Figure 1.26): [CD(−)314]-(*S*,*S*,*S*,*S*,^{f}*A*)-**108**, [CD(+)314]-(*S*,*S*,*S*,*S*,^{f}*C*)-**109**, [CD(−)314]-(*R*,*R*,*R*,*R*,^{f}*A*)-**109**, and [CD(+)314]-(*R*,*R*,*R*,*R*,^{f}*C*)-**108**.[54]

Further cyclopropanation of bis-adducts was undertaken in order to explore the regiochemistry in the formation of higher adducts as well as the relation between the chiroptical contributions of chirally functionalized fullerene chromophores and the degree of addition. Whereas the addition of diethyl 2-bromomalonate to C_{2v}-symmetric **102** (Figure 1.26) afforded a C_{2v}-symmetric tetrakis-adduct (1,2:31,32:41,58:65,66-adduct; for the numbering, cf. Figure 1.6), a C_2-symmetric tetrakis-adduct was obtained from C_2-symmetric bis-adduct (±)-**103** (Figure 1.26),[54] and a high degree of regioselectivity was observed in tetrakis-adduct formation.[35,54] The inherently chiral addition pattern of the latter tetrakis-adduct corresponds to that of the four stereoisomeric tetrakis-adducts (*S*,*S*,*S*,*S*,^{f}*A*)-**110**, (*R*,*R*,*R*,*R*,^{f}*C*)-**110**, (*S*,*S*,*S*,*S*,^{f}*C*)-**111**, and (*R*,*R*,*R*,*R*,^{f}*A*)-**111**, obtained in separate reactions from bis-adducts (*S*,*S*,*S*,*S*,^{f}*C*)-**107**, (*R*,*R*,*R*,*R*,^{f}*A*)-**107**, (*S*,*S*,*S*,*S*,^{f}*A*)-**106**, and (*R*,*R*,*R*,*R*,^{f}*C*)-**106**, respectively (Figure 1.28; note that in order to meet the requirement of lowest locants, the configurational descriptor formally changes on the transition from a bis- to the corresponding tetrakis-adduct).[54] The CD spectra of all four tetrakis-adducts are very similar in shape and show intensities comparable to those of the bis-adducts ($\Delta\varepsilon$ up to 85 $cm^2\,mmol^{-1}$). However, whereas the CD bands of bis- and emanating tetrakis-adducts are similar in shape and sign below around 400 nm, this agreement is less good in the longer wavelength region which may represent a more characteristic fingerprint of the particular π-chromophore involved.[54]

In the polar solvent Me_2SO, a higher reactivity was observed for the Bingel reaction, and hexakis- to octakis-adducts were obtained in the addition of diethyl 2-bromomalonate to **102** and (±)-**103** (Figure 1.26) via the selective

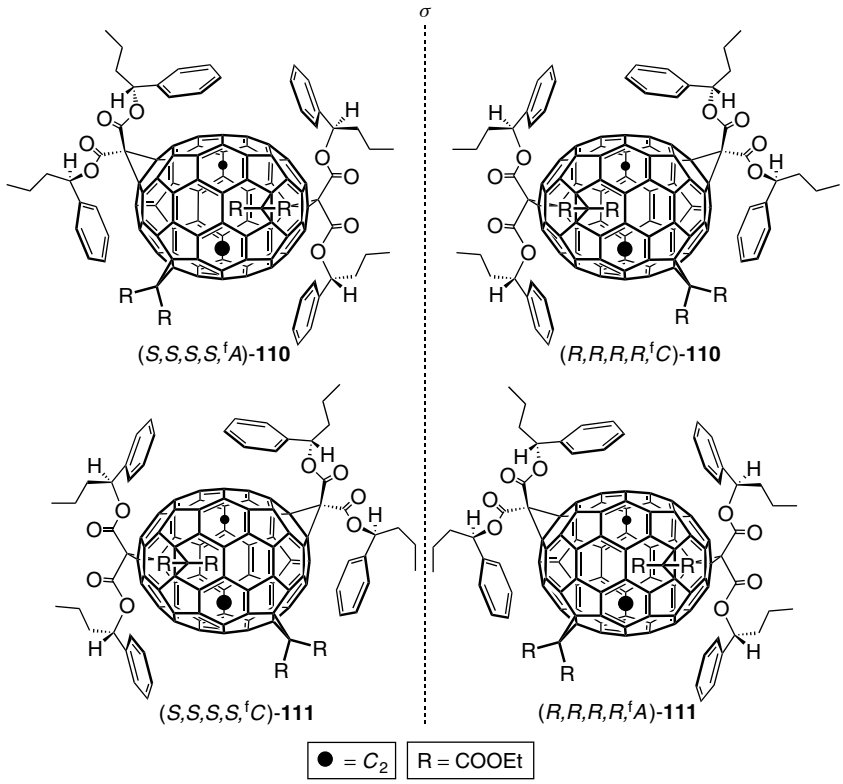

Figure 1.28. Stereoisomeric tetrakis-adducts of C_{70} prepared by diethyl 2-bromomalonate addition to stereoisomerically pure bis-adducts (*S*,*S*,*S*,*S*,^{f}*C*)-**107**, (*R*,*R*,*R*,*R*,^{f}*A*)-**107**, (*S*,*S*,*S*,*S*,^{f}*A*)-**106**, (*R*,*R*,*R*,*R*,^{f}*C*)-**106** (cf. Figure 1.26). The black dots mark intersections of the symmetry axis with the [70]fullerene spheroid.

intermediacy of the mentioned tetrakis-adduct regioisomers.[54] This regioselectivity was observed for the kinetically controlled reaction up to the stage of the hexakis-adducts, but it became strongly reduced at higher degrees of addition. Starting from bis-adduct (±)-**103** (Figure 1.26), the singular hexakis-adduct (±)-**112** (Figure 1.29) was isolated as a major product. By combining the analysis of the experimental ^{13}C-NMR data with steric considerations, with known reactivity patterns in C_{70},[17] as well as with theoretical predictions based on a correlation between the sites of preferred attack of nucleophiles and the coefficients of fullerene frontier orbitals (LUMO and LUMO+1)[109–111] obtained by ab initio calculations,[54] the structure of (±)-**112** (Figure 1.29) could be confidently elucidated. The unprecedented C_2-symmetrical hexakis-adduct contains four "6–6 closed" methanofullerene units in its polar regions in addition to two

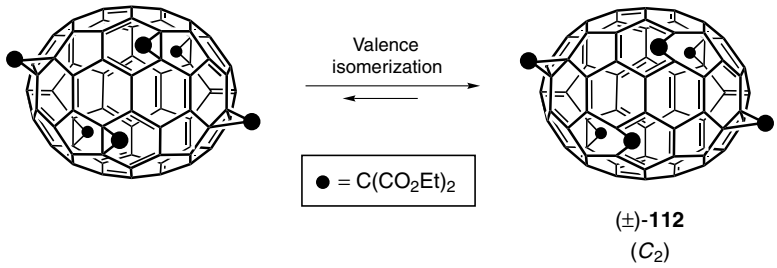

Figure 1.29. Valence isomerization of a primary C_2-symmetric Bingel type hexakis-adduct of C_{70} with two "6–5 closed" bonds (*left side*), initially formed in the cyclopropanation of bis-adduct (±)-**103** (Figure 1.26), to the more stable C_2-symmetric structure (±)-**112**, containing two "6–5 open" bonds. The molecules are viewed along the C_2-axis.

"6–5 open" homofullerene substructures.[54] The "6–5 open" substructures are formed by malonate additions to near-equatorial "6–5" bonds with enhanced LUMO coefficients,[253] followed by valence isomerization, a reactivity pattern unknown in the chemistry of C_{60}.

f. Addition of Alkynes. Zhang and Foote reported thermal [2 + 2] cycloaddition of electron-rich bis(diethylamino)ethyne and of 1-alkylthio-2-(diethylamino)ethynes to C_{60} and C_{70}.[254] Twofold addition of the diamine to C_{70} yielded two isomeric products, tentatively assigned as (±)-**113** and (±)-**114** (Figure 1.30). The inherently chiral addition patterns of these C_2-symmetric structures are typical for many bis-adducts of C_{70}.[17] The regioselectivity observed in their formation is even more pronounced than that of the double Bingel reaction,[35,54,107] and the C_{2v}-symmetric bis-adduct corresponding to **102**[35] (Figure 1.26) was not observed.[254] Self-sensitized photooxygenation of the mixture of (±)-**113** and (±)-**114**, both including a photosensitizer moiety (dihydrofullerene)[255] and an easily photooxydizable group (enamine), yielded the tetrakis(carboxamide) (±)-**115**.

g. Transition-Metal Complexes. Transition-metal complexes with fullerenes[256] are often characterized by reversible, thermodynamically controlled association. A high selectivity for η^2-complexation by Ir and Pt at the most curved polar 6–6 bonds is found in mono-[257,258] and multi-adducts of C_{70}.[259–261] In accordance with this preference, C_2-symmetric C(1)–C(2):C(56)–C(57) adduct (±)-**116** (Figure 1.30) was obtained as crystalline bis-adduct from the reaction of C_{70} with $[Ir(CO)Cl(PPhMe_2)_2]$.[259]

$[Ru_3(CO)_9]$ units are known for the hexahapto complexation of arenes and they also bind to C_{60}[262] and C_{70}[261] in this mode. Among the three types of hexagons in [70]fullerene, trinuclear ruthenium moieties add preferentially

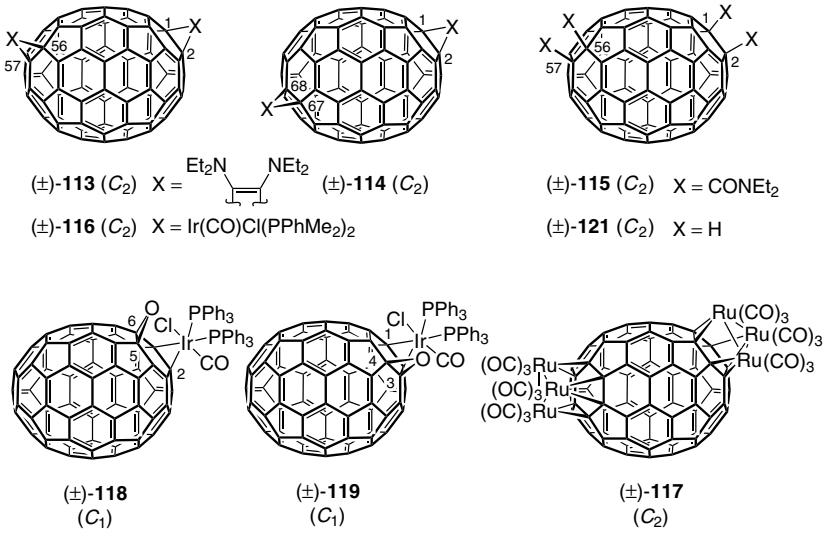

Figure 1.30. C_{70} derivatives with various chiral addition patterns.

to the near-polar one which displays the most marked bond alternation. Given their high degree of pyramidalization, the corresponding C-atoms require little further deformation to coordinate favorably to the Ru_3-triangle.[261] Addition of two $[Ru_3(CO)_9]$ units at opposite poles led to a singular chiral bis-adduct $[\{Ru_3(CO)_9\}_2(\mu_3\text{-}\eta^2 : \eta^2\text{-}C_{70})]$ for which three constitutional isomers (one of C_{2v}-symmetry and two of C_2-symmetry) are possible in analogy to the addition of achiral divalent addends to C(1)–C(2) type bonds (cf. Section IV.A.2.e).[35,54,107] Of the three formed isomers, the major one yielded crystals suitable for X-ray analysis and was found to correspond to structure (±)-**117** (Figure 1.30).[261]

Different types of chiral functionalization patterns occur in the iridium complexes[263] co-crystallized from a solution containing the two known $C_{70}O$ isomers (C(1)–C(2)- and C(5)–C(6)-adduct; cf. Figure 1.6).[264] In (±)-**118** as well as in (±)-**119** (Figure 1.30), the transition metal and the epoxy bridge are located within the same six-membered ring adjacent to the polar pentagon, a relative arrangement corresponding to the *cis*-1 addition pattern found in iridium complexes of $C_{60}O$ (cf. Section IV.B.1.c).[265,266] In both isomers of $[(\eta^2\text{-}C_{70}O)Ir(CO)Cl(PPh_3)_2]$, iridium is bound to positions C(1) and C(2) of C_{70}; this leads to an inherently chiral functionalization pattern in (±)-**118** with the epoxy function bridging positions C(5) and C(6) of the fullerene, and to a noninherently chiral functionalization pattern in (±)-**119** where the oxygen atom has added to the C(3)–C(4) bond (Figure 1.30).[263]

h. Hydro[70]fullerenes. Whereas 1,2- and 5,6-dihydro[70]fullerene, obtained by different reduction methods,[267–269] are achiral, several chiral representatives were identified among the $C_{70}H_4$ isomers.

If abstraction is made of identities/nonidentities among addends, the addition patterns of the two constitutional tetrahydro[70]fullerene isomers obtained in the reduction of C_{70} with diimide[268] correspond to those of $[(\eta^2\text{-}C_{70}O)Ir(CO)Cl(PPh_3)_2]$ isomers (±)-**118** and (±)-**119**[263] (Figure 1.30). However, the actual equality of the hydrogen addends causes the 1,2,3,4-tetrahydro[70]fullerene adduct (cf. Figure 1.6) to be achiral (C_s-symmetric), whereas it does not affect the inherent chirality of the addition pattern of C_1-symmetric (±)-1,2,5,6-tetrahydro[70]fullerene ((±)-**120**; Figure 1.31).[268]

The reduction of C_{70} by Zn(Cu) in the presence of a proton source gives completely different results: Among the formed products, a major and a minor $C_{70}H_4$ isomer were isolated and identified by ^{1}H-coupled ^{13}C NMR spectroscopy as 1,2,56,57-adduct ((±)-**121**, Figure 1.30) and 1,2,67,68-adduct ((±)-**122**, Figure 1.31), respectively.[269] Their inherently chiral addition patterns match the two C_2-symmetric ones generated by twofold Bingel addition to C_{70} and realized, for example, in (±)-**103** and (±)-**104** (Figure 1.26).[35,54,107] The difference in the product composition as compared to the diimide reduction was explained by the preferred charge distribution in the intermediate fulleride ions which are protonated irreversibly under kinetic control.[269] This reaction course should also be responsible for the isomeric product distribution observed in the corresponding reduction of C_{60} (cf. Section IV.A.1.f).[171,172]

For completeness it should be added that Spielmann, Meier, and coworkers have also isolated and characterized an achiral, C_s-symmetric isomer of $C_{70}H_8$,[269] whose addition pattern is not related to those of the above-mentioned di- and tetrahydro[70]fullerenes but corresponds to that of $C_{70}Ph_8$ (cf. Section IV.B.2.c).[270] Different structures have finally been proposed for $C_{70}H_{36}$,[179,183,271] another hydrogenated C_{70} derivative of major interest,[272] but no conclusive assignment was possible so far.

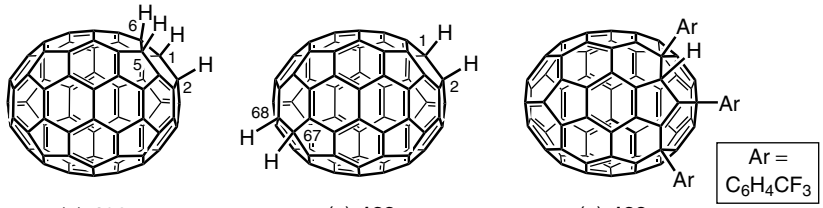

Figure 1.31. Two $C_{70}H_4$ regioisomers and a triarylhydro[70]fullerene with inherently chiral addition patterns.

i. Arylcuprate Adduct. Five aryl groups from organocopper reagents add in a 1,4-addition mode to the outer hexagon-hexagon fusion sites of a corannulene substructure in C_{60}, and protonation of the resulting anion leads to a compound[273,274] having the C_s-symmetric addition pattern of $C_{60}Ph_5H$ (**77**, Figure 1.20).[199] It can be used as a precursor to pentahapto metal complexes of the type $[M(\eta^5\text{-}C_{60}Ph_5)]$ (M = Li, K, Tl, Cu·PEt_3) with the metal bound to a cyclopentadienide substructure that is surrounded by the aryl addends and conjugatively decoupled from the remaining fullerene chromophore.[273] In C_{70}, arylcuprate addition took a slightly different course: Only three groups added in a 1,4-fashion across hexagons surrounding an equator-near pentagon. Protonation during the workup afforded C_1-symmetric adduct $C_{70}[4\text{-}(CF_3)C_6H_4]_3H$ ((±)-**123**, Figure 1.31) displaying an inherently chiral addition pattern. The corresponding C_s-symmetric anion has been shown by ab initio MO calculations and by X-ray crystal structure analysis to act as a π-indenyl type ligand in pentahapto metal complexes with K and Tl.[275]

3. Derivatives of the Higher Fullerenes beyond C_{70}

Although the first sample of pure D_2-C_{76}[2] was isolated almost a decade ago, a relatively small number of well-characterized derivatives of the fullerenes beyond C_{70} is known.[17] This is mainly due to the low abundance of these carbon cages in fullerene soot as well as to the tediousness of their isolation by HPLC. On the other hand, the lower symmetry of most of the higher homologues of C_{60} and C_{70}, and in particular the inherent chirality of a number of them is at the origin of a large fraction of chiral compounds among their derivatives.[17,22]

D_2-C_{76}, D_3-C_{78}, and D_2-C_{84} are the inherently chiral higher fullerenes of which defined derivatives have been isolated and in part structurally characterized.[17,60] As a consequence of their inherent chirality, all derivatives of these fullerenes are chiral, except for as yet unknown *meso* type combinations of both optical antipodes of a given constitution.

a. Diels-Alder Adducts of C_{76}. In the addition of 3,4-dimethoxy-*o*-quinodimethane to racemic D_2-C_{76}, at least 6 out of the 15 possible, constitutionally isomeric 6–6 adducts were formed.[50] ^{1}H NMR spectroscopy, together with the assumption of a high bond reactivity in regions of strong local curvature,[50] led to the proposition of the C_1-symmetric C(2)–C(3) adduct structure (±)-**124** (Figure 1.32; for the numbering of C_{76}, cf. Figure 1.3) for the major product, which was isolated in pure form. A C_2-symmetric mono-adduct, which was isolated as a mixture with two C_1-symmetric isomers, was assigned the structure of the apical C(1)–C(6)-adduct (±)-**125** (Figure 1.32).[50] The C(2)–C(3) and C(1)–C(6) addition patterns of (±)-**124** and (±)-**125** involve the most

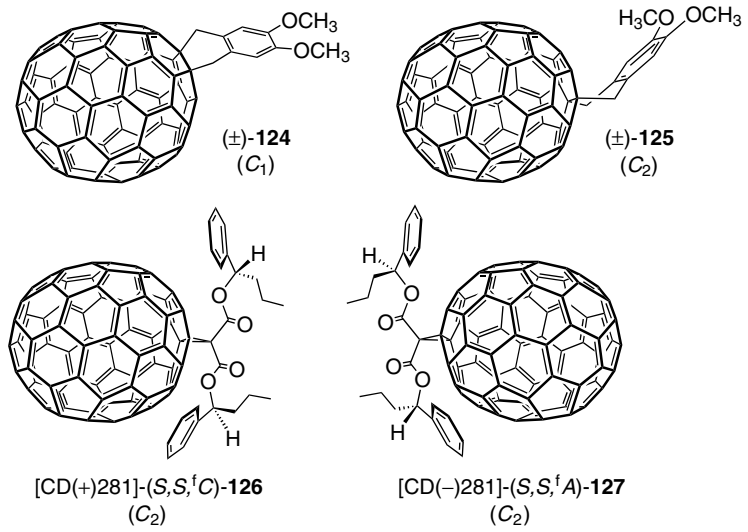

Figure 1.32. Confidently assigned C_{76} adduct structures: Two constitutional isomers of Diels-Alder adducts (*top*) and a diastereoisomeric pair of Bingel adducts (*bottom*). The latter have enantiomeric C_{76} cores and could be configurationally assigned by comparison of their CD spectra to those of the optical antipodes of the parent fullerene.

pyramidalized C-atoms of C_{76} and correspond to those proposed by Hawkins and co-workers for the main products of the osmylation.[4]

b. Bingel Type Adducts of C_{76}, C_{78}, and C_{84}. Similarly to the cases of C_{60} and C_{70} (cf. Sections IV.A.1.b and IV.A.2.e), the relatively selective, kinetically controlled Bingel reaction was used to investigate the regiochemistry of the larger spheroids.

In a nucleophilic cyclopropanation of racemic D_2-C_{76} with bis[(*S*)-1-phenylbutyl] 2-bromomalonate, superposition of the chirality of the addend and that of the inherently chiral fullerene yielded mainly three constitutionally isomeric pairs of diastereoisomeric mono-adducts, two of C_1-, and one (**126/127**, Figure 1.32) of C_2-symmetry.[93] All six compounds, not including any pair of enantiomers, were isolated by HPLC to afford the first optically pure adducts of an inherently chiral fullerene. UV/Vis, CD, and ^{13}C NMR spectroscopy showed distinct similarities for isoconstitutional stereoisomers, thus allowing facile identification of the three pairs of diastereoisomers. Their CD spectra display very pronounced Cotton effects with maximum $\Delta\varepsilon$ values ($\approx$250 $M^{-1}\,cm^{-1}$)[93] that are comparable in intensity to those of the optically pure, parent D_2-C_{76}[6] (Figure 1.10) and twice as large as those of C_{70} derivatives with an inherently chiral addition pattern (Figure 1.27).[35,54] Retro-Bingel

reaction starting from stereoisomerically pure malonate adducts of the above type with enantiomeric fullerene cores afforded the pure optical antipodes of D_2-C_{76} (cf. Section III.C).[6] Comparison between experimental (Figure 1.10)[4,6] and calculated[7,98] CD spectra allowed the assignment of their absolute configurations (cf. Section III.C).[7] Furthermore the similarity in shape and band positions between the CD spectra of diastereoisomers **126** and **127**, on one hand,[93] and those of the pure enantiomers of D_2-C_{76}, on the other, allows a configurational assignment of the former as [CD(+)-281]-(S,S,^{f}C)-**126** and [CD(−)-281]-(S,S,^{f}A)-**127** (Figure 1.32).

Nucleophilic cyclopropanation of a 3 : 1 isomeric mixture of C_{2v}- and D_3-C_{78} with nearly two equivalents of diethyl 2-bromomalonate yielded at least eight tris-adducts as main products besides two C_1-symmetric bis-adducts.[62] Of the tris-adducts, three isomers displayed a higher symmetry than C_1 and could therefore unambiguously be assigned to the respective parent C_{78} isomers. Based on a comparison of the UV and ^{13}C NMR spectra obtained for a C_2-symmetrical tris-adduct of C_{2v}-C_{78} and those of the bis-adducts, three possible structures ((±)-**128**) were proposed for one of the C_1-symmetric bis-adducts, identified as direct precursor to the corresponding tris-adduct (±)-**129** (3 possible structures, Figure 1.33). Both (±)-**128** and (±)-**129** are derived from achiral C_{2v}-C_{78} and have an inherently chiral functionalization pattern. For reason of symmetry, a common addend position in the two adducts has to be the bond C(39)–C(40) located at the intersection of the two mirror planes of the parent fullerene (Figure 1.33). For the second addend, one out of three positions within a six-membered ring containing the formal double bonds C(1)–C(2), C(9)–C(10), and C(11)–C(12) is most likely.[62] π-Bond order considerations,[276] taking into account steric effects, favor the bonds C(9)–C(10) and C(69)–C(70) as most likely positions for the homotopic second and third addends in (±)-**129**.

Two constitutionally isomeric structures, (±)-**130** or (±)-**131**, were proposed for a C_3-symmetrical pure tris-adduct of D_3-C_{78} (Figure 1.33); each structure includes three homotopic addends showing the same relative, pairwise arrangement as it is observed within a hemisphere of tetrakis-adducts of C_{70} (cf. Section IV.A.2.e).[62] According to π-bond order considerations,[276] (±)-**131** should be formed preferentially.

Following our protocol to separate fullerene isomers by the intermediacy of defined covalent adducts, the C_{84} fraction of fullerene soot was subjected to Bingel cyclopropanation with bis[(*S*)-1-phenylbutyl]malonate (cf. Section III.C).[60] Among the products two chiral mono-adducts and four chiral bis-adducts were isolated in pure state and characterized. An analysis taking into consideration the symmetries of the compounds as deduced from ^{1}H- or ^{13}C NMR spectroscopy, the magnitudes of their Cotton effects (these are relatively large, between ca. 10 and 200 $M^{-1}\,cm^{-1}$ in the case of chiral fullerene

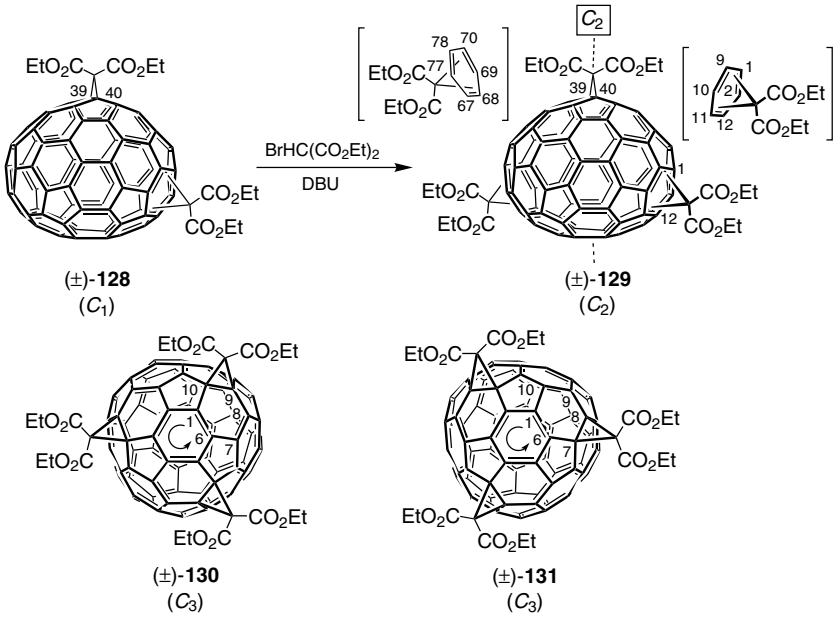

Figure 1.33. Structures proposed for a tris-adduct of C_{2v}-C_{78} and its bis-adduct precursor (*top*, 3 possible constitutional isomers, insert shows the locants of the homotopically functionalized six-membered rings), and for a tris-adduct of D_3-C_{78} (*bottom*, two possible constitutional isomers).

chromophores; cf. Sections IV.A.1.b and IV.A.2.e), and a comparison among their CD spectra (detection of mirror-image relationships) as well as their UV/Vis spectra (these are similar if the fullerene chromophores are comparable), allowed the structural assignment of a C_2-symmetric mono- (**132**) and a D_2-symmetric bis-adduct (**133**, Scheme 1.26) of D_{2d}-C_{84}. The chirality of both derivatives originates exclusively from the stereogenic centers in the ester groups (Section IV.C.3.b). Similarly, the structures of two C_2-symmetric bis-adducts were recognized as a diastereoisomeric pair (six possible constitutions) of D_2-C_{84} derivatives with enantiomeric fullerene cores (**3** and **4**; Figure 1.11). Each of the two diastereoisomers was subjected to the electrochemical retro-Bingel reaction[6] to afford optically pure enantiomers of D_2-C_{84} (cf. Section III.C).[60] The retro-Bingel reaction of the last two isolated products, a C_1-symmetric mono-adduct and a C_1-symmetric bis-adduct, yielded a novel, CD-inactive C_{84} isomer whose UV/Vis spectra differ from those of the D_2- and D_{2d}-C_{84} isomers.

c. Fluorination and Hydrogenation of Higher Fullerenes. Following earlier mass spectrometric observations of different fluorinated higher

fullerenes,[193,277–280] the formation of these derivatives was recently reinvestigated by reaction of either pure C_{76} and C_{84}, or a mixture of higher fullerenes, with different fluorinating agents, such as K_2PtF_6, MnF_3 or CeF_4.[281,282] HPLC purification of the crude materials allowed the isolation and a partial characterization of a number of compounds. Among the isolated carbon fluorides were $C_{76}F_{36}$, $C_{76}F_{38}$ (main component, C_1-symmetric), $C_{76}F_{40}$ (five isomers, one of them C_2-symmetric), $C_{76}F_{42}$, $C_{76}F_{44}$, $C_{78}F_{42}$,[282] $C_{84}F_{40}$ (a favored level of fluorination, 2 isomers), and $C_{84}F_{44}$.[281] Besides, unresolved mixtures were shown to contain $C_{76}F_{32}$, $C_{76}F_{36}$, $C_{76}F_{38}$, $C_{76}F_{40}$, $C_{76}F_{42}$, $C_{78}F_{38}$, and $C_{82}F_{44}$. Assignment of specific structures was not possible with the small amounts of material available, but in two cases, the symmetry was determined by ^{19}F NMR spectroscopy (*vide supra*).[282]

Hydrogenation of a mixture of higher fullerenes in toluene solution with Zn/conc. HCl — conditions that give $C_{60}H_{36}$ from [60]fullerene and $C_{70}H_{2x}$ ($x = 18–20$) from [70]fullerene — yielded as most abundant species $C_{76}H_{2x}$ ($x = 23–25$), $C_{78}H_{2x}$ ($x = 18–24$), and $C_{84}H_{2x}$ ($x = 24–26$).[283] A notable feature of this reduction is a substantial cage breakdown of the higher fullerenes to $C_{60}H_{36}$ and $C_{70}H_{2x}$ ($x = 18–20$) as most prominent species. At high mass spectrometer probe temperatures, the main hydro[84]fullerene species detected was $C_{84}H_{40}$, which parallels the preferred addition degree in the fluorination reaction.[284]

As to the chirality of the observed fluoro- and hydrofullerenes, it is evident that those derived from chiral parent fullerenes, such as C_{76}, have an inherently chiral functionalization pattern. In the other cases no further information is currently available.

d. Further Adducts of Higher Fullerenes and Metal Incarceranes Thereof. The addition of photochemically generated $(i\text{-PrO})_2OP$ radicals generated seven out of the 19 possible chiral $(i\text{-PrO})_2OP(C_{76})\bullet$ regioisomers. On removing the irradiation source, one of them dimerized, whereas six radicals persisted in solution.[285]

Osmates with an inherently chiral functionalization pattern have been synthesized by Hawkins and co-workers as intermediates in the kinetic resolution of D_2-C_{76},[4,5] D_3-C_{78}, and D_2-C_{84} (cf. Section III.C).[5]

Because of the rareness of pure endohedral metallofullerenes which are partly sensitive to air and even more difficult to isolate than higher fullerenes, the chemistry of these species is barely explored.[76,286] Photo-induced addition of 1,1,2,2-tetramesityl-1,2-disilirane to endohedral metallofullerenes such as iLaC$_{82}$ (also functionalized with 1,1,2,2-tetrakis(2,6-diethylphenyl)-1,2-digermirane[287]), iGdC$_{82}$, iLa$_2$C$_{80}$, and iSc$_2$C$_{84}$ yielded isomeric mixtures of mono-adducts.[288] In contrast to the empty cages, most of the endohedral metallofullerenes also react thermally with the disilirane reagent. This reactivity

seems to be related to the stronger electron acceptor as well as the stronger electron donor properties of the metal incarceranes.[76] Further derivatizations[289] include the reaction of iLaC$_{82}$ with diphenyldiazomethane[290] and the transformation of iPrC$_{82}$ (Pr@C$_{82}$) into a water-soluble derivative by treatment with nitric acid followed by hydrolysis.[291]

Finally, it may be mentioned that product mixtures from ozonation,[292] hydrogenation,[283] and methylenation[293] of higher fullerenes have been reported.

B. Fullerene Derivatives with a Noninherently Chiral Addition Pattern

1. Derivatives of C_{60}

a. "Monomeric" 1,4-Adducts of C_{60}. The introduction of bulky groups into C_{60} often occurs as intrahexagonal 1,4-addition with functionalization of positions C(1) and C(4) (cf. Figure 1.12*a*).[14–16] In case the introduced groups are homomorphic and achiral, a 1,4-adduct of C_{60} is C_s-symmetric. If, however, both groups differ in constitution, there is no mirror plane reflecting the addends into each other and the symmetry is reduced to C_1 (cf. Figure 1.12*a*). As the chirality of the resulting functionalization pattern is due uniquely to the nonidentity of the addends, it is termed noninherently chiral. Although many other noninherently chiral functionalization patterns are theoretically conceivable for mono-adducts of C_{60}, the only one encountered so far corresponds to the 1,4-adduct.

Similarly to other molecules with isoconstitutional chiral substructures, the combination of distinct fullerene addition patterns with enantiomorphic or homomorphic chiral addends can lead to steric arrangements with a certain complexity. However, these can be easily analyzed with the substitution test delineated in Figure 1.1. In the case of the 1,4-addition pattern of C_{60}, we may consider the following cases (Figure 1.34): If both chiral addend moieties are homomorphic (structure A), the resulting addition pattern is achiral

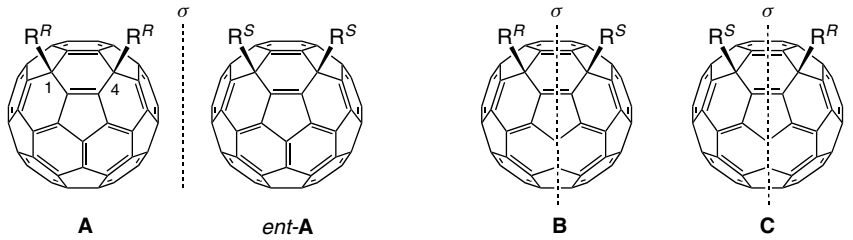

Figure 1.34. Different combinations of the 1,4-addition pattern of C_{60} and enantiomorphic addends R^R and R^S, resulting in a *d*, *l* pair (**A** and *ent*-**A**) and two *meso* forms (**B** and **C**).

and the chirality of the adduct resides in the chiral elements of the addends only; changing the configuration of both residues leads to the enantiomeric C_{60} derivative (*ent*-A). If the addend moieties are enantiomorphic, a *meso* structure results and the functionalization pattern can be called *pseudoasymmetric* (structure B). Inverting the configuration of each residue, in this case, leads to a diastereoisomeric molecule combining the same types of chiral units as its predecessor (structure C). Obviously B and C are also diastereoisomers of A and *ent*-A (Figure 1.34).

By addition of organolithium or Grignard reagents to C_{60} and subsequent in situ protonation, Hirsch and co-workers isolated isomerically pure 1,2-adducts of the type $C_{60}RH$.[294,295] The addition pattern was corroborated by electron density calculations for intermediate RC_{60}^- anions showing the highest negative Mulliken charges to be localized at C(2)(−0.29) with a significantly lower, yet enhanced charge at C(4)(−0.14) (cf. Figures 1.2 and 1.12*a*).[294] On the other hand, Fagan and co-workers, upon protonation of the isolated salt $Li[(t\text{-Bu})C_{60}] \cdot 4\ CH_3CN$, obtained the C_s-symmetric 1,2- as well as the C_1-symmetric 1,4-isomer,[296] with the latter slowly rearranging to the thermodynamically more stable 1,2-adduct.[53,296,297] 1-*tert*-Butyl-4-hydro[60]fullerene ((±)-**134**, Figure 1.35) was, to our knowledge, the first fullerene derivative with a noninherently chiral addition pattern reported in literature. As mentioned in Section IV.A.1.h, the 1,4-addition pattern was also proposed for some of the products isolated after addition of silyllithium reagents, such as $(t\text{-Bu})_2(4\text{-MeC}_6H_4)SiLi$ or $(t\text{-Bu})(4\text{-MeC}_6H_4)_2SiLi$, to C_{60} and subsequent quenching with ethanol.[195] A notable feature of 1,4-adducts is a UV/Vis band

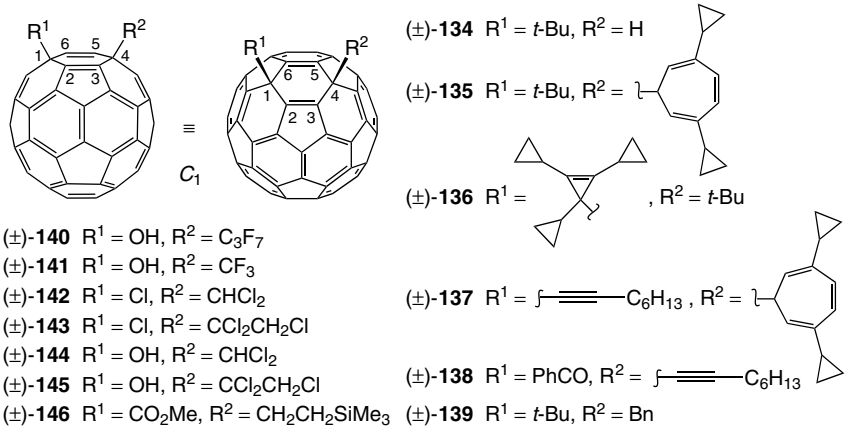

Figure 1.35. C_1-symmetric 1,4-adducts of C_{60} with a noninherently chiral functionalization pattern. The general structural formula is depicted in two different views of which the right one illustrates well that there is no mirror plane including the two added residues.

around 445 nm[53,298–300] contrasting with the nearly 430 nm absorption of 1,2-adducts.[15,301]

Whereas 1,2-addition preserves the favorable π-electron system of C_{60} to a large extent, the generally lower thermodynamic stability of the 1,4-adduct can be associated with the necessary introduction of an intrapentagonal double bond which costs ca. 8.5 kcal mol^{-1}.[167,302] However, this unfavorable electronic effect can be compensated by unfavorable steric (eclipsing) interactions that exist between bulky addends in 1,2-position.

Such a situation is encountered in the ionically dissociative hydrocarbon (±)-**135** (Figure 1.35) obtained by Kitagawa, Takeuchi, and co-workers as a single constitutional isomer.[303] In contrast to the rapid isomerization of 1-*tert*-butyl-4-hydro[60]fullerene ((±)-**134**), it does not rearrange, even at 75°C in $CDCl_3$, to the 1,2-adduct which PM3 calculations predict to be 18 kcal mol^{-1} less stable than the 1,4-adduct. A notable feature of (±)-**135** is its partial heterolytic dissociation in a polar solvent like DMSO, giving a greenish-yellow solution of two stabilized species, the *tert*-butyl[60]fullerenide and the dicyclopropylcycloheptatrienyl ions.[303] Besides the charge stabilization in each of the ions, the steric repulsion between the bulky groups on the fullerene surface seems to favor the unusual heterolytic C–C bond dissociation. Similar reversibly dissociative systems were obtained by varying the substituents on the cycloheptatriene ring,[300] or by replacing the whole residue by a 1,2,3-tricyclopropylcycloprop-2-enyl moiety ((±)-**136**, Figure 1.35).[304] If the cyclopropyl rings of the latter are substituted by 5-isopropyl-3,8-dimethylazulenyl units, the resulting C_{60}-derived hydrocarbon can be isolated as an ionic solid.[305]

The importance of the bulkiness of the two addend moieties in the preferred formation of either the 1,2- or the 1,4-adduct (cf. Figure 1.12*a*) was nicely evidenced by work of Komatsu and co-workers who reacted the oct-1-ynyl[60]fullerenide ion with different electrophiles.[306] Whereas treatment with methyl iodide afforded only the 1,2-adduct, the addition of tropylium tetrafluoroborate gave a 55 : 45 mixture of 1,2- and 1,4-adduct ((±)-**137**, Figure 1.35), and the 1,4-addition only (product (±)-**138**) was observed in the reaction with benzoyl chloride.

Kinetic studies by Fukuzumi, Kadish, and co-workers suggest that the formation of organofullerenes of the type R_2C_{60} or $RR'C_{60}$, such as (±)-**139**, by reaction of C_{60}^{2-} with alkyl halides in acetonitrile occurs in two steps, of which the first one involves an electron transfer mechanism leading to the organofullerenide ion RC_{60}^{-}, followed by a nucleophilic substitution (S_N2) of the second halide molecule by RC_{60}^{-}.[53]

Another major group of 1,4-adducts of C_{60} includes polyhaloalkyl side chains as one of the added residues. Treatment of C_{60} with bis(heptafluorobutanoyl)peroxide or bis(trifluoroacetyl)peroxide in dichlorobenzene at 40°C under degassed conditions yielded the C_1-symmetrical (±)-**140** and (±)-**141**

as major and minor products, respectively (Figure 1.35).[298] A second study involved the first addition to C_{60} of a carbon electrophile by treatment of the fullerene with $AlCl_3$ in $CHCl_3$ or $Cl_2HCCHCl_2$.[307] In both cases single, C_1-symmetric products resulted which were identified as 1,4-adducts (±)-**142** and (±)-**143**. The latter structure indicates that the cation initially formed from $Cl_2HCCHCl_2$ with $AlCl_3$ underwent a rapid hydride shift. The (±)-**142** and (±)-**143** adducts are readily hydrolyzed to the fullerenols (±)-**144** and (±)-**145**, suggesting a relatively high stability of the intermediate [60]fullerenylium ion. This was substantiated by the dissolution of the fullerenols in F_3CSO_3H, resulting in reddish-purple solutions of the cations which were stable over several weeks. ^{13}C NMR spectroscopy nicely demonstrated that the generation of the fullerenylium ion from (±)-**144** was accompanied by an increase in symmetry from C_1 to C_s.[307] The preparation of compounds (±)-**142** to (±)-**145** points out the potential utility of electrophilic addition reactions as a means of C–C bond formation in the derivatization of fullerenes.

In the context of a completely different type of chemistry, an unexpected rearrangement occurred upon reaction of C_{60} with 1-methoxy-1-[2-(trimethylsilyl)ethoxy]carbene and afforded a mixture of 1,4-adduct (±)-**146** (Figure 1.35) and the corresponding 1,2-adduct instead of the anticipated methanofullerene.[299] A crucial role in this reaction course was ascribed by Wudl, Warkentin, and co-workers to the nucleophilicity of the dialkoxycarbene, the electrophilicity of the fullerene and the β-stabilization of a positive charge by the trimethylsilyl group.

b. "Dimeric" 1,4-Adducts of C_{60}. As early as 1991 it was found that alkyl radicals add rapidly and multiply to C_{60} to give products R_nC_{60} which were investigated for odd n by ESR spectroscopy.[308] A remarkable feature of the ESR signals observed for RC_{60}• was a dramatic and reversible increase in intensity with rising temperature.[309,310] Such a behavior is in contrast to the Curie law, and it reflects an equilibrium between a radical and its dimer. A discernible correlation between the strength of the formed intercage bond, as reflected by the position of the RC_{60}• dimerization equilibrium, and the steric requirements of the added group R suggested that the fullerene-fullerene bond was formed at a position close to that bearing the residue R. Of the three positions C(2), C(4), and C(6) (cf. Figure 1.35) exhibiting the highest spin density,[311] C(4) is the only one allowing bonding to another fullerene moiety on steric grounds, and consequently structure **147** (Figure 1.36) was proposed for the dimer $(t\text{-}BuC_{60})_2$.[296,309] Based on data from dilution experiments, the interfullerene bond enthalpy in $(t\text{-}BuC_{60})_2$ was estimated to 22.1 kcal mol^{-1}.[309]

The "dimeric" 1,4-adducts of C_{60} are very interesting with respect to possible stereoisomerism: combining two isoconstitutional, directly linked

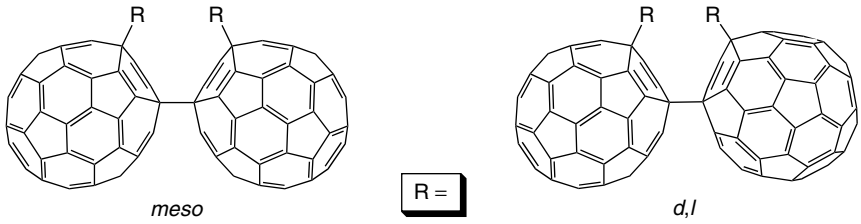

147	*t*-Bu	(±)-**148**
149	$\int$—≡—C_6H_{13}	(±)-**150**
151	C_3F_7	(±)-**152**
153	CF_3	(±)-**154**
155	C_2F_5	(±)-**156**
157	$\int$–N⟨O⟩	(±)-**158**

Figure 1.36. "Dimeric" 1,4-adducts of C_{60} with a noninherently chiral functionalization pattern in each spheroid. Whereas the combination of homochiral moieties leads to a *d*, *l* pair of enantiomers, that of heterochiral cages gives rise to a *meso* form.

[60]fullerene substructures with a noninherently chiral addition pattern, they can give rise to three stereoisomers (for a related case involving C_{70} derivatives with a noninherently chiral functionalization pattern, cf. Section IV.A.2.b): A *d*, *l*-pair of enantiomers (e.g., (±)-**148**) containing either two ^{f}A- or two ^{f}C-configured spheroids, as well as a *meso* form (**147**) combining an ^{f}A- and an ^{f}C-configured cage.[22] Although most reports on "dimeric" 1,4-adducts do not include any information on the obtained stereoisomer(s), both the *meso*- and the *d*, *l*-form are included in the following discussion as well as in Figure 1.36 to illustrate their possible formation. As to the preferred conformations resulting from rotation around the interfullerene bond, molecular mechanics calculations predict those with R groups close to each other (*syn*) to be more stable than those with the residues R at maximal distance (*anti*).[312]

"Dimeric" C_{60} derivatives[313] of this type are formed in many reactions involving radical intermediates which can be generated easily not only by addition of radicals to C_{60}, but also through oxidation of RC_{60}^- ions.[296] Thus, when the oct-1-ynyl[60]fullerenide ion ($(H_{13}C_6C{\equiv}C)C_{60}^-$) was oxidized with iodine in THF, an immediate color change from dark green to brown accompanied the formation of **149**/(±)-**150**.[306] As judged from the absence of ^{1}H NMR line broadening, no homolytic dissociation seemed to take place, and this contrasts the behavior of (t-BuC_{60})$_2$ (**147**/(±)-**148**)[309] with its bulkier side chains.

"Dimeric" 1,4-adducts of C_{60} with perfluoroalkyl side chains (**151**/(±)-**152**, **153**/(±)-**154**,[298,314] and **155**/(±)-**156**[310]) were obtained by reaction of C_{60} with

perfluoroalkanoyl peroxides, the former two as byproducts in the synthesis of the "monomeric" adducts (±)-**140** and (±)-**141** (Figure 1.35).[298,314] Such dimers with perfluoroalkyl side chains can also be synthesized by photoirradiation of a solution of C_{60} and a perfluoroalkyl iodide,[310] eventually in the presence of a hexaalkyldistannane.[315] Treatment of the dumbbells **151**/(±)-**152**[314] or **147**/(±)-**148**[296] with Bu_3SnH afforded the corresponding "monomeric" compounds $RC_{60}H$ by reduction of the RC_{60}• species present in the solution of the starting material. Yoshida and co-workers have also isolated mixed "dimeric" 1,4-adducts of C_{60} with different perfluoroalkyl side chains in the fullerene moieties.[315] Such compounds can, in principle, occur as two diastereoisomeric pairs of enantiomers which can be considered as an *erythro*- and a *threo*-form.

Reaction of an excess of morpholine with C_{60} in the presence of oxygen afforded the "dimeric" **157**/(±)-**158** as main product precipitating from the benzene solution.[316] "Dimeric" 1,4-adducts were finally observed besides the "monomeric" species among the products isolated after addition of certain silyllithium reagents to C_{60} and subsequent quenching with ethanol (cf. Section IV.A.1.h).[195]

c. Bis-adducts with *cis*-1, *cis*-2, *trans*-4, and *e* Addition Patterns. The addition patterns of *cis*-1, *cis*-2, *trans*-4, and *e* (cf. Figure 1.12*b*) adducts are either achiral or, if nonidentical residues are located at appropriate positions on the fullerene surface, noninherently chiral. Whereas noninherently chiral *cis*-2 and *trans*-4 addition patterns are hardly known (*vide infra*), this is not the case for the *cis*-1 addition pattern which represents one of the electronically preferred arrangements of nonbulky addends.[111] A particularity of the *cis*-1 addition pattern is the proximity of the four involved reaction sites C(1) to C(4) (cf. Figure 1.37) which allows the introduction of certain bridging addends that are incompatible with functionalization patterns having the addends further apart on the fullerene sphere. This also explains the greater structural diversity of chiral *cis*-1 bis-adducts as compared to their 1,4-mono-adduct counterparts (cf. Sections IV.B.1.a and IV.B.1.b). As to *e* bis-adducts, noninherently chiral addition patterns have been described in the context of templated macrocyclizations (cf. Section IV.A.1.c). In such cases, both addends or, as a minimum requirement, at least the e_{edge}[104] addend has to be no more than C_s-symmetric.[102] This leads to the absence of a mirror plane in the molecule and makes that particular *e* addition pattern noninherently chiral.

1,2,3,4-Adducts (*cis*-1 bis-adducts) of C_{60} are C_1-symmetric and have a noninherently chiral addition pattern under the condition that there is a difference between the residues attached to C(1) and C(4), or to C(2) and C(3) (Figure 1.37). This situation is realized in the [60]fullerene derivative (±)-**159** (Figure 1.37), which was obtained from ethyl azidoformate addition

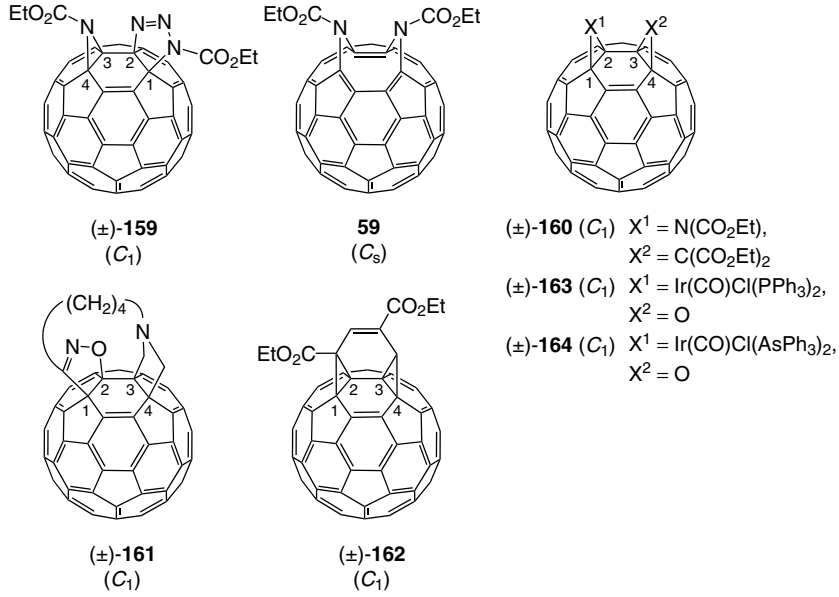

Figure 1.37. Noninherently chiral addition patterns in *cis*-1 type 1,2,3,4-bis-adducts of C_{60}.

to ethyl 1,2-epimino[60]fullerene-61-carboxylate and contains fullerene-fused aziridine and triazoline heterocycles.[160] Nitrogen extrusion from the triazoline ring of (±)-**159** and concomitant rearrangement afforded a 1,2:3,4-bis(epimino)[60]fullerene derivative and ultimately, after valence isomerization within the functionalized six-membered ring, the corresponding *cis*-1 bis-adduct **59** (Figure 1.37) with two "6–6 open bonds." It represents the first C_{60} derivative with this type of structurally modified carbon core that can be re-isomerized to the "6–6 closed" valence isomer by exchange of the CO_2R groups of the *tert*-butyl ester corresponding to **59** against hydrogen.[160] The related bis-adduct (±)-**160** bearing an epimino as well as a methano bridge, was found to occur only as the 6–6 closed valence isomer. Its *cis*-1 addition pattern was unambiguously proved by ^{13}C NMR spectroscopy using 100% ^{15}N-labeled material.[111] HPLC on the chiral Whelk-O1 phase allowed the separation of the enantiomers of (±)-**160** as well as of several methano[60]fullerene derivatives with an inherently chiral addition pattern such as the *e*,*e*,*e* tris-adduct (±)-**10** and the *trans*-3,*trans*-3,*trans*-3 adduct (±)-**11** (Figure 1.14).[115]

Structure (±)-**161** (Figure 1.37) was proposed for the adduct resulting from [3 + 2] cycloaddition an azomethine ylide tethered via a butane-1,4-diyl chain to a fullerene-fused isoxazoline anchor.[317] In a subsequent reaction with $Mo(CO)_6$, the latter could be removed from the fullerene cage, thus

demonstrating the use of isoxazolines as reversible protecting and directing groups in the regioselective functionalization of C_{60}. Also, a C_{60}-fused isoxazoline with a chiral side chain derived from enantiomerically pure D-glyceraldehyde was synthesized to illustrate the potential of a reversible introduction of a chiral auxiliary in the resolution of chiral fullerenes or fullerene derivatives via diastereoisomeric adducts.[317]

A C_1-symmetric *cis*-1 bis-adduct with an additional bridge between the addends was obtained in the reaction between two molecules of ethyl propiolate and C_{60} in the presence of triphenylphosphane.[318] Its structure ((±)-**162**, Figure 1.37) was established with the help of the HMBC- (heteronuclear multiple bond correlation) NMR technique and includes stereogenic centers in the addend moiety as well as a noninherently chiral addition pattern. The latter can be related to the head-to-tail connectivity of the two propiolate units.

Noninherently chiral *cis*-1 addition patterns were also found in two iridium complexes of $C_{60}O$.[265,266] Whereas some deoxygenation, presumably by PPh_3, appears to have occurred in $[(\eta^2\text{-}C_{60}O)Ir(CO)Cl(PPh_3)_2] \cdot 0.53\ CHCl_3 \cdot 4.47\ C_6H_6$ ((±)-**163**, Figure 1.37),[265] the X-ray crystal structure of $[(\eta^2\text{-}C_{60}O)Ir(CO)Cl(AsPh_3)_2] \cdot 0.18\ CHCl_3 \cdot 4.82\ C_6H_6$ ((±)-**164**), in which the phosphane ligand has been replaced by $AsPh_3$, shows a greater degree of disorder with respect to the position of the epoxide oxygen atom.[266] But even in the latter structure the major oxygen occupancies indicate bonding of both addends within the same hexagon.

$C_{120}O$[319] was prepared by Krätschmer and co-workers in a solid phase reaction between C_{60} and $C_{60}O$.[320] A by-product of this reaction is $C_{120}O_2$, of which the authors isolated two HPLC fractions. One of them consisted of two closely related C_1-symmetric isomers, and based on ^{13}C NMR and FT-Raman spectroscopy, calculation of heats of formation as well as of ^{13}C NMR chemical shifts, and a correlation between the latter and Mulliken atomic charges, the structure (±)-**165** (Figure 1.38) was proposed for the major component.[320] It can be considered as an epoxide derived from $C_{120}O$ in which two C_{60}

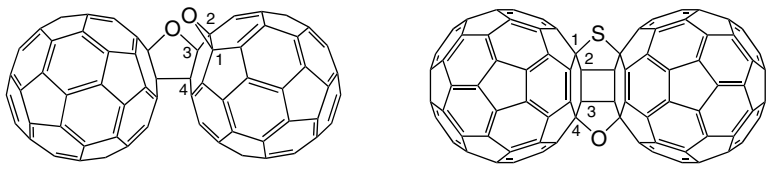

(±)-**165** (C_1) **166** (C_s)

Figure 1.38. Multiply bridged "dimeric" derivatives of C_{60} with noninherently chiral functionalization patterns in spheroids of the 1,2,3,4-adduct type.

cages are fused to an oxolane heterocycle.[319] The oxirane and the oxolane ring are fused to 6–6 junctions of the same hexagon in one of the fullerene units which displays a noninherently chiral addition pattern. A constitutionally isomeric *cis*-1 adduct structure, having the epoxy bridge located at the remaining reactive site of the bis-anellated hexagon, was proposed for the minor component.[320] In a similar type of reaction, $C_{120}O$ was heated with sulfur under Ar at 230°C. The analytical data of the main product are consistent with C_s-symmetric **166** (Figure 1.38)[321] which is a structural homologue of another, C_{2v}-symmetric isomer of $C_{120}O_2$.[320,322] Although the $C_{120}OS$ molecule is achiral as a whole, the replacement of one oxygen bridge of C_{2v}-$C_{120}O_2$ by a sulfur atom leads to a noninherently chiral *cis*-1 addition pattern in each carbon spheroid. As the two fullerene moieties are enantiomorphic, their combination results in the achiral structure **166**.

A C_1-symmetric 1,2,3,4-adduct with a C_s-symmetric bridge[102] between C(2) and C(3) ((±)-**167**, Figure 1.39) has been reported as minor product resulting from the reaction between 2-methylpropan-2-ol and $C_{60}^{\bullet+}$, generated by irradiation in the presence of the PET-(photoinduced electron transfer) sensitizer 2,4,6-triphenylpyrylium tetrafluoroborate.[323] Its formation can be understood in terms of a further transformation of the initially formed monoadduct 1-([60]fullerene-1(2*H*)-yl)-2-methylpropan-2-ol.

A complex, multiply bridged 1,2,3,4-adduct of C_{60} (**168**) (Scheme 1.11) including a noninherently chiral addition pattern as well as a multitude of stereogenic centers in the addend moiety was obtained in a tandem reaction between the alkaloid scandine and C_{60}.[324] The sequence included a photoinduced addition of the tertiary amine subunit of the alkaloid and a [2 + 2] cycloaddition of its vinyl group to the adjacent intrahexagonal formal double bond of the fullerene. The structural elucidation included ^{1}H-^{1}H COSY-, HMQC- (heteronuclear multiple quantum coherence), HMBC-, and ROESY-(rotating frame Overhauser enhancement spectroscopy) NMR experiments and

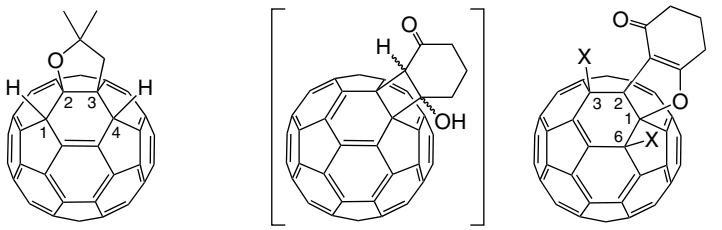

(±)-**167** (C_1) (±)-**173**/(±)-**174** (C_1) **171** X = — (C_s) (±)-**172** X = H (C_1)

Figure 1.39. Two different noninherently chiral functionalization patterns realized in a 1,2,3,4-((±)-**167**) and a 1,2,3,6-adduct ((±)-**172**) of C_{60}.

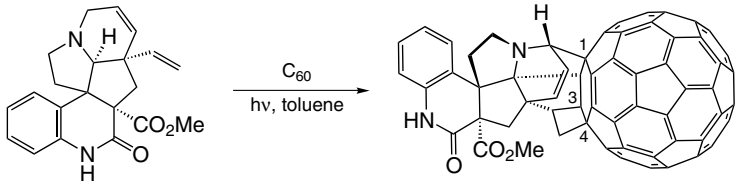

168
(C_1)

Scheme 1.11. Diastereoselective synthesis of a C_{60}-scandine conjugate by tandem reaction sequence involving a photoinduced addition of a tertiary amine and a [2 + 2] cycloaddition. The structure of the product includes a noninherently chiral functionalization pattern in addition to stereogenic centers in the alkaloid moiety.

allowed individual assignments of all protons and of a number of C-atoms. As no stereoisomer of C_1-symmetric **168** was reported, a high diastereoselectivity in its formation can be assumed.

The stereoselective addition of a series of electron-rich *N*-buta-1,3-dienyl-*O*-silyl ketene *N*,*O*-acetals to C_{60} under formation of 1,2,3,4-adducts (e.g., (±)-**169**, Scheme 1.12) with a noninherently chiral addition pattern by another tandem reaction, consisting of a nucleophilic addition–Diels-Alder reaction sequence was investigated in detail by Rubin, Neier, and co-workers.[325] The context of this study were efforts aiming at the functionalization of contiguous reactive centers in C_{60}, possibly leading to a fully saturated planar cyclohexane substructure that is prone to spontaneous ring-opening in a retro-[2 + 2 + 2] fashion under creation of a large orifice in the fullerene cage. As no reaction intermediates could be isolated, a number of model reactions were used to demonstrate that the tandem sequence starts with a nucleophilic Michael type addition, presumably involving a SET (single-electron transfer) followed by a radical recombination. The second step consists of an intramolecularly accelerated [4 + 2] cycloaddition leading to diastereoisomerically pure octahydroquinolines (e.g., (±)-**169**, Scheme 1.12) fused to two adjacent sides of a six-membered ring of C_{60}. These C_1-symmetric adducts, including a variety of functionalities in the addend moiety, are predisposed for further chemical transformations. An example is the abstraction of the acidic fullerene-attached proton of (±)-**169** by a base and subsequent alkylation of the resulting anion to afford products like C_1-symmetric (±)-**170** (Scheme 1.12).[325] Interestingly the alkylation did not take place at the original site of deprotonation (C(4) in (±)-**169**) but at C(16); as a consequence the addition pattern changes from noninherently chiral in (±)-**169** to inherently chiral in (±)-**170**. It may be of interest to mention that the complex configurational assignments in this study rely on 2D T-ROESY- (Transverse ROESY) NMR spectroscopy.

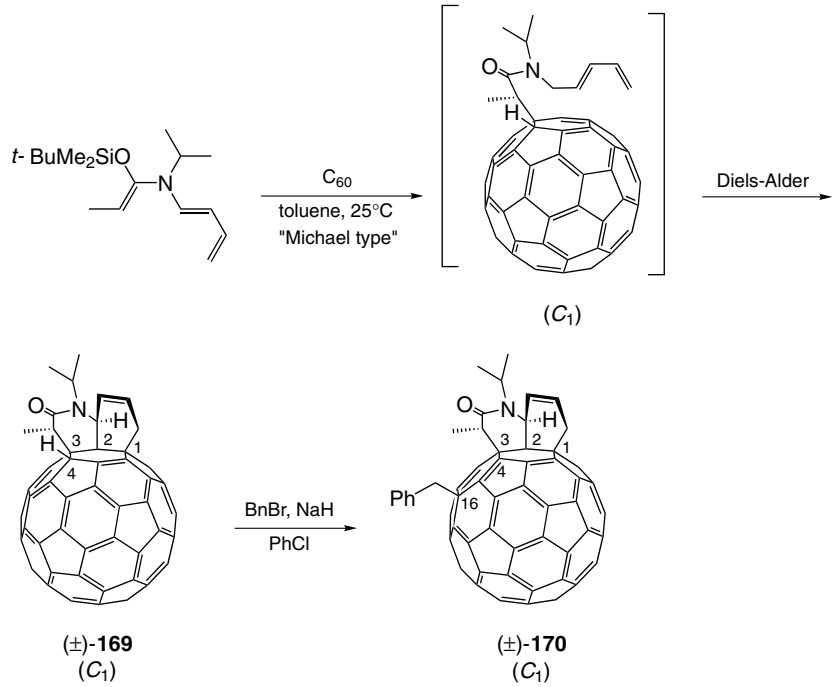

Scheme 1.12. A tandem sequence of Michael-type addition and [4 + 2] cycloaddition diastereoselectively affords highly functionalized 1,2,3,4-derivatives of C_{60} (type (±)-**169**) with two adjacent bridges and a noninherently chiral functionalization pattern. Deprotonation of (±)-**169** and subsequent alkylation leads to an inherently chiral addition pattern in (±)-**170**.

d. 1,2,3,6-Adduct of C_{60}. Photocycloaddition of cyclohexane-1,3-dione or related compounds to C_{60} did not give the expected De Mayo-type cyclooctane-1,4-dione derivatives after workup.[326] Instead, a C_s-symmetric (**171**) and a C_1-symmetric ((±)-**172**) compound (Figure 1.39), each including an enone and a vinyl ether substructure, were obtained, and the enantiomers of the latter could be separated on an (*S*,*S*)-Whelk-O column. Whereas the achiral compound (**171**) is a mono-adduct of C_{60}, ^{3}He NMR spectroscopy of the ^{3}He incarcerane of the chiral derivative ((±)-**172**) was rather indicative of a bis-adduct structure, and further experiments showed that it could be dehydrogenated to C_s-symmetric **171**. In combination with mechanistic considerations, the bis-adduct was assigned the structure (±)-**172** displaying a noninherently chiral addition pattern.[326] It should be noted that (±)-**172** does not represent a *cis*-1 type 1,2,3,4-adduct of C_{60}, a fact that can be understood in terms of the proposed mechanism of formation: It involves an intramolecular hydrogen abstraction from the addend of the initial [2 + 2] photocycloadduct

(±)-**173**/(±)-**174** (Figure 1.39) by the triplet fullerene moiety, and both H-atoms are bound to intrahexagonal positions adjacent to the initial addend. It ensues that the addition pattern comprises one 6–6 and two 6–5 junctions which leads to an intrapentagonal double bond in the formal 1,2,3,6-adduct of C_{60}.

e. 1,2,7,21- and 1,2,34,35-Adducts of C_{60}. In a study on the regiochemistry of twofold additions to 6–6 bonds of C_{60}, Hirsch and co-workers synthesized a series of bis-adducts bearing two constitutionally different addends.[111] As a result of this nonidentity the addition patterns of the otherwise achiral *cis*-2 and *trans*-4 bis-adducts become noninherently chiral, a situation realized in the C_1-symmetric 1,2,7,21-adducts (±)-**175** and (±)-**176**, as well as in the C_1-symmetric 1,2,34,35-adducts (±)-**177** and (±)-**178** (Figure 1.40). On the other hand, the *e* isomers of this series with mixed addends, including symmetric addend bridges, are achiral and occur as pairs of constitutional isomers. These differ in the occupation of the constitutionally heterotopic e_{edge} and e_{face} positions[104] by the nonidentical addends. It is interesting to compare this situation to that of *e* adducts containing two identical addends with C_s-symmetric bridges,[102] described in Sections IV.A.1.a.-c. A tethered *cis*-2 bis-adduct with a noninherently chiral addition pattern and two stereogenic centers represented by the methano bridge C-atoms ((±)-**179**) was finally reported by Nierengarten and co-workers. Its chirality originates from the "unsymmetric" tether between the cyclopropane rings.[127]

f. 1,2,3,4,5,6-Adduct of C_{60}. Investigating the binding of ruthenium clusters to fullerenes,[261,262] Shapley and co-workers synthesized a number of face-coordinated C_{60} complexes with carbido-pentaruthenium cluster cores.[256,327,328] Reaction of $[Ru_5C(CO)_{15}]$ with C_{60} in refluxing chlorobenzene,

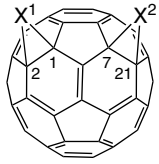

(*cis*-2)

(±)-**175** (C_1)
(±)-**176** (C_1)

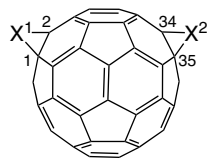

(*trans*-4)

(±)-**177** (C_1)
(±)-**178** (C_1)

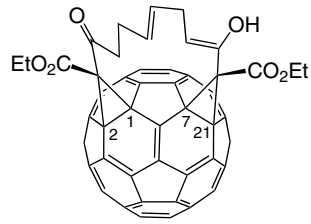

(±)-**179** (C_1)

$X^1 = N(CO_2Et)$, $X^2 = C(CO_2Et)_2$
$X^1 = C(CO_2Et)_2$, $X^2 = C(p\text{-}C_6H_4OCH_3)_2$

Figure 1.40. Noninherently chiral addition patterns in *cis*-2 and *trans*-4 adducts of C_{60}.

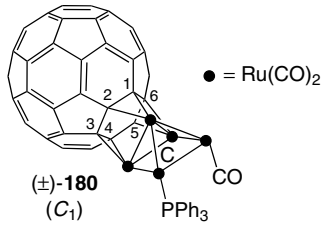

Figure 1.41. The μ_3-η^2:η^2:η^2-ligation of C_{60} to the carbido-pentaruthenium cluster of (±)-**180** results in a noninherently chiral functionalization pattern of the *cis*-1,*cis*-1,*cis*-1 type.

followed by chromatographic purification, afforded a sparingly soluble compound $[Ru_5C(CO)_{12}(C_{60})]$. Treatment of the reaction mixture with PPh_3 led to a ligand exchange, thus giving a more soluble compound, the structure of which was determined by X-ray crystallography as $[Ru_5C(CO)_{11}(PPh_3)(\mu_3$-$\eta^2$:$\eta^2$:$\eta^2$-$C_{60})]$ ((±)-**180**, Figure 1.41).[327] The metal framework consists of a square pyramid, and the fullerene ligand is bound to one of its triangular faces as μ_3-η^2:η^2:η^2-ligand. The C–C distances in the fullerene hexagon bound to the metal framework, as well as the Ru–C distances in (±)-**180** alternate in length which results in a slight twist of the Ru_3-triangle with respect to the bonded hexagon of C_{60}. Due to the presence of a single phosphane ligand, the two basal ruthenium atoms, which do not interact directly with the fullerene core, are constitutionally heterotopic, and as a result the addition pattern of the C_1-symmetric 1,2,3,4,5,6-adduct of C_{60} is noninherently chiral.

g. Hexakis-Adduct with a Pseudo-octahedral Addend Arrangement. A series of mixed hexakis-adducts of C_{60} with a pseudo-octahedral general addition pattern was recently reported by Hirsch and co-workers.[329] These compounds include two types of Bingel addends, one derived from diethyl malonate and the other one containing Fréchet type dendritic residues[330] as alcohol component of the esters (Figure 1.42).[331] When the C_3-symmetric *e*,*e*,*e* tris-adduct (±)-**10** (Figure 1.14),[51,96,110,115] was reacted with second- or third-generation dendritic 2-bromomalonates in a 9,10-dimethylanthracene-template-mediated cyclopropanation,[332] mixed hexakis-adducts, such as (±)-**181** (Figure 1.42), with a pseudo-octahedral arrangement of addends were obtained.[329] Both types of addends are grouped in oppositely configured *e*,*e*,*e* arrangements, and the combination of these substructures in C_3-symmetric (±)-**181** results in a noninherently chiral addition pattern.

2. *Derivatives of C_{70}*

a. General Considerations on Noninherently Chiral Addition Patterns in Higher Fullerenes. Considering the common types of C_{70}-mono-adducts,[17]

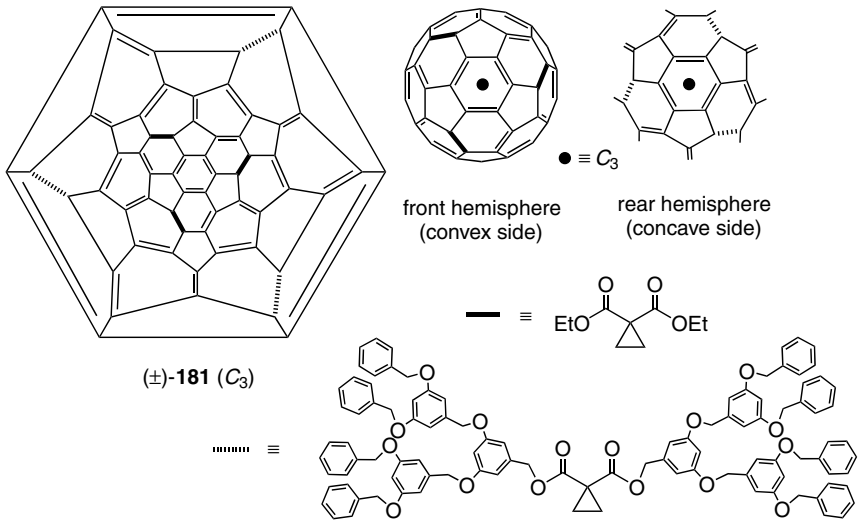

Figure 1.42. Schlegel diagram and individual hemispheres of a hexakis-adduct of C_{60} with a pseudooctahedral general functionalization pattern which is noninherently chiral due to two different sets of three addends arranged in a relative *e*,*e*,*e*-fashion. It should be noted that the front hemisphere is viewed from the convex side (extra-cage view) and the rear hemisphere from the concave side (intra-cage view).

the addition pattern arising from functionalization of the bond C(5)–C(6) (cf. Figure 1.6) is noninherently chiral if the addend is C_s-symmetric.[102] Similarly this type of chirality can in principle occur in C(7)–C(8) adducts[219,220] with C_s-symmetric bridges[102] or, generally speaking and neglecting bond reactivities, in all derivatives resulting from "unsymmetrical" addition across bonds that are perpendicular to the fivefold symmetry axis of the parent C_{70}.

It should be noted that some C_{70} derivatives with a noninherently chiral addition pattern, such as $[(\eta^2\text{-}C_{70}O)Ir(CO)Cl(PPh_3)_2]$ isomer (±)-**119** (Section IV.A.2.g, Figure 1.30), or the compounds (±)-**82** and (±)-**89** (Section IV.A.2.b, Scheme 1.9), resulting from [3 + 2] cycloaddition of diazomethane and an alkyl azide, respectively, have already been discussed in the context of chemically related compounds with an inherently chiral functionalization pattern. Besides, derivatives with a noninherently chiral addition pattern are not known so far of the fullerenes beyond C_{70}. This is due, on one hand, to the inherent chirality of many higher homologues and, on the other hand, to the hardly explored chemistry of the achiral larger carbon cages.[17,60–63]

b. 5,6-Adducts Resulting from [3 + 2] Cycloadditions. Independent studies by Meier and co-workers[333] and Irngartinger and co-workers[334]

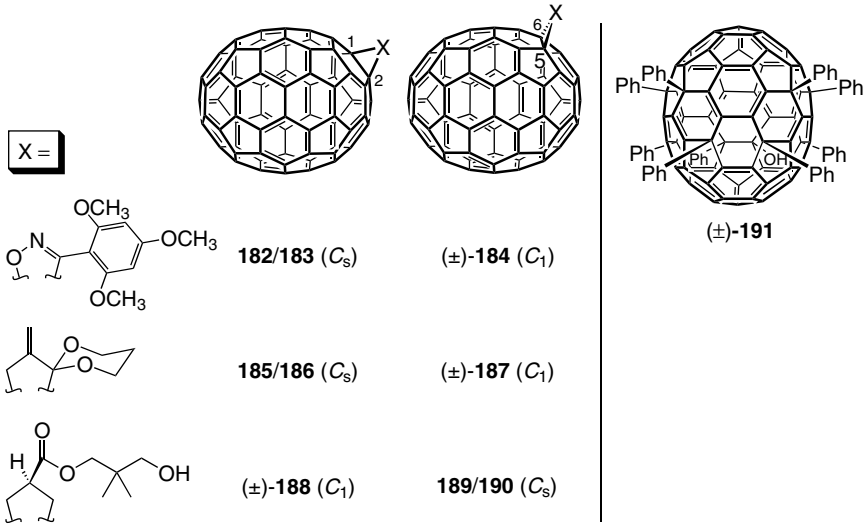

Figure 1.43. C(5)–C(6)-adducts ((±)-**184** and (±)-**187**), and a decakis-adduct ((±)-**191**) of C_{70} with noninherently chiral functionalization patterns, together with other congeners formed in the respective syntheses.

showed that isonitrile oxides add to the same bonds (C(1)–C(2) and C(5)–C(6); Figure 1.43) of C_{70} as diazomethane or alkyl azides (cf. Section IV.A.2.b),[43,226,227] albeit with a lower regioselectivity. Thus the addition of 2,4,6-trimethoxybenzonitrile oxide across C(1)–C(2) gives rise to similar amounts of two C_s-symmetric constitutional isomers (**182** and **183**, Figure 1.43), whereas the C_1-symmetric C(5)–C(6)-adducts, such as (±)-**184**, occur as enantiomers with a noninherently chiral functionalization pattern.

A relatively complex stereochemical cascade ensued from the initial [3 + 2] cycloaddition to C_{70} of a dipolar trimethylenemethane derivative generated by thermolytic ring opening of a methylidenecyclopropanone acetal.[335] Primary addition of the C_s-symmetric addend,[102] presumably involving a SET from the trimethylenemethane unit to the fullerene, occurs across the bonds C(1)–C(2) and C(5)–C(6) of C_{70}, thus giving rise to the C_s-symmetric achiral regioisomers **185** and **186**, as well as a to a third, C_1-symmetric constitutional isomer formed as a pair of enantiomers ((±)-**187**) with a noninherently chiral addition pattern (Figure 1.43). Rearrangement of the primary adducts, taking place via an achiral intermediate with a C_{2v}-symmetric addend,[102] and hydrolysis of the latter yielded a pair of enantiomers with a stereogenic center in the side chain ((±)-**188**)[336] as well as a pair of achiral *cis*/*trans* isomers (**189** and **190**; *cis* and *trans* with respect to the faces of the fullerene-fused pentagon). In summary, there was a formal transformation of a pair of achiral

constitutional isomers (C(1)–C(2)-adduct regioisomers **185** and **186**) into a pair of enantiomers ((±)-**188**), and of a constitutionally different pair of enantiomers (C(5)–C(6) adduct (±)-**187**) into a pair of achiral diastereoisomers (**189** and **190**).[335]

c. Decakis-adduct. The fullerenol $C_{70}Ph_9OH$ ((±)-**191**; Figure 1.43) is a by-product of the Friedel-Crafts alkylation of benzene by $C_{70}Cl_{10}$, giving as main product $C_{70}Ph_{10}$ via the intermediacy of $C_{70}Ph_8$.[337] The noninherently chiral functionalization pattern of the C_1-symmetric fullerenol (±)-**191** can be ascribed to the formal addition of two different residues (OH and Ph) across the bond C(7)–C(8) (cf. Figure 1.6). In $C_{70}Ph_8$ this site remains an intact 6–5 double bond,[270] whereas its formal functionalization by "symmetrical" addition of Cl or Ph leads to C_s-symmetric addition patterns in $C_{70}Cl_{10}$[338] and $C_{70}Ph_{10}$,[270] respectively.

C. Fullerene Derivatives with Chiral Elements in the Addends

In this section we will discuss chiral derivatives of achiral parent fullerenes that do not include a chiral addition pattern but have stereogenic elements located exclusively in the addends. Among the plethora of publications dealing with derivatives of this type, only a small fraction explicitly addresses stereochemical questions. The following survey, which does not intend to be comprehensive, focuses on the latter cases and, besides, tries to illustrate the most common types of fullerene derivatives having chiral pendant groups with a number of representative examples. It starts with adducts of C_{60} that include stereogenic centers newly created in the course of the addition reaction. The second part treats the coupling of a chiral addend, often an enantiomerically pure natural product derivative, with a functionalized [60]fullerene. Finally, we will present the relatively few derivatives of C_{70} and higher fullerenes with stereogenic elements residing exclusively in the addends.

1. Functionalization of C_{60} with Generation of New Stereogenic Elements in the Addends

a. [2 + 1] Cycloadditions. In the presence of ambient light, the carbene generated from the (*R*,*S*)-configured, *meso*-type tosylhydrazone lithium salt **192** reacts with [60]fullerene under formation of a mixture of homofullerene (±)-**193** and methanofullerene **194** (Scheme 1.13).[339] The proportion of the latter increases with increasing reaction time, and the kinetic "6–5 open" adduct (±)-**193** can be converted to the thermodynamic "6–6 closed" isomer by irradiation. Both structures are quite interesting from a stereochemical viewpoint:

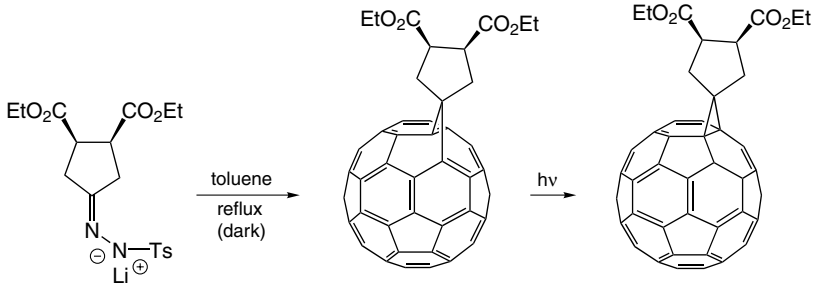

192 (±)-**193** (C_1) **194** (C_s)

Scheme 1.13. Addition of a *meso* cyclopentylidene species to C_{60} under formation of a chiral spiro-type homofullerene that can be rearranged photochemically to the corresponding achiral methanofullerene.

Whereas a mirror plane, including the cyclopropane ring and reflecting the stereogenic centers of the five-membered ring into each other, bisects achiral **194**, the homo[60]fullerene derivative (±)-**193** is chiral due to the insertion of the *cis*-disubstituted pentagon via a spiro linkage into the junction between two different rings, namely a pentagon and a hexagon of the fullerene. In (±)-**193**, the carbon cage and the addend moieties — taken for themselves — are bisected by a mirror plane. However, these planes are orthogonal, and the C_1-symmetric homofullerene (±)-**193** represents a particular kind of chiral spiro structure. If one stereogenic center of the starting hydrazone is formally inverted (e.g., leading to the (*R*,*R*)-analogue of **192**), the resulting cyclopentane substructure becomes C_2-symmetric, and both of the adducts (analogues of (±)-**193** and **194**) will be chiral.

b. [2 + 2] Cycloadditions. Fullerene-derived ketones with chiral addends have been generated in a number of cases by photocycloaddition of cyclic α,β-unsaturated ketones to C_{60} (cf. Figure 1.44). The used starting materials include cyclohex-2-enone,[248,340] substituted and anellated cyclohex-2-enones,[238,242,340] and cyclohept-2-enone.[248] In a number of cases, diastereoisomeric adducts with *cis*- and *trans*-fused rings could be distinguished by ^{3}He NMR spectroscopy of the corresponding noble gas incarceranes.[84,248] The proposed reaction mechanism involves the addition of enones in their triplet excited state to ground state [60]fullerene via triplet 1,4-biradical intermediates, as in typical enone-alkene photocycloadditions.[248]

Addition of 3-methylcyclohex-2-enone to C_{60} afforded four stereoisomers comprising the diastereoisomeric *cis*- and *trans* racemates (±)-**195** and (±)-**196** (ratio 40 : 60), respectively, which were identified by ^{1}H-NMR coupling constant analysis (Figure 1.44).[238] The separation of the enantiomers of

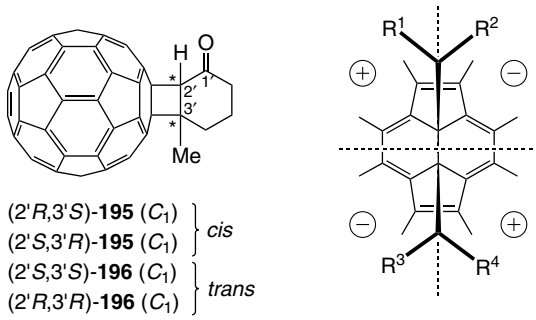

Figure 1.44. The different stereoisomers obtained by [2 + 2] photocycloaddition of 3-methylcyclohex-2-enone to C_{60} (*left*, the newly formed stereogenic centers are marked by an asterisk), and illustration of a sector rule devised for the correlation of the absolute configuration of a "6–6 closed" 1,2-adduct of C_{60} to the CD band around 430 nm (*right*). According to the sign ((+) or (−)) of the sector in which an addend moiety (R^1,R^2,R^3, or R^4) is located, it is postulated to add a positive or negative contribution to the Cotton effect associated with the ca. 430 nm UV/Vis absorption of the fullerene chromophore.

(±)-**195** and (±)-**196** by HPLC on a chiral (*S*,*S*)-Whelk-O stationary phase was the first chromatographic resolution of chiral fullerene adducts.[238] Much larger optical rotations were found for the *trans*- ((±)-**196**) in comparison to the *cis*-isomers ((±)-**195**), and the UV/Vis and CD spectra of the former also displayed additional long-wavelength bands.

Wilson, Welch, Schuster, and co-workers proposed a sector rule for the determination of the absolute configuration of C_{60} derivatives showing Cotton effects due to the perturbation of an achiral fullerene chromophore by chiral elements in the addends.[242] The method is based on the CD contribution associated with the nearly 430 nm UV/Vis absorption typical of "6–6 closed" adducts of C_{60},[15,301] and as a model compound for assigning the sign of the sectors, the authors used an optically pure adduct obtained by diastereoselective Diels-Alder addition of an enantiomerically pure (+)-α-pinene derivative. The sectors are defined by three orthogonal planes intersecting at the center of the functionalized 6–6 bond; one is tangential to the carbon cage, a second plane includes the functionalized 6–6 bond and bisects the fullerene, and the third one bisects both the functionalized bond and the fullerene (Figure 1.44). Positive or negative contributions to the above-mentioned Cotton effect are expected for adduct moieties residing in according regions of space as shown in Figure 1.44.[242] Application of this rule to the isolated *trans* enantiomer (+)-**196** suggests its absolute configuration to be (2′*R*,3′*R*).

[2 + 2] Photocycloaddition of the deuterated *p*-methoxystyrene (*Z*)-**197**, led to a mixture of *cis*- and *trans* adducts (±)-**198** and (±)-**199**, respectively, with complete lack of diastereoselectivity (Scheme 1.14).[341] Combining this

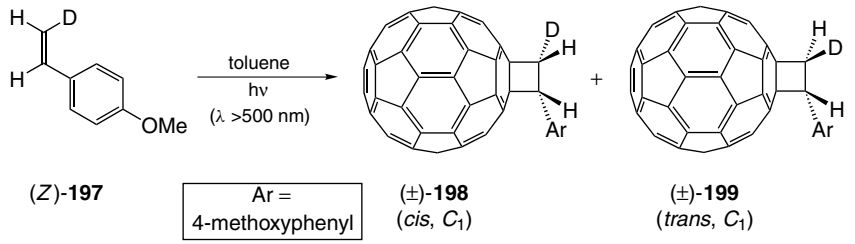

Scheme 1.14. The unselective formation of diastereoisomeric adducts by [2 + 2] photocycloaddition of a *cis*-substituted styrene to C_{60} is indicative of a stepwise reaction.

observation with a detailed study of secondary isotope effects, Orfanopoulos and co-workers concluded on a two-step mechanism involving a dipolar or a diradical adduct intermediate in the rate-determining step of the reaction between the triplet excited state of C_{60} and the styrene derivative.[341,342] Further mechanistic studies by the same group dealt with the regio- or stereoselectivity of the [2 + 2] photocycloaddition of acyclic enones and alkyl-substituted buta-1,3-dienes to C_{60}.[343]

c. [3 + 2] Cycloadditions. Next to the Bingel[94] and Diels-Alder reactions,[344] [3 + 2] cycloaddition of azomethine ylides is one of the most versatile reactions to functionalize carbon cages; it leads to fullerene-fused pyrrolidines that can easily be further derivatized.[214,345] A cornucopia of pyrrolidinofullerenes has consequently been described in literature, and as a great deal of them were formed by addition of "unsymmetrically" substituted azomethine ylides to C_{60}, most of them are chiral. Again, a very limited number of publications report on the isolation of enantiomerically pure compounds or the investigation of chiroptical properties. The first fullerene-fused pyrrolidines (e.g., fulleroproline methyl ester (±)-**200**; Figure 1.45) were synthesized in 1993 by Maggini, Scorrano, and Prato.[213] An optically pure fulleroproline derivative was obtained by diastereoselective reaction of (5*R*,6*S*)-5,6-diphenyl-*N*-octyloxymethyl-1,4-oxazin-2-one with C_{60} in the presence of *p*-toluenesulfonic acid (for a related reaction, cf. Scheme 1.15).[346]

In a subsequent study a number of fulleroproline-containing dipeptides and other derivatives, such as **201** and **202** (Scheme 1.15), were prepared and isolated as optically pure diastereoisomers or resolved into the enantiomers.[241] The most distinctive feature in the CD spectra of these adducts is a sharp extremum at 428 nm, the sign of which is characteristic of the absolute configuration of the newly generated stereogenic center at the α-C-atom of the proline unit. To establish this relationship, the absolute configuration of the isolated diastereoisomers **201** and **202** (Scheme 1.15), synthesized by reaction of azomethine ylides generated from enantiomerically pure **203** and

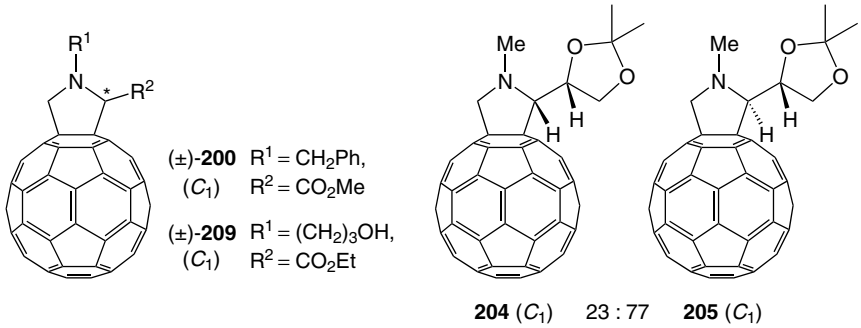

Figure 1.45. Racemic mixtures of fullerene-fused pyrrolidines obtained by [3 + 2] cycloaddition of azomethine ylides to C_{60} (*left*, the newly formed stereogenic center is marked by an asterisk); if the azomethine ylide is generated from optically pure (+)-2,3-*O*-isopropylidene-D-glyceraldehyde and *N*-methylglycine, the cycloaddition reaction is diastereoselective (*right*).

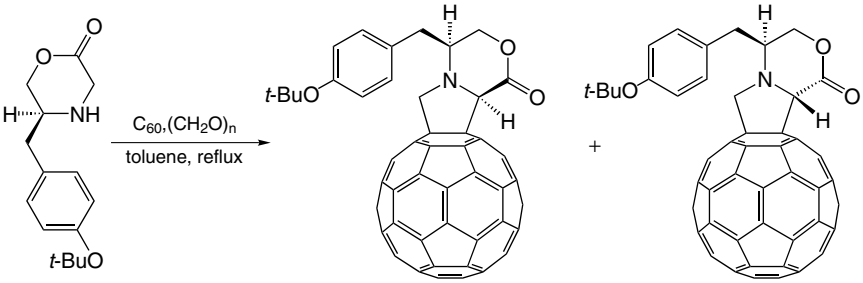

Scheme 1.15. Diastereoisomeric fulleroproline derivatives used (among other compounds) to establish the empirical relationship between the absolute configuration of the stereogenic center of the pyrrolidine ring and the sign of the ca. 428 nm CD band displayed by fulleroprolines.

paraformaldehyde, was first determined by studying NOE effects between the H-atoms connected to the stereogenic centers of **201** and **202**. Measurement of the near-mirror image CD spectra of the diastereoisomers **201** and **202** allowed to associate a positive CD maximum at 428 nm with the (*R*)-configuration of the fulleroproline unit. This correlation was experimentally confirmed by other derivatives and also corroborated by the calculation of CD spectra.[241]

When azomethine ylides are generated by condensation of aldehydes with chiral α-amino acids, the stereogenic center of the latter is lost in the planar 1,3-dipole structure. To achieve diastereoselection in the addition to C_{60}, an additional chiral element is therefore needed. An optically pure azomethine ylide was generated by reaction of (+)-2,3-*O*-isopropylidene-D-glyceraldehyde with

N-methylglycine, and its addition to C_{60} diastereoselectively afforded pyrrolidino[60]fullerenes **204** and **205** (Figure 1.45) in a 23 : 77 ratio.[245] As the bulky 2,2-dimethyl-1,3-dioxolane unit prevents free rotation around the bond connecting the two heterocycles, configurational assignments were possible by ^{1}H NMR coupling constant analysis and NOE measurements. They were in accordance with those based on the Cotton effects observed around 428 nm (*vide supra*[241]).[245]

Pyrrolidino[60]fullerenes bearing methyl substituents at C(2) and C(5) of the heterocycle can exist as a C_s-symmetrical *meso* form (*cis* compound) and a C_2-symmetrical *d*, *l* pair of enantiomers (*trans* compounds) (cf. Figure 1.46). Reaction of the isomeric mixture with an enantiomerically pure isocycanate afforded three diastereoisomeric urea derivatives (**206**, **207**, **208**, Figure 1.46).[250] Whereas the *cis* compound **206** was almost CD-silent, the configuration of the *trans* isomers **207** and **208**, displaying near-mirror image CD spectra, was assigned on the base of the sector rule devised for chiral monoadducts of C_{60} resulting from functionalization of a 6–6 bond.[242] Because of the lower symmetry of C_{70}, its fusion to 2,5-disubstituted pyrrolidines afforded a complex mixture of regio- and stereoisomers.[250]

trans-*N*-Ethyl-2′,5′-dimethylpyrrolidino[3′,4′:1,2][60]fullerene (cf. Figure 1.46) and related compounds have also been obtained from C_{60} and triethylamine in a reaction involving sequential inter- and intramolecular photoinduced electron transfer processes.[347,348] Similarly fulleroproline derivatives have been produced in a photochemical reaction from amino acid esters and C_{60}.[349]

An enantioselectivity of 45% *e.e.* (at 15% conversion) was observed in the enzymatic transesterification of 2,2,2-trifluoroethyl palmitate by the [60]fulleroproline-derived alcohol (±)-**209** (Figure 1.45), catalyzed by lipoprotein lipase (LPL) from *Pseudomonas specie*.[350] The modest enantioselectivity may be related to the distance between the stereogenic center of the substrate and its reactive OH group. If, on the other hand, the group reacting with the enzyme is located closer to the fullerene spheroid, reaction rates slow down

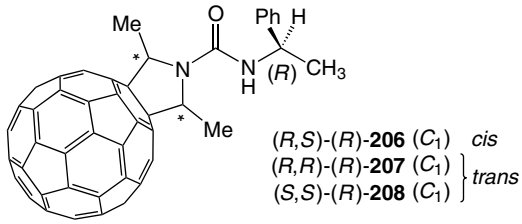

Figure 1.46. Three diastereoisomeric urea derivatives of C_{60} obtained by reaction of an optically pure isocyanate with the *meso*- and *d*, *l*-forms of fullerene-fused 2,5-dimethylpyrrolidine.

dramatically, which is probably due to the C_{60} moiety hindering productive fitting in the active site of the enzyme.[350]

For further information on synthesis, properties, and applications of pyrrolidinofullerenes, the chiral representatives of which were generally prepared and used as racemates, we refer to a recent review by Prato and Maggini.[214] Fields in which many fullerene-fused pyrrolidines have been studied are biological and medicinal chemistry[351] and, above all, advanced materials science.[352,353] In the latter context, dyads and triads used for photoinduced charge separation between a fullerene acceptor moiety and electron donors like porphyrins, tetrathiafulvalenes, ferrocenes, or polyenes, are worth particular mentioning.[354–356]

One of the first reactions studied on fullerenes was the [3 + 2] cycloaddition of diazoalkanes leading to the formation of pyrazolinofullerenes which loose N_2 thermally under formation of the "6–5 open" homofullerenes as kinetic products.[41,121,339,357,358] If the starting 1,3-dipole bears two different substituents, the intermediate pyrazoline is chiral. The racemate of such an adduct ((±)-**210**, Scheme 1.16) was reported by Schick and Hirsch as the only representative (besides the adduct of unsubstituted diazomethane)[41] of the thermally labile pyrazolino[60]fullerenes that could be isolated and characterized so far.[359] In agreement with earlier investigations on the isomeric distribution of the products resulting from addition of "unsymmetrically" substituted diazomethanes to C_{60},[301,360–363] the authors showed that the extrusion-rearrangement reaction of (±)-**210** and other pyrazolino[60]fullerenes is highly diastereoselective, leading to the homofullerene with the bulkier substituent of the bridge located above the former five-membered ring (**211**, Scheme 1.16). The diastereoisomeric homofullerene **212** was only formed in traces, and no methanofullerene was detected. The origin of the regioselectivity in the dinitrogen extrusion from pyrazolinofullerenes was investigated theoretically by

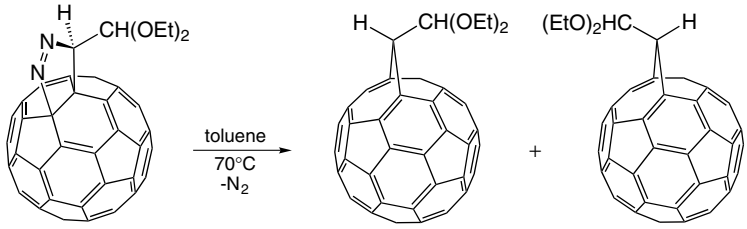

(±)-**210** (C_1) **211** (C_s) (major product) **212** (C_s) (traces)

Scheme 1.16. Thermal extrusion-rearrangement of the first isolated fullerene-fused pyrazoline substituted at C(3), affording diastereoisomeric "6–5 open" homo[60]fullerene derivatives, of which the major isomer has the bulkier group located above the former pentagon.

Diederich and co-workers,[121] and the above observations were rationalized by Schick and Hirsch in terms of a minimization of repulsive interactions between the substituent of the methylene unit and the departing N_2 moiety during the formation of the homo type methylene bridge.[359]

Wudl, Padwa, and co-workers found that the Rh(II)-catalyzed 1,3-dipolar cycloaddition of several isomünchnone precursors with C_{60} readily affords the [3 + 2] cycloadducts, such as (±)-**213** (Scheme 1.17).[364] On thermolysis, the adducts cleanly regenerated the mesoionic heterocycles, for which they may be used as a repository (Scheme 1.17). When a chiral, racemic isomünchnone precursor was used as starting material, the diastereoisomeric adducts with C_{60} were formed in unequal amounts which, in the absence of significant steric effects, points toward subtle electronic interactions between the reaction partners.[364]

Various other [3 + 2] cycloadditions, affording chiral, anellated C_{60} derivatives with stereogenic centers in the addends are reported in literature. The products were generally obtained as racemates and resulted from reaction of buckminsterfullerene with species like 2,3-disubstituted 2*H*-azirines (via nitrile ylides [under direct irradiation] or via 2-azaallenyl radical cations [sensitization by photoinduced electron transfer]),[365] 1-substituted 5-diazopentane-1,4-diones (via cyclic carbonyl ylides),[366] 7-alkylidene-2,3-diazabicyclo[2.2.1] hept-2-ene (via a diradicaloid trimethylenemethane derivative),[367] 1-benzylpyrazolidine-3-ones in the presence of aldehydes (via pyrazolidinium ylides),[368] 2-trifluoromethyl-2,5-dihydro-1,3-oxazol-5-ones (via nitrile ylides),[369] nitroalkanes in the presence of triethylamine and trimethylsilyl chloride (via *N*-silyloxynitrones),[370] or *cis*-$HOCH_2CH{=}CHCH_2OCO_2Et$ in the presence of

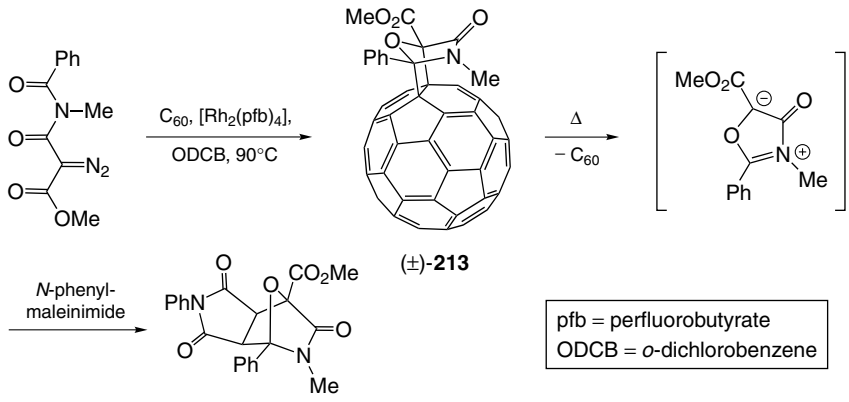

Scheme 1.17. Rhodium-catalyzed addition of an isomünchnone precursor to C_{60}. The adduct readily undergoes thermal cycloreversion under liberation of the mesoionic heterocycle, as shown by its trapping with *N*-phenylmaleinimide.

$Pd(PPh_3)_4$ and 1,2-bis(diphenylphosphano)ethane (dppe) (presumably via an oxymethyl-allylpalladium complex).[371]

d. [4 + 2] Cycloadditions. The Diels-Alder reaction has been one of the most frequently applied reactions in the derivatization of fullerenes which always act as the dienophile component.[344] The used 1,3-dienes include acyclic and cyclic dienes, exocyclic dienes such as *o*-quinodimethanes,[372] and heterodienes.[373] This variety, in combination with the fact that new stereogenic centers are generally created by addition of dienes bearing two different substituents at C(1) or C(4), gives a hint at the many chiral Diels-Alder adducts of C_{60} that have been synthesized. However, stereochemical investigation or the isolation of stereoisomerically pure adducts has been the object of only a few studies. We will focus on these studies here.

A very useful intermediate for the attachment of further functionalities to C_{60} is obtained by reaction of the fullerene with 2-[(trimethylsilyl)oxy]buta-1,3-diene, followed by hydrolysis of the resulting silyl enol ether under formation of a fullerene-fused cyclohexanone (**214**) which is reduced to the racemic alcohol (±)-**215** (Scheme 1.18).[374] Because of their great synthetic potential, silyloxy-substituted dienes, such as Danishefsky diene type systems,[375–377] have been widely used in the preparation of fullerene derivatives, mostly in the form of stereoisomeric mixtures.[378–383]

Addition of the Danishefsky diene derivative (1*E*,3*Z*)-1-methoxy-2-methyl-3-[(trimethylsilyl)oxy]penta-1,3-diene **216** (Scheme 1.19), was shown by Mikami, Fukuzumi, and co-workers to proceed in a stepwise process,

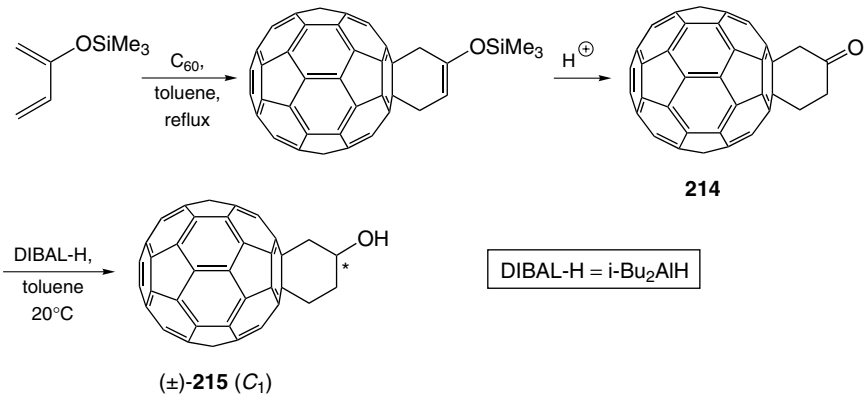

Scheme 1.18. Diels-Alder addition of 2-[(trimethylsilyl)oxy]buta-1,3-diene to C_{60}, followed by hydrolysis of the resulting silyl enol ether to the ketone **214** and reduction of the latter, affording the racemic alcohol (±)-**215** as a versatile fullerene-containing building block for the attachment of further functionalities.

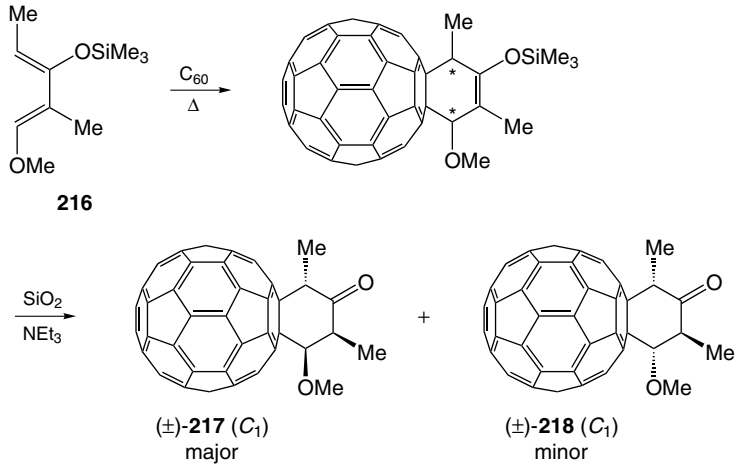

Scheme 1.19. Diastereoselective addition of a Danishefsky diene derivative (**216**) to C_{60}. The product distribution is indicative of a stepwise reaction, because the major diastereoisomer ((±)-**217**) obtained after hydrolysis of the silyl enol ether function of the primary adduct cannot result from a concerted [4 + 2] cycloaddition.

presumably involving a SET.[376] Reaction of the diene with C_{60} in the dark, followed by hydrolysis of the trimethylsilyl enol ether intermediate, afforded the diastereoisomeric adducts (±)-**217** and (±)-**218** as major and minor isomers, respectively, with the intraannular configurational relationships being deduced from NOE measurements. Because of the orbital symmetry constraint of the Diels-Alder reaction, the major stereoisomer ((±)-**217**) cannot be formed in a thermal, concerted process. When the reaction was carried out under irradiation, (±)-**217** was formed as the only product, presumably via PET and a stepwise bond formation and thus leading to the thermodynamically more stable diastereoisomer.

Configurationally homogeneous, substituted fullerene-fused cyclohexanones derived from **214** (Scheme 1.18) were prepared by Rubin, Kenyon, and coworkers in a double Michael type addition.[378] As the attempted Diels-Alder reaction with (3*Z*,5*E*)-4-[(*tert*-butyldimethyl)silyl]-2,7-dimethylocta-3,5-diene to afford the sterically congested *cis*-disubstituted analogue of (±)-**219** (Scheme 1.20) failed, they devised an alternative synthesis starting with the addition of dienolate **220** to C_{60} (Scheme 1.20), followed by intramolecular reaction of the resulting fullerenide with the enone moiety of the primary adduct (±)-**221** under formation of the thermodynamically more stable *trans*-disubstituted adduct (±)-**222**, as demonstrated by NOE measurements on the corresponding trimethylsilyl enol ether. Ketone (±)-**219** could be reduced stereoselectively by DIBAL-H to the alcohol (±)-**223** showing a *cis*-relationship

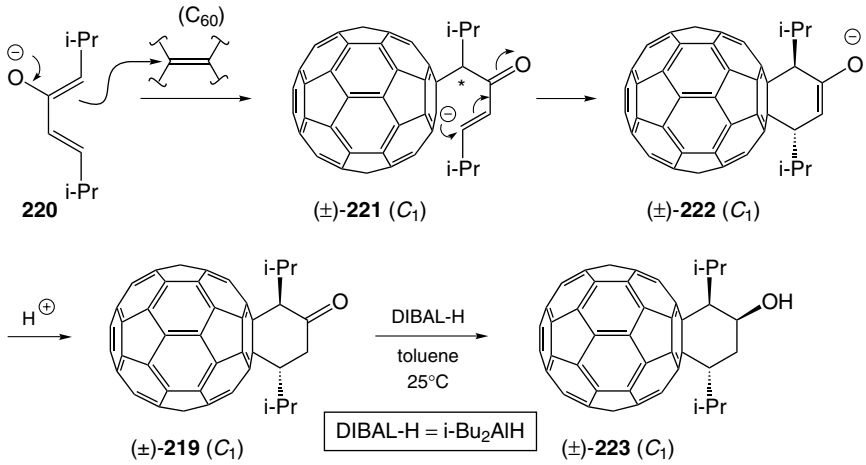

Scheme 1.20. Double Michael-type addition of dienolate **220** to C_{60}, affording after workup the thermodynamically more stable *trans*-disubstituted ketone (±)-**219**. Due to steric congestion, the corresponding *cis*-adduct is not available through Diels-Alder reaction with the silyl enol ether corresponding to **220**. Reduction of the racemic ketone (±)-**219** with DIBAL-H diastereoselectively affords alcohol (±)-**223**.

between the OH group and the vicinal isopropyl residue, resulting from stereoselective attack of the hydride reagent. Together with a number of other derivatives of C_{60}, alcohol (±)-**223** was tested for its inhibition of the HIV protease.[384]

Enantiomerically pure Diels-Alder adducts of C_{60} were prepared by Tsuji and co-workers by use of a chiral auxiliary in the diene component and separation of the diastereoisomeric intermediates.[385] The starting material for the diene component was a cyclic cyclopentenone acetal (**224**, Scheme 1.21) derived from L-threitol, reacting via its cyclopentadiene-containing enol ether isomer.[385,386] The diastereoisomeric products **225** and **226**, formed without significant diastereoselectivity, were isolated as the acetals, separated and subsequently hydrolyzed to afford the enantiomeric ketones (+)-**227** and (−)-**227**. NOE measurements allowed the determination of the absolute configuration of the diastereoisomeric intermediates **225** and **226** and, therefore, also of the enantiomeric ketones (+)-(*R*,*R*)-**227** and (−)-(*S*,*S*)-**227** (Scheme 1.21).[385]

The cyclohexene substructure resulting from Diels-Alder addition of acyclic dienes to fullerenes can adopt two boat conformations.[50,387–389] If a new stereogenic center is generated during the cycloaddition, the boat-to-boat interconversion leads to conformational diastereoisomerism in each configurational stereoisomer.[389,390] Such a case was studied by Zhang and Foote who performed VT (variable temperature) ^{1}H NMR and NOE measurements on

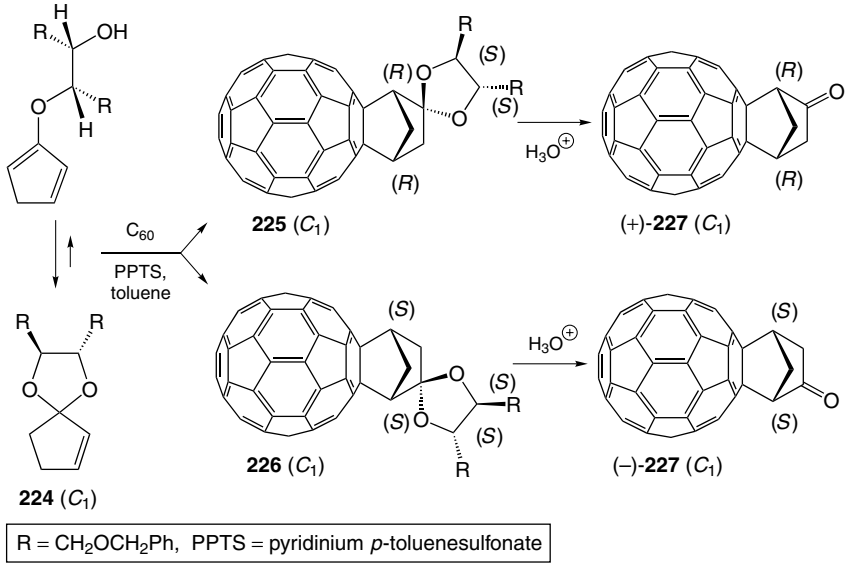

Scheme 1.21. Diels-Alder addition of an enatiomerically pure cyclopentadiene derived from (*S*,*S*)-threitol to C_{60}. Separation of the diastereoisomeric adducts **225** and **226**, followed by cleavage of the acetal protecting group, afforded enantiomerically pure ketones which were configurationally assigned as (+)-(*R*,*R*)-**227** and (−)-(*S*,*S*)-**227**.

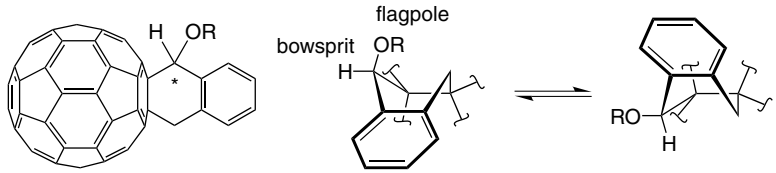

Figure 1.47. Conformational diastereoisomerism shown for one enantiomer of two Diels-Alder adducts of C_{60} including a stereogenic center newly generated in the course of the cycloaddition.

compounds (±)-**228** and (±)-**229**, obtained by *o*-quinodimethane addition to C_{60} (Figure 1.47).[389] From the coalescence temperature, they deduced activation barriers of 17.6 ± 0.3 and 19.3 ± 0.3 kcal/mol for the boat inversion of (±)-**228** and (±)-**229**, respectively. These relatively high values can be attributed to the torsional and angular constraints imparted by the rigid C_{60} backbone, enforcing a nearly planar cyclohexene ring in the transition state. A further contribution originates from the *peri*-interactions between the substituent in benzylic position ((±)-**229**) and the *ortho*-protons of the aromatic

ring. The latter also account for the fact that the substituent in (±)-**229** and a number of other adducts (not (±)-**228**!) prefer the flagpole over the bowsprit position in the cyclohexene boat.[389]

Other [4 + 2] cycloadducts including bridged cycles as chiral addends were obtained by reaction of the fullerene with cyclohepta-1,3,5-trienes,[391] tropones,[392] 2*H*-pyran-2-one,[393] norcaradienes,[394] and ethyl 1*H*-azepine-1-carboxylate (photoinduced cycloaddition).[395] A strategy developed by Rubin and co-workers for the removal of fullerene-fused cyclohexene rings involves a self-sensitized photooxygenation producing chiral hydroperoxides and a reduction to the corresponding alcohols.[49,377,396,397] Two chiral, bichromophoric, rigid ball-and-chain systems devised for the study of intramolecular electron and energy transfer processes, including a number of Diels-Alder reactions in their synthesis and having the source of chirality located very remote from the carbon cage, should be mentioned here, even though their stereogenic centers are already included in the starting materials.[398] For many other Diels-Alder and hetero–Diels-Alder adducts of fullerenes, we refer to the reviews mentioned in the introductory paragraph of this section.

e. [8 + 2] Cycloaddition. C_{60} was reported by Daub and co-workers to react with 8-methoxyheptafulvene in an [8 + 2] cycloaddition, affording a chiral, fullerene-fused tetrahydroazulene ((±)-**230**, Scheme 1.22).[399] As to the diastereoisomeric assignment, NOE measurements showed the two protons attached to sp^3-C-atoms to be *cis*-configured.

f. Miscellaneous Reactions and Adducts. Photoinduced addition of ketene silyl acetals (KSA) to C_{60} affords [60]fulleren-1(2*H*)-yl acetates (Scheme 1.23) in a reaction that probably proceeds via SET from the strongly electron-donating KSA to triplet excited C_{60}, recombination of the resulting radical ion pair, and cleavage of the silyl group by traces of water.[400,401] If the starting KSA is mono-substituted at C(2), a chiral adduct, such as (±)-**231** (Scheme 1.23) results.

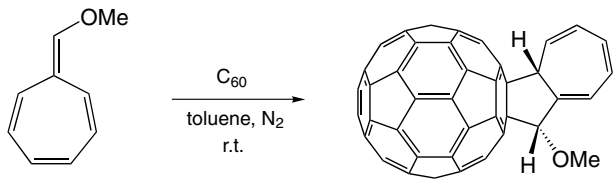

(±)-**230** (C_1)

Scheme 1.22. [8 + 2] Cycloaddition of 8-methoxyheptafulvene to C_{60}.

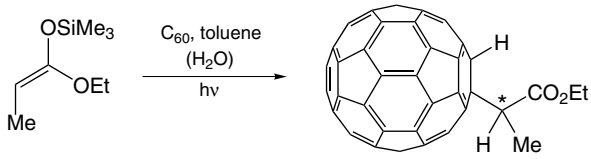

(±)- **231** (C_1)

Scheme 1.23. Photoinduced addition to C_{60} of ketene silyl acetals with two different substituents at C(2) and concomitant cleavage of the silyl group affords chiral fullerenylacetates.

Unexpected chiral adducts were formed in the thermal reaction of C_{60} with enamines such as *N*-cyclopent-1-enylpiperidine and *N*-cyclohex-1-enylpyrrolidine.[402] Fullerene derivatives with chiral side chains can also be obtained in nucleophilic substitution reactions between fullerenide ions and electrophiles such as halides having the leaving group attached to a stereogenic center.[403]

The photochemically induced addition of bulky disilanes to C_{60} has already been discussed in Section IV.A.1.h, as it affords the unusual inherently chiral 1,16-addition pattern ((±)-**72**, Figure 1.20). In this reaction some phenyl-substituted disilanes give rearranged adducts of the type (±)-**73** (Figure 1.20).[197,404] Further [60]fullerene derivatives with stereogenic centers in the addends were obtained in photoinduced addition-rearrangement reactions with 3,4-bis(alkylidene)-1,2-disilacyclobutanes,[405] and with octaaryl-substituted cyclotetrasilanes and -germanes.[406]

One of the obtained constitutional isomers of the trinuclear complex $[Os_3(CO)_{10}(MeCN)(\eta^2\text{-}C_{60})]$, in which the fullerene occupies an equatorial and the acetonitrile ligand an axial position at the same metal center of the Os_3-triangle, has been shown by VT ^{13}C NMR studies to exist at r.t. in a dynamic equilibrium between two enantiomeric forms. At 193 K the racemization process, formally consisting in a switching of the fullerene and a CO ligand between the two equatorial positions at the same metal center, becomes slow on the NMR time scale, and this is reflected by the appearance of 10 CO resonances in a sample prepared from ^{13}C-enriched carbon monoxide.[407]

A very interesting case of atropisomerism was detected by Komatsu and co-workers for (±)-**232** (Figure 1.48) obtained by nucleophilic addition of potassium fluorenide to C_{60}, carried out in the context of the preparation of the corresponding (uncharged) tetrakis-adduct which represents the first fullerene derivative with a fulvene substructure on the carbon spheroid.[408] After a reaction time of 24 hours, the pentakis-adduct anion (±)-**232** was formed as the main product. MM2 optimization of its structure shows the fluorene units to adopt a propeller type arrangement which, in conjunction with a sterically inhibited rotation, leads to a rare C_5-symmetric molecular structure as proved by ^1H and ^{13}C NMR spectroscopy. Protonation of the central

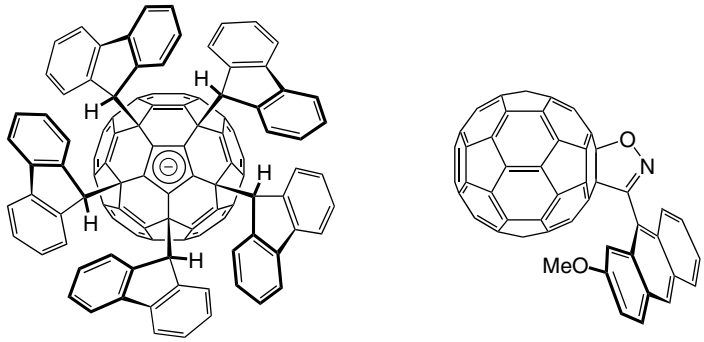

(±)-**232** (C_5) (±)-**233** (C_1)

Figure 1.48. C_5- ((±)-**232**) and C_1-symmetric ((±)-**233**) atropisomeric adducts of C_{60}.

cyclopentadienide substructure of (±)-**232** afforded an isolable adduct with the addition pattern of C_s-symmetric $C_{60}Ph_5H$ (**77**; Figure 1.20). Due to the persisting atropisomerism, however, the chiral fluorenide analogue of $C_{60}Ph_5H$ is C_1-symmetric. The formation of the above-mentioned C_s-symmetric fulvene derivative from potassium fluorenide and C_{60} after a reaction time of 72 h presumably occurs by irreversible one-electron oxidation of (±)-**232** by traces of oxygen and subsequent loss of a fluorene radical.[408]

Atropisomers exhibiting axial chirality[409] were obtained by Irngartinger and co-workers upon reaction of C_{60} with 2-methoxyanthracene-9-carbonitrile oxide.[410] Because of its close proximity to the fullerene sphere, the "unsymmetrically" substituted anthracene moiety of (±)-**233** (Figure 1.48) cannot rotate freely around the bond connecting it to the isoxazoline heterocycle, which leads to conformational enantiomers at r.t. Similarly addition of the "symmetrically" substituted bifunctional reagent 2,3,6,7-tetramethoxyanthracene-9,10-bis(carbonitrile oxide) to two C_{60} cages afforded two achiral dumbbell-shaped adducts presumed to be atropisomeric *syn*- and *anti* diastereoisomers.[410] Other chiral fullerene-fused isoxazolines with inherently and noninherently chiral addition patterns ((±)-**161**, Figure 1.37; (±)-**184**, Figure 1.43) or with a chiral appended group have been discussed in Sections IV.A.1.k, IV.B.1.c, and IV.B.2.b. (For a further case of fullerene-related conformational diastereoisomerism, cf. Section IV.C.2.g.)

2. *Attachment of Chiral Residues to C_{60} and C_{60} Derivatives*

In this section we present a number of C_{60} derivatives that have been prepared by addition of a chiral reagent to C_{60} or by coupling a chiral residue to a C_{60} derivative without creation of new stereogenic elements. Whereas most of

the fullerene-containing starting materials used in these transformations were either achiral or racemic, the added residues were often enantiomerically pure and included natural product constituents. Many of the obtained fullerene compounds were used to study biological activities and potential medicinal chemistry applications,[351,411] or advanced materials properties.[352,353]

a. Amino Acid and Peptide Conjugates. A large variety of amino acids and even a number of peptides derived from C_{60} have been prepared, and this class of compounds was recently reviewed.[412] A versatile fullerene building block for their synthesis is the achiral 1,2-methano[60]fullerene-61-carboxylic acid (**234**, Figure 1.49) which, upon coupling with enantiomerically pure amino acids under nonracemizing conditions, affords optically pure products, such as the L-phenylalanine derivative **235**.[237] Whereas the coupling of **234** with the amino acid occurs via the amino function of the latter, an ester-linkage can be achieved with alcohol (±)-**215** (Scheme 1.18) under formation of diastereoisomeric derivatives of enantiomerically pure amino acids, such as **236/237** (Figure 1.49).[374] A third, widely used building block for amino acid coupling includes fulleropyrrolidines[213] and fulleroprolines, the latter constituting themselves amino acids connected to the fullerene via their α-C-atom (cf. Figure 1.45).[241,346] Next to the direct coupling of amino acids to a functionalized fullerene, a number of amino acid syntheses starting from unmodified C_{60} have been reported. Examples, generally affording racemic amino acids, include the above-mentioned fulleroproline synthesis (cf. Scheme 1.15),[241,346] the addition of diazoamides to C_{60} followed by dinitrogen extrusion,[362] the cyclopropanation of C_{60} with *tert*-butyl *N*-(diphenylmethylene)glycinate/CBr_4/DBU and subsequent treatment of the adduct with $NaBH_3CN$ in mildly acidic medium,[413] hydrolysis of the [2 + 2] photocycloadduct of 1-(diethylamino)propyne and C_{60},[414] and the thermal or photochemical reaction of C_{60} with amino acid esters.[349]

The first fullerene-peptide conjugate, was reported by Prato and co-workers,[239] who contributed most of the work in this area.[249] Similarly to other

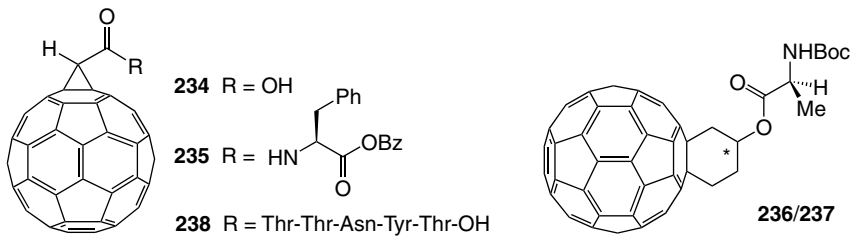

Figure 1.49. 1,2-methano[60]fullerene-61-carboxylic acid (**234**), C_{60}-amino acid conjugates (**235**, **236/237**), and C_{60}-peptide conjugate **238**.

Aib-rich (Aib = α-aminoisobutyric acid) short peptides, the pentapeptide H-(L-Ala-Aib)$_2$-L-Ala-OMe acylated at its N-terminus by a methano[60]fullerene-61-yl-substituted benzoic acid was shown by ^{1}H NMR and IR spectroscopy to predominantly adopt a 3_{10}-helix as secondary structure in $CDCl_3$ solution. The subsequently studied pentapeptide **238** (Figure 1.49)[240] corresponds to the hydrophilic residues 4 through 8 of peptide T which binds to the surface glycoprotein CD_4. It showed a remarkable chemotactic potency and efficiently stimulated monocyte-directed migration. Guldi, Maggini, and co-workers demonstrated that solvent-dependent conformational changes of a peptide spacer separating a $[Ru(bpy)_3]^{2+}$ donor unit from a fulleropyrrolidine acceptor dramatically influences the electron-transfer process occurring in the dyad upon excitation of the ruthenium chromophore.[415] A C_{60} derivative has finally been used as a thiol-selective reagent to label a surface cysteine-containing redox protein (azurin mutant S118C).[416] Electrochemical studies pointed toward the existence of interactions between the fullerene and the protein redox center.

b. Oligonucleotide Conjugates. Hélène and co-workers investigated a water-soluble oligonucleotide–C_{60} conjugate able to bind to complementary linear oligonucleotides (under duplex formation) or duplexes and hairpin structures (under triple-helix formation).[417] Upon irradiation the complementary strand was cleaved specifically at guanine sites close to the fullerene, and the experimental results were consistent with a cleavage by $^1O_2$ generated through C_{60}-mediated photosensitization. In a study by Rubin and co-workers, the [60]fullerene-linked deoxyoligonucleotide **239/240** (Figure 1.50) was hybridized with a complementary single-stranded DNA. In the presence of light and oxygen, it specifically cleaved guanosines in the proximity of the fullerene.[418] By comparison experiments with an eosin-oligonucleotide conjugate and by the use of singlet oxygen quenchers, the authors demonstrated that the cleavage

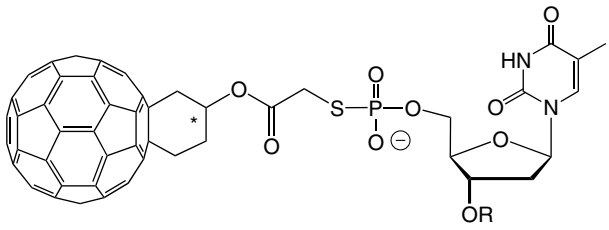

239/240 R = CTAACGACAATATGTACAAGCCTAATTGTGTAGCATCT-3′

Figure 1.50. Diastereoisomeric C_{60}-oligonucleotide conjugates **239/240** including the racemic fullerene-alcohol buliding block (±)-**215** (Scheme 1.18).

did not involve $^1O_2$ as the active agent but rather implied a SET between guanosine and $^3C_{60}$, followed by hydrolytic degradation.

c. Glycoconjugates. In 1992 Diederich, Vasella, and co-workers prepared the first fullerene-sugar derivatives by addition of nucleophilic glycosilidene carbenes to C_{60}.[23] The spiro-linked *C*-glycosides, such as **241** (Figure 1.51), represent the first enantiomerically pure fullerene adducts, and their deprotection was expected to generate amphiphiles able to form stable monolayers at the air-water interface. Systematic Langmuir-Blodgett and thin-film investigations on various systems showed that next to a strong hydrophilicity, a voluminous head group is useful in preventing irreversible association of the fullerene spheres, which have a strong tendency to aggregate.[419] This goal was best achieved by attachment of carbohydrate-containing dendrons to the carbon cage, leading to stable and reversible monolayers that could be transferred onto quartz slides by the Langmuir-Blodgett technique.[420]

Another practical synthetic approach to fullerene glycoconjugates consists in the [3 + 2] cycloaddition of protected glycosylazides to C_{60} with subsequent nitrogen extrusion, affording *N*-glycosyl-substituted 1(6)a-aza-1(6)a-homo[60]fullerenes.[421,422] Using this route, Kobayashi and co-workers reacted C_{60} with per-*O*-acetylated azides of D-glucopyranose, D-galactopyranose, lactose, maltose, and maltotriose, and obtained a mixture of two stereoisomers in each case.[421] A third method for the attachment of a sugar moiety to unmodified C_{60} uses the azomethine ylide [3 + 2] cycloaddition,[213] starting from a formyl *C*-glycoside and, for example, *N*-methylglycine (sarcosine); it affords diastereoisomeric adducts.[423] The coupling of sugar derivatives to functionalized fullerenes, on the other hand, has been achieved by reaction of 1,2:3,4-di-*O*-isopropylidene-D-galactopyranose-6-chloroformate to 1,2-epimino[60]fullerene[424] or by acid-catalyzed addition of a fullerene-alcohol conjugate to an acetyl-protected glycal. The latter reaction yielded a mixture of the anomers **242** and **243**, Figure 1.51.[425]

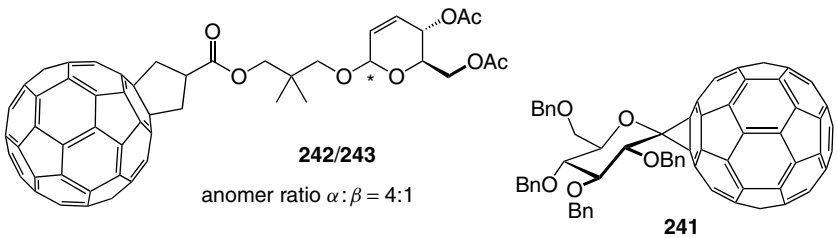

Figure 1.51. *C*-Glycoside **241**, the first enantiomerically pure adduct of C_{60}, and a fullerene-glycoconjugate obtained as a mixture of anomers (**242/243**).

The use of D-glyceraldehyde derivatives in the preparation of an enantiomerically pure C_{60}-fused isoxazoline[317] or in a diastereoselective [3 + 2] cycloaddition of an azomethine ylide (cf. Figure 1.45)[245] has been described in Sections IV.B.1.c and IV.C.1.c, respectively. L-Threitol and other sugar derivatives have been used as imprinting templates in the regio- and diastereoselective functionalization of C_{60} (cf. Scheme 1.6 and Section IV.A.1.c).[147–149] It should finally be mentioned that much work has been devoted to the study of the 2 : 1 inclusion complexes between γ-cyclodextrin and C_{60}.[426,427] Medium-intensity Cotton effects (Δε-values up to 12 M^{-1} cm^{-1} at $\lambda = 230$ and 258 nm) were proposed to be induced by the nonchromophoric cyclodextrin molecules in the achiral fullerene chromophore.[427]

d. Terpene Conjugates. Chiral methyl([60]fulleren-1(2*H*)-yl)phenylphosphane ((±)-**244**, Figure 1.52) was synthesized by Nakamura and coworkers by addition of $MePhPLi \cdot BH_3$ to C_{60}, followed by protonation and removal of the borane unit with DABCO (1,4-diazabicyclo[2.2.2]octane).[428] As the optically active reagent racemized even at a reaction temperature of −40°C, the adduct was obtained as an enantiomeric mixture. Optically pure phosphinites (**245** and **246**, Figure 1.52) were obtained on the other hand by addition of the diastereoisomerically pure, *P*-chiral (+)-menthyl phosphinite-borane complexes **247** and **248**, respectively, to C_{60} and subsequent removal of the borane group. As proved by ^1H NMR spectroscopy, addition took place stereospecifically, most probably with retention of configuration at the phosphorus atom. A palladium complex of **245**, prepared by treatment with 0.5 eq. $PdCl_2(PhCN)_2$, catalyzed, albeit with low enantiomeric excess (8%), an enantioselective cross-coupling of 1-phenyl-1-ethylmagnesium bromide and β-bromostyrene to 1,3-diphenylbut-1-ene.[428]

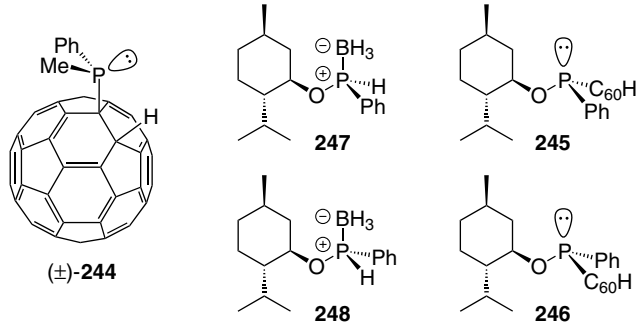

Figure 1.52. Racemic fullerenyl-substituted phosphane (±)-**244**, and stereoisomerically pure *P*-chiral fullerenyl-substituted phosphinites **245** and **246**, obtained via addition to C_{60} of diastereoisomerically pure, (+)-menthyl phosphinite-borane complexes **247** and **248**, respectively.

Further C_{60} derivatives of menthol include a menthyl malonate adduct[119] and a carbamate derived from 1,2-epimino[60]fullerene.[429] Resin acid derivatives have been prepared by Diels-Alder reaction of C_{60} with methyl levopimarate, whose parent acid can be isolated from rosin.[430] Finally, a derivative of α-pinene was synthesized in the context of a study on the photochemically induced addition of allyl stannanes to C_{60}, a reaction presumably proceeding via SET from the stannane to the triplet excited fullerene.[431]

e. Steroid Conjugates. Cholesterol, the most frequently used steroid in fullerene derivatization, was appended to C_{60} in several cases to illustrate the synthetic versatility of a reactive fullerene-containing building block.[432] Deschenaux and co-workers incorporated this steroid in the first fullerene-derived thermotropic liquid crystal (**249**, Figure 1.53).[433] In combination with additional, electroactive groups like ferrocene, C_{60}-containing liquid crystals[434,435] are attractive in view of the construction of novel electro-optical devices.[436] Cholesteryl esters derived from 1,2-methano- and 1,2-homo[60]fullerene were synthesized by Hummelen and co-workers and blended with conjugated polymers such as MEH-PPV (poly[2-methoxy-5-(2′-ethylhexyloxy)-1,4-phenylene vinylene]) to investigate the photoinduced electron transfer between the two components.[363,437]

4,5-Dihydrotestosterone was used as a spacer component in the preparation of the [60]fullerene-tris(2,2′-bipyridine)ruthenium(II) dyad **250/251** (Figure 1.54) which was obtained as a diastereoisomeric mixture and used for photoinduced electron transfer studies.[438] The rigid structure of the steroid backbone favors a "through-bond"-mediated electron transfer between the donor and the acceptor chromophores, in contrast to an "intramolecular exciplex" mechanism active in a related dyad with a flexible polyethylene glycol-based spacer.[439] As a consequence, the lifetime of the radical pair $C_{60}^{\bullet -}/[Ru(bpy)_3]^{3+}$ in the latter dyad is negligible compared to the 304 ns measured for **250/251** (CH_2Cl_2 solutions).[356,438] Investigating

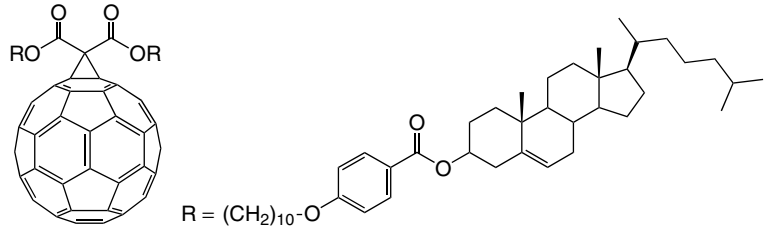

249

Figure 1.53. A C_{60}-cholesterol conjugate, representing the first fullerene-containing thermotropic liquid crystal.

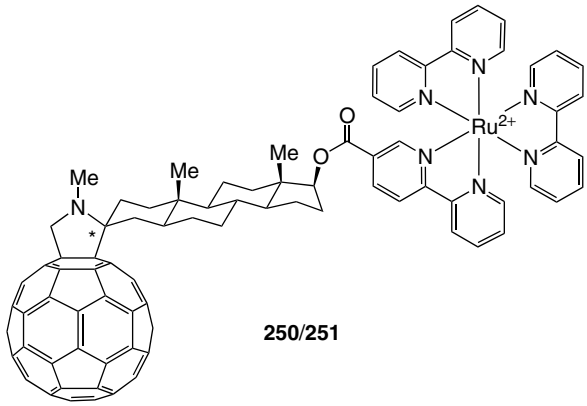

250/251

Figure 1.54. A bichromophoric dyad used for photoinduced electron transfer studies and obtained as a mixture of diastereoisomers. It includes a 1,2-dihydro[60]fullerene acceptor, a $[Ru(bpy)_3]^{2+}$ donor unit, and a rigid spacer derived from 4,5-dihydrotestosterone. (The asterisk marks the stereogenic center giving rise to the diastereoisomerism.)

the quenching of the porphyrin fluorescence in three dyads connecting a tetraphenylporphyrin to a [60]fullerene-fused pyrrolidine via spacers derived from 5α-dihydrotestosterone, testosterone, or 6-dehydrotestosterone, Schuster and co-workers concluded on significant through-bond interactions between the rigidly fixed chromophores.[440]

Addition of the enolate of the hindered 17-*tert*-butyldimethylsilyl-protected testosterone was successfully used by Rubin, Kenyon, and co-workers to prove the efficiency of sequential double Michael-type additions to C_{60} (cf. Section IV.C.1.d and Scheme 1.20).[378] Fullerene-steroid conjugates derived from vitamin D, cholesterol, testosterone, and estrone were, finally, reported by Wilson, Schuster, and co-workers.[411]

For the addition to C_{60} of two *o*-quinodimethane groups linked by tethers including methyl deoxycholate, hyodeoxycholate, and chenodeoxycholate units, we refer to Section IV.A.1.c.[151]

f. Derivatives of Tartaric Acid and Threitol. Most of the compounds discussed in this section include an optically pure threitol(-derived) unit, which can easily be obtained from the corresponding tartaric acid. The use of threitol derivatives as chiral auxiliaries in a diastereoselective Diels-Alder addition to C_{60} (cf. Section IV.C.1.d and Scheme 1.21),[385] and in templated regio- and diastereoselective double Bingel additions to C_{60} (cf. Section IV.A.1.c, and Schemes 1.4 and 1.6)[117,125,129,147–149] has already been addressed.

Rare examples of organometallic fullerene derivatives with a chiral ligand are the enantiomerically pure complexes $[(\eta^2\text{-}C_{60})Pt((+)\text{-DIOP})]$ (DIOP =

4,5-bis[(diphenylphosphano)methyl]-2,2-dimethyl-1,3-dioxolane), its palladium analogue, as well as the C_{70}-adduct [(η^2-C_{70})Pt((+)-DIOP)].[251] The crystal structure of the first complex was solved in the form of its solvate with (*Z*)-cyclooctene.

By addition of enantiomeric bis-azides derived from (+)- and (−)-threitol to C_{60} and subsequent dinitrogen extrusion, Luh and co-workers obtained optically pure 1(6)a,7(8)a-diaza-1(6)a,7(8)a-bishomo[60]fullerene derivatives with bridged nitrogen atoms inserted in the two 6–5 junctions of a fluorene substructure on the fullerene surface (adducts related to **252**, Scheme 1.24).[244] Accordingly, the use of bis-azide **253** (Scheme 1.24), prepared from 2,3-*O*-isopropylidene-L-threitol, afforded C_1-symmetric bis-adduct **252** which is stable for weeks in the dark.[252] Under the influence of ambient light, however, the bridged diaza-bishomo[60]fullerene **252** rearranges regioselectively to **254**, as shown among others by analysis of ^{13}C NMR C–N couplings of ^{15}N-labeled material. Thermolysis of **254**, finally, cleanly converts the molecule back to the isomeric **252**, thus providing the first example of interconvertible azahomo-/epiminofullerene isomers.

Addition of α-diazoketones derived from (*R*,*R*)-tartaric and (*S*)-glutamic acids, followed by dinitrogen extrusion, afforded enantiomerically pure 1,2-methano[60]fullerenes with an acylated methylene bridge.[441] Bestmann and co-workers showed that these adducts can be thermally rearranged to substituted fullerene-fused dihydrofurans.

g. Chlorin Conjugates. Among the many C_{60}-porphyrin electron donor-acceptor dyads[130,354–356] there is hardly an example in which chiral elements are located in the porphyrin moiety.[442] Recently, however, some achiral[443] and chiral[444,445] chlorin-based dyads have been reported. Chlorin-based dyads

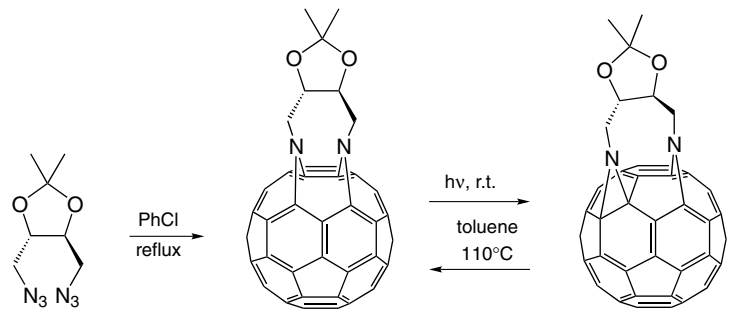

253 (C_2) **252** (C_1) **254** (C_1)

Scheme 1.24. Regioselective addition to C_{60} of a 2,3-*O*-isopropylidene-L-threitol-tethered bis-azide under formation of diaza-bishomo-[60]fullerene **252**, and regioselective interconversion between the azahomo- (**252**) and the epiminofullerene (**254**) isomers.

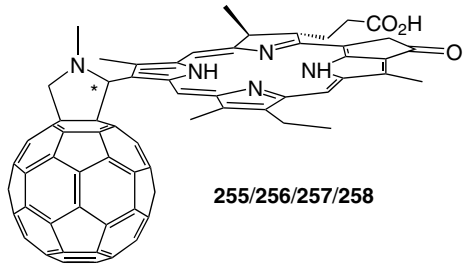

Figure 1.55. C_{60}-chlorin dyad obtained as mixture of four diastereoisomers that result from configurational (the asterisk marks the stereogenic center in question) and conformational diastereoisomerism (resulting from hindered rotation around the bond connecting the chlorin unit to the pyrrolidine ring).

have the photophysical advantage over the more symmetric porphyrins of substantially stabilized S_1 energies and a long-wavelength Q_y band that can be used for excitation. From a stereochemical viewpoint, one of these systems (**255**–**258**, Figure 1.55) is particularly interesting: Synthesized via azomethine ylide addition to the fullerene,[213] starting from an enantiomerically pure, phytochlorin-derived aldehyde and sarcosine, it gives rise to diastereoisomerism related to the configuration of the newly formed stereogenic center in the C_{60}-fused pyrrolidine ring.[444] In addition, hindered rotation around the bond connecting the latter to the chlorin unit causes each of the configurational diastereoisomers to occur as two atropisomers, thus leading to a total of four diastereoisomers at r.t. ^{1}H NMR ROESY spectroscopy allowed a complete assignment of the resonances of each isomer. Among the total of four rotational barriers determined by dynamic NMR measurements, one amounted to 21.4(5) kcal/mol and the other three to 23.0(8) kcal/mol.[444]

3. Higher Fullerene Derivatives with Stereogenic Elements Located Exclusively in the Addends

This category comprises only a handful of compounds, most of which are adducts of C_{70}, such as (*S*,*S*,*S*,*S*)-**105** and (*R*,*R*,*R*,*R*)-**105** (Figure 1.26),[35,54] presented in Section IV.A.2.e together with congeners displaying an inherently chiral addition pattern; (±)-**188** (Figure 1.43) resulting from rearrangement of the achiral primary adducts **185** and **186** (cf. Section IV.B.2.b);[335,336] and a transition metal complex with an optically pure ligand, [(η^2-C_{70})Pt((+)-DIOP)] (cf. Section IV.C.2.f).[251] Among the higher fullerenes beyond C_{70}, only the achiral homologues can give rise to the type of adducts discussed here, and a unique example, derived from D_{2d}-C_{84}, is known so far.

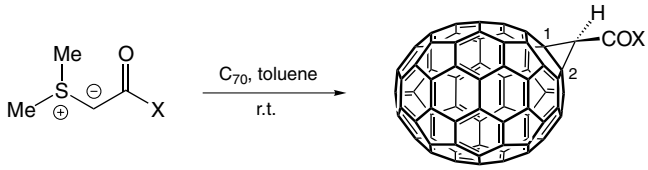

(±)-**259** X = NEt_2 (C_1)
(±)-**260** X = O*t*-Bu (C_1)

Scheme 1.25. Racemic amide ((±)-**259**) and ester ((±)-**260**) of 1,2-methano[70]fullerene-71-carboxylic acid obtained through addition of the corresponding sulfonium ylides to C_{70}.

a. Adducts of C_{70}. 1,2-Methano[60]fullerene derivatives are C_{2v}-symmetric if the substituents of the methylene bridge are achiral and identical, and C_s-symmetric if they are different. Due to a lower local symmetry of the reaction site, the corresponding C_{70} derivatives in which addition took place across the most reactive 6–6 bond C(1)–C(2) (cf. Scheme 1.25), are C_s- and C_1-symmetrical for two identical and two different achiral methano-bridge substituents, respectively. The latter case was realized by Wang, Schuster, Wilson, and Welch through addition of stabilized sulfoniun ylides to [70]fullerene which yielded various derivatives of 1,2-methano[70]fullerene-71-carboxylic acid (Scheme 1.25).[243] Among these, the *N*,*N*-diethyl amide (±)-**259** could be resolved by HPLC on an (*S*,*S*)-Whelk-O column.

Condensing racemic 1,2-methano[70]fullerene-71-carboxylic acid obtained by hydrolysis of its *tert*-butyl ester ((±)-**260**, Scheme 1.25),[243] with an amino derivative of zinc tetraphenylporphyrin, Imahori, Yamazaki, Sakata, and co-workers synthesized a C_{70}-containing dyad.[355,446] Comparison with the C_{60}-analogue showed that photoinduced electron transfer from the singlet excited Zn-porphyrin to the fullerene is faster in the C_{70} derivative.

A racemic, bichromophoric C_{70}-pyrene conjugate showing intramolecular photo-induced energy transfer from the excited singlet state of the PAH to the fullerene has been reported by Daub and co-workers.[383] Its chirality is based on the stereogenic center resulting from reduction of a fullerene-fused cyclohexanone, itself obtained by Diels-Alder addition of 2-[(trimethylsilyl)oxy]buta-1,3-diene to the C(1)–C(2) bond of C_{70} and subsequent hydrolysis of the formed silyl enol ether (cf. Section IV.C.1.d and Scheme 1.18).

From the [8 + 2] cycloaddition of 8-methoxyheptafulvene to C_{70}, the same group isolated a chiral isomer for which they proposed a C(1)–C(2) adduct structure (C_{70}-analogue of (±)-**230**; cf. Scheme 1.22).[246] The same regioisomer was identified by Taylor and co-workers as the main product of the [4 + 2] cycloaddition of pentamethyl cyclopentadiene to C_{70}.[447] A C_1-symmetric Diels-Alder adduct is, finally, expected from the reaction of C_{70} with 2-[(ferrocenyl)methylene]-3-methylenequinuclidine.[448]

b. Adducts of D_{2d}-C_{84}. In our work on the isolation and characterization of constitutional and configurational isomers of C_{84} by use of the Bingel-retro-Bingel strategy (cf. Section III.C), we reacted the isomeric mixture of this fullerene with optically pure, C_2-symmetric bis[(*S*)-1-phenylbutyl] malonate in the presence of DBU and isolated, among others (cf. Sections III.C and IV.A.3.b), a C_2-symmetric mono-adduct and a D_2-symmetric bis-adduct of [84]fullerene.[60] The weak Cotton effects ($\Delta\varepsilon$ up to 3 M^{-1} cm^{-1}) of the mono-adduct were indicative of a derivative of the achiral parent D_{2d}-C_{84} (cf. Sections III.C, IV.A.1.b, and IV.A.2.e). Furthermore analysis of the structures resulting from addition of a C_2-symmetric addend to one of the 10 most curved bonds of D_{2d}-C_{84} left **132** (Scheme 1.26) as the only possible structure for the C_2-symmetric mono-adduct. It results from addition across the same C(32)–C(53) bond as the previously reported complex [[η^2-(D_{2d}-C_{84})]Ir(CO)Cl(PPh_3)$_2$]· 4C_6H_6.[67] The D_2-symmetric bis-adduct afforded D_{2d}-C_{84} in the retro-Bingel reaction (Scheme 1.26) and also displayed weak Cotton effects ($\Delta\varepsilon < 3$ M^{-1} cm^{-1}). Therefore it had to be a derivative of D_{2d}-C_{84} with an achiral functionalization pattern, and in combination with the NMR data, this unambiguously supported the formation of **133** (Scheme 1.26). The regioisomer results from cyclopropanation of the bonds C(32)–C(53) and C(42)–C(43), each of which is included in one and bisected by the other mirror plane of the parent fullerene.[60] It is reasonable to assume that **133** is formed by cyclopropanation of **132**. Compounds **132** and **133** are the first fully characterized organic derivatives of C_{84}.

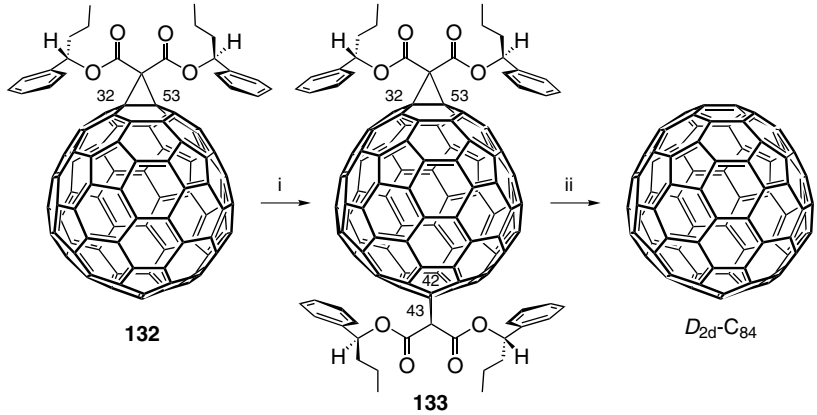

i = bis[(*S*)-1-phenylbutyl]-2-bromomalonate, DBU, *o*-DCB
ii = controlled potential electrolysis, CH_2Cl_2

Scheme 1.26. Formation of the D_2-symmetric bis-adduct **133** of D_{2d}-C_{84} from C_2-symmetric mono-adduct **132** and generation of the parent fullerene by electrochemical retro-Bingel reaction.

V. CONCLUSION

Although fullerene chemistry has only been pursued for a decade, it has produced an exceptional variety of achiral as well as chiral compounds, a fact reflected by a great deal of the nearly 10^4 papers published on the carbon spheroids since 1990.[449] The distinction between inherently chiral and non-inherently chiral fullerene functionalization patterns has been very helpful in the analysis of many chiral structures derived from the three-dimensional fullerene building blocks having geometries that were unfamiliar to many chemists. Furthermore the configurational description of chiral fullerenes and fullerene derivatives with a chiral functionalization pattern by a single, easily computable descriptor, independently of the number of addends or core-resident stereogenic centers, allows a convenient condensation of structural information.

On the other hand, the experimental investigation of the chiroptical properties of chiral fullerenes and fullerene derivatives has been hampered by the difficult resolution of many compounds. An original solution to this problem has been the generation of chiral, enantiomeric fullerene addition patterns by introduction of configurationally homogeneous chiral addends, leading to a series of (generally) separable isomers not including any enantiomeric pair. Repetition of the reaction with a reagent of opposite configuration separately affords an enantiomeric set to the first. Another technique that, besides the kinetic resolution, has proved very valuable in the separation of right- and left-handed carbon cages is the reversible introduction of a chiral auxiliary and the separation of the diastereoisomeric intermediates. Conceptually this strategy may appear as classical, but it has to be kept in mind that the synthetic methodology for the reversible functionalization of fullerenes, such as the Bingel-retro-Bingel sequence, is available only for a relatively short time. An advantage in the investigation of the chiroptical properties of fullerene derivatives including a chiral π-chromophore in addition to stereogenic centers in the addends is the enormity of the Cotton effects of the former, outranging the contribution of the latter often by two orders of magnitude. This means that stereogenic centers in the side chains can often be neglected, or that diastereoisomeric fullerene derivatives with enantiomeric functionalization patterns but identically configured addend moieties show (nearly) mirror-image-shaped CD spectra.

Further explorations should be done in the stereoselective synthesis of chiral fullerene derivatives, a field initiated by the kinetic resolution of D_2-C_{76} through diastereoselective osmylation with OsO_4 in the presence of alkaloid-derived ligands. Besides, a few diastereoselective macrocyclizations by bridging of C_{60} with enantiomerically pure, bifunctional reagents have been achieved with high *d.e.*'s. The use of optically pure fullerene derivatives as bulky chiral auxiliaries

with uncommon steric arrangements of functionalities has barely been tested so far.

Configurational assignments of chiral fullerenes or of fullerene derivatives with a chiral addition pattern by comparison of the experimental to theoretically calculated CD spectra have been possible in only a few cases. Practicable and reliable methods for the calculation of the Cotton effects of the large fullerene chromophores are only beginning to emerge. We hope that their further development will be spurred by these encouraging first results.

ACKNOWLEDGMENTS

We pleasantly remember stimulating discussions on chirality and configurational descriptors with Professor Vladimir Prelog. Our work was supported by the Swiss National Science Foundation. We thank Hoechst AG for samples of pure C_{70} and fullerene-soot extract enriched in higher fullerenes.

REFERENCES

1. Diederich, F.; Ettl, R.; Rubin, Y.; Whetten, R. L.; Beck, R.; Alvarez, M.; Anz, S.; Sensharma, D.; Wudl, F.; Khemani, K. C.; Koch, A. *Science* **1991**, *252*, 548–551.
2. Ettl, R.; Chao, I.; Diederich, F.; Whetten, R. L. *Nature* **1991**, *353*, 149–153.
3. Krätschmer, W.; Lamb, L. D.; Fostiropoulos, K.; Huffman, D. R. *Nature* **1990**, *347*, 354–358.
4. Hawkins, J. M.; Meyer, A. *Science* **1993**, *260*, 1918–1920.
5. Hawkins, J. M.; Nambu, M.; Meyer, A. *J. Am. Chem. Soc.* **1994**, *116*, 7642–7645.
6. Kessinger, R.; Crassous, J.; Herrmann, A.; Rüttimann, M.; Echegoyen, L.; Diederich, F. *Angew. Chem. Int. Ed. Engl.* **1998**, *37*, 1919–1922.
7. Goto, H.; Harada, N.; Crassous, J.; Diederich, F. *J. Chem. Soc., Perkin Trans. 2* **1998**, 1719–1723.
8. Manolopoulos, D. E. *J. Chem. Soc., Faraday Trans.* **1991**, *87*, 2861–2862.
9. Fowler, P. W.; Batten, R. C.; Manolopoulos, D. E. *J. Chem. Soc., Faraday Trans.* **1991**, *87*, 3103–3104.
10. Manolopoulos, D. *Scientist* **1993**, *7*, 16.
11. Fowler, P. W.; Manolopoulos, D. E. *An Atlas of Fullerenes*. Clarendon Press, Oxford, **1995**.
12. Special Issue on Nanotubes *Carbon* **1995**, *33*, 869–1016. Dresselhaus, M. S.; Dresselhaus, G.; Eklund, P. C. *Science of Fullerenes and Carbon Nanotubes*. Academic Press, San Diego, **1996**. Ebbesen, T. W. *Acc. Chem. Res.* **1998**, *31*, 558–566. Ajayan, P. M. *Chem. Rev.* **1999**, *99*, 1787–1799. Edelmann, F. T. *Angew. Chem. Int. Ed. Engl.* **1999**, *38*, 1381–1387.
13. Hu, J. T.; Odom, T. W.; Lieber, C. M. *Acc. Chem. Res.* **1999**, *32*, 435–445.
14. Hirsch, A. *The Chemistry of the Fullerenes*. Thieme Verlag, Stuttgart, **1994**.
15. Diederich, F.; Thilgen, C. *Science* **1996**, *271*, 317–323. Diederich, F. *Pure Appl. Chem.* **1997**, *69*, 395–400.
16. Hirsch, A. *Top. Curr. Chem.* **1999**, *199*, 1–65.
17. Thilgen, C.; Herrmann, A.; Diederich, F. *Angew. Chem. Int. Ed. Engl.* **1997**, *36*, 2269–2280. Thilgen, C.; Diederich, F. *Top. Curr. Chem.* **1999**, *199*, 135–171.

18. Rapenne, G.; Crassous, J.; Echegoyen, L. E.; Echegoyen, L.; Flapan, E.; Diederich, F. *Helv. Chim. Acta* **2000**, *83*, 1209–1223.
19. Diederich, F.; Whetten, R. L.; Thilgen, C.; Ettl, R.; Chao, I.; Alvarez, M. M. *Science* **1991**, *254*, 1768–1770.
20. Kikuchi, K.; Nakahara, N.; Wakabayashi, T.; Suzuki, S.; Shiromaru, H.; Miyake, Y.; Saito, K.; Ikemoto, I.; Kainosho, M.; Achiba, Y. *Nature* **1992**, *357*, 142–145.
21. Taylor, R.; Langley, G. J.; Dennis, T. J. S.; Kroto, H. W.; Walton, D. R. M. *J. Chem. Soc., Chem. Commun.* **1992**, 1043–1046.
22. Diederich, F.; Thilgen, C.; Herrmann, A. *Nachr. Chem. Tech. Lab.* **1996**, *44*, 9–16.
23. Vasella, A.; Uhlmann, P.; Waldraff, C. A. A.; Diederich, F.; Thilgen, C. *Angew. Chem. Int. Ed. Engl.* **1992**, *31*, 1388–1390. Uhlmann, P.; Harth, E.; Naughton, A. B.; Vasella, A. *Helv. Chim. Acta* **1994**, *77*, 2335–2340.
24. This is valid for the geometrical arrangement not only of addends, but also of heteroatoms or specific isotopes replacing C-atoms of the fullerene core. For the ease of reading, this will not be stressed each time in the following discussions.
25. Thilgen, C.; Herrmann, A.; Diederich, F. *Helv. Chim. Acta* **1997**, *80*, 183–199.
26. *Tetrahedron Symposia-in-Print Number 60, Fullerene Chemistry*. Elsevier Science, Oxford, **1996**.
27. Samal, S.; Sahoo, S. K. *Bull. Mater. Sci.* **1997**, *20*, 141–230.
28. *Topics in Current Chemistry,* Vol. 199 *(Fullerenes and Related Structures)*. Springer-Verlag, Berlin, **1999**.
29. *Proceedings of the Symposium on Recent Advances in the Chemistry and Physics of Fullerenes and Related Materials*, Vol. 1–6; Kadish, K. M.; Ruoff, R. S., eds. The Electrochemical Society Inc., Pennington, NJ, **1994–1998**. *Proceedings of the Symposium on Recent Advances in the Chemistry and Physics of Fullerenes and Related Materials*, Vol. 7. Kadish, K. M.; Kamat, P. V., eds. The Electrochemical Society Inc., Pennington, NJ, **1999**.
30. Taylor, R. *Lecture Notes on Fullerene Chemistry: A Handbook for Chemists*. Imperial College Press, London, **1999**.
31. Cahn, R. S.; Ingold, S. C.; Prelog, V. *Angew. Chem. Int. Ed. Engl.* **1966**, *5*, 385–415; errata ibid. p. 511.
32. Prelog, V.; Helmchen, G. *Angew. Chem. Int. Ed. Engl.* **1982**, *21*, 567–583.
33. A nomenclature system proposed for C_{60} derivatives, which is based on edge labeling of the icosahedron and allows even a configurational description of chiral molecules, does not appear to lead to a more intuitive operation; cf. Nakamura, Y.; Taki, M.; Nishimura, J. *Chem. Lett.* **1995**, 703–704.
34. The potential situation of addends pointing toward the center of the spheroid could be handled in analogy to that of bridgehead substituents of macrobi- or -polycyclic systems by additional stereodescriptors, such as *in/out*, or *endo/exo*.
35. Herrmann, A.; Rüttimann, M.; Thilgen, C.; Diederich, F. *Helv. Chim. Acta* **1995**, *78*, 1673–1704.
36. Godly, E. W.; Taylor, R. *Pure Appl. Chem.* **1997**, *69*, 1411–1434.
37. Goodson, A. L.; Gladys, C. L.; Worst, D. E. *J. Chem. Inform. Comput. Sci.* **1995**, *35*, 969–978.
38. A proposed structural description of chiral fullerene derivatives using a bond-labeling algorithm eventually also relies on the helicity of the fullerene numbering schemes.[110]
39. Panico, R.; Powell, W. H. In *A Guide to IUPAC Nomenclature of Organic Compounds*. Richer, J.-C., ed. Blackwell Scientific, Oxford, **1993**.
40. The configuration of C_{60} and C_{70} derivatives with a chiral functionalization pattern can easily be computed via the interactive Website *www.diederich.chem.ethz.ch/chirafull*.
41. Suzuki, T.; Li, Q. C.; Khemani, K. C.; Wudl, F. *J. Am. Chem. Soc.* **1992**, *114*, 7301–7302.
42. Diederich, F.; Isaacs, L.; Philp, D. *Chem. Soc. Rev.* **1994**, *23*, 243–255.

43. Smith III, A. B.; Strongin, R. M.; Brard, L.; Furst, G. T.; Romanow, W. J.; Owens, K. G.; Goldschmidt, R. J.; King, R. C. *J. Am. Chem. Soc.* **1995**, *117*, 5492–5502.
44. Haldimann, R. F.; Klärner, F. G.; Diederich, F. *Chem. Commun.* **1997**, 237–238.
45. Birkett, P. R.; Avent, A. G.; Darwish, A. D.; Kroto, H. W.; Taylor, R.; Walton, D. R. M. *J. Chem. Soc., Chem. Commun.* **1995**, 1869–1870.
46. Hummelen, J. C.; Bellavia-Lund, C.; Wudl, F. *Top. Curr. Chem.* **1999**, *199*, 93–134.
47. Hirsch, A.; Nuber, B. *Acc. Chem. Res.* **1999**, *32*, 795–804.
48. Rubin, Y. *Chem. Eur. J.* **1997**, *3*, 1009–1016.
49. Rubin, Y. *Chimia* **1998**, *52*, 118–126.
50. Herrmann, A.; Diederich, F.; Thilgen, C.; ter Meer, H.-U.; Müller, W. H. *Helv. Chim. Acta* **1994**, *77*, 1689–1706.
51. Hirsch, A.; Lamparth, I.; Karfunkel, H. R. *Angew. Chem. Int. Ed. Engl.* **1994**, *33*, 437–438.
52. If the difference consists only in the enantiomorphism of addends, pseudo-asymmetric addition patterns may result (cf. Section IV.B.1.a).
53. Fukuzumi, S.; Suenobu T.; Hirasaka, T.; Arakawa R.; Kadish, K. M. *J. Am. Chem. Soc.* **1998**, *120*, 9220–9227.
54. Herrmann, A.; Rüttimann, M. W.; Gibtner, T.; Thilgen, C.; Diederich, F.; Mordasini, T.; Thiel, W. *Helv. Chim. Acta* **1999**, *82*, 261–289.
55. Kroto, H. W.; Heath, J. R.; O'Brien, S. C.; Curl, R. F.; Smalley, R. E. *Nature* **1985**, *318*, 162–163. Schmalz, T. G.; Seitz, W. A.; Klein, D. J.; Hite, G. E. *Chem. Phys. Lett.* **1986**, *130*, 203–207. Kroto, H. W. *Nature* **1987**, *329*, 529–531.
56. Diederich, F.; Whetten, R. L. *Acc. Chem. Res.* **1992**, *25*, 119–126. Thilgen, C.; Diederich, F.; Whetten, R. L. In *Buckminsterfullerenes*. Billups, W. E.; Ciufolini, M. A., eds. VCH Publishers, New York, **1993**, pp. 59–81.
57. Taylor, R.; Langley, G. J.; Avent, A. G.; Dennis, T. J. S.; Kroto, H. W.; Walton, D. R. M. *J. Chem. Soc., Perkin Trans. 2* **1993**, 1029–1036.
58. Achiba, Y.; Kikuchi, K.; Aihara, Y.; Wakabayashi, Y.; Miyake, Y.; Kainosho M. in *Higher Fullerenes: Structure and Properties (Mater. Res. Soc. Symp. Proc.*, Vol. 359). Bernier, P.; Bethune, D. S.; Chiang, L. Y.; Ebbesen, T. W.; Metzger, R. M.; Mintmire, J. W., eds. Materials Research Society, Pittsburgh, **1995**, pp. 3–9.
59. Michel, R. H.; Kappes, M. M.; Adelmann, P.; Roth, G. *Angew. Chem. Int. Ed. Engl.* **1994**, *33*, 1651–1654.
60. Crassous, J.; Rivera, J.; Fender, N. S.; Shu, L. H.; Echegoyen, L.; Thilgen, C.; Herrmann, A.; Diederich, F. *Angew. Chem. Int. Ed. Engl.* **1999**, *38*, 1613–1617.
61. Wakabayashi, T.; Kikuchi, K.; Suzuki, S.; Shiromaru, H.; Achiba, Y. *J. Phys. Chem.* **1994**, *98*, 3090–3091.
62. Herrmann, A.; Diederich, F. *J. Chem. Soc., Perkin Trans. 2* **1997**, 1679–1684.
63. Boudon, C.; Gisselbrecht, J.-P.; Gross, M.; Herrmann, A.; Rüttimann, M.; Crassous, J.; Cardullo, F.; Echegoyen, L.; Diederich, F. *J. Am. Chem. Soc.* **1998**, *120*, 7860–7868.
64. Hennrich, F. H.; Michel, R. H.; Fischer, A.; Richard-Schneider, S.; Gilb, S.; Kappes, M. M.; Fuchs, D.; Bürk, M.; Kobayashi, K.; Nagase, S. *Angew. Chem. Int. Ed. Engl.* **1996**, *35*, 1732–1734.
65. Kobayashi, K.; Nagase, S.; Akasaka, T. *Chem. Phys. Lett.* **1995**, *245*, 230–236.
66. The present notation for the isomers corresponds to that proposed by Godly and Taylor.[36] The correspondence with the designations of Fowler[11] is the following: D_2(IV)–C_{84} = D_2(22)–C_{84} and D_{2d}(II)–C_{84} = D_{2d}(23)–C_{84}. In our discussions we will just use the designations D_2–C_{84} and D_{2d}–C_{84} for these constitutional isomers.
67. Balch, A. L.; Ginwalla, A. S.; Lee, J. W.; Noll, B. C.; Olmstead, M. M. *J. Am. Chem. Soc.* **1994**, *116*, 2227–2228.
68. Dennis, T. J. S.; Kai, T.; Tomiyama, T.; Shinohara, H. *Chem. Commun.* **1998**, 619–620.

69. Saunders, M.; Jiménez-Vázquez, H. A.; Cross, R. J.; Billups, W. E.; Gesenberg, C.; Gonzalez, A.; Luo, W.; Haddon, R. C.; Diederich, F.; Herrmann, A. *J. Am. Chem. Soc.* **1995**, *117*, 9305–9308.
70. Avent, A. G.; Dubois, D.; Pénicaud, A.; Taylor, R. *J. Chem. Soc., Perkin Trans. 2* **1997**, 1907–1910.
71. Dennis, T. J. S.; Kai, T.; Asato, K.; Tomiyama, T.; Shinohara, H.; Yoshida, T.; Kobayashi, Y.; Ishiwatari, H.; Miyake, Y.; Kikuchi, K.; Achiba, Y. *J. Phys. Chem. A* **1999**, *103*, 8747–8752.
72. The assignment for the C_s-symmetric isomers is provisional as 1D NMR spectroscopy does not allow an unambiguous symmetry determination.
73. Achiba, Y.; Kikuchi, K.; Aihara, Y.; Wakabayashi, T.; Miyake, Y.; Kainosho, M. In *Trends in Large Fullerenes: Are They Balls or Tubes?* Andreoni, W., ed. Kluwer Academic, Dordrecht, **1996**, pp. 139–147.
74. Gromov, A.; Ballenweg, S.; Giesa, S.; Lebedkin, S.; Hull, W. E.; Krätschmer, W. *Chem. Phys. Lett.* **1997**, *267*, 460–466.
75. Heath, J. R.; O'Brien, S. C.; Zhang, Q.; Liu, Y.; Curl, R. F.; Kroto, H. W.; Tittel, F. K.; Smalley, R. E. *J. Am. Chem. Soc.* **1985**, *107*, 7779–7780. Chai, Y.; Guo, T.; Jin, C.; Haufler, R. E.; Chibante, L. P. F.; Fure, J.; Wang, L.; Alford, J. M.; Smalley, R. E. *J. Phys. Chem.* **1991**, *95*, 7564–7568. Bethune, D. S.; Johnson, R. D.; Salem, J. R.; de Vries, M. S.; Yannoni, C. S. *Nature* **1993**, *366*, 123–128. Edelmann, F. T. *Angew. Chem. Int. Ed. Engl.* **1995**, *34*, 981–985. Nakane, T.; Xu, Z.; Yamamoto, E.; Sugai, T.; Tomiyama, T.; Shinohara, H. *Fullerene Sci. Technol.* **1997**, *5*, 829–838. Shinohara, H. *Adv. Met. Semicond. Clusters* **1998**, *4*, 205–226.
76. Nagase, S.; Kobayashi, K.; Akasaka, T. *Bull. Chem. Soc. Jpn.* **1996**, *69*, 2131–2142.
77. Ross, M. M.; Callahan, J. H. *J. Phys. Chem.* **1991**, *95*, 5720–5723. Caldwell, K. A.; Giblin, D. E.; Gross, M. L. *J. Am. Chem. Soc.* **1992**, *114*, 3743–3756. Weiske, T.; Böhme, D. K.; Hrusák, J.; Krätschmer, W.; Schwarz, H. *Angew. Chem. Int. Ed. Engl.* **1991**, *30*, 884–886. Weiske, T.; Wong, T.; Krätschmer, W.; Terlouw, J. K.; Schwarz, H. *Angew. Chem. Int. Ed. Engl.* **1992**, *31*, 183–185. Schwarz, H.; Weiske, T.; Böhme, D. K.; Hrusák, J. In *Buckminsterfullerenes*. Billups, W. E.; Ciufolini, M. A., eds. VCH Publishers, New York, **1993**, pp. 257–283.
78. Saunders, M.; Jiménez-Vázquez, H. A.; Cross, R. J.; Poreda, R. J. *Science* **1993**, *259*, 1428–1430. Saunders, M.; Jiménez-Vázquez, H. A.; Cross, R. J.; Mroczkowski, S.; Gross, M. L.; Giblin, D. E.; Poreda, R. J. *J. Am. Chem. Soc.* **1994**, *116*, 2193–2194.
79. Khong, A.; Jiménez-Vázquez, H. A.; Saunders, M.; Cross, R. J.; Laskin, J.; Peres, T.; Lifshitz, C.; Strongin, R.; Smith, A. B. *J. Am. Chem. Soc.* **1998**, *120*, 6380–6383. Shabtai, E.; Weitz, A.; Haddon, R. C.; Hoffman, R. E.; Rabinovitz, M.; Khong, A.; Cross, R. J.; Saunders, M.; Cheng, P.-C.; Scott, L. T. *J. Am. Chem. Soc.* **1998**, *120*, 6389–6393. Komatsu, K.; Wang, G.-W.; Murata, Y.; Tanaka, T.; Fujiwara, K.; Yamamoto, K.; Saunders, M. *J. Org. Chem.* **1998**, *63*, 9358–9366. Yamamoto, K.; Saunders, M.; Khong, A.; Cross, R. J.; Grayson, M.; Gross, M. L.; Benedetto, A. F.; Weisman, R. B. *J. Am. Chem. Soc.* **1999**, *121*, 1591–1596.
80. Pietzak, B.; Waiblinger, M.; Murphy, T. A.; Weidinger, A.; Höhne, M.; Dietel, E.; Hirsch, A. *Chem. Phys. Lett.* **1997**, *279*, 259–263. Mauser, H.; van Eikema Hommes, N. J. R.; Clark, T.; Hirsch, A.; Pietzak, B.; Weidinger, A.; Dunsch, L. *Angew. Chem. Int. Ed. Engl.* **1997**, *36*, 2835–2838. Knapp, C.; Weiden, N.; Käss, H.; Dinse, K.-P.; Pietzak, B.; Waiblinger, M.; Weidinger, A. *Mol. Phys.* **1998**, *95*, 999–1004. Dietel, E.; Hirsch, A.; Pietzak, B.; Waiblinger, M.; Lips, K.; Weidinger, A.; Gruss, A.; Dinse, K.-P. *J. Am. Chem. Soc.* **1999**, *121*, 2432–2437.
81. Akasaka, T.; Nagase, S.; Kobayashi, K.; Walchli, M.; Yamamoto, K.; Funasaka, H.; Kako, M.; Hoshino, T. Erata, T. *Angew. Chem. Int. Ed. Engl.* **1997**, *36*, 1643–1645.

82. Yamamoto, E.; Tansho, M.; Tomiyama, T.; Shinohara, H.; Kawahara, H.; Kobayashi, Y. *J. Am. Chem. Soc.* **1996**, *118*, 2293–2294.
83. Saunders, M.; Jiménez-Vázquez, H. A.; Cross, R. J.; Mroczkowski, S.; Freedberg, D. I.; Anet, F. A. L. *Nature* **1994**, *367*, 256–258.
84. Saunders, M.; Cross, R. J.; Jiménez-Vázquez, H. A.; Shimshi, R.; Khong, A. *Science* **1996**, *271*, 1693–1697.
85. Smith III, A. B.; Strongin, R. M.; Brard, L.; Romanov, W. J.; Saunders, M.; Jiménez-Vázquez, H. A.; Cross, R. J. *J. Am. Chem. Soc.* **1994**, *116*, 10831–10832.
86. Saunders, M.; Jiménez-Vázquez, H. A.; Bangerter, B. W.; Cross, R. J.; Mroczkowski, S.; Freedberg, D. I.; Anet, F. A. L. *J. Am. Chem. Soc.* **1994**, *116*, 3621–3622.
87. Cross, R. J.; Jiménez-Vázquez, H. A.; Lu, Q.; Saunders, M.; Schuster, D. I.; Wilson, S. R.; Zhao, H. *J. Am. Chem. Soc.* **1996**, *118*, 11454–11459.
88. Rüttimann, M.; Haldimann, R. F.; Isaacs, L.; Diederich, F.; Khong, A.; Jiménez-Vázquez, H.; Cross, R. J.; Saunders, M. *Chem. Eur. J.* **1997**, *3*, 1071–1076.
89. Iijima, S. *Nature* **1991**, *354*, 56–58. Iijima, S.; Ichihashi, T. *Nature* **1993**, *363*, 603–605.
90. Ge, M.; Sattler, K. *Science* **1993**, *260*, 515–518. Wildoer, J. W. G.; Venema, L. C.; Rinzler, A. G.; Smalley, R. E.; Dekker, C. *Nature* **1998**, *391*, 59–62. Odom, T. W.; Huang, J. L.; Kim, P.; Lieber, C. M. *Nature* **1998**, *391*, 62–64.
91. Stone, A. J.; Wales, D. J. *Chem. Phys. Lett.* **1986**, *128*, 501–503.
92. Pinto, Y.; Fowler, P. W.; Mitchell, D.; Avnir, D. *J. Phys. Chem. B* **1998**, *102*, 5776–5784.
93. Herrmann, A.; Diederich, F. *Helv. Chim. Acta* **1996**, *79*, 1741–1756.
94. Bingel, C. *Chem. Ber.* **1993**, *126*, 1957–1959.
95. Arias, F.; Yang, Y.; Echegoyen, L.; Lu, Q.; Wilson, S. R. In *Proceedings of the Symposium on Recent Advances in the Chemistry and Physics of Fullerenes and Related Materials*. Kadish, K. M.; Ruoff, R. S., eds. The Electrochemical Society Inc., Pennington, NJ, **1995**, pp. 200–212.
96. Dojo, F.; Hirsch, A. *Chem. Eur. J.* **1998**, *4*, 344–356.
97. Djojo, F.; Hirsch, A.; Grimme, S. *Eur. J. Org. Chem.* **1999**, 3027–3039.
98. Orlandi, G.; Poggi, G.; Zerbetto, F. *Chem. Phys. Lett.* **1994**, *224*, 113–117.
99. Harada, N.; Nakanishi, K. *Circular Dichroism Spectroscopy—Exciton Coupling Method in Organic Stereochemistry*. Oxford University Press, Oxford, **1983**.
100. Harada, N.; Koumura, N.; Feringa, B. L. *J. Am. Chem. Soc.* **1997**, *119*, 7256–7264, and references cited therein.
101. Fanti, M.; Orlandi, G.; Poggi, G.; Zerbetto, F. *Chem. Phys.* **1997**, *223*, 159–168.
102. Note on the use of the expression *addend*: As bridging (divalent) addends are among the most common in fullerene chemistry, the simple expression *addend* is often used in the sense of *bridging addend* and thus implies bonding to two carbon atoms on the fullerene surface. This situation can be compared to the addition of two monovalent addends like H or Cl and, in terms of symmetry, a C_{2v}-symmetric (C_s-symmetric) bridging addend corresponds to two identical (different) achiral monovalent addends. In both cases the resulting product is considered a *mono-adduct*. It is important to be aware of this use of the language in order to avoid confusion in discussing fullerene adduct isomers. Furthermore, talking about the symmetry of addends in this review, we mean the symmetry of the bound addend bridge which may differ from that of the reagent molecule prior to addition.
103. Kusukawa, T.; Ando, W. *Angew. Chem. Int. Ed. Engl.* **1996**, *35*, 1315–1317.
104. Isaacs, L.; Seiler, P.; Diederich, F. *Angew. Chem. Int. Ed. Engl.* **1995**, *34*, 1466–1469.
105. Hawkins, J. M.; Meyer, A.; Lewis, T. A.; Bunz, U.; Nunlist, R.; Ball, G. E.; Ebbesen, T. W.; Tanigaki, K. *J. Am. Chem. Soc.* **1992**, *114*, 7954–7955.
106. Hawkins, J. M.; Meyer, A.; Nambu, M. *J. Am. Chem. Soc.* **1993**, *115*, 9844–9845.
107. Bingel, C.; Schiffer, H. *Liebigs Ann.* **1995**, 1551–1553.
108. Hirsch, A. *J. Phys. Chem. Solids* **1997**, *58*, 1729–1740.

109. Hirsch, A.; Lamparth, I.; Grösser, T.; Karfunkel, H. R. *J. Am. Chem. Soc.* **1994**, *116*, 9385–9386.
110. Hirsch, A.; Lamparth, I.; Schick, G. *Liebigs Ann.* **1996**, 1725–1734.
111. Djojo, F.; Herzog, A.; Lamparth, I.; Hampel, F.; Hirsch, A. *Chem. Eur. J.* **1996**, *2*, 1537–1547.
112. Wilson, S. R.; Lu, Q. *Tetrahedron Lett.* **1995**, *36*, 5707–5710.
113. Kessinger, R.; Gómez-López, M.; Boudon, C.; Gisselbrecht, J.-P.; Gross, M.; Echegoyen, L.; Diederich, F. *J. Am. Chem. Soc.* **1998**, *120*, 8545–8546.
114. Lamparth, I.; Hirsch, A. *J. Chem. Soc., Chem. Commun.* **1994**, 1727–1728.
115. Gross, B.; Schurig, V.; Lamparth, I.; Herzog, A.; Djojo, F.; Hirsch, A. *Chem. Commun.* **1997**, 1117–1118.
116. Gross, B.; Schurig, V.; Lamparth, I.; Hirsch, A. *J. Chromatogr. A* **1997**, *791*, 65–69.
117. Nierengarten, J.-F.; Gramlich, V.; Cardullo, F.; Diederich, F. *Angew. Chem. Int. Ed. Engl.* **1996**, *35*, 2101–2103.
118. Nierengarten, J.-F.; Herrmann, A.; Tykwinski, R. R.; Rüttimann, M.; Diederich, F.; Boudon, C.; Gisselbrecht, J.-P.; Gross, M. *Helv. Chim. Acta* **1997**, *80*, 293–316.
119. Camps, X.; Hirsch, A. *J. Chem. Soc., Perkin Trans. 1* **1997**, 1595–1596.
120. Lamparth, I.; Herzog, A.; Hirsch, A. *Tetrahedron* **1996**, *52*, 5065–5075.
121. Wallenborn, E. U.; Haldimann, R. F.; Klärner, F. G.; Diederich, F. *Chem. Eur. J.* **1998**, *4*, 2258–2265.
122. Breslow, R. *Acc. Chem. Res.* **1980**, *13*, 170–177.
123. Isaacs, L.; Haldimann, R. F.; Diederich, F. *Angew. Chem. Int. Ed. Engl.* **1994**, *33*, 2339–2342. Isaacs, L.; Diederich, F.; Haldimann, R. F. *Helv. Chim. Acta* **1997**, *80*, 317–342.
124. Diederich, F.; Kessinger, R. *Acc. Chem. Res.* **1999**, *32*, 537–545. Diederich, F.; Kessinger, R. In *Templated Organic Synthesis*. Diederich, F.; Stang, P. J., eds. Wiley-VCH, Weinheim, **2000**, pp. 189–218.
125. Nierengarten, J.-F.; Habicher, T.; Kessinger, R.; Cardullo, F.; Diederich, F.; Gramlich, V.; Gisselbrecht, J.-P.; Boudon, C.; Gross, M. *Helv. Chim. Acta* **1997**, *80*, 2238–2276.
126. Li, J.; Yoshizawa, T.; Ikuta, M.; Ozawa, M.; Nakahara, K.; Hasegawa, T.; Kitazawa, K.; Hayashi, M.; Kinbara, K.; Nohara, M.; Saigo, K. *Chem. Lett.* **1997**, 1037–1038.
127. Nierengarten, J.-F.; Felder, D.; Nicoud, J.-F. *Tetrahedron Lett.* **1998**, *39*, 2747–2750.
128. Kemp, C. M.; Mason, S. F. *Tetrahedron* **1966**, *22*, 629–635.
129. Nierengarten, J.-F.; Schall, C.; Nicoud, J.-F.; Heinrich, B.; Guillon, D. *Tetrahedron Lett.* **1998**, *39*, 5747–5750.
130. Diederich, F.; Gómez-López, M. *Chimia* **1998**, *52*, 551–556. Diederich, F.; Gómez-López, M. *Chem. Soc. Rev.* **1999**, *28*, 263–277.
131. Bourgeois, J.-P.; Diederich, F.; Echegoyen, L.; Nierengarten, J.-F. *Helv. Chim. Acta* **1998**, *81*, 1835–1844.
132. Dietel, E.; Hirsch, A.; Eichhorn, E.; Rieker, A.; Hackbarth, S.; Röder, B. *Chem. Commun.* **1998**, 1981–1982.
133. Asthon, P. R.; Diederich, F.; Gómez-López, M.; Nierengarten, J.-F.; Preece, J. A.; Raymo, F. M.; Stoddart, J. F. *Angew. Chem. Int. Ed. Engl.* **1997**, *36*, 1448–1451.
134. Philp, D.; Stoddart, J. F. *Angew. Chem. Int. Ed. Engl.* **1996**, *35*, 1154–1196.
135. Bourgeois, J.-P.; Echegoyen, L.; Fibbioli, M.; Pretsch, E.; Diederich, F. *Angew. Chem. Int. Ed. Engl.* **1998**, *37*, 2118–2121. Bourgeois, J.-P.; Seiler, P.; Fibbioli, M.; Pretsch, E.; Diederich, F.; Echegoyen, L. *Helv. Chim. Acta* **1999**, *82*, 1572–1595.
136. Collet, A.; Gabard, J.; Jacques, J.; Cesario, M.; Guilhem, J.; Pascard, C. *J. Chem. Soc., Perkin Trans. 1* **1981**, 1630–1638.
137. Rapenne, G.; Crassous, J.; Collet, A.; Echegoyen, L.; Diederich, F. *Chem. Commun.* **1999**, 1121–1122.

138. Steed, J. W.; Junk, P. C.; Atwood, J. L.; Barnes, M. J.; Raston, C. L.; Burkhalter, R. S. *J. Am. Chem. Soc.* **1994**, *116*, 10346–10347. Atwood, J. L.; Barnes, M. J.; Gardiner, M. G.; Raston, C. L. *Chem. Commun.* **1996**, 1449–1450. Matsubara, H.; Hasegawa, A.; Shiwaku, K.; Asano, K.; Uno, M.; Takahashi, S.; Yamamoto, K. *Chem. Lett.* **1998**, 923–924. Matsubara, H.; Shimura, T.; Hasegawa, A.; Semba, M.; Asano, K.; Yamamoto, K. *Chem. Lett.* **1998**, 1099–1100.
139. Frisch, H. L.; Wasserman, E. *J. Am. Chem. Soc.* **1961**, *83*, 3789–3795. Walba, D. M. *Tetrahedron* **1985**, *41*, 3161–3212. Chambron, J.-C.; Dietrich-Buchecker, C. O.; Sauvage, J.-P. *Top. Curr. Chem.* **1993**, *165*, 131–162. Liang, C.; Mislow, K. *J. Math. Chem.* **1994**, *15*, 245–260. Breault, G. A.; Hunter, C. A.; Mayers, P. C. *Tetrahedron* **1999**, *55*, 5265–5293.
140. Dietrich-Buchecker, C.; Rapenne, G.; Sauvage, J.-P. In *Molecular Catenanes, Rotaxanes and Knots*. Sauvage, J.-P.; Dietrich-Buchecker, C., eds. Wiley-VCH, New York, **1999**, pp. 107–142.
141. Nakamura, E.; Isobe, H.; Tokuyama, H.; Sawamura, M. *Chem. Commun.* **1996**, 1747–1748.
142. Isobe, H.; Tokuyama, H.; Sawamura, M.; Nakamura, E. *J. Org. Chem.* **1997**, *62*, 5034–5041.
143. Isobe, H.; Sawamura, M.; Nakamura, E. *Fullerene Sci. Technol.* **1999**, *7*, 519–528.
144. Taki, M.; Sugita, S.; Nakamura, Y.; Kasashima, E.; Yashima, E.; Okamoto, Y.; Nishimura, J. *J. Am. Chem. Soc.* **1997**, *119*, 926–932. Taki, M.; Nakamura, Y.; Uehara, H.; Sato, M.; Nishimura, J. *Enantiomer* **1998**, *3*, 231–239.
145. Nakamura, Y.; Taki, M.; Tobita, S.; Shizuka, H.; Yokoi, H.; Ishiguro, K.; Sawaki, Y.; Nishimura, J. *J. Chem. Soc., Perkin Trans. 2* **1999**, 127–130.
146. Okamoto, Y.; Yashima, E. *Angew. Chem. Int. Ed. Engl.* **1999**, *37*, 1021–1043.
147. Ishi-i, T.; Nakashima, K.; Shinkai, S. *Chem. Commun.* **1998**, 1047–1048.
148. Ishi-i, T.; Iguchi, R.; Shinkai, S. *Tetrahedron* **1999**, *55*, 3883–3892.
149. Ishi-i, T.; Nakashima, K.; Shinkai, S.; Ikeda, A. *J. Org. Chem.* **1999**, *64*, 984–990.
150. The absolute configurations are based on a configurational assignment made for a *cis*-3 adduct by Goto and co-workers.[7]
151. Ishi-i, T.; Shinkai, S. *Tetrahedron* **1999**, *55*, 12515–12530.
152. Grösser, T.; Prato, M.; Lucchini, V.; Hirsch, A.; Wudl, F. *Angew. Chem. Int. Ed. Engl.* **1995**, *34*, 1343–1345.
153. Hummelen, J. C.; Prato, M.; Wudl, F. *J. Am. Chem. Soc.* **1995**, *117*, 7003–7004.
154. Hummelen, J. C.; Knight, B.; Pavlovich, J.; González, R.; Wudl, F. *Science* **1995**, *269*, 1554–1556.
155. Bellavia-Lund, C.; Keshavarz-K., M.; Collins, T.; Wudl, F. *J. Am. Chem. Soc.* **1997**, *119*, 8101–8102.
156. Keshavarz-K., M.; González, R.; Hicks, R. G.; Srdanov, G.; Srdanov, V. I.; Collins, T. G.; Hummelen, J. C.; Bellavia-Lund, C.; Pavlovich, J.; Wudl, F.; Holczer, K. *Nature* **1996**, *383*, 147–150.
157. Hummelen, J. C.; Keshavarz-K., M.; van Dongen, J. L. J.; Janssen, R. A. J.; Meijer, E. W.; Wudl, F. *Chem. Commun.* **1998**, 281–282.
158. Lamparth, I.; Nuber, B.; Schick, G.; Skiebe, A.; Grösser, T.; Hirsch, A. *Angew. Chem. Int. Ed. Engl.* **1995**, *34*, 2257–2259.
159. Nuber, B.; Hirsch, A. *Chem. Commun.* **1996**, 1421–1422.
160. Schick, G.; Hirsch, A.; Mauser, H.; Clark, T. *Chem. Eur. J.* **1996**, *2*, 935–943.
161. Elemes, Y.; Silverman, S. K.; Sheu, C.; Kao, M.; Foote, C. S.; Alvarez, M. M.; Whetten, R. L. *Angew. Chem. Int. Ed. Engl.* **1992**, *31*, 351–353.
162. Creegan, K. M.; Robbins, J. L.; Robbins, W. K.; Millar, J. M.; Sherwood, R. D.; Tindall, P. J.; Cox, D. M.; Smith III, A. B.; McCauley, J. P.; Jones, D. R.; Gallagher, R. T. *J. Am. Chem. Soc.* **1992**, *114*, 1103–1105.
163. Hamano, T.; Mashino, T.; Hirobe, M. *J. Chem. Soc., Chem. Commun.* **1995**, 1537–1538.

164. Fusco, C.; Seraglia, R.; Curci, R.; Lucchini, V. *J. Org. Chem.* **1999**, *64*, 8363–8368.
165. Balch, A. L.; Costa, D. A.; Noll, B. C.; Olmstead, M. M. *J. Am. Chem. Soc.* **1995**, *117*, 8926–8932.
166. Henderson, C. C.; Rohlfing, C. M.; Cahill, P. A. *Chem. Phys. Lett.* **1993**, *213*, 383–388. Cahill, P. A.; Rohlfing, C. M. *Tetrahedron* **1996**, *52*, 5247–5256.
167. Matsuzawa, N.; Dixon, D. A.; Fukunaga, T. *J. Phys. Chem.* **1992**, *96*, 7594–7604.
168. Henderson, C. C.; Cahill, P. A. *Science* **1993**, *259*, 1885–1887.
169. Henderson, C. C.; Rohlfing, C. M.; Assink, R. A.; Cahill, P. A. *Angew. Chem. Int. Ed. Engl.* **1994**, *33*, 786–788.
170. Billups, W. E.; Luo, W.; Gonzalez, A.; Arguello, D.; Alemany, L. B.; Marriott, T.; Saunders, M.; Jiménez-Vázquez, H. A.; Khong, A. *Tetrahedron Lett.* **1997**, *38*, 171–174.
171. Meier, M. S.; Weedon, B. R.; Spielmann, H. P. *J. Am. Chem. Soc.* **1996**, *118*, 11682–11683.
172. Bergosh, R. G.; Meier, M. S.; Laske Cooke, J. A.; Spielmann, H. P.; Weedon, B. R. *J. Org. Chem.* **1997**, *62*, 7667–7672.
173. Meier, M. S.; Corbin, P. S.; Vance, V. K.; Clayton, M.; Mollman, M.; Poplawska, M. *Tetrahedron Lett.* **1994**, *35*, 5789–5792.
174. Weedon, B. R.; Haddon, R. C.; Spielmann, H. P.; Meier, M. S. *J. Am. Chem. Soc.* **1999**, *121*, 335–340.
175. Diederich, F.; Isaacs, L.; Philp, D. *J. Chem. Soc., Perkin Trans. 2* **1994**, 391–394.
176. Haddon, R. C.; Raghavachari, K. *Tetrahedron* **1996**, *52*, 5207–5220.
177. Haufler, R. E.; Conceicao, J.; Chibante, L. P. F.; Chai, Y.; Byrne, N. E.; Flanagan, S.; Haley, M. M.; O'Brien, S. C.; Pan, C.; Xiao, Z.; Billups, W. E.; Ciufolini, M. A.; Hauge, R. H.; Margrave, J. L.; Wilson, L. J.; Curl, R. F.; Smalley, R. E. *J. Phys. Chem.* **1990**, *94*, 8634–8636.
178. Taylor, R.; Langley, G. J.; Brisdon, A. K.; Holloway, J. H.; Hope, E. G.; Kroto, H. W.; Walton, D. R. M. *J. Chem. Soc., Chem. Commun.* **1993**, 875–878.
179. Fowler, P. W.; Sandall, J. P. B.; Taylor, R. *J. Chem. Soc., Perkin Trans. 2* **1997**, 419–423.
180. Boltalina, O. V.; Street, J. M.; Taylor, R. *J. Chem. Soc., Perkin Trans. 2* **1998**, 649–653.
181. Darwish, A. D.; Avent, A. G.; Taylor, R.; Walton, D. R. M. *J. Chem. Soc., Perkin Trans. 2* **1996**, 2051–2054.
182. Austin, S. J.; Batten, R. C.; Fowler, P. W.; Redmond, D. B.; Taylor, R. *J. Chem. Soc., Perkin Trans. 2* **1993**, 1383–1384. Rathna, A.; Chandrasekhar, J. *Chem. Phys. Lett.* **1993**, *206*, 217–224. Dunlap, B. I.; Brenner, D. W.; Schriver, G. W. *J. Phys. Chem.* **1994**, *98*, 1756–1757. Clare, B. W.; Kepert, D. L. *J. Mol. Struct. (Theochem)* **1994**, 304, 181. Bühl, M.; Thiel, W.; Schneider, U. *J. Am. Chem. Soc.* **1995**, *117*, 4623–4627.
183. Book, L. D.; Scuseria, G. E. *J. Phys. Chem.* **1994**, *98*, 4283–4286.
184. Okotrub, A. V.; Bulusheva, L. G.; Asanov, I. P.; Lobach, A. S.; Shulga, Y. M. *J. Phys. Chem. A* **1999**, *103*, 716–720.
185. Hall, L. E.; Mc Kenzie, D. R.; Davis, R. L.; Attalla, M. I.; Vassallo, A. M. *Acta Crystallogr. Sect. B* **1998**, *54*, 345–350.
186. Bensasson, R. V.; Hill, T. J.; Land, E. J.; Leach, S.; McGarvey, D. J.; Truscott, T. G.; Ebenhoch, J.; Gerst, M.; Rüchardt, C. *Chem. Phys.* **1997**, *215*, 111–123.
187. Billups, W. E.; Gonzalez, A.; Gesenberg, C.; Luo, W.; Marriott, T.; Alemany, L. B.; Saunders, M.; Jiménez-Vázquez, H. A.; Khong, A. *Tetrahedron Lett.* **1997**, *38*, 175–178.
188. Boltalina, O. V.; Bühl, M.; Khong, A.; Saunders, M.; Street, J. M.; Taylor, R. *J. Chem. Soc., Perkin Trans. 2* **1999**, 1475–1479.
189. Boltalina, O. V.; Markov, V. Y.; Taylor, R.; Waugh, M. P. *Chem. Commun.* **1996**, 2549–2550.
190. Gakh, A. A.; Tuinman, A. A.; Adcock, J. L.; Sachleben, R. A.; Compton, R. N. *J. Am. Chem. Soc.* **1994**, *116*, 819–820.

191. Balasubramanian, K. *J. Phys. Chem.* **1993**, *97*, 6990–6998.
192. Austin, S. J.; Fowler, P. W.; Sandall, J. P. B.; Zerbetto, F. *J. Chem. Soc., Perkin Trans. 2* **1996**, 155–157.
193. Boltalina, O. V.; Sidorov, L. N.; Bagryantsev, V. F.; Seredenko, V. A.; Zapol'skii, A. S.; Street, J. M.; Taylor, R. *J. Chem. Soc., Perkin Trans. 2* **1996**, 2275–2278.
194. Schick, G.; Levitus, M.; Kvetko, L.; Johnson, B. A.; Lamparth, I.; Lunkwitz, R.; Ma, B.; Khan, S. I.; Garcia-Garibay, M. A.; Rubin, Y. *J. Am. Chem. Soc.* **1999**, *121*, 3246–3247.
195. Kusukawa, T.; Ando, W. *J. Organomet. Chem.* **1998**, *561*, 109–120.
196. Akasaka, T.; Suzuki, T.; Maeda, Y.; Ara, M.; Wakahara, T.; Kobayashi, K.; Nagase, S.; Kako, M.; Nakadaira, Y.; Fujitsuka, M.; Ito, O. *J. Org. Chem.* **1999**, *64*, 566–569.
197. Kusukawa, T.; Ando, W. *J. Organomet. Chem.* **1998**, *559*, 11–22.
198. Birkett, P. R.; Avent, A. G.; Darwish, A. D.; Kroto, H. W.; Taylor, R.; Walton, D. R. M. *J. Chem. Soc., Chem. Commun.* **1993**, 1230–1232.
199. Avent, A. G.; Birkett, P. R.; Crane, J. D.; Darwish, A. D.; Langley, G. J.; Kroto, H. W.; Taylor, R.; Walton, D. R. M. *J. Chem. Soc., Chem. Commun.* **1994**, 1463–1464.
200. Birkett, P. R.; Avent, A. G.; Darwish, A. D.; Kroto, H. W.; Taylor, R.; Walton, D. R. M. *J. Chem. Soc., Perkin Trans. 2* **1997**, 457–461. The structural assignment of unsymmetrical $C_{60}Ar_4$ was revised in 2001: Darwish, A. D.; Avent, A. G.; Birkett, P. R.; Kroto, H. W.; Taylor, R.; Walton, D. R. M. *J. Chem. Soc., Perkin Trans. 2* **2001**, 1038–1044.
201. Birkett, P. R.; Bühl, M.; Khong, A.; Saunders, M.; Taylor, R. *J. Chem. Soc., Perkin Trans. 2* **1999**, 2037–2039.
202. Avent, A. G.; Birkett, P. R.; Darwish, A. D.; Kroto, H. W.; Taylor, R.; Walton, D. R. M. *Chem. Commun.* **1997**, 1579–1580.
203. For the direct synthesis of benzo[*b*]furano-fused fullerene derivatives, starting from $C_{60}Cl_6$ or $C_{70}Cl_{10}$ and phenols; cf. Darwish, A. D.; Avent, A. G.; Kroto, H. W.; Taylor, R.; Walton, D. R. M. *J. Chem. Soc., Perkin Trans. 2* **1999**, 1983–1988.
204. Darwish, A. D.; Birkett, P. R.; Langley, G. J.; Kroto, H. W.; Taylor, R.; Walton, D. R. M. *Fullerene Sci. Technol.* **1997**, *5*, 705–726.
205. Hirsch, A. *Synthesis* **1995**, 895–913.
206. Kampe, K.-D.; Egger, N.; Vogel, M. *Angew. Chem. Int. Ed. Engl.* **1993**, *32*, 1174–1176.
207. Kampe, K.-D.; Egger, N. *Liebigs Ann.* **1995**, 115–124.
208. Balch, A. L.; Cullison, B.; Fawcett, W. R.; Ginwalla, A. S.; Olmstead, M. M.; Winkler, K. *J. Chem. Soc., Chem. Commun.* **1995**, 2287–2288.
209. Balch, A. L.; Ginwalla, A. S.; Olmstead, M. M.; Herbst-Irmer, R. *Tetrahedron* **1996**, *52*, 5021–5032.
210. Maggini, M.; Scorrano, G.; Bianco, A.; Toniolo, C.; Prato, M. *Tetrahedron Lett.* **1995**, *36*, 2845–2846.
211. Irngartinger, H.; Fettel, P. W. *Tetrahedron* **1999**, *55*, 10735–10752.
212. Sinyashin, O. G.; Romanova, I. P.; Sagitova, F. R.; Pavlov, V. A.; Kovalenko, V. I.; Badeev, Y. V.; Azancheev, N. M.; Ilyasov, A. V.; Chernova, A. V.; Vandyukova, I. I. *Mendeleev Commun.* **1998**, 79–81.
213. Maggini, M.; Scorrano, G.; Prato, M. *J. Am. Chem. Soc.* **1993**, *115*, 9798–9799.
214. Prato, M.; Maggini, M. *Acc. Chem. Res.* **1998**, *31*, 519–526.
215. Lu, Q.; Schuster, D. I.; Wilson, S. R. *J. Org. Chem.* **1996**, *61*, 4764–4768.
216. Pasimeni, L.; Hirsch, A.; Lamparth, I.; Herzog, A.; Maggini, M.; Prato, M.; Corvaja, C.; Scorrano, G. *J. Am. Chem. Soc.* **1997**, *119*, 12896–12901.
217. Foote, C. S. *Top. Curr. Chem.* **1994**, *169*, 347–363.
218. Cf. publications cited by Schick and co-workers.[194]
219. Meier, M. S.; Wang, G.-W.; Haddon, R. C.; Pratt Brock, C.; Lloyd, M. A.; Selegue, J. P. *J. Am. Chem. Soc.* **1998**, *120*, 2337–2342.

220. Kiely, A. F.; Haddon, R. C.; Meier, M. S.; Selegue, J. P.; Pratt Brock, C.; Patrick, B. O.; Wang, G.-W.; Chen, Y. *J. Am. Chem. Soc.* **1999**, *121*, 7971–7972.
221. Akasaka, T.; Mitsuhida, E.; Ando, W.; Kobayashi, K.; Nagase, S. *J. Am. Chem. Soc.* **1994**, *116*, 2627–2628.
222. Darwish, A. D.; Avent, A. G.; Taylor, R.; Walton, D. R. M. *J. Chem. Soc., Perkin Trans. 2* **1996**, 2079–2084.
223. Hawkins, J. M.; Meyer, A.; Lewis, T. A.; Loren, S.; Hollander, F. J. *Science* **1991**, *252*, 312–313.
224. Hawkins, J. M.; Meyer, A.; Solow, M. A. *J. Am. Chem. Soc.* **1993**, *115*, 7499–7500.
225. Smith III, A. B.; Strongin, R. M.; Brard, L.; Furst, G. T.; Romanow, W. J.; Owens, K. G.; Goldschmidt, R. J. *J. Chem. Soc., Chem. Commun.* **1994**, 2187–2188.
226. Nuber, B.; Hirsch, A. *Fullerene Sci. Technol.* **1996**, *4*, 715–728.
227. Bellavia-Lund, C.; Wudl, F. *J. Am. Chem. Soc.* **1997**, *119*, 943–946.
228. Hasharoni, K.; Bellavia-Lund, C.; Keshavarz-K., M.; Srdanov, G.; Wudl, F. *J. Am. Chem. Soc.* **1997**, *119*, 11128–11129.
229. Bellavia-Lund, C.; Hummelen, J.-C.; Keshavarz-K. M.; González, R.; Wudl, F. *J. Phys. Chem. Solids* **1997**, *58*, 1983–1990.
230. Wilson, S. R.; Lu, Q. *J. Org. Chem.* **1995**, *60*, 6496–6498.
231. Keizer, P. N.; Morton, J. R.; Preston, K. F. *J. Chem. Soc., Chem. Commun.* **1992**, 1259–1261.
232. Borghi, R.; Lunazzi, L.; Placucci, G.; Krusic, P. J.; Dixon, D. A.; Knight Jr., L. B. *J. Phys. Chem.* **1994**, *98*, 5395–5398.
233. Borghi, R.; Guidi, B.; Lunazzi, L.; Placucci, G. *J. Org. Chem.* **1996**, *61*, 5667–5669.
234. Morton, J. R.; Negri, F.; Preston, K. F. *Magn. Reson. Chem.* **1995**, *33 Special Issue*, S20–S27.
235. Borghi, R.; Lunazzi, L.; Placucci, G.; Krusic, P. J.; Dixon, D. A.; Matsuzawa, N.; Ata, M. *J. Am. Chem. Soc.* **1996**, *118*, 7608–7617.
236. Morton, J. R.; Negri, F.; Preston, K. F. *Chem. Phys. Lett.* **1994**, *218*, 467–474.
237. Isaacs, L.; Diederich, F. *Helv. Chim. Acta* **1993**, *76*, 2454–2464.
238. Wilson, S. R.; Wu, Y.; Kaprinidis, N. A.; Schuster, D. I.; Welch, C. J. *J. Org. Chem.* **1993**, *58*, 6548–6549.
239. Prato, M.; Bianco, A.; Maggini, M.; Scorrano, G.; Toniolo, C.; Wudl, F. *J. Org. Chem.* **1993**, *58*, 5578–5580.
240. Toniolo, C.; Bianco, A.; Maggini, M.; Scorrano, G.; Prato, M.; Marastoni, M.; Tomatis, R.; Spisani, S.; Palú, G.; Blair, E. D. *J. Med. Chem.* **1994**, *37*, 4558–4562.
241. Bianco, A.; Maggini, M.; Scorrano, G.; Toniolo, C.; Marconi, G.; Villani, C.; Prato, M. *J. Am. Chem. Soc.* **1996**, *118*, 4072–4080.
242. Wilson, S. R.; Lu, Q.; Cao, J.; Wu, Y.; Welch, C. J.; Schuster, D. I. *Tetrahedron* **1996**, *52*, 5131–5142.
243. Wang, Y.; Schuster, D. I.; Wilson, S. R.; Welch, C. J. *J. Org. Chem.* **1996**, *61*, 5198–5199.
244. Shen, C. K.-F.; Chien, K.-M.; Juo, C.-G.; Her, G.-R.; Luh, T.-Y. *J. Org. Chem.* **1996**, *61*, 9242–9244.
245. Novello, F.; Prato, M.; Da Ros, T.; De Amici, M.; Bianco, A.; Toniolo, C.; Maggini, M. *Chem. Commun.* **1996**, 903–904.
246. Gareis, T.; Köthe, O.; Beer, E.; Daub, J. In *Proceedings of the Symposium on Recent Advances in the Chemistry and Physics of Fullerenes and Related Materials*. Kadish, K. M.; Ruoff, R. S., eds. The Electrochemical Society Inc., Pennington, NJ, **1996**, pp. 1244–1253.
247. Smith, H. E.; Neergaard, J. R. *J. Am. Chem. Soc.* **1996**, *118*, 7694–7701.
248. Schuster, D. I.; Cao, J.; Kaprinidis, N.; Wu, Y.; Jensen, A. W.; Lu, Q.; Wang, H.; Wilson, S. R. *J. Am. Chem. Soc.* **1996**, *118*, 5639–5647.

249. Bianco, A.; Bertolini, T.; Crisma, M.; Valle, G.; Toniolo, C.; Maggini, M.; Scorrano, G.; Prato, M. *J. Pept. Res.* **1997**, *50*, 159–170.
250. Tan, X.; Schuster, D. I.; Wilson, S. R.; Khong, A.; Saunders, M. In *Proceedings of the Symposium on Recent Advances in the Chemistry and Physics of Fullerenes and Related Materials*. Kadish, K. M.; Ruoff, R. S., eds. The Electrochemical Society Inc., Pennington, NJ, **1998**, pp. 1079–1087.
251. Sokolov, V. I. *Pure Appl. Chem.* **1998**, *70*, 789–798.
252. Kanakamma, P. P.; Huang, S.-L.; Juo, C.-G.; Her, G.-R.; Luh, T.-Y. *Chem. Eur. J.* **1998**, *4*, 2037–2042.
253. For another C_{70} derivative with such a substructure cf. ref. 220.
254. Zhang, X.; Foote, C. S. *J. Am. Chem. Soc.* **1995**, *117*, 4271–4275.
255. Anderson, J. L.; An, Y.-Z.; Rubin, Y.; Foote, C. S. *J. Am. Chem. Soc.* **1994**, *116*, 9763–9764.
256. Balch, A. L.; Olmstead, M. M. *Chem. Rev.* **1998**, *98*, 2123–2165.
257. Balch, A. L.; Catalano, V. J.; Lee, J. W.; Olmstead, M. M.; Parkin, S. R. *J. Am. Chem. Soc.* **1991**, *113*, 8953–8955.
258. Iyoda, M.; Ogawa, Y.; Matsuyama, H. *Fullerene Sci. Technol.* **1995**, *3*, 1–9.
259. Balch, A. L.; Lee, J. W.; Olmstead, M. M. *Angew. Chem. Int. Ed. Engl.* **1992**, *31*, 1356–1358.
260. Balch, A. L.; Hao, L.; Olmstead, M. M. *Angew. Chem. Int. Ed. Engl.* **1996**, *35*, 188–190.
261. Hsu, H.-F.; Wilson, S. R.; Shapley, J. R. *Chem. Commun.* **1997**, 1125–1126.
262. Hsu, H.-F.; Shapley, J. R. *J. Am. Chem. Soc.* **1996**, *118*, 9192–9193.
263. Balch, A. L.; Costa, D. A.; Olmstead, M. M. *Chem. Commun.* **1996**, 2449.
264. Smith, A. B.; Strongin, R. M.; Brard, L.; Furst, G. T.; Atkins, J. H.; Romanow, W. J.; Saunders, M.; Jiménez-Vázquez, H. A.; Owens, K. G.; Goldschmidt, R. J. *J. Org. Chem.* **1996**, *61*, 1904–1905. Bezmelnitsin, V. N.; Eletskii, A. V.; Schepetov, N. G.; Avent, A. G.; Taylor, R. *J. Chem. Soc., Perkin Trans. 2* **1997**, 683–686.
265. Balch, A. L.; Costa, D. A.; Lee, J. W.; Noll, B. C.; Olmstead, M. M. *Inorg. Chem.* **1994**, *33*, 2071–2072.
266. Balch, A. L.; Costa, D. A.; Noll, B. C.; Olmstead, M. M. *Inorg. Chem.* **1996**, *35*, 458–462.
267. Henderson, C. C.; Rohlfing, C. M.; Gillen, K. T.; Cahill, P. A. *Science* **1994**, *264*, 397–399.
268. Avent, A. G.; Darwish, A. D.; Heimbach, D. K.; Kroto, H. W.; Meidine, M. F.; Parsons, J. P.; Remars, C.; Roers, R.; Ohashi, O.; Taylor, R.; Walton, D. R. M. *J. Chem. Soc., Perkin Trans. 2* **1994**, 15–22.
269. Spielmann, H. P.; Wang, G.-W.; Meier, M. S.; Weedon, B. R. *J. Org. Chem.* **1998**, *63*, 9865–9871.
270. Avent, A. G.; Birkett, P. R.; Darwish, A. D.; Kroto, H. W.; Taylor, R.; Walton, D. R. M. *Tetrahedron* **1996**, *52*, 5235–5246.
271. Taylor, R. *J. Chem. Soc., Perkin Trans. 2* **1994**, 2497–2498. Fowler, P. W.; Sandall, J. P. B.; Austin, S. J.; Manolopoulos, D. E.; Lawrenson, P. D. M.; Smallwood, J. M. *Synth. Met.* **1996**, *77*, 97–101.
272. Gerst, M.; Beckhaus, H.-D.; Rüchardt, C.; Campbell, E. E. B.; Tellgmann, R. *Tetrahedron Lett.* **1993**, *34*, 7729–7732. Attalla, M. I.; Vassallo, A. M.; Tattam, B. N.; Hanna, J. V. *J. Phys. Chem.* **1993**, *97*, 6329–6331. Shigematsu, K.; Abe, K. *Chem. Express* **1992**, *7*, 905–908. Shigematsu, K.; Abe, K.; Mitani, M.; Tanaka, K. *Chem. Express* **1992**, *7*, 957–960. Shigematsu, K.; Abe, K.; Mitani, M.; Tanaka, K. *Fullerene Sci. Technol.* **1993**, *1*, 309–318. Darwish, A. D.; Abdul-Sada, A. K.; Langley, G. J.; Kroto, H. W.; Taylor, R.; Walton, D. R. M. *J. Chem. Soc., Perkin Trans. 2* **1995**, 2359–2365. Darwish, A. D.; Abdul-Sada, A. K.; Langley, G. J.; Kroto, H. W.; Taylor, R.; Walton, D. R. M. *Synth. Met.* **1996**, *77*, 303–307.

273. Sawamura, M.; Iikura, H.; Nakamura, E. *J. Am. Chem. Soc.* **1996**, *118*, 12850–12851.
274. Iikura, H.; Mori, S.; Sawamura, M.; Nakamura, E. *J. Org. Chem.* **1997**, *62*, 7912–7913.
275. Sawamura, M.; Iikura, H.; Hirai, A.; Nakamura, E. *J. Am. Chem. Soc.* **1998**, *120*, 8285–8286.
276. Taylor, R. *J. Chem. Soc., Perkin Trans. 2* **1993**, 813–824.
277. Boltalina, O. V.; Sidorov, L. N.; Sukhanova, E. V.; Sorokin, I. D. *Chem. Phys. Lett.* **1994**, *230*, 567–570.
278. Boltalina, O. V.; Ponomarev, D. B.; Borschevskii, A. Y.; Sorokin, I. D.; Sidorov, L. N. In *Proceedings of the Symposium on Recent Advances in the Chemistry and Physics of Fullerenes and Related Materials*. Kadish, K. M.; Ruoff, R. S., eds. The Electrochemical Society Inc., Pennington, NJ, **1996**, pp. 108–120.
279. Borschevskii, A. Y.; Boltalina, O. V.; Sidorov, L. N.; Markov, V. Y.; Ioffe, I. N. In *Proceedings of the Symposium on Recent Advances in the Chemistry and Physics of Fullerenes and Related Materials*. Kadish, K. M.; Ruoff, R. S., eds. The Electrochemical Society Inc., Pennington, NJ, **1996**, pp. 509–521.
280. Boltalina, O. V.; Dashkova, E. V.; Sidorov, L. N. *Chem. Phys. Lett.* **1996**, *256*, 253–260.
281. Boltalina, O. V.; Avakyan, T. V.; Markov, V. Y.; Dennis, T. J. S.; Abdul-Sada A. K.; Taylor, R. *J. Phys. Chem. B* **1999**, *103*, 8189–8191.
282. Abdul-Sada A. K.; Avakyan, T. V.; Boltalina, O. V.; Markov, V. Y.; Street, J. M.; Taylor, R. *J. Chem. Soc., Perkin Trans. 2* **1999**, 2659–2666.
283. Darwish, A. D.; Kroto, H. W.; Taylor, R.; Walton, D. R. M. *J. Chem. Soc., Perkin Trans. 2* **1996**, 1415–1418.
284. Taylor, R. In *Lecture Notes on Fullerene Chemistry: A Handbook for Chemists*. Imperial College Press, London, **1999**, p. 66.
285. Kalina, O. G.; Tumanskii, B. L.; Bashilov, V. V.; Chistyakov, A. L.; Stankevich, I. V.; Sokolov, V. I.; Dennis, T. J. S.; Taylor, R. *J. Chem. Soc., Perkin Trans. 2* **1999**, 2655–2657.
286. Kato, T.; Akasaka, T.; Kobayashi, K.; Nagase, S.; Kikuchi, K.; Achiba, Y.; Suzuki, T.; Yamamoto, K. *J. Phys. Chem. Solids* **1997**, *58*, 1779–1783.
287. Akasaka, T.; Kato, T.; Nagase, S.; Kobayashi, K.; Yamamoto, K.; Funasaka, H.; Takahashi, T. *Tetrahedron* **1996**, *52*, 5015–5020.
288. Akasaka, T.; Kato, T.; Kobayashi, K.; Nagase, S.; Yamamoto, K.; Funasaka, H.; Takahashi, T. *Nature* **1995**, *374*, 600–601. Akasaka, T.; Nagase, S.; Kobayashi, K.; Suzuki, T.; Kato, T.; Yamamoto, K.; Funasaka, H.; Takahashi, T. *J. Chem. Soc., Chem. Commun.* **1995**, 1343–1344. Akasaka, T.; Nagase, S.; Kobayashi, K.; Suzuki, T.; Kato, T.; Kikuchi, K.; Achiba, Y.; Yamamoto, K.; Funasaka, H.; Takahashi, T. *Angew. Chem. Int. Ed. Engl.* **1995**, *34*, 2139–2141.
289. Sun, D.; Liu, Z.; Liu, Z.; Guo, X.; Hao, C.; Xu, W.; Liu, S. *Fullerene Sci. Technol.* **1997**, *5*, 1461–1477.
290. Suzuki, T.; Maruyama, Y.; Kato, T.; Akasaka, T.; Kobayashi, K.; Nagase, S.; Yamamoto, K.; Funasaka, H.; Takahashi, T. *J. Am. Chem. Soc.* **1995**, *117*, 9606–9607.
291. Sun, D.; Huang, H.; Yang, S.; Liu, Z.; Liu, S. *Chem. Mater.* **1999**, *11*, 1003–1006.
292. Heymann, D.; Chibante, L. P. F. *Recl. Trav. Chim. Pays-Bas* **1993**, *112*, 639–642.
293. Birkett, P. R.; Darwish, A. D.; Kroto, H. W.; Langley, G. J.; Taylor, R.; Walton, D. R. M. *J. Chem. Soc., Perkin Trans. 2* **1995**, 511–514.
294. Hirsch, A.; Soi, A.; Karfunkel, H. R. *Angew. Chem. Int. Ed. Engl.* **1992**, *31*, 766–768.
295. Hirsch, A.; Grösser, T.; Skiebe, A.; Soi, A. *Chem. Ber.* **1993**, *126*, 1061–1067.
296. Fagan, P. J.; Krusic, P. J.; Evans, D. H.; Lerke, S. A.; Johnston, E. *J. Am. Chem. Soc.* **1992**, *114*, 9697–9699.
297. Banim, F.; Cardin, D. J.; Heath, P. *Chem. Commun.* **1997**, 25–26.

298. Yoshida, M.; Morinaga, Y.; Iyoda, M.; Kikuchi, K.; Ikemoto, I.; Achiba, Y. *Tetrahedron Lett.* **1993**, *34*, 7629–7632.
299. González, R.; Wudl, F.; Pole, D. L.; Sharma, P. K.; Warkentin, J. *J. Org. Chem.* **1996**, *61*, 5837–5839.
300. Kitagawa, T.; Tanaka, T.; Takata, Y.; Takeuchi, K.; Komatsu, K. *Tetrahedron* **1997**, *53*, 9965–9976.
301. Isaacs, L.; Wehrsig, A.; Diederich, F. *Helv. Chim. Acta* **1993**, *76*, 1231–1250.
302. Dixon, D. A.; Matsuzawa, N.; Fukunaga, T.; Tebbe, F. N. *J. Phys. Chem.* **1992**, *96*, 6107–6110.
303. Kitagawa, T.; Tanaka, T.; Takata, Y.; Takeuchi, K.; Komatsu, K. *J. Org. Chem.* **1995**, *60*, 1490–1491.
304. Kitagawa, T.; Tanaka, T.; Murakita, H.; Takeuchi, K. *J. Org. Chem.* **1999**, *64*, 2–3.
305. Tanaka, T.; Kitagawa, T.; Komatsu, K.; Takeuchi, K. *J. Am. Chem. Soc.* **1997**, *119*, 9313–9314.
306. Murata, Y.; Motoyama, K.; Komatsu, K.; Wan, T. S. M. *Tetrahedron* **1996**, *52*, 5077–5090.
307. Kitagawa, T.; Sakamoto, H.; Takeuchi, K. *J. Am. Chem. Soc.* **1999**, *121*, 4298–4299.
308. Morton, J. R.; Negri, F.; Preston, K. F. *Acc. Chem. Res.* **1998**, *31*, 63–69.
309. Morton, J. R.; Preston, K. F.; Krusic, P. J.; Hill, S. A.; Wasserman, E. *J. Am. Chem. Soc.* **1992**, *114*, 5454–5455.
310. Fagan, P. J.; Krusic, P. J.; McEwen, C. N.; Lazar, J.; Parker, D. H.; Herron, N.; Wasserman, E. *Science* **1993**, *262*, 404–407.
311. Morton, J. R.; Preston, K. F.; Krusic, P. J.; Hill, S. A.; Wasserman, E. *J. Phys. Chem.* **1992**, *96*, 3576–3578.
312. Osawa, S.; Osawa, E.; Harada, M. *J. Org. Chem.* **1996**, *61*, 257–265.
313. Segura, J. L.; Martín, N. *Chem. Soc. Rev.* **2000**, *29*, 13–25.
314. Yoshida, M.; Morishima, A.; Morinaga, Y.; Iyoda, M. *Tetrahedron Lett.* **1994**, *35*, 9045–9046.
315. Yoshida, M.; Sultana, F.; Uchiyama, N.; Yamada, T.; Iyoda, M. *Tetrahedron Lett.* **1999**, *40*, 735–736.
316. Schick, G.; Kampe, K.-D.; Hirsch, A. *J. Chem. Soc., Chem. Commun.* **1995**, 2023–2024.
317. Da Ros, T.; Prato, M.; Novello, F.; Maggini, M.; De Amici, M.; De Micheli, C. *Chem. Commun.* **1997**, 59–60.
318. Hsiao, T. Y.; Chidambareswaran, S. K.; Cheng, C. H. *J. Org. Chem.* **1998**, *63*, 8617–8620.
319. Lebedkin, S.; Ballenweg, S.; Gross, J.; Taylor, R.; Krätschmer, W. *Tetrahedron Lett.* **1995**, *36*, 4971–4974. Smith III, A. B.; Tokuyama, H.; Strongin, R. M.; Furst, G. T.; Romanow, W. J.; Chait, B. T.; Mirza, U. A.; Haller, I. *J. Am. Chem. Soc.* **1995**, *117*, 9359–9360. Taylor, R.; Barrow, M. P.; Drewello, T. *Chem. Commun.* **1998**, 2497–2498.
320. Gromov, A.; Lebedkin, S.; Hull, W. E.; Krätschmer, W. *J. Phys. Chem. A* **1998**, *102*, 4997–5005.
321. Giesa, S.; Gross, J. H.; Hull, W. E.; Lebedkin, S.; Gromov, A.; Gleiter, R.; Krätschmer, W. *Chem. Commun.* **1999**, 465–466.
322. Gromov, A.; Lebedkin, S.; Ballenweg, S.; Avent, A. G.; Taylor, R.; Krätschmer, W. *Chem. Commun.* **1997**, 209–210.
323. Siedschlag, C.; Luftmann, H.; Wolff, C.; Mattay, J. *Tetrahedron* **1999**, *55*, 7805–7818.
324. Guo, L.-W.; Gao, X.; Zhang, D.-W.; Wu, S.-H.; Wu, H.-M.; Li, Y.-J. *Chem. Lett.* **1999**, 411–412.
325. Rubin, Y.; Ganapathi, P. S.; Franz, A.; An, Y.-Z.; Qian, W.; Neier, R. *Chem. Eur. J.* **1999**, *5*, 3162–3184.
326. Jensen, A. W.; Khong, A.; Saunders, M.; Wilson, S. R.; Schuster, D. I. *J. Am. Chem. Soc.* **1997**, *119*, 7303–7307.
327. Lee, K.; Hsu, H.-F.; Shapley, J. R. *Organometallics* **1997**, *16*, 3876–3877.

328. Lee, K.; Shapley, J. R. *Organometallics* **1998**, *17*, 3020–3026.
329. Herzog, A.; Hirsch, A.; Vostrowsky, O. *Eur. J. Org. Chem.* **2000**, 171–180.
330. Hawker, C. J.; Fréchet, J. M. J. *J. Am. Chem. Soc.* **1990**, *112*, 7638–7647.
331. Camps, X.; Schonberger, H.; Hirsch, A. *Chem. Eur. J.* **1997**, *3*, 561–567.
332. Lamparth, I.; Maichle-Mössmer, C.; Hirsch, A. *Angew. Chem. Int. Ed. Engl.* **1995**, *34*, 1607–1609.
333. Meier, M. S.; Poplawska, M.; Compton, A. L.; Shaw, J. P.; Selegue, J. P.; Guarr, T. F. *J. Am. Chem. Soc.* **1994**, *116*, 7044–7048.
334. Irngartinger, H.; Köhler, C.-M.; Baum, G.; Fenske, D. *Liebigs Ann.* **1996**, 1609–1614.
335. Yamago, S.; Nakamura, E. *Chem. Lett.* **1996**, 395–396.
336. Irie, K.; Nakamura, Y.; Ohigashi, H.; Tokuyama, H.; Yamago, S.; Nakamura, E. *Biosci. Biotechnol. Biochem.* **1996**, *60*, 1359–1361.
337. Birkett, P. R.; Avent, A. G.; Darwish, A. D.; Kroto, H. W.; Taylor, R.; Walton, D. R. M. *Chem. Commun.* **1996**, 1231–1232.
338. Birkett, P. R.; Avent, A. G.; Darwish, A. D.; Kroto, H. W.; Taylor, R.; Walton, D. R. M. *J. Chem. Soc., Chem. Commun.* **1995**, 683–684.
339. Li, Z.; Bouhadir, K. H.; Shevlin, P. B. *Tetrahedron Lett.* **1996**, *37*, 4651–4654. Li, Z.; Shevlin, P. B. *J. Am. Chem. Soc.* **1997**, *119*, 1149–1150.
340. Wilson, S. R.; Kaprinidis, N.; Wu, Y.; Schuster, D. I. *J. Am. Chem. Soc.* **1993**, *115*, 8495–8496.
341. Vassilikogiannakis, G.; Orfanopoulos, M. *J. Am. Chem. Soc.* **1997**, *119*, 7394–7395.
342. Vassilikogiannakis, G.; Orfanopoulos, M. *Tetrahedron Lett.* **1997**, *38*, 4323–4326.
343. Vassilikogiannakis, G.; Chronakis, N.; Orfanopoulos, M. *J. Am. Chem. Soc.* **1998**, *120*, 9911–9920. Vassilikogiannakis, G.; Orfanopoulos, M. *J. Org. Chem.* **1999**, *64*, 3392–3393.
344. Sliwa, W. *Fullerene Sci. Technol.* **1995**, *3*, 243–281. Sliwa, W. *Fullerene Sci. Technol.* **1997**, *5*, 1133–1175.
345. Prato, M.; Maggini, M.; Giacometti, C.; Scorrano, G.; Sandonà, G.; Farnia, G. *Tetrahedron* **1996**, *52*, 5221–5234.
346. Maggini, M.; Scorrano, G.; Bianco, A.; Toniolo, C.; Sijbesma, R. P.; Wudl, F.; Prato, M. *J. Chem. Soc., Chem. Commun.* **1994**, 305–306.
347. Lawson, G. E.; Kitaygorodskiy, A.; Ma, B.; Bunker, C. E.; Sun, Y. P. *J. Chem. Soc., Chem. Commun.* **1995**, 2225–2226. Lawson, G. E.; Kitaygorodskiy, A.; Sun, Y. P. *J. Org. Chem.* **1999**, *64*, 5913–5920.
348. Wu, S. H.; Zhang, D. W.; Wang, G. W.; Shu, L. H.; Wu, H. M.; Xu, J. F.; Lao, X. F. *Synth. Commun.* **1997**, *27*, 2289–2298.
349. Gan, L.; Zhou, D.; Luo, C.; Tan, H.; Huang, C.; Lu, M.; Pan, J.; Wu, Y. *J. Org. Chem.* **1996**, *61*, 1954–1961. Zhang, W.; Su, Y.; Gan, L.; Jiang, J.; Huang, C. *Chem. Lett.* **1997**, 1007–1008.
350. Schergna, S.; Da Ros, T.; Linda, P.; Ebert, C.; Gardossi, L.; Prato, M. *Tetrahedron Lett.* **1998**, *39*, 7791–7794.
351. Da Ros, T.; Prato, M. *Chem. Commun.* **1999**, 663–669.
352. Prato, M. *J. Mater. Chem.* **1997**, *7*, 1097–1109.
353. Prato, M. *Top. Curr. Chem.* **1999**, *199*, 173–187.
354. Gust, D.; Moore, T. A.; Moore, A. L. *Pure Appl. Chem.* **1998**, *70*, 2189–2200.
355. Imahori, H.; Sakata, Y. *Eur. J. Org. Chem.* **1999**, 2445–2457.
356. Guldi, D. M. *Chem. Commun.* **2000**, 321–327.
357. Wudl, F. *Acc. Chem. Res.* **1992**, *25*, 157–161.
358. Smith III, A. B.; Strongin, R. M.; Brard, L.; Furst, G. T.; Romanow, W. J.; Owens, K. G.; King, R. C. *J. Am. Chem. Soc.* **1993**, *115*, 5829–5830.
359. Schick, G.; Hirsch, A. *Tetrahedron* **1998**, *54*, 4283–4296.

360. Prato, M.; Lucchini, V.; Maggini, M.; Stimpfl, E.; Scorrano, G.; Eiermann, M.; Suzuki, T.; Wudl, F. *J. Am. Chem. Soc.* **1993**, *115*, 8479–8480.
361. Osterodt, J.; Nieger, M.; Windscheif, P.-M.; Vögtle, F. *Chem. Ber.* **1993**, *126*, 2331–2336.
362. Skiebe, A.; Hirsch, A. *J. Chem. Soc., Chem. Commun.* **1994**, 335–336.
363. Hummelen, J. C.; Knight, B. W.; LePeq, F.; Wudl, F.; Yao, J.; Wilkins, C. L. *J. Org. Chem.* **1995**, *60*, 532–538.
364. González, R.; Knight, B. W.; Wudl, F.; Semones, M. A.; Padwa, A. *J. Org. Chem.* **1994**, *59*, 7949–7951.
365. Averdung, J.; Albrecht, E.; Lauterwein, J.; Luftmann, H.; Mattay, J.; Mohn, H.; Müller, W. H.; ter Meer, H.-U. *Chem. Ber.* **1994**, *127*, 787–789. Averdung, J.; Mattay, J. *Tetrahedron* **1996**, *52*, 5407–5420. Averdung, J.; Torres Garcia, G.; Luftmann, H.; Schlachter, I.; Mattay, J. *Fullerene Sci. Technol.* **1996**, *4*, 633–654.
366. Nair, V.; Sethumadhavan, D.; Sheela, K. C.; Eigendorf, G. K. *Tetrahedron Lett.* **1999**, *40*, 5087–5090.
367. Prato, M.; Suzuki, T.; Foroudian, H.; Li, Q.; Khemani, K.; Wudl, F.; Leonetti, J.; Little, R. D.; White, T.; Rickborn, B.; Yamago, S.; Nakamura, E. *J. Am. Chem. Soc.* **1993**, *115*, 1594–1595.
368. Duczek, W.; Niclas, H. J. *Tetrahedron Lett.* **1995**, *36*, 2457–2458.
369. Wu, F. H.; Yu, X. D.; Wu, S. H.; Wu, H. M.; Xu, J. F.; Lao, X. F. *J. Fluorine Chem.* **1998**, *90*, 57–58.
370. Ohno, M.; Yashiro, A.; Eguchi, S. *Synlett* **1996**, 815–816. Ohno, M.; Yashiro, A.; Tsunenishi, Y.; Eguchi, S. *Chem. Commun.* **1999**, 827–828.
371. Shen, C. K. F.; Chien, K. M.; Liu, T. Y.; Lin, T. I.; Her, G. R.; Luh, T. Y. *Tetrahedron Lett.* **1995**, *36*, 5383–5384.
372. Segura, J. L.; Martín, N. *Chem. Rev.* **1999**, *99*, 3199–3246.
373. Eguchi, S.; Ohno, M.; Kojima, S.; Koide, N.; Yashiro, A.; Shirakawa, Y.; Ishida, H. *Fullerene Sci. Technol.* **1996**, *4*, 303–327. Eguchi, S. *Fullerene Sci. Technol.* **1997**, *5*, 977–987.
374. An, Y.-Z.; Anderson, J. L.; Rubin, Y. *J. Org. Chem.* **1993**, *58*, 4799–4801.
375. Wilson, S. R.; Lu, Q. *Tetrahedron Lett.* **1993**, *34*, 8043–8046.
376. Mikami, K.; Matsumoto, S.; Okubo, Y.; Suenobu, T.; Fukuzumi, S. *Synlett* **1999**, 1130–1132.
377. An, Y.-Z.; Ellis, G. A.; Viado, A. L.; Rubin, Y. *J. Org. Chem.* **1995**, *60*, 6353–6361.
378. Ganapathi, P. S.; Friedman, S. H.; Kenyon, G. L.; Rubin, Y. *J. Org. Chem.* **1995**, *60*, 2954–2955.
379. Arce, M.-J.; Viado, A. L.; An, Y.-Z.; Khan, S. I.; Rubin, Y. *J. Am. Chem. Soc.* **1996**, *118*, 3775–3776.
380. Ohno, M.; Azuma, T.; Kojima, S.; Shirakawa, Y.; Eguchi, S. *Tetrahedron* **1996**, *52*, 4983–4994.
381. Torres-Garcia, G.; Luftmann, H.; Wolff, C.; Mattay, J. *J. Org. Chem.* **1997**, *62*, 2752–2756.
382. Kawaguchi, M.; Ikeda, A.; Hamachi, I.; Shinkai, S. *Tetrahedron Lett.* **1999**, *40*, 8245–8249.
383. Gareis, T.; Köthe, O.; Daub, J. *Eur. J. Org. Chem.* **1998**, 1549–1557.
384. Friedman, S. H.; Ganapathi, P. S.; Rubin, Y.; Kenyon, G. L. *J. Med. Chem.* **1998**, *41*, 2424–2429.
385. Ohkita, M.; Ishigami, K.; Tsuji, T. *J. Chem. Soc., Chem. Commun.* **1995**, 1769–1770.
386. Takeshita, H.; Liu, J. F.; Kato, N.; Mori, A.; Isobe, R. *Chem. Lett.* **1995**, 377–378.
387. Rubin, Y.; Khan, S.; Freedberg, D. I.; Yeretzian, C. *J. Am. Chem. Soc.* **1993**, *115*, 344–345.
388. Tago, T.; Minowa, T.; Okada, Y.; Nishimura, J. *Tetrahedron Lett.* **1993**, *34*, 8461–8464.
389. Zhang, X.; Foote, C. S. *J. Org. Chem.* **1994**, *59*, 5235–5238.
390. Martín, N.; Martínez-Grau, A.; Sánchez, L.; Seoane, C.; Torres, M. *J. Org. Chem.* **1998**, *63*, 8074–8076. Tomioka, H.; Yamamoto, K. *J. Chem. Soc., Chem. Commun.* **1995**, 1961–1962.

391. Liu, J.-F.; Kato, N.; Mori, A.; Takeshita, H.; Isobe, R. *Bull. Chem. Soc. Jpn.* **1994**, *67*, 1507–1509.
392. Takeshita, H.; Liu, J.-F.; Kato, N.; Mori, A.; Isobe, R. *J. Chem. Soc., Perkin Trans. 1* **1994**, 1433–1437. Liu, J. F.; Mori, A.; Kato, N.; Takeshita, H. *Fullerene Sci. Technol.* **1995**, *3*, 45–58. Mori, A.; Takamori, Y.; Takeshita, H. *Chem. Lett.* **1997**, 395–396.
393. Mori, S.; Karita, T.; Komatsu, K.; Sugita, N.; Wan, T. S. M. *Synth. Commun.* **1997**, *27*, 1475–1482.
394. Duczek, W.; Radeck, W.; Niclas, H.-J.; Ramm, M.; Costisella, B. *Tetrahedron Lett.* **1997**, *38*, 6651–6654.
395. Banks, M. R.; Cadogan, J. I. G.; Gosney, I.; Hodgson, P. K. G.; Langridge-Smith, P. R. R.; Millar, J. R. A.; Parkinson, J. A.; Sadler, I. H.; Taylor, A. T. *J. Chem. Soc., Chem. Commun.* **1995**, 1171–1172.
396. An, Y.-Z.; Viado, A. L.; Arce, M.-J.; Rubin, Y. *J. Org. Chem.* **1995**, *60*, 8330–8331.
397. Cardullo, F.; Isaacs, L.; Diederich, F.; Gisselbrecht, J.-P.; Boudon, C.; Gross, M. *Chem. Commun.* **1996**, 797–799. Cardullo, F.; Seiler, P.; Isaacs, L.; Nierengarten, J.-F.; Haldimann, R. F.; Diederich, F.; Mordasini-Denti, T.; Thiel, W.; Boudon, C.; Gisselbrecht, J.-P.; Gross, M. *Helv. Chim. Acta* **1997**, *80*, 343–371.
398. Lawson, J. M.; Oliver, A. M.; Rothenfluh, D. F.; An, Y.-Z.; Ellis, G. A.; Ranasinghe, M. G.; Khan, S. I.; Franz, A. G.; Ganapathi, P. S.; Shephard, M. J.; Paddon-Row, M. N.; Rubin, Y. *J. Org. Chem.* **1996**, *61*, 5032–5054. Jolliffe, K. A.; Langford, S. J.; Ranasinghe, M. G.; Shephard, M. J.; Paddon-Row, M. N. *J. Org. Chem.* **1999**, *64*, 1238–1246. Paddon-Row, M. N. *Fullerene Sci. Technol.* **1999**, *7*, 1151–1173.
399. Beer, E.; Feuerer, M.; Knorr, A.; Mirlach, A.; Daub, J. *Angew. Chem. Int. Ed. Engl.* **1994**, *33*, 1087–1089.
400. Tokuyama, H.; Isobe, H.; Nakamura, E. *J. Chem. Soc., Chem. Commun.* **1994**, 2753–2754.
401. Mikami, K.; Matsumoto, S. *Synlett* **1995**, 229–230. Mikami, K.; Matsumoto, S.; Ishida, A.; Takamuku, S.; Suenobu, T.; Fukuzumi, S. *J. Am. Chem. Soc.* **1995**, *117*, 11134–11141. Mikami, K.; Matsumoto, S.; Tonoi, T.; Okubo, Y.; Suenobu, T.; Fukuzumi, S. *Tetrahedron Lett.* **1998**, *39*, 3733–3736.
402. Gao, X.; Ma, S. L.; Guo, L. W.; Zhang, D. W.; Wu, S. H.; Wu, H. M.; Li, Y. J. *Chem. Lett.* **1999**, 671–672.
403. Okamura, H.; Murata, Y.; Minoda, M.; Komatsu, K.; Miyamoto, T.; Wan, T. S. M. *J. Org. Chem.* **1996**, *61*, 8500–8502.
404. Kusukawa, T.; Ando, W. *Organometallics* **1997**, *16*, 4027–4029.
405. Kusukawa, T.; Kabe, Y.; Erata, T.; Nestler, B.; Ando, W. *Organometallics* **1994**, *13*, 4186–4188.
406. Kusukawa, T.; Kabe, Y.; Ando, W. *Organometallics* **1995**, *14*, 2142–2144. Kusukawa, T.; Shike, A.; Ando, W. *Tetrahedron* **1996**, *52*, 4995–5005.
407. Park, J. T.; Cho, J. J.; Song, H. *J. Chem. Soc., Chem. Commun.* **1995**, 15–16. Park, J. T.; Song, H.; Cho, J. J.; Chung, M. K.; Lee, J. H.; Suh, I. H. *Organometallics* **1998**, *17*, 227–236.
408. Murata, Y.; Shiro, M.; Komatsu, K. *J. Am. Chem. Soc.* **1997**, *119*, 8117–8118.
409. Osterodt, J.; Vögtle, F. *Fullerene Sci. Technol.* **1996**, *4*, 729–741.
410. Irngartinger, H.; Weber, A.; Escher, T.; Fettel, P. W.; Gassner, F. *Eur. J. Org. Chem.* **1999**, 2087–2092.
411. Jensen, A. W.; Wilson, S. R.; Schuster, D. I. *Bioorg. Med. Chem.* **1996**, *4*, 767–779.
412. Burley, G. A.; Keller, P. A.; Pyne, S. G. *Fullerene Sci. Technol.* **1999**, *7*, 973–1001.
413. Burley, G. A.; Keller, P. A.; Pyne, S. G.; Ball, G. E. *Chem. Commun.* **1998**, 2539–2540.
414. Zhang, X.; Romero, A.; Foote, C. S. *J. Am. Chem. Soc.* **1993**, *115*, 11024–11025.
415. Polese, A.; Mondini, S.; Bianco, A.; Toniolo, C.; Scorrano, G.; Guldi, D. M.; Maggini, M. *J. Am. Chem. Soc.* **1999**, *121*, 3446–3452.

416. Kurz, A.; Halliwell, C. M.; Davis, J. J.; Hill, H. A. O.; Canters, G. W. *Chem. Commun.* **1998**, 433–434.
417. Boutorine, A. S.; Tokuyama, H.; Takasugi, M.; Isobe, H.; Nakamura, E.; Hélène, C. *Angew. Chem. Int. Ed. Engl.* **1994**, *33*, 2462–2465.
418. An, Y.-Z.; Chen, C.-H. B.; Anderson, J. L.; Sigman, D. S.; Foote, C. S.; Rubin, Y. *Tetrahedron* **1996**, *52*, 5179–5189.
419. Jonas, U.; Cardullo, F.; Belik, P.; Diederich, F.; Gügel, A.; Harth, E.; Herrmann, A.; Isaacs, L.; Müllen, K.; Ringsdorf, H.; Thilgen, C.; Uhlmann, P.; Vasella, A.; Waldraff, C. A. A.; Walter, M. *Chem. Eur. J.* **1995**, *1*, 243–251.
420. Cardullo, F.; Diederich, F.; Echegoyen, L.; Habicher, T.; Jayaraman, N.; Leblanc, R. M.; Stoddart, J. F.; Wang, S. P. *Langmuir* **1998**, *14*, 1955–1959.
421. Yashiro, A.; Nishida, Y.; Ohno, M.; Eguchi, S.; Kobayashi, K. *Tetrahedron Lett.* **1998**, *39*, 9031–9034.
422. Ahn, Y. H.; Yoo, J. S.; Kim, S. H. *Synth. Commun.* **1998**, *28*, 4201–4206. Marco-Contelles, J.; Jagerovic, N.; Alhambra, C. *J. Chem. Research (S)* **1999**, 680–681.
423. Dondoni, A.; Marra, A. *Chem. Commun.* **1999**, 2133–2145.
424. Banks, M. R.; Cadogan, J. I. G.; Gosney, I.; Hodgson, P. K. G.; Langridge-Smith, P. R. R.; Millar, J. R. A.; Taylor, A. T. *J. Chem. Soc., Chem. Commun.* **1995**, 885–886.
425. Yamago, S.; Tokuyama, H.; Nakamura, E.; Prato, M.; Wudl, F. *J. Org. Chem.* **1993**, *58*, 4796–4798.
426. Andersson, T.; Nilsson, K.; Sundahl, M.; Westman, G.; Wennerström, O. *J. Chem. Soc., Chem. Commun.* **1992**, 604–606. Braun, T. *Fullerene Sci. Technol.* **1997**, *5*, 615–626.
427. Yoshida, Z. I.; Takekuma, H.; Takekuma, S. I.; Matsubara, Y. *Angew. Chem. Int. Ed. Engl.* **1994**, *33*, 1597–1599.
428. Yamago, S.; Yanagawa, M.; Nakamura, E. *J. Chem. Soc., Chem. Commun.* **1994**, 2093–2094. Yamago, S.; Yanagawa, M.; Mukai, H.; Nakamura, E. *Tetrahedron* **1996**, *52*, 5091–5102.
429. Mattay, J.; Torres-Garcia, G.; Averdung, J.; Wolff, C.; Schlachter, I.; Luftmann, H.; Siedschlag, C.; Luger, P.; Ramm, M. *J. Phys. Chem. Solids* **1997**, *58*, 1929–1937.
430. Gigante, B.; Santos, C.; Fonseca, T.; Curto, M. J. M.; Luftmann, H.; Bergander, K.; Berberan-Santos, M. N. *Tetrahedron* **1999**, *55*, 6175–6182.
431. Mikami, K.; Matsumoto, S.; Tonoi, T.; Suenobu, T.; Ishida, A.; Fukuzumi, S. *Synlett* **1997**, 85–87.
432. Belik, P.; Gügel, A.; Kraus, A.; Walter, M.; Müllen, K. *J. Org. Chem.* **1995**, *60*, 3307–3310. Nagashima, H.; Terasaki, H.; Saito, Y.; Jinno, K.; Itoh, K. *J. Org. Chem.* **1995**, *60*, 4966–4967.
433. Chuard, T.; Deschenaux, R. *Helv. Chim. Acta* **1996**, *79*, 736–741.
434. Chuard, T.; Deschenaux, R.; Hirsch, A.; Schönberger, H. *Chem. Commun.* **1999**, 2103–2104.
435. Tirelli, N.; Cardullo, F.; Habicher, T.; Suter, U. W.; Diederich, F. *J. Chem. Soc., Perkin Trans. 2* **2000**, 193–198.
436. Deschenaux, R.; Even, M.; Guillon, D. *Chem. Commun.* **1998**, 537–538.
437. Hasharoni, K.; Keshavarz-K., M.; Sastre, A.; González, R.; Bellavia-Lund, C.; Greenwald, Y.; Swager, T.; Wudl, F.; Heeger, A. J. *J. Chem. Phys.* **1997**, *107*, 2308–2312.
438. Maggini, M.; Guldi, D. M.; Mondini, S.; Scorrano, G.; Paolucci, F.; Ceroni, P.; Roffia, S. *Chem. Eur. J.* **1998**, *4*, 1992–2000.
439. Maggini, M.; Donò, A.; Scorrano, G.; Prato, M. *J. Chem. Soc., Chem. Commun.* **1995**, 845–846.
440. Fong, R.; Schuster, D. I.; Wilson, S. R. *Org. Lett.* **1999**, *1*, 729–732.
441. Bestmann, H. J.; Moll, C.; Bingel, C. *Synlett* **1996**, 729–730.
442. Liddell, P. A.; Sumida, J. P.; Macpherson, A. N.; Noss, L.; Seely, G. R.; Clark, K. N.; Moore, A. L.; Moore, T. A.; Gust, D. *Photochem. Photobiol.* **1994**, *60*, 537–541.
443. Montforts, F. P.; Kutzki, O. *Angew. Chem. Int. Ed. Engl.* **2000**, *39*, 599–601.

444. Helaja, J.; Tauber, A. Y.; Abel, Y.; Tkachenko, N. V.; Lemmetyinen, H.; Kilpeläinen, I.; Hynninen, P. H. *J. Chem. Soc., Perkin Trans. 1* **1999**, 2403–2408. Tkachenko, N. V.; Rantala, L.; Tauber, A. Y.; Helaja, J.; Hynninen, P. H.; Lemmetyinen, H. *J. Am. Chem. Soc.* **1999**, *121*, 9378–9387.
445. Zheng, G.; Dougherty, T. J.; Pandey, R. K. *Chem. Commun.* **1999**, 2469–2470.
446. Tamaki, K.; Imahori, H.; Nishimura, Y.; Yamazaki, I.; Shimomura, A.; Okada, T.; Sakata, Y. *Chem. Lett.* **1999**, 227–228.
447. Meidine, M. F.; Avent, A. G.; Darwish, A. D.; Kroto, H. W.; Ohashi, O.; Taylor, R.; Walton, D. R. M. *J. Chem. Soc., Perkin Trans. 2* **1994**, 1189–1193.
448. García, M. M.; Cruz-Almanza, R.; Lara-Ochoa, F.; Almehua, J. G.; Ochoa, A. T.; Zentella-Dehesa, A.; Vidales, V. G. *Fullerene Sci. Technol.* **1999**, *7*, 897–908.
449. Braun, T.; Schubert, A. P.; Kostoff, R. N. *Chem. Rev.* **2000**, *100*, 23–37.

Chapter 2

Transition-Metal-Templated Synthesis of Rotaxanes

MARÍA-JESÚS BLANCO, JEAN-CLAUDE CHAMBRON, M. CONSUELO JIMÉNEZ, AND JEAN-PIERRE SAUVAGE

Laboratoire de Chimie Organo-Minérale, UMR 7513 du CNRS, Université Louis Pasteur, Institut Le Bel, 4, rue Blaise Pascal, 67070 Strasbourg Cedex, France

Topics in Stereochemistry, Volume 23, Edited by Scott E. Denmark.
ISBN 0-471-17622-2

I. INTRODUCTION: DEFINITION OF A ROTAXANE

Chemists' long-standing fascination with rotaxanes, catenanes, and knots[1] (Figure 2.1) stems from the unique topology of catenanes and knots, and the fact that rotaxanes and catenanes contain two or more independent portions that are not bonded to each other by any covalent bond and yet remain linked. This mode of bonding, typical of rotaxanes and catenanes, is called a mechanical link. Whereas catenanes are composed of interlocked rings only, the simplest rotaxanes are molecules made from a macrocycle threaded onto a dumbbell-shaped molecule consisting of an axle bearing large, bulky end-groups (or stoppers) to prevent the macrocycle from slipping out. The term "rotaxane" (from the Latin words *rota* and *axis* meaning wheel and axle, respectively) was coined in 1967 by Schill and Zollenkopf,[2] and replaced the term "hooplane" suggested the same year by Harrison and Harrison.[3]

The preparation of even relatively simple catenanes and rotaxanes was a formidable synthetic challenge in the 1960s, which was when the first syntheses of rotaxanes were published.[2,3] However, this is no longer true at the dawn of the twentyfirst century, thanks to the introduction of template effects in newer preparative approaches.

This chapter will be concerned mainly with the transition-metal-templated synthesis of rotaxanes. General features of these compounds, including stereochemical issues, will be addressed at first. The intent, however, is not to

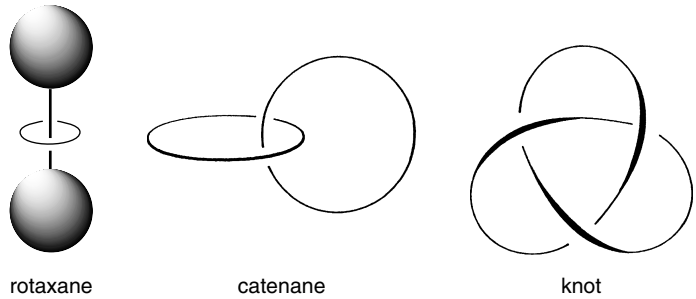

Figure 2.1. The prototypical [2]-rotaxane, [2]-catenane, and one enantiomer of the trefoil knot.

present a comprehensive review of the rotaxanes that have been made using the transition-metal-templated route. Rather, we present an analytical and concise approach, that helps rationalize this chemistry by way of selected examples. Further detail on the work can be found in the references.

II. GENERAL ASPECTS OF ROTAXANE CHEMISTRY

A. Topological Stereochemistry: Catenanes and Knots, the Topological Link

The importance of geometry in understanding molecular structure was illustrated long ago by the pioneering work of Louis Pasteur, Achille Joseph Le Bel, and Jacobus Henricus van't Hoff. However, it was only after Harry L. Frisch and Edel Wasserman's now classic paper,[4] a century later, that the topology of molecular structures is also being considered to be significant.

Molecules can be seen as three-dimensional objects possessing Euclidean geometrical and topological properties.[5] Euclidean geometric properties are those to which chemists usually refer in describing the stereostructure of a molecule, namely bond lengths and bond angles. Topological properties are classified as "intrinsic" and "extrinsic." The extrinsic topology is simply the atom connectivity (called the molecular graph), and the intrinsic topology is described by embedding the molecular graph in the three-dimensional space (e.g., interlocking rings in the case of catenanes, and knotting and closing a curve in the case of knots). Unlike Euclidean properties of rigid structures, topological properties of molecules are invariant when the molecules are subjected to continuous deformation in three-dimensional space.

The idea of topological diastereoisomers was introduced by comparing the catenane made with two interlocking macrocycles to the set of the separate rings (with same atomic composition). As for Euclidean diastereoisomers, the two systems have the same atom connectivity, and their physical and chemical properties may be very different: complexing[6] and chromatographic behavior, melting points, acid-base properties,[7] colligative properties (e.g., molar volume[8]). The expression "topological isomers" was proposed by Walba,[5] and is best exemplified using a single closed curve: normal (topologically trivial) or knotted cycle (the simplest knot being the trefoil knot). The three objects *a*, *b*, and *c* of Figure 2.2 are *topological diastereoisomers*. Although they may consist of exactly the same atoms and chemical bonds connecting these atoms, they cannot be interconverted by any type of continuous deformation in three-dimensional space. In addition the objects *b* and *c* are *topological enantiomers*, since the mirror image of *b* is identical to *c*.

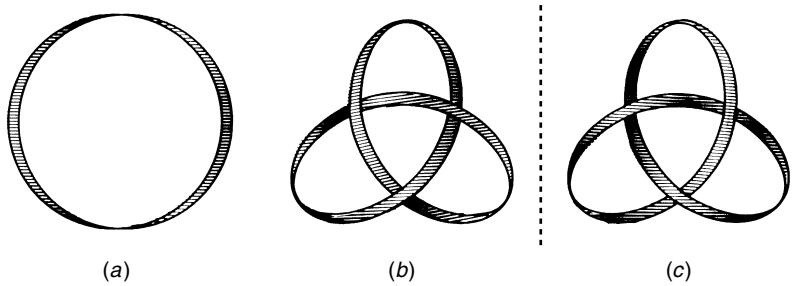

Figure 2.2. The trivial knot (single curve, a) and the two enantiomers of the trefoil knot (*b* and *c*). All three knots are topological stereoisomers.

B. Rotaxanes and Catenanes: The Mechanical Link

From a purely topological point of view, rotaxanes have never been considered as noble as interlocking ring systems and knots, although they have been associated with these species since the first published discussions and experimental work on catenanes.[4,9] A rotaxane was not classified as a topological isomer of a free ring and a dumbbell, since both states might be interconverted without breaking a covalent bond, either by expansion of the ring diameter or by contraction of the dumbbell stoppers (Figure 2.3).

In catenanes the mechanical bond that holds the components together is also a *topological bond* (the interlocked rings cannot be separated without cleavage of one ring), whereas in rotaxanes only deformations of one of the components are required to dissociate the system. Therefore rotaxanes owe their existence to the larger size of the stoppers as compared to the ring diameter, that is, to *steric factors*.

In other words, rotaxanes can be described as threaded species stabilized by steric interactions. The relative size of the different components must be carefully controlled. The cross section of the macrocycle must be large enough to allow a free motion along the thread and small enough to ensure efficient stoppering.[10] The thread must protrude from the rims of the macrocycle to prevent steric hindrance of the stoppering reaction.[11] On the

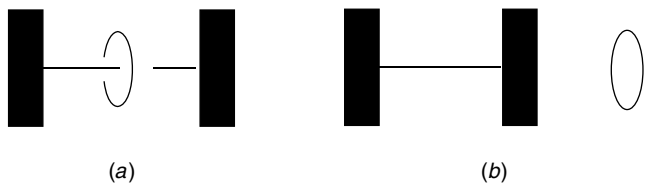

Figure 2.3. A [2]-rotaxane (*a*) and the set of separated components, ring and dumbbell (*b*).

contrary, pseudorotaxanes[12] (or prerotaxanes = precursors to rotaxanes) are unlocked threaded species. Pseudorotaxanes owe their long-term stability to intercomponent chemical interactions, such as hydrogen[1h,i] or coordination bonds,[1b,c,d,g] hydrophobic,[11] or donor-acceptor electronic interactions.[1f]

C. Nomenclature, Morphologies, and Constitution of Rotaxanes

The simplest rotaxane morphology, as defined in the Introduction and represented in Figure 2.1, is noted as [2]-rotaxane to express that it is made up with two components: a ring and a dumbbell.[1a] More generally, an [*n*]-rotaxane contains $n - 1$ rings threaded onto a dumbbell component. Figure 2.4 shows several relatively simple rotaxane morphologies that have been realized.

Two higher homologues of the [2]-rotaxane are represented: the [3]-rotaxane and the [4]-rotaxane. Whereas [3]-rotaxanes are relatively common,[13] this is not the case for the linear [4]-rotaxane[14] and its branched or dendritic analogue.[15] An important system in the recent developments of rotaxane chemistry is the [2]-rotaxane whose dumbbell contains two separated sites for interaction of the threaded macrocycle. In response to an external trigger, the macrocycle can move between the two sites of the dumbbell.[16] If the sites (sometimes called stations) are identical, the rotaxanes are degenerate,[17] whereas if the sites are different the interconversion of the isomeric rotaxanes may be controlled by different means, depending on the nature of the driving force that governs the interaction between the ring and the stations. For example, electronic donor-acceptor or coordination (metal-ligand) interactions can be controlled electrochemically,[16a,b,f] while hydrogen-bonding interactions can be controlled by the polarity of the solvent,[16d,g] or the acidity of the medium.[16e,g] Light has also been used for the control of molecular motions.[16e,f]

The chemical constitution of rotaxanes will depend, of course, on the methods used for their elaboration. Whereas the statistical synthesis (*vide infra*)

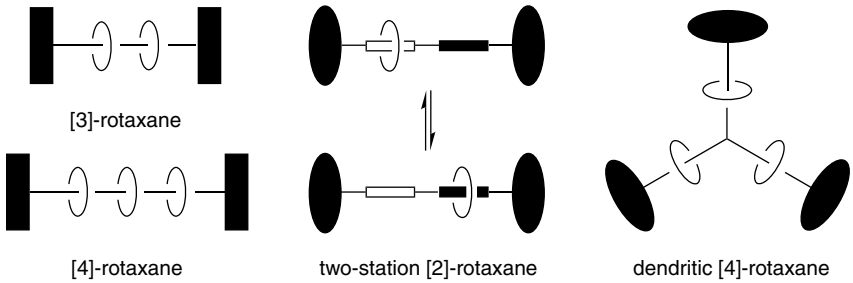

Figure 2.4. Examples of morphologies of rotaxanes.

is not demanding in terms of functionality, template methods require that the components (i.e., the rod and the macrocycle in the case of the threading route) be able to interact. Therefore the components should contain all the necessary complementary chemical information, such as chelating subunits, functional groups able to form hydrogen bonds, and electron donor and acceptor moieties. Cyclodextrins,[11,18,19] cationic[1f] or amide-based[1h,16d,g] cyclophanes, electron-rich benzo-crown ethers[1f] or simple crown-ethers[1e,f] have been extensively used as macrocycles, as shown in the examples developed below. Rarer is the use of cucurbituril.[20] The most common stoppers are derived from the bulky triphenylmethyl (trityl) group, because the size of the trityl group can be easily controlled by peripheral substitution.[21] Transition-metal complexes are also a very versatile material for making stoppers of various size, since one simply controls the number and nature of the ligands around the metal.[11,18,22] Another important group of stoppers is the porphyrins,[23,24] which are electro- and photo-active moieties that can mimic the properties of natural cofactors such as hemes or chlorophylls. Porphyrins have also been used as parts of the threaded rings.[24,25]

D. Synthetic Approaches of Rotaxanes

Because of the intriguing structure of rotaxanes much effort has been devoted to develop efficient synthetic methods to make such compounds. Three principles known as *threading*, *slipping*, and *clipping*[26] have been conceived (Figure 2.5*a*–*c*). In *threading* (Figure 2.5*a*), a preformed macrocycle is first threaded onto the molecular axle and then the stoppers are chemically attached to the end of the thread. The *slipping* principle (Figure 2.5*b*) consists in the assembly of a presynthesized-size complementary ring and a string achieved by applying a certain amount of thermal energy. In the *clipping* principle (Figure 2.5*c*), the macrocyclization of the ring component takes place in the presence of the preformed dumbbell component.

In accord with these three principles, three synthetic methods — *statistical, directed*, and *template* — have been developed to make rotaxanes. Figure 2.5*d*–*f* gives an example of the combination of the threading principle and these methods. In the *statistical* synthesis (Figure 2.5*e*) the molecular axle is inserted through the macrocycle by statistical threading. Usually the portion inserted is very small, but it can be quite large if the ring is used as the solvent. Statistical slipping was the strategy used in the early 1970s by Harrison and co-workers to synthesize rotaxanes.[3,27] The *directed* method, developed by Schill and co-workers[2,28] (Figure 2.5*d*), involves the construction of a prerotaxane in which linear and cyclic components are linked covalently. Once the rotaxane backbone is constructed, the covalent bonds are cleaved. In the *template* method (Figure 2.5*f*) the components

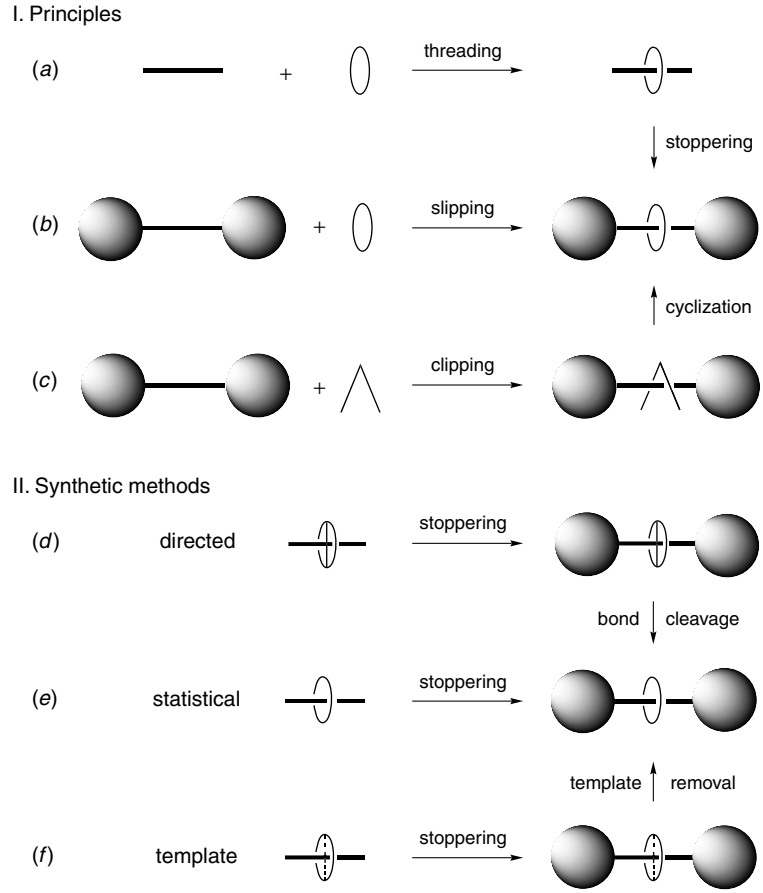

Figure 2.5. (*a*–*c*) The three principles of rotaxane assembly, and (*d*–*f*) the three synthetic methods corresponding to the threading/stoppering principle.

interact through noncovalent bonds (e.g., van der Waals,[11,13c,18,19] hydrogen-bonding,[1h,i,16d,g,20,22] π-π stacking,[1f] or metal-ligand interactions[1b–d,g] in the assembled prerotaxane. The free rotaxane is obtained by suppression of the interactions behind the formation of the prerotaxane once the stoppers have been attached. In hydrogen-bonded systems this can be done by changing the solvent.[16d,g] In principle, as illustrated later, metal templates are the easiest to remove, by competitive decomplexation.

The different strategies and methods can be combined according to their particular features. Thus the statistical synthesis relies on the threading or slipping principle, while the directed method relies only on the clipping method.

The template method is the most general, since it can be accomplished a priori with all the strategies.

The earliest syntheses of rotaxanes were largely based on the statistical or directed methods.[2,3] Statistical methods require very precise reaction conditions, and directed methods involve numerous chemicals steps. However, the use of templates allows high control of these synthetic methods resulting in efficient and precise assemblies of rotaxanes that incorporate a wide range of chemical functionalities. Two types of interactions occur in synthetic template methods: (1) purely organic and (2) transition-metal-templated. In this latter case, the template can easily be removed at the end of the synthesis, whereas in the former, the interactions between the template and the components of the final rotaxane will often be maintained. Selected examples will now illustrate the statistical, the directed, and templated strategies outlined above. The transition-metal-templated route will be developed separately.

E. Selected Examples of Rotaxane Synthesis

1. Statistical Synthesis: Threading and Slipping

One of the earliest rotaxane syntheses was based on statistical threading (Figure 2.6).[3] Harrison and Harrison coupled the 30-membered macrocycle **1** bearing a pendent carboxylic group to a Merrifield's peptide resin, forming

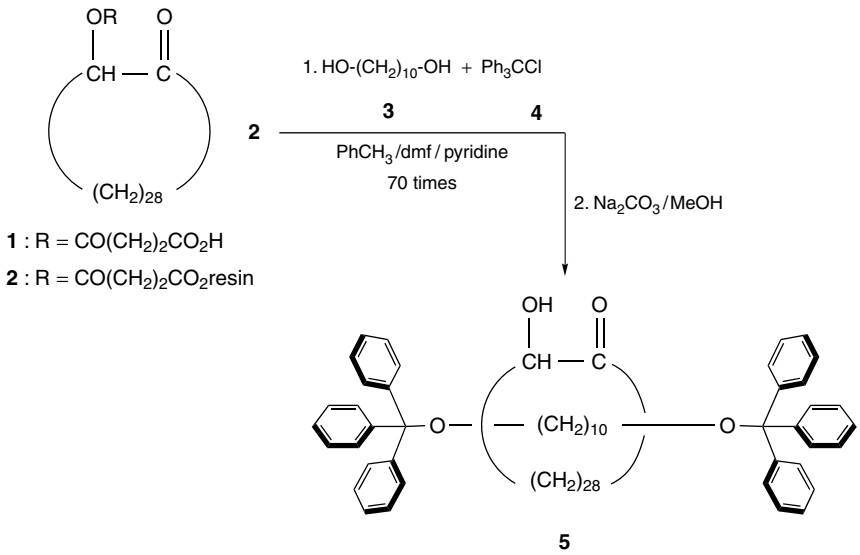

Figure 2.6. Statistical threading: Preparation of [2]-rotaxane **5**.

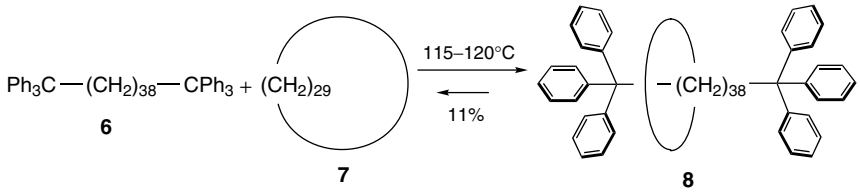

Figure 2.7. Statistical slipping: Preparation of [2]-rotaxane **8**.

the resin adduct **2**. Next, a column was charged with this material and treated with a solution of decane-1,10-diol **3** and triphenylmethyl chloride **4** in a mixture of pyridine, dimethylformamide, and toluene. The process was repeated 70 times. Then the column was washed, and treatment of the resin with sodium carbonate liberated all the macrocycle-containing species. Then rotaxane **5** was isolated in 6% yield. The slipping method was investigated in detail by Schill and co-workers,[29] following initial investigations by Harrison[27,30] and Zilkha and co-workers[31]. As shown in Figure 2.7, [2]-rotaxane **8** was prepared in 11% yield by simple heating of a solvent-free mixture of macrocycle **7** and dumbbell component **6** followed by cooling of the reaction mixture.[29]

2. *Directed Synthesis: Clipping*

So-called directed synthesis involves the control of the selective formation of *intra*-annular or *extra*-annular species by way of covalent bonds. The earliest attempts were undertaken by Lüttringhaus and co-workers but were not successful. An example is shown in Figure 2.8. As reported by Schill in his book,[32] Lüttringhaus and Schill reacted the macrocyclic ketone **9** and the diol **10** in an attempt to obtain the threaded species **11** by the formation of a ketal. They could show that only the extraannular species **12** was obtained in this process. These studies helped much in the development of the multistep procedure of Schill and Zollenkopf.[28] In this approach the components are elaborated at a rigid core, an aromatic ketal (Figure 2.9). The ketal tetrahedral carbon atom in intermediate **16**, obtained in several steps from guaiacoldialdehyde **13** via **14** and **15**, was designed to maintain at right angles the precursor to the thread (a benzene ring bearing two functionalized alkyl chains at *meta* positions) and the precursor to the macrocycle (two functionalized alkyl chains ready to react with a primary amino group placed in between the precursors of the thread). The cyclization reaction (clipping) provided the intermediate "threaded" compound **17** in 26% yield. The stoppers were then grafted, affording **18**, and the bonds linking the dumbbell to the macrocycle cleaved by hydrolysis of the ketal, and subsequent reductive acetylation of the intermediate **19**, to produce the [2]-rotaxane **20**.

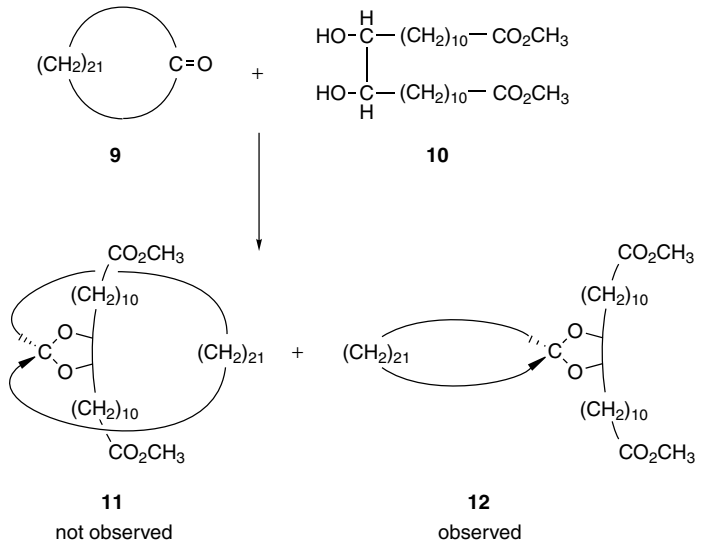

Figure 2.8. Attempts to threading by covalent bond formation. Only the extra-annular conformer **12** was obtained. The intra-annular conformer (**11**) was not observed.

3. Templated Syntheses: Threading, Slipping, and Clipping

Stoddart and co-workers have developed a template strategy for the construction of catenanes and rotaxanes based primarily on donor-acceptor interactions between electron releasing and electron withdrawing aromatic moieties, and relying secondarily on CH•••O hydrogen bonds.[33] The following illustration of their principle of rotaxane synthesis is the stepwise preparation of a [3]-rotaxane containing two different rings, and it involves consecutive threading and slipping steps (Figure 2.10).[13e] The functionalized stopper **21** and linear component **22** were at first allowed to react in the presence of the smaller macrocycle **23** in dimethylformamide at room temperature, but under 12 kbar pressure. The intermediate degenerate two-stations [2]-rotaxane **24** was isolated in 19% yield. In the next step the larger macrocycle **25** was added to a solution of the [2]-rotaxane in acetonitrile, and the reaction mixture heated to 55°C. The target [3]-rotaxane **26** was obtained in 49% yield.

Rotaxanes in which the macrocyclic and dumbbell components are assembled by hydrogen bonds were usually prepared by the threading and stoppering method.[22,34,16g] An exception is the slipping experiment at 350°C performed by Vögtle and co-workers.[35] Another is illustrated in Figure 2.11. In this example the macrocycle is constructed around the dumbbell, the latter serving as a template by use of a clipping procedure. As shown by Leigh and

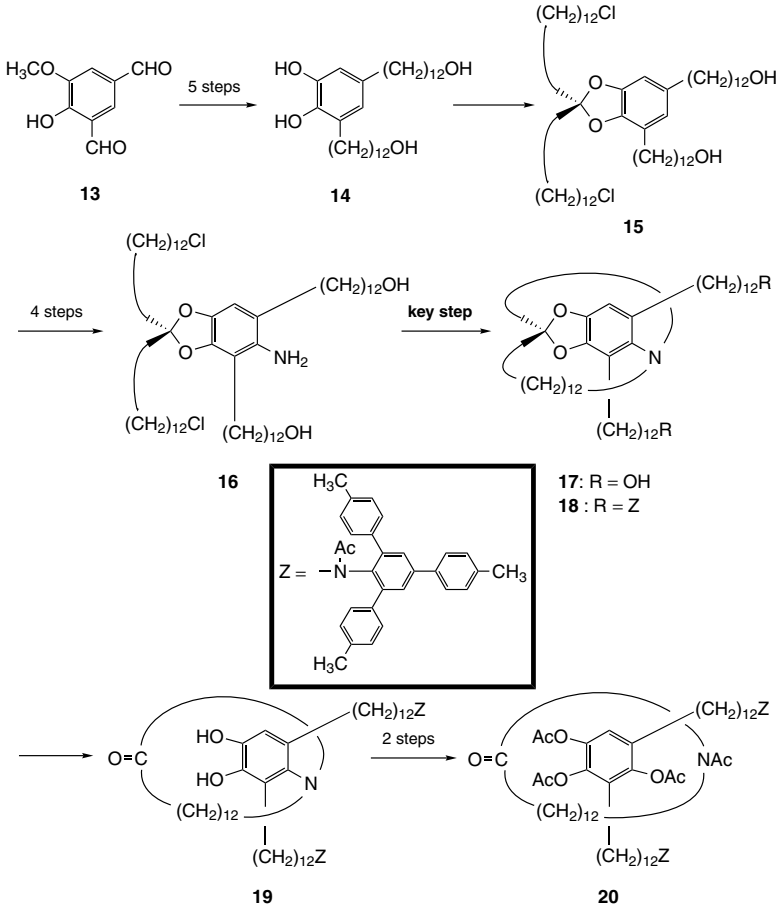

Figure 2.9. Directed clipping. The directed synthesis of [2]-rotaxane **20** by cyclization of the key intermediate **16**.

co-workers, when the glycylglycine-containing dumbbell **27** was reacted with α,α′-diamino-*p*-xylene **28** and isophthaloyl dichloride **29**, rotaxane **30** was obtained in a yield as high as 62%.[34d] This was explained by the fact that adjacent amide groups of the dumbbell adopt transoid conformations that favorably interact via hydrogen bonding with the macrocycle precursors.

F. Stereochemistry of Rotaxanes

Rotaxanes are three-dimensional molecules made from two mechanically linked components: a ring (macrocycle) and a dumbbell subunit. In this section

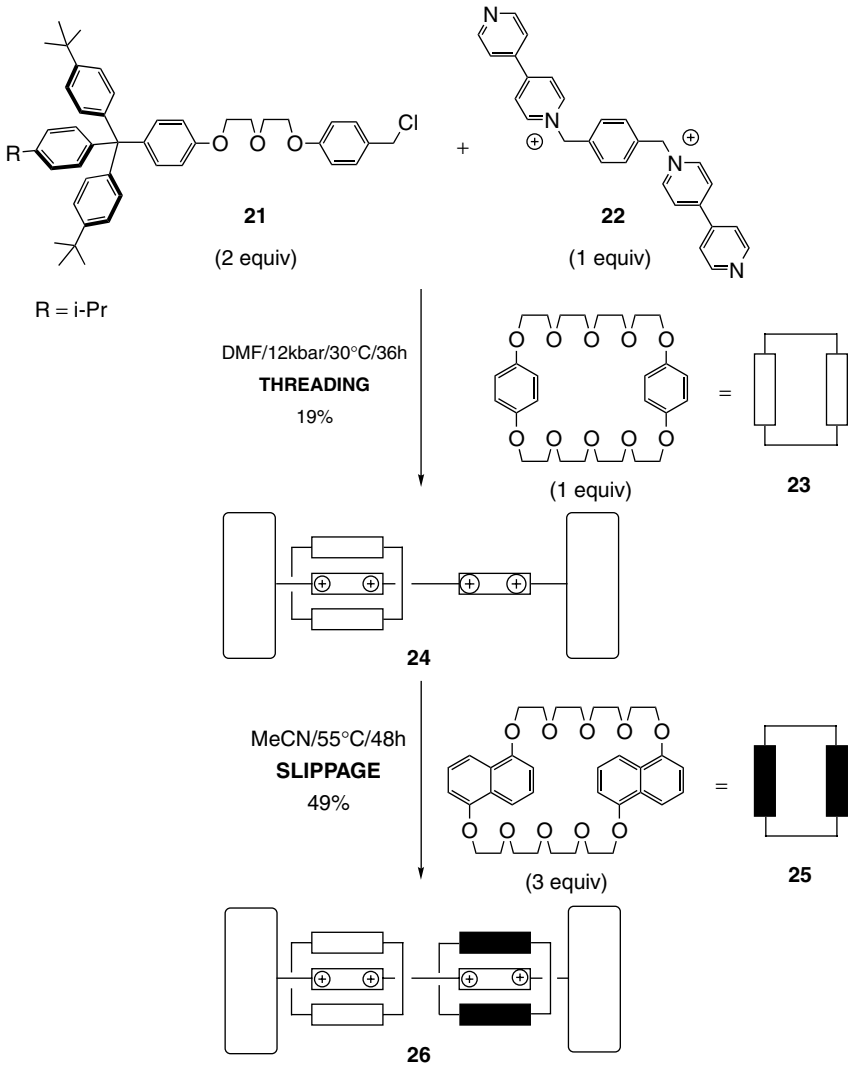

Figure 2.10. Templated threading and slipping. π-donor/π-acceptor interactions control the preparation of [3]-rotaxane **26** containing two different rings.

we discuss the stereochemical features that arise from the mechanical bonding, that is, the combination of ring(s) and dumbbell by threading of the former onto the latter. The different possibilities are represented schematically in Figure 2.12 but many other interesting systems can be created.

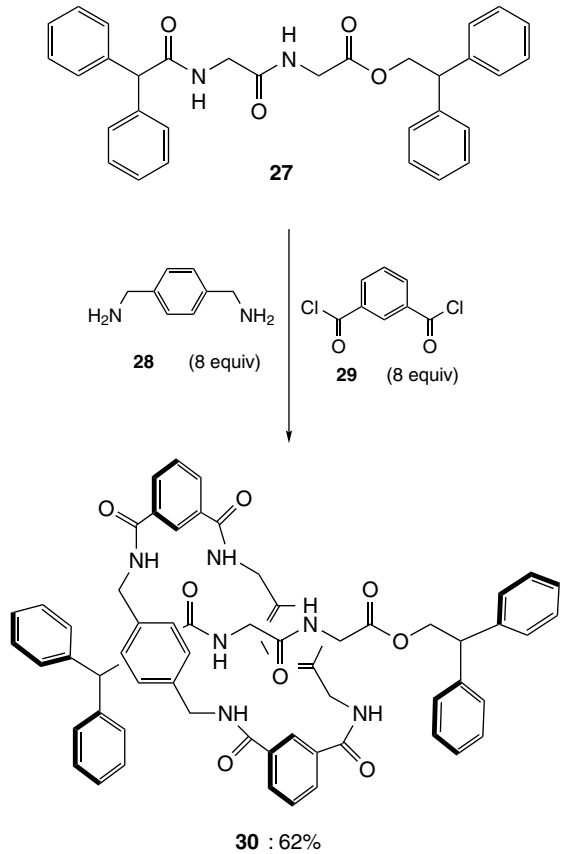

Figure 2.11. Templated clipping. H-bonding interactions control the preparation of [2]-rotaxane **30**.

Undoubtedly, the most important stereochemical feature is chirality. The [2]-rotaxane depicted schematically in Figure 2.12*a* is made with a macrocycle and a dumbbell that are not themselves chiral but *oriented* by appropriate substitution patterns on these components. Vögtle and co-workers described *cycloenantiomeric* rotaxanes that are based on the amide templating functionality (Figure 2.13).[36] Racemic [2]-rotaxane **34** was synthesized in 20% yield by reaction of unsymmetrical acid dichloride **32** with trityl aniline **33** in the presence of macrocycle **31**. The object and its mirror image are created by different sequences of the amide and sulfonamide linkers in both the dumbbell and the macrocyclic component. If the order of the atoms within the dumbbell is examined, in one enantiomer the sulfonamide nitrogen atom is

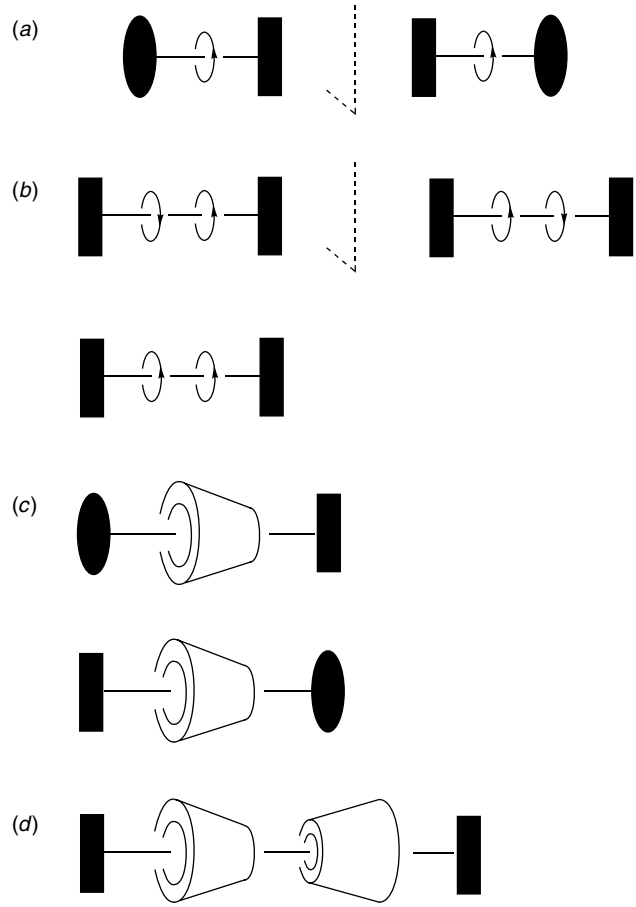

Figure 2.12. Different stereochemistries of rotaxanes that have been realized: (*a*) Chiral rotaxane; (*b*, *c*, and *d*) diastereomeric rotaxanes. Arrows mark macrocycle orientation. The cone-shaped bead represents a cyclodextrin.

passed before the sulfonamide sulfur, whereas in the other enantiomer the order of the atoms is reversed. The enantiomers could be separated by HPLC chromatography on chiral column materials, despite the high conformational flexibility of the molecular parts of the rotaxane, by comparison with more rigid molecules.[37]

[3]-Rotaxanes made with two oriented macrocycles, but a symmetrical dumbbell will also display interesting stereochemical features. Depending on the mutual orientations of the two threaded rings, a pair of enantiomers and a *meso* form of the [3]-rotaxane are obtained, as shown schematically in

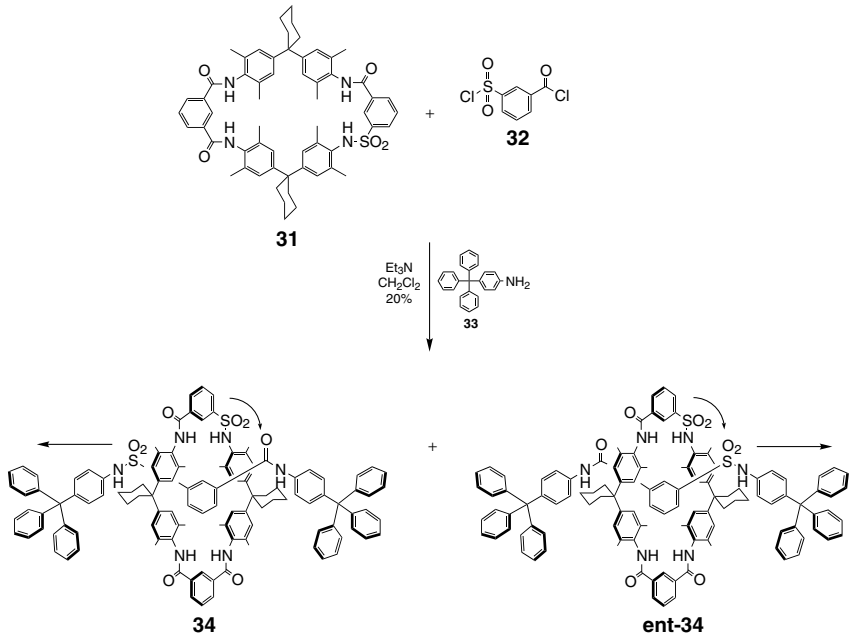

Figure 2.13. Preparation, by templated threading, of the chiral, cycloenantiomeric [2]-rotaxane **34** using H-bonding interactions.

Figure 2.12*b*. These molecules were described by Vögtle and co-workers as *cyclodiastereomeric* [3]-rotaxanes (Figure 2.14).[38] Thus [3]-rotaxanes **37a,b** were prepared in 29% yield by reaction of dibromide **35** with trityl phenol **36** in the presence of the oriented macrocycle **31** and a base. (Threading is driven by hydrogen bonding between the phenate generated in situ and the amide hydrogen atoms of the macrocycle[39]). The three stereoisomers **37a**, **37b**, and ent-**37b**, were nearly completely separated employing again chiral HPLC. As expected, the *meso* form was optically inactive, whereas the enantiomers showed significant circular dichroism activity.

Cyclodextrins (CDX) were used as rings in the earliest template synthesis developed by Ogino[11,18a,d] and others.[18b,c,e,19] These cyclic oligosaccharides are constructed from glucose units as hollow, cone-shaped molecules with a wide rim (secondary OH groups), a narrow rim (primary OH groups), and a nonpolar hydrophobic cavity (Figure 2.15).[40] The size of the cavity, ranging from 5.7 to 9.5 Å, depends on the number of glucose units (6 to 8). The most common cyclodextrins are known as α-, β-, and γ-CDX. Their characteristics are indicated in Figure 2.15. They form inclusion compounds with lipophilic materials in very polar solvents, such as water or dimethylsulfoxide.

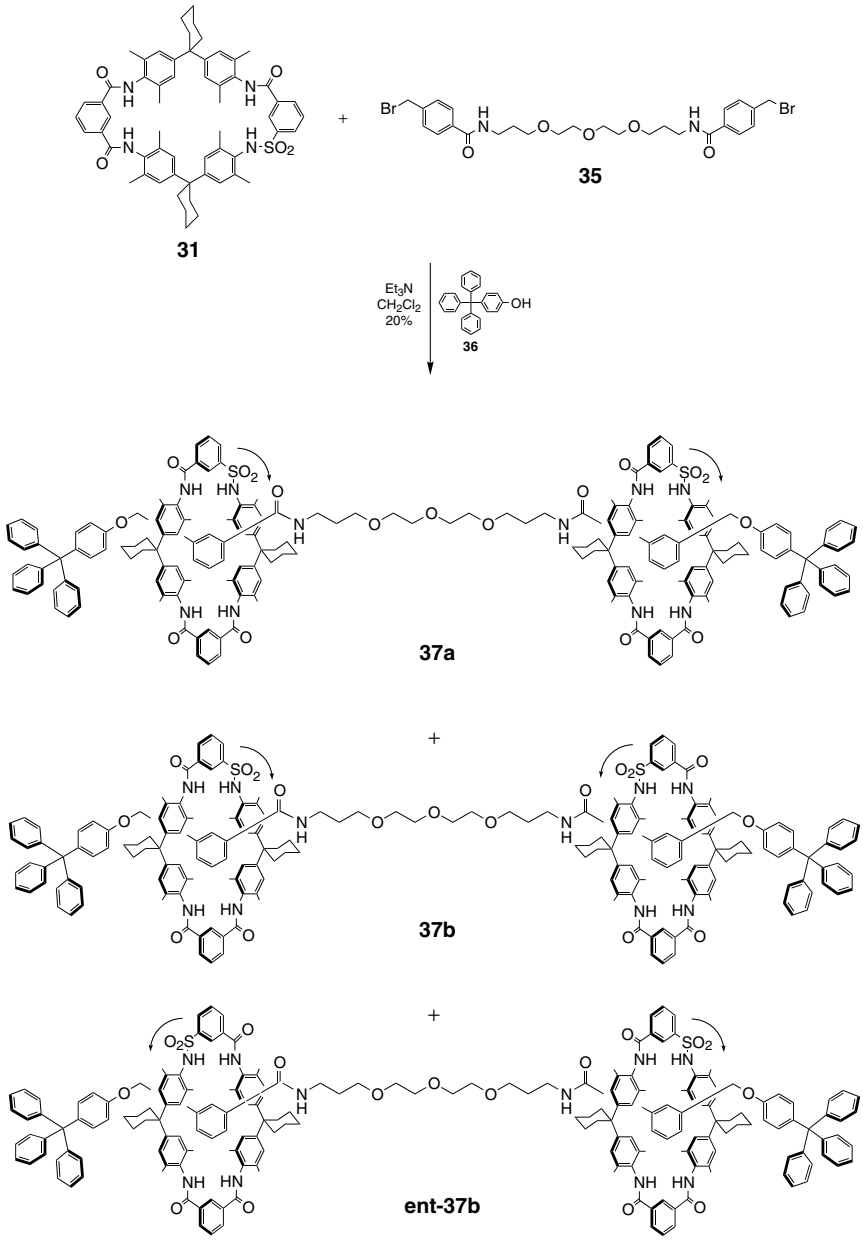

Figure 2.14. Preparation, by templated threading, of the cyclodiastereomeric [3]-rotaxane **37a** and **37b** based on H-bonding interactions.

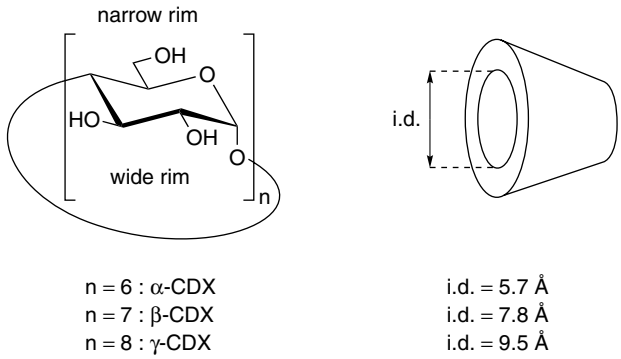

Figure 2.15. Cyclodextrin family.

Cyclodextrins have remarkable stereochemical properties: They are at the same time optically active and oriented rings, with the orientation parallel to the ring axis. These stereochemical properties of CDX work to endow the corresponding rotaxanes with original stereochemical features.

The first cyclodextrin-based rotaxanes were prepared by Ogino in 1981.[18a] The idea was to use kinetically inert Co(III) complex fragments as stoppers. Therefore the molecular thread had to be functionalized with coordinating end groups. One of the synthetic routes is depicted in Figure 2.16*a*.

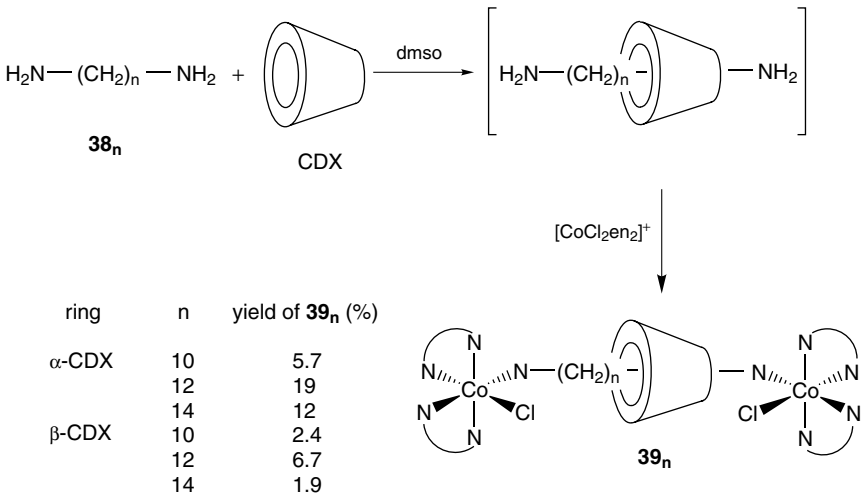

ring	n	yield of **39$_n$** (%)
α-CDX	10	5.7
	12	19
	14	12
β-CDX	10	2.4
	12	6.7
	14	1.9

Figure 2.16. Preparation of the cyclodextrin-based [2]-rotaxane **39$_n$** by stoppering with Co(III) complexes.

Diamino-1,12-dodecane $\mathbf{38_{12}}$ was first equilibrated with β-CDX in dmso, allowing for the formation of the threaded species [$\mathbf{38_{12}}$,β-CDX]. Two equivalents of $[CoCl_2en]^+$ were then added to the reaction mixture. The desired [2]-rotaxane $\mathbf{39_{12}}$ could be isolated in about 7% yield after chromatography on Sephadex. Next, Ogino and Ohata showed that the yield could be increased up to 19% when the smaller α-CDX was used.[11]

Octahedral Co(III) complexes with ethylenediamine (en) are chiral. Working on related rotaxanes, Yamanari and Shimura studied the stereoselectivity of the stoppering reaction induced by the chirality of the cyclodextrin.[18b] When α-CDX and a racemic mixture of Co(III) precursor complexes were used, they observed that the (Δ,Δ) configuration at the stoppers was predominant. More

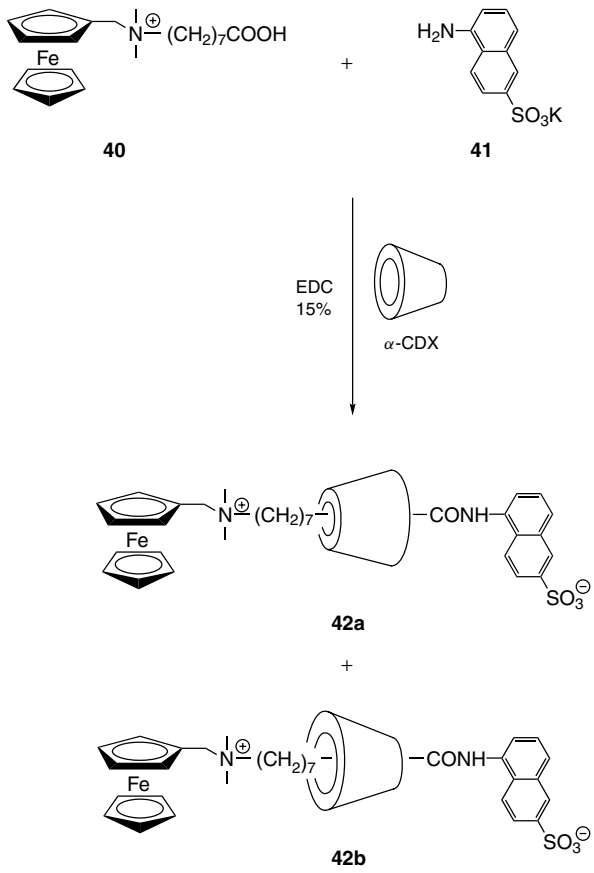

Figure 2.17. Preparation, by templated threading, of diastereomeric [2]-rotaxane **42a** and **42b**, using hydrophobic interactions.

original stereochemical properties of CDX-based rotaxanes are described in the following examples.

Threading such an oriented ring onto a dumbbell end capped with two different stoppers will give rise to two diastereoisomers, as shown schematically in Figure 2.12*c*. Such rotaxanes were actually described by Isnin and Kaifer, and were characterized as CDX-positional isomers (Figure 2.17).[41] Thus reaction of ferrocenyl derivative **40** (1 equiv) with 2 equiv of α-CDX, and potassium 5-amino-2-naphthalene sulfonate **41** in water, in the presence of EDC (EDC = 1-(3-[dimethylamino)propyl]-3-ethylcarbodiimide hydrochloride) as a catalyst, afforded a mixture of diastereoisomeric [2]-rotaxanes **42a** and **42b** in 15% yield and 6 : 4 ratio.

Threading of two cyclodextrins onto a symmetrical dumbbell can occur head-to-head, head-to-tail, or tail-to-tail, defining a new class of diastereoisomeric [3]-rotaxanes, as shown schematically in Figure 2.12*d*. Anderson and co-workers have shown that end-capping of 4,4′-bis(diazonio)azobenzene chloride **43** with 2,6-dimethylphenol **44** in the presence of α-CDX produced the [3]-rotaxane **45** in 12% yield, in addition to the [2]-rotaxane **46** in 9% yield, and free dumbbell **47** in trace amounts (Figure 2.18).[42] The stereochemistry of the [3]-rotaxane species is remarkable because the two cyclodextrin beads have their smallest rims facing to each other. Therefore the threading reaction was stereoselective. The reasons for the exclusive formation of the tail-to-tail stereoisomer are not clearly established.

This work can be interestingly related to earlier studies of Harada and coworkers, who prepared a polyrotaxane from a poly(ethyleneglycol) polymer bearing amino end groups and α-CDX.[43] The stoppering reaction involved

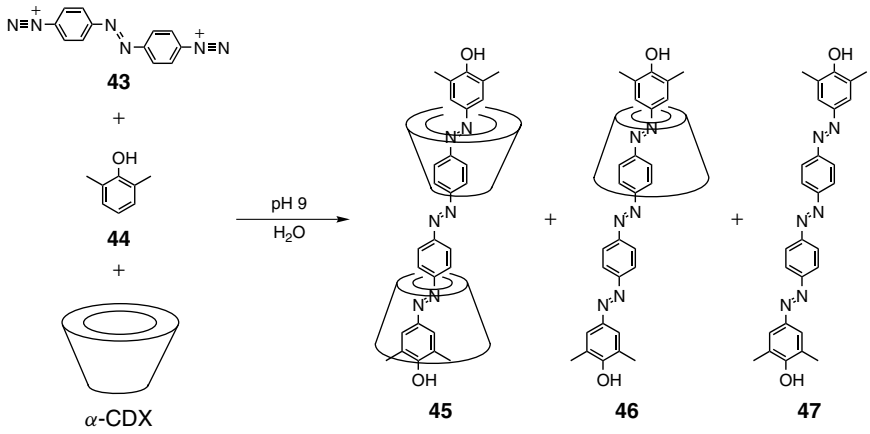

Figure 2.18. Diastereoselective preparation, by templated threading, of [3]-rotaxane **45**, using hydrophobic interactions. [2]-rotaxane **46** and free-dumbbell **47** are also produced in this reaction.

coupling with 2,4-dinitrofluorobenzene in dmf at room temperature, and the polyrotaxane was obtained in 60% yield. Spectroscopic experiments indicated that around 20 to 23 α-CDX rings had threaded onto the poly(ethyleneglycol) chain. More important, consecutive CDXs were shown to be linked by hydrogen bonds, indicating that an *alternation* of the cone-shaped rings had taken place. This tubular assembly was further stabilized by covalently linking the threaded CDXs.[44] After cleavage of the stoppers and extrusion of the poly(ethyleneglycol) backbone, a molecular tube constructed from linked cyclodextrins was produced. Therefore a poly(ethyleneglycol) chain was used as a template to generate a tubular cyclodextrin polymer.

III. TRANSITION-METAL-TEMPLATED SYNTHESIS

A. Principle and Examples

A template is a pattern used in making or duplicating something. The word is derived from old French *temple*, the name for a device in a loom.[45] In Roman antiquity, *templum* was the virtual rectangular field that the augur laid out in the sky with his bent stick. He used then to note favorable (from his right, *dexter*) or unfavorable (from his left, *sinister*) bird crossings. Only later was *templum* the name given for shrine. In chemistry a template is an ion or a molecule used generally as a core for the construction of another molecule around it. Historically transition-metal cations were the first species to be used in templated effects, thanks to their ability to gather and dispose ligands in a given predictable geometry.[46] The archetypical template synthesis is the condensation reaction between copper(II) or nickel(II) diamine complexes and aliphatic ketones or aldehydes to produce Schiff-base complexed macrocycles.[47] An early example is shown in Figure 2.19: biacetylbis(mercaptoethylimino)nickel(II) **48** reacts with α,α′-dibromo-*o*-xylene **49** to produce the macrocyclic Ni(II) complex **50**.[48] However, most of the template syntheses reported involve a transition metal bound to four coordination sites in a square-planar geometry, and thus occur in two-dimensional space.[49] By comparison, relatively few syntheses rely on the reaction between ligands preorganized around the metal in three-dimensional space.[47c] Such syntheses become possible, for example, with transition metals that are hexacoordinated in a preferentially octahedral geometry. In particular, cobalt(III) complexes have been extensively used to induce a three-dimensional, or generalized, templated effect,[50] a prototypical example being the Co(III) sepulchrate synthesis performed by Sargeson and co-workers.[51] The reaction of $[Co(en)_3]^{3+}$ (**51**), HCHO, and NH_3 leads, in a single step, with 74% yield, to the macrobicyclic cobalt(III) sepulchrate complex **52** in which the ligand completely encapsulates

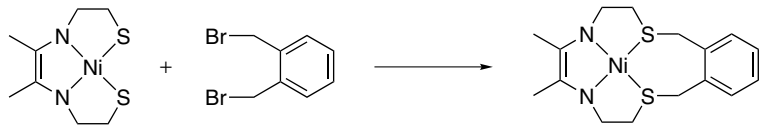

48 **49** **50**

Figure 2.19. Early use of a metal template. Ni(II)-templated preparation of macrocycle **50**.

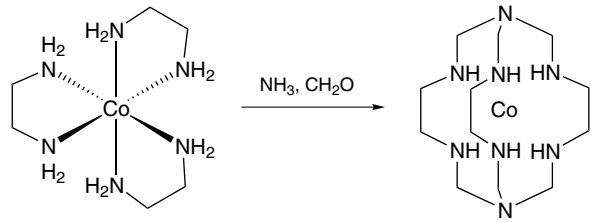

51 **52**

Figure 2.20. Co(III)-templated preparation of the macrobicyclic Co(III)-sepulchrate complex **52**.

the cobalt ion (Figure 2.20). Three-dimensional template syntheses are not restricted to cobalt(III), additional examples involve iron(III) tris-catecholate[52] and ruthenium(II) tris-bipyridine[53] precursor complexes.

B. Template Synthesis of Catenates

The generalized template effect was developed in this laboratory to build up catenane structures.[1b–d,g,54] It was based on the fact that copper(I), a d^{10} transition metal ion, forms very stable complexes with the 2,9-diphenyl-1,10-phenanthroline (dpp) chelate.[55] Two such ligands are entwined around the Cu^{+} cation, the nitrogen atoms of the chelate forming a tetrahedral coordination sphere, as required for the d^{10} electronic configuration. This three-dimensional template synthesis is unique because it relies on a transition metal with a *tetrahedral geometry*. Figure 2.21 shows the synthetic route that was followed to prepare [2]-catenane **57**, starting from a functionalized dpp ligand, 2,9-di(*p*-hydroxyphenyl)-1,10-phenanthroline **53**.[56] In the key intermediate complex **54**, the two ligands **53** are perpendicular to each other, the phenol groups of one ligand extending beyond the phenanthroline nucleus of the other. The molecule seems therefore designed "to ring close with the formation of a catenane."[46b] This was performed by reaction with the diodo-derivative of pentaoxyethylene glycol **55** under high dilution conditions. Copper(I)-complexed [2]-caten*ate* **56** was obtained in 27% yield by this route. The metal template was then released

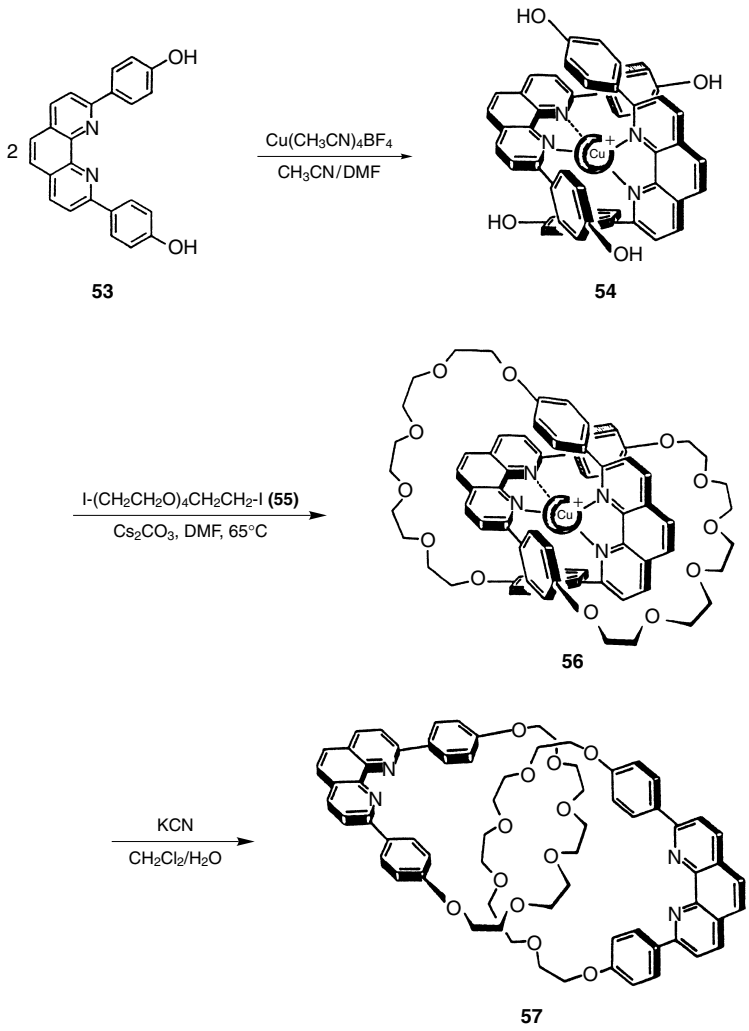

Figure 2.21. Copper(I)-templated synthesis of [2]-caten*ate* **56** and its demetallation to the corresponding [2]-caten*and* **57**.

by competitive complexation with cyanide, affording the [2]-catenane or caten*and* **57** quantitatively.

The synthetic route described above corresponds to strategy I of Figure 2.22. Strategy II was in fact tested at first, since it involves well-controlled steps.[54a,56] This approach requires the preliminary preparation of one single chelate macrocyclic component. However, once intermediate (*F*)

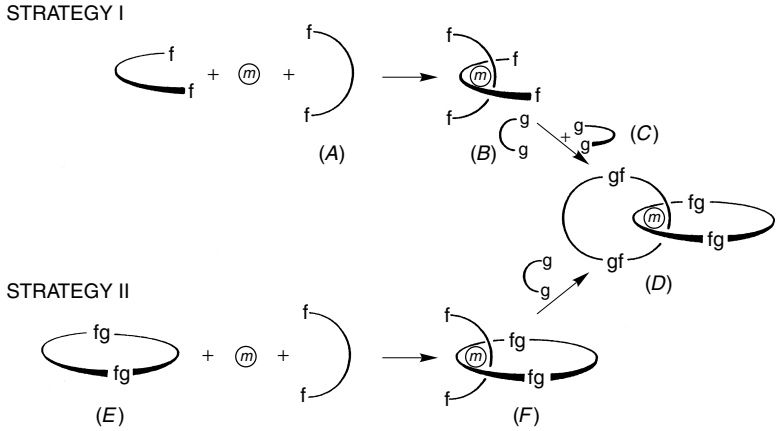

Figure 2.22. Strategies for the transition metal-templated synthesis of catenanes. The metal (m) predisposes two fragments as open chelates (A) (strategy I) or as a macrocyclic chelate (E) and an open chelate (strategy II) in intermediates (B) and (F), respectively. Cyclization of these intermediate complexes with the chain fragments (C) provides the [2]-catenate complex (D).

(called precatenate) is formed, only a single cyclization reaction is needed to afford the interlocked species. Accordingly, yields as high as 42% were observed in this last step.

The clean and selective formation of precatenate (F) deserves some comment. Of course, a homoleptic complex like (B) of Figure 2.22 could also have been formed. However, as shown in Figure 2.23, this would imply that

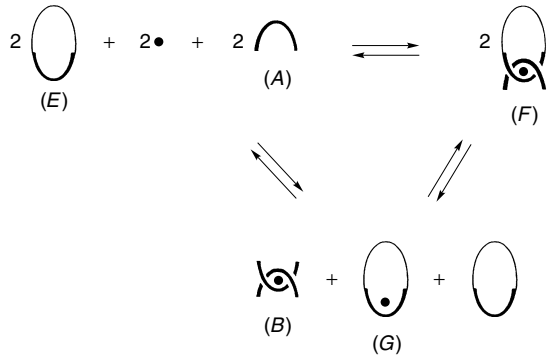

Figure 2.23. The equilibria shown here involve a mixture of macrocyclic chelate (E), open chelate (A), and metal cation (black disk), on the one hand, and different complexed species, on the other hand: The "threaded" complex (F) or a mixture of homoleptic complex (B), metal-complexed macrocycle (G), and free-macrocycle (E).

the remaining fraction of copper(I) be complexed by the single chelate macrocycle (*E*), as in complex (*G*). Obviously two such macrocycles cannot entwine around a Cu^+ cation, and since $Cu(dpp)_2^+$ complexes are much more stable than the $Cu(dpp)^+$ homologues,[55] bis-chelate complex (*F*) forms exclusively.

IV. TRANSITION-METAL-CONTROLLED THREADING: A NEW PRINCIPLE OF ROTAXANE SYNTHESIS

The precatenate intermediate (*F*) of Figure 2.22 can be regarded as a threaded complex that is thermodynamically stabilized by coordination to the metal. In recognition of this feature, a transition-metal-templated synthesis of rotaxanes was devised as shown in Figure 2.24.[23b,57] The threading step (*i*) is a complexation reaction involving (1) a macrocycle that incorporates a dpp chelate (*A*), (2) a linear fragment incorporating the same dpp chelate (*B*) and that is also end-functionalized by the appropriate reactive groups X. As a consequence of its stereoelectronic requirements, the copper(I) cation templates the assembly of the threaded complex or prerotaxane (*C*). After stoppering (*ii*), a copper(I)-complexed [2]-rotaxane (*D*) is produced. Release of the Cu^+ cation leaves the template-free [2]-rotaxane (*E*).

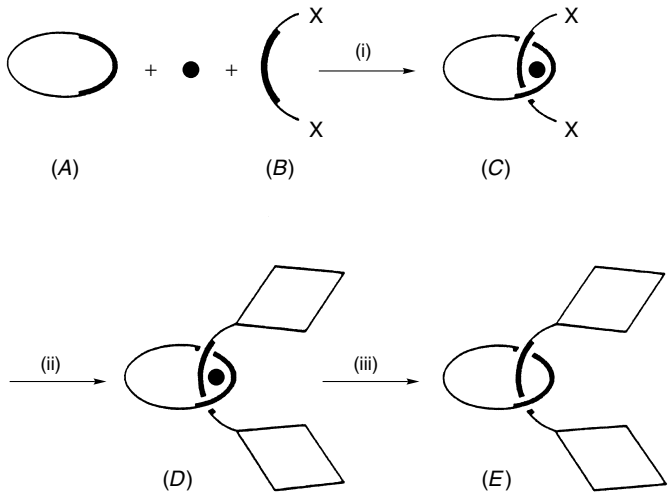

Figure 2.24. Schematic representation of the principle of transition-metal-templated synthesis of [2]-rotaxanes from macrocyclic chelate (*A*), metal cation (black disk) and open chelate (*B*). The latter bears functions X at its extremities, which will be used for anchoring or constructing the stoppers (represented as diamonds). (*i*) Threading step; (*ii*) stoppering step; (*iii*) removal of the metal template.

V. MULTITHREADING EXPERIMENTS: INVESTIGATING PRE[N]ROTAXANE FORMATION

Initial multithreading experiments involved macrocycle **58** and the various molecular threads of Figure 2.25, containing two chelating subunits.[58] These

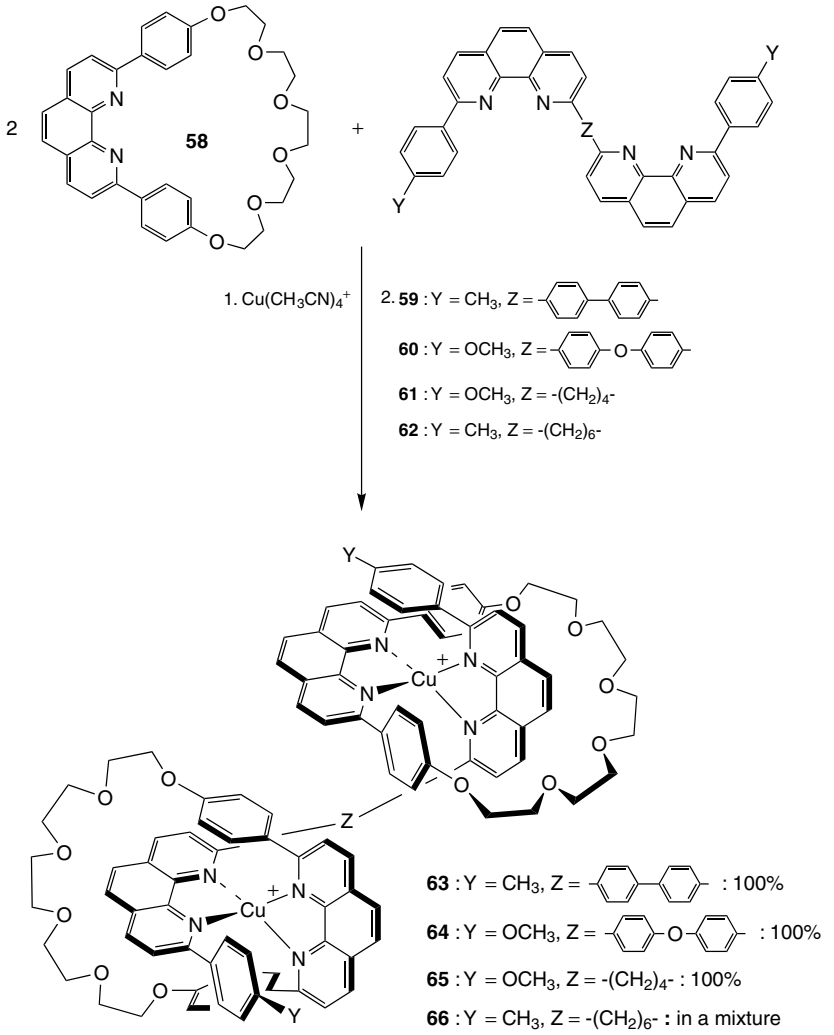

Figure 2.25. Copper(I)-templated threading of macrocycle **58** onto 1,10-phenanthroline-based molecular threads containing two such chelates: **59**, **60**, **61**, and **62**, to afford threaded complexes **63**, **64**, **65**, and **66** respectively.

linear components incorporate 2-*p*-anisyl, or 2-*p*-tolyl-1,10-phenanthroline chelates linked by biphenyl (**59**) biphenylether (**60**), $-(CH_2)_4-$(**61**) or $-(CH_2)_6-$(**62**) spacers. Mixing **59**, **60**, or **61** (1 equiv) with macrocycle **58** (2 equiv) and $[Cu(CH_3CN)_4]PF_6$ (2 equiv) in CH_3CN/CH_2Cl_2 mixtures produced a single complex in all three cases: respectively, **63**, **64**, and **65**. The

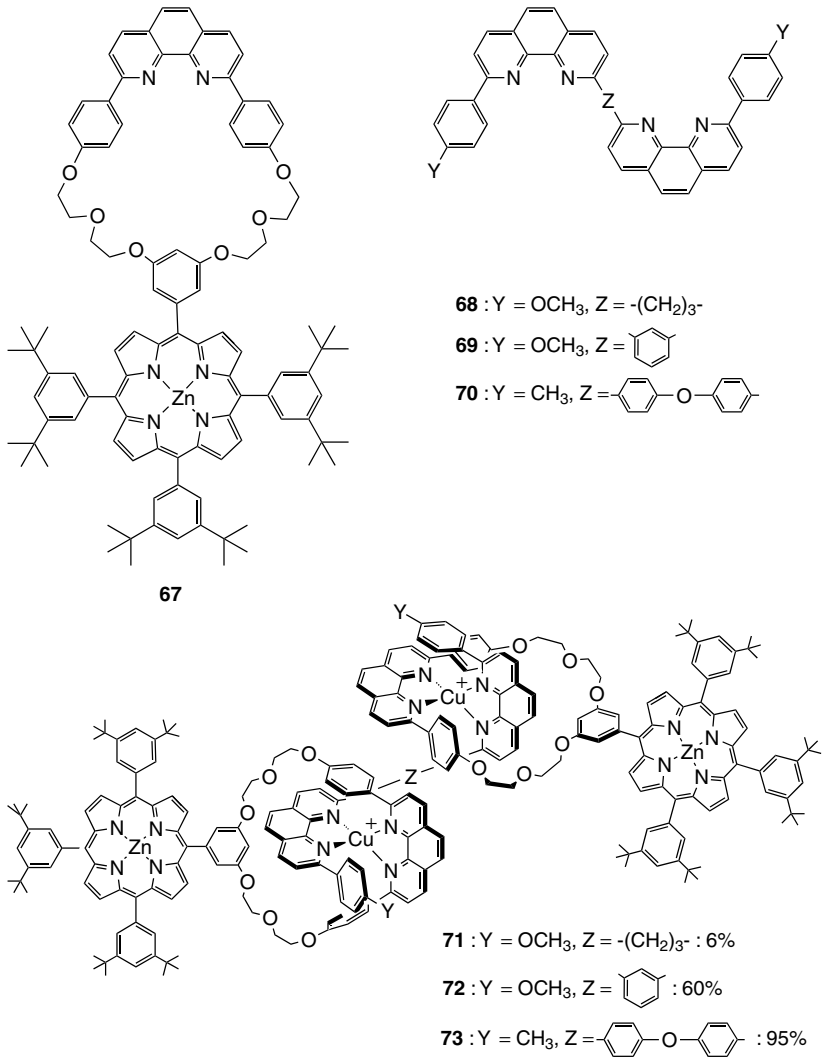

Figure 2.26. Assembly, by Cu(I)-templated threading, of two zinc porphyrins appended to a chelating macrocycle (**67**). Bis-chelate molecular threads **68**, **69**, and **70** provide threaded complexes **71**, **72**, and **73** respectively.

threaded structure was supported by mass-spectroscopy and particularly, ^{1}H-NMR spectroscopy. When the $-(CH_2)_6-$bridged bis-chelate **62** was involved, a mixture of complexes (**66**) was formed. This suggests that the spacer plays an important role in the control of the complexation properties of the bis-chelate threads. This result was taken into account for the synthesis of [3]-rotaxanes (see Section VI.D).

This multithreading process was realized in the construction of multiporphyrin assemblies from macrocycles with pendent zinc(II) or gold(III) *meso*-tetraarylporphyrins.[59] These assemblies are shown in Figure 2.26,

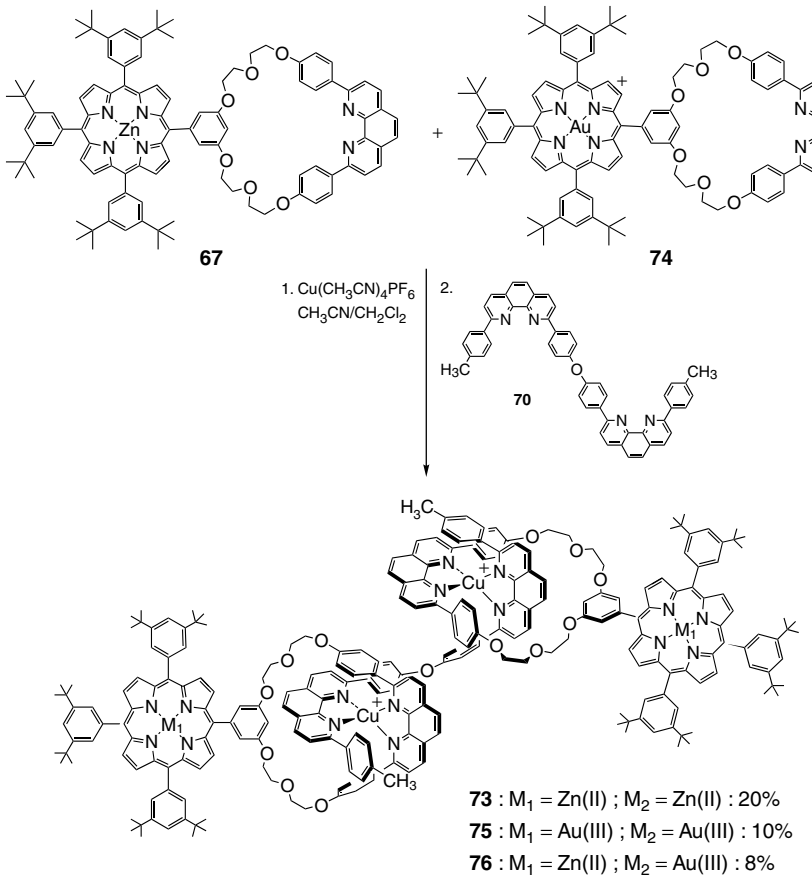

Figure 2.27. Assembly, by Cu(I)-templated threading, of a zinc(II) porphyrin (**67**) and a gold(III) porphyrin (**74**) appended to a chelating macrocycle. The bis-chelate molecular thread **70** affords a mixture of homoleptic complexes **73** and **75**, and heteroleptic complex **76**, which can be separated by chromatography.

together with the linear components used. Mixing **68**, **69**, or **70** with macrocycle **67** under the same conditions as above produced mixtures of complexes in the case of bis-chelates **68** and **69**, from which the desired threaded compounds could be isolated in 6% (for **71**) and 60% (for **72**) yields, respectively, after chromatography. As noted above, competing complexation reactions, like formation of a 1 : 1 complex in the case of the $-(CH_2)_3-$bridged thread **68**, or a dinuclear double helix for the *m*-xylyl-bridged bis-chelate **69**, decreased the yields of threaded compound. Nevertheless, when **70** was used as the linear component, the yield of the threaded complex **73** was nearly quantitative. Therefore this compound was used for threading two different porphyrin-containing macrocycles (Figure 2.27). The macrocycles **67** and **74** (1 : 1 stoichiometry) incorporating zinc(II) and gold(III) porphyrins, respectively, were combined with a stoichiometric amount of $[Cu(CH_3CN)_4]PF_6$, and the required amount of the molecular thread **70** was added to the solution of complexed macrocycles. As expected, the threaded complexes **73**, **75**, and **76** had formed quantitatively in the 1 : 1 : 2 statistical ratio. They were separated by chromatography and isolated in 20%, 10%, and 8% yields for **73**, **75**, and **76**, respectively. A remarkable feature of the heteroporphyrinic system **76** is its kinetic stability: It does not detectably "scramble" to either **73** or **75** when kept in CD_2Cl_2 solution at room temperature for 24 hours.

VI. ROTAXANE FORMATION

A. Stoppering by Capping or Generation In Situ

It is obvious that if the acyclic fragment that threads the ring does not bear blocking groups at its ends, dethreading will occur in the absence of any interactions between the thread and the ring. The general approach is to attach one, or better two bulky groups at the extremities of the string in order to prevent unthreading. Two main strategies have been employed to stopper the prerotaxane or threaded species, either attaching a preformed bulky group to the end of the rod of the prerotaxane, or use a functional group at the end of the string to build the stopper in situ. Examples of both types can be found in the literature cited in this chapter. They are illustrated below in the case of the copper(I) template route. Both approaches require that the threaded complex is stable under the reaction conditions used for the stoppering.

B. Removal of the Metal Template by Competitive Decomplexation

Release of the Cu^+ cation (step *iii* of Figure 2.22) is performed by competitive complexation with the CN^- anion, which binds Cu^+ avidly.[6] This

process leaves the template-free rotaxane. It should be noted again that this decomplexation step is unique to the transition metal-template approach. Neither hydrophobic nor hydrogen-bonding interactions can be canceled so easily, except by changing the solvent.

C. Example of [2]-Rotaxane Synthesis by Capping

The [2]-rotaxane **81** of Figure 2.28 owes its existence to transition metal-complex fragments as stoppers.[60] The thread **77** designed for its synthesis

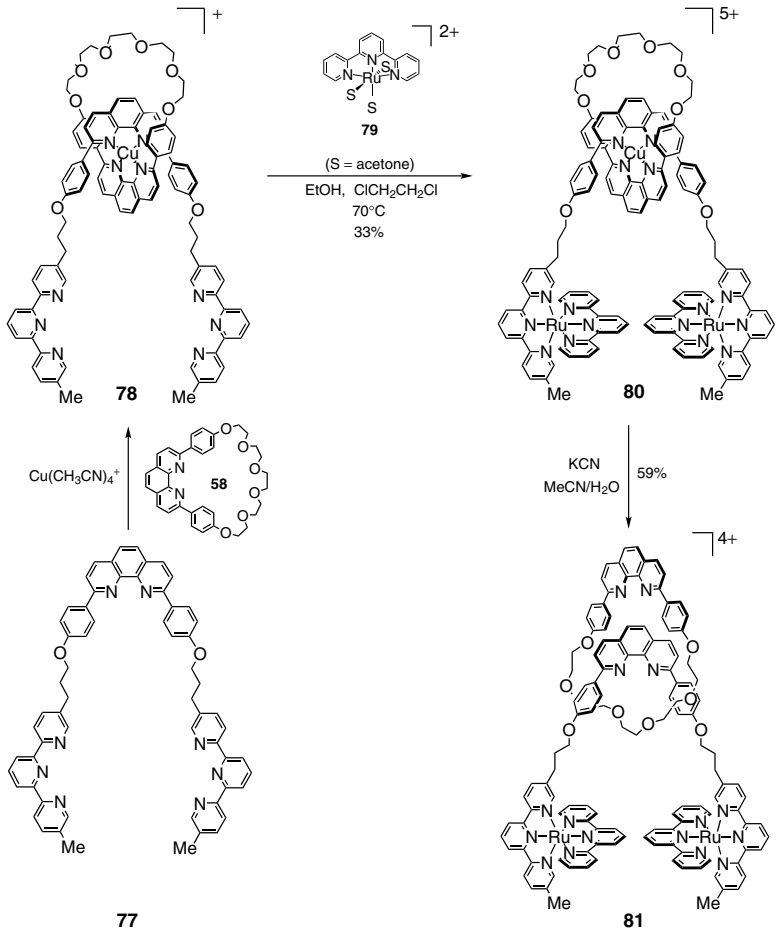

Figure 2.28. Copper(I)-templated synthesis of [2]-rotaxane **81** from the thread **77**, macrocycle **58**, and Ru(II)-complex precursor **79**.

contains a central dpp chelate bearing two pendent terpyridyl units. This tris-chelate-containing linear component reacted with stoichiometric amounts of $[Cu(CH_3CN)_4]PF_6$ and the macrocycle **58** to produce the prerotaxane **78** in which Cu(I) is selectively bound to the dpp subunit of the thread. Stoppering was performed by coordinating the pendent terpyridyl subunits to a $[Ru(terpy)]^{2+}$ complex fragment (**79**) under relatively mild conditions (neutral medium). The resulting copper(I)-complexed [2]-rotaxane **80** was obtained in 33% yield. Removal of the metal template with KCN afforded [2]-rotaxane **81** in 59% yield. ^{1}H-NMR experiments established that release of Cu^+ was accompanied by a pirouetting motion of the macrocyclic component, placing the dpp subunit far away from the ruthenium stoppers.

D. Example of [3]-Rotaxane Synthesis by Construction of the Stoppers

It was shown earlier that the Cu(I)-templated threading of two macrocycles onto a bis-phenanthroline-containing thread was possible, provided that the spacer linking the two chelates was well chosen. The principle of the construction of a [3]-rotaxane is shown in Figure 2.29.[13d] The first step is the transition metal-templated threading of two macrocycles (*A*) incorporating a chelate subunit onto a bis-chelate thread (*B*), to afford the prerotaxane species (*C*). Construction of the porphyrin stoppers using the reactive end-groups X of (*C*) is achieved in the next step, producing the desired [3]-rotaxane species (*D*). The formation of a compartmental [5]-rotaxane (*E*) may also be observed.

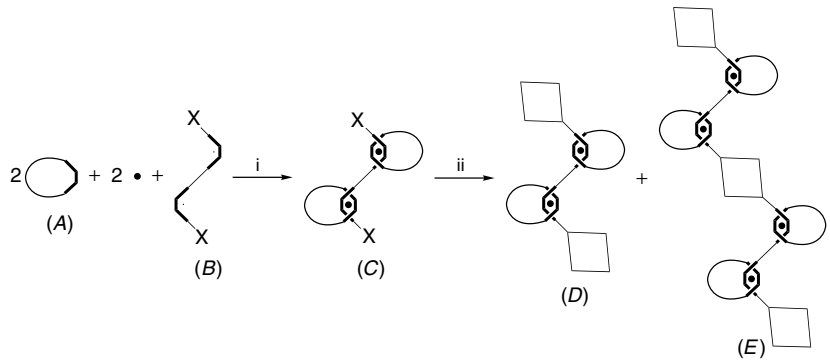

Figure 2.29. Schematic representation of the principle of transition-metal-templated synthesis of [3]-rotaxanes and compartmental [5]-rotaxanes from macrocyclic chelate (*A*), metal cation (black disk) and open chelate (*B*). The latter bears functions X at its extremities, which will be used for anchoring or constructing the stoppers (represented as diamonds). (*i*) Threading step; (*ii*) stoppering step.

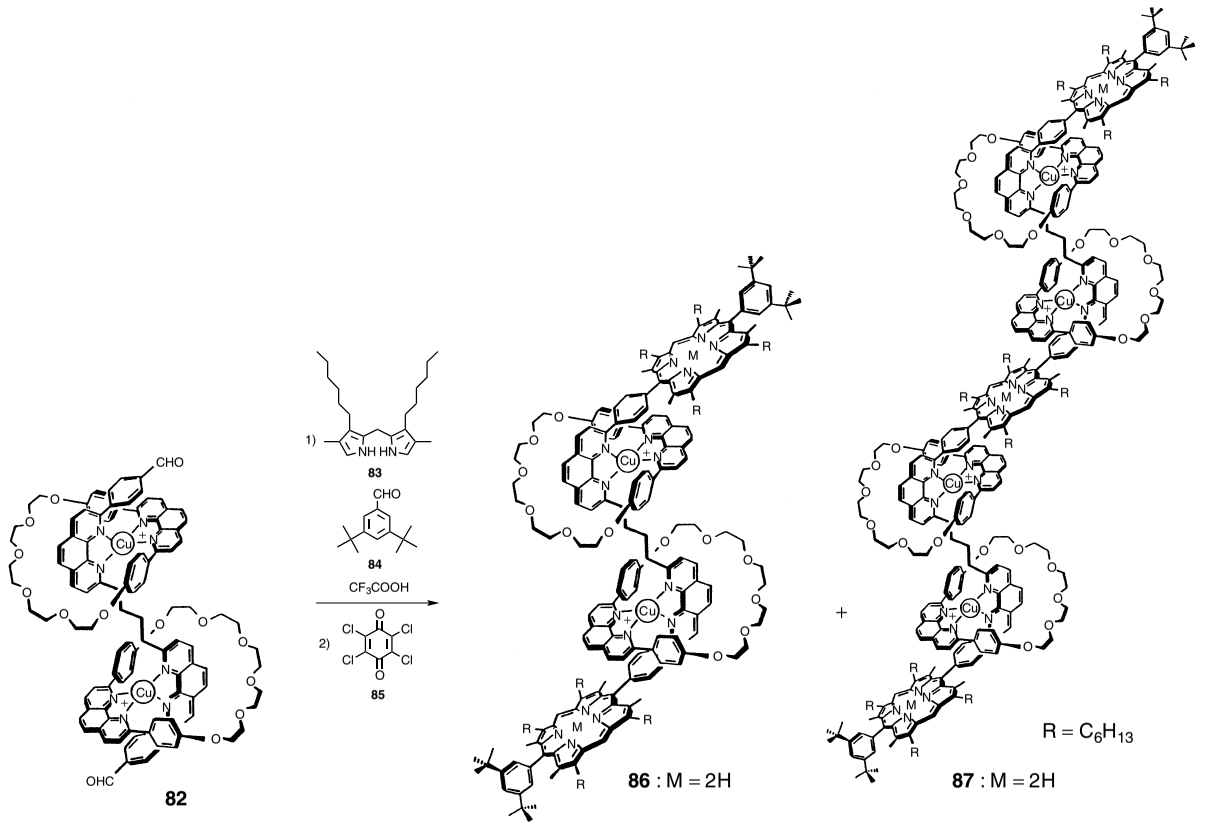

Figure 2.30. Copper(I)-templated synthesis of Cu(I)-complexed [3]-rotaxane **86** and compartmental [5]-rotaxane **87**, bearing free-base porphyrins as stoppers.

The illustration of the process is provided in Figure 2.30.[13d] At first, prerotaxane **82** was generated in a manner similar to that of Figure 2.25. The prerotaxane was subsequently combined with 4,4′-dimethyl-3,3′-dihexyl-2,2′-dipyrrylmethane **83** (10 equiv), and 3,5-di-*tert*-butylbenzaldehyde **84** (8 equiv) using trifluoroacetic acid catalysis, followed by oxidation of the porphyrinogen intermediates with chloranil **85** to afford bis-copper(I)-complexed [3]-rotaxane **86** in 35% yield. Remarkably, a copper(I)-complexed [5]-rotaxane (**87**) could be isolated from the reaction mixture in 8% yield.

Because porphyrins bind metal cations avidly, we found it necessary to "protect" the porphyrin stoppers by complexation prior to template removal studies. The sequence of reactions are shown schematically in Figure 2.31.[61]

Reaction of Cu(I)-complexed [3]-rotaxane **86** with either $Zn(OAc)_2 \cdot 2H_2O$ (2 equiv) or $[Au(tht)_2]BF_4$ (6 equiv; tht = tetrahydrothiophene) afforded the [3]-rotaxanes **87** and **88** respectively, in 83% and 42% isolated yields. Subsequent reaction of **88** with a slight excess of KCN afforded the free [3]-rotaxane **89** in 62% yield. Surprisingly, the same reaction performed on **87** resulted in the removal of only one of the two template cations, affording the Cu(I) complex **90** in essentially quantitative yield.

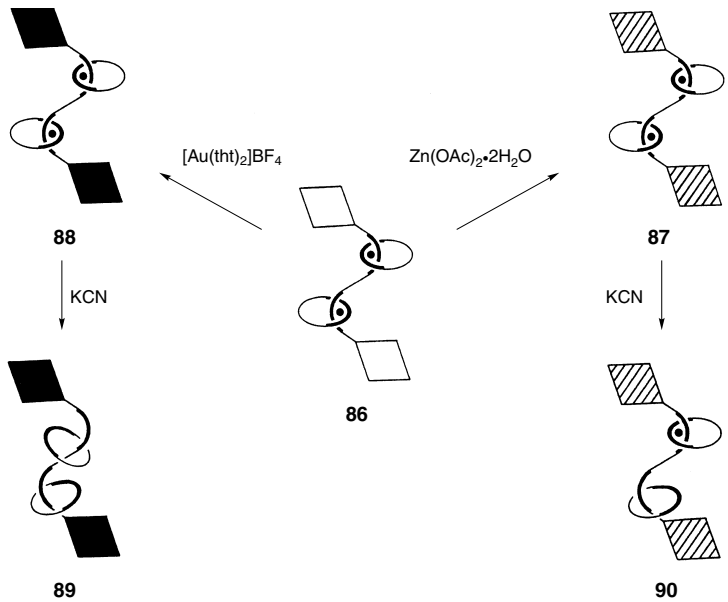

Figure 2.31. Schematic representation of some coordination chemistry studies performed on bis-porphyrin-stoppered [3]-rotaxane **86**. The black disk is Cu(I); black and hatched diamonds represent Au(III) and Zn(II) porphyrins, respectively. The thick lines represent chelate (phenanthroline) fragments.

VII. FUNCTIONAL ROTAXANES

With the introduction of the transition-metal-templated synthesis of rotaxanes at the beginning of the 1980s, these compounds have become more and more accessible. This fact has completely changed the stature of rotaxanes molecules, and nowadays rotaxanes are no longer considered as laboratory curiosities but as compounds of real interest that can be used as models for mimicking natural processes such as photo-induced electron transfer or certain motions that occur in biological systems. Potential uses of rotaxanes can be envisioned as components of long-term information storage or processing devices.

A. Rotaxanes Capable of Triggered Molecular Motions

Linear and rotary motors of several types are very common in biology.[62] Some examples of linear motors are the myosin-actin complex present in muscles[63] or the kinesin-containing systems,[64] while examples of rotary motors are provided by the enzyme ATP synthase[65] or the motor responsible of mobility of bacterial flagella.[66]

Rotaxanes that incorporate transition metals are suitable systems for building nanoscale machines and motors. Their interlocked components can be moved relative to one another without breaking covalent bonds, such dynamic processes being triggered by the influence of external stimuli. Two cases of rotaxanes containing a metal center, and in which molecular motions are triggered electrochemically, are described below: the gliding of a ring along a string and the rotation of a wheel around an axle.

1. Gliding of a Ring along a String

The metallorotaxane **96** in Figure 2.32 is formed by a macrocycle containing a 2,9-diphenyl-1,10-phenanthroline chelate and a dumbbell component that possesses two different chelate subunits (a 1,10-phenanthroline and a 2,2′:6′,2″-terpyridine) and that is terminated at both extremities by bulky trityl groups.[16b,f,67] The presence of two different coordinating sites in the string (bi- and tridentate) together with the different stereoelectronic requirements of Cu(I) (four-coordinate tetrahedral geometry) and Cu(II) (pentacoordinate square-pyramid geometry) were used to study the electrochemically controlled translational motion of the macrocycle between the phenanthroline and the terpyridine fragments of the thread.

Cu(I)-complexed [2]-rotaxane **96** was synthesized as follows (Figure 2.32)[16f,67]: 2-methyl-9-(*p*-anisyl)-1,10-phenanthroline **91** was deprotonated (lithium diisopropylamide) and the resulting anion was alkylated with the

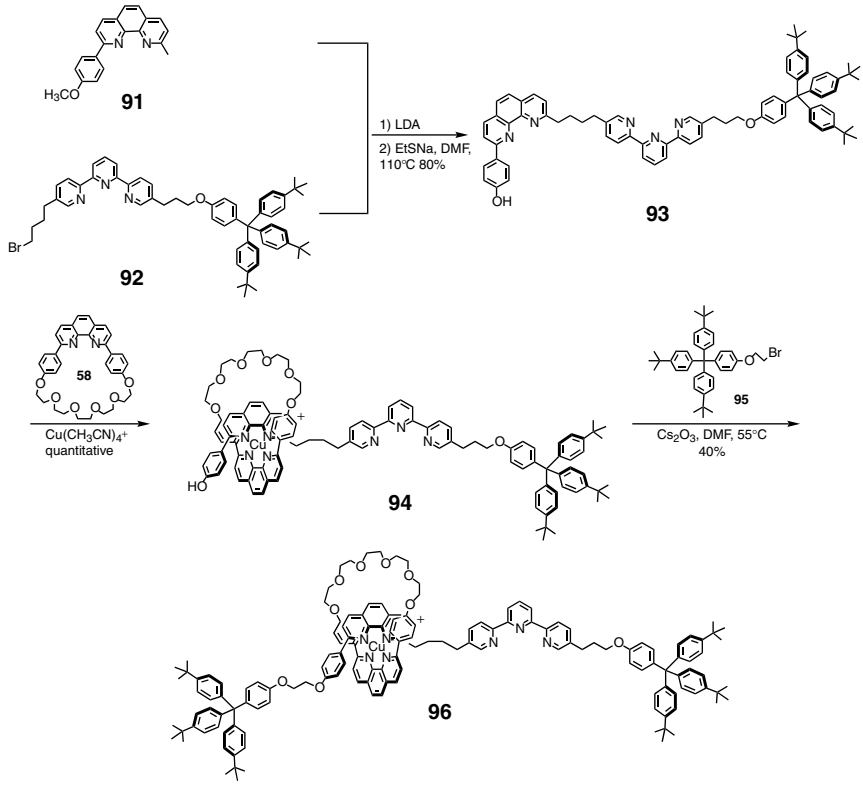

Figure 2.32. Copper(I)-templated synthesis of Cu(I)-complexed [2]-rotaxane **96** whose thread contains a terpyridine and a phenanthroline chelate.

monostoppered terpyridine **92**. Subsequent demethylation of the hydroxy group led to the semidumbbell **93**, which incorporates phenanthroline and terpyridine subunits and a stopper at one end. Macrocycle **58** was then threaded quantitatively into the semidumbbell **93**, using $[Cu(CH_3CN)_4]PF_6$, to afford **94**. Alkylation of **94** with the blocking group **95** produced rotaxane **96** in 40% yield.

The controlled motion of the ring between the two coordinating sites of the string (schematically represented in Figure 2.33) in Cu(I)-complexed [2]-rotaxane **96** takes place as follows: in the initial metallorotaxane the complexed ring stays at the phenanthroline site, because of the stereoelectronic requirements (tetrahedral coordination sphere) of Cu(I). Electrochemical oxidation of Cu(I) to Cu(II) resulted in the movement of the macrocycle to the terpyridine site, since Cu(II) requires higher coordination numbers than Cu(I). This translational motion occurs at a rate of 1.5×10^{-4} s^{-1} at room temperature

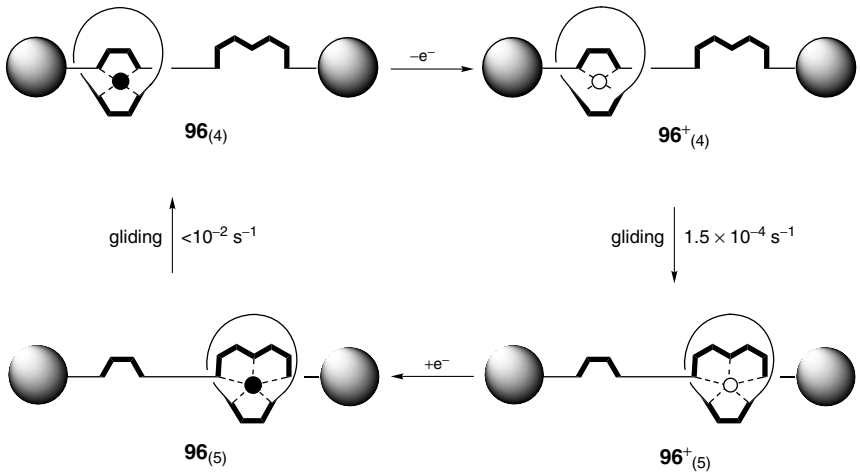

Figure 2.33. Diagram of the molecular motions in copper(I)-complexed [2]-rotaxane **96** controlled by the redox state dependence of the stereoelectronic requirements of Cu. Cu(I) and Cu(II) are represented by black and white circles, respectively. Chelating sites are represented by thick lines. Initially the macrocycle coordinates Cu(I) together with the bidentate site of the dumbbell in a tetrahedral geometry, affording the state $\mathbf{96}_{(4)}$. Electrochemical oxidation of Cu(I) to Cu(II) produces the state $\mathbf{96}^{+}{}_{(4)}$, which slowly converts into the state $\mathbf{96}^{+}{}_{(5)}$, after transfer of the Cu(II)-complexed macrocycle to the terdentate chelate of the rod. The cycle is completed by reduction of Cu(II), which produces the state $\mathbf{96}_{(5)}$, converting to the initial state by back motion of the Cu(I)-complexed macrocycle.

in CH_3CN. Electrochemical reduction of Cu(II) to Cu(I) led to a movement of the ring along the dumbbell back to the phenanthroline site, giving the starting Cu(I)-complexed [2]-rotaxane. This last process takes place at a rate of approximately 10^{-2} s^{-1}.

2. *Rotation of a Wheel around an Axle*

The metallorotaxane **101** shown in Figure 2.34 consists of a thread possessing a 2,9-diphenyl-1,10-phenanthroline ligand fragment capped at both extremities by trityl bulky groups, and a ring which contains two chelates: a 2,9-diphenyl-1,10-phenanthroline and a 2,2′:6′,2″-terpyridine.[68] As in the case of rotaxane **96**, the presence of different coordinating sites together with the different stereoelectronic requirements of Cu(I) and Cu(II) is the driving force of the motion, which again can be induced electrochemically.

The synthetic strategy leading to **101** is to use a monostoppered species, to form the prerotaxane intermediate, and to add the second stopper afterward (Figure 2.34). The advantage of this method is to limit dethreading of the macrocycle during the stoppering reaction. Rotaxane **101** was synthesized as

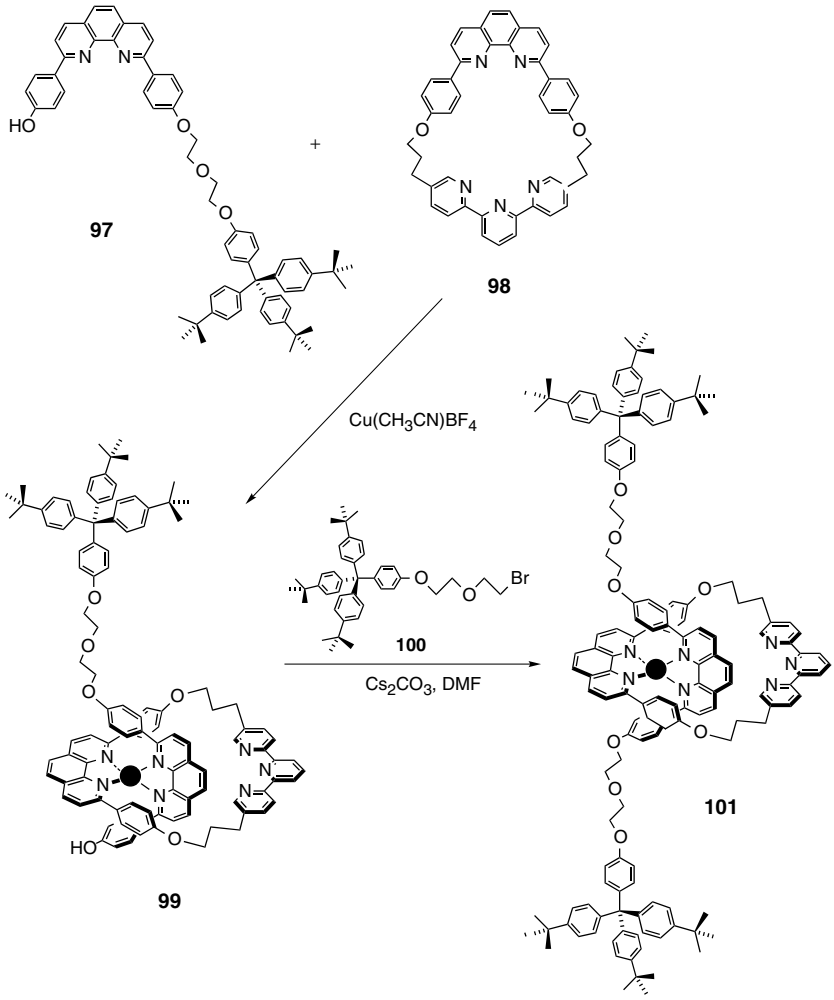

Figure 2.34. Copper(I)-templated synthesis of Cu(I)-complexed [2]-rotaxane **101**, whose ring contains a terpyridine and a phenanthroline chelate.

follows: Prerotaxane **99** was prepared quantitatively by consecutive addition of $[Cu(CH_3CN)_4]BF_4$ and macrocycle **98** to a solution of mono-stoppered phenanthroline **97** in CH_2Cl_2/CH_3CN. The second stopper was attached by alkylation of **99** with terminator unit **100** in the presence of cesium carbonate in dmf. The overall yield for the two step synthesis of **101** was 30%.

The pirouetting motion of the wheel around its axle in the Cu(I)-complexed [2]-rotaxane **101** is schematically represented in Figure 2.35. In the initial

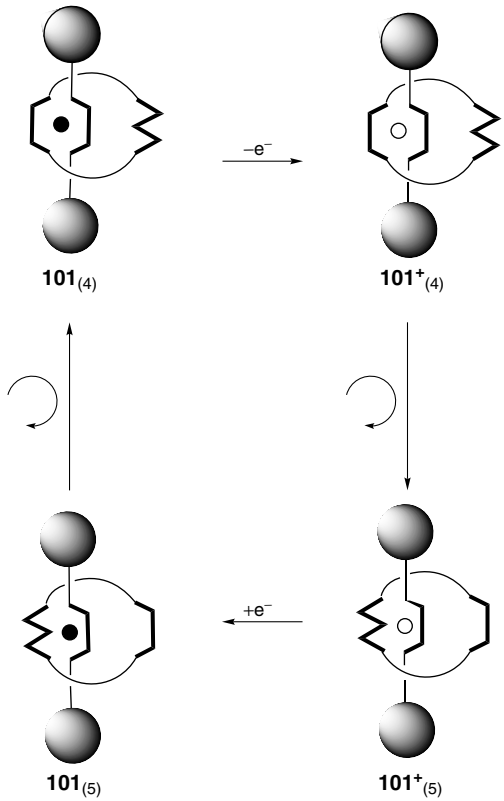

Figure 2.35. Diagram of the molecular motions in copper(I)-complexed [2]-rotaxane **101** controlled by the redox state dependence of the stereoelectronic requirements of Cu. Cu(I) and Cu(II) are represented by black and white circles, respectively. Chelating sites are represented by thick lines. Initially, the string coordinates Cu(I) together with the bidentate site of the macrocycle in a tetrahedral geometry, affording the state $\mathbf{101}_{(4)}$. Electrochemical oxidation of Cu(I) to Cu(II) produces the state $\mathbf{101}^{+}{}_{(4)}$, which slowly converts into the state $\mathbf{101}^{+}{}_{(5)}$ after rotation of the Cu(II)-complexed macrocycle. The cycle is completed by reduction of Cu(II), which produces the state $\mathbf{101}_{(5)}$, converting to the initial state by back motion of the Cu(I)-complexed macrocycle.

Cu(I) state the phenanthroline of the ring and that of the rod interact with the metal in a tetrahedral geometry. Electrochemical oxidation of Cu(I) to Cu(II) triggers a change in the coordination sphere of the copper atom, involving a pirouetting of the wheel around its axle to give a five-coordinate Cu(II) complex whose geometry is imposed by the phenanthroline of the string and the terpyridine of the ring. Electrochemical reduction of Cu(II) back to Cu(I) afforded the initial situation. The rate constant values determined for the rotaxane are 0.007 s^{-1} for the forward step and 17 s^{-1} for the back process. When

these results are compared to those obtained above, it appears that the pirouetting of a macrocycle around its axle induced by changing the redox state of the central metal is much faster than the translation of a macrocycle along a molecular thread using the same triggering process. In addition, in these two different types of molecular motion, gliding and pirouetting, the process triggered by oxidation of Cu(I) to Cu(II) is slower than the process triggered by reduction of Cu(II) to Cu(I); this means that the reorganization process around Cu(I) is much faster than around Cu(II), which can be attributed to the higher activation barrier for the decoordination step in the change from a tetracoordinated Cu(II) to pentacoordinated Cu(II) state as compared to the change from a pentacoordinated Cu(I) to tetracoordinated Cu(I) state.

B. Rotaxanes as Models of the Photosynthetic Reaction Centers

The reaction centers (RC) of photosynthetic bacteria are protein aggregates containing tetrapyrrole- and quinone- type cofactors, where vectorial photoinduced electron transfer (ET) leads to effective charge separation. The 1984 publication of the high-resolution X-ray crystal structure of the RC of *Rh. viridis*[69] inspired many research groups and initiated the design and synthesis of various multicomponent systems expected to display structural analogy with the RC and also to exhibit some of its photochemical and ET functions.[70] For example, gable bis-porphyrins were designed to mimic the fact that the natural co-factors are mostly organized in an oblique fashion to one another.[70e–g] The required electronic properties were controlled by the nature of the metal center of each porphyrin. Zinc(II) and gold(III) were selected as metals for the donor component and the acceptor subunit respectively, for two reasons: (1) energy transfer following ET is avoided in these systems, because the excited states of Au(III) porphyrins are higher in energy than those of Zn(II) porphyrins; (2) chemical events following ET are also avoided, because reduction takes place in the porphyrin system, and not at gold trication.

1. Through-Bond Electron Transfer

A view of the core of the reaction center of *Rh. viridis*[69] is shown in Figure 2.36. It consists of three tetrapyrrolic cofactors: the so-called special pair (SP), which is a dimer of bacteriochlorophylls, a monomeric bacteriochlorophyll (BCh), and a bacteriopheophytin (BPh). As noted above, all these chromophores are arranged within the protein structure with oblique orientations to one another. In this bacterial triad, SP functions as the electron donor in

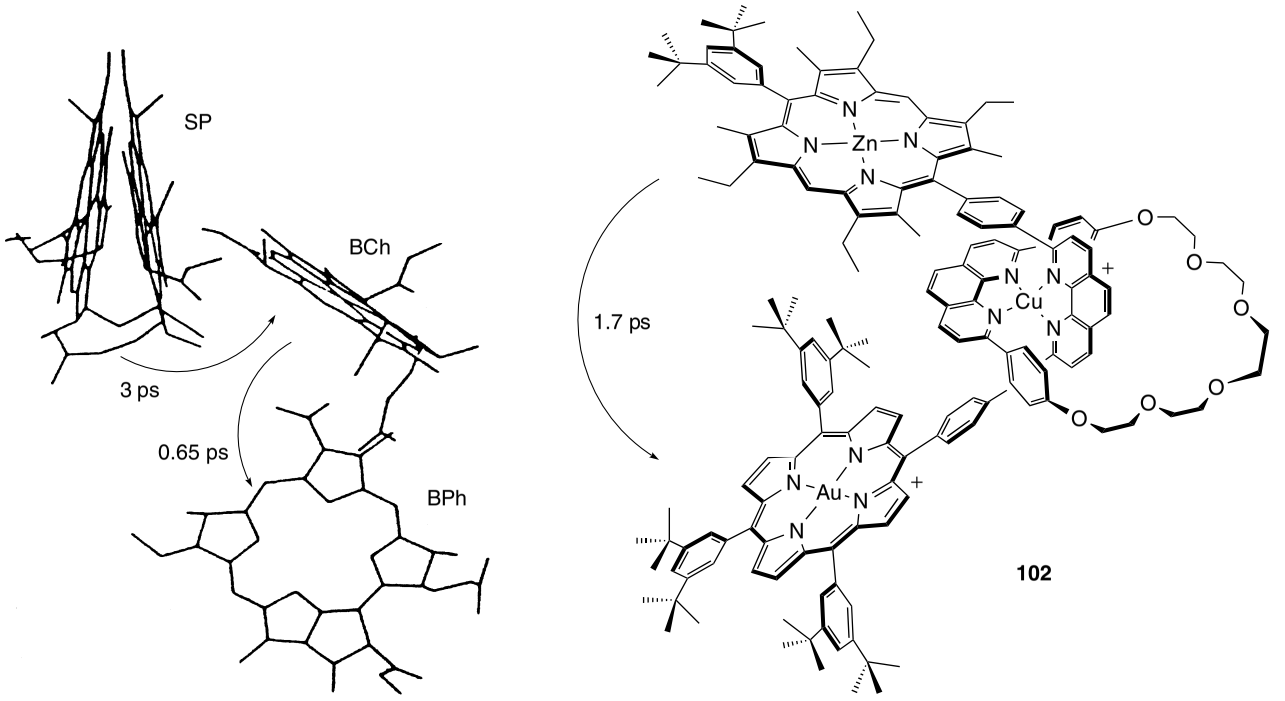

Figure 2.36. (*a*) Fragment of the reaction center of *Rh. viridis*, with the rates of the individual electron transfer steps following light excitation of the special pair (SP). The terminal acceptor is a bacteriopheophytin (BPh). BCh is the so-called accessory bacteriochlorophyll, that plays the role of an electron relay between SP and BPh. (*b*) Cu(I)-complexed [2]-rotaxane **102**. The time constant for photoinduced electron transfer between the zinc and the gold porphyrins is indicated by an arrow.

the excited state, BCh is an electronic relay, and BPh is the terminal electron acceptor. The role of the triad is to supply ubiquinone with two electrons, following light excitation either directly or indirectly (via the bacteriochlorophyll light-harvesting complexes LH1 and LH2[71]). The reduced ubiquinone then pumps protons across the photosynthetic membrane, in a process that converts light energy in proton gradient. Recent fast kinetic studies have shown that electron transfer between the tetrapyrrole components takes place at very high rates, with an order of magnitude of about 1 to 3 ps.[72]

The Cu(I)-complexed [2]-rotaxane **102** of Figure 2.36, containing Zn(II) and Au(III) porphyrins as stoppers, was designed and synthesized with the purpose of mimicking the ET processes occurring within the SP/BCh/BPh trichromophoric fragment described above.

The precursors and the synthetic route leading to rotaxane **102** are represented in Figure 2.37.[57b] First macrocycle **58** was threaded onto the presynthesized Au(III) porphyrin-substituted phenanthroline **103**, a semidumbbell molecule, in the presence of Cu(I), to afford prerotaxane **104** quantitatively. The second stopper (and functional end cap) was installed by the *meso*-porphyrin construction method. Thus reaction of **104** with 4,4′-dimethyl-3,3′-diethyl-2,2′-dipyrrylmethane **105** and 3,5-di-*tert*-butylbenzaldehyde **84**, followed by oxidation of the intermediate porphyrinogen with chloranil **85**, gave the free-base Cu(I)-complexed [2]-rotaxane **106** in 25% yield. After metallation with $Zn(OAc)_2 \cdot 2H_2O$ and exhaustive purification, Cu(I) complex **102** was obtained. It was subsequently demetallated with KCN, to afford the free [2]-rotaxane **107** in quantitative yield.

Kinetic studies have demonstrated that photo-induced electron transfer between the zinc and the gold porphyrin occurs at a rate of $(1.7\ \text{ps})^{-1}$ in Cu(I)-complexed [2]-rotaxane **102**, which is much higher than in the case of the free rotaxane **107** $(36\ \text{ps})^{-1}$.[73] The higher photoinduced electron transfer rate in the Cu(I) complex **102** than in the demetallated system **107** was explained also in terms of a superexchange mechanism.

2. *Electron Transfer across Mechanical Bonds*

An important question in biological electron transfer is related to "through-space" and "through-bond" processes.[74] Whereas through-bond processes were studied with [2]-rotaxanes **102** and **107**, [2]-rotaxane **111** of Figure 2.38 was synthesized with the purpose of addressing the through-space question in a novel approach.[75,76] In such a rotaxane the donor (Zn porphyrin stoppers) and the acceptor (Au porphyrin appended to the macrocycle) components are maintained in the same molecule by mechanical bonds only. It is therefore

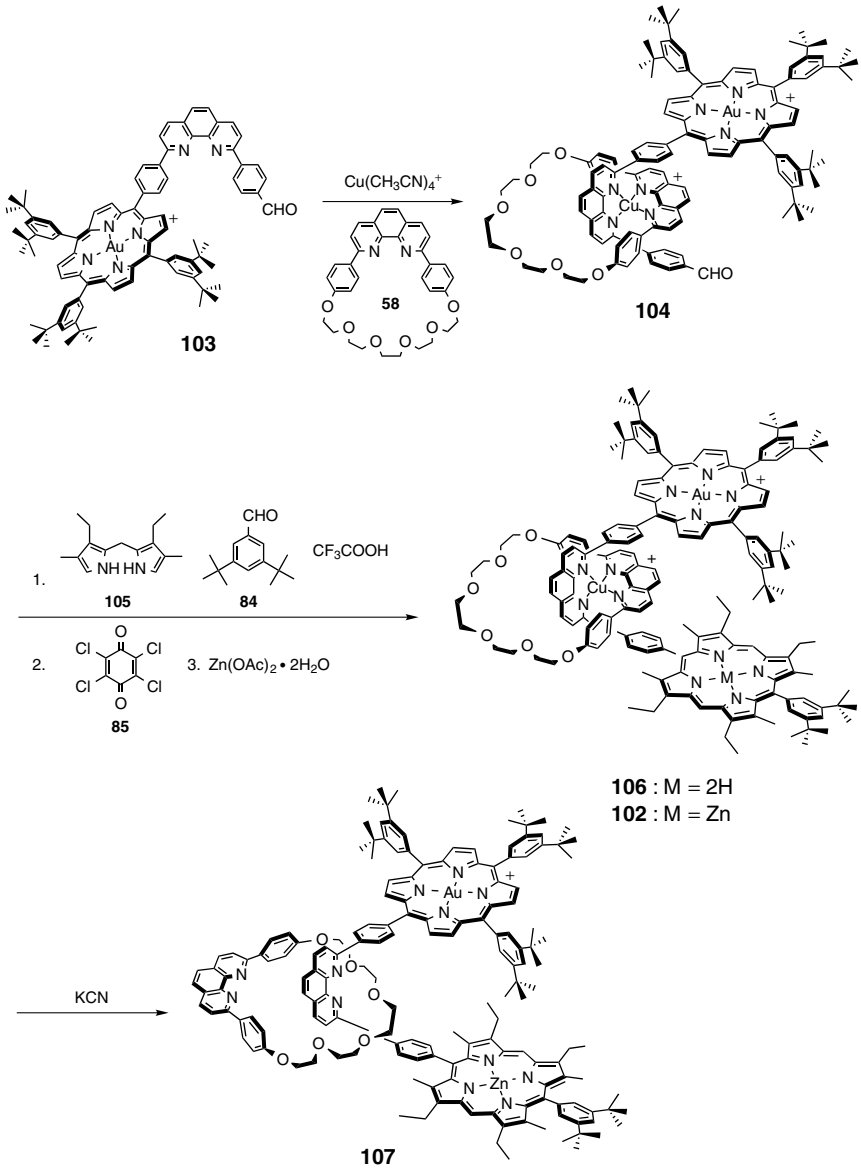

Figure 2.37. Copper(I)-templated synthesis of a Zn(II)/Au(III) bis-porphyrin-stoppered [2]-rotaxane as its Cu(I) complex (**102**) and as free [2]-rotaxane (**107**).

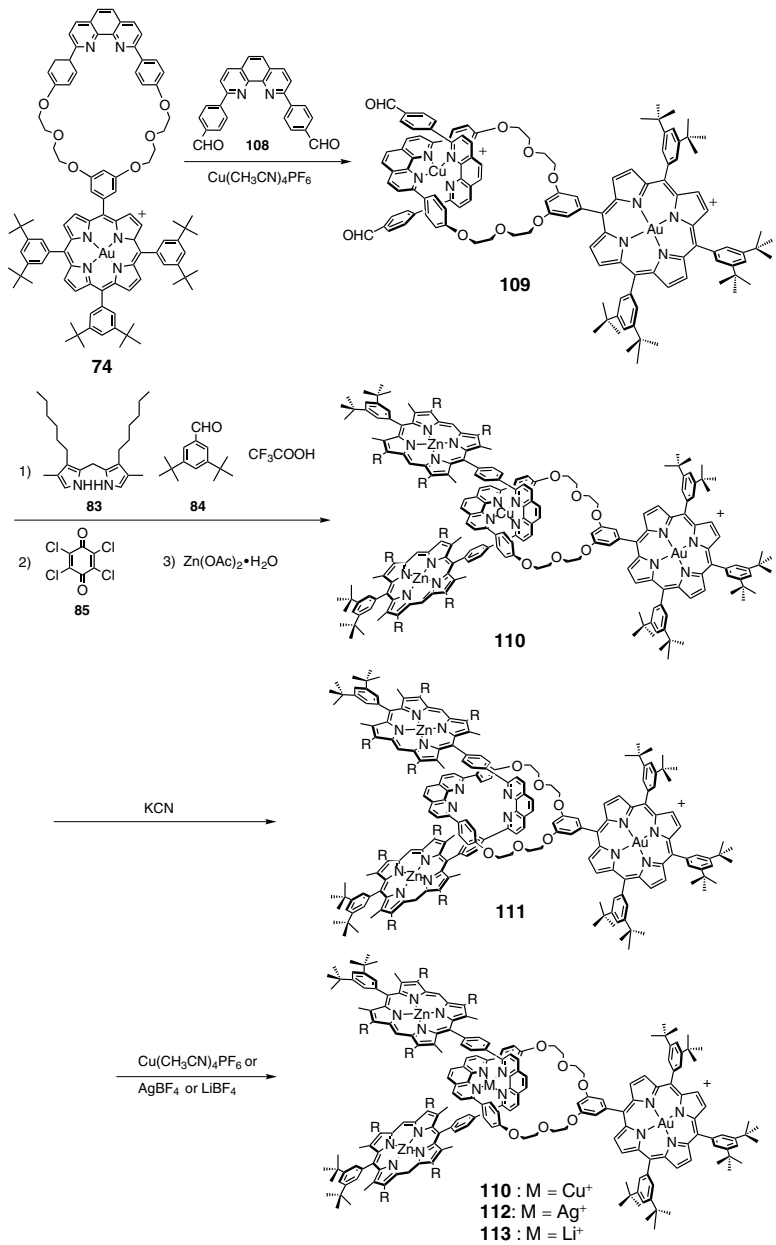

Figure 2.38. Copper(I)-templated synthesis of a Zn(II)/Zn(II) bis-porphyrin-stoppered [2]-rotaxane with Au(III) porphyrin-containing ring as its Cu(I), Ag(I), and Li(I) complexes (**110**,**112**, and **113**, respectively), and as the free [2]-rotaxane **111**.

impossible to follow an electron transfer pathway involving a sequence of chemical bonds between the donor and acceptor porphyrins.

The precursors and the synthetic steps in the synthesis of the Cu(I)-complexed [2]-rotaxane **110** are shown in Figure 2.38.[24a] Cu(I)-directed threading of Au(III) porphyrin-containing macrocycle **74** onto 2,9-di(*p*-formylphenyl)-1,10-phenanthroline **108** led to prerotaxane **109** quantitatively. The two porphyrin stoppers were appended by the one-pot procedure from reaction of **109** with 3,5-di-*tert*-butylbenzaldehyde **84** and 4,4′-dimethyl-3,3′-dihexyl-2,2′-dipyrrylmethane **83**. After oxidation of the porphyrinogens with chloranil **85** and metallation of the resulting porphyrinic stoppers with $Zn(OAc)\cdot 2H_2O$, Cu(I)-complexed [2]-rotaxane **110** was obtained in 17% yield. Removal of Cu(I) leading to **111** was done by treatment with KCN, as usual. Rotaxane **111** was remetallated with monocations such as Ag^+ and Li^+, to afford metal-complexed [2]-rotaxanes **112** and **113** respectively.

Selective excitation of the Zn porphyrin unit of [2]-rotaxane **111** at 575 nm resulted in photo-induced electron transfer from the singlet excited state ^{1}ZnP to the ground state AuP^+. Two rates of electron transfer could be extracted from the fast kinetic studies, $(83\ ps)^{-1}$ and $(770\ ps)^{-1}$, with 35% and 65% contributions respectively.[75] These rates probably correspond to different conformations of the [2]-rotaxane. In any case the electron transfer rates are much slower than those measured for through bond processes in rotaxanes **102** and **107**. Related [2]-rotaxanes with Au porphyrin incorporated into, rather than appended to, the macrocyclic component have been synthesized and studied.[24b] Similar conclusions could be drawn from the photophysical studies.[76]

C. Polymers Incorporating Threaded Rings as Novel Materials

Linear and branched poly([2]-rotaxanes) have been synthesized by electropolymerization of prerotaxane species assembled by the metal template strategy.[77] The synthesis of electroactive films with a poly([2]-rotaxane) backbone structure is represented in Figure 2.39.[77a] Cu(I)- or Co(II)-templated threading of macrocycle **58** onto the pyrrole-substituted dpp ligand **114**, afforded prerotaxanes **115** and **116**, respectively. The electropolymerization process took place only in the case of Co(II), affording poly([2]-rotaxane) **117**. Surprisingly the Cu(I) analogue **119** could not be obtained directly. A demetallation-remetallation procedure was used instead. Removal of Co(II) from the branched polymer **117** was performed with SCN^-, and the resulting metal-free poly([2]-rotaxane) **118** was remetallated with Cu(I), leading to Cu(I)-complexed poly([2]-rotaxane) **119**.

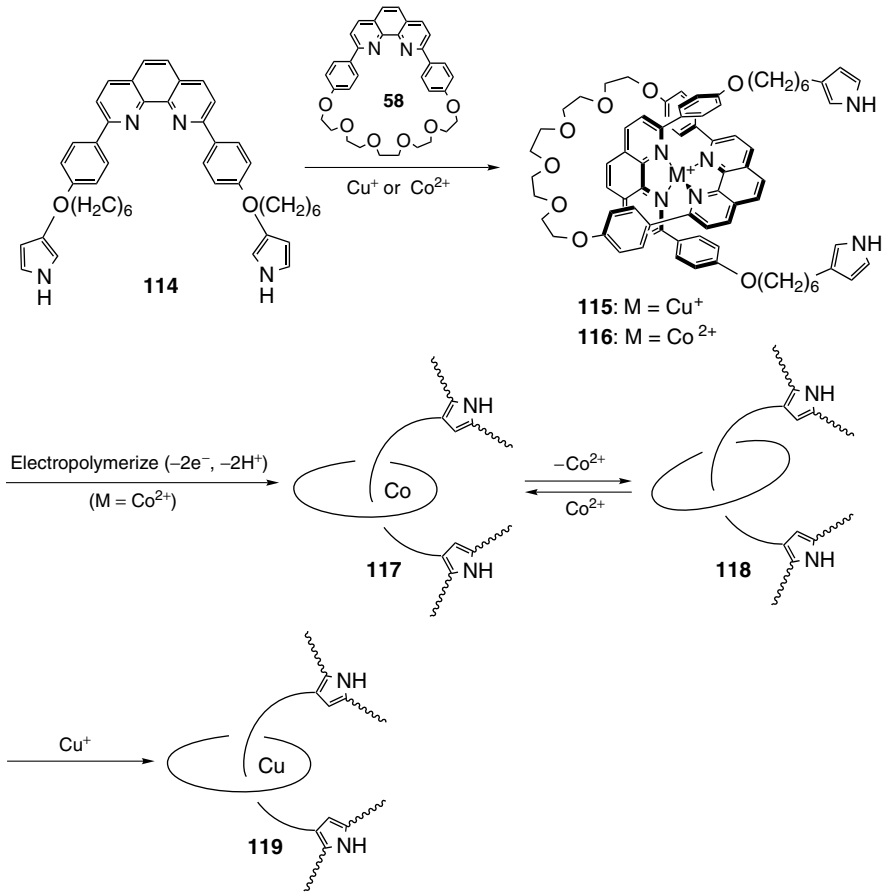

Figure 2.39. Preparation of poly([2]-rotaxane) **118** by electropolymerization of Co(II)-complexed pre[2]-rotaxane **117**, formed by cobalt(II)-templated threading of macrocycle **58** onto the dpp-based thread **114**. Cu(I) turned out to be ineffective as template for the electropolymerization process. The Cu(I)-complexed polymer (**119**) was obtained by successive demetallation-remetallation processes.

VIII. CONCLUSION

The goal of this chapter was several-fold: (1) to provide a comprehensive definition of rotaxanes, with emphasis on their main stereochemical features; (2) to present the various methods that have been devised to prepare them; (3) to show, with selected examples, how the transition-metal-templated method has been used to prepare various [2]-, [3]-, and poly([2]-rotaxanes); (4) to present the rotaxanes in action, from controlled motions of the

ring along, or around the string, to electron transfer between mechanically linked components.

ACKNOWLEDGMENTS

We wish to thank all the talented co-workers whose names appear in the references.

REFERENCES

1. (a) Schill, G. *Catenanes, Rotaxanes and Knots*. Academic Press, New York, **1971**. (b) Dietrich-Buchecker, C. O.; Sauvage, J.-P. *Chem. Rev.* **1987**, *87*, 795. (c) Sauvage, J.-P. *Acc. Chem. Res.* **1990**, *23*, 319. (d) Dietrich-Buchecker, C. O.; Sauvage, J.-P. *Bioorganic Chemistry Frontiers* **1991**, *2*, 195. (e) Gibson, H. W.; Bheda, M. C.; Engen, P. T. *Progr. Polym. Sci.* **1994**, *19*, 843. (f) Amabilino, D. B.; Stoddart, J. F. *Chem. Rev.* **1995**, *95*, 2725. (g) Chambron, J.-C.; Dietrich-Buchecker, C. O.; Sauvage, J.-P., In *Comprehensive Supramolecular Chemistry*; Vol. 9. Sauvage, J.-P.; Hosseini, M. W., eds. Pergamon, New York, **1996**, pp. 44–84. (h) Vögtle, F.; Dünnwald, T.; Schmidt, T. *Acc. Chem. Res.* **1996**, *29*, 451. (i) Jäger, R.; Vögtle, F. *Angew. Chem. Int. Ed. Engl.* **1997**, *36*, 930. (j) For a representative collection of papers on molecular topology, see *New J. Chem.* (Special Issue, Sauvage, J.-P. guest ed.) **1993**, *17*; (k) Sauvage, J.-P.; Dietrich-Buchecker, C., eds. *Molecular Catenanes, Rotaxanes and Knots: A Journey through the World of Molecular Topology*. Wiley-VCH, New York, **1999**.
2. Schill, G.; Zollenkopf, H. *Nachr. Chem. Techn.* **1967**, *15*, 149.
3. Harrison, I. T.; Harrison, S. *J. Am. Chem. Soc.* **1967**, *89*, 5723.
4. Frisch, H. L.; Wasserman, E. *J. Am. Chem. Soc.* **1961**, *83*, 3789.
5. Walba, D. M. *Tetrahedron* **1985**, *41*, 3161.
6. (a) Dietrich-Buchecker, C.; Sauvage, J.-P.; Kern, J.-M. *J. Am. Chem. Soc.* **1989**, *111*, 7791. (b) Albrecht-Gary, A.-M.; Dietrich-Buchecker, C.; Saad, Z.; Sauvage, J.-P. *J. Am. Chem. Soc.* **1988**, *110*, 1467.
7. Cesario, M.; Dietrich, C. O.; Edel, A.; Guilhem, J.; Kintzinger, J.-P.; Pascard, C.; Sauvage, J.-P. *J. Am. Chem. Soc.* **1986**, *108*, 6250.
8. Morel-Desrosiers, N.; Morel, J.-P.; Dietrich-Buchecker, C. O.; Weiss, J.; Sauvage, J.-P. *New J. Chem.* **1988**, *12*, 205.
9. Sokolov, V. I. *Russ. Chem. Rev. (Engl. transl.)* **1972**, *41*, 452.
10. Gibson, H. W. In *Large Ring Molecules*. Semlyen J. A., ed., Wiley, New York, **1997**, pp. 191–262.
11. Ogino, H.; Ohata, K. *Inorg. Chem.* **1984**, *23*, 3312.
12. (a) Ashton, P. R.; Philp, D.; Reddington, M. V.; Slawin, A. M. Z.; Spencer, N.; Stoddart, J. F.; Williams, D. J. *J. Chem. Soc., Chem. Commun.* **1991**, 1680. (b) Anelli, P. L.; Ashton, P. R.; Spencer, N.; Slawin, A. M. Z.; Stoddart, J. F.; Williams, D. J. *Angew. Chem. Int. Ed. Engl.* **1991**, *30*, 1036. (c) Ashton, P. R.; Iqbal, S.; Stoddart, J. F.; Tinker, N. D. *Chem. Commun.* **1996**, 479.
13. (a) Ashton, P. R.; Glink, P. T.; Stoddart, J. F.; Tasker, P. A.; White, A. J. P.; Williams, D. J. *Chem. Eur. J.* **1996**, *2*, 729. (b) Vögtle, F.; Dünnwald, T.; Händel, M.; Jäger, R.; Meier, S.; Harder, G. *Chem. Eur. J.* **1996**, *2*, 640. (c) Anderson, S.; Anderson, H. L. *Angew. Chem. Int. Ed. Engl.* **1996**, *35*, 1956. (d) Solladié, N.; Chambron, J.-C.; Dietrich-Buchecker, C. O.; Sauvage, J.-P. *Angew. Chem. Int. Ed. Engl.* **1996**, *35*, 906. (e) Asakawa, M.; Ashton, P. R.;

Ballardini, R.; Balzani, V.; Belohradsky, M.; Gandolfi, M. T.; Kocian, O.; Prodi, L.; Raymo, F. M.; Stoddart, J. F.; Venturi, M. *J. Am. Chem. Soc.* **1997**, *119*, 302. (f) Kolchinski, A. G.; Alcock, N. W.; Roesner, R. A.; Busch, D. H. *Chem. Commun.* **1998**, 1437. (g) Loeb, S. J.; Wisner, J. A. *Chem. Commun.* **2000**, 845.

14. Ashton, P. R.; Ballardini, R.; Balzani, V.; Belohradsky, M.; Gandolfi, M. T.; Philp., D.; Prodi, L.; Raymo, F. M.; Reddington, M. V.; Spencer, N.; Stoddart, J. F.; Venturi, M.; Williams, D. J. *J. Am. Chem. Soc.* **1996**, *118*, 4931.
15. Amabilino, D. B.; Ashton, P. R.; Belohradsky, M.; Raymo, F. M.; Stoddart, J. F. *J. Chem. Soc., Chem. Commun.* **1995**, 751.
16. (a) Bissell, R. A.; Córdova, E.; Kaifer, A.; Stoddart, J. F. *Nature* **1994**, *369*, 133. (b) Collin, J.-P.; Gaviña, P.; Sauvage, J.-P. *New J. Chem.* **1997**, *21*, 525. (c) Murakami, H.; Kawabuchi, A.; Kotoo, K.; Kunitake, M.; Nakashima, N. *J. Am. Chem. Soc.* **1997**, *119*, 7605. (d) Lane, A. S.; Leigh, D. A.; Murphy, A. *J. Am. Chem. Soc.* **1997**, *119*, 11092. (e) Ashton P. R.; Ballardini, R.; Balzani, V.; Baxter, I.; Credi, A.; Fyfe, M. C. T.; Gandolfi, M. T.; Gomez-Lopez, M.; Martinez-Diaz, M.-V.; Piersanti, A.; Spencer, N.; Stoddart, J. F.; Venturi, M.; White, A. J. P.; Williams, D. J. *J. Am. Chem. Soc.* **1998**, *120*, 11932. (f) Armaroli, N.; Balzani, V.; Collin, J.-P.; Gaviña, P.; Sauvage, J.-P.; Ventura, B. *J. Am. Chem. Soc.* **1999**, *121*, 4397. (g) Clegg, W.; Gimenez-Saiz, C.; Leigh, D. A.; Murphy, A.; Slawin, A. M. Z.; Teat, S. J. *J. Am. Chem. Soc.* **1999**, *121*, 4124.
17. (a) Anelli, P. L.; Spencer, N.; Stoddart, J. F. *J. Am. Chem. Soc.* **1991**, *113*, 5131. (b) Ashton, P. R.; Philp, D.; Spencer, N.; Stoddart, J. F. *J. Chem. Soc., Chem. Commun.* **1992**, 1124. (c) Amabilino, D. B.; Ashton, P. R.; Balzani, V.; Brown, C. L.; Credi, A.; Fréchet, J. M. J.; Leon, J. W.; Raymo, F. M.; Spencer, N.; Stoddart, J. F.; Venturi, M. *J. Am. Chem. Soc.* **1996**, *118*, 12012. (d) Leigh, D. A.; Troisi, A.; Zerbetto, F. *Angew. Chem. Int. Ed.* **2000**, *39*, 350. (e) Cao, J.; Fyfe, M. C. T.; Stoddart, J. F.; Cousins, G. R. L.; Glink, P. T.; *J. Org. Chem.* **2000**, *65*, 1937.
18. (a) Ogino, H. *J. Am. Chem. Soc.* **1981**, *103*, 1303. (b) Yamanari, K.; Shimura, Y. *Bull. Chem. Soc. Jpn* **1983**, *56*, 2283. (c) Wylie, R. S.; Macartney, D. H. *J. Am. Chem. Soc.* **1992**, *114*, 3136. (d) Ogino, H. *New J. Chem.* **1993**, *17*, 683. (e) Beer, A. J.; Macartney, D. H. *Inorg. Chem.* **2000**, *39*, 1410.
19. (a) Wenz, G.; von der Bey, E.; Schmidt, L. *Angew. Chem. Int. Ed. Engl.* **1992**, *31*, 783. (b) Wenz, G.; Wolf, F.; Wagner, M.; Kubik, S. *New J. Chem.* **1993**, *17*, 729. (c) Anderson, S.; Claridge, T. D. W.; Anderson, H. L. *Angew. Chem. Int. Ed. Engl.* **1997**, *36*, 1310. (d) Murakami, H.; Kawabuchi, A.; Kotoo, K.; Kunitake, M.; Nakashima, N. *J. Am. Chem. Soc.* **1997**, *119*, 7605. (e) Harada, A.; Li, J.; Kamachi, M. *Chem. Commun.* **1997**, 1413. (f) Buston, J. E. H.; Young, J. R.; Anderson, H. L. *Chem. Commun.* **2000**, 905. (g) Skinner, P. J.; Blair, S.; Kataky, R.; Parker, D. *New J. Chem.* **2000**, *24*, 265.
20. Jeon, Y.-M.; Whang, D.; Kim, J.; Kim, K. *Chem. Lett.* **1996**, 503.
21. Gibson, H. W.; Lee, S.-H.; Engen, P. T.; Lecavalier, P.; Sze, J.; Shen, Y. X.; Bheda, M. *J. Org. Chem.* **1993**, *58*, 3748.
22. Loeb, S. J.; Wisner, J. A. *Chem. Commun.* **1998**, 2757.
23. (a) Ashton, P. R.; Johnston, M. R.; Stoddart, J. F.; Tolley, M. S.; Wheeler, J. W. *J. Chem. Soc., Chem. Commun.* **1992**, 1128. (b) Chambron, J.-C.; Heitz, V.; Sauvage, J.-P. *J. Chem. Soc., Chem. Commun.* **1992**, 1131. (c) Vögtle, F.; Ahuis, F.; Baumann, S.; Sessler, J. L. *Liebigs Ann.* **1996**, 921. (d) Chichak, K.; Walsh, M. C.; Branda, N. R. *Chem. Commun.* **2000**, 847. (e) Gunther, M. J.; Bampos, N.; Johnstone, K.; Sanders, J. K. M. *New J. Chem.* **2001**, 166.
24. (a) Linke, M.; Chambron, J.-C.; Heitz, V.; Sauvage, J.-P. *J. Am. Chem. Soc.* **1997**, *119*, 1132. (b) Linke, M.; Chambron, J.-C.; Heitz, V.; Sauvage, J.-P.; Semetey, V. *Chem. Commun.* **1998**, 2469. (c) Blanco, M.-J.; Chambron, J.-C.; Heitz, V.; Sauvage, J.-P. *Org. Lett.* **2000**, *2*, 3051;

25. Rowan, A. E.; Aarts, P. P. M.; Koutstaal, K. W. M. *Chem. Commun.* **1998**, 611.
26. The terms "slipping" and "threading" were initially coined as "threading", without differentiating the presence or absence of stopper. Thus, "slipping" could be viewed as a particular case of the general "threading". In this chapter we use the current nomenclature.
27. Harrison, I. T. *J. Chem. Soc., Chem. Commun.* **1972**, 231.
28. Schill, G.; Zollenkopf, H. *Liebigs Ann. Chem.* **1969**, *721*, 53.
29. Schill, G.; Beckmann, W.; Schweickert, N.; Fritz, H. *Chem. Ber.* **1986**, *119*, 2647.
30. Harrison, I. T. *J. Chem. Soc. Perkin Trans. I* **1974**, *301*.
31. Agam, G.; Graiver, D.; Zilkha, A. *J. Am. Chem. Soc.* **1976**, *98*, 5206.
32. Schill (ref. 1a), pp. 41–46.
33. (a) Ashton, P. R.; Grognuz, M.; Slawin, A. M. Z.; Stoddart, J. F.; Williams, D. J. *Tetrahedron Lett.* **1991**, *32*, 6235. (a) Anelli, P. L.; Ashton, P. R.; Ballardini, R.; Balzani, V.; Delgado, M.; Gandolfi, M. T.; Goodnow, T. T.; Kaifer, A. E.; Philp, D.; Pietraszkiewicz, M.; Prodi, L.; Reddington, M. V.; Slawin, A. M. Z.; Spencer, N.; Stoddart, J. F.; Vicent, C.; Williams, D. J. *J. Am. Chem. Soc.* **1992**, *114*, 193. (b) Ashton, P. R.; Ballardini, R.; Balzani, V.; Belohradsky, M.; Gandolfi, M. T.; Philp, D.; Prodi, L.; Raymo, F. M.; Reddington, M. V.; Spencer, N.; Stoddart, J. F.; Venturi, M.; Williams, D. J. *J. Am. Chem. Soc.* **1996**, *118*, 4931. (c) Asakawa, M.; Ashton, P. R.; Iqbal, S.; Stoddart, J. F.; Tinker, N. D.; White, A. J. P.; Williams, D. J. *Chem. Commun.* **1996**, 483.
34. (a) Vögtle, F.; Händel, M.; Meier, S.; Ottens-Hildebrandt, S.; Ott, F.; Schmidt, T. *Liebigs Ann.* **1995**, 739. (a) Ashton, P. R.; Glink, P. T.; Stoddart, J. F.; Tasker, P. A.; White, A. J. P.; Williams, D. J.; *Chem. Eur. J.* **1996**, *2*, 729. (b) Vögtle, F.; Dünnwald, T.; Händel, M.; Jäger, R.; Meier, S.; Harder, G. *Chem. Eur. J.* **1996**, *2*, 640. (c) Vögtle, F.; Jäger, R.; Händel, M.; Ottens-Hildebrandt, S.; Schmidt, W. *Synthesis* **1996**, 353. (d) Leigh, D. A.; Murphy, A.; Smart, J. P.; Slawin, A. M. Z. *Angew. Chem. Int. Ed. Engl.* **1997**, *36*, 728. (e) Takata, T.; Kawasaki, H.; Asai, S.; Furusho, Y.; Kihara, N. *Chem. Lett.* **1999**, 111. (f) Seel, C.; Parham, A. H.; Safarowsky, O.; Hübner, G. M.; Vögtle, F. *J. Org. Chem.* **1999**, *64*, 7236.
35. Händel, M.; Plevoets, M.; Gestermann, S.; Vögtle, F. *Angew. Chem. Int. Ed. Engl.* **1997**, *36*, 1199.
36. Jäger, R.; Händel, M.; Harren, J.; Rissanen, K.; Vögtle, F. *Liebigs Ann.* **1996**, 1201.
37. Yamamoto, C.; Okamoto, Y.; Schmidt, T.; Jäger, R.; Vögtle, F. *J. Am. Chem. Soc.* **1997**, *119*, 10547.
38. Schmieder, R.; Hubner, G.; Seel, C.; Vögtle, F. *Angew. Chem. Int. Ed.* **1999**, *38*, 3528.
39. Hübner, G. M.; Gläser, J.; Seel, C.; Vögtle, F. *Angew. Chem. Int. Ed.* **1999**, *38*, 383. Reuter, C.; Wienand, W.; Hübner, G. M.; Seel, C.; Vögtle, F. *Chem. Eur. J.* **1999**, *5*, 2692.
40. Saenger, W. *Angew. Chem. Int. Ed. Engl.* **1980**, *19*, 344.
41. Isnin, R.; Kaifer, A. E. *J. Am. Chem. Soc.* **1991**, *113*, 8188.
42. Craig, M. R.; Claridge, T. D. W.; Hutchings, M. G.; Anderson, H. L. *Chem. Commun.* **1999**, 1537.
43. Harada, A.; Li, J.; Kamachi, M. *Nature*, **1992**, *356*, 325.
44. Harada, A.; Li, J.; Kamachi, M. *Nature*, **1993**, *364*, 516.
45. *The American heritage Dictionary*, Dell Publishing, New York, **1983**.
46. (a) Melson, G. A., ed. *Coordination Chemistry of Macrocyclic Compounds*. Plenum, New York. (b) Busch, D. H.; Vance, A. L.; Kolchinski, A. G. In *Comprehensive Supramolecular Chemistry*, Vol. 9. Sauvage, J.-P.; Hosseini, M. W. eds. Pergamon, New York, **1996**, pp. 1–42.
47. (a) Curtis, N. F. *J. Chem. Soc.* **1960**, 4409. (b) Curtis, N. F.; House, D. A. *Chem. Ind. (London)* **1961**, 1708. (c) Curry, J. D.; Busch, D. R. *J. Am. Chem. Soc.* **1964**, *86*, 592. (d) Busch, D. R. *Helv. Chim. Acta, Fasciculus Extraordinarius Alfred Werner* **1967**, 174 and references therein. (e) Busch, D. H. *Pure Appl. Chem.* **1980**, *52*, 2477.

48. Thompson, M. C.; Busch, D. H. *J. Am. Chem. Soc.* **1964**, *86*, 3651.
49. (a) Nelson, S. M. *Pure Appl. Chem.* **1980**, *52*, 2461. (b) Alexander, V. *Chem. Rev.* **1995**, *95*, 273.
50. (a) Boston, D. R.; Rose, N. J. *J. Am. Chem. Soc.* **1968**, *90*, 6859. (b) Parks, J. E.; Wagner, B. E.; Holm, R. H. *J. Am. Chem. Soc.* **1970**, *92*, 3500. (c) Parks, J. E.; Wagner, B. E.; Holm, R. H. *Inorg. Chem.* **1971**, *10*, 2472.
51. (a) Creaser, I. I.; Harrowfield, J. MacB.; Herlt, A. J.; Sargeson, A. M.; Springborg, J.; Geue, R. J.; Snow, M. R. *J. Am. Chem. Soc.* **1977**, *99*, 3181. (b) Creaser, I. I.; Geue, R. J.; Harrowfield, J. MacB.; Herlt, A. J.; Sargeson, A. M.; Snow, M. R.; Springborg, J. *J. Am. Chem. Soc.*, **1982**, *104*, 6016.
52. (a) McMurry, T. J.; Rodgers, S. J.; Raymond, K. N. *J. Am. Chem. Soc.* **1987**, *109*, 3451. (b) McMurry, T. J.; Hosseini, M. W.; Garrett, T. M.; Hahn, F. E.; Reyes, Z. E., Raymond, K. N. *J. Am. Chem. Soc.* **1987**, *109*, 7196. (c) Garrett, T. M.; McMurry, T. J.; Hosseini, M. W.; Reyes, Z. E.; Hahn, F. E.; Raymond, K. N. *J. Am. Chem. Soc.* **1991**, *113*, 2965.
53. (a) Belser, P.; De Cola, L.; von Zelewsky, A. *J. Chem. Soc., Chem. Commun.* **1988**, 1057. (b) Barigelletti, F.; De Cola, L.; Balzani, V.; Belser, P.; von Zelewsky, A.; Vögtle, F.; Ebmeyer, F.; Grammenudi, S. *J. Am. Chem. Soc.* **1989**, *111*, 4662.
54. (a) Dietrich-Buchecker, C. O.; Sauvage, J.-P.; Kintzinger, J.-P. *Tetrahedron Lett.* **1983**, *24*, 5095. (b) Dietrich-Buchecker, C. O.; Sauvage, J.-P.; Kern, J.-M. *J. Am. Chem. Soc.* **1984**, *106*, 3043.
55. Arnaud-Neu, F; Marques, E.; Schwing-Weill, M.-J.; Dietrich-Buchecker, C.; Sauvage, J.-P.; Weiss, J. *New J. Chem.* **1988**, *12*, 15.
56. Dietrich-Buchecker, C. O.; Sauvage, J.-P. *Tetrahedron* **1990**, *46*, 503.
57. (a) Wu, C.; Lecavalier, P. R.; Shen, Y. X.; Gibson, H. W. *Chem. Mater.* **1991**, *3*, 569. (b) Chambron, J.-C.; Heitz, V.; Sauvage, J.-P. *J. Am. Chem. Soc.* **1993**, *115*, 12378.
58. (a) Chambron, J.-C.; Dietrich-Buchecker; C. O.; Nierengarten, J.-F.; Sauvage, J.-P. *J. Chem. Soc., Chem. Commun.* **1993**, 801. (b) Chambron, J.-C.; Dietrich-Buchecker, C.; Nierengarten, J.-F.; Sauvage, J.-P.; Solladié, N.; Albrecht-Gary, A.-M.; Meyer, M. *New J. Chem.* **1995**, *19*, 409.
59. Amabilino, D. B.; Dietrich-Buchecker, C. O.; Sauvage, J.-P. *J. Am. Chem. Soc.* **1996**, *118*, 3285.
60. (a) Cárdenas, D. J.; Gaviña, P.; Sauvage, J.-P. *Chem. Commun.* **1996**, 1915. (b) Cárdenas, D. J.; Gaviña, P.; Sauvage, J.-P. *J. Am. Chem. Soc.* **1997**, *119*, 3521.
61. Solladié, N.; Chambron, J.-C.; Sauvage, J.-P. *J. Am. Chem. Soc.* **1999**, *121*, 3684.
62. Howard, J. *Nature* **1997**, *389*, 561.
63. (a) Kitamura, K; Tokunaga, M.; Iwane, A. H.; Yanagida, T. *Nature* **1999**, *397*, 129. (b) Rayment, I.; Holden, H. M.; Whittaker, M.; Yohn, C. B.; Lorenz, M.; Holmes, K. C.; Milligan, R. A. *Science* **1993**, *261*, 58. (c) Rayment, I; Rypniewski, W. R.; Schmid-Bäse, K.; Smith, R.; Tomchick, D. R.; Benning, M. M.; Winkelmann, D. A.; Wasenberg, G.; Holden, H. M. *Science* **1993**, *261*, 50. (d) Dobbie, I.; Linari, M.; Piazzesi, G.; Reconditi, M.; Koubassova, N.; Ferenczi, M. A.; Lombardi, V.; Irving, M. *Nature* **1998**, *396*, 383.
64. Hirokawa, N. *Science*, **1998**, *279*, 519.
65. (a) Abrahams, J. P.; Leslie, A. G. W.; Lutter, R.; Walker, J. E. *Nature* **1994**, *370*, 621. (b) Noji, H.; Yasuda, R.; Yoshida, M.; Kinosita, K. *Nature* **1997**, *386*, 299. (c) Walker, J. E. *Angew. Chem. Int. Ed.* **1998**, *37*, 2308. (d) Boyer, P. D. *Angew. Chem. Int. Ed.* **1998**, *37*, 2296.
66. Stryer, L. *Biochemistry*, 2nd ed. Freeman, San Francisco **1981**, pp. 906–907.
67. Gaviña, P.; Sauvage, J.-P. *Tetrahedron Lett.* **1997**, *38*, 3521.
68. Raehm, L.; Kern, J.-M.; Sauvage, J.-P. *Chem Eur. J.* **1999**, *5*, 3310.

69. (a) Deisenhofer, J.; Epp, O.; Miki, K.; Huber, R.; Michel, H. *J. Mol. Biol.* **1984**, *180*, 385. (b) Deisenhofer, J.; Epp, O.; Miki, K.; Huber, R.; Michel, H. *Nature* **1985**, *318*, 618.
70. Some early and representative examples : (a) Boxer, S. G.; Bucks, R. R. *J. Am. Chem. Soc.* **1979**, *101*, 1883. (b) Gust, D.; Moore, T. A.; Moore, A.; Makings, L. R.; Seely, G. R.; Ma, X.; Trier, T. T.; Gao, F. *J. Am. Chem. Soc.* **1988**, *110*, 7567. (c) Nagata, T.; Osuka, A.; Maruyama, K. *J. Am. Chem. Soc.* **1990**, *112*, 3054. (d) Harriman, A.; Magda, D. J.; Sessler, J. L. *J. Chem. Soc., Chem. Commun.* **1991**, 345. (e) Chardon-Noblat, S.; Dietrich-Buchecker, C. O.; Sauvage, J.-P. *Tetrahedron Lett.*, **1987**, *47*, 5829. (f) Chardon-Noblat, S.; Sauvage, J.-P. *Tetrahedron*, **1991**, *47*, 5123. (g) Brun, A. M.; Atherton, S.; Harriman, A.; Heitz, V.; Sauvage, J.-P. *J. Am. Chem. Soc.* **1992**, *114*, 4632.
71. (a) Kühlbrandt, W.; Wang, D. N.; Fuji, Y. *Nature* **1994**, *367*, 614. (b) Mc Dermott, G.; Prince, S. M.; Freer, A. A.; Hawthornthwaitelawless, A. M.; Papiz, M. Z.; Cogdell, R. J.; Isaacs, N. W. *Nature*, **1995**, *374*, 517. (c) Kühlbrandt, W. *Nature* **1995**, *374*, 497. (d) Pullerits, T.; Sundström, V. *Acc. Chem. Res.* **1996**, *29*, 381.
72. (a) Arlt, T.; Schmidt, S.; Kaiser, W.; Lauterwasser, C.; Meyer, M.; Scheer, H.; Zinth, W. *Proc. Natl. Acad. Sci. USA* **1993**, *90*, 11757. (b) Dressler, K.; Umlauf, E.; Schmidt, S.; Hamm, W.; Zinth, W.; Buchanan, S.; Michel, H. *Chem. Phys. Lett.* **1991**, *183*, 270.
73. (a) Chambron, J.-C.; Harriman, A.; Heitz, V.; Sauvage, J.-P. *J. Am. Chem. Soc.* **1993**, *115*, 6109. (b) Chambron, J.-C.; Harriman, A.; Heitz, V.; Sauvage, J.-P. *J. Am. Chem. Soc.* **1993**, *115*, 7419.
74. Moser, C. C.; Keske, J. M.; Warne, K.; Farid, R. S.; Dutton, P. L. *Nature* **1992**, *355*, 796.
75. Andersson, M.; Linke, M.; Chambron, J.-C.; Davidsson, J.; Heitz, V.; Sauvage, J.-P.; Hammarström, L. *J. Am. Chem. Soc.* **1999**, *122*, 3526.
76. Linke, M.; Chambron, J.-C.; Heitz, V.; Sauvage, J.-P.; Encinas, S.; Barigelletti, F.; Flamigni, L. *J. Am. Chem. Soc.* **2000**, *122*, 11834.
77. (a) Kern, J.-M.; Sauvage, J.-P.; Bidan, G.; Billon, M.; Divisia-Blohorn, B. *Adv. Mater.* **1996**, *8*, 580. (b) Zhu, S. S.; Swager, T. M. *J. Am. Chem. Soc.* **1997**, *119*, 12568. (c) Vidal, P. L.; Billon, M.; Divisia-Blohorn, B.; Bidan, G.; Kern, J.-M.; Sauvage, J.-P. *Chem. Commun.* **1998**, 629. (d) Vidal, P. L.; Divisia-Blohorn, B.; Bidan, G.; Kern, J.-M.; Sauvage, J.-P.; Hazemann, J.-L. *Inorg. Chem.* **1999**, *38*, 4203. (e) Buey, J.; Swager, T. M. *Angew. Chem. Int. Ed.* **2000**, *39*, 608.

Chapter 3

Memory of Chirality: Asymmetric Induction Based on the Dynamic Chirality of Enolates

TAKEO KAWABATA AND KAORU FUJI

Institute for Chemical Research, Kyoto University, Uji Kyoto 611-0011, Japan

I. INTRODUCTION: MEMORY OF CHIRALITY

Is it possible to retain the chirality of a stereogenic carbon center at which deprotonation takes place upon formation of an enolate? Usually not. For example, α-methylation of either (*S*)-**1** or (*R*)-**1** gives racemic **3** via an enolate

Topics in Stereochemistry, Volume 23, Edited by Scott E. Denmark.
ISBN 0-471-17622-2

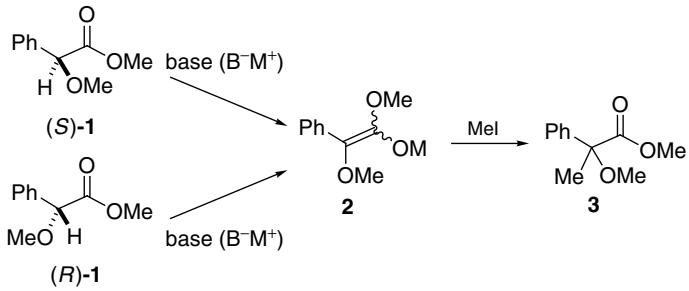

Scheme 3.1.

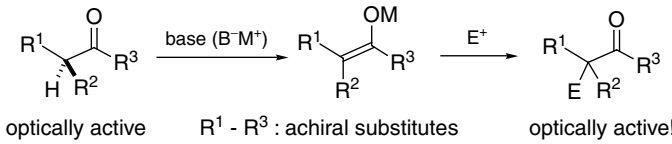

Scheme 3.2.

intermediate **2**. Since the enolate structure is achiral, enolate **2** generated from (*S*)-**1** is identical to that from (*R*)-**1**. Thus the chirality of ester **1** is lost upon formation of the enolate **2**.

In this chapter we show that the chirality of a ketone and some α-amino acid esters can, however, be preserved in their enolate forms, and asymmetric synthesis via the strategy shown in Scheme 3.2 becomes possible. In these reactions the chirality of the starting material appears to be *memorized* in the enolate intermediates, so we call this type of asymmetric transformation "memory of chirality." The design, development, and rationale of the memory of chirality are described.[1]

II. ASYMMETRIC SYNTHESIS VIA ENOLATE INTERMEDIATES

Asymmetric synthesis via enolate intermediates has been extensively studied. Asymmetric induction can be divided into five main categories: (1) a chiral auxiliary covalently linked to an enolate moiety,[2,3] (2) a chiral ligand of a countercation of an enolate,[4–6] (3) a chiral electrophile,[7,8] (4) a chiral Lewis acid,[9,10] and (5) a chiral phase-transfer catalyst.[11,12] Rather than reviewing these examples, we introduce here the principle of asymmetric induction for

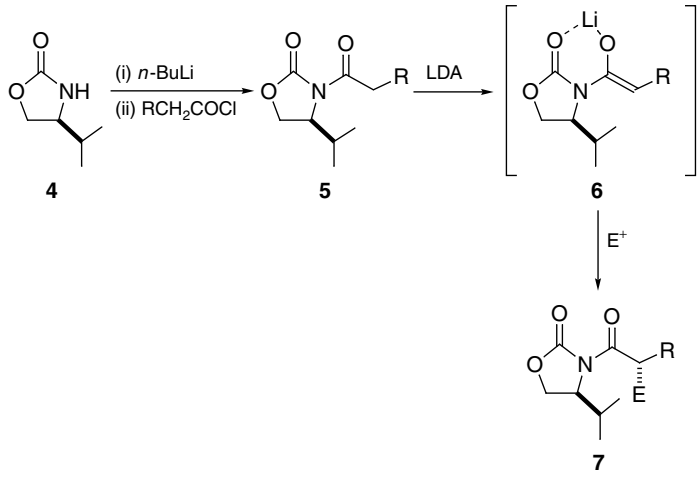

Scheme 3.3.

each category with a leading reference. This will reveal the difference in methodology between these examples and Scheme 3.2.

1. Evans and co-workers developed chiral auxiliary **4**.[3] Imide **5**, obtained by the condensation of **4** and an acid chloride, was treated with LDA to generate chiral enolate intermediate **6**. Since the upper face of the enolate plane is blocked by the bulky isopropyl substituent, the reaction with an electrophile takes place from the bottom face of the enolate **6** to give **7** highly selectively. Chiral auxiliary **4** can be removed by the reaction of **7** with benzyloxy lithium without noticeable racemization.

2. Koga and co-workers found that benzylation of the lithium enolate generated from **8** and methyl lithium proceeds in 92% *ee* in the presence of chiral ligand **9**. A ternary complex consisting of lithium enolate, lithium bromide, and **9** is assumed to be responsible for the asymmetric induction.[5] A possible structure of the ternary complex is shown in **A**. Since the enantioface of the lithium enolate is discriminated by strongly coordinated chiral ligand **9**, the approach of an electrophile (benzyl bromide) occurs selectively from the upper face of the enolate to give **10**. This method was further developed as a catalytic asymmetric synthesis. Benzylation of the lithium enolate of tetralone with a catalytic amount (ca. 5 mol%) of chiral ligand **11** in the presence of *N*,*N*,*N*′,*N*′-tetramethylpropanediamine gives 2-benzyl-1-tetralone in 96% *ee* and 76% yield.[6]

3. Enantiofacial discrimination of achiral enolates by chiral electrophiles is also possible. Duhamel and co-workers reported that the reaction of the

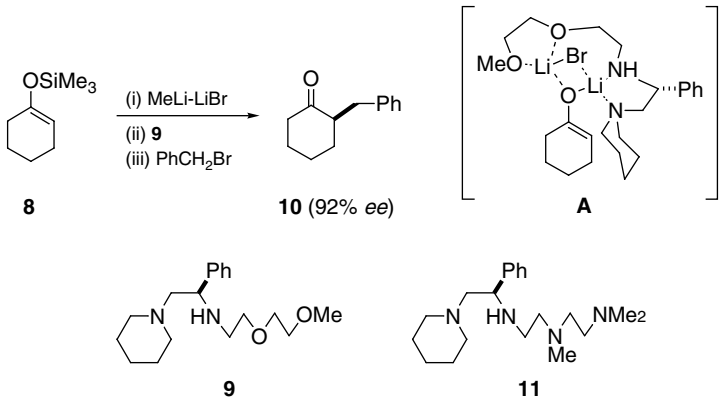

Scheme 3.4.

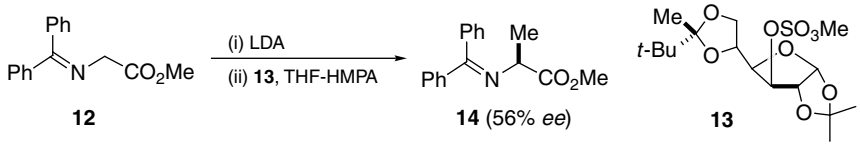

Scheme 3.5.

lithium enolate of glycine derivative **12** with chiral methylating agent **13** proceeds enantioselectively to afford **14** in 56% *ee*. Better selectivity (76% *ee*) was reported with the corresponding Schiff base derived from *t*-butyl *p*-dimethylaminophenyl ketone and glycine methyl ester.[7]

4. Mukaiyama and co-workers developed a chiral Lewis acid complex **15** consisting of tin (II) triflate and a chiral diamine. An aldol reaction of enol silyl ether **16** and octanal is promoted by **15** to give **17** in a highly diastereo- and enantioselective manner. The enantioface of the aldehyde is selectively activated by coordination with **15**. This method is similar to method 3, in that an aldehyde-chiral Lewis acid complex can be regarded as a chiral electrophile. An advantage of method 4 over method 3 is the possible catalytic use of a chiral Lewis acid. In the reaction of Scheme 3.6, 20 mol% of **15** effects the aldol reaction in 76% yield with excellent selectivity.[9]

5. Enolates with a chiral countercation are also useful intermediates for asymmetric synthesis. An inorganic countercation of an enolate can be replaced by a chiral quaternary ammonium cation under phase-transfer conditions. Dolling and co-workers reported that α-methylation of ketone **18** took place in 92% *ee* by the treatment of **18** with MeCl in the presence of 10 mol%

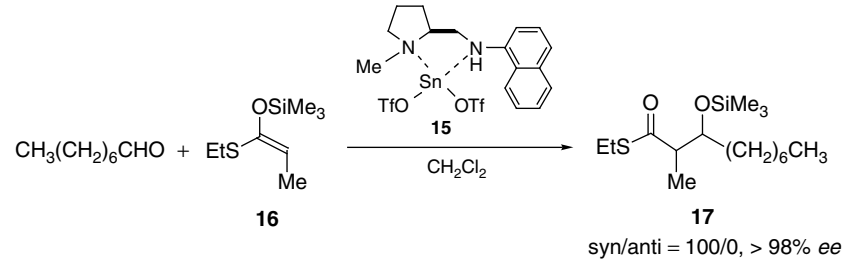

Scheme 3.6.

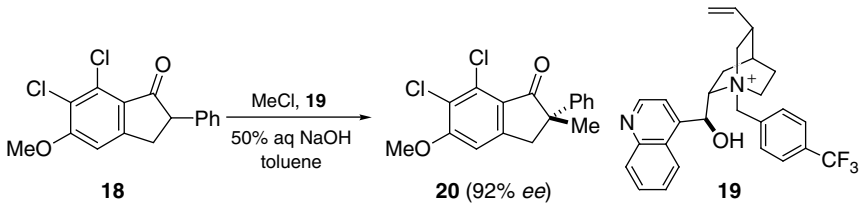

Scheme 3.7.

of chiral phase-transfer catalyst **19** in a 50% aqueous NaOH-toluene two-phase system.[11] The asymmetric alkylation of enolates with the aid of chiral phase-transfer catalysts has been developed most successfully.[13]

All of the methods in categories 2 to 5 have been designed and developed on the basis of the achiral enolate structure. The methods in category 1 involve chiral enolates where the enolate subunit (achiral on its own) covalently links to a chiral element. In contrast to these methodologies, the next section describes a novel asymmetric induction based on dynamic chirality of the enolate structure.

III. DYNAMIC CHIRALITY

Even a simple molecule such as *n*-butane has many chiral conformations. When rotation about the C–C bond is fixed, enantiomers of *n*-butane exist (Figure 3.1*a*). Chiral *n*-butane, even if it could be isolated, readily racemizes through C–C bond rotation with a barrier of around 3 kcal/mol. The corresponding half-life of racemization is expected to be shorter than 10^{-9} s at -78°C. The molecule behaves as an achiral molecule beyond this time scale. 2,2′-Dimethylbiphenyl is another example of a chiral molecule in a limited time (Figure 3.1*b*). Enantiomers with axial chirality exist when rotation of the C(1)–C(1′) bond is restricted. Racemization takes place through C–C bond

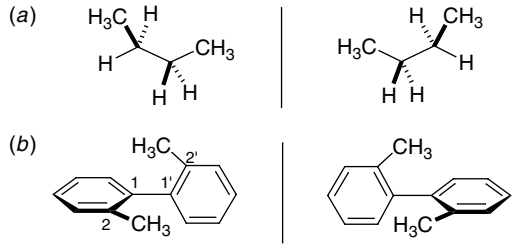

Figure 3.1. Dynamic chirality of (*a*) *n*-butane and (*b*) 2,2′-dimethylbiphenyl.

rotation with a barrier of around 18 kcal/mol,[14] which corresponds to the half-life of racemization, about 7 days at −78°C or about 2 s at 20°C. Since the chiral properties of these molecules are time and temperature dependent, we prefer to call this type of chirality rather than conformational chirality.[1,15]

At a rudimentary level of analysis, simple enolates devoid of remote elements of chirality are achiral because all four substituents are in the same plane as the enolate double bond. However, the enolate subunit on its own is capable of existing in chiral conformations by virtue of slow rotation about one or more bonds between the substituents and the enolate double bond. For example, enolate **21** has axial chirality due to slow rotation about the C(1)–C(2) axis, and **22** possesses planar chirality resulting from the disposition of the metal cation with respect to the enolate plane (Figure 3.2). Racemization of these chiral enolates takes place readily through rotation of the C(1)–C(2) and C(1)–O bonds for **21** and **22**, respectively. For a limited time at low temperature, these enolates can exist in chiral, nonracemic forms. Since reactions involving enolate intermediates are usually performed at cryogenic temperatures, chiral enolates with sufficiently long half-lives are expected to be generated and may

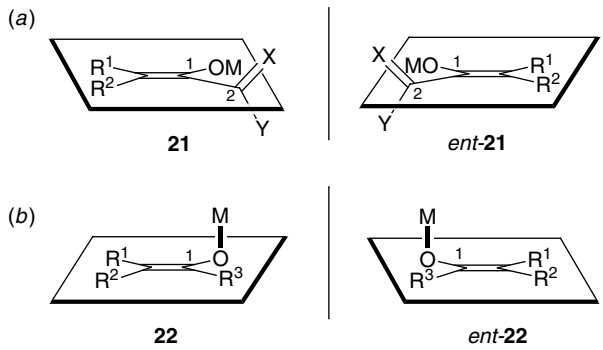

Figure 3.2. Dynamic chirality of enolate structure: (*a*) Axial chirality, (*b*) planar chirality.

be used for asymmetric synthesis. Several asymmetric reactions based on this hypothesis are described below.

IV. DESIGNED "MEMORY OF CHIRALITY" IN ALKYLATION OF A KETONE

Although chiral nonracemic enolates of type **21** and **22** are expected to exist under particular conditions, their half-lives to racemization are usually too short to effect actual asymmetric reactions. To realize an asymmetric transformation via a chiral enolate of type **21**, chiral ketone **23** was designed that would generate a chiral enolate with a significantly long half-life to racemization (Scheme 3.8). Steric interactions of C(2)–OMe with C(2′)–OEt and C(8′)–H in the enolate would prevent free rotation of the C(1)–C(1′) bond as well as coplanarity of the enolate double bond with the naphthalene ring. Thus the enolate was expected not to exist as an achiral planar enolate, but it could be a chiral enolate with a chiral C(1)–C(1′) axis. The rotational barrier about the C(1)–C(1′) bond may be estimated by analogy with 2,2′-disubstituted biphenys because of similarity of the local steric environment around the chiral axes. The half-life to racemization was assumed to be about a few years at -78°C from the reported rotational barrier of various 2,2′-disubstituted biphenys (~80 kJ/mol).[16]

Treatment of **23** with potassium hydride in the presence of an alkyl halide and 18-crown-6 in fact gave optically active α-alkylated products **24** in 48% to nearly 73% *ee* in the absence of any additional chiral source (Table 3.1).[17] Thus chirality of optically active **23** was memorized in the enolate intermediate during its alkylation. The stereochemical course of α-methylation and ethylation was inversion.

The geometry of the enolate intermediate was investigated by trapping experiments. When **23** (93% *ee*) was treated with potassium hydride and acetic anhydride in the presence of 18-crown-6, *E*-enol acetate **25** (59%) and its *Z*-isomer **26** (6%) were obtained together with the recovery of **23** (27%). The *ee* of the recovered **23** was unchanged. These observations indicate that the *E*-enolate is the major intermediate under conditions of kinetic control. HPLC analysis of **25** with a chiral stationary phase indicated the existence of a pair of enantiomers (Figure 3.3*a*). Rapid interconversion between

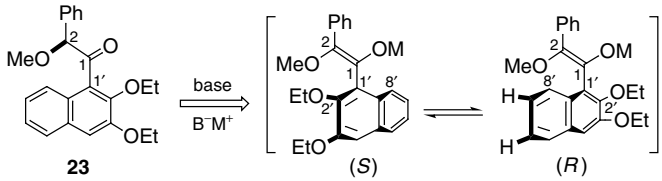

23

Scheme 3.8.

Table 3.1
Enantioselective Alkylation of **23**

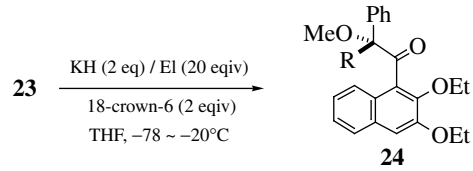

Entry	El	R	Yield (%)	*ee* (%)[a]	Configuration
1	Me-I	Me	48	66	*R*
2[b]	Me-I	Me	54	73	*R*
3	Et-I	Et	27	65	*R*
4	$PhCH_2$-Br	CH_2Ph	31	67	*c*
5	$CH{=}CHCH_2$-Br	$CH_2CH{=}CH_2$	36	48	*c*
6	$CH_2CHCOCH_3$	$CH_2CH_2COCH_3$	25	70	*c*

[a]Determined by HPLC analysis (Chiralpak AD, hexane : 2-propanol = 95 : 5).
[b]Reaction was carried out in toluene.
[c]Not determined

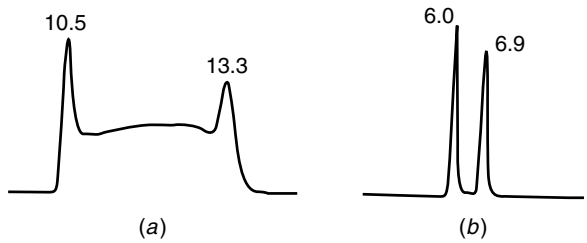

Figure 3.3. HPLC analysis of (*a*) **25** with Chiralpak AD, *i*PrOH : hexane = 7 : 93, (*b*) **27** with Chiralpak AD, *i*PrOH : hexane = 3 : 97.

the enantiomers seems to occur, which is indicated by the plateau observed between the enantiomer peaks. In accordance with this observation, **25** isolated from the reaction of **23** (93% *ee*) did not show optical rotation at either 589 or 405 nm. On the other hand, enol ether **27**, obtained as a by-product in 15% to nearly 27% yield in the transformation of **23** into **24** (R=Me), showed a clear separation of enantiomer peaks in an HPLC analysis at 21°C (Figure 3.3b). Although interconversion between the enantiomers of **27** should take place even during the HPLC analysis, the short retention time (6.0, 6.9 min) of both enantiomers minimized the epimerization of **27** and made near-baseline

separation possible in the HPLC analysis (*cf.* the half-life of racemization of **27** which is 53 min at 21°C; see below).

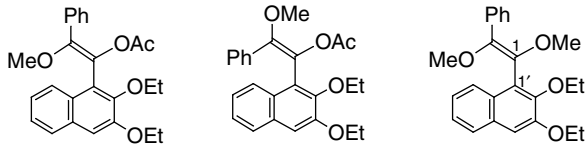

25 **26** **27**

Isolation of chiral nonracemic enol ether **27** is possible by rapid workup followed by purification. Isolated **27** showed $[\alpha]_D^{20}$ +21 (*c* 0.15, $CHCl_3$) and 43% *ee* by HPLC analysis. The enantiomeric purity of **27** decreased gradually at 21°C with a barrier, $\Delta G_{294}^{\neq} = 22.6$ kcal/mol ($t_{1/2} = 53$ min). Direct HPLC analysis of the reaction mixture showed that the *ee* of **27** was at least 65% in reaction medium below −20°C.[17] Thus intervention of the potassium enolate intermediate with the chiral C(1)–C(1′) axis seems logical (Scheme 3.9). It appears that the central chirality at C(2) in **23** is *memorized* in the enolate intermediate as dynamic axial chirality and then regenerated as central chirality in product **24**. The rotational barrier of the C(1)–C(1′) bond of the potassium enolate may be close to that of **27** (22.6 kcal/mol). The rotational barrier of the C(1)–C(1′) bond of **23** could not be measured by variable-temperature NMR within the range of +20 to almost −100°C, and is assumed to be ∼11 kcal/mol by analogy to that reported for the related alkyl naphthyl ketone **28**.[18] Thus the increase in the rotational barrier is roughly estimated to be about 10 kcal/mol, as sp^3 hybridization at C(2) in **23** is converted into sp^2 hybridization in the corresponding enolate. This enables the existence of an axially chiral enolate intermediate with a significantly long half-life to racemization. The half-life to racemization of the potassium enolate intermediate may be estimated to be about 20 days at −20°C, provided that the enolate has the rotational barrier close to that of **27**. The lifetime of the chiral nonracemic enolate is sufficiently long for the asymmetric alkylation to take place.

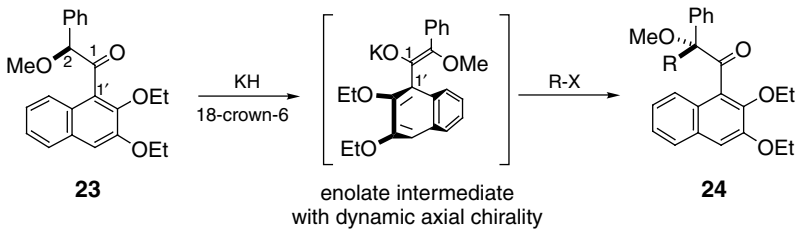

23 enolate intermediate with dynamic axial chirality **24**

Scheme 3.9.

For the memory effect of chirality during the alkylation, the naphthalene ring in **23** is essential. The benzene analogue **29** gave a completely racemized product on its α-methylation under the identical reaction conditions.

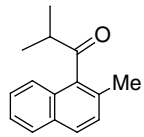

28

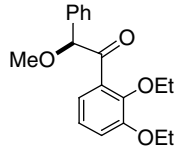

29

The potassium enolate generated from **23** is regarded as an enantiomeric atropisomer. Recently non-biaryl atropisomers have been receiving more attention in asymmetric synthesis.[19] Most of them employ atropisomers that are configurationally stable at room temperature, while attention in this chapter is focused on asymmetric reactions that proceed via chiral nonracemic enolate intermediates that can exist only in a limited time. An application of configurationally stable atropisomeric amide to a chiral auxiliary for stereoselective alkylation has been reported by Simpkins and co-workers (Scheme 3.10).[20]

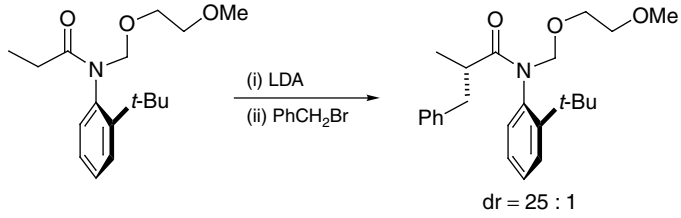

Scheme 3.10.

V. DIRECT ASYMMETRIC α-ALKYLATION OF PHENYLALANINE DERIVATIVES

It is worthwhile to apply the "memory of chirality" principle to asymmetric alkylation of α-amino acids because nonproteinogenic α,α-disubstituted-α-amino acids are important class of compounds in the fields of medicinal and biological chemistry.[21] Typical methods for their asymmetric synthesis involve chiral auxiliary-based enolate chemistry.[22–24] However, the most straightforward synthesis would be direct asymmetric α-alkylation of the parent α-amino acids in the absence of external chiral sources. Asymmetric

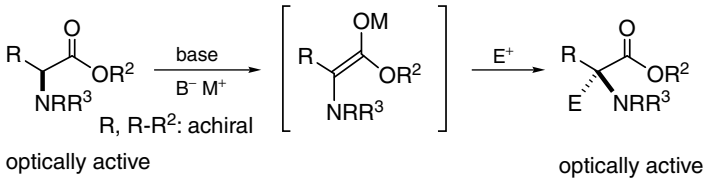

Scheme 3.11.

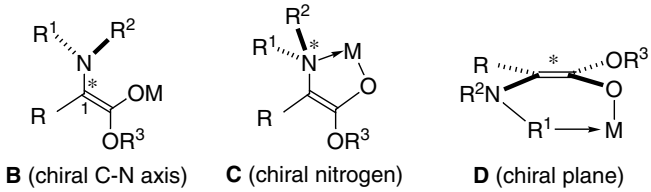

Figure 3.4. Dynamic chirality of enolates derived from α-amino acids.

synthesis in Scheme 3.11 was developed based on dynamic chirality of the enolate structure.

Enolates derived from α-amino acids are not always achiral, but they can exhibit dynamic chirality (Figure 3.4).[1,15] As shown in **B**, an enolate with axial chirality resulting from slow rotation about the C(1)–N bond is expected if R^1 is different from R^2. An enolate with a stereogenic nitrogen atom is shown in **C**, where tight coordination of nitrogen to a metal cation creates a new stereocenter.[25] An enolate with planar chirality that comprises the enolate plane and a metal cation (**D**) is also possible. Accordingly the choice of R^1 and R^2 in **B**, **C**, or **D** is crucial for the generation of a chiral enolate as well as its asymmetric environment. Table 3.2 shows the effects of the nitrogen substituents of phenylalanine derivatives **30** on enantioselectivity in their α-methylation.[26,27]

Phenylalanine derivatives with various nitrogen substituents R^1 and R^2 (**30**) were prepared and their α-methylation was examined (Table 3.2). It turned out that derivatives with an alkoxycarbonyl group on the nitrogen undergo α-methylation with modest asymmetric induction (entries 5–7). The presence of two substituents on the nitrogen seems to be essential for asymmetric induction (entries 1 vs. 7).

This asymmetric induction is strongly affected by the base. Asymmetric methylation of **32** occurred with retention of configuration when lithium 2,2,6,6-tetramethylpiperidide (LTMP) or LDA was used, while inversion of configuration was observed with potassium hexamethyldisilazide (KHMDS)

Table 3.2
Effects of Nitrogen Substituents on Enantioselectivity of α-Methylation of **30**[a]

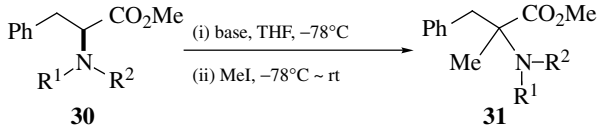

30 **31**

Entry	R^1	R^2	*ee* of **30** (%)	Base	Yield (%)	*ee* (%) of **31**
1	H	CO_2t-Bu	96	LDA	57	~0
2	Me	CH_2tPh	98	LDA	45	~0
3	Me	CHO	94	LHMDS[b]	66	~0
4	Me	COPh	96	LDA	50	12
5[c]	Me	CO_2CH_2Ph	94	LHMDS	40	26
6	Me	CO_2Ad[d]	94	LHMDS	38	35
7	Me	CO_2t-Bu	96	LHMDS	30	36

[a] Substrate **30** was treated with the base (11 ~ 1.8 equiv) at −78°C for 30 to 60 minutes followed by methyl iodide at −78°C to room temp.
[b] Lithium hexamethyldisilazide.
[c] Run in THF-DMF (10 : 1).
[d] 1-Adamantyl ester.

(entries 1–3). The highest enantioselectivity (82% *ee*) was obtained with 1.0 equiv of LTMP in 40% yield (entry 3). A ^{13}C-NMR study using ^{13}C(2),^{15}N-labeled derivative of **32** indicated that enolate formation is in the range of only 50% to nearly 60% when 1.1 equiv of LTMP was used. Enolate formation was complete with 2 to 4 equiv of LTMP, but it did not improve the yield of **33** (entries 3–5). Asymmetric α-allylation of **32** occurred in 88% *ee* by similar treatment (entry 6).[26]

Thus the hypothesis in Figure 3.4 is indeed effective for designing asymmetric synthesis. However, the main drawbacks in the transformation of **32** into **33** are low chemical yield and difficulty in removing the *N*-methyl protective group. Further investigation of other (readily removable) nitrogen substituents and conditions for asymmetric induction are shown in Table 3.4. The best result was obtained with *N*-methoxymethyl(MOM)-*N*-Boc derivative **40**. Treatment of **40** with KHMDS in toluene-THF (4 : 1) at −78°C for 30 minutes followed by the addition of methyl iodide afforded **41** in 96% yield and 81% *ee* (entry 9).[27,28] Use of a toluene-THF (4 : 1) mixture as a solvent is crucial for both high yield and enantioselectivity (entries 7–9).

Table 3.3
Asymmetric α-Alkylation of *N*-Me-*N*-Boc-Phenylalanine Derivative **32**[a]

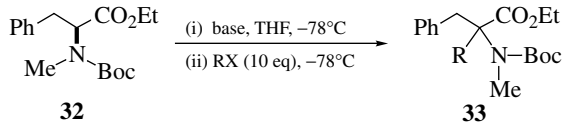

32 **33**

Entry	Base		Rx	Yield (%)	*ee* (%) [b]
1	KHMDS[c]	(1.2 equiv)	MeI	79	20 (*R*)
2	LDA	(1.2 equiv)	MeI	57	22 (*S*)
3	LTMP[d]	(1.0 equiv)	MeI	40	82 (*S*)
4	LTMP	(2.0 equiv)	MeI	42	73 (*S*)
5	LTMP	(4.0 equiv)	MeI	36	66 (*S*)
6	LTMP	(1.0 equiv)	CH_2=$CHCH_2Br$	15	88
7	LTMP	(1.0 equiv)	MOMCI	24	69

[a] **32** (98% *ee*) was treated with the base in THF at −78°C for 15 minutes followed by alkyl halide at −78°C for 4 hours.
[b] Letter in parentheses indicates the absolute configuration of **33**.
[c] Potassium hexamethyldisilazide.
[d] Lithium 2,2,6,6-tetramethylpiperidide.

Table 3.4
Asymmetric α-Methylation of *N*-Boc-Phenylalanine Derivatives

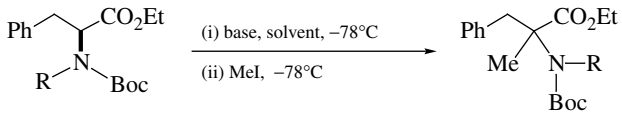

Entry	Substrate	R	Base	Solvent	Product	Yield (%)	*ee* (%)
1	**34**	CH_2CH=CH	LTMP	THF	**35**	24	54
2	**34**	CH_2CH=CH	KHMDS	Toluene-THF (4 : 1)	**35**	66	31
3	**36**	CH_2OCO^tBu	KHMDS	THF	**37**	70	20
4	**36**	CH_2OCO^tBu	KHMDS	Toluene-THF (4 : 1)	**37**	68	60
5	**38**	$CH_2OCH_2CH_2OMe$	LTMP	THF	**39**	51	10
6	**38**	$CH_2OCH_2CH_2OMe$	KHMDS	Toluene-THF (4 : 1)	**39**	79	73
7	**40**	CH_2OMe	KHMDS	THF	**41**	93	36
8	**40**	CH_2OMe	KHMDS	Toluene	**41**	47	75
9	**40**	CH_2OMe	KHMDS	Toluene-THF (4 : 1)	**41**	96	81

VI. ASYMMETRIC α-METHYLATION OF VARIOUS α-AMINO ACID DERIVATIVES

Thorough investigation of nitrogen substituents of phenylalanine for asymmetric induction disclosed that *N*-MOM-*N*-Boc derivative **40** gives α-methylated product in 81% *ee* and in 96% yield without the aid of any external chiral

Table 3.5
Asymmetric α-Methylation of *N*-Boc-*N*-MOM-α-Amino Acid Derivatives[a]

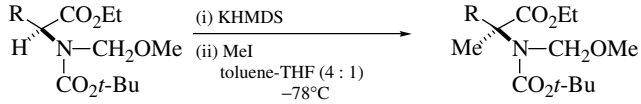

Entry	R	Substrate[b]	Product	Yield (%)	*ee* (%)[c]	Configuration[d]
1	$PhCH_2-$	**40**	**41**	96	81	*S*
2	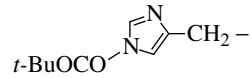	**42**	**43**	83	93	*e*
3	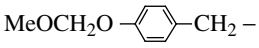	**44**	**45**	94	79	*S*
4	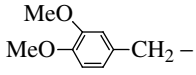	**46**	**47**	95	80	*S*
5	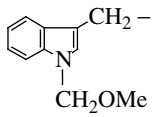	**48**	**49**	88	76	*e*
6	Me_2CH-	**50**	**51**[f]	81	87	*S*
7	Me_2CHCH_2-	**52**	**53**[f]	78	78	*S*

[a] A substrate (0.5 mmol) was treated with 1.1 mol equiv of KHMDS at −78°C for 30 minutes (for **40**, **42**, **44**, **46**, and **48**) or 60 minutes (for **50** and **52**) followed by 10 mol equiv of methyl iodide for 16 to 17 hours at −78°C.
[b] *ee* of each substrate is >99%.
[c] Determined by CSP HPLC analysis.
[d] Absolute configuration of the corresponding α methyl α-amino acid.
[e] Not determined.
[f] Obtained as an inseparable mixture with the substrate. Yield was determined based on the ratio of signals observed in 400 MHz ^{1}H NMR. Complete separation was achieved with the corresponding *N*-benzoyl derivative.

source. α-Amino acids with *N*-MOM-*N*-Boc substituents (>99% *ee*) can be readily prepared through esterification of the amino acid ($SOCl_2$/EtOH) and *t*-butoxycarbonylation ($(Boc)_2O$/*i*PrNEt$_2$), followed by *N*-methoxymethylation (MOMCl/KHMDS). α-Methylation of several *N*-MOM-*N*-Boc α-amino acid derivatives is shown in Table 3.5. The derivatives with aromatic side chains (Phe, **40**; His, **42**; Tyr, **44**; Dopa, **46**; and Trp, **48**) as well as aliphatic side chains (Val, **50** and Leu, **52**) undergo α-methylation in a highly enantioselective manner (76 ~ 93% *ee*) and in good yields (78 ~ 96%) upon treatment with KHMDS in toluene-THF (4 : 1) followed by methyl iodide.[28] Removal of the protective groups of **41**, **45**, **51**, and **53** is readily accomplished in one step by treatment with 6 M aq HCl to give the corresponding α-methyl α-amino acids in 51% to 86% yields. Antihypertensive α-methyldopa was obtained from **47** through the sequential removal of the protective groups.[29] In each case the α-methylation proceeds with retention of configuration. The degree of asymmetric induction is comparable among several different amino acids. This implies that the MOM and Boc groups at the nitrogen have a decisive effect on the stereochemical course of the α-methylation.

VII. MECHANISM OF MEMORY OF CHIRALITY IN ASYMMETRIC ALKYLATION OF α-AMINO ACID DERIVATIVES

A possible rationale for the asymmetric α-methylation of **40** involves the participation of mixed aggregate **E** in which the undeprotonated starting material functions as a chiral ligand of the potassium cation of the *achiral enolate*. To test the feasibility of **E**, a crossover experiment between **40** and **44** was conducted (Scheme 3.12). A 1 : 1 mixture of *racemic* **40** and (*S*)-**44** (>99% *ee*) was treated with KHMDS (1.1 equiv of the total amount of **40** and **44**) followed by methyl iodide according to the protocol in Table 3.5, to give *racemic* **41** (79% yield) and (*S*)-**45** (74% *ee*, 79% yield). This means that transfer of chirality between substrates did not occur. Thus mixed aggregate **E** is not responsible for the present asymmetric induction.

The structure and chiral properties of the enolate intermediate were then investigated. Treatment of **40** with KHMDS (1.1 equiv) in toluene-THF (4 : 1) at −78°C for 30 minutes followed by *t*-butyldimethylsilyl (TBS) triflate gave *Z*-enol silyl ether **54** and its *E*-isomer **55** in respective isolated yields of 57% and 27%.[30] In the ^{1}H NMR spectra of both **54** and **55**, methylene protons of the MOM groups appeared as AB quartets, which indicates restricted rotation of the C(1)–N bonds. The rotational barrier of the C(1)–N bond of the major *Z*-isomer **54** was determined to be 16.8 kcal/mol at 92°C by variable-temperature NMR measurements in toluene-d_8 (400 MHz ^{1}H

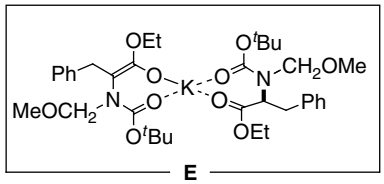

E

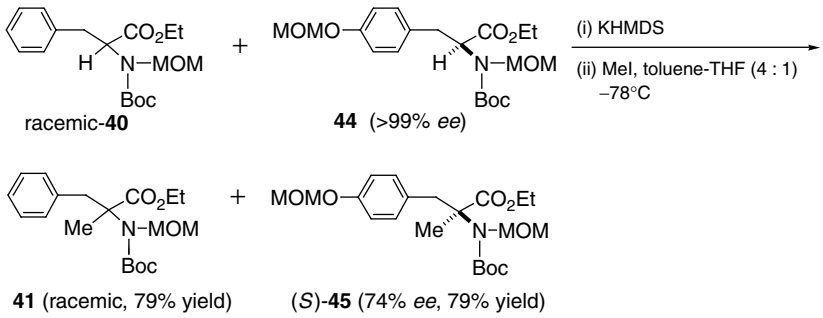

Scheme 3.12.

NMR, $J_{AB} = 9.9$ Hz, $\Delta\nu_{AB} = 228.4$ Hz, Tc = 92°C). The restricted bond rotation brings about axial chirality in **54** (chiral C(1)–N axis), as shown in Scheme 3.13. The half-life to racemization of **54** was estimated to be 5×10^{-4} sec at 92°C, which corresponds to a half-life of about 7 days at −78°C.[31] This implies that the corresponding potassium enolate could also exist in an axially chiral form with a relatively long half-life to racemization at low temperatures.

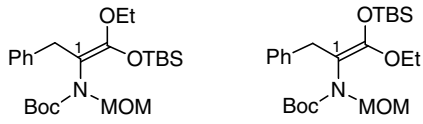

54 **55**

The behavior of the potassium enolate intermediate toward racemization was investigated (Table 3.6). When **40** was treated with KHMDS for 24 hours at −78°C, the reaction of the resulting enolate with methyl iodide gave **41** in 36% *ee*, while **41** in 81% *ee* was obtained by 30 minute treatment with base (entries 1 vs. 2). When the enolate was prepared at −78°C for 30 minutes, and then kept at −40°C for 30 minutes, its reaction with methyl iodide at −78°C produced **41** in 5% *ee* (entry 3). These results clearly indicate that the enolate intermediate underwent racemization.

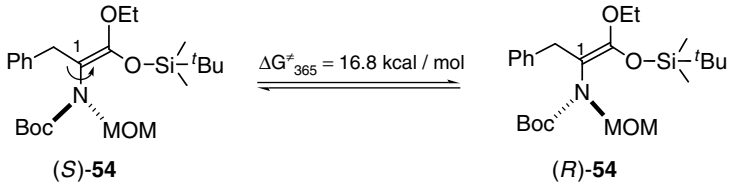

Scheme 3.13.

Table 3.6
Effects of Time and Temperature for Enolate Formation of **40** on *ee* of **41**

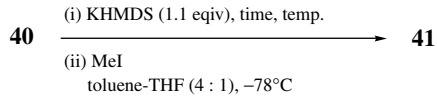

Entry	Conditions for Enolate Formation	Yield (%)	*ee* (%)
1	−78°C, 30 minutes	96	81
2	−78°C, 24 hours	84	36
3	−78°C, 30 minutes, then −40°C, 30 minutes	88	5
4	−78°C, 30 minutes, then 0°C, 30 minutes	58	∼0

The barrier to racemization of the chiral enolate intermediate generated from **40** was determined through periodic quenching of the enolate generated at −78°C with methyl iodide. Figure 3.5 shows the logarithm of the relative *ee*'s of **41** as a function of time for base treatment of **40**, and indicates a linear relationship between them ($r = 0.999$), although the enolate is a 2 : 1 mixture of the *Z*- and *E*-forms. This suggests that the rates of racemization of the *Z*- and *E*-enolates are very close to each other. The barrier was calculated from the slope ($2k = 5.34 \times 10^{-4}$/min) to be 16.0 kcal/mol at −78°C. This racemization barrier of the potassium enolate matches the rotational barrier (16.8 kcal/mol) of the C(1)–N bond of enol silyl ether **54**. This suggests that the chirality of the enolate intermediate also originates in the restricted rotation of the C(1)–N bond. It is concluded that *a chiral nonracemic enolate with dynamic axial chirality (**F**) is the origin of the present asymmetric induction*.[28,32,33] The half-life to racemization of the chiral enolate was 22 hours at −78°C, which is sufficiently long for the chiral enolate to undergo asymmetric methylation without significant racemization.

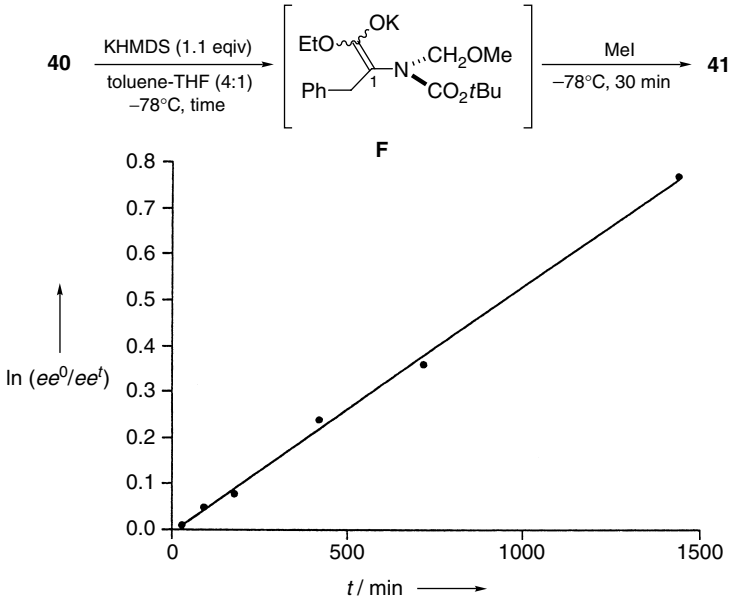

Figure 3.5. Determination of racemization barrier of the enolate generated from **40** and KHMDS. ee^0: The *ee* value of **41** obtained by the reaction of the enolate immediately after its generation ($t = 5$ min) from **40** with methyl iodide. ee^t: The *ee* value of **41** obtained by treatment of **40** with KHMDS for the time indicated, followed by addition of methyl iodide. 0.25 mmol of **40** was employed for each run. Reactions were quenched 30 minutes after the addition of methyl iodide in order to minimize racemization of the enolate intermediate during alkylation: $ee^0 = 80\%$ ($t = 5$ min), $ee^{t=30\ \text{min}} = 79\%$, $ee^{t=90\ \text{min}} = 76\%$, $ee^{t=180\ \text{min}} = 74\%$, $ee^{t=420\ \text{min}} = 63\%$, $ee^{t=720\ \text{min}} = 56\%$, $ee^{t=1440\ \text{min}} = 37\%$.

Support for this novel mechanism was obtained from the reactions of **56** and **58** (Scheme 3.14). Upon α-methylation according to the protocol in Table 3.5, *N*,*N*-diBoc derivative **56** (>99% *ee*) gave racemic **57** (95% yield). Similarly methylene acetal derivative **58** (>99% *ee*) gave racemic **59** (95% yield). These results are consistent with the conclusions above, since enolates **G** and **H** generated from **56** and **58**, respectively, are *not* expected to be axially chiral along the C(1)–N axis. Enolate **G** is not axially chiral even if rotation about the C(1)–N bond is restricted at −78°C. The 2,3-dihydrooxazole ring in **H** is supposed to be nearly planar.

A possible rationale for the stereochemical course of the transformation of (*S*)-**40** into (*S*)-**41** is shown in Scheme 3.15. Note that this is a speculation without experimental proof. (1) deprotonation occurs from the stable conformer **I**[34] where the C(1)–H bond is eclipsed with the N–C (MOM) bond to produce enantiomerically enriched chiral enolate **F** and (2) an electrophile

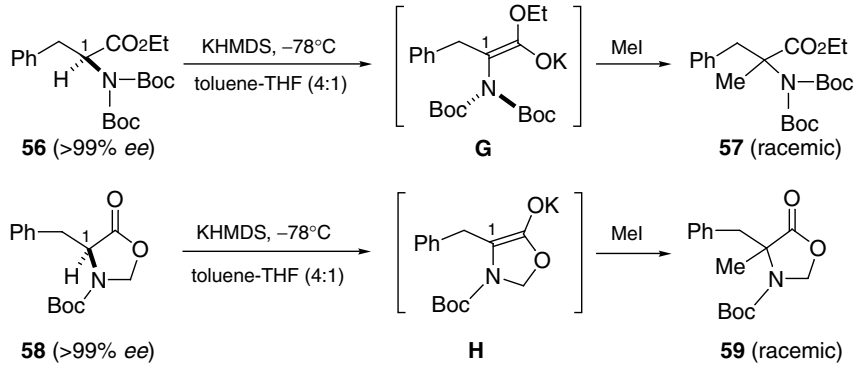

Scheme 3.14.

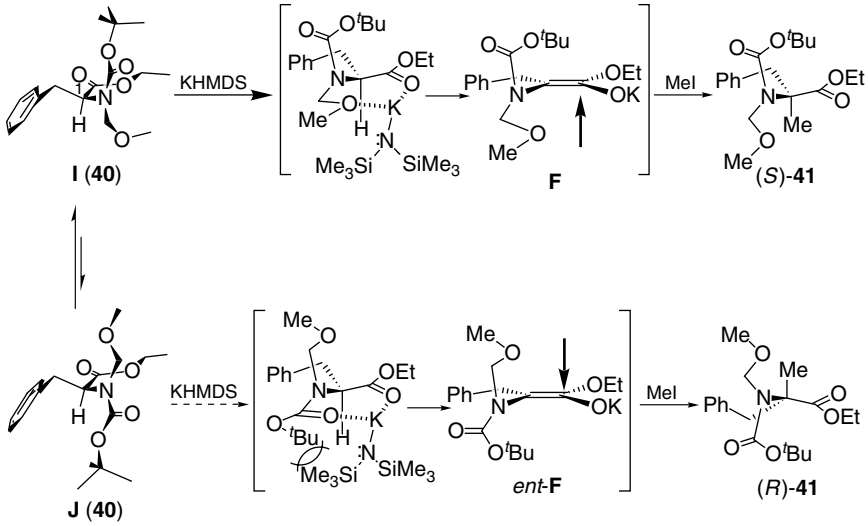

Scheme 3.15.

(methyl iodide) approaches from the sterically less demanding face (MOM) of the enolate double bond of **F**. When deprotonation takes place from the second-most stable conformation **J**, where the C(1)–H bond is eclipsed with the N–C(Boc) bond, enolate *ent*-**F** is produced. This leads to (*R*)-**41** via electrophilic attack from the face of the MOM group. Besides the conformational preference of **40**, the steric interaction between KHMDS and the Boc or MOM

group at the transition state for deprotonation should critically affect the enantioselectivity (**F**/*ent*–**F** ratio) of formation of the chiral enolate. While this is merely a speculation, it is consistent with the experimental result that **60** undergoes α-methylation in only 22% *ee* under the same treatment as that for **40**. This could be ascribed to the smaller difference in steric bulk between MOM and CO_2Me groups than that between MOM and Boc groups in **40**. Table 3.5 also shows that the enantioselectivity of α-methylation is comparable among several α-amino acid derivatives irrespective of the side-chain structure. These results indicate that the difference in steric bulk between Boc and MOM groups is crucial for the asymmetric induction.

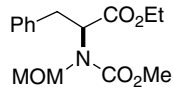

60

VIII. MEMORY OF CHIRALITY IN DIASTEREOSELECTIVE α-ALKYLATION OF β-BRANCHED α-AMINO ACID DERIVATIVES

Several *N*-Boc-*N*-MOM-α-amino acid derivatives undergo α-methylation in 78% to nearly 93% *ee* with retention of the configuration upon treatment with KHMDS followed by methyl iodide at −78°C. The substituents of the nitrogen are essential for control of the stereochemistry. How much is the stereochemical course of the reaction affected by an additional chiral center at C(3) of substrates? α-Alkylation of *N*-Boc-*N*-MOM-L-isoleucine derivative **61** and its C(2)-epimer, D-*allo*-isoleucine derivative **62**, were investigated (Scheme 3.16). If the chirality at C(2) is completely lost with formation of the enolate, α-methylation of either **61** or **62** should give a mixture of **63** and **64** with an identical diastereomeric composition via common enolate intermediate **K**. On the other hand, if the chirality of C(2) is *memorized* in enolate intermediates, **61** and **62** should give products with independent diastereomeric compositions via diastereomeric enolate intermediates.

Treatment of **61** with 1.1 mol equiv of KHMDS in THF at −78°C for 60 minutes followed by the addition of methyl iodide gave a mixture of diastereomers **63** and **64** in a ratio of 93 : 7 in a combined yield of 93%. On the other hand, the same treatment of **62** gave a mixture of **63** and **64** in a ratio of 14 : 86 in a combined yield of 91%. Although **63** and **64** were obtained as an inseparable mixture, each of the pure diastereomers was obtained after conversion to the corresponding *p*-nitrobenzamides **65** and **66**, respectively.

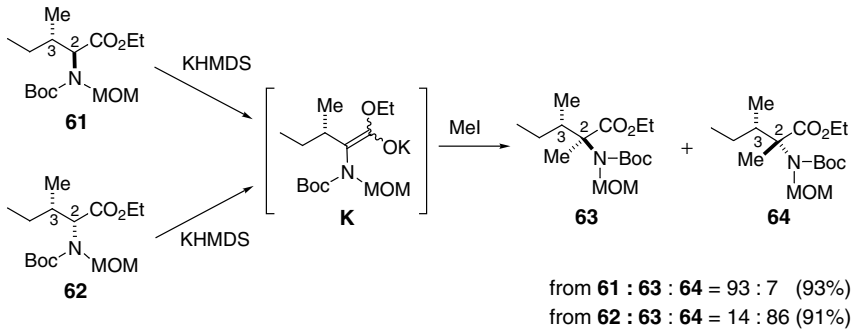

Scheme 3.16.

The configuration of **66** was unambiguously determined to be (2*R*,3*S*) by an X-ray crystallographic analysis.[35]

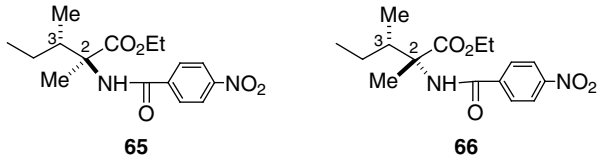

α-Methylation of both **61** and **62** proceeds with retention of configuration at C(2) with comparable diastereoselectivities (dr = 93 : 7 for **61** vs. dr = 86 : 14 for **62**). The configuration of C(2) makes a decisive contribution to the stereochemical course of α-methylation even in the presence of the adjacent chiral center C(3). **L** and **M** are proposed for the possible structures of chiral enolate intermediates generated from **61** and **62**, respectively, by analogy to phenylalanine derivative **40**. The central chirality at C(2) in **61** and **62** appears to be preserved in **L** and **M** as dynamic axial chirality due to restricted rotation of the C(2)–N bond.

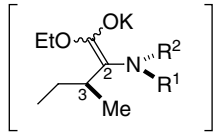

L : R^1 = Boc, R^2 = MOM
M : R^1 = MOM, R^2 = Boc

Since the Boc and MOM groups at the nitrogen seem to be essential for the axial chirality in **L** and **M**, the reactions of *N*,*N*-diBoc derivatives **67** and **68** that do not generate axially chiral enolates were next investigated (Scheme 3.17). Upon α-methylation under conditions identical to those for **61**

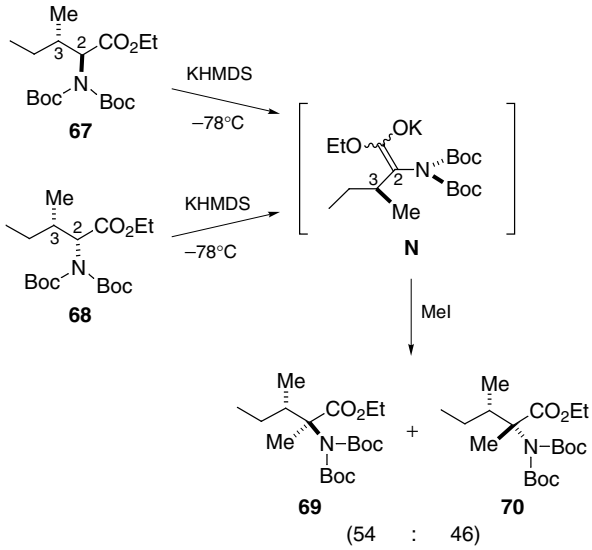

Scheme 3.17.

and **62**, **67** gave a 54 : 46 mixture of **69** and **70** in 83% yield. The structure of **69** and **70** was determined after their conversion to **65** and **66**, respectively. An identical diastereomer ratio of **69** and **70** was observed in α-methylation of **68** (87% yield). Thus the stereochemical course of the α-methylation of **67** and **68** is completely controlled by the chirality at C(3) regardless of the chirality at C(2), which is in sharp contrast to the reactions of **61** and **62**. These results suggest that the reactions of both **67** and **68** share a common enolate intermediate **N**. Enolate **N** does not possess a chiral axis about the C(2)–N bond even if the bond rotation is restricted at −78°C.

α-Allylation of **61** and **62** gave results that paralleled those of α-methylation (Scheme 3.18). Treatment of **61** with KHMDS for 60 minutes followed by the

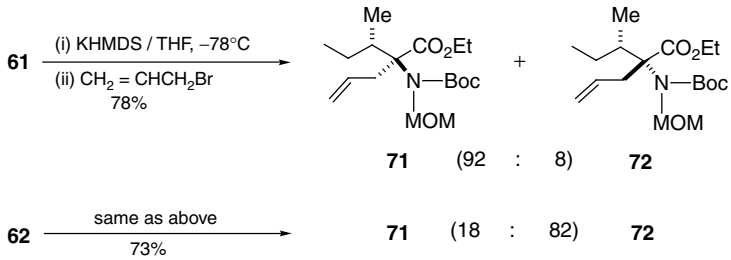

Scheme 3.18.

addition of allyl bromide in THF at −78°C gave **71** and **72** in a 92 : 8 ratio with a combined yield of 78%, while the same treatment of **62** gave **71** and **72** in a 18 : 82 ratio with a combined yield of 73%.

The stereochemical course of α-alkylation of both L-isoleucine and D-alloisoleucine derivatives **61** and **62** is controlled predominantly by the chiral axis in the enolate intermediate, whereas the adjacent chiral center C(3) has little effect.

IX. MEMORY OF CHIRALITY IN THE LITERATURE

"Memory of chirality" signifies asymmetric transformation in which the chirality of the starting materials is preserved in the configurationally labile intermediates (typically enolates) during the transformation. A typical example of memory of chirality is the alkylation of ketone **23** and α-amino acid ester **40**. Before and after our first report on the memory of chirality in 1991, several related phenomena have been reported.

A. Chlorination of Optically Active 2-Substituted 1-Indanone Derivatives

In the early twentieth century Leuchs reported a surprising example of the α-chlorination of chiral ketone **73**, which gave optically active **74** in the absence of additional chiral sources.[36] From a mechanistic point of view, however, there remains some ambiguity. Possible mechanisms for the formation of optically active **74** include (1) asymmetric chlorination via an enol intermediate (i.e., memory of chirality), (2) direct electrophilic chlorination of the C–H bond at the stereogenic carbon center, (3) complex formation of an achiral enol intermediate with optically active **73**, (4) resolution of *dl*-**74** by co-crystallization with optically active **73**, and (5) simultaneous resolution of *dl*-**74**.

Bromination of **73** was also reported to produce an optically active product.[37] Ingold and Wilson investigated the kinetics of the bromination and racemization of optically active **73**.[38] Under carefully controlled conditions the rate of bromination is essentially the same as that of racemization. Since bromination takes place via an enol intermediate under the given conditions (Br_2/HBr/AcOH–H_2O), the kinetic study suggested that possibility 1 is unlikely. In the 1960s Ronteix and Marquet re-examined the chlorination of **73**.[39] They focused on intramolecular participation of the carboxylic group of **73**, which seemed crucial if the enol intermediate could preserve chirality. Chlorination of both methyl ester **75** and the *para*-carboxylic acid derivative **76** gave optically active products under similar reaction conditions. This

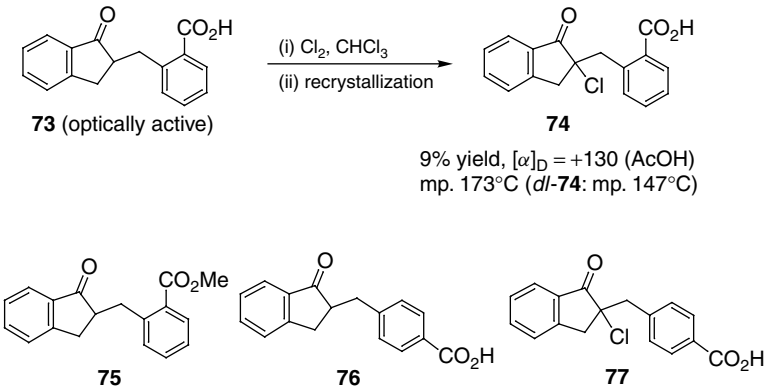

Scheme 3.19.

again suggests that possibility 1 above is unlikely. Crossover experiments with racemic **73** and optically active **76** gave racemic **74** and optically active **77**. These results exclude possibility 3 above. They proposed direct electrophilic chlorination (possibility 2) as the origin for the asymmetric chlorination, although there was no direct evidence. Direct electrophilic chlorination would compete with chlorination via an enol intermediate that gives the racemic product.[39]

B. Retention of Chirality of Optically Active α-Amino Acid Derivatives during α-Alkylation

Seebach and Wasmuth reported an alkylation of diethyl malate (**78**) via dilithio intermediate **79**.[40] The reaction took place at C(3) to give erythro product **80** selectively. Extension of this method to alkylation of aspartic acid derivative **81** gave an unexpected asymmetric induction. In addition to the expected β-alkylated product **82**, α-alkylated product **83** was obtained as a minor product in an optically active form! (ca. 60% *ee*).[41] This appears to be the first example of the retention of chirality of optically active α-amino acid derivatives during α-alkylation.[42] Chiral enolate **84** is assumed to be the intermediate in the formation of **82**. The authors proposed possible intermediates for the production of optically active **83**: (1) *Axially chiral enolate* **85** with a chiral C(2)–N axis or (2) a mixed aggregate of *achiral enolate* **85** with chiral enolate **84**. Possibility 1 does not seem likely since the rotational barrier of the C–N bond may be too small to retain chirality during alkylation. They comment that simple amino acids might also be alkylated via analogues of **85** without racemization, if possibility 1 is valid.[41] In Table 3.2, we observed that the alkylation of **30** (R^1=H, R^2=CO_2t-Bu) gave racemic **31**, probably via enolate

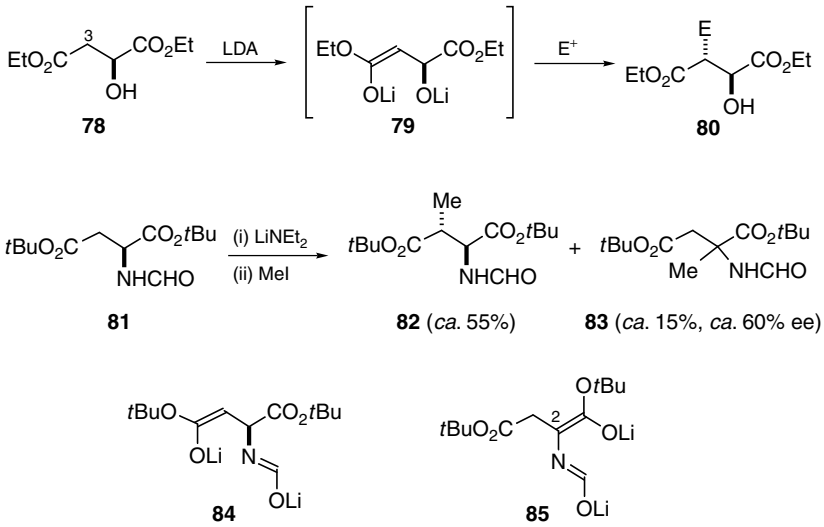

Scheme 3.20.

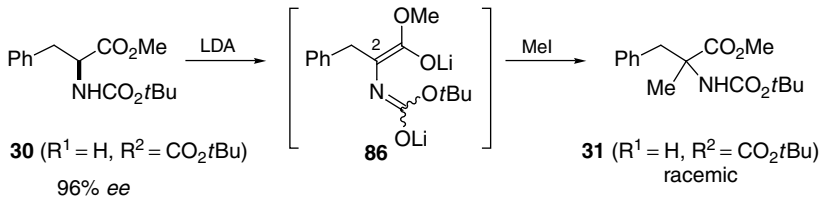

Scheme 3.21.

intermediate **86**. This also indicates that enolates such as **85** and **86** are not likely to be axially chiral about the C(2)–N axis. Accordingly we feel that the mixed aggregate mechanism 2 above is responsible for the formation of **83**.

C. Memory of Chirality in a Cyclization Reaction via an Enolate Intermediate

Stoodley and co-workers found retention of chirality in a cyclization reaction of **87**.[43] The reaction of **87** with triethylamine gave **89** in an enantiomerically pure form. They suggested that axially chiral enolate **88** with a chiral C(4)–N axis may be the origin of the asymmetric induction. Because of the high reactivity of the electrophilic diazo group, the cyclization of **87** would proceed before racemization of the axially chiral enolate.

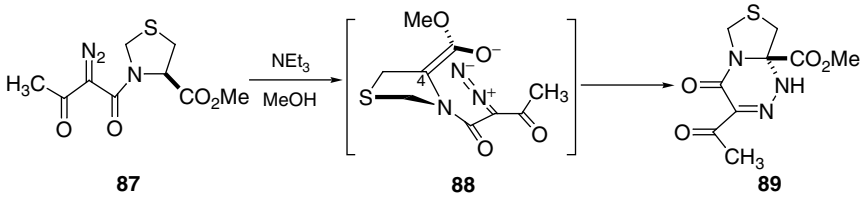

Scheme 3.22.

D. Memory of Chirality in Reactions via Radical Intermediates

Koning and co-workers found a memory effect of chirality in electron-transfer-mediated benzylic substitution.[44] Treatment of arene-chromium complex **90** (91% *ee*) with 4,4′-di-*tert*-butylbiphenyl (LiDBB) followed by trimethylsilyl chloride (TMSCl) gave **91** in 87% *ee*. The radical intermediate formed by a single-electron reduction of **90** with LiDBB is assumed to have 17 valence electron (VE) resonance structure **O**. The barrier to racemization of planar chiral arene-chromium intermediate **O** is estimated by calculation to be about 13 kcal/mol, which corresponds to the half-life of racemization, about one minute at −78°C. The second electron transfer to **O** produces configurationally stable 18 VE anionic species **92** that should react with TMSCl to give **91**. The radical intermediate **O** is expected to undergo a rapid electron transfer from LiDBB before racemization takes place.

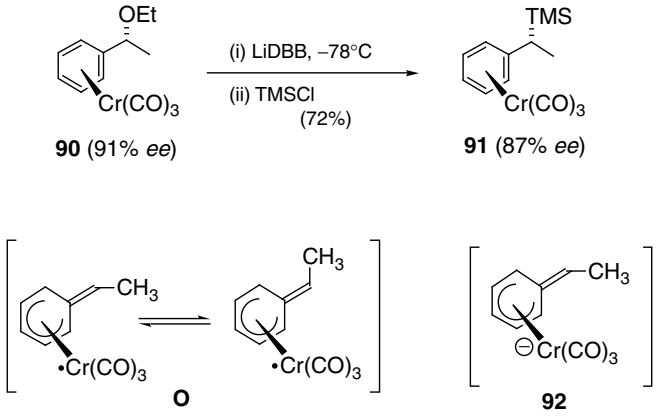

Scheme 3.23.

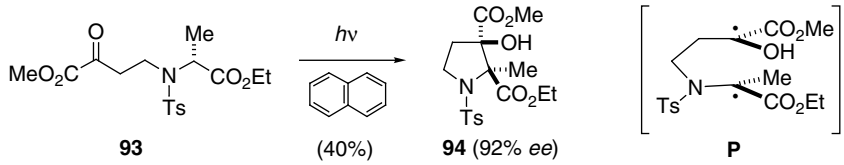

Scheme 3.24.

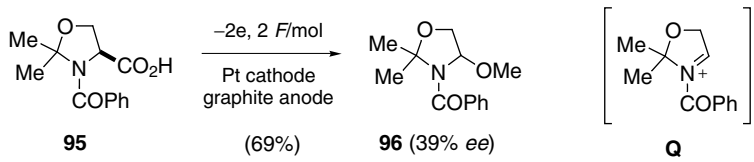

Scheme 3.25.

Giese and co-workers reported the asymmetric photo-cyclization of **93** via short-lived diradical intermediate **P** in the presence of a triplet quencher, naphthalene. Because of the extremely fast cyclization of the singlet diradical **P**, racemization through bond rotation was minimized.[45]

E. Memory of Chirality in Electrochemical Oxidation

Matsumura and co-workers reported a memory effect of chirality in the electrochemical oxidation of **95** to give **96**, although the enantioselectivity was modest (Scheme 3.25). The reaction is assumed to proceed via carbenium ion intermediate **Q**.[46] The mechanism for asymmetric induction is not clear. A possible mechanism involves chiral acid (**95**)-mediated deracemization of racemic **96** produced by the electrochemical oxidation of **95**. However, this suggestion may be eliminated based on the finding that treatment of racemic **96** with **95** in methanol containing 5% formic acid did not produce optically active **96**.

F. Memory of Chirality in Host-Guest Chemistry

Fully substituted porphyrin **97** has been prepared by Aida and co-workers. Porphyrin **97** does not adopt an achiral planar conformation, but rather adopts a chiral saddle-shaped conformation. A rapid saddle-to-saddle inversion, that is, racemization, readily takes place at room temperature. In the presence of a chiral guest molecule such as mandelic acid, **97** retains an enantiomeric saddle-shaped conformation by the formation of a hydrogen-bonded complex with two molecules of mandelic acid. When mandelic acid is replaced by achiral acetic acid, **97** still retains the enantiomeric saddle-shaped conformation. Thus the

chirality of the initial chiral guest molecule was memorized by host molecule **97**. The memory effect lasts for a long time, with a half-life of about 200 hours at 23°C.[47]

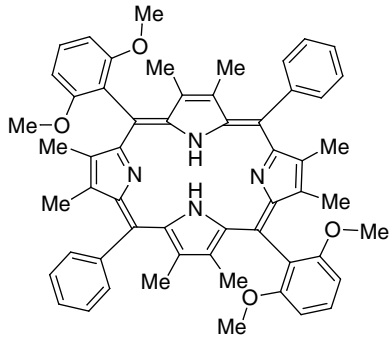

97

Yashima and co-workers reported the memory of macromolecular helicity of poly((4-carboxyphenyl)acetylene) (poly-**98**). Poly-**98** itself possesses a large number of short helical units with many helix-reversal points, and is therefore achiral. However, in the presence of optically active amine **99**, which can interact with the polymer's carboxyl groups, one-handed macromolecular helicity is induced in the polymer. When achiral amino alcohol **100** is added to the helical complex, chiral amine **99** bound to poly-**98** is replaced by stronger base **100**. Nevertheless, the newly formed complex still shows a one-handed helical conformation. Even after the removal of **99** by gel permeation chromatography, the poly-**98**-**100** complex retains a one-handed helical conformation without a loss of helical intensity. Thus the helicity of poly-**98** induced by complexation with a chiral amine was memorized after replacement by an achiral one. The half-life of the chiral memory is as long as four years at room temperature.[48]

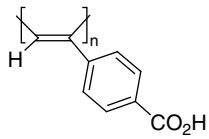

poly-**98**

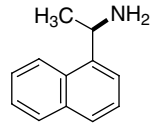

99

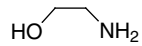

100

X. PERSPECTIVES AND CONCLUSIONS

A principle for asymmetric Synthesis based on the dynamic chirality of the enolate structure is introduced (Scheme 3.26). Following this principle,

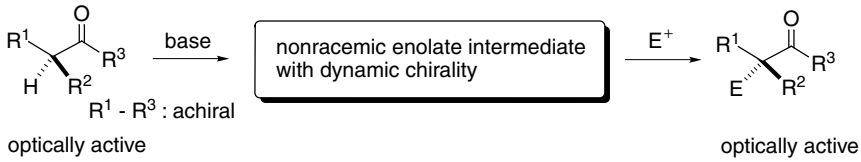

Scheme 3.26.

optically active α-amino acids can be directly converted into optically active α,α-disubstituted α-amino acids in the absence of any additional chiral source. The lower limit of the racemization barrier of the chiral enolate intermediate to achieve significant asymmetric induction is about 14 kcal/mol ($t_{1/2}$ = ca. 10 min) for intermolecular reactions and about 10 kcal/mol ($t_{1/2}$ = ca. 0.01 s) for intramolecular reactions at −78°C. Since the racemization barrier and the chiral environment of enolates can be controlled by introducing substituents into substrates and/or by adding ligands (even achiral ligands) of enolates, the present method may have potentially general applicability in enolate chemistry and asymmetric synthesis.

ACKNOWLEDGMENTS

We are grateful to our co-workers, Dr. Hideo Suzuki, Dr. Thomas Wirth, Dr. Kiyoshi Yahiro, Dr. Jianyong Chen, and Mr. Yoshikazu Nagae, for their excellent contributions to the present study. This work was supported by a Grant-in-Aid for Scientific Research on Priority Areas (No. 706: Dynamic Control of Stereochemistry) from the Ministry of Education (Monbusho), Japan.

REFERENCES

1. Kawabata, T. *Yakugaku Zasshi* **1995**, *115*, 700–715.
2. Trost, B. M.; Fleming, I., eds. *Comprehensive Organic Synthesis*, Vol. 3. Pergamon Press, Oxford **1991**, pp. 1–63.
3. Evans, D. A.; Ennis, M. D.; Mathre, D. J. *J. Am. Chem. Soc.* **1982**, *104*, 1737–1739.
4. (a) Heathcock, C. H. *Asymmetric Synthesis,* Vol. 3. Morrison, D. J., ed. Academic Press, New York, **1984**, p. 200.
5. Murakata, M.; Nakajima, M.; Koga, K. *J. C. S. Chem. Comm.* **1990**, 1657–1658.
6. Imai, M.; Hagihara, A.; Kawasaki, H.; Manabe, K.; Koga, K. *J. Am. Chem. Soc.* **1994**, *116*, 8829–8830.
7. Duhamel, P.; Valnot, J.-Y.; Eddine, J. J. *Tetrahedron Lett.* **1982**, *23*, 2863–2866.
8. (a) Davis, F. A.; Weismiller, M. C.; Lal, G. S.; Chen, B. C.; Przeslawski, R. M. *Tetrahedron Lett.* **1989**, *30*, 1613–1616. (b) Fuji, K.; Node, M.; Nagasawa, H.; Naniwa, Y.;

Taga, T.; Machida, K.; Snatzke, G. *J. Am. Chem. Soc.* **1989**, *111*, 7921–7925. (c) Shibata, N.; Suzuki, E.; Takeuchi, Y. *J. Am. Chem. Soc.* **2000**, *122*, 10728–10729.
9. Mukaiyama, T.; Kobayashi, S.; Uchiro, H.; Shiina, I. *Chem. Lett.* **1990**, 129–132.
10. Krauss, R.; Koert, U. *Organic Synthesis Highlights IV*. Schmalz, H.-G. ed. Wiley-VCH, Weinheim, **2000**, pp. 144–154.
11. Dolling, U.-H.; Davis, P.; Grabowski, E. J. J. *J. Am. Chem. Soc.* **1984**, *106*, 446–447.
12. Nelson, A. *Angew. Chem. Int. Ed.* **1999**, *38*, 1583–1585.
13. For examples, see: (a) Corey, E. J.; Xu, F.; Noe, M. C. *J. Am. Chem. Soc.* **1997**, *119*, 12414–12415. (b) Ooi, T.; Takeuchi, M.; Kameda, M.; Maruoka, K. *J. Am. Chem. Soc.* **2000**, *122*, 5228–5229.
14. Activation parameters for racemization of optically active 2,2′-dimethylbiphenyl has been reported; $\Delta H^{\neq} = 14.6 \pm 0.4$ kcal/mol, $\Delta S = -11.6 \pm 1.8$ eu. The barrier for racemization is calculated to be 16.8 kcal/mol at -78°C and 18.0 kcal/mol at 20°C. Theilacker, W.; Böhm, H. *Angew. Chem. Int. Ed. Engl.* **1967**, *6*, 251.
15. Fuji, K.; Kawabata, T. *Chem. Eur. J.* **1998**, *4*, 373–397.
16. Bott, G.; Field, L. D.; Sternhell, S. *J. Am. Chem. Soc.* **1980**, *102*, 5618–5626.
17. Kawabata, T.; Yahiro, K.; Fuji, K. *J. Am. Chem. Soc.* **1991**, *113*, 9694–9696.
18. Casarini, D.; Lunazzi, L.; Pasquali, F.; Gasparrini, F.; Villani, C. *J. Am. Chem. Soc.* **1992**, *114*, 6521–6527.
19. Clayden, J. *Angew Chem. Int. Ed. Engl.* **1997**, *36*, 949–951.
20. Hughes, A. D.; Price, D. A.; Shishkin, O.; Simpkins, N. S. *Tetrahedron Lett.* **1996**, *37*, 7607–7610.
21. (a) Horwell, D. C.; Hughes, J.; Hunter, J. C.; Pritchard, M. C.; Richardson, R. S.; Roberts, E.; Woodruff, G. N. *J. Med. Chem.* **1991**, *34*, 404–414. (b) Altmann, K.-H.; Altmann, E.; Mutter, M. *Helv. Chim. Acta.* **1992**, *75*, 1198–1210. (c) Mendel, D.; Ellman, J.; Schultz, P. G. *J. Am. Chem. Soc.* **1993**, *115*, 4359–4360. (d) Stilz, H. U.; Jablonka, B.; Just, M.; Knolle, J.; Paulus, E. F.; Zoller, G. *J. Med. Chem.* **1996**, *39*, 2118–2122. (e) Chinchilla, R.; Falvello, L. R.; Galindo, N.; Nájera, C. *Angew. Chem. Int. Ed.* **1997**, *36*, 995–997.
22. For example, Williams, R. M.; Im., M.-N. *J. Am. Chem. Soc.* **1991**, *113*, 9276–9286. For examples of *advanced* chiral auxiliaries that utilize chirality of parent α-amino acids, see: (a) Seebach, D.; Boes, M.; Naef, R.; Schweizer, W. B. *J. Am. Chem. Soc.* **1983**, *105*, 5390–5398. (b) Vedejs, E.; Fields, S. C.; Schrimpf, M. R. *J. Am. Chem. Soc.* **1993**, *115*, 11612–11613. (c) Ferey, V.; Toupet, L.; Gall, T. L.; Mioskowski, C. *Angew. Chem. Int. Ed. Engl.* **1996**, *35*, 430–432. (d) Vedejs, E.; Fields, S. C.; Hayashi, R.; Hitchcock, S. R.; Powell, D. R.; Schrimpf, M. R. *J. Am. Chem. Soc.* **1999**, *121*, 2460–2470.
23. Recent progress in asymmetric synthesis of α,α-disubstituted α-amino acids has been reviewed; see: Wirth, T. *Angew. Chem. Int. Ed. Engl.* **1997**, *36*, 225–227.
24. Recently excellent catalytic methods for asymmetric synthesis of α,α-disubtituted α-amino acid derivatives have been developed; see: (a) Kuwano, R.; Ito, Y. *J. Am. Chem. Soc.* **1999**, *121*, 3236–3237. (b) Ooi, T.; Takeuchi, M.; Kameda, M.; Maruoka, K. *J. Am. Chem. Soc.* **2000**, *122*, 5228–5229.
25. Formation of a stereogenic nitrogen atom by coordination with a metal cation has been claimed: Sato, D.; Kawasaki, H.; Shimada, I.; Arata, Y.; Okamura, K.; Date, T.; Koga, K. *J. Am. Chem. Soc.* **1992**, *114*, 761–763.
26. Kawabata, T.; Wirth, T.; Yahiro, K.; Suzuki, H.; Fuji, K. *J. Am. Chem. Soc.* **1994**, *116*, 10809–10810.
27. Kawabata, T.; Fuji, K. *J. Syn. Org. Chem. Jpn.* **2000**, *58*, 1095–1099.
28. Kawabata, T.; Suzuki, H.; Nagae, Y.; Fuji, K. *Angew. Chem. Int. Ed.* **2000**, *39*, 2155–2157.
29. Conversion of **47** into α-methyldopa was accomplished in the following three-step sequence, since the treatment of **47** with 6 M HCl gave the corresponding tetrahydroisoquinoline derivative: (1) TMSBr/Me_2S, (2) 1 M NaOH, (3) 47% aq. HBr.

30. *N*-Boc-*N*-MOM Enol ethers **54** and **55** exist as a 4 : 1 and 5 : 1 mixture of *N*-Boc *E*/*Z* isomers, respectively at 21°C.
31. The half-life at −78°C was roughly estimated on the assumption that $\Delta S^{\neq}$ of the restricted bond rotation is nearly zero.
32. The absolute configuration of **F** is shown provisionally.
33. The *Z*- and *E*-enolate intermediates should afford α-methylated products of the same absolute configuration. Assuming that *Z*-enolate gives the product of the opposite absolute configuration to that from *E*-enolate and the *Z*/*E* ratio is 2 : 1, the theoretical maximum *ee* of the product is 67% at about 100% conversion or about 100% at <67% conversion. Experimentally, **41** of 81% *ee* was obtained at about 100 conversion (96% yield) (Table 3.5, entry 1).
34. The most stable conformation **I** and the second-stable conformation **J** of **40** were generated by MCMM search with MM3* force field using MacroModel V6.0 (a,b). The difference in potential energies between **I** and **J** is estimated to be 1.0 kcal/mol: (a) Chang, G.; Guida, W. C.; Still, W. C. *J. Am Chem. Soc.* **1989**, *111*, 4379–4386. (b) Kolossváry, I.; Guida, W. C. *J. Am. Chem. Soc.* **1996**, *118*, 5011–5019.
35. Kawabata, T.; Chen, J.; Suzuki, H.; Nagae, Y.; Kinoshita, T.; Chancharunee, S.; Fuji, K. *Org. Lett.* **2000**, *2*, 3883–3885.
36. Leuchs, H. *Ber.* **1915**, *48*, 1015–1021.
37. Leuchs, H. *Ber.* **1913**, *46*, 2435–2442.
38. Ingold, C. K.; Wilson, C. L. *J. Chem. Soc.* **1934**, 773–776.
39. Ronteix, M. J.; Marquet, A. *Tetrahedron Lett.* **1966**, 5801–5806.
40. Seebach, D.; Wasmuth, D. *Hel. Chim. Acta.* **1980**, *63*, 197–200.
41. Seebach, D.; Wasmuth, D. *Angew. Chem. Int. Ed. Engl.* **1981**, *20*, 971.
42. Prior to Seebach's report in 1981, Braña and co-workers had reported that α-methylation of an L-tryptophan derivative furnished optically active product (a). The reported rotation of the product, $[\alpha]_D^{30} - 3.8$ ($CHCl_3$), corresponds to about 60% *ee*. However, re-examination of this reaction independently done by us and Schöllkopf (b) both gave totally racemized product: (a) Braña, M. F.; Garrido, M.; López, M. L.; Sanz, A. M. *J. Heterocycl. Chem.*, **1980**, *17*, 829–830. (b) Schöllkopf, U.; Lonsky, R.; Lehr, P. *Liebigs Ann. Chem.* **1985**, 413–417.
43. (a) Beagley, B.; Betts, M. J.; Pritchard, R. G.; Schofield, A.; Stoodley, R. J.; Vohra, S. *J. Chem. Soc. Chem. Comm.* **1991**, 924–925. (b) Beagley, B.; Betts, M. J.; Pritchard, R. G.; Schofield, A.; Stoodley, R. J.; Vohra, S. *J. C. S. Perkin 1* **1993**, 1761–1770. (c) Betts, M. J.; Pritchard, R. G.; Schofield, A.; Stoodley, R. J.; Vohra, S. *J. C. S. Perkin 1* **1999**, 1067–1072.
44. Schmaltz, H.-G.; Koning, C. B.; Bernicke, D.; Siegel, S.; Pfletschinger, A. *Angew. Chem. Int. Ed.* **1999**, *38*, 1620–1623.
45. Giese, B.; Wettstein, P.; Stähelin, C.; Barbosa, F.; Neuburger, M.; Zehnder, M.; Wessig, P. *Angew. Chem. Int. Ed.* **1999**, *38*, 2586–2587.
46. Matsumura, Y.; Shirakawa, Y.; Satoh, Y.; Umino, M.; Tanaka, T.; Maki, T.; Onomura, O. *Org. Lett.* **2000**, *2*, 1689–1691.
47. (a) Furusho, Y.; Kimura, T.; Mizuno, Y.; Aida, T. *J. Am. Chem. Soc.* **1997**, *119*, 5267–5268. (b) Mizuno, Y.; Aida, T.; Yamaguchi, K. *J. Am. Chem. Soc.* **2000**, *122*, 5278–5285.
48. Yashima, E.; Maeda, K.; Okamoto, Y. *Nature* **1999**, *399*, 449–451.

Chapter 4

Chiral Discrimination during Crystallization

KAZUSHI KINBARA AND KAZUHIKO SAIGO

Department of Chemistry and Biotechnology, School of Engineering, The University of Tokyo, 7-3-1, Hongo, Bunkyo-ku, Tokyo, 113-8656, Japan

I. INTRODUCTION

A. Chiral Discrimination Phenomena during Crystallization

Chiral discrimination during the crystallization of chiral compounds was discovered by Pasteur in the mid nineteenth century. He reported two kinds of chiral

Topics in Stereochemistry, Volume 23, Edited by Scott E. Denmark.
ISBN 0-471-17622-2

discrimination phenomena individually.[1,2] One is called spontaneous resolution whereby (+)- and (−)-enantiomers of a racemate crystallize independently to afford a mechanical mixture of enantiomeric crystals.[1] The other is called diastereomeric resolution whereby a mixture of a pair of diastereomers derived from a racemate and an enantiopure compound (called a resolving agent) is separated simply by crystallization. In a successful case, one of the enantiomers of a racemate selectively forms a diastereomer with a resolving agent and the diastereomer preferentially crystallizes out from a solution, while the other enantiomer remains in the solution.[2,3] After removal of the resolving agent from the precipitated crystals, the target enantiomer can be isolated in an enantiopure form. The diastereomeric resolution is most frequently applied to the separation of various racemates in laboratorial and industrial scales even at present.[4–6]

Although the basic principle and procedure of diastereomeric resolution are not difficult to understand, the chiral discrimination mechanism involved in the selective crystallization of one diastereomer from the mixture is very complicated. The chiral discrimination mechanism for diastereomeric resolution changes in accord with the resolving system, since not only the properties of diastereomeric crystals but also the conditions for crystallization strongly influence the chiral discrimination mechanism. In particular, the polymorphism of crystal, the severe solvent effect on solubility, and the kinetic factor for crystal growth are still not perfectly understood regarding this chiral discrimination phenomenon. The study is therefore limited in its investigation of the chiral discrimination mechanism for the diastereomeric resolution, as the mechanism involves both the crystal and solution properties of diastereomers.[7]

For convenience, a phase diagram of a pair of diastereomeric crystals is ordinarily studied in detail, and the mechanism of the diastereomeric resolution is interpreted in terms of the thermodynamic and physical properties of the bulk of the diastereomeric crystals.[4,7–10] Such studies reveal the importance for diastereomeric resolution of the type of mixture of diastereomers in a target system. There are three types of diastereomer mixtures: an eutectic mixture, a 1 : 1 addition compound, and a solid solution. To achieve successful resolution, it is essential that the mixture of the diastereomeric crystals of a target racemate with a resolving agent be an eutectic mixture. The classic studies are thoroughly reviewed by Collet and co-workers.[4,12]

When a diastereomeric mixture is an eutectic mixture, the difference in solubility between the diastereomers can be roughly correlated to the difference in thermodynamic stability between them if the conditions for crystallization, such as temperature and solvent, are unchanged. Then it becomes meaningful to estimate the stabilities of a pair of diastereomeric crystals and to observe the correlation between the difference of the stability of the pair of diastereomeric crystals and the efficiency of the chiral discrimination.

Knowledge about intermolecular interactions that play a large role in the stabilization of a crystal, along with the development of crystallographic techniques, is being continuously accumulated.[13,14] At the same time the number of solved crystal structures of diastereomeric crystals is rapidly increasing. These solutions afford us valuable information on how molecules interact in a crystal so as to stabilize their packing and what kind of interaction is effective for the discrimination of a pair of enantiomers in the crystalline state. In some systems use of the same resolving agent has produced some common patterns of intermolecular networks. This kind of information helps us to see how systematically the functional group(s) of a racemate and that of a resolving agent, involved in diastereomers, interact and how their interaction works in the discrimination of a pair of the enantiomers of the racemate by the resolving agent. Thus we can expect such studies to lead to some practical criterion for the selection and molecular design of a resolving agent suitable for a target racemate.

In the next section we describe some successful designs of resolving agents that were developed in studies of diastereomeric resolution using crystallographic analyses. In later sections we will consider the common characteristics observed in the crystal structures of the diastereomeric salts of chiral compounds with conventional resolving agents. We will especially focus on the characteristic interactions and supramolecular systems formed between the enantiomers and the resolving agents in these crystals.

II. MOLECULAR DESIGN OF NOVEL NONNATURAL RESOLVING AGENTS IN DIASTEREOMERIC RESOLUTION

Research up to the present time has reported on the phenomenon that one resolving agent can usually resolve a series of structurally related compounds. For example, ephedrine has been shown to be effective for the resolution of mandelic acid derivatives.[15] Likewise 1-phenylethylamine can effectively resolve a series of 2-arylalkanoic acids.[16] However, the correlation between the efficiency of the resolutions and the molecular and/or crystal structures of the resulting diastereomeric salts has not been studied until quite recently, although such a study would be valuable for understanding the chiral discrimination mechanism of the diastereomeric resolution and for designing a novel resolving agent. Our objective is to draw attention to this present situation and to demonstrate the importance of a systematic study on the diastereomeric resolution for the design of a novel resolving agent. This section is devoted to examples of such systematic studies and their application to the design of more effective resolving agents.

A. Design of Acidic Resolving Agents

1. Systematic Study on the Diastereomeric Resolution by Mandelic Acid

Mandelic acid (**1**), which consists of a carboxyl group, a hydroxy group, and a phenyl group on a carbon atom, is one of the most popular resolving agents. Because of its simple structure and the easy availability of both enantiomers, there is much literature on the resolutions of chiral amines with enantiomerically pure **1**, and the chiral discrimination mechanism for the resolutions has been the subject of some study. For example, Zingg and co-workers produced detailed studies of the complexation energy, enthalpy, and entropy, and the crystal structures of ephedrinium and pseudoephedrinium salts of **1**.[6] In addition there are some studies on the crystal structures of a pair of less and more soluble diastereomeric salts and on the difference in stability between the diastereomeric salts.[17,18] These studies suggest the importance of hydrogen-bond interaction in the chiral discrimination. However, no comprehensive study on the diastereomeric resolution of systematically selected racemates by **1** has been carried out.

For these reasons our group performed the resolution of 1-arylethylamines, which are a series of simple chiral amines, by enantiomerically pure **1**[19] and determined the crystal structures of the resulting diastereomeric salts in order to clarify whether there is a correlation between the efficiency of the diastereomeric resolution by **1** and the crystal and/or molecular structure of the diastereomeric salts.[19,20] We found that the efficiency of resolution (tentatively defined as yield $\times$ *ee*) in the diastereomeric resolution of 1-arylethylamines by **1** is strongly affected by the substituent on the aromatic group of the amines; **1** shows a high-resolution ability for the non- and *o*-substituted amines while a low-resolution ability for the *p*-substituted amines (Table 4.1). This result indicates that the efficiency of resolution in this series of diastereomeric resolutions depends on the relative molecular length of the amines to **1**, namely **1** shows a high-resolution ability for the amines having a molecular length similar to that of **1** and a low-resolution ability for the amines having a molecular length longer than that of **1** (Figure 4.1).

The crystal structures of the diastereomeric salts of **1** with 1-arylethylamines revealed that a quite characteristic hydrogen-bond network is often formed in the less soluble diastereomeric salts when high efficiency of resolution is achieved; all of the less soluble salts are commonly stabilized by two kinds of interactions, hydrogen-bonding and van der Waals interactions. The typical hydrogen-bond network formed in the less soluble salts is shown in Figure 4.2*a*. The carboxylate and ammonium moieties form a columnar hydrogen-bond network stabilized by strong hydrogen bonds (2_1-column)

Table 4.1
Resolution of 1-Arylethylamines by Enantiopure **1**[a]

Entry	Amine (R)	Yield[b]	*ee*
1	H	76	87
2	*o*-Me	71	100
3	*o*-OMe	69	81
4	*m*-Me	94	12
5	*m*-OMe	70	89
6	*p*-Me	88	4
7	*p*-OMe	84	4

[a] Solvent: Aqueous alcohol or H_2O.
[b] Yield of the deposited salt by the first crystallization on the basis of a half amount of the racemate.

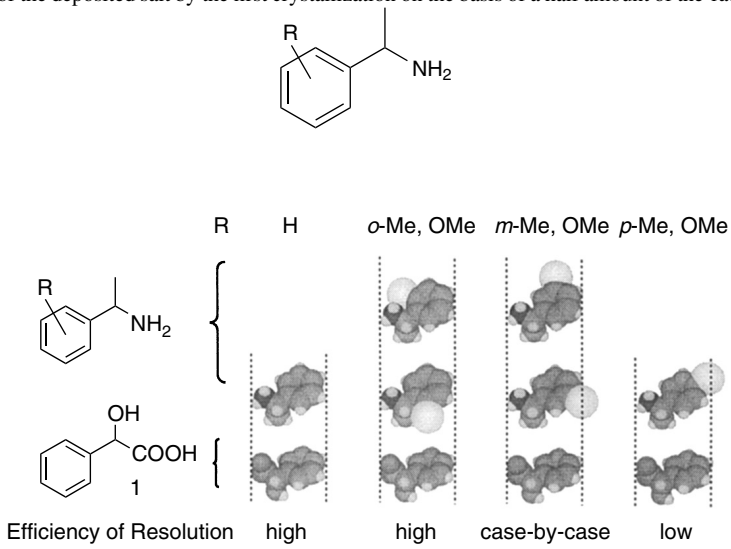

Figure 4.1. Schematic representations of the correlation between the result of resolution and the relative molecular length of the racemic amines and **1**.

whose pattern is almost the same as that commonly found in the crystals of primary ammonium carboxylates.[21] The hydroxy groups of (**1**-H)$^-$ molecules link the columns by other hydrogen bonds, resulting in the formation of a quite tightly hydrogen-bonded supramolecular sheet. Furthermore the hydrophobic surfaces of the supramolecular hydrogen-bond sheet are planar (Figure 4.2*b*), and are favorable for the close packing of these supramolecular sheets. Thus the less soluble salts in success are stable with regard to hydrogen-bonding and van der Waals interactions.

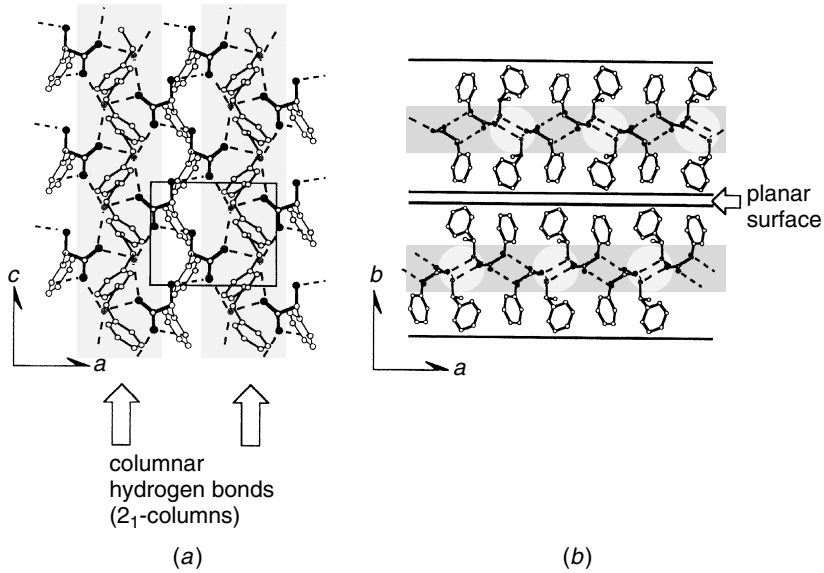

Figure 4.2. Crystal structure of less soluble (*R*)-**1**•(*R*)-1-phenylethylamine. (*a*) Hydrogen-bond sheet viewed down the *b* axis. (*b*) Edge-on view of the hydrogen-bond sheets and their packing.

On the other hand, such a stable crystal structure is not realized in the corresponding more soluble diastereomeric salts; in some cases the substituent in the aromatic group of the amines projects out from the surface of the supramolecular sheet to disturb the close packing of the sheets (Figure 4.3*b*), although the same stable pattern of hydrogen-bond network as that formed in the less soluble salts is attained (Figure 4.3*a*). In other cases, the hydrogen-bonding interaction in the more soluble salts is apparently less stable than the less soluble salts (Figure 4.4*a*), although the close packing of the supramolecular sheets is achieved (Figure 4.4*b*). These facts indicate that the more soluble salts are stabilized only by hydrogen-bonding or van der Waals interaction.

Thus we suggest that there are two factors for the stabilization of the diastereomeric crystals of the present system, hydrogen-bonding and van der Waals interactions. The difference in crystal stability between the less and more soluble diastereomeric salts, which are successfully separated upon crystallization, arises from the difference in magnitude of the interactions between them (Figure 4.5). Namely the crystals of the less soluble diastereomeric salts are stabilized by the two factors, while the crystals of the more soluble diastereomeric salts are stabilized by only one of the two factors.

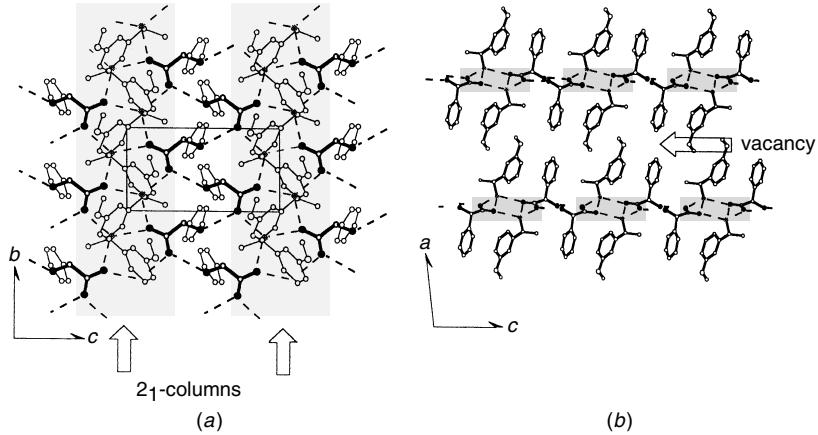

Figure 4.3. Crystal structure of more soluble (*R*)-**1**•(*S*)-1-(*m*-methoxyphenyl)ethylamine. (*a*) Hydrogen-bond sheet viewed down the *a*-axis. (*b*) Edge-on view of the hydrogen-bond sheets and their packing.

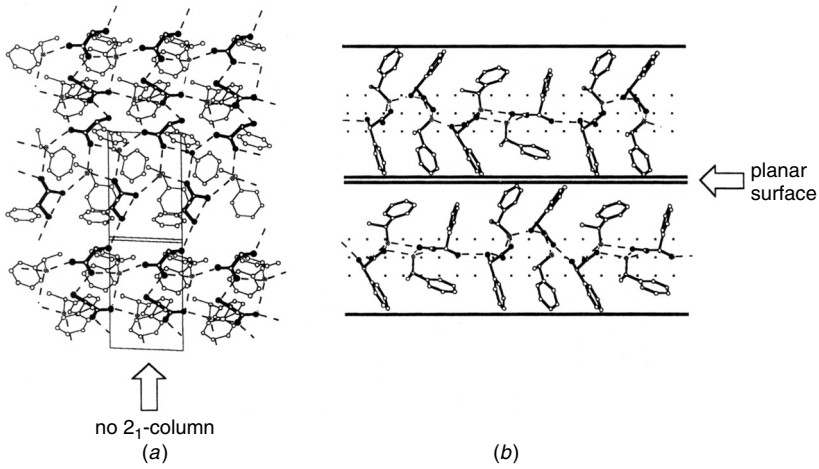

Figure 4.4. Crystal structure of more soluble (*R*)-**1**•(*S*)-1-phenylethylamine. (*a*) Hydrogen-bond sheet. (*b*) Edge-on view of the hydrogen-bond sheets and their packing.

The authors' group also determined the crystal structures of a pair of diastereomeric salts of **1** with 1-*p*-tolylethylamine (**2**), which could not be efficiently resolved by **1**. We found that both diastereomeric crystals ((*R*)-**1**•(*R*)-**2** and (*R*)-**1**•(*S*)-**2**) do not satisfy the two factors that are found in the

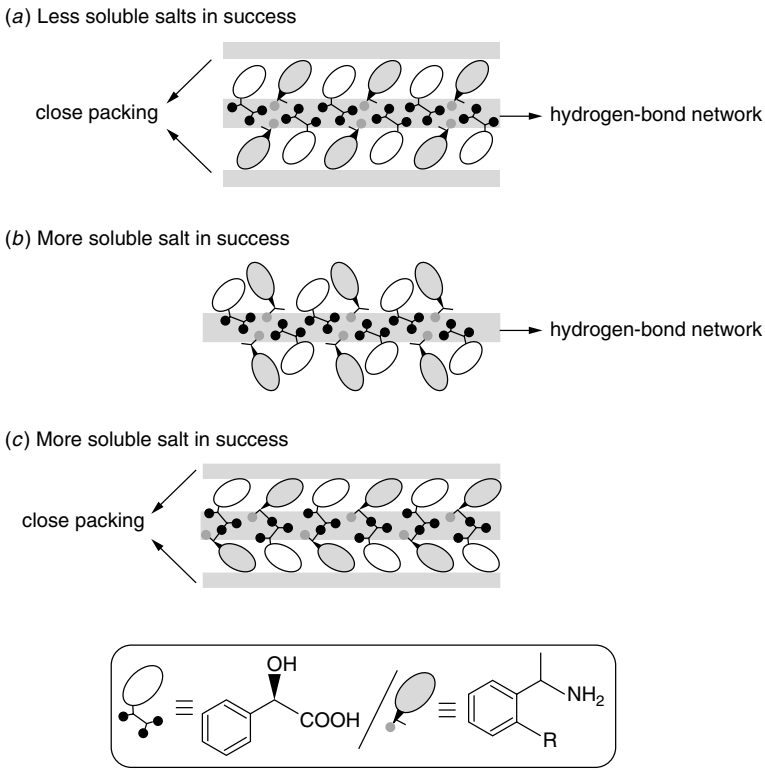

Figure 4.5. Schematic representations of the crystal structures of the less and more soluble salts of enantiopure **1** with 1-arylethylamines in success. (*a*) Less soluble salts, which are stable from the viewpoint of hydrogen-bonding and van der Waals interactions. (*b*) More soluble (*R*)-**1**•(*S*)-1-(*m*-methoxyphenyl)ethylamine, in which a stable hydrogen-bond sheet is formed while the close packing of the sheets is not achieved. (*c*) More soluble (*R*)-**1**•(*S*)-1-phenylethylamine, in which a stable hydrogen-bond sheet is not formed while the close packing of the sheets is achieved.

less soluble diastereomeric salts (Figure 4.5*a*); in the case of (*R*)-**1**•(*R*)-**2**, hydrogen-bonding interaction is less stable than that in the less soluble salts, although the close packing of the sheets is achieved (Figure 4.6*a*). On the other hand, in the case of (*R*)-**1**•(*S*)-**2**, a stable pattern of the hydrogen-bond network is attained, although the substituent on the aromatic group of **2** projects out from the surface of the supramolecular sheet to disturb the close packing of the sheets (Figure 4.6*b*). Thus each crystal is considered to be stable only in terms of hydrogen-bonding or van der Waals interaction just like the crystals of the more soluble diastereomeric salts. The unstable structures are caused by the *p*-methyl substituent in the aromatic group of the amine. The *p*-substituent

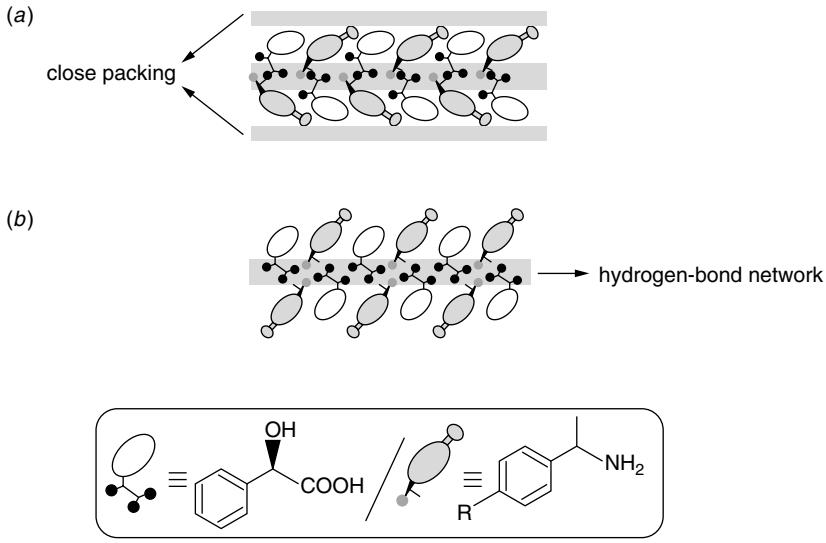

Figure 4.6. Schematic representations of the crystal structures of the salt of enantiomerically pure **1** with **2**. (*a*) (*R*)-**1**•(*R*)-**2**, in which a stable hydrogen-bond sheet is not formed while the close packing of the sheets is achieved. (*b*) (*R*)-**1**•(*S*)-**2**, in which a stable hydrogen-bond sheet is formed while the close packing of the sheets is not achieved.

in the aromatic group of **2** makes the surfaces of the supramolecular sheet irregular, which disturbs the close packing of these sheets as observed in (*R*)-**1**•(*S*)-**2**. This can lead to the formation of a less stable hydrogen-bond network as observed in (*R*)-**1**•(*R*)-**2** in order to regain the close packing of the sheets. The occurrence of this phenomenon would be possible in the case of an amine whose molecular length is longer than that of **1**.

The observations above indicate that the correlation between the relative molecular length of a racemate/resolving agent and the efficiency of resolution in an optical resolution can be elucidated by crystal structural analyses of the diastereomeric salts. It is noteworthy that a failure is possible due not only to little or no difference in solubility between a pair of the diastereomeric salts of a racemate and a resolving agent but also due to the formation of a double salt consisting of both enantiomers of a racemate and a resolving agent, as in the combination of **1** and **2**.[22]

2. *p-Methoxymandelic Acid and 2-Naphthylglycolic Acid: Tailor-Made Resolving Agents for 1-Arylethylamines*

The results described in the preceding section indicate that the size-match of a resolving agent and a target racemate is important to achieve high efficiency of

resolution. On the basis of this observation, the authors and their co-workers attempted the design of resolving agents for *p*-substituted 1-arylethylamines, which could not be efficiently resolved by **1**. They assumed that the realization of a stable crystal structure, found commonly in the above-mentioned less soluble diastereomeric salts, is essential for achieving high efficiency of resolution, and that the complementarity in molecular length between a target racemate and a resolving agent is important for this realization. Thus *p*-methyl and *p*-methoxymandelic acids (**3** and **4**) were designed with the expectation that the *p*-substituent on the aromatic group of **3** or **4** would make the surface of a supramolecular sheet planar in the diastereomeric salt with one of the enantiomers of **2**, as is found in the less soluble salts of **1** (Figure 4.7*a*), and that the efficiency of resolution would subsequently be improved by using such resolving agents. Actually the designed **3** and **4** show a much higher resolving ability than **1** for *p*-substituted 1-arylethylamines (Table 4.2). In addition the crystallographic analysis of less soluble (*R*)-**4**•(*R*)-**2** revealed that its structure is quite similar to that (Figure 4.2) found in the less soluble salts of **1**.

This success prompted the authors' group to further design a novel resolving agent that could be applied even in practical use, for *p*-substituted

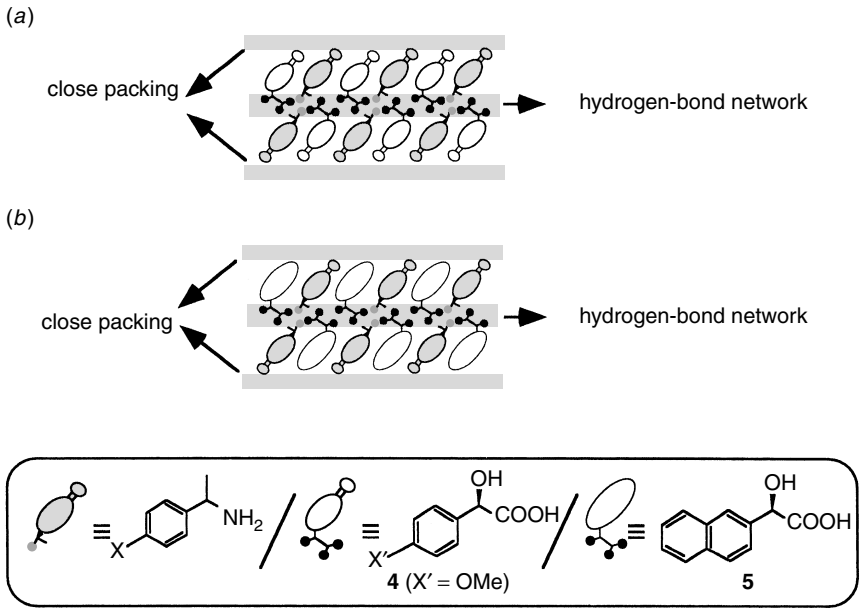

Figure 4.7. Schematic representations of the hypothetical crystal structures of the salts of enantiomerically pure **4** and **5** with **2**. (*a*) Less soluble **4●2.** (*b*) Less soluble **5●2**.

Table 4.2
Resolution of 1-Arylethylamines by Enantiopure **3** and **4**[a]

Entry	Resolving Agent	Amine(R)	Yield[b]	*ee*
1	**3**	H	74	80
2	**4**	H	70	89
3	**3**	*p*-Me	85	63
4	**4**	*p*-Me	72	85
5	**4**	*p*-OMe	62	46

[a] Solvent: Aqueous alcohol or H_2O.
[b] Yield of the deposited salt by the first crystallization on the basis of a half amount of the racemate.

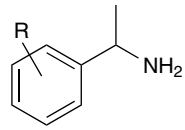

1-arylethylamines. The authors' group designed 2-naphthylglycolic acid (**5**) with expectations not only that **5** has complementary molecular length with the target amines, but also that the naphthyl group of **5** would fill the spaces at the hydrophobic region of a supramolecular sheet (Figure 4.7*b*).[23]

Indeed, **5** has an excellent resolution ability for *p*-substituted 1-arylethylamines (Table 4.3). The efficiency of resolution is sufficiently high in almost of all cases. Furthermore, **5** shows high-resolution ability not only for amines having complementary molecular length with **5** (Table 4.3, entries 2–7) but also for amines with shorter or longer molecular length than that of **5** (Table 4.3, entries 1 and 8).

X-ray crystallographic analyses of the less and more soluble diastereomeric salts of 1-arylethylamines with **5** revealed that a characteristic hydrogen-bond sheet, which is similar to that observed in the less-soluble diastereomeric salts of **1**, **3**, and **4**, is also formed in these crystals (Figure 4.8). In the cases of the amines that have similar molecular length to that of **5**, the surfaces of the supramolecular sheet are planar to achieve the close packing of these sheets. In addition an infinite chain of CH•••π interaction is formed by the naphthyl group and the aromatic group of the amines in the hydrophobic region, which stabilizes the less soluble salts to a considerable extent. Thus, in these cases, the less soluble salts are stabilized by three kinds of interactions, such as hydrogen-bonding, CH•••π, and van der Waals interactions (Figure 4.9*a*). On the other hand, in the more soluble salts, of which the crystal structures are solved so far, a supramolecular hydrogen-bond sheet, having a similar hydrogen-bonding pattern to that of the less soluble salt and

Table 4.3
Resolution of 1-Arylethylamines by Enantiopure **5**[a]

Entry	Amine (R)	Yield[b]	*ee*
1	H	61	96
2	*p*-Me	81	95
3	*p*-OMe	58	87
4	*p*-Cl	77	98
5	*p*-Br	81	93
6	*p*-NO_2	80	70
7	*p*-1-Naphthyl	77	96
8	*p*-Cyclohexyl	50	91

[a] Solvent: Aqueous alcohol or H_2O.
[b] Yield of the deposited salt by the first crystallization on the basis of a half amount of the racemate.

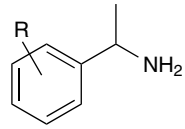

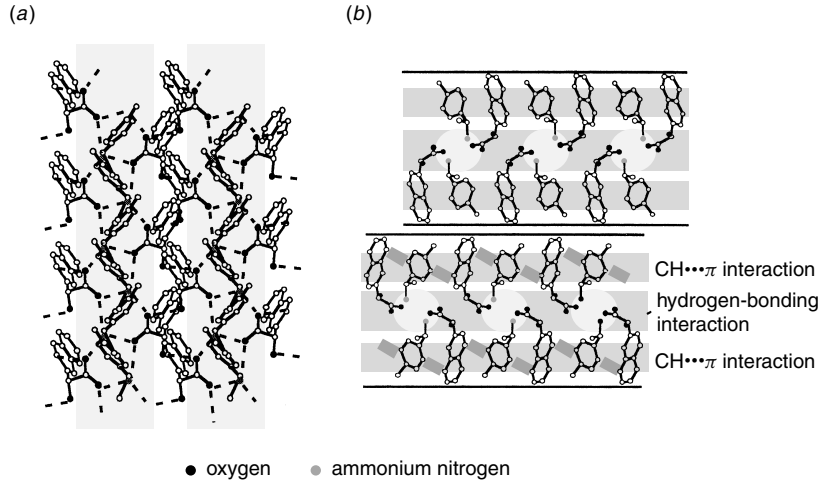

Figure 4.8. Crystal structure of less soluble (*R*)-**5**•(*R*)-**2**. (*a*) Hydrogen-bond sheet. (*b*) Edge-on view of the hydrogen-bond sheets and their packing.

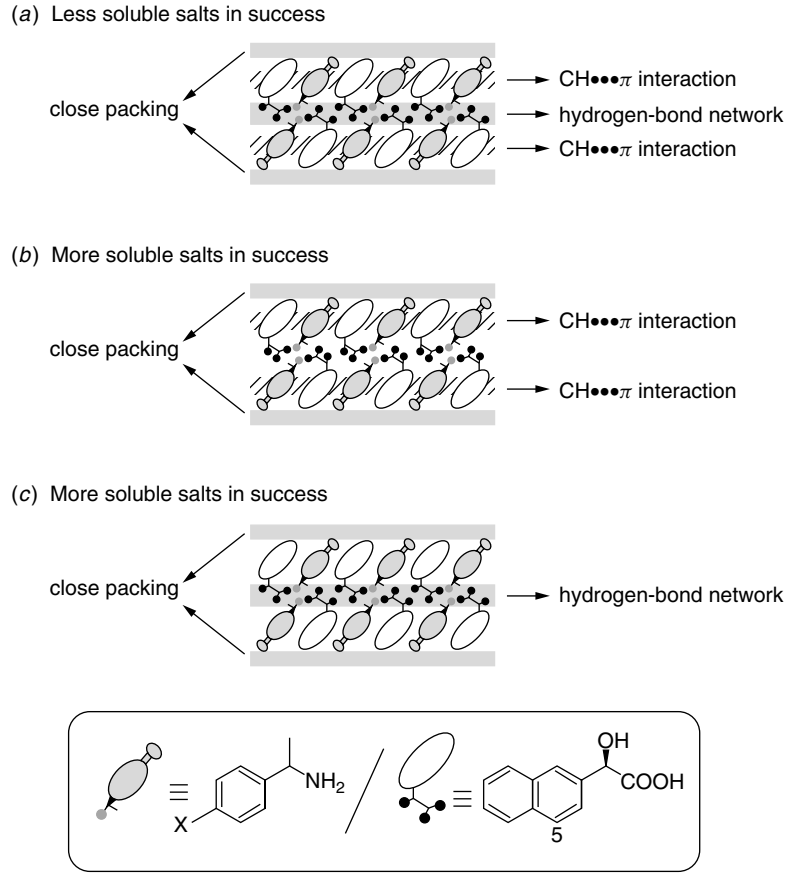

Figure 4.9. Schematic representations of the crystal structures of the salts of enantiopure **5** with *p*-substituted 1-arylethylamines in success. (*a*) Less soluble salts, in which the formation of a stable supramolecular hydrogen-bond sheet, the realization of efficient CH•••π interaction, and the close packing of the sheets are achieved. (*b*) More soluble salts, in which efficient CH•••π interaction is not realized and the close packing of the supramolecular sheets a stable supramolecular hydrogen-bond sheet is not formed. (*c*) More soluble salts, in which a stable supramolecular hydrogen-bond sheet is formed and the close packing of the supramolecular sheets is achieved, while efficient CH•••π interaction is not realized.

having planar surfaces, is also commonly formed (Figure 4.10). However, the difference in stereochemistry of the ammonium part reflects the direction of the aromatic group of the ammonium part or that of the hydroxy group of **5** in the supramolecular sheet to significantly weaken the CH•••π or hydrogen-bonding interaction, respectively. Thus, in this system, the difference in stability between the less and more soluble diastereomeric salts

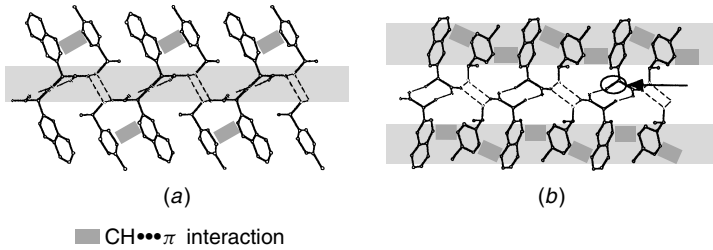

Figure 4.10. Edge-on views of the hydrogen-bond sheets in (*a*) more soluble (*R*)-**5**•(*S*)-**2** and (*b*) more soluble (*R*)-**5**•(*S*)-1-(*p*-chlorophenyl)ethylamine.

comes from the difference in magnitude of the hydrogen-bonding and CH•••π interactions.

In the case of 1-(*p*-cyclohexylphenyl)ethylamine (entry 8), its molecular length should obviously be longer than that of **5**; the planar surfaces of a supramolecular hydrogen-bond sheet would be no longer realized. Therefore the successful result of the resolution of 1-(*p*-cyclohexylphenyl)ethylamine by enantiopure **5** would indicate that van der Waals interaction, which is correlated with the close packing of supramolecular sheets, is less important than the other two interactions. This idea is also supported by the result of the resolution of 1-phenylethylamine (**6**), of which the molecular length is obviously shorter than that of **5**, and by the crystal structure of the corresponding less soluble diastereomeric salt. Thus the excellent resolution ability of **5** arises from the stabilization of the less soluble diastereomeric crystals by the formation of a stable supramolecular hydrogen-bond sheet, which is reinforced by the formation of an infinite chain of CH•••π interaction between the naphthyl group of **5** and the aromatic group of the target amines in the hydrophobic region of the supramolecular hydrogen-bond sheet (Figure 4.9).

Noteworthy is that throughout the present studies, special care has been paid in controlling the conditions of crystallization as close as possible, since it is well known that the polymorphism of crystal sometimes makes the explanation for the chiral discrimination during crystallization complicated. The combination of **1** and **6** is one of the typical examples, which demonstrates the complexity of polymorphism. For (*R*)-**1**•(*R*)-**6**, two polymorphic crystals, belonging to space groups of $P2_1$ and $P2_12_12_1$, are reported.[24,25] Each crystal can be prepared by controlling the solvent for recrystallization. On the other hand, only one crystal structure of more soluble (*R*)-**1**•(*S*)-**6** is reported.[26] Usually, when a mixture of enantiomerically pure **1** and racemic **6** is crystallized, a mixture of diastereomeric salts (*R*)-**1**•(*R*)-**6** and (*R*)-**1**•(*S*)-**6** precipitates. However, under special conditions, a double salt, in which both (*R*)-**6** and (*S*)-**6** are included in a unit cell, can precipitate from a mixture of enantiomerically pure **1** and racemic **6**.[27] In addition, when the ratio of **6** to **1** changes, a 1 : 3

crystal of **6** and **1** can be prepared.[28] Thus important factors for polymorphism are solvent, temperature, and stoichiometry of a resolving agent to a racemate. At least these conditions must be tuned for a systematic study on the diastereomeric resolution in order to compare the results with each other.

B. Design of Basic Resolving Agents

1. Systematic Study on the Diastereomeric Resolution of 2-Arylalkanoic Acids by 2-Amino-1,2-diphenylethanol

As is described in the previous sections, in the cases of the resolutions of 1-arylethylamines by enantiopure arylglycolic acids, the hydroxy group of the resolving agents plays a significant role in the discrimination of the enantiomers of the racemates; the hydroxy group forms a hydrogen bond between hydrogen-bonded 2_1-columns so as to form a supramolecular hydrogen-bonded sheet in the less soluble diastereomeric salts. From these results the authors expected that a similar system of chiral discrimination would be realized even in an opposite situation, that is, in the resolution of acidic racemates by a basic resolving agent.[29,30] Thus the resolutions of racemic acids by enantiopure amino alcohols were carried out with an expectation that the hydroxy group of the amino alcohols would interlink hydrogen-bonded columns, formed by the carboxylate oxygens of the target acids and the ammonium hydrogens of the amino alcohols by strong hydrogen bonds, so as to construct a hydrogen-bonded sheet and to efficiently stabilize the less soluble diastereomeric salt (Figure 4.11). As target racemates for the present systematic study, 2-arylalkanoic acids were selected, because they are a family of rather simple chiral acids and because some of them are valuable as pharmaceuticals. Moreover, as a resolving agent, enantiopure erythro-2-amino-1,2-diphenylethanol (**7**) was selected,[31] since **7** showed the highest resolution ability for 2-phenylpropionic acid as a result of the survey of various amino alcohols. Thus the resolution of a series of racemic 2-arylalkanoic acids was carried out by using enantiopure **7** as a resolving agent under conditions arranged for the experiments as close as possible to each other.

The results are summarized in Table 4.4. Enantiopure **7** has a moderate to excellent resolution ability for a variety of 2-arylalkanoic acids. In addition the efficiency of the resolutions strongly depends on the substituent on the aromatic group of the 2-arylalkanoic acids. There appears a weak correlation between the position of the substituent and the efficiency of resolution; the non- or *o*-substituted acids are resolved with high efficiency of resolution while the *p*-substituted acids are not resolved effectively.

The crystal structures of these less soluble diastereomeric salts revealed that there are some common characteristics. A typical crystal structure

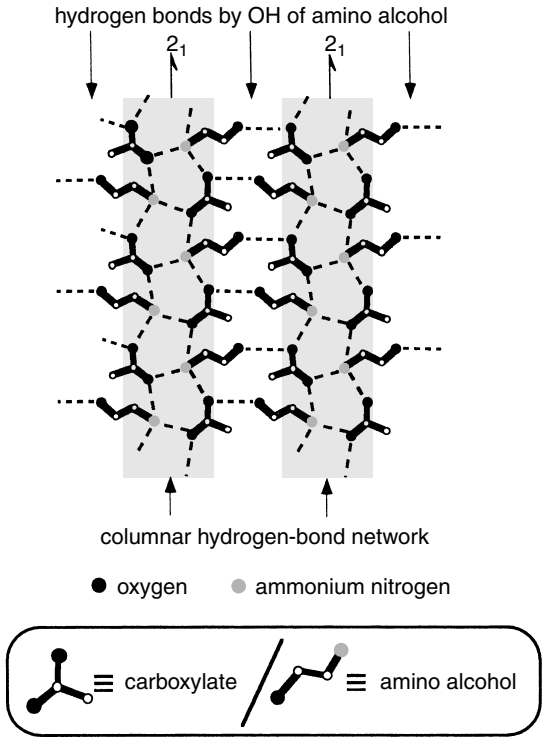

Figure 4.11. Schematic representation of a hypothetical hydrogen-bond network in the diastereomeric salts of enantiopure amino alcohols with carboxylic acids.

of the less soluble salts is shown in Figure 4.12. The first characteristic in these crystal structures is the existence of a columnar hydrogen-bond network formed by hydrogen bonds between the ammonium hydrogens and the carboxylate oxygens (Figure 4.13), whose pattern is the same as that found in the less soluble diastereomeric salts of enantiopure arylglycolic acids with 1-arylethylamines.[20,22] The second common characteristic is the incorporation of water molecules, which form hydrogen bonds with the hydroxy group of **7**•H^+ and the carboxylate oxygens. These hydrogen bonds do not form a supramolecular hydrogen-bond sheet, contrary to our expectation, but reinforce the columnar structure to a considerable extent to realize a strongly hydrogen-bonded supramolecular column. These tightly hydrogen-bonded water molecules are found in all of the less soluble salts. In connection with this phenomenon, noteworthy is the conformation of the **7**•H^+ molecule in the less soluble salts. In each case the conformation of the hydroxy and ammonium groups of **7**•H^+ is *gauche*, and this conformation enables **7**•H^+ to

Table 4.4
Resolution of 2-Arylalkanoic Acids by (1*R*, 2*S*)-**7**[a]

Entry	R^1	R^2	Yield (%)[a]	*ee* (%)
1	Me	H	89	77
2	Et	H	70	70
3	Pr	H	75	79
4	Pr^i	H	77	9
5	Me	*o*-Me	65	37
6	Me	*m*-Me	71	57
7	Me	*p*-Me	74	6
8	Et	*o*-Me	87	49
9	Et	*m*-Me	72	36
10	Et	*p*-Me	77	13

[a] Yield of the deposited salt by the first crystallization on the basis of a half amount of the racemate.

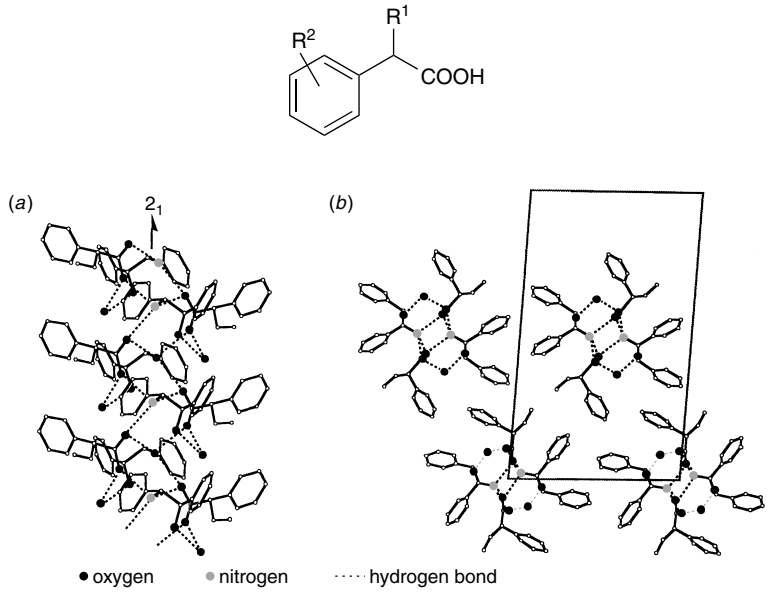

Figure 4.12. Crystal structure of less soluble (1*R*, 2*S*)-**7**•(*R*)-2-phenylpropanoic acid•H_2O. (*a*) Columnar hydrogen-bond network. (*b*) Viewed down the 2_1-axis of the hydrogen-bond column (*b*-axis). The solid square shows the unit cell.

form strong hydrogen bonds upon incorporating water molecules. The third common characteristic of the less soluble salts is the absence of any strong interaction between the hydrogen-bond columns, except for weak van der Waals interaction; it is in contrast to the fact that the columns are built up by

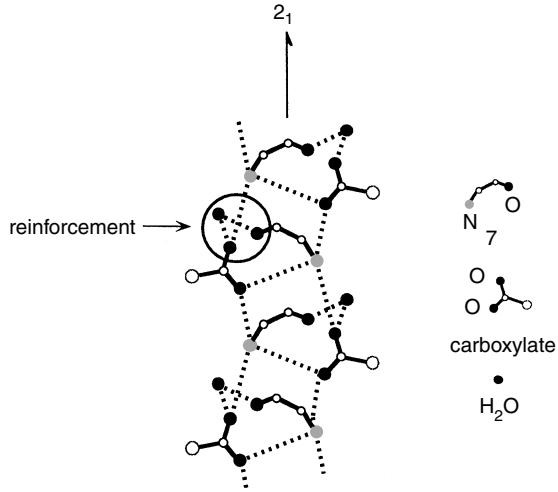

Figure 4.13. Schematic representation of the common pattern of the hydrogen-bond network in the less soluble salts of enantiopure **7** with 2-arylalkanoic acids in success.

strong hydrogen-bonding and electrostatic interactions. Thus the crystals can be regarded as assemblies of these supramolecular hydrogen-bond columns held together by van der Waals interactions.

In contrast to the less soluble diastereomeric salts, no water molecule is incorporated in a columnar hydrogen-bond network in the corresponding more-soluble salts (Figure 4.14). In addition the hydroxy group of **7**•H^+ forms no hydrogen bond in the more soluble salts. On the basis of these observations, the authors concluded that the incorporation of water molecules, which enhances the stability of a supramolecular hydrogen columns to a considerable extent, plays an important role in increasing the difference in stability between the less and more soluble salts and in achieving high efficiency of resolution.

On the other hand, the crystal structures of a pair of diastereomeric salts, which gave an unsatisfactory result on the resolution upon crystallization (Table 4.4, entry 10, and Figure 4.15), revealed that in this case no stable supramolecular column is formed in both less and more soluble diastereomeric salts. In one diastereomeric salt, no water molecule is incorporated in the column, although a columnar hydrogen-bond network is formed by the hydrogen bonds between the ammonium hydrogens and the carboxylate oxygens (Figure 4.15*a*). Instead of the incorporation of a water molecule, direct hydrogen-bonding of the hydroxy group of **7**•H^+ to the carboxylate oxygen so as to reinforce the columnar hydrogen-bond network is observed. However, the O···O distance in this crystal is much longer than those in less soluble

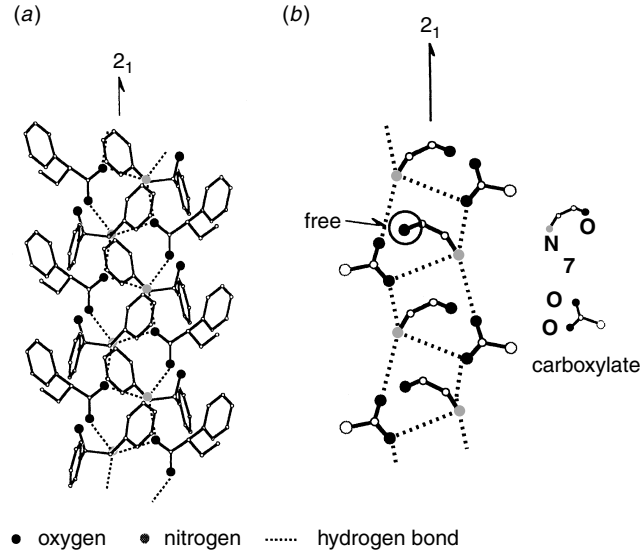

Figure 4.14. (*a*) Hydrogen-bond network of more soluble (1*R*, 2*S*)-**7**•(*S*)-2-phenylpropanoic acid and (*b*) its schematic representation.

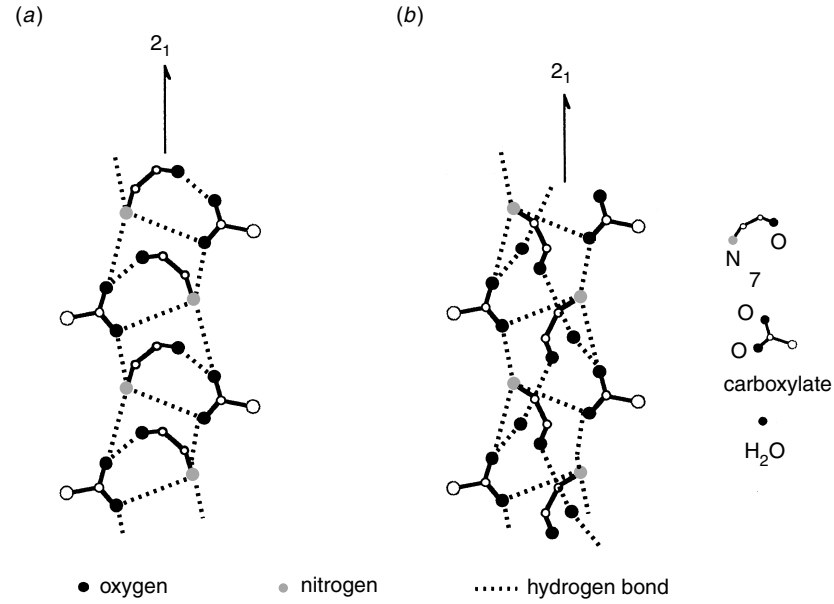

Figure 4.15. Schematic representation of the hydrogen-bond network of (*a*) (1*R*, 2*S*)-**7**•(*R*)-2-*p*-tolylpropionic acid and (*b*) (1*R*, 2*S*)-**7**•(*S*)-2-*p*-tolylpropionic acid•H_2O.

salts, meaning that the reinforcement by the hydrogen bond is not so sufficient. In addition the conformation of **7**•H^+ is less favorable than that in the less soluble salts. On the other hand, in the case of the other diastereomeric salt with low resolution efficiency, water molecules are incorporated, just as in the cases of less soluble salts (Figure 4.15*b*). However, the bond lengths of the hydrogen bonds involving the water molecules are longer than those in the less soluble salts, suggesting that the hydrogen-bonding interaction related to the water molecules is rather weak in the hydrogen-bond columns. The DSC-TG analysis showed that the diastereomeric salt with low resolution efficiency releases the water molecules at a much lower temperature than the less soluble salts with high resolution efficiency (difference is ca. 80°C); this result also supports the fact that the OH· · ·O hydrogen bonds are rather weak in this crystal.

Thus, in the cases of these diastereomeric salts which could not be efficiently separated by crystallization, the columnar hydrogen-bond network is not reinforced by additional hydrogen bonds formed by the hydroxy group as that in the less-soluble salts in success. This makes the difference in stability between the pair of diastereomeric salts small, resulting in low efficiency of resolution for this combination.

2. *Design of Basic Resolving Agents for 2-Arylalkanoic Acids*

As mentioned in the preceding section, in the resolution of 2-arylalkanoic acids by enantiomerically pure **7**, the formation of a columnar hydrogen-bond network, and the reinforcement of the resulting supramolecular column by hydrogen bonds with an assist of water molecules are essential in chiral discrimination. These results suggest that the increase of interactions in a columnar supramolecular hydrogen-bond network in less soluble diastereomeric salts would be effective in order to discriminate the enantiomers of racemic 2-arylalkanoic acids by an enantiopure amino alcohol with high efficiency. However, for the formation of a rigid columnar structure, the conformational flexibility of **7** would be unfavorable. Then the authors selected *cis*-1-amino-2-indanol (**8**) as a new resolving agent for 2-arylalkanoic acids on the basis of the following considerations: Amino alcohol **8** has a more rigid skeleton than does **7**, and the amino and hydroxy groups are in a fixed *cis*-conformation, which mimics the conformation of **7** in its less soluble diastereomeric salts with 2-arylalkanoic acids in success. These characteristics of **8** would be favorable for the formation and reinforcement of a rigid columnar hydrogen-bond network.

In Table 4.5 the results of the resolutions of 2-arylalkanoic acids by (1*S*,2*R*)-**8** are summarized. It is apparent from this table that **8** has high-resolution ability for a variety of racemic 2-arylalkanoic acids having a substituent on the

Table 4.5
Resolution of 2-Arylalkanoic Acids by (1*S*, 2*R*)-**8**[a]

Entry	R^1	R^2	Yield (%)[a]	*ee* (%)
1	Me	H	65	95
2	Et	H	48	78
3	Pr	H	80	44
4	Pr^i	H	67	59
5	Me	*o*-Me	85	24
6	Me	*m*-Me	59	91
7	Me	*p*-Me	32	61
8	Et	*p*-Me	83	67

[a] Yield of the deposited salt by the first crystallization on the basis of a half amount of the racemate.

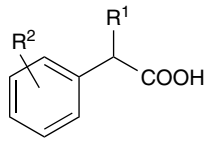

aromatic ring and/or at the α-position; the efficiency of resolution is dramatically improved by using **8** as a resolving agent, as we have expected.

The important point in these results is that the absolute configuration of the acid component in the less soluble diastereomeric salts changes depending on the bulkiness of the alkyl group at the α-position of 2-arylalkanoic acids; the (*R*)-form is predominantly obtained when the α-substituent is a methyl or ethyl group while the (*S*)-form is obtained when the α-substituent is a more bulky group.

The crystallographic analyses of the diastereomeric salts of 2-arylalkanoic acids with **8** revealed that a very similar columnar hydrogen-bond network is formed in the less soluble diastereomeric salts (Figures 4.16). In these less soluble diastereomeric crystals in success, the carboxylate oxygens, the ammonium hydrogens of **8**•$\mathbf{H}^+$, and the hydroxy group of **8**•$\mathbf{H}^+$ participate the formation of the columnar hydrogen-bond network, which is constructed around a 2_1-axis (Figures 4.17). This pattern of hydrogen bonds is different from that found in the salts of carboxylic acids with primary amines described in the previous sections. In the cases of the less soluble salts of **8**, the hydroxy group acts as both a hydrogen donor and a hydrogen acceptor, and deeply penetrates into the columnar structure so as to form a novel pattern of hydrogen-bond network.

In the hydrogen-bond column the smallest α-substituent of the carboxylate, the hydrogen, is commonly oriented parallel to the columnar axis, while the

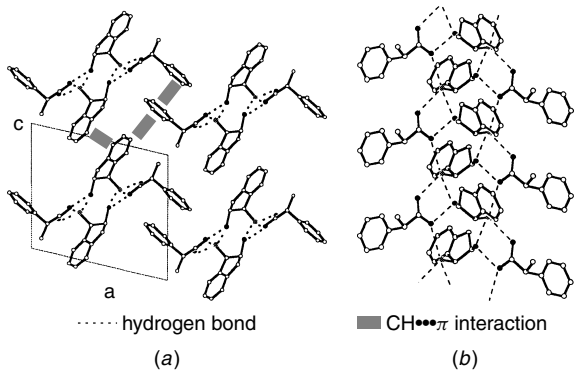

Figure 4.16. Crystal structure of less soluble (1*S*, 2*R*)-**8**•(*R*)-2-phenylpropanoic acid. (*a*) Viewed down the 2_1-axis of the hydrogen-bond column (*b*-axis). The solid square shows the unit cell. (*b*) Columnar hydrogen-bond network.

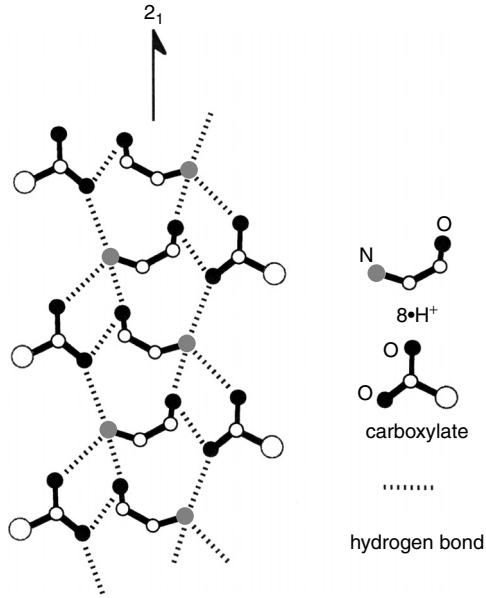

Figure 4.17. Schematic representation of the common pattern of the hydrogen-bond network in the less soluble salts of enantiopure **8** with 2-arylalkanoic acids in success.

other two substituents, the aryl and alkyl groups, are positioned vertical to the columnar axis. Moreover the largest aryl group is located apart from the aromatic group of **8●H**$^+$, while the medium alkyl group is close to **8●H**$^+$, when the acid part has a methyl or ethyl group as the α-alkyl group. However,

when the α-substituent becomes larger, the alkyl and aryl substituents in the hydrogen-bond column are replaced by each other in order to prevent serious steric repulsion in the crystals. This phenomenon would a major reason for the inversion of the absolute conformation of the 2-arylalkanoic acids incorporated in the less soluble diastereomeric salts.

In addition to the hydrogen-bonding interaction, there is an important interaction in the less soluble diastereomeric salt, namely a CH•••π interaction[32] between the aromatic groups, which results in the formation of stable herringbone packing.[33,34] This interaction works between the supramolecular columns to stabilize the assembly of the columns to build up a three-dimensional crystal (Figure 4.18).

Thus the crystallographic analyses of these less soluble diastereomeric salts revealed that the dominant interactions in the crystals are (1) the hydrogen-bonding interaction, which constructs a consistent columnar supramolecular hydrogen-bond network, and (2) the CH•••π interaction, which packs the columns tightly with each other. Thus the less soluble diastereomeric salts are efficiently stabilized by these two kinds of interactions.

On the other hand, in the more soluble diastereomeric salts, there is also a columnar supramolecular hydrogen-bond network formed by hydrogen bonds between the carboxylates and the ammoniums, of which the pattern is quite similar to that of the corresponding less soluble diastereomeric salts

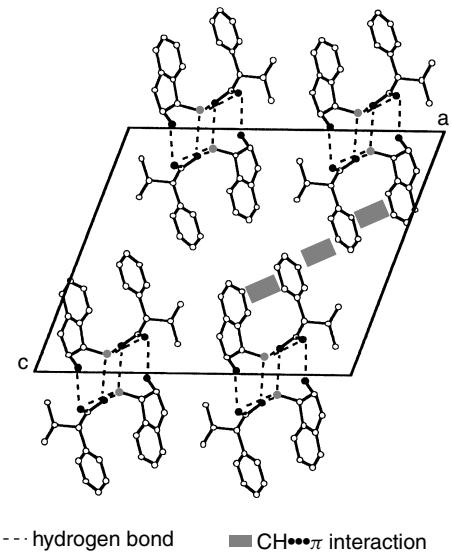

Figure 4.18. Crystal structure of less soluble (1*S*, 2*R*)-**8**•(*S*)-3-methyl-2-phenylbutyric acid viewed down the axis of the hydrogen-bond column.

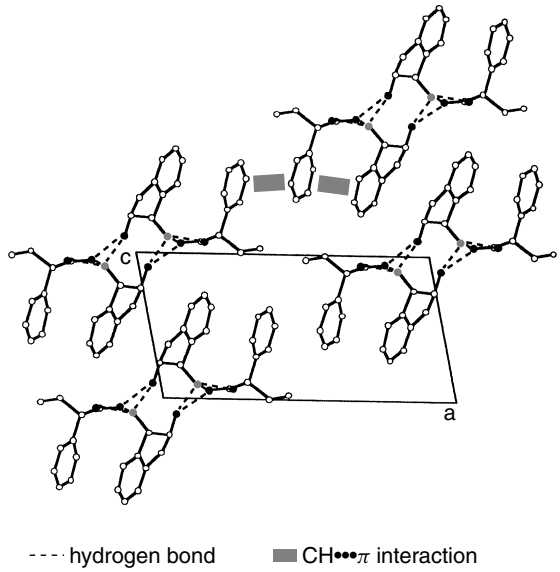

Figure 4.19. Crystal structure of more soluble (1*S*, 2*R*)-**8**•(*S*)-2-phenylpropanoic acid viewed down the axis of the hydrogen-bond column.

(Figure 4.19). However, the hydrogen-bond distance in the more soluble salts is longer than that in the less soluble salt; the IR study also revealed that the hydrogen-bonding interaction is weaker in the more soluble salts than in the less soluble salts. In addition, in the more-soluble salts the position of the aromatic and alkyl groups in the hydrogen-bond column is opposite to those in the less soluble salts. This different orientation of the aromatic group of 2-arylalkanoic acids in the columnar hydrogen-bond network decreases the number of effective herringbone packings. Although the stabilizing energy by CH•••π interaction is rather smaller than that of hydrogen-bonding interaction,[35–37] this difference should increase the difference in stability between the less and more soluble diastereomeric salts to some extent.

In order to understand the difference of the structures of columnar hydrogen-bond networks in the salts of **7** and those of **8**, it is valuable to discuss the geometrical relationship between the aromatic group(s) and the hydrogen-bond-forming groups in these amino alcohols. The most remarkable difference between the molecular structures of **7**•$\mathbf{H}^+$ and **8**•$\mathbf{H}^+$ is the orientation of the hydroxy group toward the aromatic ring at the α-position of the amino group (Figure 4.20). In the case of **7**•$\mathbf{H}^+$, the plane of the phenyl group at C2 is rather vertical to the single bond between C1 and C2, and the hydroxy group is *gauche* not only to this phenyl group but also to the ammonium group.

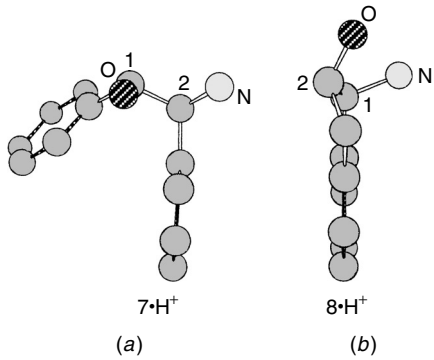

Figure 4.20. Molecular structures of (*a*) **7●H**$^+$ and (*b*) **8●H**$^+$ in the less soluble salts in success. The hydrogen atoms are omitted for clarity.

In contrast, in the case of **8●H**$^+$, the plane of the aromatic group is almost parallel to the single bond between C1 and C2, and the hydroxy group is *anti* to the aromatic group and exists almost on the same plane made by the aromatic group.

As is shown in Figure 4.21, in the hydrogen-bond column the relative position of the aromatic and ammonium groups is not so much different when the crystal structures of the salts of **7●H**$^+$ and those of **8●H**$^+$ are compared with each other. As a result the above-mentioned difference of the orientation of the hydroxy group in the molecular structures directly affects its position in the hydrogen-bond column. In the cases of the salts of **7●H**$^+$, the hydroxy group is placed apart from the hydrogen-bond column, and water molecule(s) is required in order to reinforce the columnar structure by hydrogen bonds. On the other hand, in the case of the salts of **8●H**$^+$, the hydroxy group is placed in a similar direction to that of the ammonium group toward the hydrogen-bond column, and this geometry allows the hydroxy group to penetrate deeply into

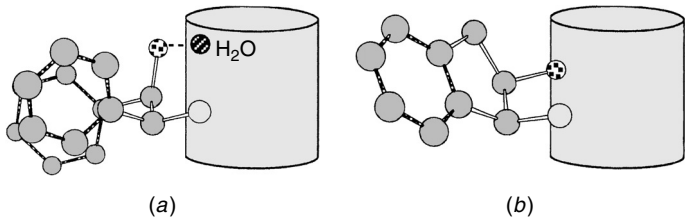

Figure 4.21. Schematic representations of the packing of (*a*) **7●H**$^+$ and (*b*) **8●H**$^+$ along the columnar axis. The hydrogen atoms are omitted. The cylinders represent a hydrogen-bond network formed by the carboxylate oxygens and the ammonium hydrogens.

the hydrogen-bond column. Thus the orientation of the hydroxy group of **8**, which is favorable for the direct hydrogen-bonding to the carboxylate oxygen in the hydrogen-bond column, results in an improved resolution ability of **8**, compared with that of **7**.

The resolving agents, **3**–**5** and **8**, are the first successful examples of tailor-made resolving agents on the basis of the structural studies on diastereomeric salt crystals. From these results it is suggested that for the design of suitable resolving agents for target racemates, it is important to increase as much as possible the number of interactions, such as hydrogen-bonding, CH•••π, and van der Waals interactions, for the stabilization of the less soluble diastereomeric salts. Under such conditions it would become possible to decrease the number of the interactions and/or weaken the interactions in the corresponding more soluble diastereomeric salts due to the difference in stereochemistry. These situations make the difference in stability between the less and more soluble diastereomeric salts larger so as to achieve high efficiency of resolution.

III. CHIRAL DISCRIMINATION OF RACEMATES BY CONVENTIONAL RESOLVING AGENTS

As is described in the previous sections, the studies on the resolution of systematically selected racemates by resolving agents and the extraction of the characteristics of the crystal structures of the resulting diastereomeric salts give us various valuable informations for understanding the chiral discrimination mechanism of the diastereomeric resolution and for designing resolving agents for target racemates. In this section common characteristics in the crystal structures of the diastereomeric salts of racemates with conventional resolving agents are reviewed. Special attention is given to the characteristic interactions and supramolecular systems formed between the enantiomers of the racemates and the resolving agents in the diastereomeric crystals.

A. Resolving Agents Used in Diastereomeric Resolution

Neutral resolving agents are not as popular as acidic and basic resolving agents, since it is generally difficult to prepare a co-crystal from a pair of neutral compounds. This fact has constrained wide use of neutral resolving agents, and special care must be taken in order to overcome this problem. Among neutral resolving agents, the most successful compounds are enantiopure alcohols shown in Figure 4.22, which were developed by Toda and co-workers. These enantiomerically pure host compounds can form various complexes with chiral guests, such as alcohols,[38,39] amides,[40,41] amines,[42,43] ketones,[44,45] phosphinates,[46] and sulfoxides,[47,48–51] through the formation of hydrogen

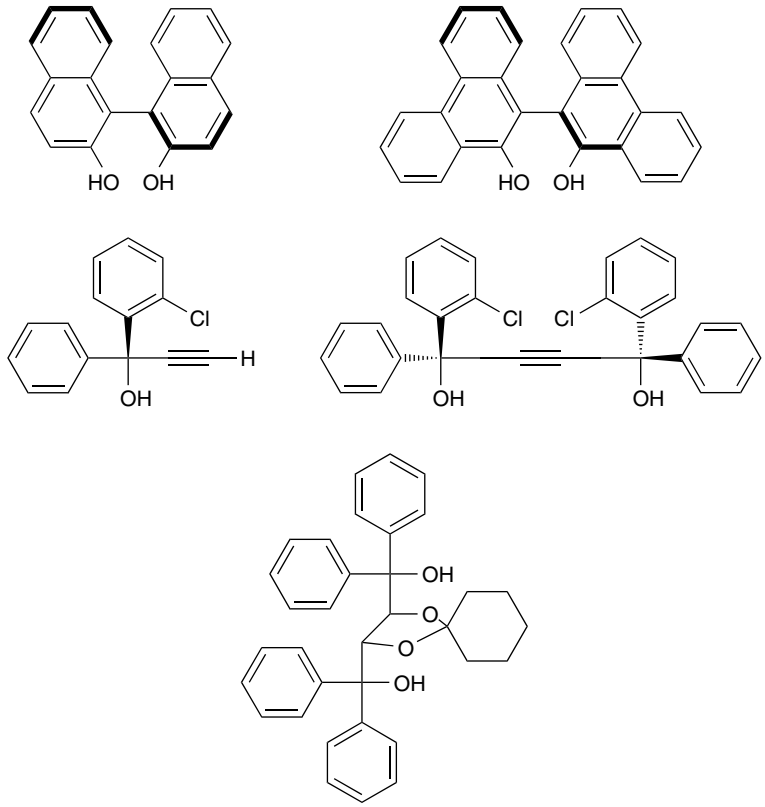

Figure 4.22. Structures of enantiopure neutral hosts.

bonds between the hydroxy group(s) of the hosts and hydrogen acceptor(s) of the guests to achieve excellent efficiency of resolution in some cases.

Thus the diastereomeric resolution is commonly carried out for acidic racemates by using basic resolving agents, and vice versa, since organic acids and bases easily form highly crystallizable salts in many cases. Figure 4.23 shows conventional acidic and basic resolving agents: mandelic acid (**1**), tartaric acid (**9**), dibenzoyl and ditoluoyltartaric acid (**10a–b**), camphorsulfonic acid (**11**), *N*-acylated amino acids (**12**), 1-phenylethylamine (**6**), brucine (**13a**), strychnine (**13b**), quinine (**14a**), cinchonidine (**14b**), quinidine (**15a**), cinchonine (**15b**), and amino acid esters (**16**). Many of them are naturally occurring compounds or their derivatives. This situation brings about serious problems in the usage of such compounds. For example, some of the basic resolving agents (**13–15**) are highly toxic, although they have a high resolution ability for a variety of racemates. Moreover only one enantiomer is usually available

Acidic Resolving Agents

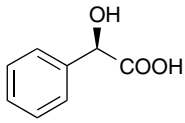

1

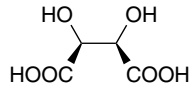

9

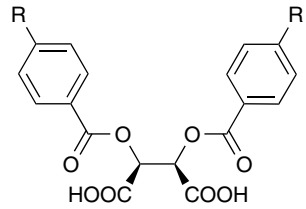

10a: R = H
10b: R = Me

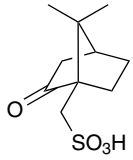

11

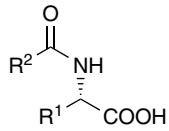

12

Basic Resolving Agents

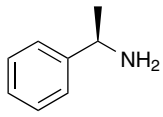

6

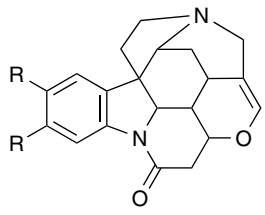

13a: R = OMe
13b: R = H

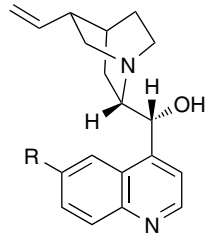

14a: R = H
14b: R = OMe

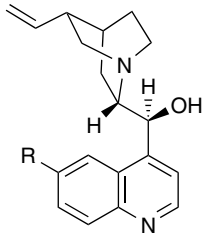

15a: R = H
15b: R = OMe

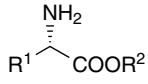

16

Figure 4.23. Structures of conventional resolving agents.

for naturally occurring compounds and their derivatives, such as **13a** and **13b**, although both enantiomers are fortunately available for **1**, **6**, **9**, and **10**. Under such circumstances another naturally occurring compound or its derivative is used as an alternative of the unavailable enantiomer, for example, **15a** and **15b** for the corresponding enantiomers of **14a** and **14b**, respectively.

In order to know the characteristic interactions and supramolecular systems formed between the enantiomers of racemates and these resolving agents in the diastereomeric crystals, the crystal structures of the diastereomeric salts with the resolving agents were searched from the Cambridge Structural Database (CSD),[52] 1999 October version. Omitted among the structures thus extracted were data analyzed only for the determination of the absolute configuration of the counter ion and those unrelated to the diastereomeric resolution. As a result of the search under these conditions, the diastereomeric salts of **9**, **10**, **6**, and **13**–**15** were picked up, and the characteristics of the crystal structures of the diastereomeric salts, which would be helpful for the design of novel resolving agents, are thoroughly investigated.

B. Acidic Resolving Agents

1. Tartaric Acid

Tartaric acid (**9**) is the most conventional acidic resolving agent for basic racemates. A great number of basic racemates have been resolved by **9** so far. In Nature, the L-form [(+)-*d*-form] is abundant and occurs in many fruits. However, not only the L-isomer but also the D-isomer are commercially available in fairly low costs. This makes the availability of this acid notable.

Since **9** is a divalent acid, the composition of a precipitated diastereomeric salt depends on the ratio of **9** to a racemic base; either a tartrate form or a hydrogen tartrate form is possible to precipitate depending on the ratio of acid/base in a solution. The structures of the cationic parts of tartrates and hydrogen tartrates, which are listed in the CSD, are summarized in Figures 4.24 and 4.25.[53–89] Most of them are less soluble diastereomeric salts, except for CIVFOC10,[67] JESCOZ,[61] JOBZAB,[62] ENGCOB,[64] KABXOA,[66] and RPEHTH.[69]

Tartaric acid (**9**) is a C_2-symmetric molecule, having two carboxyl and two hydroxy groups. These functional groups play a significant role in the chiral discrimination of the enantiomers of a racemate by hydrogen-bonding interaction. The structural studies on the diastereomeric salts of **9** showed that in the crystals there exists a common and fairly stable conformation for the anion of **9**; the four carbon atoms (C1–C4 in Figure 4.26) lie almost on the same plane, and all of the carbon and oxygen atoms in each α-hydroxy

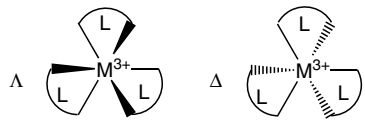

Tartrate

BELSUG[57]	*d*-**9**	Λ-Co($H_2NCH_2CH_2SO)_3$	H_2O
BUTPIP[59]	*d*-$\mathbf{9}^{2-}$	Λ-Co[$CH_3C(NHCH_2CH_2NH_2)_3]^{3+}$•$Cl^-$	$6H_2O$
ENCOCT01[58]	*d*-$\mathbf{9}^{2-}$	Λ-Co($H_2NCH_2CH_2NH_2)_3^{3+}$•Cl^-	$5H_2O$
ENCOTT[56]	2*d*-$\mathbf{9}^{2-}$	Λ-Co($H_2NCH_2CH_2NH_2)_3^{3+}$•H^+	$3H_2O$
ENCTAR[54]	*d*-$\mathbf{9}^{2-}$	Λ–δδδ-Co($H_2NCH_2CH_2NH_2)_3^{3+}$•Br^-	$5H_2O$
JESCIT[61]	*d*-$\mathbf{9}^{2-}$	Λ–*lel*$_3$–Co[(NH$_2$,NH$_2$)$_3$]$^{3+}$•Cl^-	$2H_2O$
JESCOZ[61]	*d*-$\mathbf{9}^{2-}$	Δ–*lel*$_3$–Co[(NH$_2$,NH$_2$)$_3$]$^{3+}$•Cl^-	$2H_2O$
JOBYUU[62]	*d*-$\mathbf{9}^{2-}$	Λ–*lel*$_3$–Ni[(NH$_2$,NH$_2$)$_3$]$^{2+}$	$3H_2O$
JOBZAB[62]	*d*-$\mathbf{9}^{2-}$	Δ–*lel*$_3$–Ni[(NH$_2$,NH$_2$)$_3$]$^{2+}$	$5H_2O$
LENCRT[55]	2*d*-$\mathbf{9}^{2-}$	Λ–δδδ-Cr($H_2NCH_2CH_2NH_2)_3^{3+}$•Li^+	$3H_2O$

Hydrogen Tartrate

ENGCOA[64]	*d*-**9**•$\mathbf{H}^+$	Λ–[Co($H_2NCH_2COO)_2$($H_2NCH_2CH_2NH_2$)]$^+$	$3H_2O$
ENGCOB[63]	*d*-**9**•$\mathbf{H}^+$	Δ–[Co($H_2NCH_2COO)_2$($H_2NCH_2CH_2NH_2$)]$^+$	H_2O
KABXIU[66]	*d*-**9**•$\mathbf{H}^+$	Λ–δλ-[Co($H_2NCH_2CH_2NH_2)_2$($NO_2)_2$]$^+$	H_2O
KABXOA[66]	*d*-**9**•$\mathbf{H}^+$	Δ–δλ-[Co($H_2NCH_2CH_2NH_2)_2$($NO_2)_2$]$^+$	$2H_2O$

Figure 4.24. Structures of the diastereomeric metal complex salts in the forms of a tartrate and a hydrogen tartrate listed in the CSD. The capitals are the CSD reference codes.

carboxylate moiety (C1, C2, O1–O3 and C3, C4, O4–O6, in Figure 4.26) are coplanar.[53]

The mechanism for the chiral discrimination of the enantiomers of metal cation complexes, such as $[Co(en)_3]^{3+}$, by enantiopure **9** has been studied by

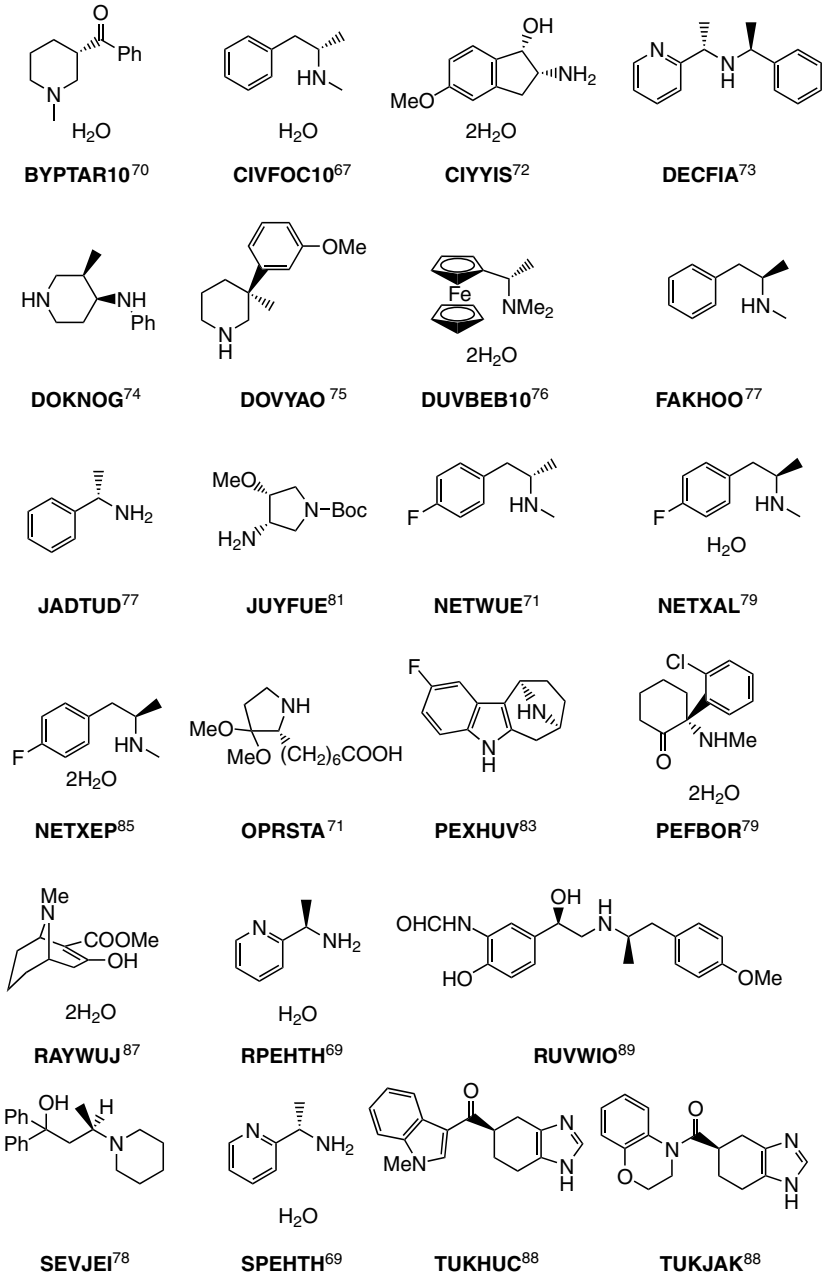

Figure 4.25. Structures of the chiral amines of the diastereomeric salts in the forms of a tartrate and a hydrogen-tartrate listed in the CSD. The capitals are the CSD reference codes.

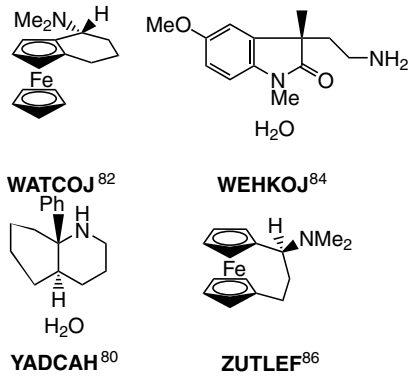

Figure 4.25. (*continued*).

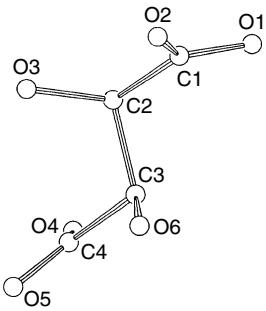

Figure 4.26. Conformation of (**9**-2H)$^{2-}$ in ENCOCT01.

Yoneda and other groups in detail.[53–66] Their studies revealed that the mechanism changes strikingly depending on the anionic species of **9** in the diastereomeric salts, a tartrate form (**9**-2H)$^{2-}$ or a hydrogen tartrate form (**9**-H)$^{-}$.

In the cases of the (**9**-2H)$^{-}$ form, the chiral discrimination of the enantiomers of a racemic metal cation complex mainly occurs through the formation of a cation-anion pair. In the diastereomeric salts, a unique face-to-face contact between (**9**-2H)$^{2-}$ and the enantiomers of the metal cation complex is commonly found (Figure 4.27).[53–62] When the cation complex has a Λ configuration, three oxygens of (**9**-2H)$^{2-}$ are placed in favorable positions for the formation of multiple hydrogen bonds with three amino hydrogens on the triangular face of the complex. On the other hand, when the complex has a Δ configuration, the fourth oxygen atom of (**9**-2H)$^{2-}$ is located closely to

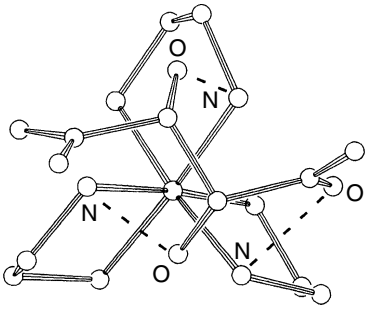

Figure 4.27. ORTEP[91] drawing of the typical face-to-face contact of (**9**-2H)$^{2-}$ with $[Co(en)_3]^{3+}$ observed in ENCOCT. The dotted lines represent hydrogen bonds.

one of the chelate rings of the complex to cause a severe steric repulsion, although the multiple hydrogen bonds are similarly formed. As a result the diastereomeric salts of (**9**-2H)$^{2-}$ with the Δ complex becomes less stable than the salt with the corresponding Λ-complex. Thus, in this case, the difference in stability between the cation-anion pairs would reflect in the difference in solubility between the diastereomeric salts.

In the cases of the salts of the (**9**-H)$^{-}$ form, an infinite hydrogen-bond chain, in which (**9**-H)$^{-}$ molecules align in a head-to-tail manner, is commonly formed in the less soluble diastereomeric salts (Figure 4.28*a*).[63–66] The guest metal cation complex forms hydrogen bonds with this supramolecular chain (Figure 4.28*b*), and the strength of the interaction between the guest cation complex and (**9**-H)$^{-}$ in the hydrogen-bond chain plays an important role in the chiral discrimination.

Foggasy's group[67] reported that this type of hydrogen-bond chain is generally found in other less soluble diastereomeric salts of (**9**-H)$^{-}$ with a variety of chiral amines. They pointed out that the length of the unit cell, which is parallel to the chain, is about 7.0 to 7.9 Å in most cases. In addition their studies showed that in many cases there are hydrogen bonds between the chains of (**9**-H)$^{-}$ to form a hydrogen-bonding layer (Figures 4.29 and 4.30). In the layer, the mode of hydrogen bonds between the neighboring hydrogen-bond chains changes according to the system. The ammonium nitrogen and other hydrogen-bonding groups in a basic part participate in the formation of the hydrogen-bond layer from outside (Figure 4.29). Therefore it is suggested that chiral discrimination of the racemates occurs on the basis of the facility of the interactions with the layer of (**9**-H)$^{-}$. In certain cases solvent molecules, such as water molecules, are included in the hydrogen-bond layer and play an important role in the stabilization of the crystal.

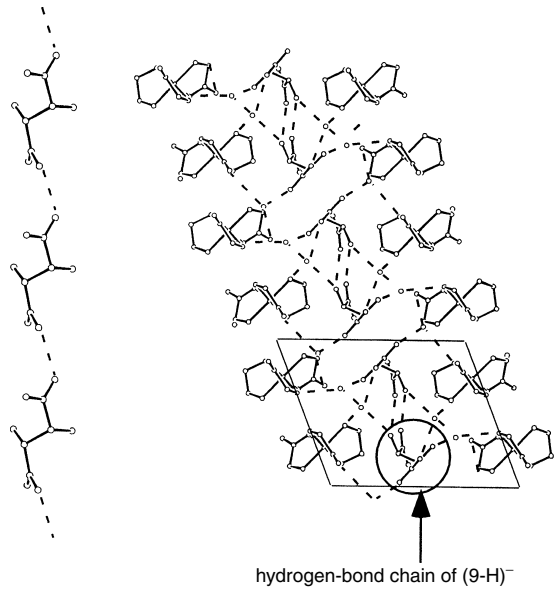

Figure 4.28. a) ORTEP drawings of (*a*) the hydrogen-bond chain formed by (**9**-H)$^-$ molecules in ENGCOA and (*b*) the crystal structure of ENGCPA viewed down the axis of the hydrogen-bond chain formed by (**9**-H)$^-$ molecules. The dotted lines represent hydrogen bonds.

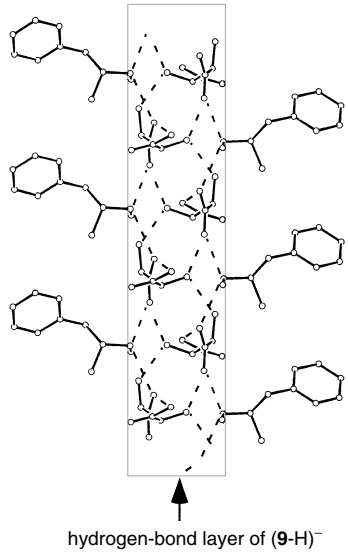

Figure 4.29. ORTEP drawing of the edge-on view of the hydrogen-bond layer formed in FAKHOO. The dotted lines represent hydrogen bonds.

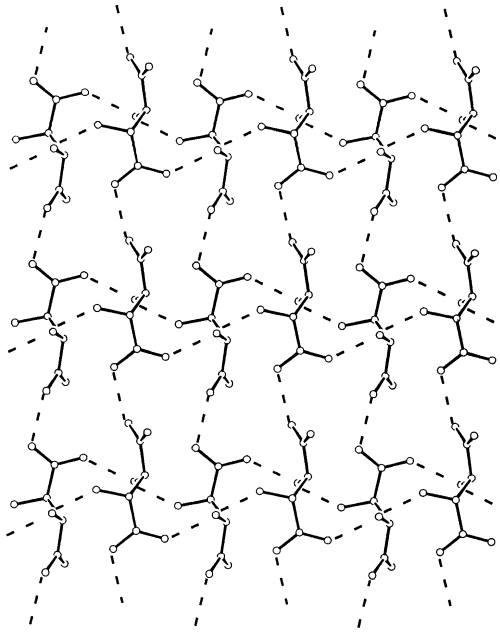

Figure 4.30. ORTEP drawing of the hydrogen-bond sheet formed by (**9**-H)$^-$ molecules in FAKHOO. The dotted lines represent hydrogen bonds.

On the basis of the comparison of the less soluble diastereomeric salts of (**9**-H)$^-$ with the corresponding more soluble salts, Larsen and co-workers[68–69] pointed out that hydrogen-bonding interaction plays the most important role in the discrimination of the enantiomers of racemates by (**9**-H)$^-$. On the other hand, Foggasy and co-workers[67] suggested that the secondary interaction, such as CH•••O interaction, plays a significant role in the discrimination of the enantiomers. Upon comparing the crystal structure of less soluble FAKHOO with that of more soluble CIVFOC10, they found their to be only a slight difference in the pattern and distance of the hydrogen bonds. On the other hand, in the less soluble salt, quite efficient CH•••O interaction is found, while less efficient CH•••O interaction is observed in the more soluble salt. On the basis of these observations, they concluded that the apparent difference in crystal structure between the less and more soluble salts arises not from hydrogen bonds but from rather weak CH•••O interaction between the carboxylate oxygens and the aromatic hydrogens.

The tendency to form a hydrogen-bond chain consisting of (**9**-H)$^-$ molecules is observed in many subsequently reported crystals of the less soluble salts of (**9**-H)$^-$ with chiral amines, as is listed in Figure 4.25.[70–90] In most cases, one of the unit cell lengths is also 7.0 to 8.0 Å, as was pointed by

Foggasy and co-workers. In many cases, the hydrogen-bond chains form a supramolecular sheet. Thus it is strongly suggested that the chiral discrimination of racemic amines by enantiopure **9** mainly occurs through the formation of a supramolecular hydrogen-bond sheet (chain) of (**9**-H)$^-$, which interact with the amine to discriminate its chirality.

2. *Dibenzoyl- and Ditoluoyltartaric Acids*

Dibenzoyltartaric acid (**10a**) and ditoluoyltartaric acid (**10b**) are prepared from tartaric acid. Both enantiomeric forms are readily available for **10a** and **10b**. Unlike **9**, there are no hydrogen-bonding group other than carboxyl group in **10**. However, **10** has two aryl groups that can bring about rather weak but distinct intermolecular interaction, such as π•••π or CH•••π interaction, in crystals. The combination of the strong hydrogen bond and weak π•••π or CH•••π interaction sometimes exerts an excellent effect on the chiral discrimination of enantiomers in the crystal. Although the molecular structures of these acids are quite similar to each other, they sometimes exhibit a different resolving ability toward the same basic racemate.

Since **10** are divalent acids, either a tartrate form or a hydrogen tartrate form is possible to precipitate, depending on the ratio of acid to base in a solution, just as the case of **9**. In the case of the resolution of mono-basic racemates, equimolar amounts of **10** and the racemates are usually mixed to afford hydrogen tartrate-type salts.

The crystal structures of the salts of **10** with racemic amines showed that there is a favorable and common conformation for the anions of **10** [(**10a**-H)$^-$, (**10b**-H)$^-$, (**10a**-2H)$^{2-}$, and (**10b**-2H)$^{2-}$] in the crystalline state (Figure 4.31); four carbon atoms (C1–C4) are almost on the same plane, and two carboxylate groups are in an *anti* conformation while two benzoyl or toluoyl groups are *gauche* to each other.[92]

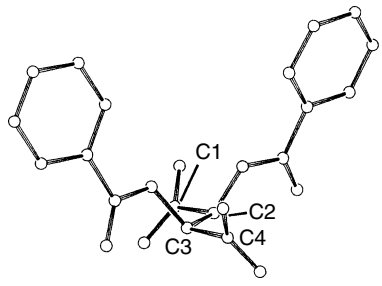

Figure 4.31. ORTEP drawing of the typical structure of (**10a**-2H)$^{2-}$ molecule in SUNWUT.

The less soluble diastereomeric salts of **10** with chiral amines, which are listed in the CSD, are summarized in Table 4.6, Figure 4.32, and Figure 4.33.[92–114] Most of these less soluble salts are hydrogen tartrate-type salts (Table 4.6); tartrate-type salts are rather rare, compared to hydrogen tartrate-type salts (Figure 4.33).

Ogura's group reported that there is a common characteristic in the crystal structures of the hydrogen tartrate-type salts of **10** with amines.[93] A characteristic hydrogen-bond chain of (**10**-H)$^-$ molecules, which align in a head-to-tail manner just as the salts of **9** (Figure 4.34), is commonly formed in these crystals. There are two types of hydrogen-bond chains according to the symmetrical relationship between the neighboring anion molecules in a single hydrogen-bond chain. One case is that the molecules align simply by translation as is

Table 4.6
Summary of the Diastereomeric Salts of **10a** or **10b** with Chiral Amines

CSD Reference Code	Anion	Space Group	Type of the Hydrogen-Bond Chain	Cell Length Parallel to the Hydrogen-Bond Chain	Reference
FEZPAB	(**10a-H**)$^-$	$P2_12_12_1$	Translational	7.478	94
LAZLAZ	(**10a-H**)$^-$	$P1$	Translational	7.467	95
NEYLEI01	(**10a-H**)$^-$	$P2_12_12_1$	Translational	8.0096	96
NINKEA	(**10a-H**)$^-$	$P2_1$	Translational	7.765	97
PIVDUT	(**10a-H**)$^-$	$P2_12_12_1$	Translational	7.993	98
PUTMUM	(**10a-H**)$^-$	$P2_12_12_1$	Translational	7.752	99
TUKHOW	(**10a-H**)$^-$	$P2_1$	Translational	7.517	100
TUKJEO	(**10a-H**)$^-$	$P2_1$	[a]	7.545	100
ZUTLUV	(**10a-H**)$^-$	$P2_12_12_1$	Translational	7.873	101
PIHCIS	(**10b-H**)$^-$	$P2_12_12_1$	2_1	14.1699	102
POKFEA	(**10b-H**)$^-$	$P2_12_12_1$	2_1	13.400	103
TEVMUC	(**10b-H**)$^-$	$P2_1$	[a]	7.887	104
VARBEV	(**10b-H**)$^-$	$P1$	Translational	7.628	105
YADBUA	(**10b-H**)$^-$	$P1$	Translational	7.765	106
YAGRAZ	(**10b-H**)$^-$	$P2_12_12_1$	2_1	13.932	107
ZAJDAP	(**10b-H**)$^-$	$P2_1$	2_1	13.8816	108
ZUNPON	(**10b-H**)$^-$	$P2_1$	[a]	7.882	109
PABGOO	**10a**$^{2-}$	$P2_1$	1 : 2 Pair	—	110
PIWMOX	**10a**$^{2-}$	$P2_1$	1 : 1 Pair	—	111
SUNWUT	**10a**$^{2-}$	$P4_3$	1 : 2 Pair	—	112
YABTAW	**10a**$^{2-}$	$C2$	1 : 2 Pair	—	113
YIBYEN	**10a**$^{2-}$	$C2$	1 : 2 Pair	—	114

[a] Atomic coordinates are not available.

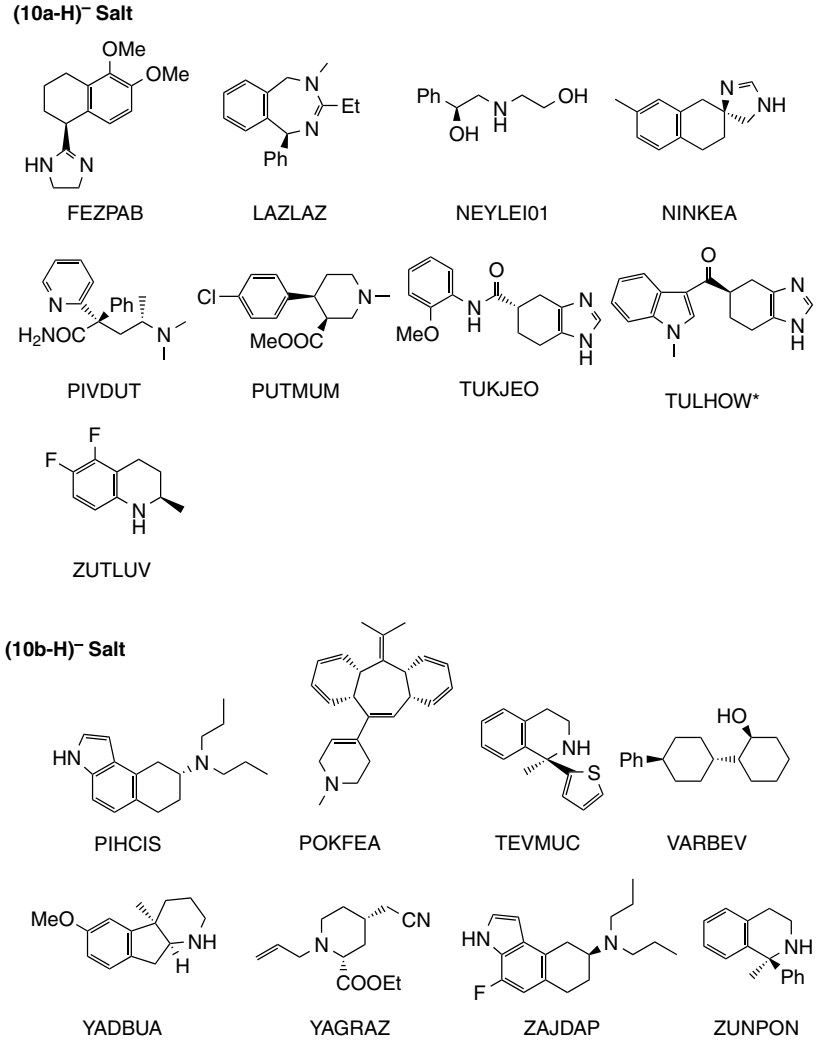

Figure 4.32. Structures of the ammonium parts of the less soluble diastereomeric salts with (**10**-H)$^-$. The capitals are the CSD reference codes.

shown in Figure 4.34*a*, and the other case is that the molecules align around a 2_1-axis as is shown in Figure 4.34*b*. It is noteworthy that (**10a**-H)$^-$ molecules highly tend to form a translation-type hydrogen-bond chain while (**10b**-H)$^-$ molecules form a 2_1-type hydrogen-bond chain more frequently than (**10a**-H)$^-$ molecules (Table 4.6). It seems that the methyl groups of the aromatic groups

(10a-2H)⁻ Salt

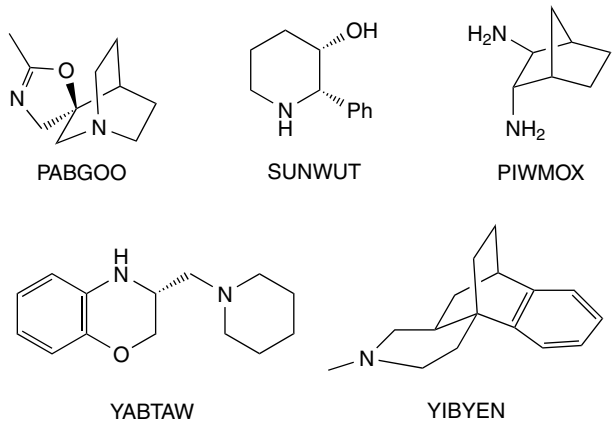

Figure 4.33. Structures of the ammonium parts of the less soluble diastereomeric salts of (**10a**-2H)⁻. The capitals are the CSD reference codes.

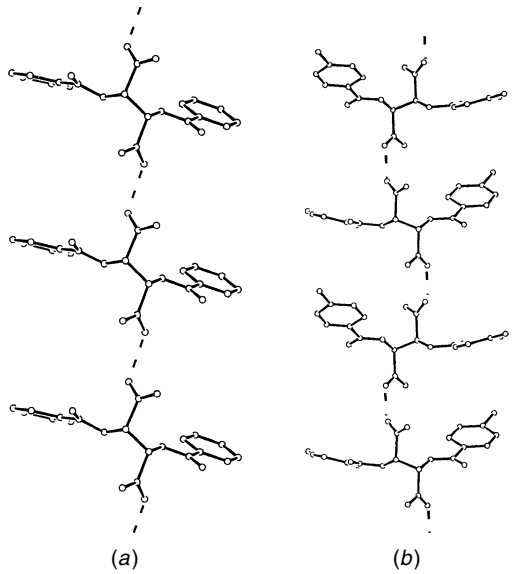

Figure 4.34. Hydrogen-bond chains of (**10a**-H)⁻ molecules formed in the less soluble diastereomeric salts. (*a*) Translational chain formed in NINKEA and (*b*) 2_1-type chain formed in YAGRAZ. The dotted lines represent hydrogen bonds.

in **10b** give some effect on the mode of hydrogen-bond network formed by the anions. One of the unit cell lengths, which is parallel to the hydrogen-bond chain, is about 7.5 to 8.0 Å for the salt crystals consisting of translational-type chains, and 13.4 to 14.1 Å for the salt crystals consisting of 2_1-type chains. Thus the cell parameter helps deduce the type of hydrogen-bond chain formed in the diastereomeric salts of **10** with racemic amines.

The whole crystal of less soluble diastereomeric salts is constructed by assembly of these types of hydrogen-bond chains and guest molecules which are surrounded by the chains (Figure 4.35*a*). In certain cases, the chains exist in a puckered layer structure, and the guest molecules are sandwiched by the layers (Figure 4.35*b*). However, the packing mode of the chains shows versatility, which is sensitive to the structure of the chiral guest amine to a considerable extent. The major interaction between **10** and a racemate is hydrogen-bonding interaction between the carboxylate oxygen of (**10**-H)$^-$ and the ammonium hydrogen of the racemate. In addition, the secondary interaction such as CH•••π or π•••π interaction, which is observed between the aromatic groups in (**10**-H)$^-$ and in the ammonium part, also plays some role in the discrimination of the enantiomers of the amine.[93]

Tartrate-type salt crystals are rather rare, compared with hydrogen tartrate-type salt crystals, as was mentioned above. In the CSD, five kinds of less soluble salts of (**10a**-2H)$^{2-}$ are listed. In the crystals of four of them (PABGOO,[110] SUNWUT,[112] YABTAW,[113] and YIBYEN[114]), two carboxylate groups in one (**10a**-2H)$^{2-}$ molecule make strong hydrogen bonds with the ammonium hydrogens of two guest molecules to form a 1 : 2 anion-cation pair (Figure 4.36). Although there are no data for the corresponding more soluble salts, it is supposed that the chiral discrimination occurs in the stage of the formation of a 1 : 2 anion-cation pair, like the case of (**9**-H)$^-$ with a metal cation complex. On the other hand, in the crystal of PIWMOX,[111] one (**10a**-2H)$^{2-}$ molecule forms a pair with one diammonium cation molecule. In this case the geometry of the two amino groups of the diammonium cation is essential for the formation of the 1 : 1 pair. There are hydrogen bonds between the pairs, resulting in the formation of a stable hydrogen-bond sheet consisting of (**10a**-2H)$^{2-}$ molecules and the guest molecules.

C. Basic Resolving Agents

1. 1-Phenylethylamine

1-Phenylethylamine (**6**), one of simple chiral amines, has been widely used as a resolving agent in the resolution of various kinds of racemic acids. There is a chiral carbon at the α-position, and a large phenyl group, a middle methyl group, and a small hydrogen atom are bonded to the carbon atom. One of

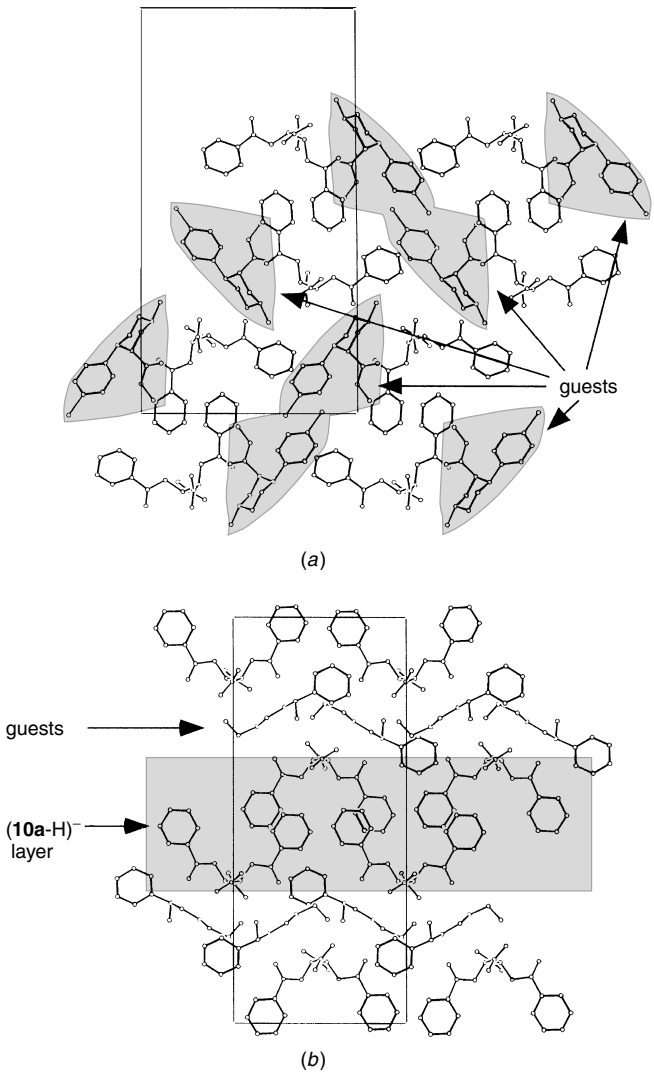

Figure 4.35. ORTEP drawings of the crystal structures of the less soluble salts of (*a*) OUTMUM and (*b*) NEYLEI01.

the notable advantages in the usage of this amine as a resolving agent is that unlike naturally occurring basic resolving agents, both enantiomers are readily available in fairly large quantities. Because of high availability and simple structure of **6**, the chiral discrimination mechanism concerned with **6** is widely studied.

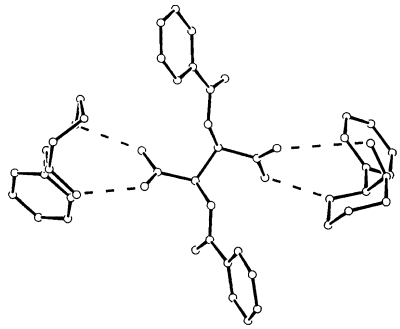

Figure 4.36. ORTEP drawing of the cation-anion 2 : 1 pair formed in SUNWUT. The dotted lines represent hydrogen bonds.

More than one hundred crystal structures of the diastereomeric salts of **6** with chiral carboxylic acids are listed in the CSD. About 20% of them are related to the results of the studies on the diastereomeric resolution. The chemical structures of the acidic parts in these salts and the corresponding CSD reference codes are shown in Figure 4.37.[115–125]

Of these crystal structures, 1-phenylethylammonium 2-phenylpropionate (NMACEP, PMACEP, Figure 4.38)[115] and 2-phenylbutyrate (PEAPEA, PBUPEA)[115,116] are the earliest examples reported by Brianso. The less soluble salt is the combination of the *S*-acid with the *R*-amine (PMACEP and PEAPEA) in each case. The crystal structures of both pairs of the diastereomeric salts (less and more soluble salts) have been determined to show that these two systems have quite similar crystalline characteristics. In both less and more soluble salts a columnar hydrogen-bond network, formed by the carboxylate and ammonium groups, is commonly built around a two fold screw axis; two molecules of the carboxylate part and two molecules of the ammonium part form a unit, which is piled up along a 2_1-axis to form a supramolecular hydrogen-bond column.

The stereochemistry of the carboxylate part reflects the relative orientation of the aromatic group in the hydrogen-bond column; in the less soluble salts (PMACEP and PEAPEA), four aromatic groups in a unit are perpendicular to each other, while in the corresponding more-soluble salts (NMACEP and PBUPEA), the aromatic groups are parallel. Since there is no significant difference in the hydrogen-bonding pattern between the less and more soluble salts, it is suggested that this difference in aromatic packing may lead to the difference in stability of the packing of the supramolecular columns between the less and more soluble salts, resulting in the difference in solubility between the less and more soluble salts. However, in the practical resolution processes of 2-phenylpropionic acid[126] and 2-phenylbutyric acid with enantiomerically pure

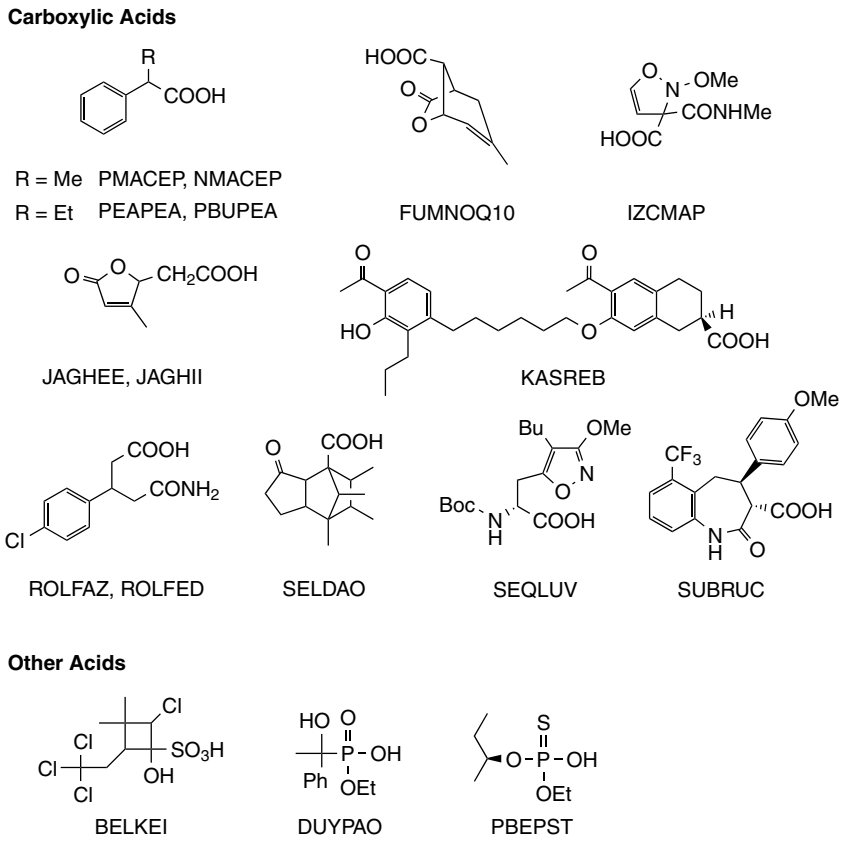

Figure 4.37. Structures of the acidic parts of the diastereomeric salts with **6**. The capitals are the CSD reference codes.

6,[127] recrystallizations must be repeated four to five times in order to obtain the enantiopure acids. Hence in these systems it is considered that the difference in stability between the less and more soluble salts is not so sufficient.

The crystal structures of the diastereomeric salts of 1-phenylethylamine with chiral carboxylic acids are subsequently reported by other groups (Table 4.7). The comparison of the crystal structure of JAGHEE with that of JAGHII also indicates that columnar hydrogen-bond networks are formed in these crystals, respectively, and that the difference between them can be found in the relative orientation of the substituent on the chiral carbon of the carboxylate moiety in the supramolecular column.

It is noteworthy that there is high tendency to form a common columnar hydrogen-bond network especially in the less soluble salts (Figure 4.39). This

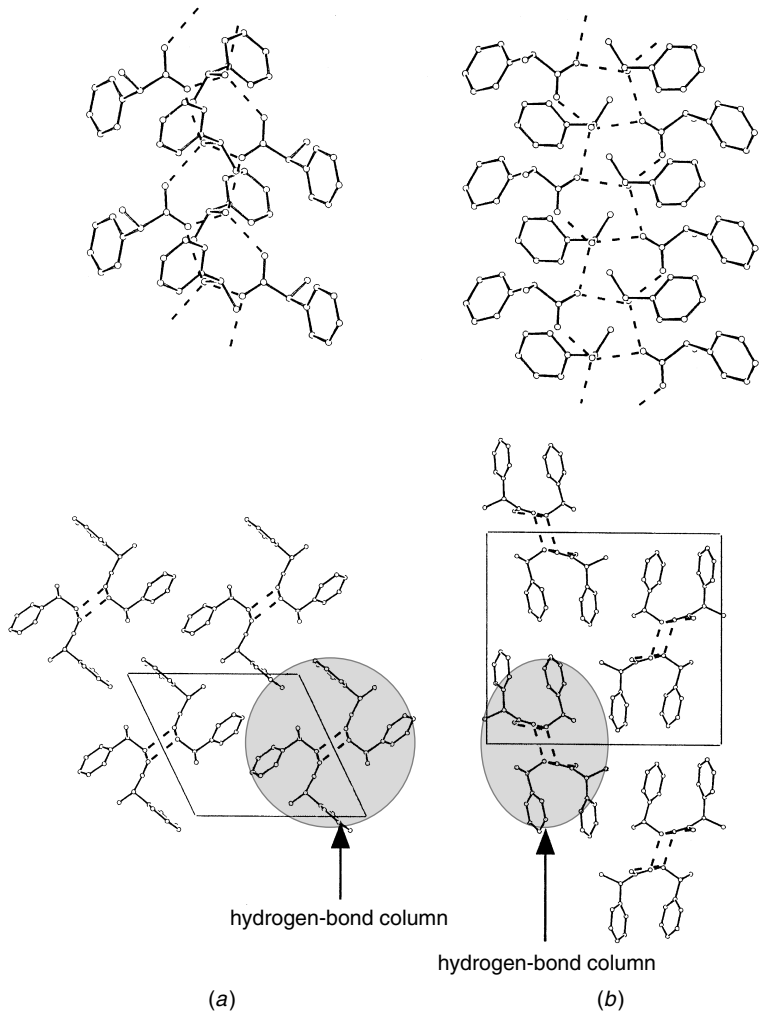

Figure 4.38. ORTEP drawings of the crystal structures of (*a*) NMACEP and (*b*) PMACEP. The upper and lower figures show the hydrogen-bond columns and the packing of the columns viewed down the columnar axis, respectively. The dotted lines represent hydrogen bonds.

tendency is preserved even for the diastereomeric salts containing a chiral acid having strong hydrogen-bonding group(s) other than carboxylate group(s) such as KASREB,[121] SEQLUV,[124] and SUBROC.[125] Thus it is suggested that in the cases of the resolutions of racemic carboxylic acids by 1-phenylethylamine, the chiral discrimination occurs through the formation and packing of supramolecular hydrogen-bond columns.

Table 4.7
Hydrogen-Bond Network Formed in the Diastereomeric Salts of **6**

CSD Reference Code	Less or More Soluble Salt	Hydrogen-Bond Network	Reference
FUMNOQ10	Less	2_1-Column[a]	118
IZCMAP	Less	Another column	119
JAGHEE	More	2_1-Column	120
JAGHII	Less	2_1-Column	120
KASREB	Less	2_1-Column	121
NMACEP	More	2_1-Column	115
PMACEP	Less	2_1-Column	115
PBUPEA	More	2_1-Column	116
PEAPEA	Less	2_1-Column	117
ROLFAZ	Less	Another column	122
ROLFED	More	2_1-Column	122
SELDAO	Less	2_1-Column	123
SEQLUV	Less	2_1-Column	124
SUBRUC	Less	2_1-Column	125
BELKEI	Less	Another column	128
DUYPAO	Less	Another column	129
PBEPST	Less	Another column	130

[a] 2_1-Column: The hydrogen-bond pattern shown in Figure 4.38.

Although examples are rather less than those of chiral carboxylic acids, the crystal structures of diastereomeric less soluble salts of **6** with chiral sulfonic acid (BELKEI),[128] phosphoric acid (DUYPAO),[129] and thiophosphoric acid (PBEPST)[130] are also reported. Here, noteworthy is that in each case a columnar hydrogen-bond network is formed whose pattern of hydrogen bonds is similar to that in carboxylate salts (Figure 4.40). In each case the anionic functional group plays a similar role to a carboxylate group in the columnar hydrogen-bond network (Figure 4.41).

2. *Brucine and Strychnine*

Brucine (**13a**) is an alkaloid isolated from *Strychnos* seeds,[131] which has great versatility in forming complexes with a wide variety of compounds. This compound has one basic nitrogen and four oxygens, which can be hydrogen acceptors, and form complexes with acidic compounds and alcohols mainly by electrostatic and/or hydrogen-bonding interaction (Figure 4.42). The most variable part of **13a** is the amido group, while the other functional groups are situated in a similar conformation throughout a variety of crystals.

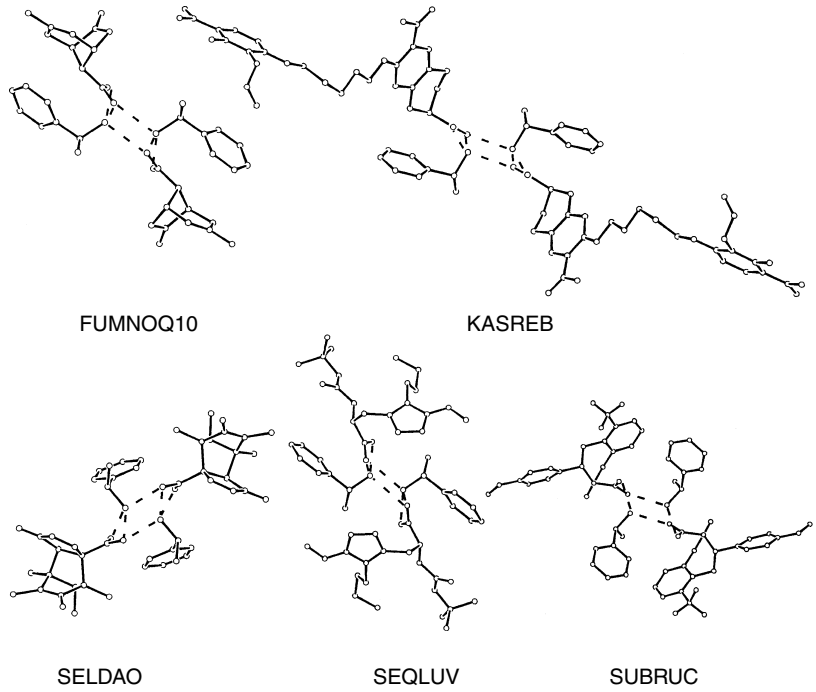

Figure 4.39. ORTEP drawings of the columnar hydrogen-bond networks viewed down the columnar axis. The dotted lines represent hydrogen bonds. The capitals are the CSD reference codes.

Gould and Walkinshaw thoroughly studied the crystal structures of **13a** salts with *N*-protected amino acids, taking into account the facts that **13a** has a high resolving ability for many types of racemic acids including *N*-protected amino acids, and that **13a** usually co-crystallizes with the D-isomers of *N*-protected amino acids to form the less soluble salts.[132] The crystal structure of the less soluble salt of **13a** with *N*-benzoyl-D-alanine shows that the protonated cations of **13a** (**13a•H**$^+$) form a corrugated monolayer-type sheet in the less soluble salt (Figures 4.43, and 4.44).[131] The guest carboxylate molecules and water molecules are incorporated between the sheets, and they form strong hydrogen bonds with **13a•H**$^+$ molecules and with each other. This type of monolayer, made by **13a•H**$^+$ molecules, is observed not only in the other salts of **13a** with *N*-protected amino acids such as *N*-acetyl-D-alanine,[132] but also in the salts with various chiral acidic compounds such as α-D-glucuronic acid,[134] and β-D-glucuronic acid.[134;135,136] The distance between the layers and the number of the included solvent molecules change according to the size of the guest molecule. Such a change in interlayer distance can be usually observed in the

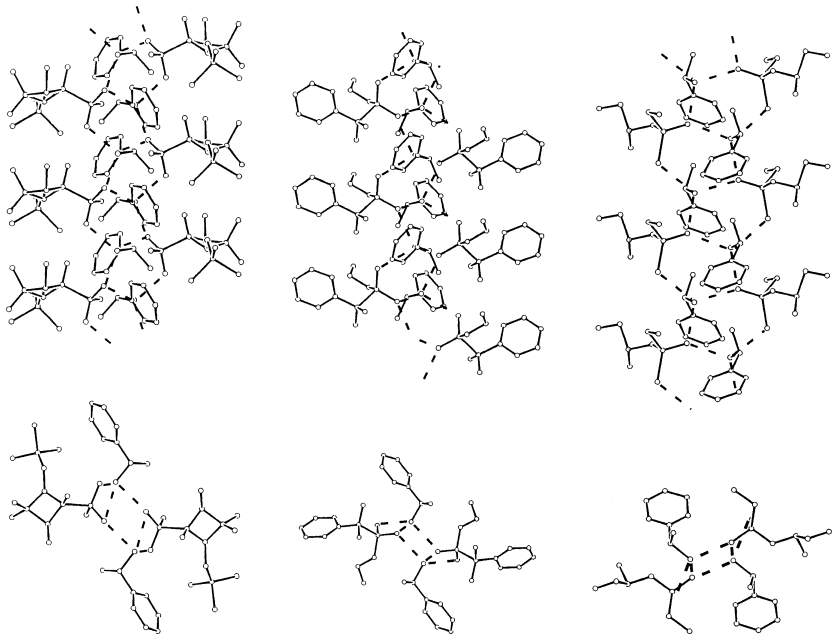

Figure 4.40. ORTEP drawings of the columnar hydrogen-bond networks formed in (*a*) BELKEI, (*b*) DUYPAO, and (*c*) PBEPST. The upper and lower figures show the side view and down view of the columns, respectively. The dotted lines represent hydrogen bonds. The capitals are the CSD reference codes.

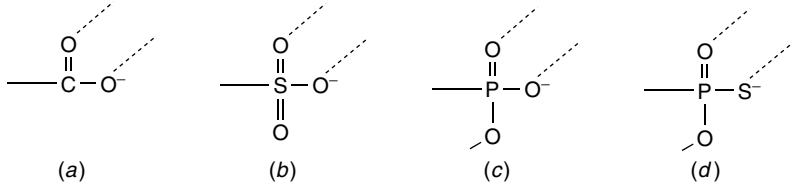

Figure 4.41. Schematic representations of the hydrogen bonds made by the anionic functional groups in the diastereomeric salts of (*a*) carboxylates, (*b*) sulfonates, (*c*) *O*-alkylphosphonates, and (*d*) *O*-alkylphosphonothioates. The dotted lines represent hydrogen bonds.

length of the *b*-axis of the unit cell with preservation of the lengths of *a*- and *c*-axes.

On the other hand, the crystal structures of the corresponding more-soluble salts of **13a** with *N*-protected amino acids show that such a monolayer of **13a●H**$^+$ molecules, found in the less soluble salts, is not formed.[136] These

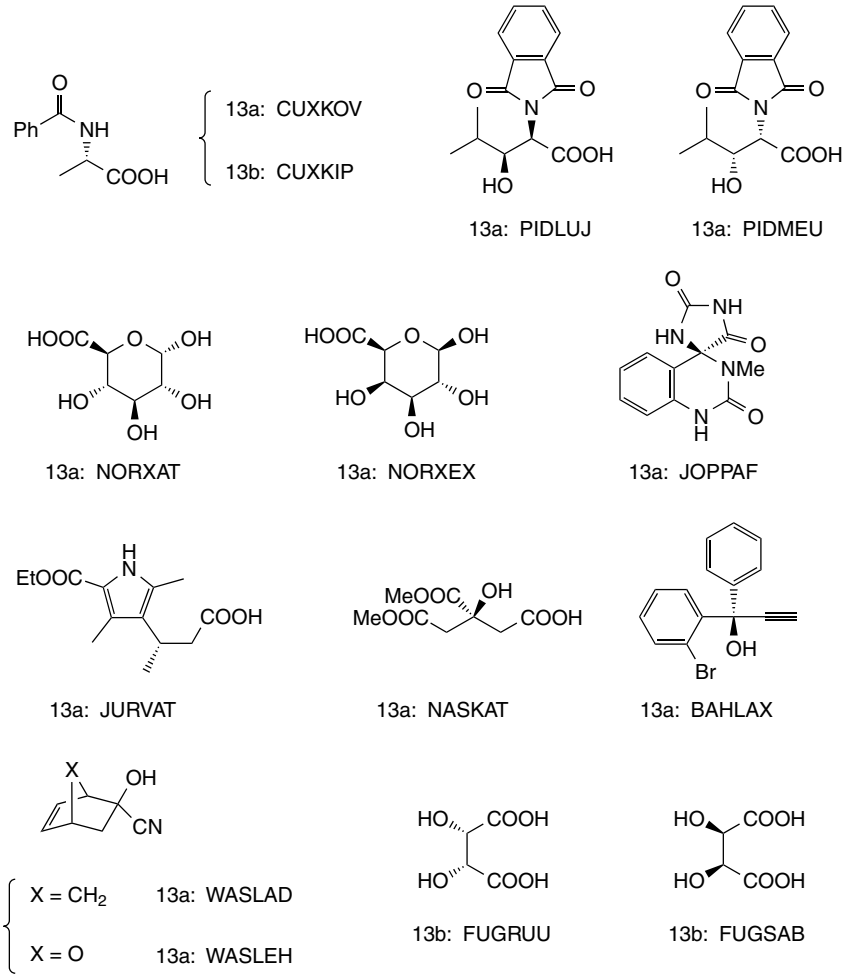

Figure 4.42. Structures of the chiral acids listed as **13a** and/or **13b** salts in the CSD and the corresponding reference codes.

facts indicate that the formation of a monolayer of **13a•H**$^+$ molecules, which lead to the selective incorporation of one of the enantiomers of a chiral carboxylic acid between the layers, is essential in the chiral discrimination by **13a**.

A monolayer structure, similar to that made by **13a•H**$^+$ molecules as is shown in Figure 4.43, is also formed even when guest chiral compounds are not acids but alcohols[137] and cyanohydrins (Figure 4.45).[138] In the cases of alcohol complexes, the basic nitrogen of **13a**, which is not protonated, can make a strong hydrogen bond with the hydroxy hydrogen of the alcohol,

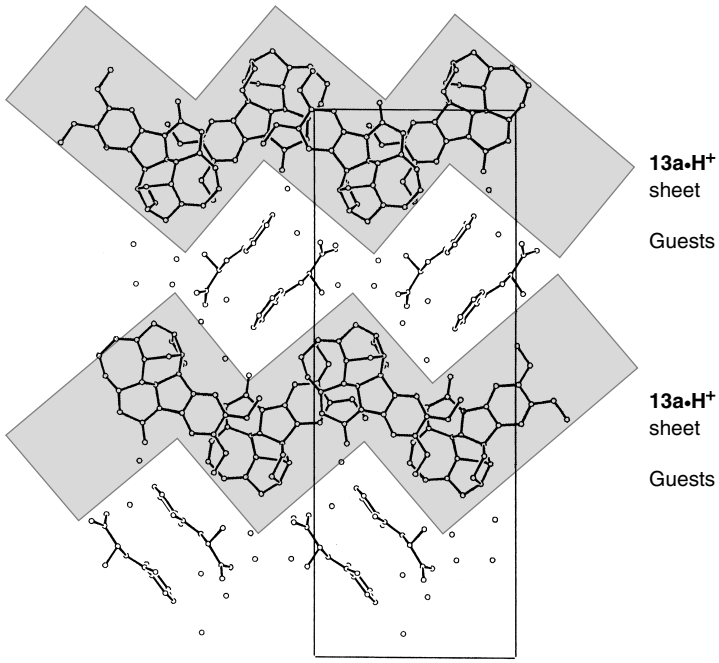

Figure 4.43. ORTEP drawing of the crystal structure of CUXKOV. The hydrogen atoms are omitted for clarity.

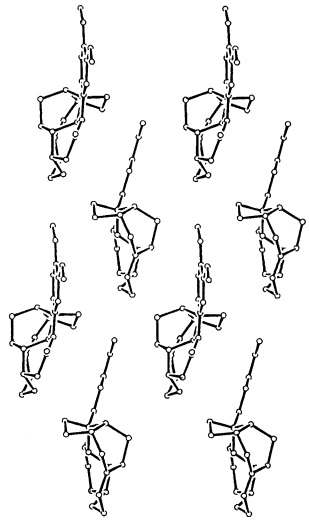

Figure 4.44. ORTEP drawing of the supramolecular sheet consisting of **7a●H**$^+$ molecules formed in CUXKOV.

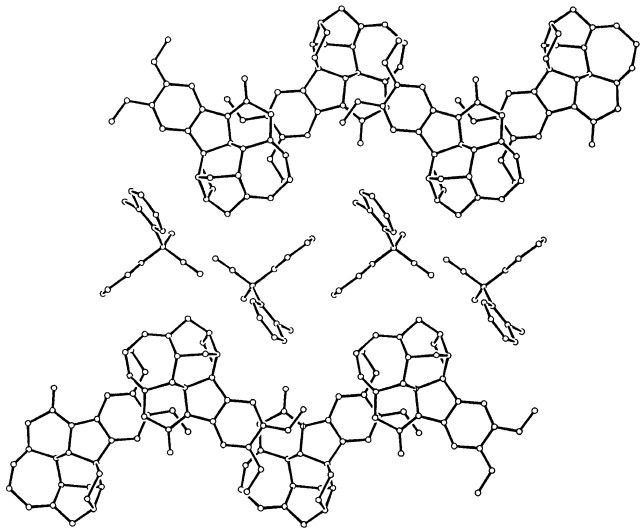

Figure 4.45. ORTEP drawing of the crystal structure of BAHLAX. The hydrogen atoms are omitted for clarity.

playing a highly significant role in the formation of the complex with the guest alcohol.

Strychnine (**13b**), which is also isolated from *Strychnos* seeds, has a similar structure to that of **13a** and has been used as a resolving agent. However, **13b** is, in general, used less frequently than **13a** because of its lower resolving ability than that of **13a**. In addition **13b** sometimes shows different preference to the enantiomers of a racemate than does **13a**.[132] It is notable that a small difference in chemical structure between **13a** and **13b**, that is, the presence or absence of two methoxy groups, causes a dramatic change in the resolution ability and in the preference to a pair of enantiomers. Gould, Walkinshaw, and their co-workers showed that this difference in resolving ability between **13a** and **13b** originates from the difference in structure of the supramolecular hydrogen-bond sheets formed in the less soluble salts.[131,138,139]

3. Quinine, Cinchonine, Quinidine, and Cinchonidine

Quinine (**14a**), cinchonine (**14b**), quinidine (**15a**), and cinchonidine (**15b**), which are so-called cinchona alkaloids, occur in cinchona barks. Although **14a** and **15a** are the diastereomers of each other, they have been used as alternatives of the corresponding enantiomers, respectively. Quininium and quinidinium ions (**14a**•$\mathbf{H}^+$ and **15a**•$\mathbf{H}^+$) have two possible hydrogen-bond donors, a ternary ammonium ion and a hydroxy group. They also have two

possible hydrogen acceptors, a hydroxy oxygen and a heterocyclic nitrogen atom. Cinchonine (**14b**) and cinchonidine (**15b**) additionally have a methoxy group on the quinoline ring, respectively, that can be a hydrogen acceptor. These hydrogen-bonding groups of **14** and **15** play an important role in the discrimination of chiral carboxylic acids in crystals.

The crystal structures of the diastereomeric salts of **14b** with (*S*)-mandelic acid (LABXOB) and (*R*)-mandelic acid (LABXUH) were studied by Larsen and co-workers[140] In this system, (*R*)-mandelate salt is the less soluble diastereomeric salt. The crystal structure of this less-soluble salt shows that the hydroxy group of **14b●H**$^+$ makes an intermolecular hydrogen bond with the quinoline nitrogen of the neighboring **14b●H**$^+$ molecule. On the other hand, there is a strong hydrogen bond between the carboxylate oxygen of a mandelate molecule and the ammonium hydrogen of **14b●H**$^+$. Thus a complicated hydrogen-bond network is formed in the less soluble salt of **14b** with mandelic acid (Figure 4.46). The important characteristic of this crystal structure is that a mandelate anion forms an intramolecular hydrogen bond between its hydroxy group and carboxylate oxygen, realizing a very stable conformation of the mandelate anion in the crystal.

On the other hand, in the more soluble salt of **14b** with (*S*)-mandelic acid (LABXOB), all of hydrogen bonds are intermolecularly formed. The carboxylate oxygens of a mandelate anion form strong hydrogen bonds with the ammonium hydrogen and hydroxy hydrogen of **14b●H**$^+$. Thus a hydrogen-bond

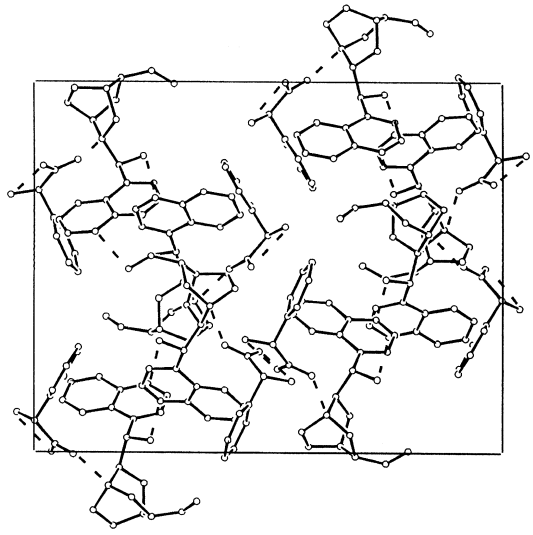

Figure 4.46. ORTEP drawing of the crystal structure of LABXUH. The hydrogen atoms are omitted for clarity. The dotted lines represent hydrogen bonds.

chain, in which **14b•H**$^+$ cations and (*S*)-mandelate anions align alternatively, is formed in this more-soluble salt (Figure 4.47). Noteworthy is that the conformation of the (*S*)-mandelate anion significantly deviates from the most stable form, which would be one of the major reasons for the destabilization of this more soluble salt compared with the corresponding less soluble salt. The DSC-TG analysis of these less and more soluble salts also suggests that the less soluble salt is more stable than the corresponding more soluble salt.

Larsen's group successively studied the crystal structures of the less and more soluble salts of **15b** with mandelic acid (RERXUH and RERYAO).[141] As a result they found that in both diastereomeric salts a characteristic hydrogen-bond chain, as is observed in the crystal of LABXOB, is commonly formed (Figure 4.48). In addition a similar hydrogen-bond network is also found in the less-soluble salt of **14a•H**$^+$ with (*S*)-mandelate[142] and in other quininium salts such as FEQZEG[144] and FIJSUM (Figure 4.49).[145]

Thus there are plenty of reports on the resolutions of a wide variety of racemates with conventional resolving agents and on the crystal structures of the diastereomeric crystals of some combinations. These studies are rarely concerned with the correlation between the difference in stability of a pair of diastereomeric crystals and the efficiency of resolutions. However, the information about supramolecular hydrogen-bond systems obtained from these studies is very valuable for understanding such relationship in the resolutions of systematically selected racemates with a resolving agent.

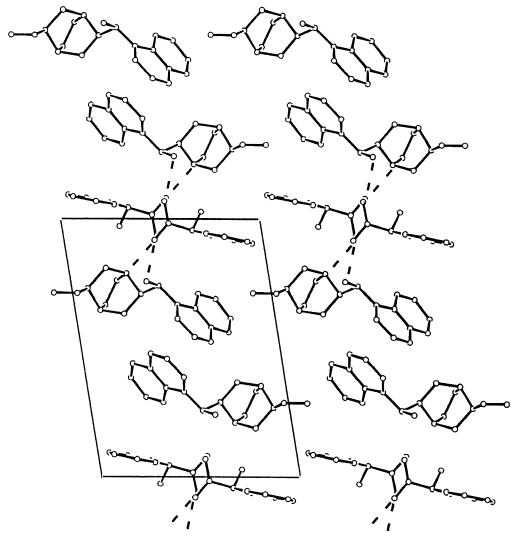

Figure 4.47. ORTEP drawing of the crystal structure of LABXOB. The hydrogen atoms are omitted for clarity. The dotted lines represent hydrogen bonds.

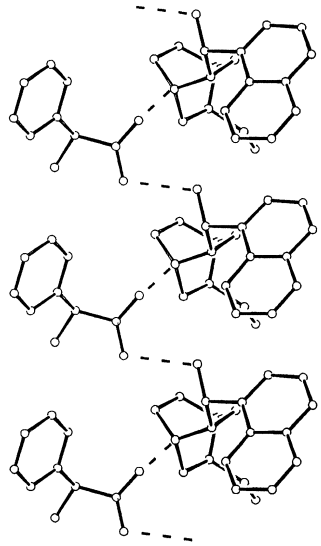

Figure 4.48. ORTEP drawing of the hydrogen-bond chain formed in RERXUH. The hydrogen atoms are omitted for clarity. The dotted lines represent hydrogen bonds.

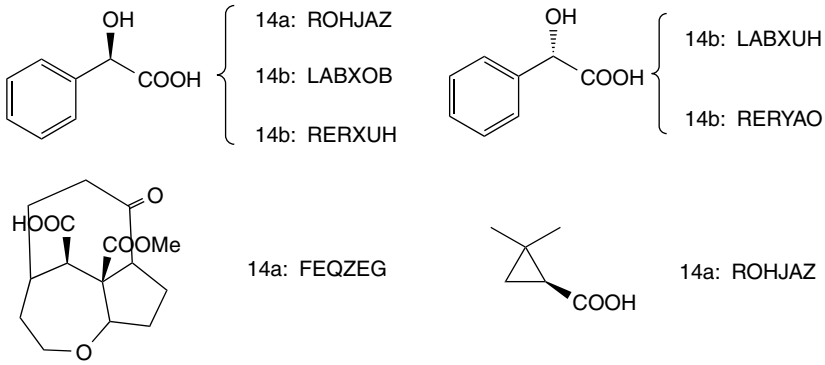

Figure 4.49. Structures of the chiral acids listed as cinchona alkaloid salts in the CSD and the corresponding reference codes.

IV. CONCLUDING REMARKS

As described in this chapter, it is useful to study the crystal structures of diastereomeric salt crystals, which precipitate upon resolution, for understanding the chiral discrimination mechanism of the diastereomeric resolution in a molecular level. The authors' studies on the crystal structures described

here revealed that each resolving agent originally contributes to the formation of a characteristic supramolecular hydrogen-bond network in the less soluble diastereomeric salt crystals that is independent of the structure of target racemates. This fact suggests that for achieving high efficiency of resolution, it is important to realize a supramolecular hydrogen-bond sheet rather than a supramolecular hydrogen-bond column in the less soluble diastereomeric salt.

Thus the information about the effects of intermolecular interactions, such as electrostatic, dipole-dipole, hydrogen-bonding, CH•••π, π•••π, and van der Waals interactions, in diastereomeric salts, which contribute to the formation of a supramolecular hydrogen-bond network and play significant roles in chiral discrimination, is very valuable. We obtained this information by systematically selecting resolutions of racemates using a single resolving agent and by making subsequent crystallographic analyses of the corresponding diastereomeric salts. At the same time we had to determine and compare the crystal structures of diastereomeric salts that could not be efficiently resolved upon crystallization. However, such studies have not yet been carried out in full, since so far almost of all studies on the diastereomeric resolution have been concerned with individual and limited target racemates. We are encouraged by our results in the resolution of a series of systematically selected racemates with modified or newly designed resolving agents. It has also been instructive to compare the crystal structures of the pairs of the diastereomeric salts for both low and high efficiency resolutions.

The importance of the formation of a supramolecular hydrogen-bond sheet in less soluble diastereomeric salts is strongly supported by the fact that conventionally used natural resolving agents can easily form such a sheet, as described in Section III, that makes them widely applicable for many racemates. These results indicate that the design of an efficient resolving agent can be regarded as the design of a stable supramolecular system to be formed in less soluble diastereomeric salt crystals.

As exemplified in this chapter, X-ray crystallographic analysis enables us to thoroughly understand intermolecular interactions that occur in a supramolecular structure and play some role in chiral discrimination in diastereomeric salt crystals. However, it is very difficult to determine the positions of the hydrogens in crystals by a conventional X-ray apparatus. This situation leads us a question the location of hydrogen bond(s) between an ammonium group and a carboxylate group. To answer this question, an explanation would be considered on the basis of the following facts: The geometries of ammonium and carboxylate groups and lone pairs on carboxylate oxygens are well established. Subsequently, when the angle of the C-N$\cdots$: O and the distance of the N$\cdots$O in a pair of an ammonium group and a carboxylate group are reasonable, the existence of a hydrogen bond should be deduced.

The present strategy for the design of a resolving agent is based on a simplified assumption and is rather qualitative. The more serious problem, which lies between the recent crystallographic and classic thermodynamic studies on the diastereomeric resolution, is that at present it is impossible to estimate the packing energy of an organic crystal precisely, and hence such thermodynamic parameters of a crystal cannot be correlated with the crystal structure, that is, the alignment of the molecules directly. Therefore, it is becoming increasingly apparent that a method should be established for the quantitative analysis of the crystal packing energy of an organic crystal. More progress in quantum chemical calculation is required for this purpose.

Another problem is explaining the mechanism of solvation of an organic molecule at a molecular level. It is well known that even for the same compound, different polymorphic crystals have different solubility characteristics. In addition the rate of solvation varies according to the face of the crystals; this is also observed in crystal growth. These phenomena could be influenced by kinetic factors, which have a significant effect on the efficiency of resolution. Thus treatment of the kinetic factors of solvation is another problem that must be explored.

As more knowledge on chiral discrimination phenomena in crystals is accumulated, more progress in the above-mentioned fields should lead to efficient tools for the design of nonnatural resolving agents. With progress on the diastereomeric resolutions of systematically selected racemates and on the X-ray structures of their diastereomeric crystals, a widely applicable criterion for the selection of a suitable resolving agent for a given target racemate could be developed.

REFERENCES

1. Pasteur, L. *Ann. Chim. Phys.* **1848**, *24*, 442.
2. Pasteur, L. *C. R. Acad. Sci.* **1853**, *37*, 162.
3. Gernez, M. *Compt. Rend.* **1866**, *63*, 843.
4. Jacques, J.; Collet, A.; Wilen, S. H. *Enantiomers, Racemates, and Resolutions*. Krieger Publishing, Malabar, FL, **1994**.
5. Newman, P. *Optical Resolution Procedures for Chemical Compounds*, Vols. 1–3. Optical Resolution Information Center, New York, **1978** (Vol. 1), **1981** (Vol. 2), and **1984** (Vol. 3).
6. Zingg, S. P.; Arnett, E. M.; McPhail, A. T.; Bothner-By, A. A.; Gilkerson, W. R. *J. Am. Chem. Soc.* **1988**, *110*, 1565.
7. Leusen, F. J. J.; Noordik, J. H.; Karfunkel, H. R. *Tetrahedron* **1993**, *49*, 5377.
8. Ács, M.; Novotny-Bregger, E.; Simon, K.; Argay, G. *J. Chem. Soc., Perkin Trans. 2* **1992**, 2011.
9. Fogassy, E.; Faigl, F.; Ács, M. *Tetrahedron* **1993**, *41*, 2837.
10. Ebbers, E. J.; Plum, B. J. M.; Ariaans, G. J. A.; Kaptein, B.; Broxterman, Q. B.; Bruggink, A.; Zwanenburg, B. *Tetrahedron: Asymmetry* **1997**, *8*, 4047.
11. Ebbers, E.; Ariaans, G. J. A.; Zwanenburg, B.; Bruggink, A. *Tetrahedron: Asymmetry* **1998**, *9*, 2745.

12. Collet, A., *Comprehensive Supramolecular Chemistry*, Vol. 10. Reinhoudt, D. N., ed. Pergamon, Oxford, **1996**, pp. 113–149.
13. Desiraju, G. R. *Crystal Engineering*. Elsevier, Amsterdam, **1989**.
14. Desiraju, G. R.; Steiner, T. *The Weak Hydrogen Bond*. Oxford University Press, Oxford, **1999**.
15. Collet, A.; Jacques, J. *Bull. Soc. Chim. Fr.* **1973**, 3330.
16. Aaron, C.; Dull, D.; Larkin Schmiegel, J.; Jaeger, D.; Ohashi, Y.; Mosher, H. S. *J. Org. Chem.* **1967**, *32*, 2797.
17. Okamura, K.; Aoe, K.; Hiramatsu, H.; Nishimura, N.; Sato, T.; Hashimoto, K. *Anal. Sci.* **1997**, *13*, 315.
18. Larsen, S.; Kozma, D.; Ács, M. *J. Chem. Soc., Perkin Trans. 2* **1994**, 1091.
19. Kinbara, K.; Sakai, K.; Hashimoto, Y.; Nohira, H.; Saigo, K. *Tetrahedron: Asymmetry* **1996**, *7*, 1539.
20. Kinbara, K.; Sakai, K.; Hashimoto, Y.; Nohira, H.; Saigo, K. *J. Chem. Soc., Perkin Trans. 2* **1996**, 2615.
21. Kinbara, K.; Hashimoto, Y.; Sukegawa, M.; Nohira, H.; Saigo, K. *J. Am. Chem. Soc.* **1996**, *118*, 3441.
22. Unpublished result.
23. Kinbara, K.; Harada, Y.; Saigo, K. *Tetrahedron: Asymmetry* **1998**, *9*, 2219.
24. de Diego, H. L. *Acta Crystallogr., Sect. C* **1995**, *51*, 253.
25. Larsen, S.; de Diego, H. L. *Acta Crystallogr., Sect. B* **1993**, *49*, 303.
26. de Diego, H. L. *Acta Chem. Scand.* **1994**, *48*, 306.
27. de Diego, H. L. *Acta Crystallogr., Sect. C* **1994**, *50*, 1995.
28. Larsen, S.; de Diego, H. L. *J. Chem. Soc., Perkin Trans. 2* **1993**, 469.
29. Kinbara, K.; Kobayashi, Y.; Saigo, K. *J. Chem. Soc., Perkin Trans. 2* **1998**, 1767.
30. Kinbara, K.; Kobayashi, Y.; Saigo, K. *J. Chem. Soc., Perkin Trans. 2* **2000**, 111.
31. Saigo, K.; Ozawa, S.; Kikuchi, S.; Kasahara, A.; Nohira, H. *Bull. Chem. Soc. Jpn.* **1982**, *55*, 1568.
32. Nishio, M.; Hirota, M.; Umezawa, Y. *The CH/π Interaction*. Wiley-VCH, New York, **1998**.
33. Gavezzotti, A.; Desiraju, G. R. *Acta. Crystallogr, Sect. B* **1988**, *44*, 427.
34. Desiraju, G. R.; Gavezzotti, A. *Acta. Crystallogr, Sect. B* **1989**, *45*, 473.
35. Karlström, G.; Linse, P.; Wallqvist, A.; Jönsson, B. *J. Am. Chem. Soc.* **1983**, *105*, 3777.
36. Burley, S. K.; Petsko, G. A. *J. Am. Chem. Soc.* **1986**, *108*, 7995.
37. Hunter, C. A.; Sanders, J. K. M. *J. Am. Chem. Soc.* **1990**, *112*, 5525.
38. Toda, F.; Tanaka, K.; Nassimbeni, L.; Niven, M. L. *Chem. Lett.* **1988**, 1371.
39. Toda, F.; Sato, A.; Nassimbeni, L. R.; Niven, M. L. *J. Chem. Soc., Perkin Trans. 2* **1991**, 1971.
40. Toda, F.; Tanaka, K.; Yagi, M.; Stein, Z.; Goldberg, I. *J. Chem. Soc., Perkin Trans. 1* **1990**, 1215.
41. Toda, F.; Soda, S.; Goldberg, I. *J. Chem. Soc., Perkin Trans. 1* **1993**, 2357.
42. Toda, F.; Tanaka, K.; Kido, M. *Chem. Lett.* **1988**, 513.
43. Toda, F.; Tanaka, K.; Ootani, M.; Hayashi, A.; Miyahara, I.; Hirotsu, K. *J. Chem. Soc., Chem. Commn.* **1993**, 1413.
44. Toda, F.; Tanaka, K.; Marks, D.; Goldberg, I. *J. Org. Chem.* **1991**, *56*, 7332.
45. Toda, F.; Tanaka, K.; Leung, C. W.; Meetsma, A.; Feringa, B. L. *J. Chem. Soc., Chem. Commn.* **1994**, 2371.
46. Toda, F.; Mori, K.; Stein, Z.; Goldberg, I. *J. Org. Chem.* **1988**, *53*, 308.
47. Toda, F.; Tanaka, K.; Mak, T. C. W. *Chem. Lett.* **1984**, 2085.
48. Lee, G.-H.; Wang, Y.; Tanaka, K.; Toda, F. *Chem. Lett.* **1988**, 781.
49. Toda, F.; Mori, K.; Stein, Z.; Goldberg, I. *Tetrahedron Lett.* **1989**, *20*, 1841.
50. Toda, F.; Sato, A.; Tanaka, K.; Mak, T. C. W. *Chem. Lett.* **1989**, 873.

51. Toda, F.; Tanaka, K.; Infantes, L.; Foces-Foces, C.; Claramunt, R. M.; Elguero, J. *J. Chem. Soc., Chem. Commn.* **1995**, 1453.
52. Allen, F. H.; Kennard, O. *Chemical Design Automation News* **1993**, *8*, 1 & 31–37.
53. Yoneda, H. *J. Chromatogr.* **1984**, *313*, 59.
54. Kushi, Y.; Kuramoto, M.; Yoneda, H. *Chem. Lett.* **1976**, 135.
55. Kushi, Y.; Kuramoto, M.; Yoshida, H. *Chem. Lett.* **1976**, 339.
56. Tada, T.; Kushi, Y.; Yoneda, H. *Chem. Lett.* **1977**, 379.
57. Kita, M.; Yamanari, K.; Kitahama, K.; Shimura, Y. *Bull. Chem. Soc. Jpn.* **1981**, *54*, 2995.
58. Magill, L. S.; Korp, J. D.; Bernal, I. *Inorg. Chem.* **1981**, *20*, 1187.
59. Okazaki, H.; Sakaguchi, U.; Yoneda, H. *Inorg. Chem.* **1983**, *22*, 1539.
60. Bernal, I.; Korp, J. D.; Creaser, I. I. *Aust. J. Chem.* **1984**, *37*, 2365.
61. Mizuta, T.; Toshitani, K.; Miyoshi, K.; Yoneda, H. *Inorg. Chem.* **1990**, *29*, 3020.
62. Mizuta, T.; Miyoshi, K. *Bull. Chem. Soc. Jpn.* **1991**, *64*, 1859.
63. Kuramoto, M.; Kushi, Y.; Yoneda, H. *Bull. Chem. Soc. Jpn.* **1978**, *51*, 3251.
64. Kuramoto, M. *Bull. Chem. Soc. Jpn.* **1979**, *52*, 3702.
65. Kuramoto, M.; Kushi, Y.; Yoneda, H. *Bull. Chem. Soc. Jpn.* **1980**, *53*, 3702.
66. Frederiksen, J. M.; Horn, E.; Snow, M. R.; Tiekink, E. R. T. *Aust. J. Chem.* **1988**, *41*, 1305.
67. Fogassy, E.; Ács, M.; Fiagl, F.; Simon, K.; Rohonczy, J.; Ecsery, Z. *J. Chem. Soc., Perkin Trans. 2* **1986**, 1881.
68. Larsen, S. *Acta Crystallogr. Sect. A* **1975**, *31*, S168.
69. Larsen, S.; Sørensen, B. *Acta Crystallogr. Sect. A* **1978**, *34*, S98.
70. Hite, G.; Soares, J. R. *Acta Crystallogr. Sect. B* **1973**, *29*, 2935.
71. Nordenson, S. *Acta Crystallogr. Sect. B* **1981**, *37*, 960.
72. Hagishita, S.; Shiro, M.; Kuriyama, K. *J. Chem. Soc., Perkin Trans. 1* **1984**, 1655.
73. Eleveld, M. B.; Hogeveen, H. *Tetrahedron Lett.* **1984**, *25*, 5187.
74. Burke Jr., T. R.; Jacobson, A. E.; Rice, K. C.; Silverton, J. V.; Simonds, W. F.; Streaty, R. A.; Klee, W. A. *J. Med. Chem.* **1986**, *29*, 1087.
75. Cheng, A.; Uyeno, E.; Polgar, W.; Toll, L.; Lawson, J. A.; DeGraw, J. I.; Loew, G.; Camerman, A.; Camerman, N. *J. Med. Chem.* **1986**, *29*, 531.
76. Luo, Y. G.; Barton, R. J.; Robertson, B. E. *Can. J. Chem.* **1987**, *65*, 2756.
77. Molins, E.; Miravitlles, C.; Lopez-Calahorra, F.; Castells, J.; Raventos, J. *Acta Crystallogr. Sect. C* **1989**, *45*, 104.
78. Schjelderup, L.; Groth, P. A.; Aasen, A. J. *Acta Chem. Scand.* **1990**, *44*, 284.
79. Ratti-Moberg, E.; Groth, P.; Aasen, A. J. *Acta Chem. Scand.* **1991**, *45*, 108.
80. Chen, C.; Kozikowski, A. P.; Wood, P. L.; Reynolds, I. J.; Ball, R. G.; Pang, Y.-P. *J. Med. Chem.* **1992**, *35*, 1634.
81. Okada, T.; Sato, H.; Tsuji, T.; Tsushima, T.; Nakai, H.; Yoshida, T.; Matsuura, S. *Chem. Pharm. Bull.* **1993**, *41*, 132.
82. Wally, H.; Kratky, C.; Weissensteiner, W.; Widhalm, M.; Schlogl, K. *J. Organomet. Chem.* **1993**, *450*, 185.
83. Mewshaw, R. E.; Abreu, M. E.; Silverman, L. S.; Mathew, R. M.; Tiffany, C. W.; Bailey, M. A.; Karbon, E. W.; Ferkany, J. W.; Kaiser, C. *J. Med. Chem.* **1993**, *36*, 3037.
84. Pallavicini, M.; Valoti, E.; Villa, L.; Lianza, F. *Tetrahedron: Asymmetry* **1994**, *5*, 111.
85. Simon, K.; Fogassy, E.; Ács, M. *ACH-Models in Chemistry* **1995**, *132*, 479.
86. Mernyi, A.; Kratky, C.; Weissensteiner, W.; Widhalm, M. *J. Organomet. Chem.* **1996**, *508*, 209.
87. Chen, Z.; Izenwasser, S.; Katz, J. L.; Zhu, N.; Klein, C. L.; Trudell, M. L. *J. Med. Chem.* **1996**, *39*, 4744.
88. Ohta, M.; Suzuki, T.; Furuya, T.; Kurihara, H.; Tokunaga, T.; Miyata, K.; Yanagisawa, I. *Chem. Pharm. Bull.* **1996**, *44*, 1707.
89. Kurihara, H.; Fujita, S.; Mase, M. *Acta Crystallogr., Sect. C* **1997**, *53*, 187.

90. Hansen, L. M.; Frydenvang, K.; Jensen, B. *J. Chem. Cryst.* **1998**, *28*, 125.
91. Burnett, M. N.; Johnson, C. K. *ORTEP-III: Oak Ridge Thermal Ellipsoid Plot Program for Crystal Structure Illustrations*. Oak Ridge National Laboratory Report ORNL-6895, **1996**.
92. Marthi, K.; Larsen, S.; Ács, M.; Bálint, J.; Fogassy, E. *Acta Chem. Scand.* **1997**, *51*, 367.
93. Tomori, H.; Yoshihara, H.; Ogura, K. *Bull. Chem. Soc. Jpn.* **1996**, *69*, 3581.
94. DeBernardis, J. F.; Kerkman, D. J.; Arendsen, D. L.; Buckner, S. A.; Kyncl, J. J.; Hancock, A. A. *J. Med. Chem.* **1987**, *30*, 1011.
95. Johnson, R. E.; Baizman, E. R.; Becker, C.; Bohnet, E. A.; Bell, R. H.; Birsner, N. C.; Busacca., C. A. Carabateas, P. M.; Chadwick, C. C.; Gruett, M. D.; Hane, J. T.; Herrmann Jr., J. L.; Josef, K. A.; Krafte, D. S.; Kulling, R. K.; Michne, W. F.; Pareene, P. A.; Perni, R. B.; O'Connor, B.; Salvador, U. J.; Sanner, M. A.; Schlegel, D. C.; Silver, P. J.; Swestock, J.; Stankus, G. P.; Tatlock, J. H.; Volberg, W. A.; Weigelt, C. C.; Erzin, A. M. *J. Med. Chem.* **1993**, *36*, 3361.
96. Marhi, K.; Larsen, S.; Ács, M.; Balint, J.; Fogassy, E. *Acta Chem Scand.* **1997**, *51*, 367.
97. Cordi, A. A.; Lacoste, J.-M.; Borgne, F. L.; Herve, Y.; Vaysse-Ludot, L.; Descombes, J.-J.; Courchay, C.; Laubie, M.; Verbeuren, T. J. *J. Med. Chem.* **1997**, *40*, 2931.
98. Oyasu, H.; Nagano, M.; Akahane, A.; Tomoi, M.; Tada, T.; Matsuo, M. *J. Med. Chem.* **1994**, *37*, 1378.
99. Kozikowski, A. P.; Araldi, G. L.; Boja, J.; Meil, W. M.; Johnson, K. M.; Flippen-Anderson, J. L.; George, C.; Saiah, E. *J. Med. Chem.* **1998**, *41*, 1962.
100. Ohta, M.; Suzuki, T.; Furuya, T.; Kurihara, H.; Tokunaga, T.; Miyata, K.; Yanagisawa, I. *Chem. Pharm. Bull.* **1996**, *44*, 1707.
101. Kido, M.; Nomi, D.; Hashimoto, K. *Chem. Pharm. Bull.* **1996**, *44*, 421.
102. Stjernolf, P.; Gullme, M.; Elebring, T.; Andersson, B.; Wikstrom, H.; Lagerquist, S.; Svensson, K.; Ekman, A.; Carlsson, A.; Sundell, S. *J. Med. Chem.* **1993**, *36*, 2059.
103. Phillips, S. T.; de Paulis, T.; Baron, B. M.; Siegel, B. W.; Seeman, P.; Van Tol, H. H. M.; Guan, H.-C; Smith, H. E. *J. Med. Chem.* **1994**, *37*, 2686.
104. Ohkubo, M.; Kuno, A.; Katsuta, K.; Ueda, Y.; Shirakawa, K.; Nakanishi, H.; Kinoshita, T.; Takasugi, H. *Chem. Pharm. Bull.* **1996**, *44*, 778.
105. Rogers, G. A.; Parsons, S. M.; Anderson, D. C.; Nilsson, L. M.; Bahr, B. A.; Kornreich, W. D.; Kaufman, R.; Jacobs, R. S.; Kirtman, B. *J. Med. Chem.* **1989**, *32*, 1217.
106. Chen, Y. L.; Nielsen, J.; Hedberg, K.; Dunaiskis, A.; Jones, S.; Russo, L.; Johnson, J.; Ives, J.; Liston, D. *J. Med. Chem.* **1992**, *35*, 1429.
107. Ornstein, P. L.; Schoepp, D. D.; Arnold, M. B.; Jones, N. D.; Deeter, J. B.; Lodge, D.; Leander, J. D. *J. Med. Chem.* **1992**, *35*, 3111.
108. Stjernlof, P.; Ennis, M. D.; Hansson, L. O.; Hoffman, R. L.; Ghazal, N. B.; Sundell, S.; Smith, M. W.; Svensson, K.; Carlsson, A.; Wikstrom, H. *J. Med. Chem.* **1995**, *38*, 2202.
109. Ohkubo, M.; Kuno, A.; Katsuta, K.; Ueda, Y.; Shirakawa, K.; Nakanishi, H.; Nakanishi, I.; Kinoshita, T.; Takasugi, H. *Chem. Pharm. Bull.* **1996**, *44*, 95.
110. Swain, C. J.; Baker, R.; Kneen, C.; Herbert, R.; Moseley, J.; Saunders, J.; Seward, E. M.; Stevenson, G. I.; Beer, M.; Stanton, J.; Watling, K.; Ball, R. G. *J. Med. Chem.* **1992**, *35*, 1019.
111. Hatano, K.; Takeda, T.; Saito, R. *J. Chem. Soc., Perkin Trans. 2* **1994**, 579.
112. Harrison, T.; Williams, B. J.; Swain, C. J.; Ball, R. G. *Bioorg. Med. Chem. Lett.* **1994**, *4*, 2545.
113. D'Ambra, T. E.; Estep, K. G.; Bell, M. R.; Eissenstat, M. A.; Josef, K. A.; Ward, S. J.; Haycock, D. A.; Baizman, E. R.; Casiano, F. M.; Beglin, N. C.; Chippari, S. M.; Grego, J. D.; Kullnig, R. K.; Daley, G. T. *J. Med. Chem.* **1993**, *35*, 124.
114. Ciganek, E.; Wuonola, M. A.; Harlow, R. L. *J. Heterocycl. Chem.* **1994**, *31*, 1251.
115. Brianso, M. C. *Acta Crystallogr., Sect. B* **1976**, *32*, 3040.
116. Brianso, M. C. *Acta Crystallogr., Sect. B* **1978**, *34*, 679.

117. Brianso, M. C. *Acta Crystallogr., Sect. B* **1981**, *37*, 740.
118. White, J. D.; Bolton, G. L.; Dantanarayana, A. P.; Fox, C. M. J.; Hiner, R. N.; Jackson, R. W.; Sakuma, K.; Warrier, U. S. *J. Am. Chem. Soc.* **1995**, *117*, 1908.
119. Kostyanovskii, R. G.; Rudchenko, V. F.; D'yachenko, O. A.; Chervin, I. I.; Zolotoi, A. B.; Atovmyan, L. O. *Tetrahedron* **1979**, *35*, 213.
120. Freer, A. A.; Kirby, G. W.; Rao, G. V.; Cain, R. B. *J. Chem. Soc., Perkin Trans. 1* **1996**, 2111.
121. Cohen, N.; Weber, G.; Banner, B. L.; Lopresti, R. J.; Schaer, B.; Focella, A.; Zenchoff, G. B.; Chiu, A.-M.; Todaro, L.; O'Donnell, M.; Welton, A. F.; Brown, D.; Garippa, R.; Crowley, H.; Morgan, D. W. *J. Med. Chem.* **1989**, *32*, 1842.
122. Caira, M. R.; Clauss, R.; Nassimbeni, L. R.; Scott, J. L.; Wildervanck, A. F. *J. Chem. Soc., Perkin Trans. 2* **1997**, 763.
123. Grieco, P. A.; Abood, N. *J. Chem. Soc., Chem. Commn.* **1990**, 410.
124. Johansen, T. N.; Ebert, B.; Brauner-Osborne, H.; Didriksen, M.; Christensen, I. T.; Soby, K. K.; Madsen, U.; Krogsgaard-Larsen, P.; Brehm, L. *J. Med. Chem.* **1998**, *41*, 930.
125. Das, J.; Floyd, D. M.; Kimball, S. D.; Duff, K. J.; Vu, T. C.; Lago, M. W.; Moquin, R. V.; Lee, V. G.; Gougoutas, J. Z.; Malley, M. F.; Moreland, S.; Brittain, R. J.; Hedberg, S. A.; Cucinotta, G. C. *J. Med. Chem.* **1992**, *35*, 773.
126. Pettersson, K. *Arkiv Kemi* **1956**, *10*, 283.
127. Gold-Aubert, Ph. *Helv. Chim. Acta* **1958**, *41*, 1512.
128. Greuter, H.; Dingwall, J.; Martin, P.; Bellus, D. *Helv. Chim. Acta* **1981**, *64*, 2812.
129. Hammerschmidt, F.; Vollenkle, H. *Liebigs Ann. Chem.* **1986**, 2053.
130. Lin, G. H. Y.; Wustner, D. A.; Fukuto, T. R.; Wing, R. M. *J. Agric. Food Chem.* **1980**, *28*, 594.
131. Geiger, H. *Arch. Pharm.* **1901**, *239*, 491.
132. Gould, R. O.; Walkinshaw, M. D. *J. Am. Chem. Soc.* **1984**, *106*, 7840.
133. Gould, R. O.; Taylor, P.; Walkinshaw, M. D. *Acta Crystallogr., Sect. A* **1984**, *40*, C85.
134. Dijlsma, F. J. J.; Gould, R. O.; Parsons, S.; Taylor, P.; Walkinshaw, M. D. *Chem. Commn.* **1998**, 745.
135. Boiadjiev, S. E.; Person, R. V.; Puzicha, G.; Knobler, C.; Maverick, E.; Trueblood, K. N.; Lightnet, D. A. *J. Am. Chem. Soc.* **1992**, *114*, 10123.
136. Kuwata, S.; Tanaka, J.; Onda, N.; Yamada, T.; Miyazawa, T.; Sugiura, M.; In, Y.; Doi, M.; Inoue, M.; Ishida, T. *Bull. Chem. Soc. Jpn.* **1993**, *66*, 1501.
137. Pinkerton, A. A.; Carrupt, P.-A.; Claret, F.; Vogel, P. *Acta Crystallogr. Sect. C* **1993**, *44*, 1632.
138. Toda, F.; Tanaka, K. *Tetrahedron Lett.* **1981**, *46*, 4669.
139. Gould, R. O.; Kelly, R.; Walkinshaw, M. D. *J. Chem. Soc., Perkin Trans. 2* **1985**, 847.
140. Gould, R. O.; Taylor, P.; Walkinshaw, M. D.; Bruins Slot, H. J. *Acta Crystallogr. Sect. C* **1987**, *43*, 2405.
141. Larsen, S.; de Diego, H. L.; Kozma, D. *Acta Crystallogr. Sect. B* **1993**, *49*, 310.
142. Gjerløv, A.; Larsen, S. *Acta Crystallogr. Sect. B* **1997**, *53*, 708.
143. Gjerløv, A.; Larsen, S. *Acta Crystallogr. Sect. C* **1997**, *53*, 1505.
144. Tochtermann, W.; Panitzsch, T.; Petroll, M.; Habeck, T.; Schlenger, A.; Wolff, C.; Peters, E.-M.; Peters, K.; von Schnering, H. G. *Eur. J. Org. Chem.* **1998**, 2651.
145. Graham, D. W.; Ashton, W. T.; Barash, L.; Brown, J. E.; Brown, R. D.; Canning, L. F.; Chen, A.; Springer, J. P.; Rogers, E. F. *J. Med. Chem.* **1987**, *30*, 1074.

Chapter 5

Asymmetric Aldol Reactions Using Aldolases

MICHAEL G. SILVESTRI, GRACE DESANTIS, MICHAEL MITCHELL, AND CHI-HUEY WONG

Department of Chemistry, The Scripps Research Institute, 10550 N. Torrey Pines Rd., La Jolla, CA 92037

I. INTRODUCTION

Stimulated by developments in natural product chemistry, organic synthesis has evolved into a well-disciplined system for the construction of carbon–carbon bonds and for the control of stereochemistry. The aldol reaction is a prominent transformation means in organic synthesis. Involved are the control of enolate geometry and facial selectivity, which has traditionally been accomplished using chiral metal complexes or chiral auxiliaries.[1] The new carbon–carbon bond is formed under the control of a chiral environment for the positioning of the acceptor and donor. This design parallels Nature's own method of accomplishing similar goals.[1n]

Topics in Stereochemistry, Volume 23, Edited by Scott E. Denmark.
ISBN 0-471-17622-2

Biocatalysis is becoming recognized as a useful method in organic synthesis. Natural enzymes, engineered protein catalysts, whole cell microbial systems, and catalytic antibodies that demonstrate high selectivity provide attractive alternatives to traditional chemical methods.[2] The reaction conditions are generally mild, and they can proceed in aqueous environments at near neutral pH. The aqueous reaction conditions, lack of heavy metals, toxic reagents, and solvents make biocatalysis an environmentally attractive alternative to standard chemical methods. Additionally, as a result of biocatalyst specificity, the use and manipulation of protecting groups is kept to a minimum. Enzymes are able to perform a multitude of chemical reactions as demonstrated by their prowess in biology. With the growing list of known enzymes, now several thousand long and over a hundred of them commercially available, a wide range of chemical reactivity has been represented. The tailoring and design of new catalysts with specific function and selectivity are moving rapidly forward as a consequence of the advancing database of protein structure and sequence, coupled with advances in molecular biology and protein engineering.

This chapter focuses on biocatalytic methods that have been demonstrated in the aldol and related reactions. Additionally strategies for enzyme engineering and future challenges faced in this field are addressed.

II. ASYMMETRIC REACTIONS

The use of enzymes for the aldol reaction complements traditional chemical approaches. In the early twentieth century a class of enzymes was recognized that catalyzes, by an aldol condensation, the reversible formation of hexoses from their three carbon components.[3] The lyases that catalyze the aldol reaction, are referred to as aldolases. More than 30 aldolases have been characterized to date. These aldolases are capable of stereospecifically catalyzing the reversible addition of a ketone or aldehyde donor to an aldehyde acceptor. Two distinct mechanistic classes of aldolases have been identified (Scheme 5.1).[4]

Type I aldolases are generally found in animals and higher plants. They use an active-site lysine to form a covalent reaction intermediate via Schiff-base formation. Following an imine-to-enamine tautomerization, this activated donor then adds stereoselectively to an acceptor aldehyde. Structures of type I aldolases have been reported for fructose-1,6-bisphosphate aldolase from a variety of sources, including rabbit muscle,[5] human muscle,[6] *Drosophila melanogaster*,[7a] and *Plasmodium falciparum*.[7b] Other type I aldolases including 2-keto-3-deoxy-6-phosphogluconate (KDPG) aldolase

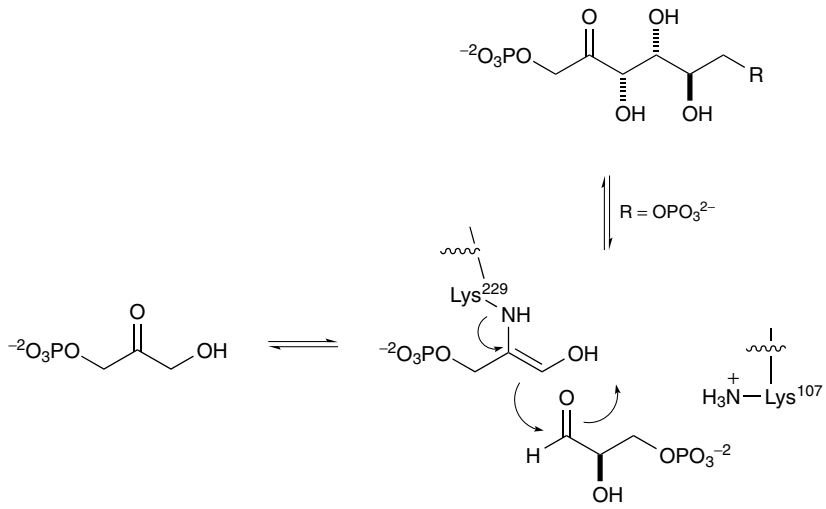

Type I Aldolase

Type II Aldolase

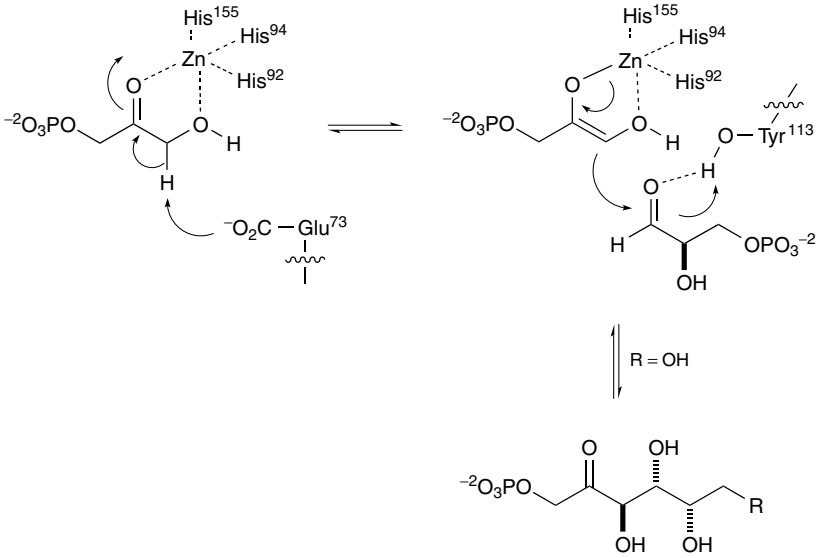

Scheme 5.1. The two types of aldolase mechanisms: The type I Schiff-base forming aldolase is represented by rabbit muscle fructose disphosphate (FDP) aldolase (RAMA, *top*), and the type II zinc enolate aldolase is represented by *E. coli* fructose diphosphate (FDP) aldolase (*bottom*).

from *Pseudomonas putida*,[9] *N*-acetylneuraminate aldolase from *Escherichia coli*,[10] 7,8-dihydroneopterin aldolase from *Staphylococcus aureus*,[11] and deoxyribose 5-phosphate aldolase (DERA)[8] from *E. coli*, have been isolated and structurally characterized.

For several enzymes the Schiff-base intermediate has been trapped by hydride reduction to an unreactive amine.[5–8,12] The X-ray crystal structures of KDPG aldolase[13a] and DERA[13b] complex with substrate have recently been determined, and the detailed mechanism of DERA has been investigated with the aid of the ultra-high-resolution structure of DERA (see the following discussion with DERA). The related Schiff-base intermediate complex of transaldolase (this enzyme catalyzes a transaldol reaction), from *E. coli*, has also been solved.[14a] The crystal structure of this transaldolase has mechanistic implication for the class I aldolases. These studies revealed that the three-dimensional structure of the transaldolase and the active-site architecture are similar to those of class I aldolases, both utilizing a Lys residue to form a Schiff-base intermediate to initiate the aldol reaction. It has been further suggested that the transaldolase may be evolved from an ancestral aldolase.[14b]

Type II aldolases are found in bacteria and fungi. In contrast to the type I aldolases, the type II aldolases require a Zn^{+2} cofactor in the active site.[15] The zinc functions as a Lewis acid to stabilize the donor such as dihydroxyacetone phosphate. Fuculose 1-phosphate aldolase was the first structurally established type II enzyme. Subsequently structures have been determined for fructose 1,6-bisphosphate aldolase and L-rhamnulose 1-phosphate aldolase from *E. coli*. and a mechanistic picture for the type II aldolases has begun to emerge.[16] The important residues that constitute the binding site for the natural substrate have been mapped by a combination of X-ray crystallographic studies (on the *E. coli* type II fructose 1,6-bisphosphate aldolase complexed with the transition state analogue, phosphoglycolhydroxamate), sequence alignments, site-directed mutagenesis, and steady state enzyme kinetics.[17] This enzyme, which catalyzes the reversible cleavage of fructose 1,6-bisphosphate into two triose sugars, dihydroxyacetone phosphate and glyceraldehyde 3-phosphate, is a member of the $(\alpha/\beta)_8$ barrel family of enzymes.[18] The barrel is composed of eight α-helices and eight β-sheets (about 10% of known proteins contain this fold as the active site for binding and catalysis). Its active site and the bound zinc ion are found at the C-terminal end of the barrel. The asymmetric unit is a homodimer of $(\alpha/\beta)_8$ barrels where the substrate is bound in a deep polar cavity at the C-terminal end of the $(\alpha/\beta)_8$ barrel, where it chelates the critical zinc ion using hydroxyl and enolate oxygen atoms of the donor substrate.[12,19] The trigonal bipyramidal coordination of the zinc ion is complexed by three histidine residues (His-110, His-226, and His-264). In the absence of substrate a glutamate residue (Glu-174) additionally binds to the Zn^{+2} ion. As has been shown for fuculose 1-phosphate aldolase, this glutamic acid may additionally

function as the proton shuttle for deprotonation of the donor and protonation of the acceptor oxygen. The rate-determining step is formation of the enolate.

Type II FDP aldolases are more stable than their type I counterparts. For example, the enzyme from *E. coli* has no thiol group in the active site and has a half-life of approximately 60 days in 0.3 mM Zn^{+2} at pH 7.0. The type I enzyme from rabbit muscle (RAMA), by contrast, has a half-life for the free enzyme of approximately 2 days in aqueous solution at pH 7.0.[20] These half-lives can be lengthened by immobilization or enclosure in dialysis membranes.

For both types of enzymes, with few exceptions, highly predictable product stereochemistry is observed, as the stereoselectivity is determined by the enzyme and does not depend on the structure or configuration of the substrate. Aldolases are fairly specific for the donor component but exhibit a more relaxed specificity for the acceptor. The aldolases that have been investigated for use in synthesis are broken down into four main groups, based on the structure of the donor substrates (Scheme 5.2).

The first group is the dihydroxyacetone phosphate (DHAP)-dependent aldolases, which use DHAP as the donor to produce 2-keto-1, 3, 4-trihydroxy motifs. The second group, the pyruvate- or phosphoenol pyruvate (PEP)-dependent aldolases, uses pyruvate to form 4-hydroxy-2-ketoacids. The third

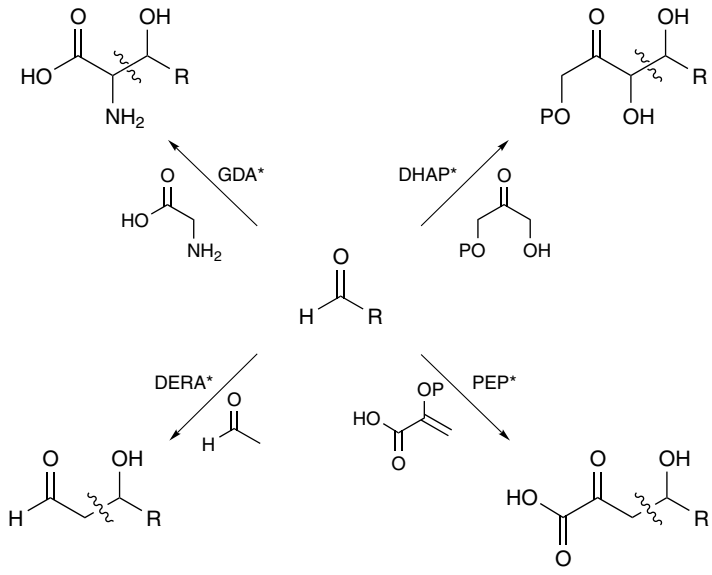

Scheme 5.2. The four main groups of aldolase reactions classified by their donor substrate: (1) Dihydroxyacetone phosphate (DHAP)- dependent aldolases, (2) phosphoenol pyruvate (PEP)- and pyruvate-dependent aldolases, (3) 2-deoxyribose-5-phosphate aldolase (DERA), a member of the acetaldehyde-dependent aldolases, and (4) glycine-dependent aldolases (GDA).

group, consisting of a single example, is the acetaldehyde-dependent aldolase, 2-deoxyribose-5-phosphate aldolase (DERA), which results in the formation of 3-hydroxyaldehydes. The fourth group, the glycine-dependent aldolases, uses glycine as the donor to produce 2-amino-3-hydroxy-acids. In addition to these four groups, the transketolases and transaldolases, capable of transferring, respectively, the C(1)–C(2) ketol or C(1)–C(3) aldol unit from one sugar to an aldehyde, share similarities with the aldolases, and selectively form aldol like products. In the following sections these six groups are discussed in more detail. In addition the proficiency of aldol-catalyzing catalytic antibodies or abzymes are compared.

A. DHAP-Dependent Aldolases

In vivo, six known DHAP-dependent aldolases are known to catalyze the reversible enanotioselective aldol addition of dihydroxyacetone phosphate to an acceptor aldehyde. The group is comprised of fructose 1,6-diphosphate (FDP) aldolase (EC 4.1.2.13), L-fuculose 1-phosphate (Fuc 1-P) aldolase (EC 4.1.2.17), tagatose 1,6-diphosphate (TDP) aldolase (EC 4.1.2.2), ketotetrose phosphate aldolase (EC 4.1.2.2), L-rhamnulose 1-phosphate (Rha 1-P) aldolase (EC 4.1.2.19), and phospho-5-keto-2-deoxygluconate aldolase (EC 4.1.2.29). The in vivo catalyzed reactions of this group are shown in Scheme 5.3.

In addition to the natural substrates as shown in Scheme 5.3, many of these enzymes are capable of reacting with a wide range of aldehyde acceptors.[2a] In general, unhindered aliphatic aldehydes and α-heteroatom substituted aldehydes, including monosaccharides and their derivatives, are suitable acceptors. Sterically hindered aldehydes, α, β-unsaturated aldehydes and aromatic aldehydes are generally not suitable substrates for these reactions. Hydroxylated aldehydes are generally superior substrates, due to their higher affinity to the enzyme active site. When α-hydroxy- or β-hydroxyaldehydes are used as acceptors, the hydroxyl group and the carbonyl of the resulting products form a stable 5- or 6-membered cyclic acetals thus driving the aldol reaction toward condensation. Additionally phosphorylated aldehydes, because of their similarity in structure with the natural substrate, D-glyceraldehyde 3-phosphate, show enhanced reactivity rates relative to their nonphosphorylated counterparts.[21]

The absolute configuration of the products from the aldolase-catalyzed reactions with unnatural substrates generally parallels that observed for the natural substrates. Fructose 1,6-diphosphate aldolase, almost without exception, generates products with the D-threo configuration for the two newly formed carbon centers as found in the natural substrate of FDP (see Scheme 5.3). With the RAMA derived FDP aldolase, Lys-229 activates the DHAP through Schiff-base formation, while the negatively charged phosphate group of DHAP interacts with the quanidinium side chain of Arg-148. Lys-107, which is

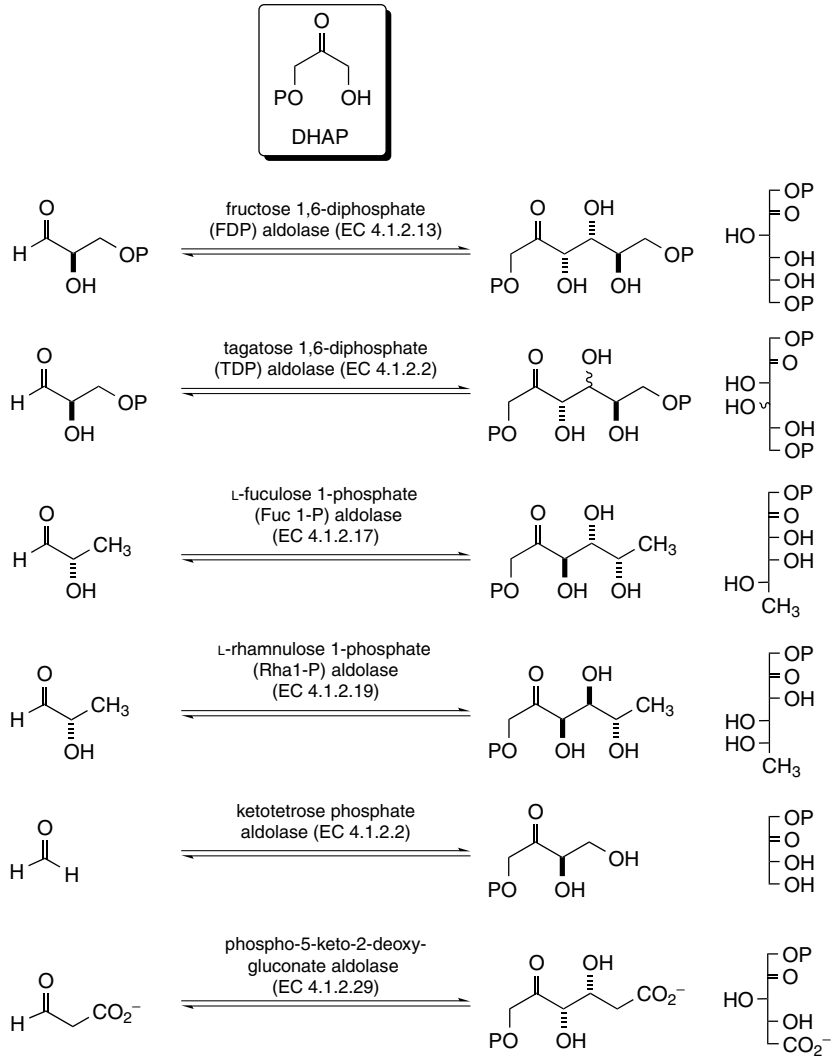

Scheme 5.3. Dihydroxyacetone phosphate (DHAP) dependent aldolases, their natural substrates and products. P = PO_3^{2-}.

approximately 8.9 Å from the site of Schiff-base formation, is thought to stabilize the phosphate group of glyceraldehyde 3-phosphate.[22] Nucleophilic *si*-face attack onto the *R*-aldehyde is favored because of the decreased steric hindrance as compared to the *S*-isomer; R_1=OH for the *R*-isomer, and R_2=OH for the *S*-isomer (Scheme 5.4).[23] By contrast, tagatose 1,6-diphosphate (TDP)

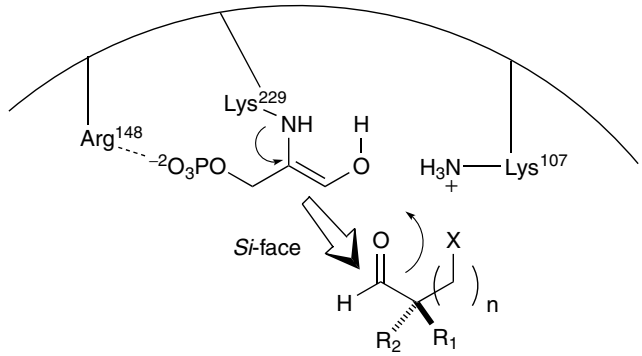

Scheme 5.4. Enzyme catalyzed *Si*-face attack is favored with the *R*-aldehyde: $R(R_1 = OH)$; $S(R_2 = OH)$.

aldolase, yields diastereomeric mixtures in most examples that have been studied.[24] As a result this enzyme has not shown itself to be synthetically valuable. L-Fuculose 1-phosphate (Fuc 1-P) aldolase and L-rhamnulose 1-phosphate (Rha 1-P) aldolase usually generate products with the D-erythro and L-threo configurations, respectively. Since the products of the DHAP aldolase reactions are phosphorylated, acid phosphatases (EC 3.1.3.2) are often utilized to produce the dephosphorylated products.

The aldehyde substrates may be used as racemic mixtures in many cases, as the aldolase catalyzed reactions can concomitantly accomplish kinetic resolution. For example, when DHAP was combined with D- and L-glyceraldehyde in the presence of FDP aldolase, the reaction proceeded 20 times faster with the D-enantiomer. Fuc 1-P aldolase and Rha 1-P aldolase show kinetic preferences (greater than 19/1) for the L-enantiomer of 2-hydroxy-aldehydes. Alternatively, these reactions may be allowed to equilibrate to the more thermodynamically favored products. This thermodynamic approach is particularly useful when the aldol products can cyclize to the pyranose form. Since the reaction is reversible under thermodynamic conditions, the product with the fewest 1,3-diaxial interactions will predominate. This was demonstrated in the formation of 5-deoxy-5-methyl-fructose-1-phosphate as a minor product (Scheme 5.5).[20*a*,25] The major product, which is thermodynamically more stable, arises from the kinetically less reaction acceptor.

Despite the broader substrate tolerance for aldehyde acceptors by DHAP-dependent aldolases, the donor substrate specificity is narrow. With the exception of DHAP, only a few donors have shown to be acceptable as weak substrates (Scheme 5.6).[20*a*,21*a*,26]

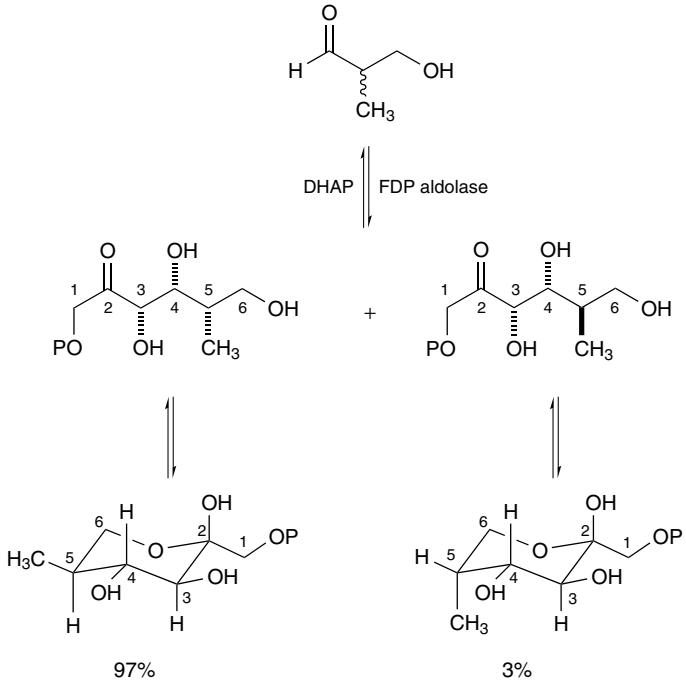

Scheme 5.5. Product stereochemistry is thermodynamically controlled. A = aldolase; P = PO_3^{2-}.

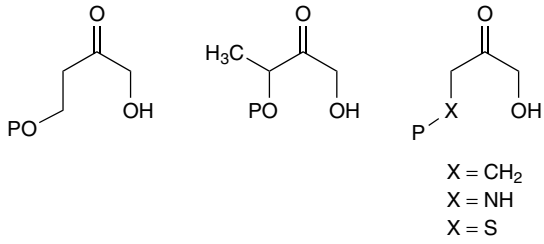

Scheme 5.6. DHAP analogues that are substrates for RAMA. P = PO_3^{2-}.

The preparation of DHAP for synthetic applications has been accomplished both enzymatically and chemically (Scheme 5.7).[27] DHAP can be generated enzymatically in situ from fructose 1,6-diphosphate, using FDP aldolase acting in its catabolic mode, and triosephosphate isomerase (TPI). Glyceraldehyde 3-phosphate (G3P) and DHAP are produced in this reaction, with the G3P rapidly undergoing isomerization to DHAP.

DHAP has also been prepared by phosphorylation of dihydroxyacetone with glycerol kinase in the presence of ATP, with in situ regeneration of ATP, giving yields in excess of 80%. The use of chemical methods[26a–c] for the preparation of DHAP generates a pure product, which results in a cleaner aldol reaction. In an improved and commonly used chemical preparation, the protected dimer of dihydroxyacetone was phosphorylated with diphenyl chlorophosphate, followed by hydrogenolysis and hydrolysis, to give clean DHAP in 61% yield (Scheme 5.8).[28]

Preparation of the DHAP analogue, 4-hydroxy-3-oxobutylphosphonic acid, which is an effective donor substrate, is accomplished in four steps from glycidol.[29] Glycidol is silyl protected; then its epoxide is opened by dimethyl methylphosphonate. The secondary alcohol was oxidized under the Dess-Martin conditions. Deprotection of the alcohol followed by phosphate hydrolysis, generated the DHAP phosphonate analogue (Scheme 5.9).

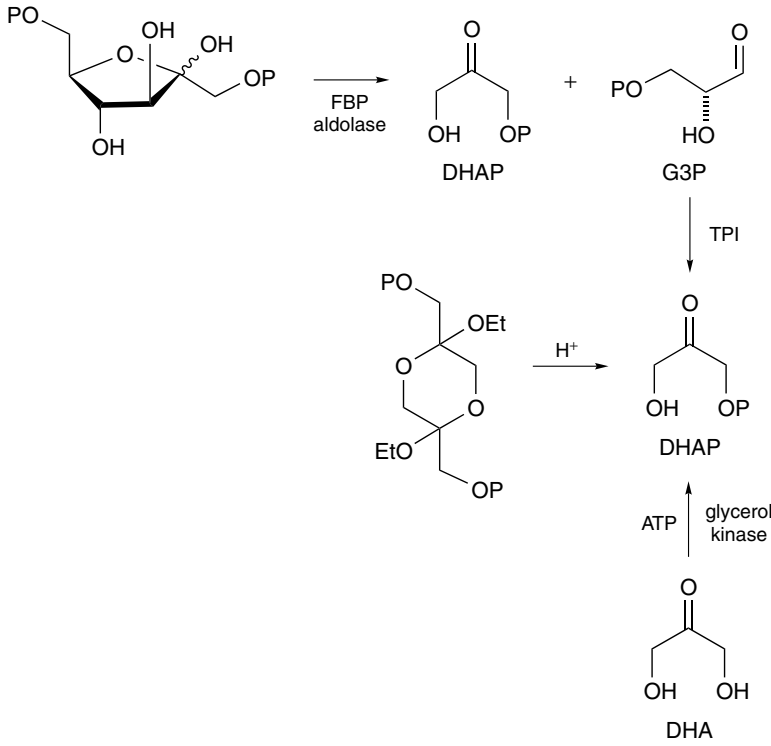

Scheme 5.7. Chemical and enzymatic preparations of DHAP. TPI = triosephosphate isomerase; ATP = adenosine triphosphate; P = PO_3^{2-}.

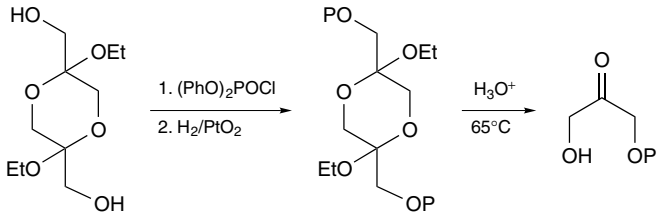

Scheme 5.8. Chemical synthesis of DHAP. $P = PO_3^{2-}$.

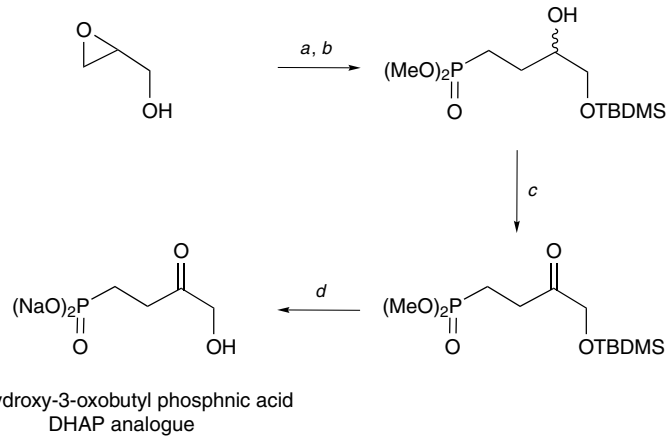

Scheme 5.9. Preparation of a DHAP analogue. Conditions: (*a*) TBDMSCI, imidazole; (*b*) $MeP(O)(OMe)_2$, BuLi, BF_3/Et_2O; (*c*) Dess-Martin reagent; (*d*) (*i*) TMSBr, (*ii*) NaOH.

As a result of the broad substrate tolerance and predictable product stereochemistry, DHAP-dependent aldolases have been frequently utilized in synthetic endeavors. With over a hundred known aldehyde substrates, DHAP-dependent aldolases have been used in the preparation of a large number of monosaccharides from simple precursors, including ^{13}C-labeled sugars, heterosubstituted sugars, deoxysugars, fluorosugars, long-chain sugars, and cyclitols.[2a,30] Additionally this enzymatic approach has been extended to a variety of noncarbohydrate natural products.

Preparation of enantiometrically pure aldehyde substrates for DHAP-dependent aldolase reactions has been accomplished by a combination of enzymatic and chemical methods. The lipase-catalyzed resolution of racemic aldehyde precursors has been accomplished by enantioselective acetate hydrolysis, as exhibited in the preparation of enantiomerically pure *R*- and *S*-glycidaldehyde acetals (Scheme 5.10).[31] Regioselective ring opening of the epoxides, followed by acetal hydrolysis, generated the aldehydes in enantiomerically pure form.

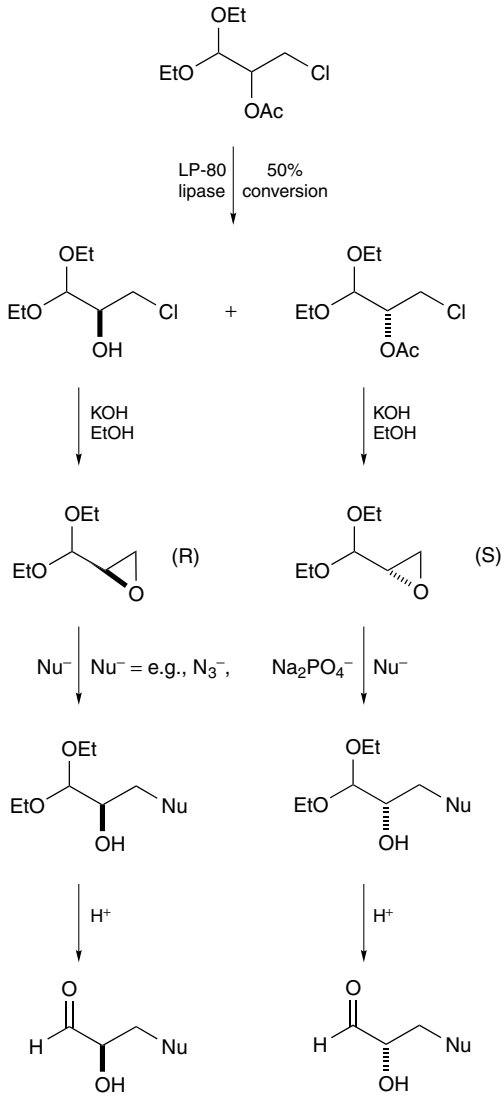

Scheme 5.10. Preparation of enantiomerically pure aldehyde substrates for DHAP-dependent aldolases.

When the Sharpless osmium-catalyzed dihydroxylation procedure is used in tandem with an aldolase-catalyzed addition, a rapid stereoselective entry to a variety of carbohydrates is achieved (Scheme 5.11).[32] By judicious choice of hydroxylation and aldolase conditions, a number of the possible hexose

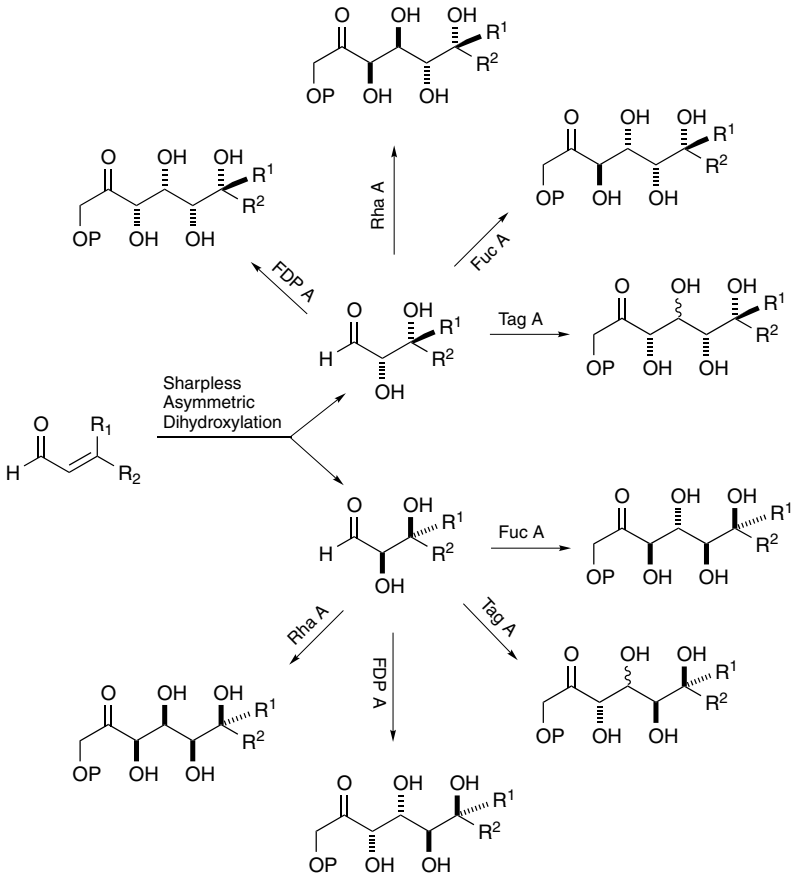

Scheme 5.11. Tandem asymmetric dihydroxylation coupled with aldolase conditions. A = aldolase, P = PO_3^{2-}.

stereoisomers are available, starting from achiral acroleins. Additionally L-sugars as well as the natural D-sugars are available by appropriate selection of aldehyde and aldolase. This is evidenced by contrasting the FDP-catalyzed reaction of D-glyceraldehyde with DHAP and the Rha 1-P-catalyzed reaction of L-glyceraldehyde with DHAP (Scheme 5.12).[33] Derivatives of sialic acid (SA) and 2-keto-3-deoxyoctanoate (KDO), a component of the cell wall of gram-negative bacteria, are both difficult to prepare by the chemical approach or from natural product augmentation. These were easily prepared by the aldolase condensation of DHAP with hexose and pentose sugars, respectively (Scheme 5.13).[21b] This procedure extends the chain length of the sugar by three carbons while concurrently introducing two new stereogenic centers.

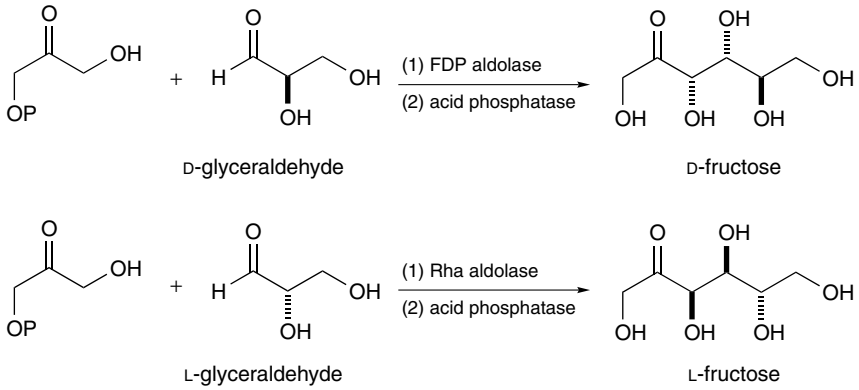

Scheme 5.12. Synthesis of D- and L-fructose catalyzed by fructose 1,6-diphosphate and rhamnulose 1-phosphate aldolases. $P = PO_3^{2-}$.

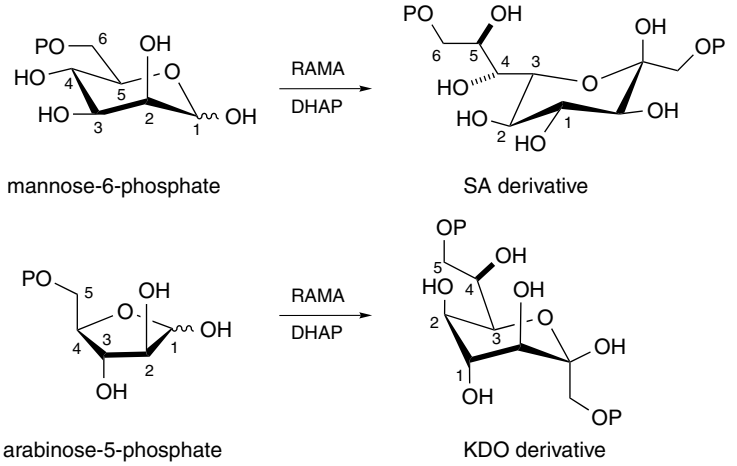

Scheme 5.13. Synthesis of sialic acid and KDO derivatives from hexose and pentose sugars, respectively. $P = PO_3^{2-}$.

The monosaccharides formed in the DHAP-dependent aldolase-catalyzed reaction described above are ketose sugars. As many of the important naturally occurring carbohydrates are aldoses, the desire to extend this methodology to allow their formation has led to the use of isomerases. Glucose isomerase (GI) catalyzes the isomerization of fructose into glucose. This procedure is used in the food industry for the production of high-fructose corn syrup. GI will also accept fructose analogs that are modified at positions 3, 5, and 6. A series of 6-substituted glucoses have been synthesized using the FDP aldolase/GI

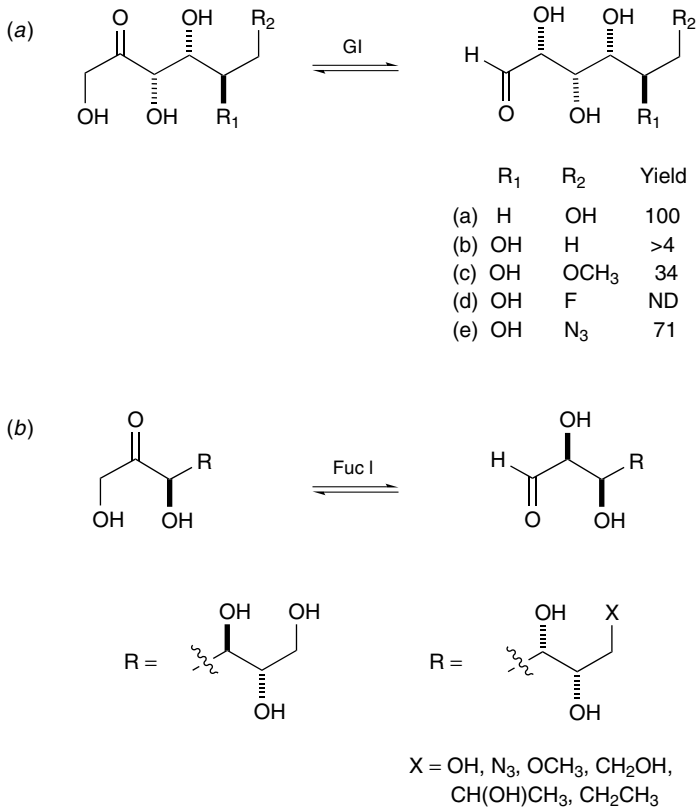

Scheme 5.14. Glucose isomerase (GI) and fuculose isomerase (Fuc I) are used in the preparation of aldoses from ketoses.

methodology (Scheme 5.14).[25b,34] Rha isomerase (Rha I; EC 5.3.1.14) and Fuc isomerase (Fuc I, EC 5.3.1.3) have been cloned and overexpressed and applied for the preparation of a variety of aldoses.[25a]

An alternate approach, the "inversion strategy," is useful for the transformation of ketose to aldose products.[35] In this procedure mono-protected dialdehydes were allowed to react with DHAP in the presence of an aldolase to generate ketoses. The ketones are then reduced either chemically or enzymatically. When the aldehyde-protecting group is removed, the aldose is revealed.[27g,36]

In the chemical synthesis of complex natural products, the concept of bi-directional chain synthesis has also been shown effective for the bi-directional backbone extension, as implemented by DHAP-dependent aldolases.[37] As such, highly complex carbohydrate mimics may be obtained in a single pot

operation. For example, when hexa-1,5-diene-3,4-diol is ozonized to a dialdehyde, and then treated with DHAP under the FruA conditions, an enantiomerically and diastereomerically pure form of a 10-carbon diketose was formed (Scheme 5.15). In both aldol reactions the (*R*)-enantiomer of the aldehyde was converted to the product with the new stereogenic centers in the same relative configurations as the natural product FDP.

This procedure has also been used to prepare a series of hydrolytically stable dipyranoid disaccharide mimetics from homologous dihydroxy-α,ω-dialdehydes[37] (Scheme 5.16). While the FruA and FucA reactions are selective for the (*R*)-aldehyde, the RhuA reactions are selective for the (*S*)-aldehydes, all giving thermodynamically more stable product with retention of the natural stereochemistry for the two newly formed carbon centers.

However, when the dialdehydes lack an α-hydroxyl substitutent, they undergo a single aldol reaction catalyzed by RAMA, leading to the synthesis of highly functionalized monoaldehydes (Scheme 5.17).[38] The enzyme does not exhibit any strong stereochemical selection and consumes all stereoisomers of the dialdehyde. Dialdehydes separated by a hydrophobic ring are not substrates for RAMA.

Heteroatom-substituted carbohydrates are efficiently assembled by the enzymatic aldol condensation of DHAP with an appropriately appended aldehyde. Iminocyclitols that are inhibitors of glycosidases, such as deoxynojirimycin and deoxymannojirimycin, are simply prepared by condensation of azo-substituted aldehydes under the FDP protocol followed by dephosphorylation and palladium mediated reductive amination (Scheme 5.18*a*).[39] In addition a number of polyhydroxylated pyrrolidines that are efficient glucosidase inhibitors have been synthesized by this chemo-enzymatic strategy (Scheme 5.18*b*).[1*n*,30,40] If the palladium mediated hydrogenation is done in the presence of hydrochloric acid, an amino-sugar intermediate is formed as its hydrochloride salt. Treatment with base then forms polyhydroxylated imines, instead of iminocyclitols (Scheme 5.19).[41]

Thiosugars can be rapidly synthesized when sulfur-substituted aldehydes are condensed with DHAP under the influence of FDP aldolase.[42] The synthesis of these heterocycles is completed by phosphate cleavage, acetylation and reduction of the resultant ketone (Scheme 5.20). Cyclitols, another interesting class of biologically active compounds, have been prepared through the reaction of phosphonate- and nitro-substituted aldehydes with DHAP under the influence of FDP aldolase (Scheme 5.21).[43,43*b*]

Aldolases have been applied to the synthesis of noncarbohydrate products. An early report demonstrated the utility of RAMA in the synthesis of (+) *exo*-brevicomin, the sex pheromone of the western bark beetle, *Dendroctonus brevicomis* (Scheme 5.22).[44] DHAP reacts with hexane-1,5-dione under the influence of RAMA. After the phosphate is cleaved, an acid-catalyzed

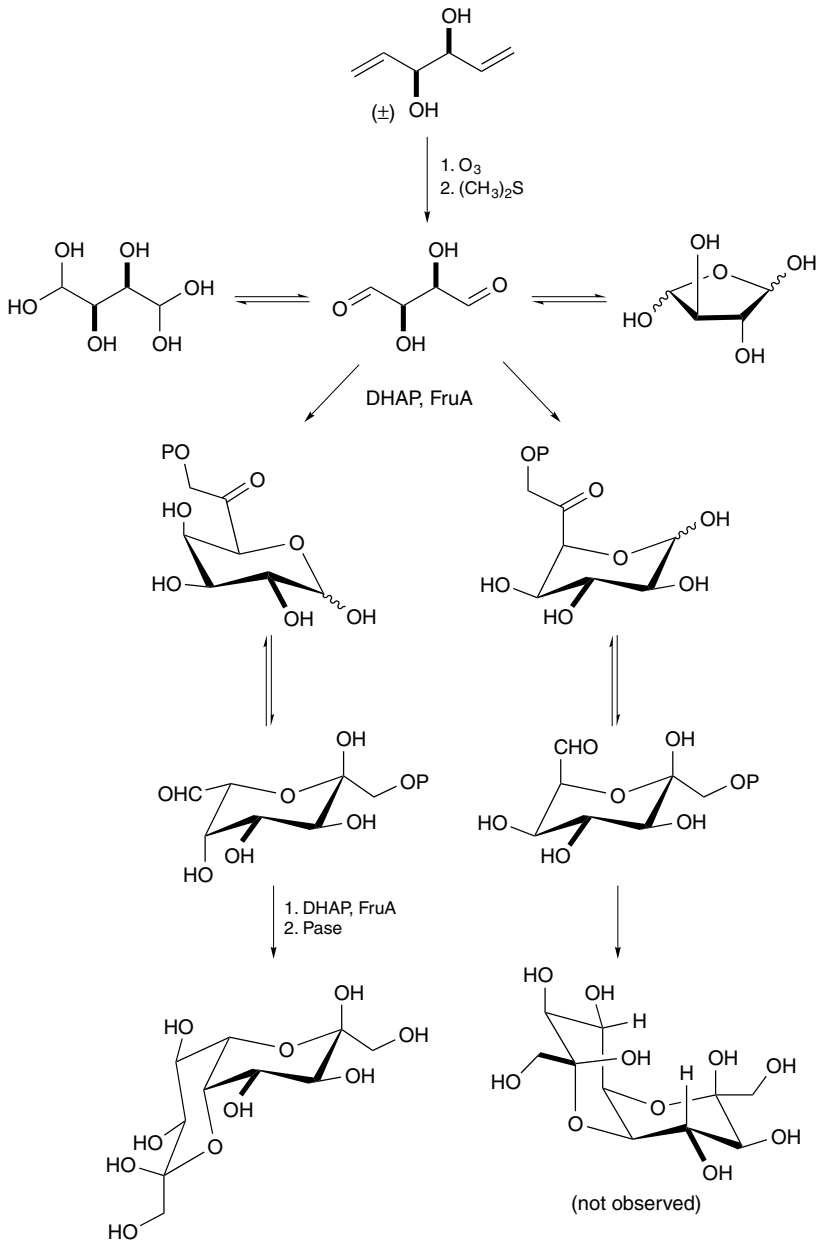

Scheme 5.15. Divergent pathways for tandem aldol additions of dihydroxyacetone phosphate (DHAP) with racemic tartaric dialdehyde, catalyzed by fructose 1,6-bisphosphate (FruA). P = PO_3^{2-}; Pase = phosphatase.

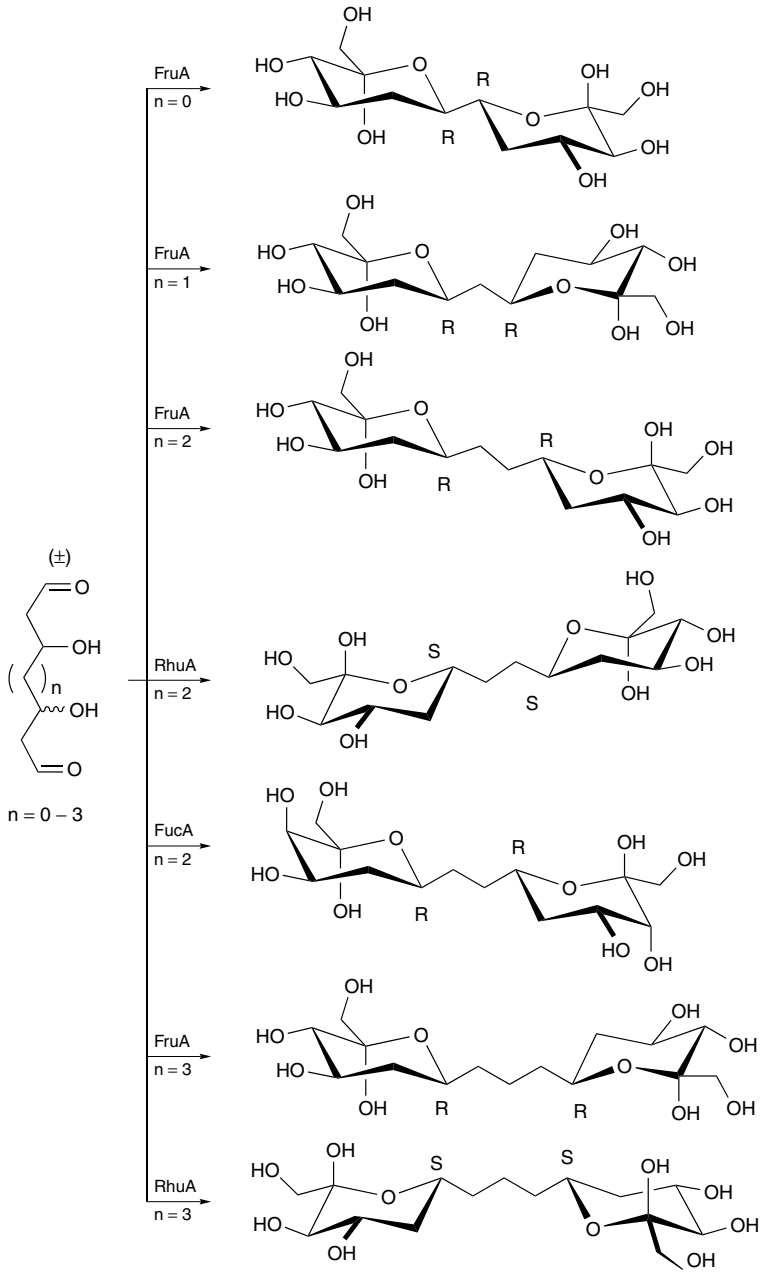

Scheme 5.16. Formation of a series of hydrolytically stable dipyranoid disaccharide mimetics from homologous dihydroxy-α,ω-dialdehydes by tandem enzymatic aldolizations. Major diastereomers are shown. Reaction conditions include sequential treatment by aldolase and phosphatase.

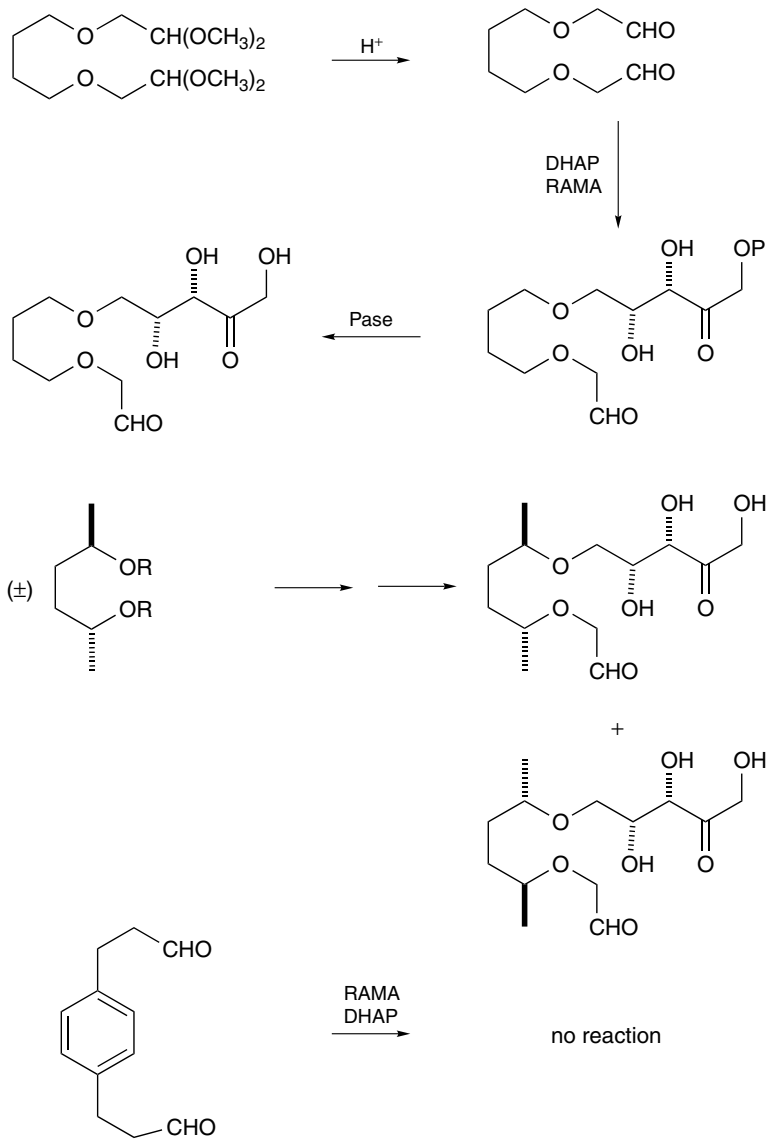

Scheme 5.17. Enzymatic single aldol reactions of remote dialdehydes. BDA = bromoacetaldehyde dimethyl acetal; Pase = phosphatase.

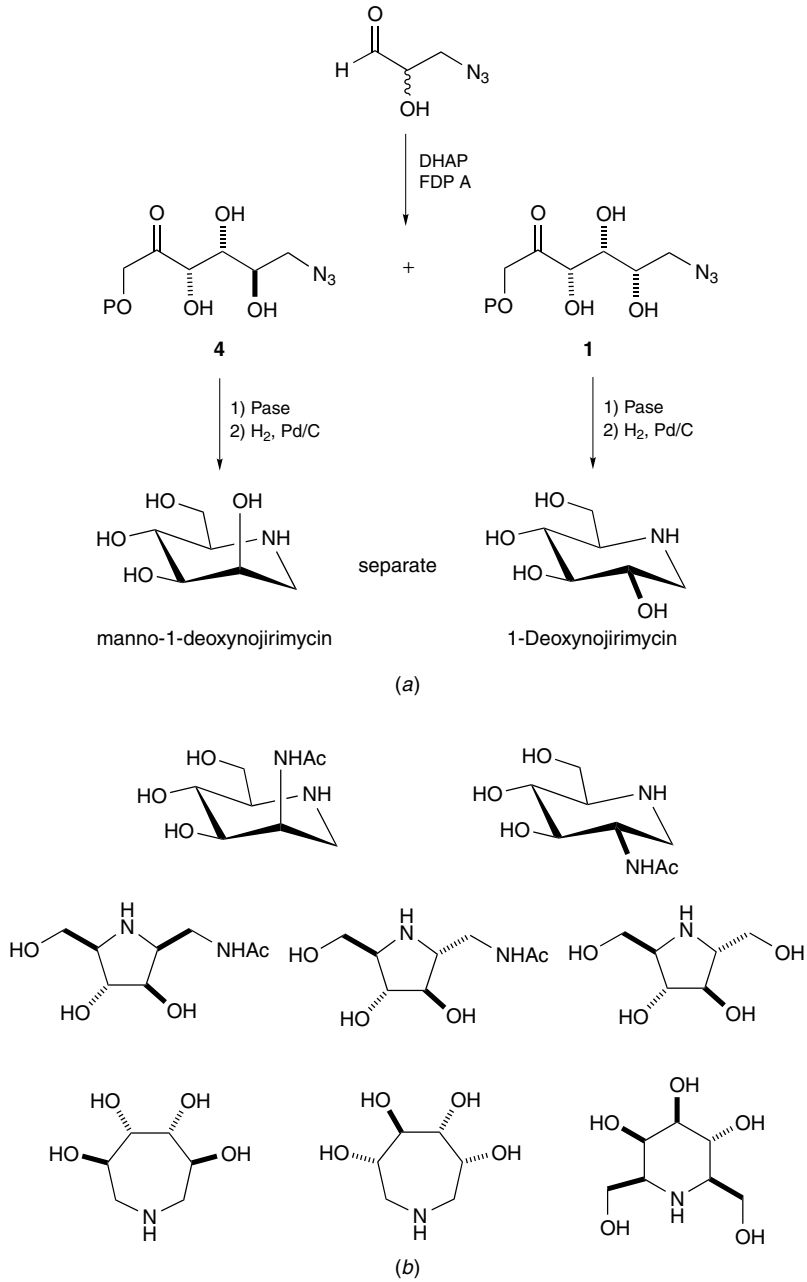

Scheme 5.18. (*a*) Synthesis of iminocyclitols from azidoaldehydes and DHAP. (*b*) Polyhydroxylated pyrrolidine inhibitors.

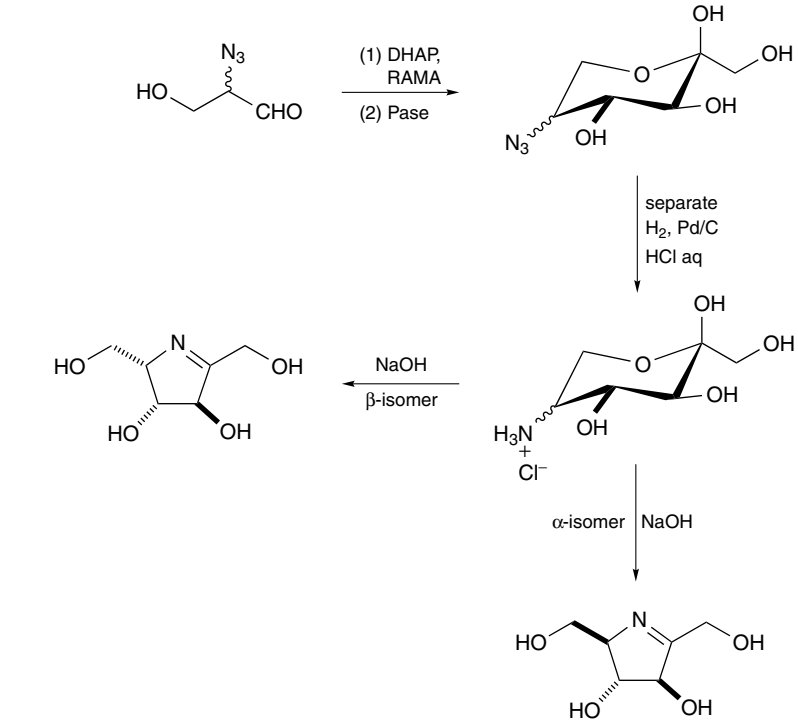

Scheme 5.19. Chemoenzymatic synthesis of novel cyclic imine sugars. Pase = phosphatase.

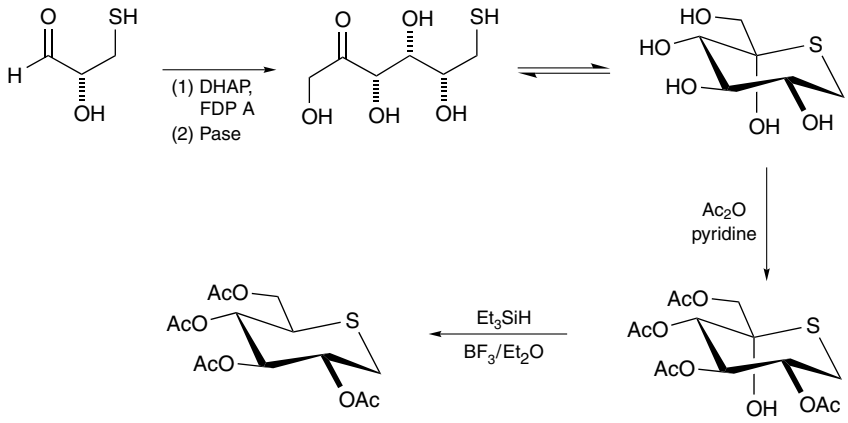

Scheme 5.20. Synthesis of thio sugars from thioaldehydes and DHAP. Pase = phosphatase.

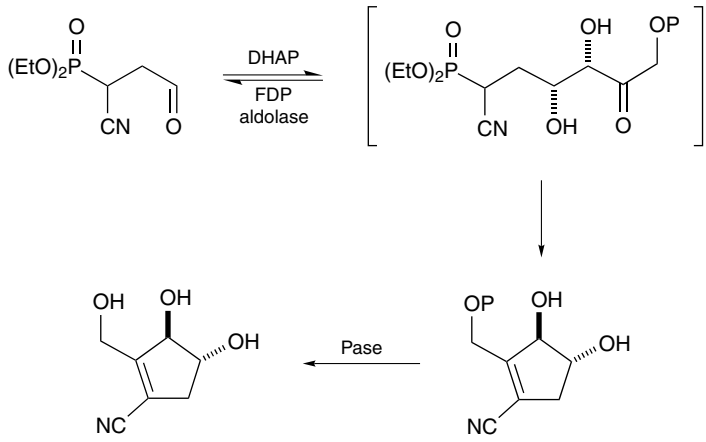

Scheme 5.21. Chemoenzymatic synthesis of cyclitols. P = PO_3^{2-}, Pase = phosphatase.

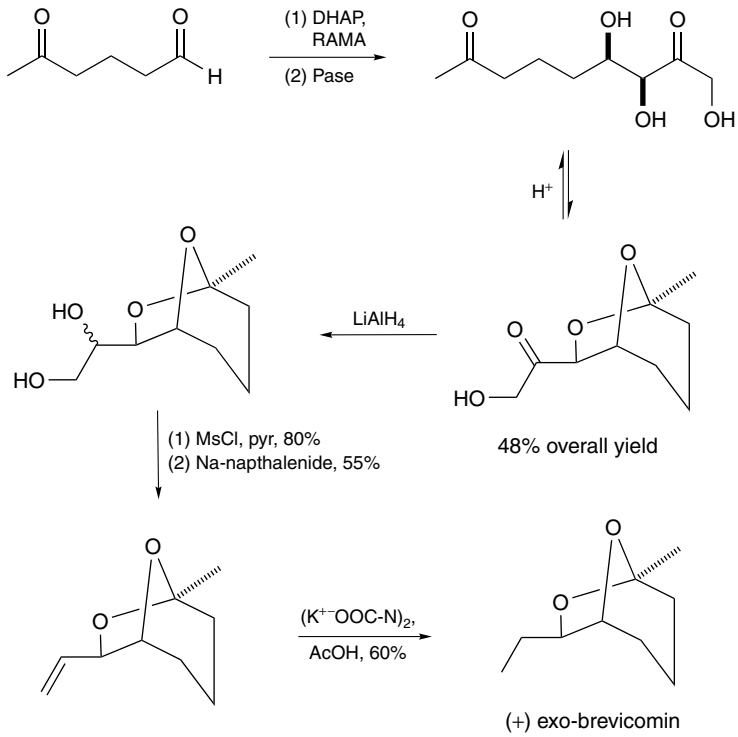

Scheme 5.22. Chemoenzymatic synthesis of (+) *exo*-breviocomin by rabbit muscle aldolase (RAMA). Pase = phosphatase.

intramolecular acetal formation generates the required bicyclic ring system. After ketone reduction and elimination of the resultant diol, the synthesis is completed with a diimide reduction of the resultant vinyl side chain.

Stereoselective synthesis of the C11–C16 fragment of the polyene macrolide antibiotic, pentamycin, has also been accomplished under the aldolase protocol.[45] A formyl and benzyl protected aldehyde, available from D-glucose by chemical methods, reacts with DHAP under the influence of FDP aldolase. After phosphatase hydrolysis the essential C11–C16 skeleton of pentamycin is generated. Removal of an additional hydroxyl group at position 1 and isolation of the C11–C16 fragment as a thioacetal, is accomplished in several steps (Scheme 5.23).

A formal total synthesis of (+)-aspicilin, an 18-membered ring lactone isolated from the lichen *Aspicilia gibbosa*, is accomplished by the FDP aldolase protocol.[46] The three carbon chain extension of benzyl protected 4-hydroxybutanal is achieved with DHAP under the influence of FDP aldolase. The acid

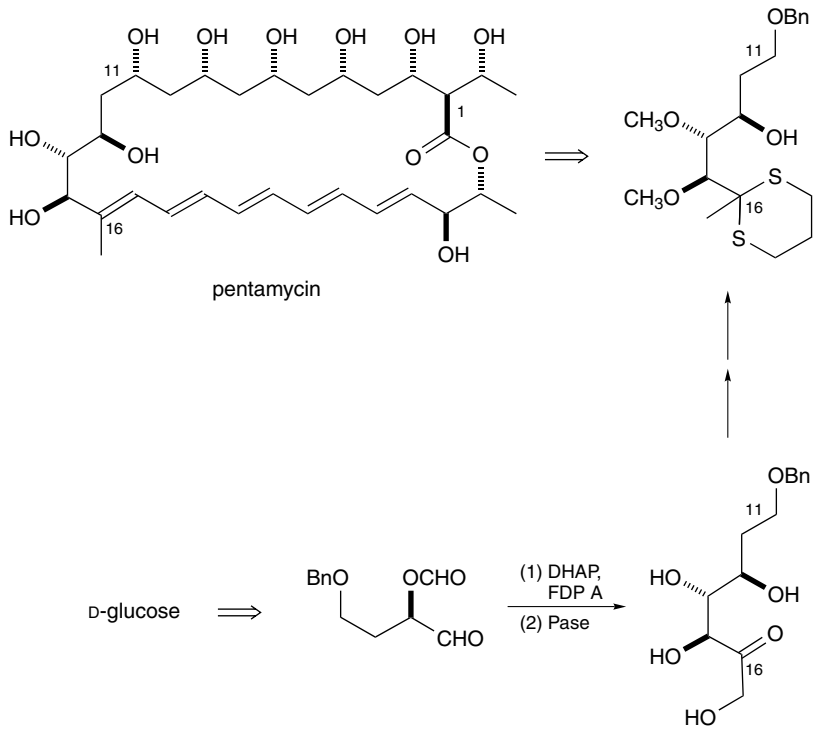

Scheme 5.23. Synthesis of the C11–C16 fragment in the formal total synthesis of Pentamycin. Pase = phosphatase.

phosphatase derived ketose is reduced by a hydride reagent to complete setting the three stereogenic centers for the C3–C9 fragment of aspicilin. After a protection sequence, the fragment that had previously been converted to aspicilin is formed, thus completing the formal total synthesis (Scheme 5.24).

An efficient five step total synthesis of (−)-syringolide, an elicitor of the bacterial plant pathogen *Pseudomonas syringae*, is accomplished by similar aldolase chemistry.[47a] The key enzymatic step involves setting the critical glycol configuration through the FDP aldolase reaction of DHAP with the 4-methoxyphenylmethyl protected 2-hydroxyacetaldehyde. The acetonide-protected product then participated in a Knoevenagel reaction with 5-(1-hydroxy-octylidene)-2,2-dimethyl-[1,3]dioxane-4,6-dione. DDQ deprotection of the MPM derivative, followed by acid catalyzed cyclization, completed the synthesis of syringolide (Scheme 5.25).

Mimetics of sialyl Lewis X, the terminal tetrasaccharide of glycoproteins and glycolipids that are known to interact with selectins in the inflammatory process, have been efficiently synthesized through the use of the enzymatic aldol condensation (Scheme 5.26).[29] This straightforward approach involved the condensation of mannosyl aldehyde derivatives with DHAP in the presence of DHAP-dependent aldolases. The aldehyde acceptors are generated from mannose by protection of the anomeric center as allyl ether, followed by

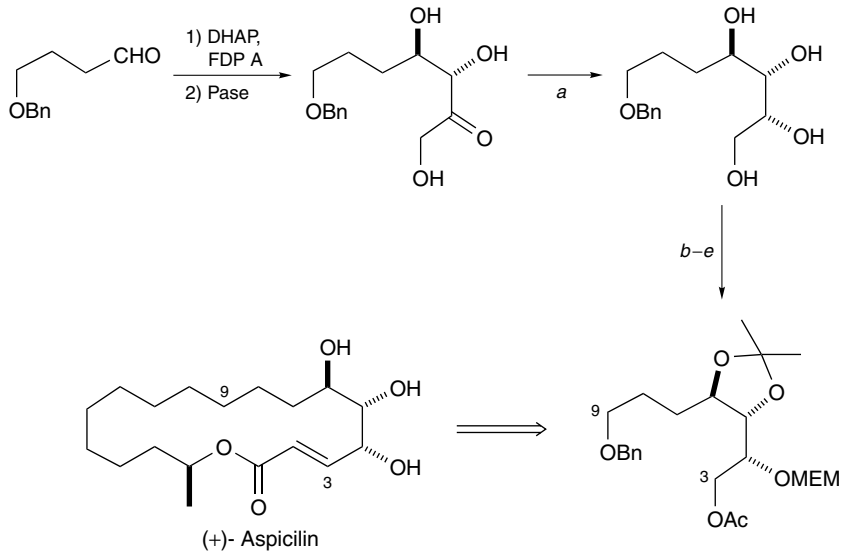

Scheme 5.24. Stereoselective synthesis of aspicilin C3–C9 fragment. Conditions: (*a*) $NaBH(OAc)_3$; (*b*) $Me_2C(OMe)_2$, H^+; (*c*) MeOH, H^+; (*d*) AcCl, collidine; (*e*) MEMCl, *N*, *N*-diisopropylethylamine. Pase = phosphatase.

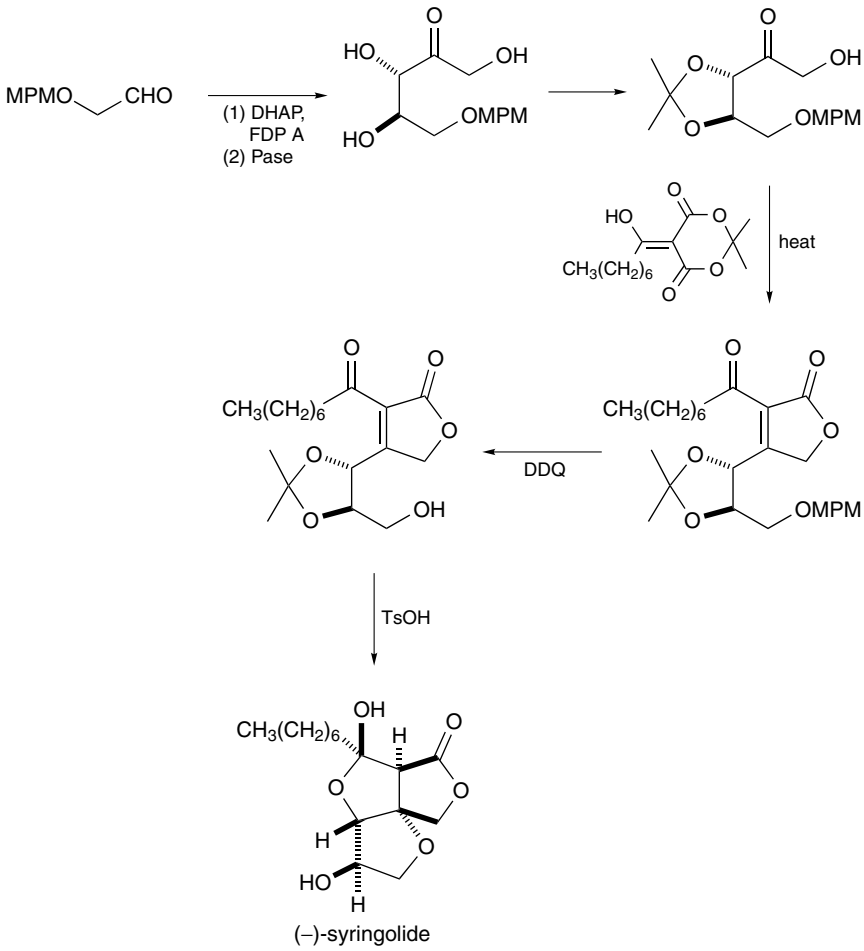

Scheme 5.25. Chemoenzymatic synthesis of (−)-Syringolide. Pase = phosphatase.

ozonolysis. These aldehydes undergo enzymatic condensation with DHAP and its 4-carbon phosphonate isostere. By a judicious choice of aldolase, the three stereoisomers were obtainable.

The double aldol reaction strategy can also be used in conjunction with palladium-mediated reductive amination to produce tetrahydroxy pyrrolizidine alkaloids, including 3-epiaustraline, australine, and 7-epialexine (Scheme 5.26(b)).[47b] These alkaloid natural products are active as glycosidase inhibitors.

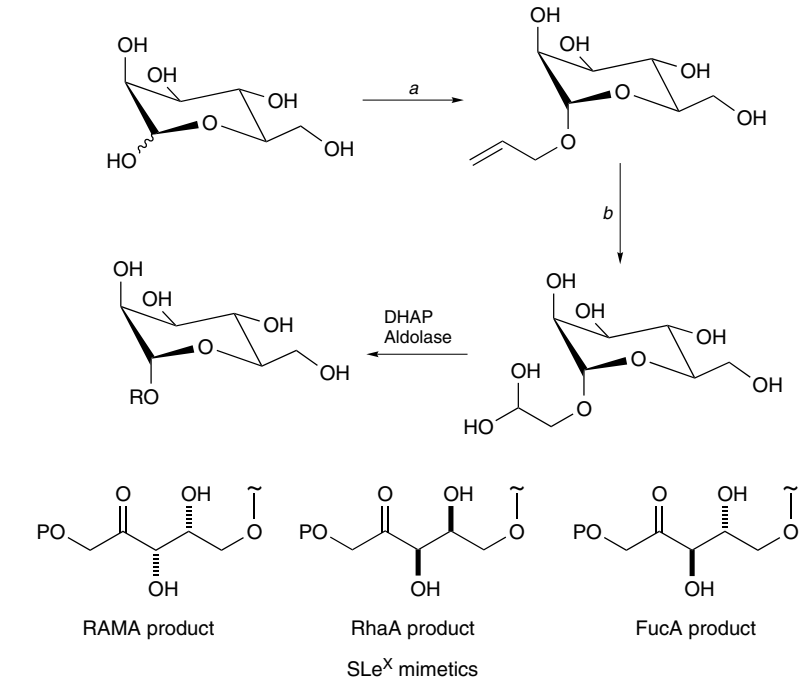

Scheme 5.26. (*a*) Synthesis of sialyl Lewis X (SLe^x) mimetics. Conditions: (*a*) allyl alcohol, CSA; (*b*) (*i*) O_3, (*ii*) PPh_3. P = PO_3^{2-}. (*b*) Tetrahydroxypyrrolizidine alkaloids prepared by double aldol reaction. (*a*) $NaIO_4/H_2O$; DHAP/RAMA; phosphatase, 30%. (*b*) O_3, $MeOH/H_2O$, then HCl, $NaOAc/NaCNBH_3$, 52%. (*c*) O_3, $MeOH/H_2O$, then HCl and H_2, Pd/C, 70%.

B. Pyruvate and Phospoenolpyruvate — Dependent Aldolases

Pyruvate-dependent aldolases have catabolic activity in vivo, whereas their counterparts utilizing phosphoenolpyruvate as the donor substrate are involved in the biosynthesis of keto acids. Both classes of enzymes have been used in synthesis to prepare similar α-keto acids. The enzymes catalzye this type of reaction in vivo and their stereoselectivity are presented together in this section (Schemes 5.27, 5.28).

In vivo, the enzyme *N*-acetylneuraminic acid (NeuAc) aldolase (EC 4.1.3.3), also known as sialic acid aldolase, catalyzes the reversible aldol reaction of *N*-acetyl-D-mannosamine (ManNAc) and pyruvate to form *N*-acetyl-5-amino-3,5-dideoxy-D-glycero-D-galacto-2-nonulosonic acid (NeuAc or sialic acid) (Scheme 5.29*a*).[48] With an equilibrium constant of 12.7 M^{-1}, the retro-aldol reaction is favored. However, for synthetic purposes, an equilibrium favoring the aldol addition reaction can be achieved by the use of excess pyruvate. In these cases the excess pyruvate can be destroyed by the use of pyruvate decarboxylase.[49] Alternatively, the use of excess pyruvate can be avoided by coupling the NeuAc synthesis to a second step, leading to a thermodynamically more stable product. For example, in the preparation of sialylsaccharides, the NeuAc aldolase was paired with CMP-sialic acid synthase and sialytransferase, which catalyze the conversion of NeuAc to a sialylsaccharide irreversibly thus driving the reaction toward condensation (Scheme 5.29*b*).[50] NeuAc aldolase has been isolated from both bacteria and animals. In both cases it has been found to be a Schiff-base forming type I aldolase. The optimum pH for enzymatic activity is 7.5, but the enzyme retains its activity from pH 6 to 9, and is stable under oxygen.[49*a*,51]

The commercially available NeuAc aldolase from *Clostridia* or *E. coli* has been extensively studied. This enzyme is highly specific for pyruvate as the donor but is flexible toward a variety of enantiomeric acceptor substrates, including hexoses, pentoses and tetroses.[30] Substitutions as C(4), C(5), and C(6) are allowed with a slight preference for the configuration of the natural substrate, *N*-acetyl-D-mannosamine (ManNAc). Relatively small substituents are tolerated at C(2), where the stereochemistry at that center is the same as the natural substrate. A free hydroxyl at position C(3) is, however, required for the success of the reaction.[52]

Unlike most aldolases, the stereochemical outcome of NeuAc-aldolase-catalyzed reactions depend on the structure of the acceptor substrates. With acceptor substrates of the natural *S*-configuration at C(3), the carbonyl group is attacked from the *Si*-face, forming the new stereogenic center of *S*-configuration. Substrates with the *R*-configuration at C(3) usually lead to attack from the *Re*-face of the carbonyl group, generating the *R*-configuration at the new

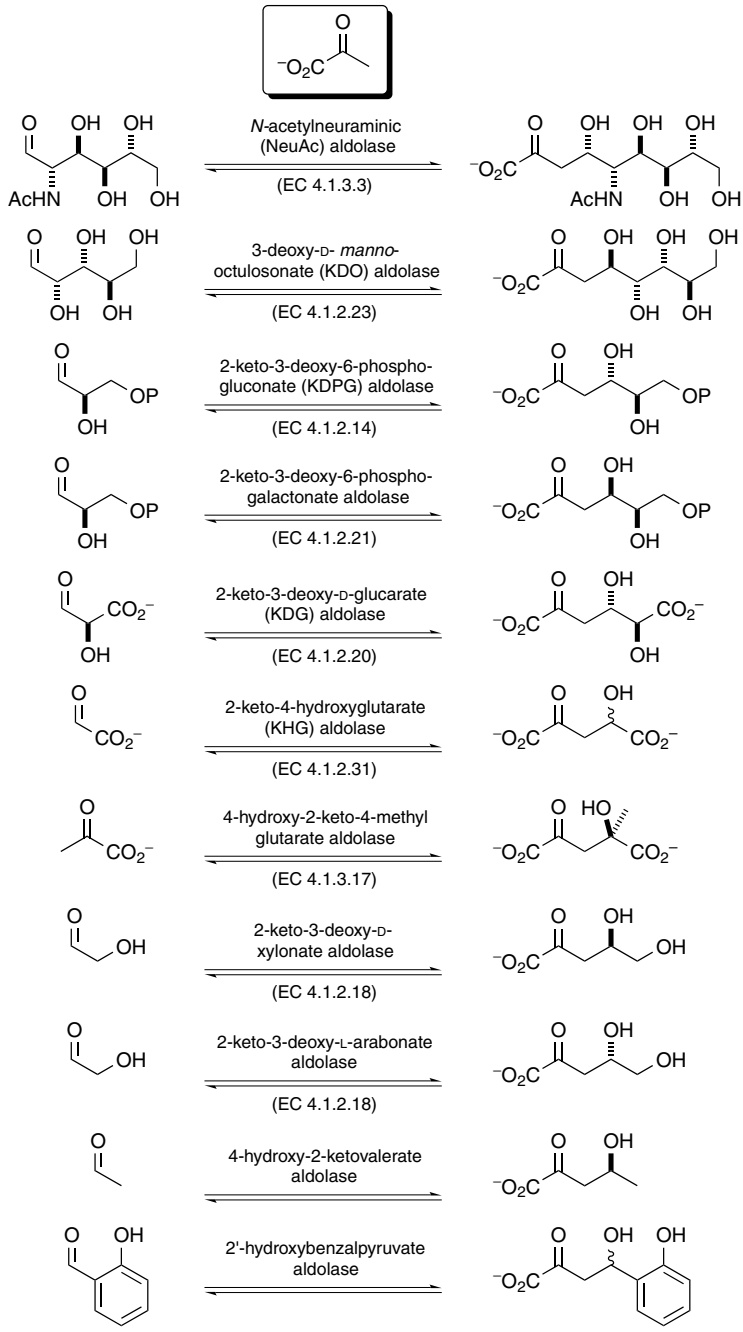

Scheme 5.27. Pyruvate-dependent aldolases and the reactions they catalyze. P = PO_3^{2-}.

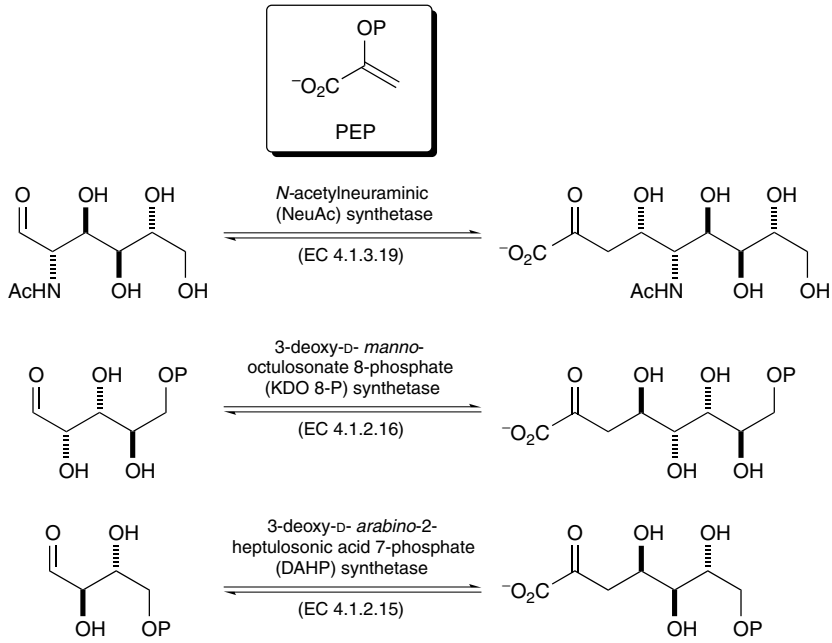

Scheme 5.28. Phospoenolpyruvate (PEP) dependent aldolases and the reactions they catalyze. $P = PO_3^{2-}$.

stereogenic center (Scheme 5.30). In general, the attack on the *Si*-face was kinetically favored over attack at the *Re*-face.[49b] The *Re*-face stereochemical outcome, however, appears to be operated under thermodynamic control when the substrate C(3) is of *R*-configuration. Thus, in all cases where the substrate C(3) is of *R*-configuration, the *Re*-face attack predominates, and the more thermodynamically favored *R*-configuration product is slowly formed, with the newly forming stereocenter in the equatorial position. A model for the active site of this enzyme, based on X-ray data and modeling of the Schiff-base and enamine intermediates of pyruvate has been proposed.[53] The proposal suggests that the reaction between the enamine of pyruvate and the aldehyde acceptor occurs through different faces of the aldehyde, with the aldehyde in different orientation in both conformations.

Because of the availability of NeuAc aldolase and its unique stereochemical features, many biologically interesting molecules have been prepared. This method has been exploited, for example, in the synthesis of D- and L-sialic acid analogues (Scheme 5.31),[54] in the synthesis of the polyhydroxylated alkaloid 3-(hydroxymethyl)-6-epi-castanospermine (Scheme 5.32),[55] and in the synthesis of the melanoma antigen 9-*O*-acetyl GD_3 from GD_3 (Scheme 5.33).[56]

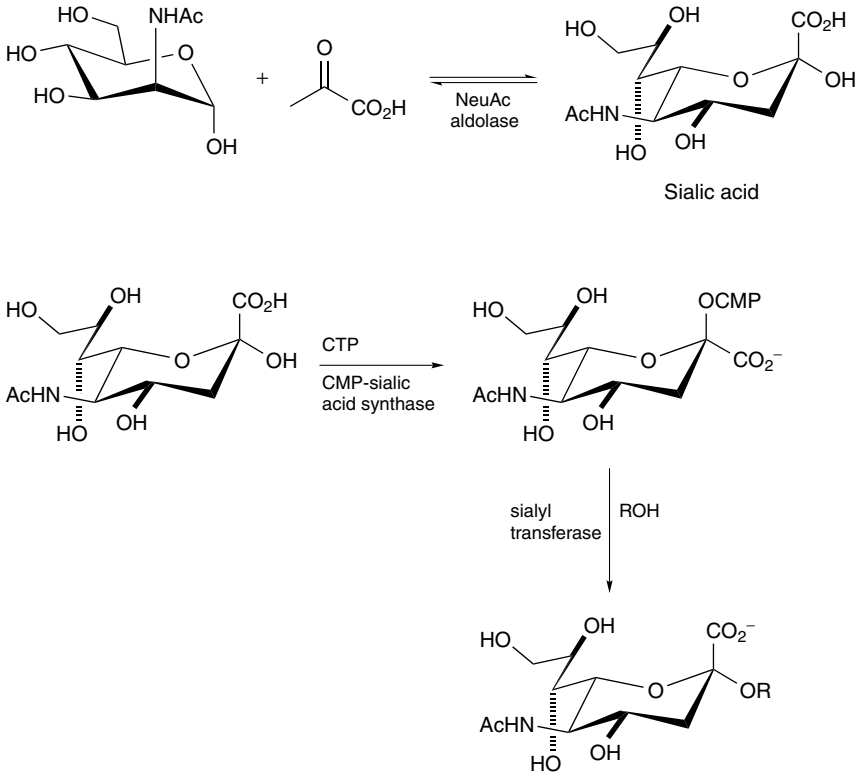

Scheme 5.29. Aldol addition reaction catalyzed in vivo by *N*-acetylneuraminic acid (NeuAc) aldolase.

The use of this enzyme system has been extended to the multi-kilogram scale as demonstrated in the paired enzyme sequence utilizing NeuAc aldolase and *N*-acetyl-D-glucosamine 2-epimerase (GlcNAc 2-epimerase) to prepare sialic acid (Scheme 5.34).[57] 3-Deoxy-D-manno-2-octulosonate aldolase (EC 4.1.2.23), also known as 2-keto-3-deoxyoctulosonate (KDO) aldolase, is the enzyme responsible in vivo for the reversible condensation of pyruvate and D-arabinose. KDO aldolase has been isolated and purified from such sources as *E. coli*, *Aerobacter cloacae*, *Aureobacter barkerei*, and *Pseudomonas aerusinosa*.[58] So far the main use of this enzyme has been in the preparation of KDO analogues,[58c] as KDO and its activated form CMP-KDO are key intermediates in the biosynthesis of the outer membrane lipopolysaccharide (LPS) of gram-negative bacteria (Scheme 5.35).[59] Such analogues may inhibit LPS biosynthesis or interact with LPS binding protein. KDO aldolase will accept D-ribose, D-xylose, D-lyxose, L-arabinose, D-arabinose-5-phosphate, and

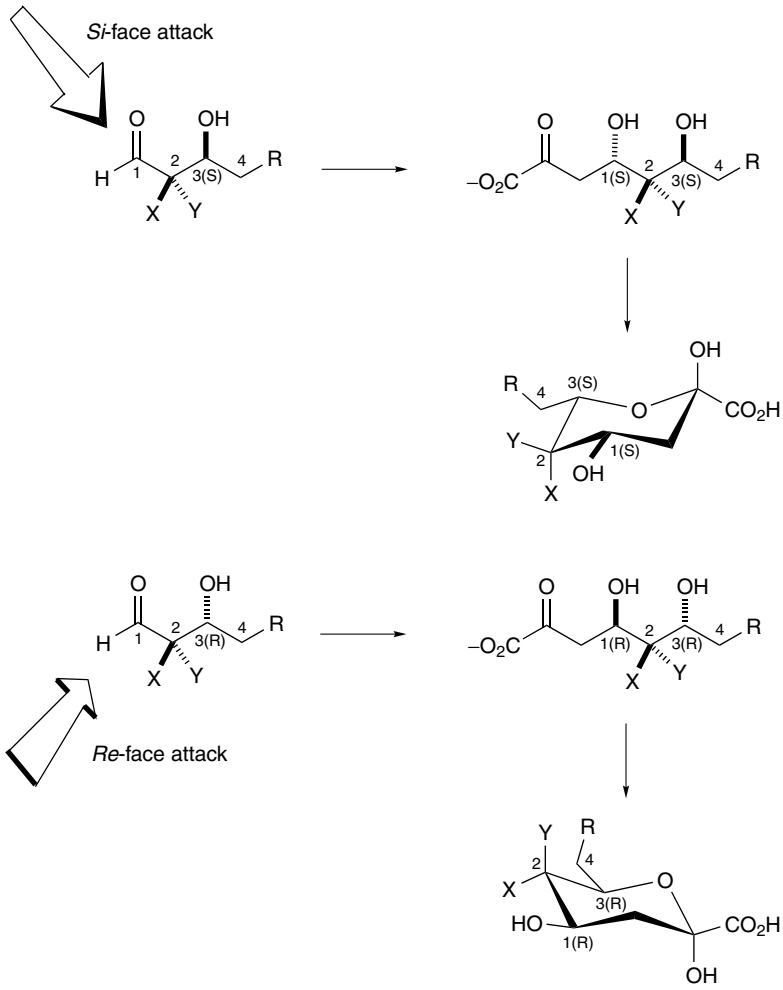

Scheme 5.30. Stereochemical result for the NeuAc-aldolase-catalyzed reaction, with attack at the *si*-face (when C3 = *S*-configuration) and *Re*-face (when C3 = *R*-configuration).

N-acetylmannosamine, but all at less than 5% of the natural substrate D-arabinose.[58a] This enzyme is specific for substrates with the *R*-configuration at C(3), and *Re*-face addition of pyruvate to the aldehyde acceptors is the normal mode of attack.[58c] Though the enzymes accept substrates with C(2) hydroxyl of *R*- and *S*-configurations, it prefers the *S*-isomer (Scheme 5.36).

Unlike other pyruvate aldolases, 2-keto-3-deoxy-6-phosphogluconate (KDPG) aldolase (EC 4.1.2.14), which catalyzes the reversible condensation

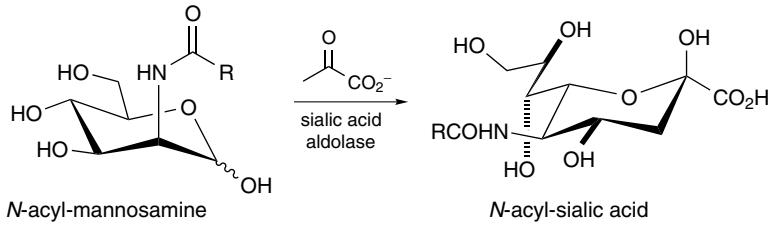

N-acyl-mannosamine

N-acyl-sialic acid

R	Yield
CH_2NHAc	70
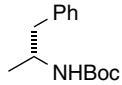	63
$(CH_2)_8CH_3$	71
$(CH_2)_2Ph$	71
GlyGlyCbz	60
Dansyl	72
Biotin	55

Scheme 5.31. Synthesis of sialic acid analogues.

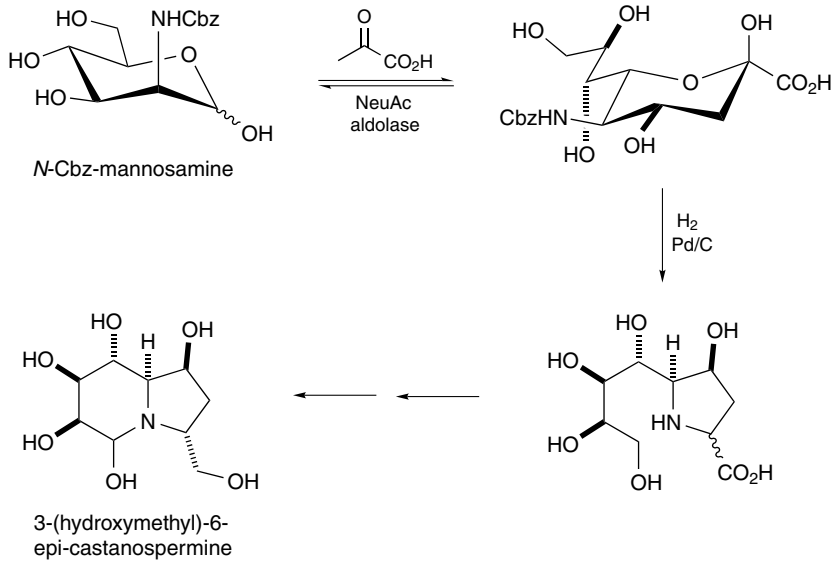

N-Cbz-mannosamine

3-(hydroxymethyl)-6-
epi-castanospermine

Scheme 5.32. Preparation of aza sugars by NeuAc aldolase catalysis.

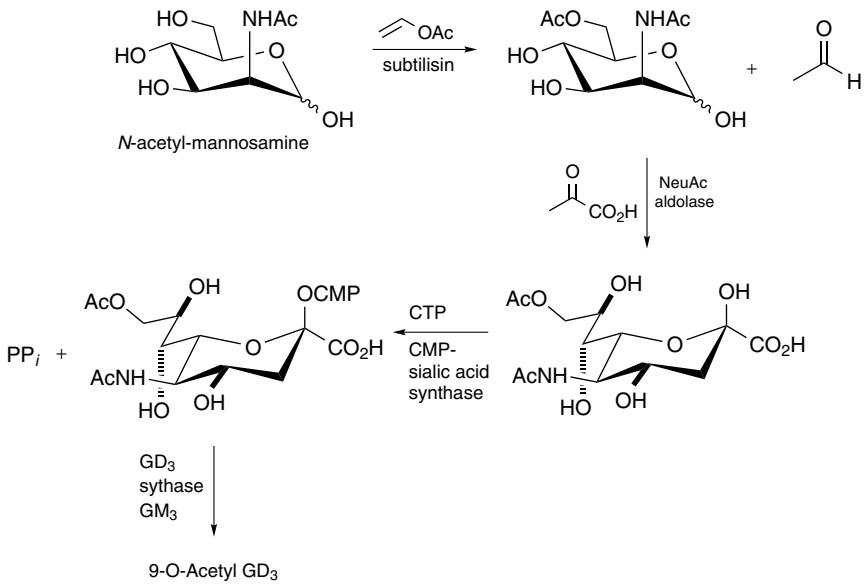

Scheme 5.33. Enzymatic synthesis of the melanoma antigen 9-*O*-acetyl GD_3.

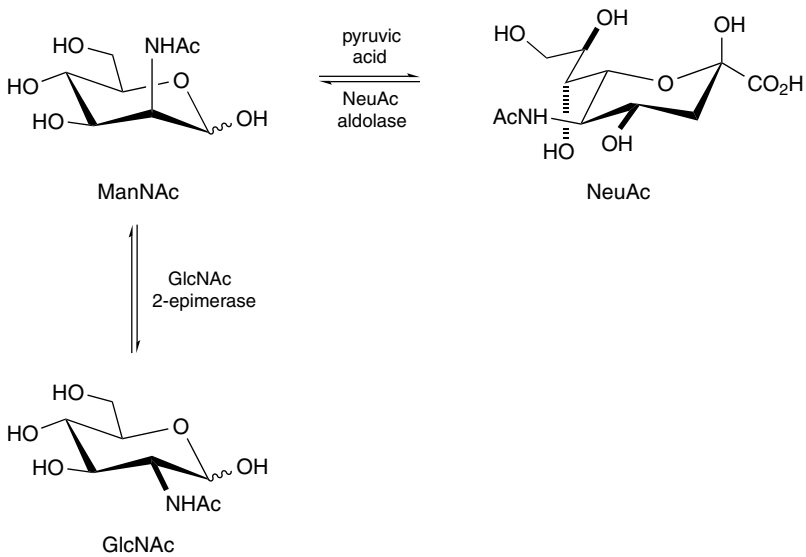

Scheme 5.34. Preparative scale synthesis of sialic acid (NeuAc) from *N*-acetyl glucosamine (GlcNAc) and pyruvate.

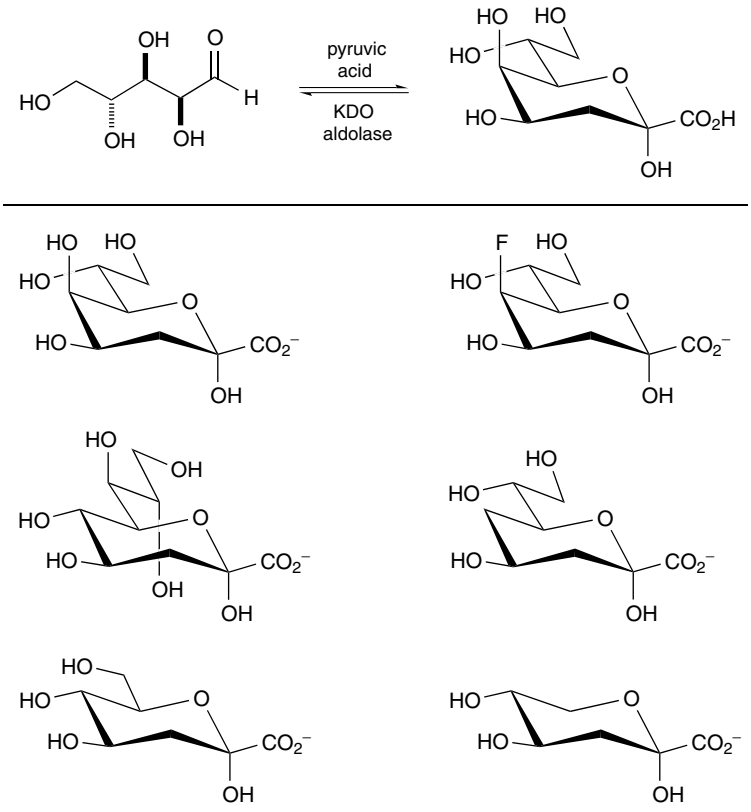

Scheme 5.35. KDP analogues synthesized on a preparative scale using KDO aldolase.

of pyruvate with glyceraldehyde 3-phosphate (G3P), will accept short-chain noncarbohydrate aldehydes as substrates but at very low rates (Scheme 5.37).[60] D-Glyceraldehyde is itself accepted as an electrophile by KDPG aldolase but at a rate of 1% that for D-glyceraldehyde 3-phosphate. Although it may have been expected that the addition of a phosphate moiety at C(3) or C(4) in unnatural substrates would enhance their activity, studies have shown that phosphorylation failed to provide a general rate enhancement.[61]

KDPG aldolase has been shown to be highly stereoselective when pyruvate is used as donor, affording products possessing the *S*-configuration at the new C(4) stereocenter. A sequential enzyme combination of KDPG aldolase, followed by a phenylalanine dehydrogenase-catalyzed reductive amination, has led to the stereospecific preparation of the N-terminal amino acid moiety of the Nikkomycin Kx and Kz (Scheme 5.38).[62] These nucleoside antifungals are

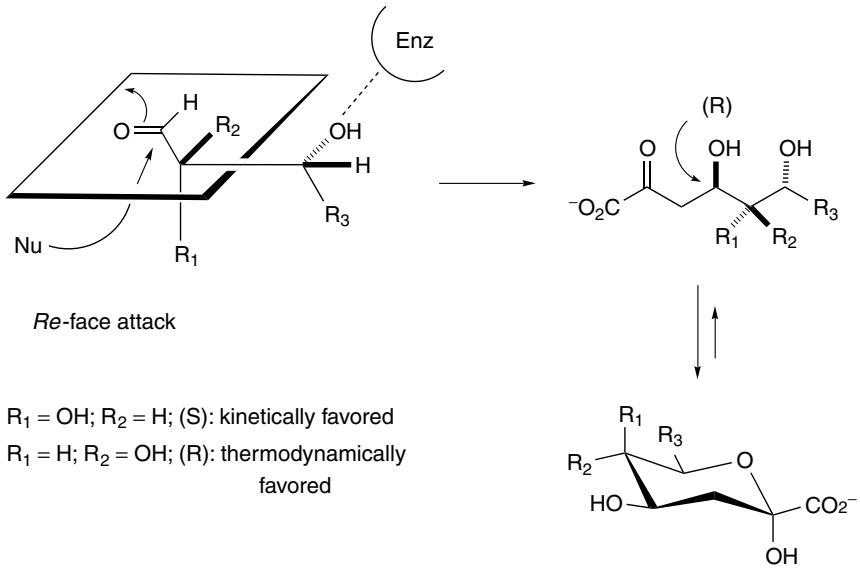

Scheme 5.36. Synthesis of higher 2-deoxysugars via *Re*-face attack, utilizing KDO aldolase.

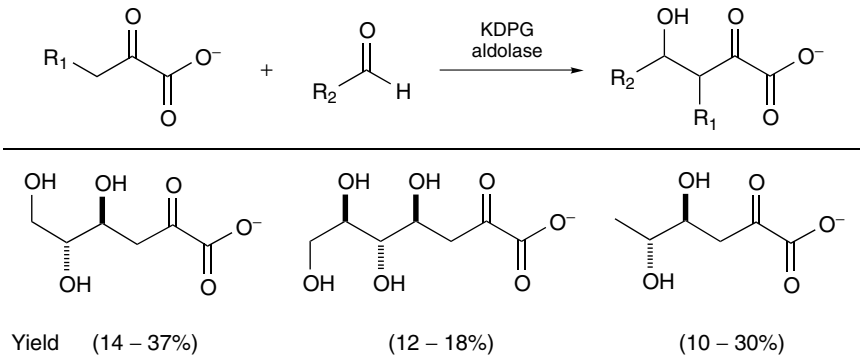

Scheme 5.37. Compounds synthesized on a preparative scale utilizing KDPG aldolase.

inhibitors of the fungal cell wall enzyme, chitin synthase. Using the technique of directed evolution, by DNA shuffling and error-prone polymerase chain reaction, a new variant of KDPG aldolase containing six site-specific mutations outside the active site has been prepared to accept enantiomeric substrates that do not possess a phosphate group (i.e., L-glyceraldehyde). This approach has additionally allowed the formation of interesting L-sugars (Scheme 5.39).[63]

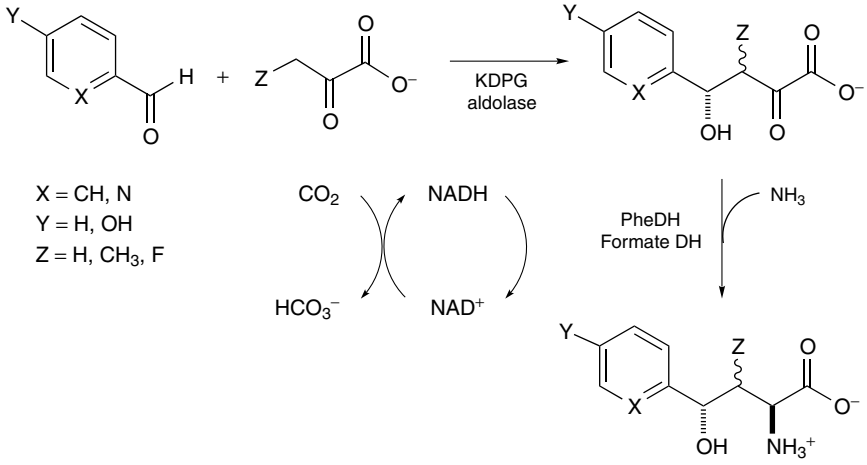

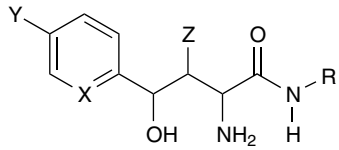

Nikkomycins B, I, J, K, Q, X and Z

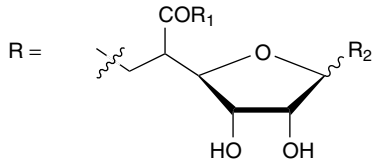

R_1 = amino acids, OH

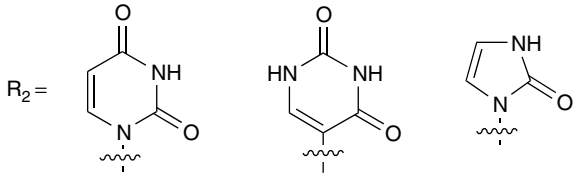

Scheme 5.38. Strategy for the synthesis of the N-terminal amino acid of Nikkomycin (*top*) and the general structure of Nikkomycins B, I, J, K, Z, X and Z (*bottom*).

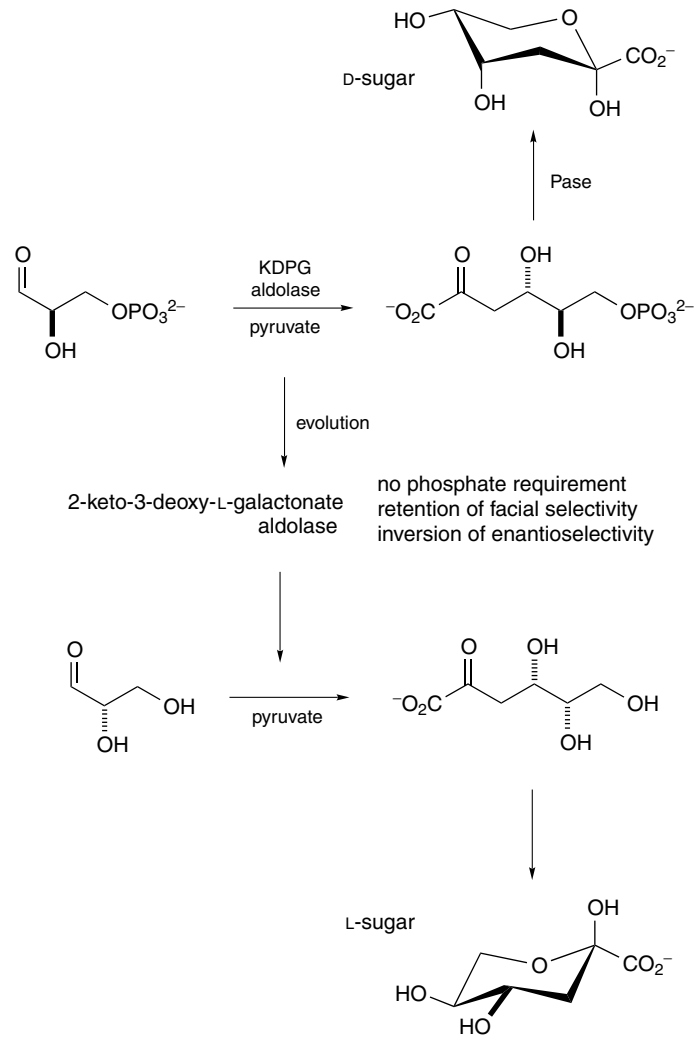

Scheme 5.39. Alteration of the acceptor enantioselectivity and phosphate dependency by directed evolution of KDPG aldolase.

Other pyruvate- and phosphoenolpyruvate-dependent aldolases have been isolated and purified, but have not yet been extensively investigated for synthetic use. Those showing promise for future applications include, 3-deoxy-D-arabino-2-heptulosonic acid 7-phosphate (DAHP) synthetase (EC 4.1.2.15), 2-keto-4-hydroxyglutarate (KHG) aldolase (EC 4.1.2.31), and 2-keto-3-deoxy-D-gluconate (KDG) aldolase (EC 4.1.2.20). DAHP synthetase has been used

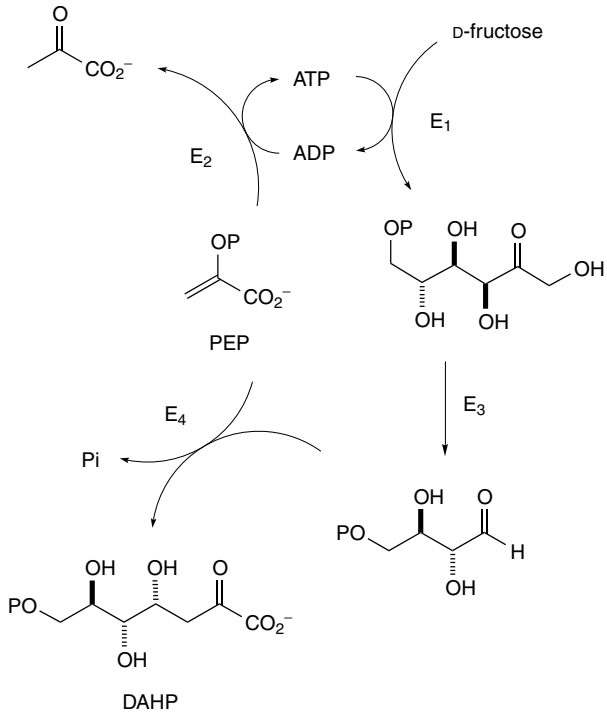

Scheme 5.40. Preparative scale production of DAHP by multi-enzyme synthesis. E_1 = hexokinase, E_2 = pyruvate kinase, E_3 = transketolase + D-ribose 5-P, E_4 = DHAP synthetase. P_i = inorganic phosphate, $P = PO_3^{2-}$.

for the preparative-scale production of DAHP, via a multi-enzyme system (Scheme 5.40).[64] The substrate specificity of this enzyme, however, is not well studied. KHG aldolase, unlike other aldolases in its class, will accept a variety of donor substrates.[65] KDG aldolase from *Aspergillus niger* has shown its applicability in the preparative scale synthesis of 2-keto-3-deoxy-D-gluconate from pyruvate and D-glyceraldehyde.[66]

C. 2-Deoxyribose-5-Phosphate Aldolases

The enzyme DERA, 2-deoxyribose-5-phosphate aldolase (EC 4.1.2.4), is unique among the aldolases in that the donor is an aldehyde. In vivo it catalyzes the reversible aldol reaction of acetaldehyde and D-glyceraldehyde 3-phosphate, forming 2-deoxyribose 5-phosphate, with an equilibrium lying in the synthetic direction (Scheme 5.41). DERA, the only well-characterized member of this type I aldolase, has been isolated from both animal tissue and microorganisms.[67]

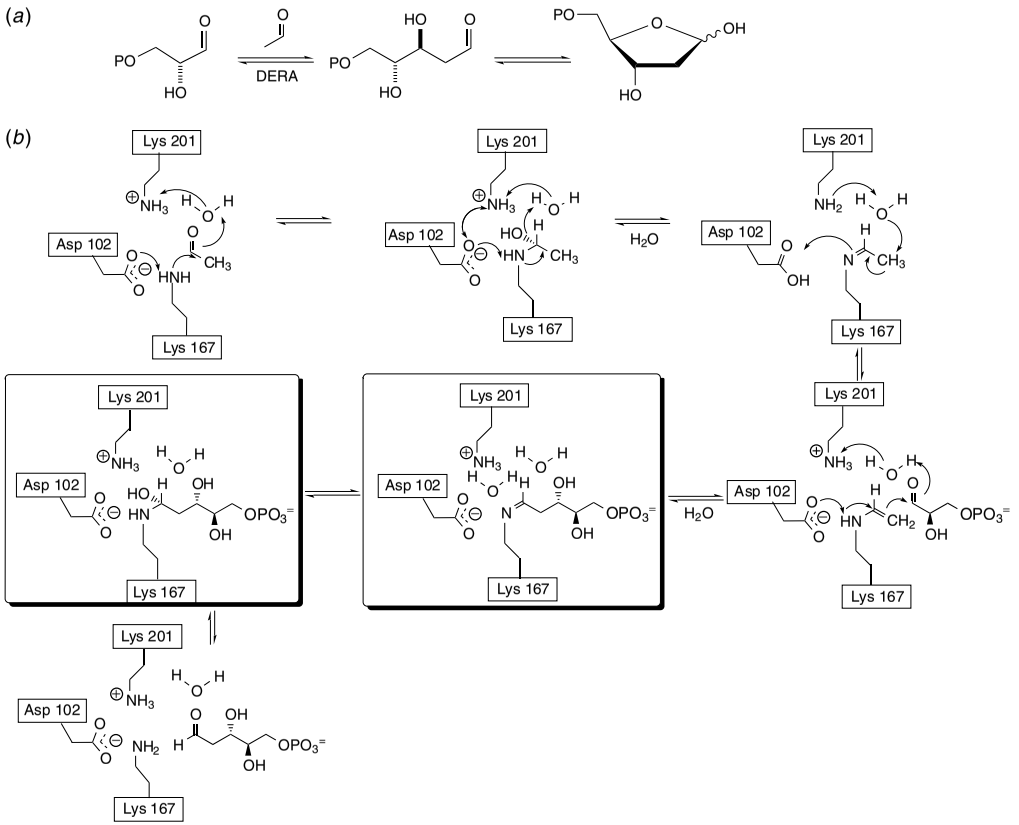

Scheme 5.41. Aldol addition reaction catalyzed in vivo by 2-deoxyribose-5-phosphate aldolase (DERA). $P = PO_3^{2-}$.

This enzyme, which is relatively stable under reaction conditions, will retain 70% of its activity after 10 days at pH 5 and 25°C. Although it is not yet commercially available, it has been overexpressed in *E. coli*, making large quantities easily accessible.[68] The detailed mechanism of DERA has been determined based on the atomic structure (ca. 1.0 Å) combined with site-directed mutagenesis, kinetic, and NMR studies[13b] (Scheme 5.41*b*). A proton relay system composed of Lys and Asp appears to activate a conserved active-site water that functions as the critical mediator for proton transfer in acid-base catalysis.

DERA can also accept propanol, acetone, and fluoroacetone as donors, albeit less efficiently than acetaldehyde. Even at slower rates of donor consumption, the high specific activity of the overexpressed enzyme allows for the rapid formation of products. This enzyme shows a broad acceptor substrate tolerance. The uptake of 2-hydroxyaldehydes appears to be more rapid for the *R*-isomers as opposed to the *S*-isomers, allowing for kinetic resolution of racemic mixtures of acceptor substrates. Glyceraldehyde is more slowly taken up by the enzyme than its natural substrate, glyceraldehyde 3-phosphate, and has a relative rate of 250-fold less. Many simple aldehydes such as azidoaldehydes, thio-substituted aldehydes and α-methylaldehydes are good acceptor substrates for the enzyme. The newly created stereogenic center is generated under control of the enzyme, giving products of the *S*-configuration. A variety of products including analogues of 2-deoxy-sugars and thiosugars, have been prepared using DERA (Table 5.1).[68b] Isotopically labeled nucleosides have been conveniently synthesized using the combined enzyme system of triosephosphate isomerase (TPI) and DERA (Scheme 5.42).[69] Several iminocyclitols have been prepared from 3-azido-2-hydroxypropanals using the DERA aldol protocol; Table 5.2.[68*a*,70]

In DERA reactions, where acetaldehyde is the donor, products are also themselves aldehydes. In certain cases a second aldol reaction will proceed until a product has been formed that can cyclize to a stable hemiacetal.[71] For example, when α-substituted aldehydes were used, containing functionality that could not cyclize to a hemiacetal after the first aldol reaction, these products reacted with a second molecule of acetaldehyde to form 2,4-dideoxyhexoses, which then cyclized to a hemiacetal, preventing further reaction. Oxidation of these materials to the corresponding lactone, provided a rapid entry to the mevinic acids and compactins (Scheme 5.43). Similar sequential aldol reactions have been studied, where two enzyme systems have been employed[72] (Scheme 5.44). The synthesis of 5-deoxy ketoses with three substitutents in the axial position was accomplished by the application of DERA and RAMA in one-pot (Scheme 5.44). The long reaction time required for the formation of these thermodynamically less stable products, results in some breakdown of the normally observed stereoselectivity of the DERA and FDP aldolases. In a two-pot procedure, DERA and NeuAc aldolase have

Table 5.1
Reactions Catalyzed by DERA

Acceptor	Donor	Product
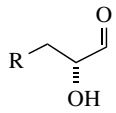		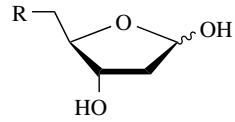 R = H R = Br R = F R = OH R = Cl R = CH_3
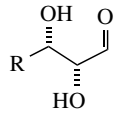		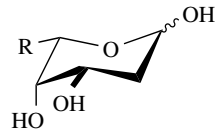 R = CH_3 R = CH_2OH R = Ph
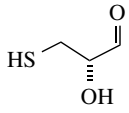		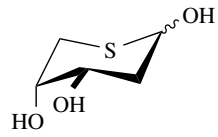
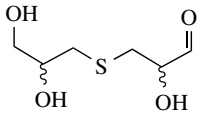		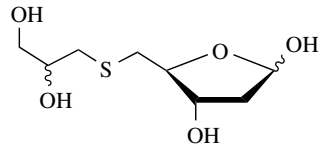
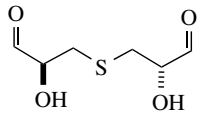		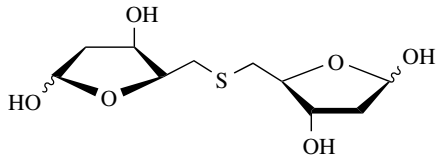

been used to prepare deoxy-sialic acid derivatives, from relatively simple starting materials (Scheme 5.45). Very recently the DERA-catalyzed reaction of acetaldehyde and L-lactaldehyde was used to prepare key fragments for the synthesis of the potent antitumor agent epothilone (Scheme 5.46).[73] The enzyme is used in the synthesis of two key intermediates for the assembly of two fragments for Suzuki's coupling.

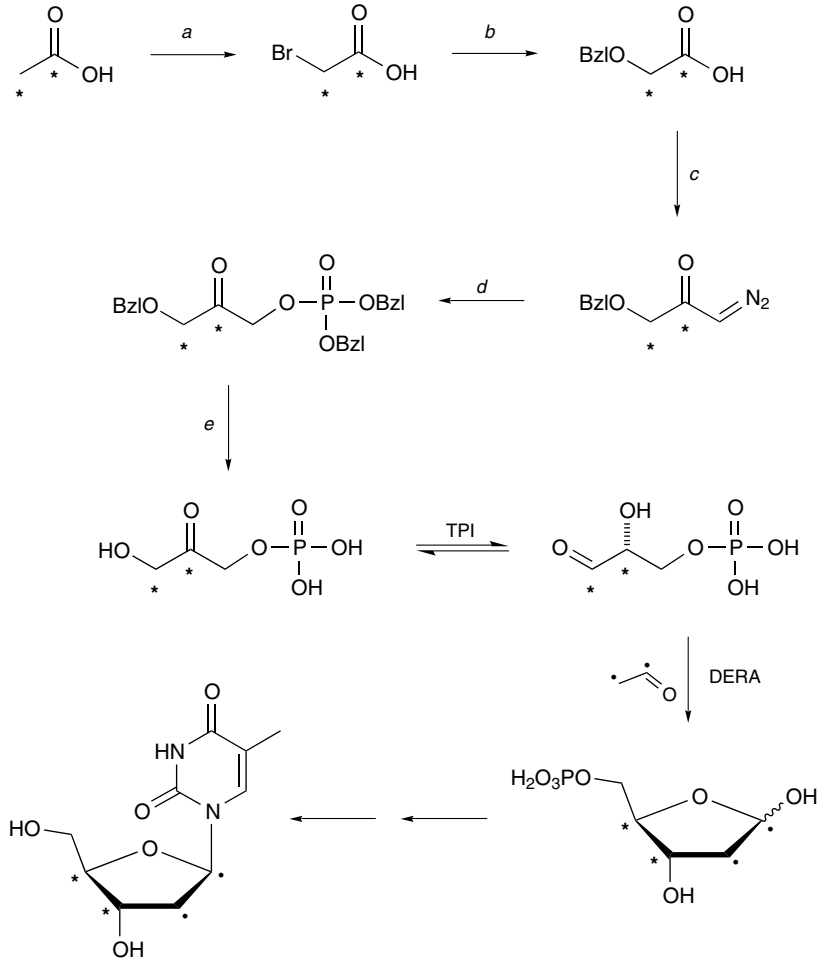

Scheme 5.42. Synthesis of isotopically labeled nucleosides using a combined enzyme system. Conditions: (*a*) TFAA/Br_2; (*b*) BzlOH/NaH; (*c*) (*i*) $SOCl_2$, (*ii*) CH_2N_2; (*d*) $(BzlO)_2P(O)OH$; (*e*) H_2 Pd/C. TPI = triosephosphate isomerase.

D. Glycine-Dependent Aldolases

The glycine-dependent aldolases are pyridoxal 5-phosphate dependent enzymes that catalyze the reversible aldol reaction, where glycine and an acceptor aldehyde form a β-hydroxy-α-amino acid (Scheme 5.47).[74] Serine hydroxymethyltransferases, SHMT (EC 2.1.2.1), and threonine aldolases, two types of glycine dependent aldolases, have been isolated. In

Table 5.2
Synthesis of Iminocyclitols Using DERA

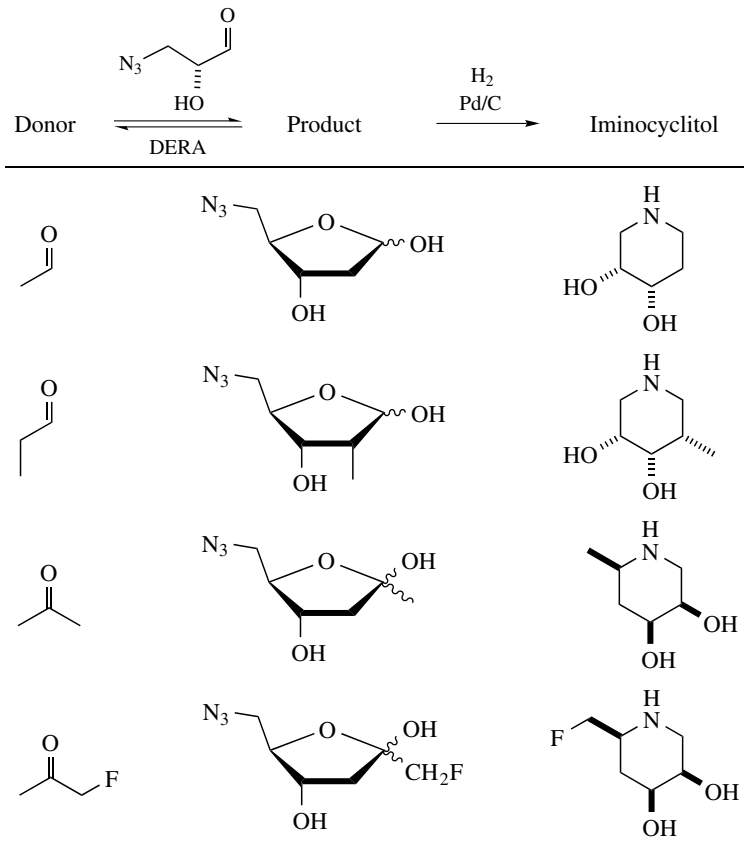

vivo, SHMT catalyzes the reversible aldol reaction between glycine and formaldehyde, giving L-serine. SHMT, which was expressed in *Klebsiella aerogenes*, has been used successfully for the high-yield kilogram-scale production of L-serine.[75] This reaction requires tetrahydrofolate as a cofactor. Tetrahydrofolate binds nonenzymatically with formaldehyde to form N^5, N^{10}-methylenetetrahydrofolate, which is then accepted by the enzyme. SHMT from rabbit liver, which was overexpressed in *E. coli* for industrial applications, has been used in the stereoselective condensation of glycine and succinic semialdehyde for the production of L-erythro-2-amino-3-hydroxy-1,6-hexanedicarboxylic acid.[76] These substituted dicarboxylic acids have been used as precursors to carbocyclic β-lactams and nucleosides (Scheme 5.48).

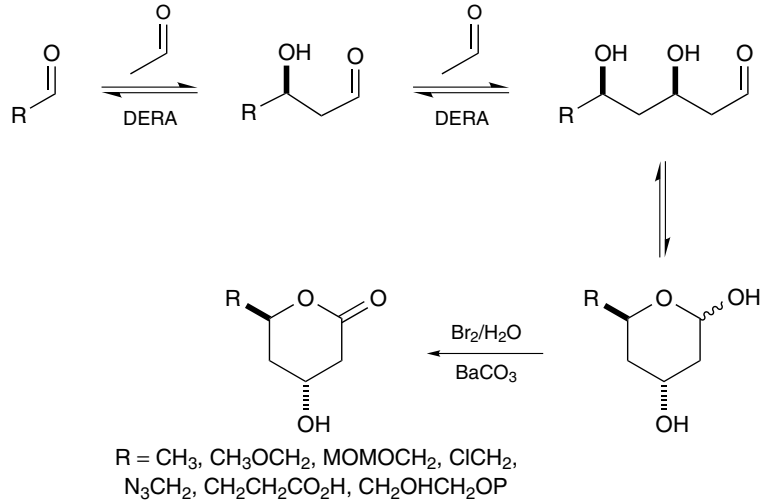

Scheme 5.43. Three-component, double-aldol condensation catalyzed by DERA. MOM = methoxymethyl.

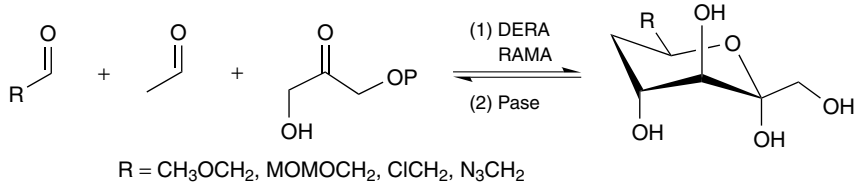

Scheme 5.44. Single-pot, three-component, double-aldol condensation catalyzed by DERA and RAMA. P = PO_3^{2-}, Pase = phosphatase.

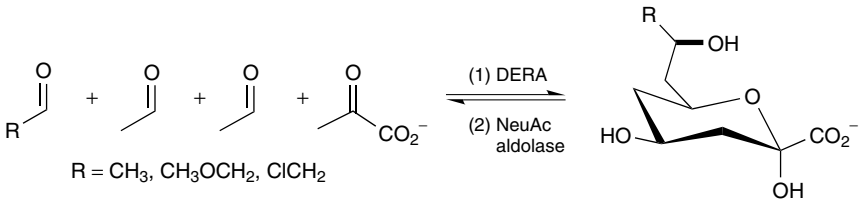

Scheme 5.45. Two-pot, triple-aldol condensation catalyzed by DERA and NeuAc, giving deoxy sialic acid derivatives.

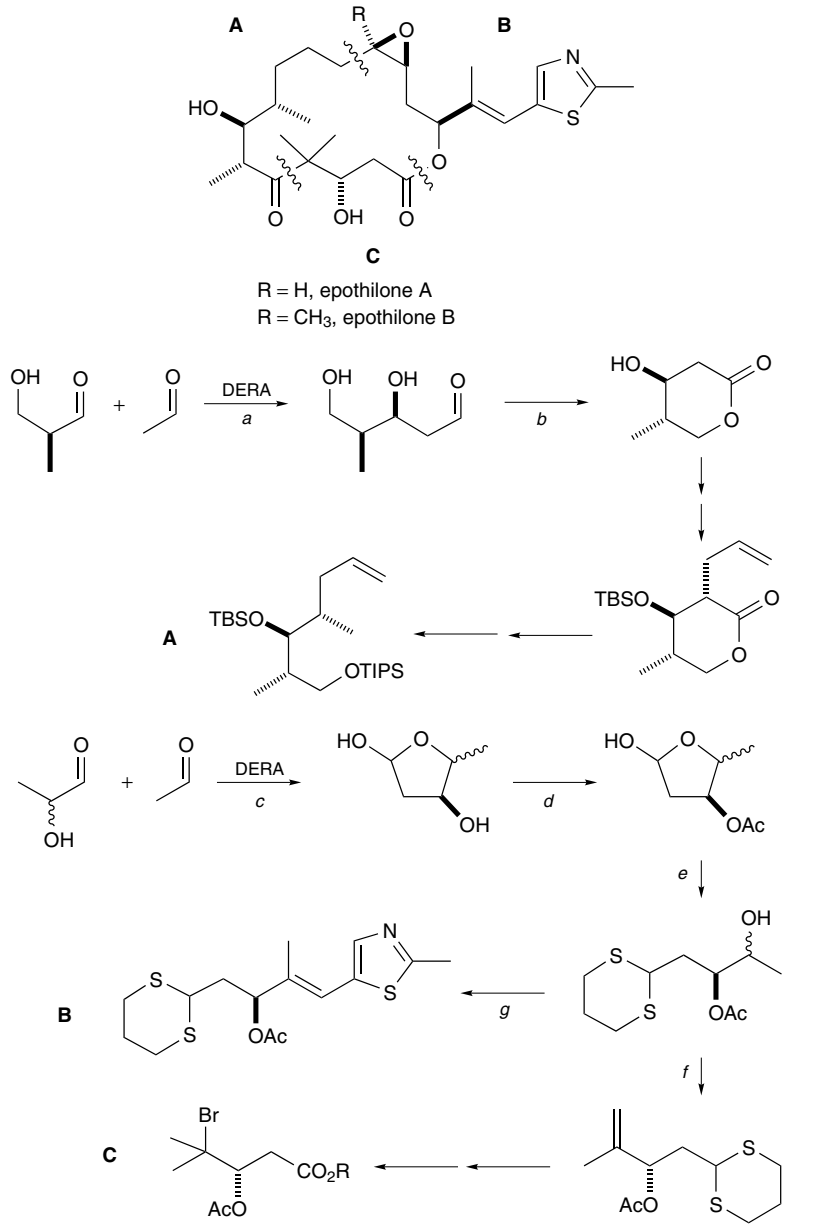

Scheme 5.46. Synthesis of key epothilone fragments using DERA. Conditions: (*a*) 42% yield; (*b*) Br_2/H_2O; (*c*) 35%; (*d*) (*i*) Ac_2O, pyridine, (*ii*) BF_3/Et_2O; (*e*) $HS(CH_2)_3SH/BF_3/Et_2O$; (*f*) (*i*) Swern oxidation, (*ii*) Wittig reaction; (*g*) (*i*) Swern oxidation, (*ii*) Wittig reaction; TBS = tert-butyldimethylsilyl; TIPS = triisopropylsilyl.

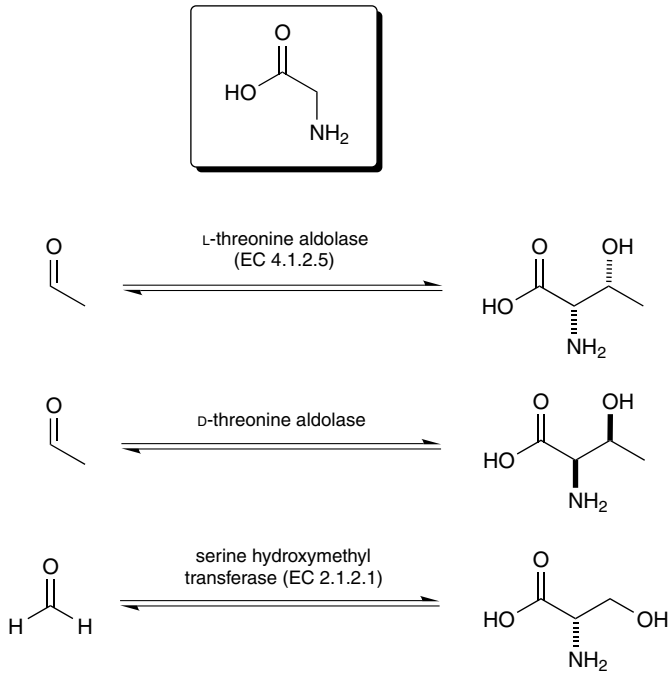

Scheme 5.47. Glycine-dependent aldolases and the reactions they catalyze.

The preparation of other β-hydroxy-α-amino acids has been less successful. This enzyme is selective for the *S*-configuration at the α-center, but in general, it displays a poor discrimination between erythro- and threo-isomers.

Threonine aldolases, both D- and L-forms, catalyze the aldol reaction between glycine and acetaldehyde to give threonine. L-Threonine aldolase (LTA) (EC 4.1.2.5) has been found to accept a broad range of substrates, producing predominantly erythro isomers (Table 5.3).[77] When α-hydroxyaldehydes are used as acceptors, a mixture of products is obtained. Through the use of hydroxyl protecting groups, however, this problem is avoided. As with other aldolases, α, β-unsaturated aldehydes were not viable acceptor substrates. The successful use of thiophenol-substituted aldehydes, however, does provide an entry into α, β-unsaturated amino acids. The threonine aldolase from *Streptomyces amakusaensis*, has been effective in the resolution of β-hydroxy-α-amino acids. For example, 3-(4-substituted-phenyl)-serines are resolved giving enantiomers with the 2(*R*)/3(*S*) configuration in greater than 95% enantiomeric excess (Scheme 5.49).[78]

LTA has been shown to catalyze the aldol reaction between glycine and (benzyloxy)-acetaldehyde or 4-benzyloxy-butanal, a process used in

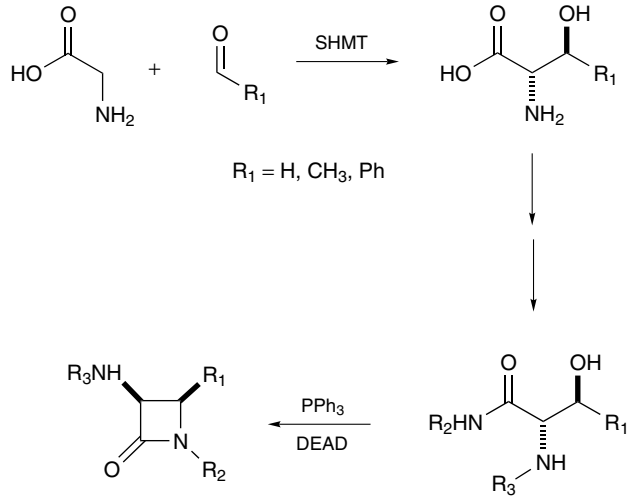

Scheme 5.48. Enzymatic synthesis of 2-amino-3-hydroxy-1,6-hexanedicarboxylic acids using serine hydroxymethyl transferases (SHMT). DEAD = diethyl azodicarboxylate.

Table 5.3
L-Threonine Aldolase (LTA)-Catalyzed Synthesis of L-β-Hydroxy-α-Amino Acids

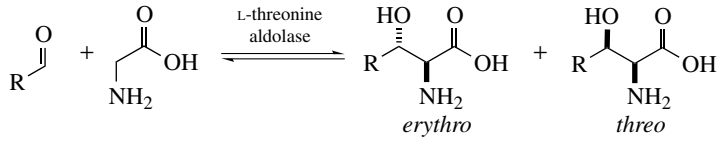

R	Yield [%]	Erythro : Threo
CH_3	38	93 : 7
Ph	87	60 : 40
N_3CH_2	45–75	70 : 30–100 : 0
$BnOCH_2$	78	92 : 8
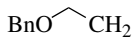	53	53 : 47
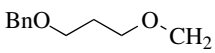	45	92 : 8
	80	50 : 50
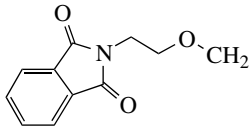	10	86 : 14

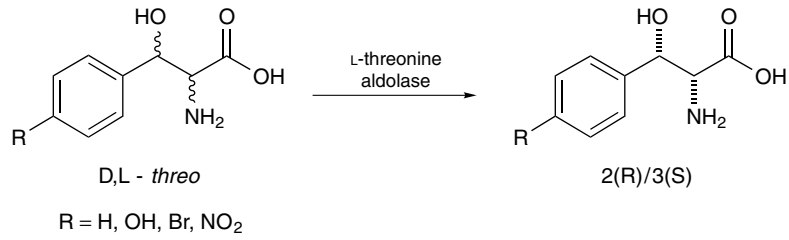

Scheme 5.49. Resolution of β-hydroxy-α-amino acids, using threonine aldolase from *Streptomyces amakusaensis*.

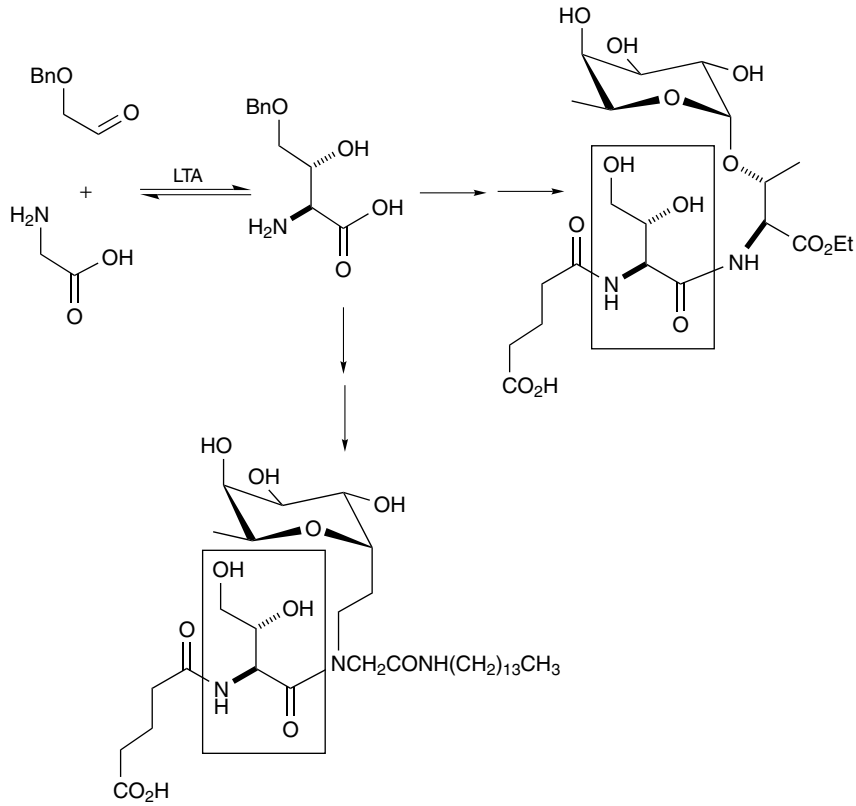

Scheme 5.50. Synthesis of sialyl Lewis X mimetics using L-threonine aldolase (LTA).

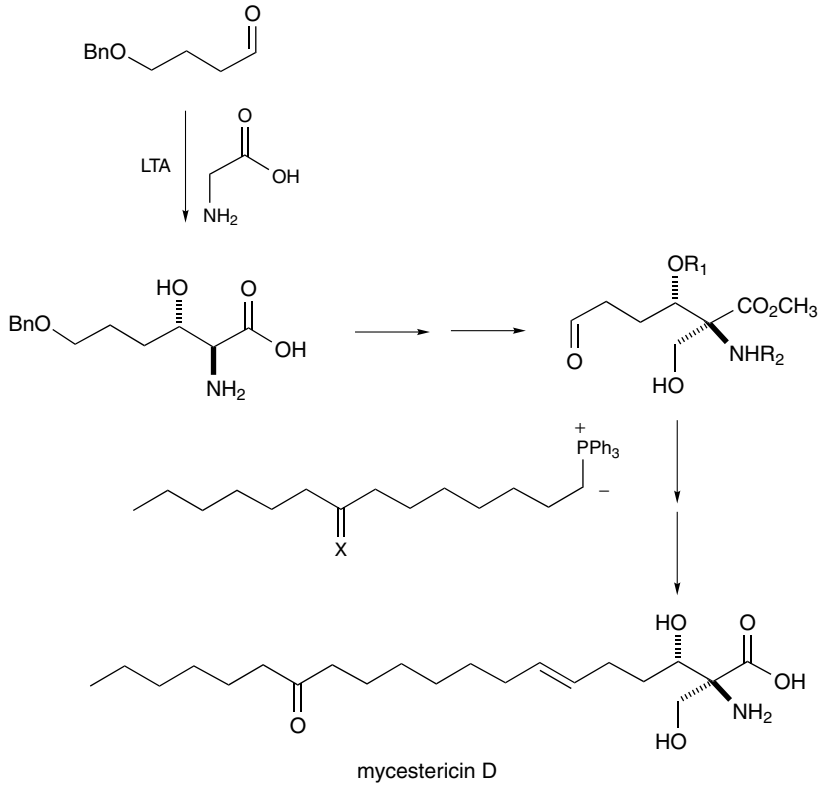

Scheme 5.51. L-Threonine aldolase approach to mycestericin D. X, R_1, R_2 = protecting groups.

the synthesis of potent sialyl Lewis X mimetics (Scheme 5.50).[79] This enzyme has also been pivotal in the asymmetric total synthesis of the potent immunosuppressants, mycestericins D and F (Scheme 5.51).[80] LTA was additionally used to prepare a peptidic RNA, having a guanine-adenine-guanine code as a base sequence that was shown to inhibit the fatal hemorrhagic colitis causative protein, Vero-toxin (Scheme 5.52).[81]

E. Transketolase

Transketolase (TK, EC 2.2.1.1), one of the enzymes in the pentose phosphate pathway, reversibly transfers an active hydroxyaldehyde group from a ketol donor to an α-hydroxyaldehyde acceptor to yield a ketose with the 3(*S*),4(*R*)-configuration.[82] TK transfers the C(1)–C(2) ketol unit of D-xylulose 5-phosphate onto D-ribose 5-P and thus generates glyceraldehyde-3-phosphate

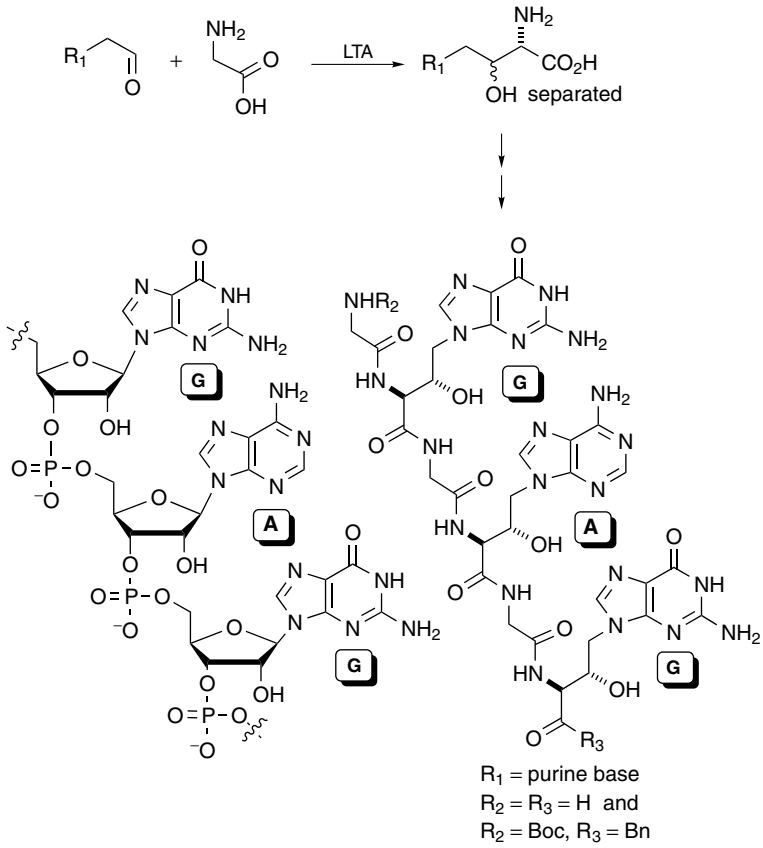

Scheme 5.52. Structure of vero-toxin recognized RNA sequence (*left*) and preparation of its peptidic mimetic (*right*) using LTA (L-threonine aldolase).

(G3P) and D-sedoheptulose 7-P as illustrated in Scheme 5.53. In addition D-erythrose 4-phosphate can function as the ketol acceptor thus producing D-fructose-6-P and G3P (Scheme 5.53). The enzyme relies on two cofactors for activity — thiamin pyrophosphate (TPP) and Mg^{2+} — and utilizes the nucleophilic catalysis mechanism outlined in (Scheme 5.54).[83] When TPP is used as a cofactor for nucleophilic catalysis, an activated aldehyde intermediate is formed. This intermediate functions as a nucleophile, and thus TK employs a strategy that is similar to the *umpolung* strategy exploited in synthetic organic chemistry.

The synthetic potential of thiamin diphosphate dependent enzymes is now recognized and has been reviewed recently.[84–85] TK has been isolated from

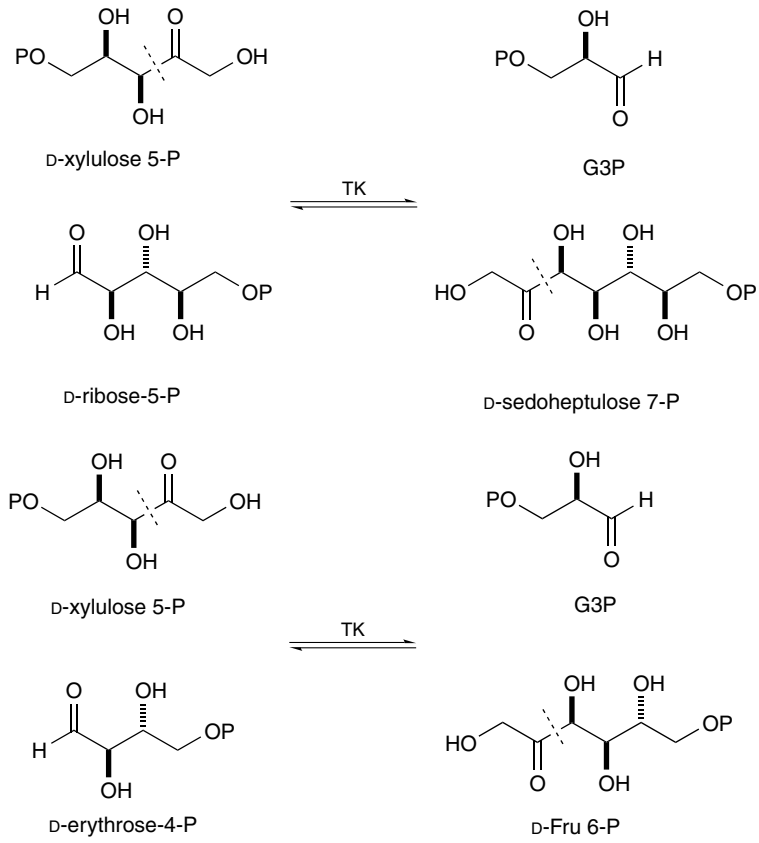

Scheme 5.53. Transketolase transfers the C1–C2 ketol unit of D-xylulose 5-phosphate onto D-ribose-5-phosphate or D-erythrose-4-phosphate generating D-sedoheptulose-7-phosphate or D-fructose-6-phosphate respectively. $P = PO_3^{2-}$.

a variety of sources including spinach, yeast, and recombinant *E. coli*. Transketolase from Baker's yeast is commercially available. It is of synthetic significance that hydroxypyruvate can function as the ketol donor for TR.[86–89] Although the ketol donor hydroxypyruvic acid (HPA) is transferred to an aldose acceptor with an activity of 4% compared to D-xylulose-5-phosphate,[90] using it as the ketol donor results in the evolution of carbon dioxide and renders the overall reaction irreversible (Scheme 5.55). Notably the 2,3-dioxopropionic acid, 2-oxo-3-hydroxybutyric acid, 2-oxomalonic acid and 2-ketogluconic acid analogues of HPA are not substrates. TK is a synthetically useful enzyme since a wide range of aldehydes including aliphatic, unsaturated, aromatic, heterocyclic, phosphorylated and unphosphorylated aldehydes function as ketol

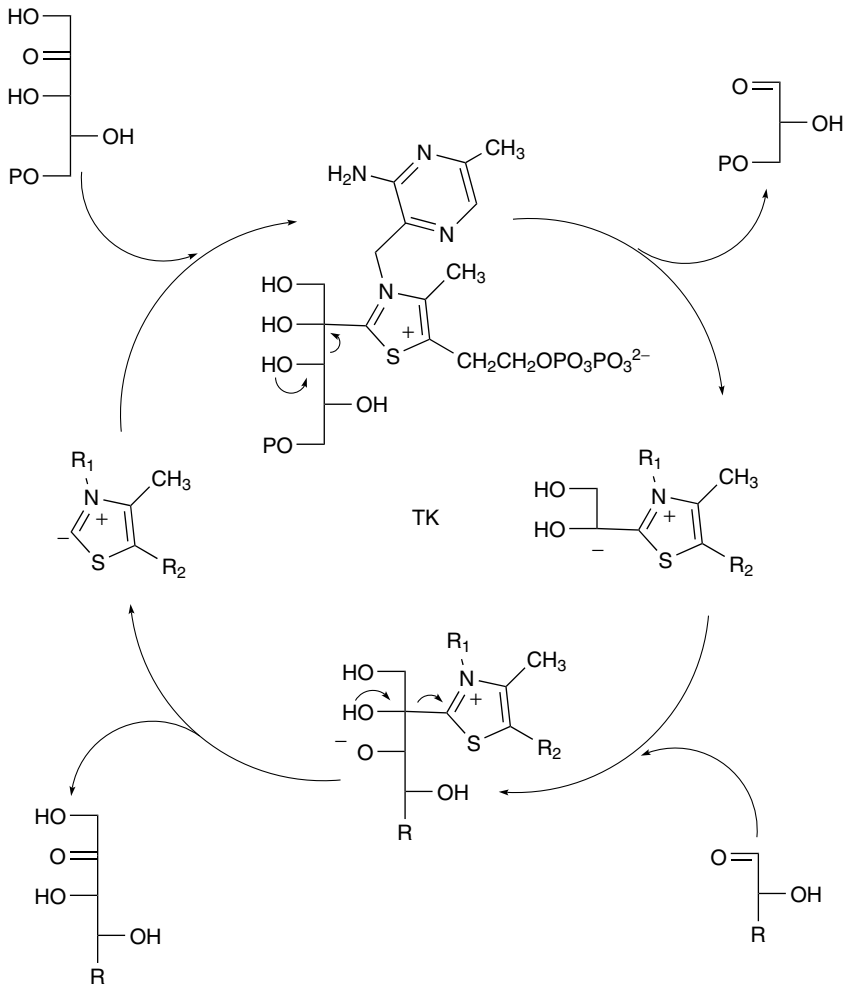

Scheme 5.54. Thiamine pyrophosphate (TPP) addition to D-xylulose-5-phosphate provides an electron sink to stabilize the incipient carbanion, which in turn reacts with the incoming aldehyde acceptor. $P = PO_3^{2-}$.

acceptors.[84–85,91–92] The presence of a hydroxy moiety or other oxygen atom containing moiety at C(2) and/or C(3) enhances the rate, while steric hindrance near the aldehyde decreases the rate. The TK from spinach, yeast, and *E. coli* can utilize aromatic aldehydes as acceptors in reaction with HPA.[93,94]

The newly formed hydroxymethine chiral center has the *S*-configuration resulting from *Re*-face addition of the hydroxyacetyl moiety to the aldehyde

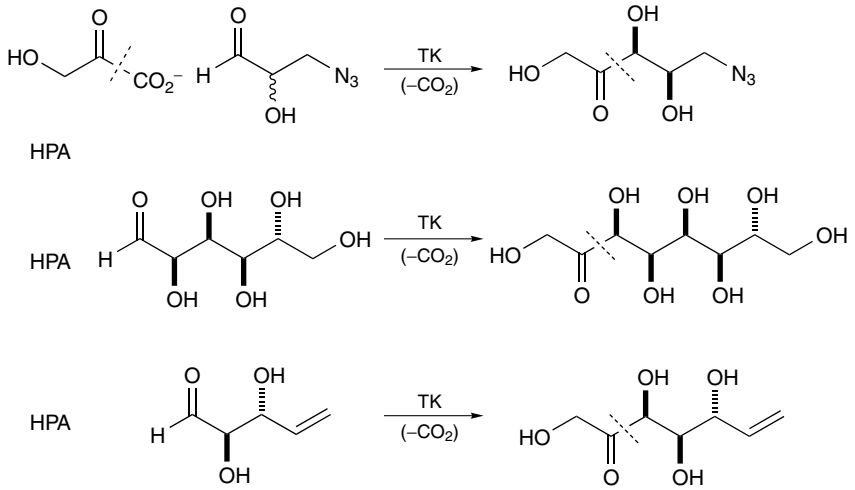

Scheme 5.55. Using hydroxypyruvic acid (HPA) as the ketol donor renders the transketolase reaction irreversible, making it of synthetic utility. Only D-hydroxyaldehyes are accepted by transketolase.

acceptor.[93] Hydroxy aldehydes epimeric at C(2) can be efficiently resolved by TK since only the (*R*)-enantiomer is a substrate, therefore giving (*R*)-*threo* products. Consequently (*S*)-hydroxyaldehydes are obtained as by-products of the kinetic resolution.[91,95] Beyond the C(2) configuration, TK appears to have no stereochemical preference. With HPA, TK from *E. coli,* spinach, and yeast have specific activities of 60 U(μmol min^{-1})/mg, 2 U/mg and 9 U/mg, respectively.[90,96]

A number of practical considerations have been investigated that may facilitate making the TK system amenable to preparative reactions of synthetic utility. Importantly, *E. coli* TK is tolerant to organic cosolvents.[97] To facilitate purification, operation under unbuffered conditions is preferred, and this may be achieved by use of a pH-autotitrator.[90] The reactive α-hydroxy aldehyde starting material, glycoaldehyde, deactivates TK. Therefore, to make large-scale synthesis with TK practical, a continuous enzyme membrane reactor is used for the preparation of L-erythrulose from HPA and glycoaldehyde. The productivity (space-time yield) of the system is thus increased to 45 g L^{-1} day^{-1} while also increasing the half-life of TK to 106 h compared to 5.6 h for the batch reactor.[98] TK immobilization on EupergitC and Amberlite XAD-7 also effects stabilization against the denaturing effects of the aldehyde acceptor. However, the addition of reducing agents is required to protect against oxidative effects.[99] Product removal in situ is accomplished by in-line borate complexation.[100] Recently a detailed and systematic approach toward the

selection of biotransformation conditions and operational design was undertaken. This permitted the design of the TK-catalyzed, batch-biotransformation synthesis of (3*S*, 4*R*)-5-oxo-benzyl-D-xylose.[94]

Several synthetic examples that successfully exploit TK for biocatalytic conversions have been reported. For example, the total synthesis of the beetle pheromone (+)-*exo*-brevicomin utilizes TK from Baker's yeast as the sole chiral reagent. Starting with racemic 2-hydroxybutanol, the ability of TK to effect kinetic resolution of substrates was exploited (Scheme 5.56). The smooth reaction of 2-hydroxybutanol with HPA was catalyzed by TK at pH 7.5 to yield the enantioenriched ketone in 90% yield. This intermediate was chemically converted into (+)-*exo*-brevicomin.[101]

TK was also utilized in the chemo-enzymatic synthesis of the polyhydroxylated piperidine and pyrrolidine glycosidase inhibitors fagomine and 1,4-dideoxy-1,4-imino-D-arabitol A (Scheme 5.56).[102] All of these syntheses involve the condensation of HPA with racemic 2-hydroxyaldehydes. Since the ketol unit is diastereoselectively transferred to only the D-enantiomer of the aldehyde, product formation is accompanied by an efficient kinetic resolution. TK was also utilized for the synthesis of polyhydroxylated piperidine and pyrrolidine products starting from reagents with azido and nitrile protecting groups, which demonstrates the substrate scope of this catalyst.[39*b*,103] Similarly the putative glycosidase inhibitor *N*-hydroxypyrrolidin, whose configuration matches that of D-glucose, was prepared chemoenzymatically by the TK mediated coupling of 3-*O*-benzylglyceraldehyde with hydroxypyruvate to yield 5-*O*-benzyl-D-xylose efficiently on a gram scale.[104] By applying spinach leaf TK to catalyze the reaction of 4-deoxy-L-threose and HPA, 6-deoxy-L-sorbose, the precursor of the industrially important aromatic product furaneol, is constructed (Scheme 5.57).[27*g*,105]

Recently the recombinant TK from *E. coli* was used in the gram-scale synthesis of D-xylulose-5-phosphate in a one-pot, enzymatic synthesis from the readily available precursors hydroxypyruvate (HPA), and fructose-1,6-bisphosphate (FBP). The fructose 1,6-bisphosphate catalyzed retroaldol of FBP was used to generate G3P and dihydroxyacetone phosphate (DHAP). DHAP could in turn be converted to G3P by triose phosphate isomerase (TPI) (Scheme 5.58*a*).[106] TK from yeast was used to prepare 4-deoxy-D-fructose-6-phosphate using L-erythrulose as the ketol donor instead of HPA. In order to drive the equilibrium toward the synthesis of the new ketose, the glycoaldehyde by-product was reduced to glycerol in situ by yeast alcohol dehydrogenase (YADH) (Scheme 5.58*b*), and cofactor recycling was accomplished by formate dehydrogenase (FDH).[107]

Because both transketolase and fructose-1,6-bisphosphate (FBP) aldolase provide ketoses of D-threo configuration on carbons 3 and 4, they are

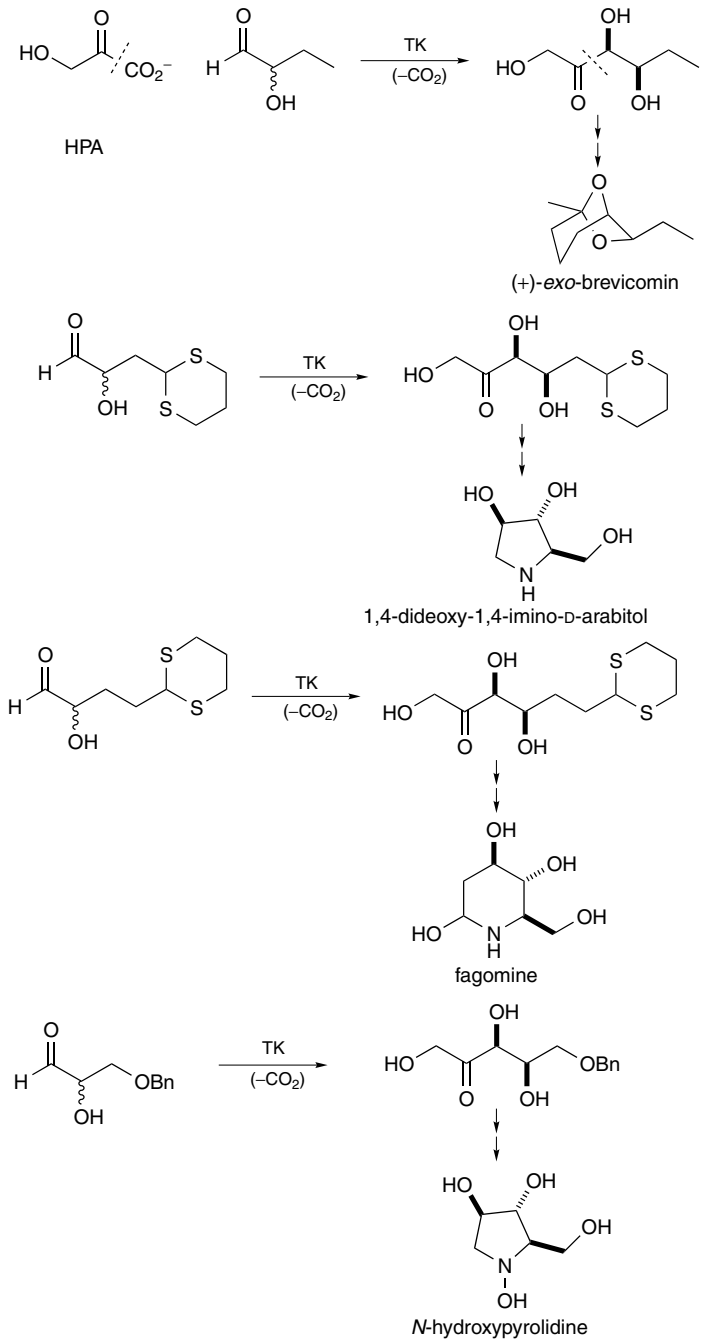

Scheme 5.56. The synthetic utility of transketolase has been demonstrated by its application in the synthesis of several natural products including: (+)-*exo*-brevicomin, 1,4-dideoxy-1,4-imino-D-arabitol, fagomine, and *N*-hydroxypyrrolidin.

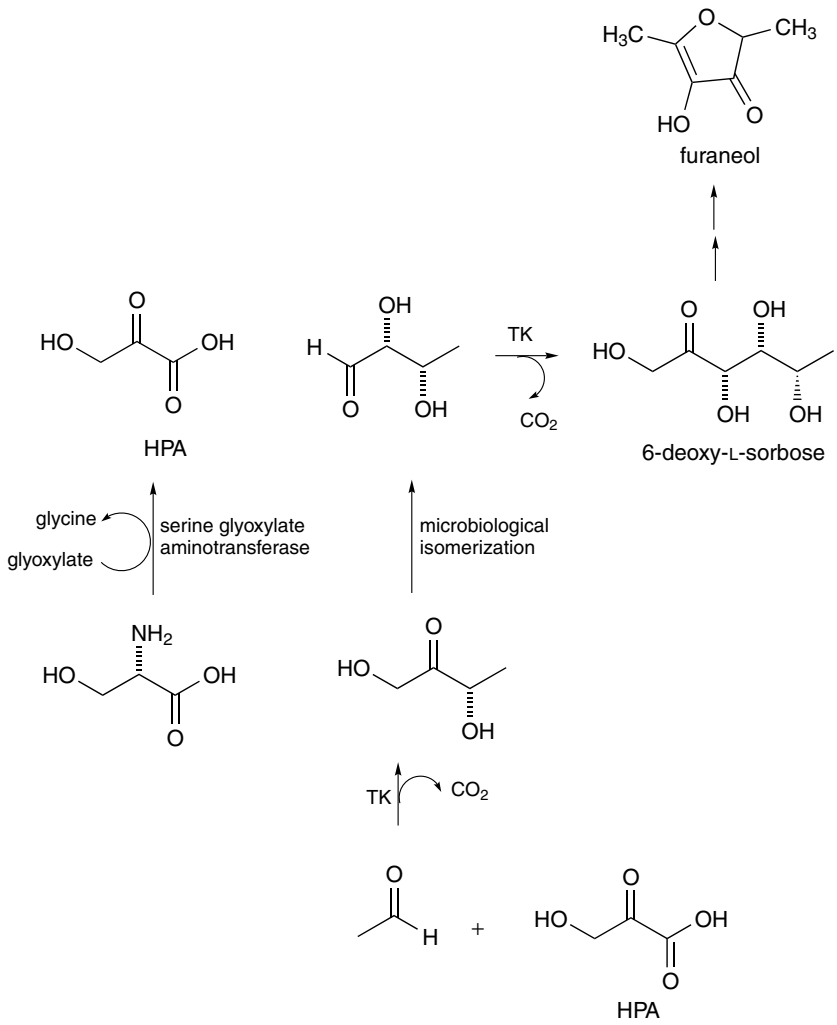

Scheme 5.57. TK catalyzed synthesis of 6-deoxy-L-sorbose, precursor to furaneol, was prepared from the readily available reagents: acetaldehyde, HPA, and serine.

complementary biocatalysts. Since TK can resolve racemic hydroxy aldehydes, it permits the use of less expensive starting materials. As well, a convenient feature of TK is that it can accept unphosphorylated substrates directly. Since FBP aldolase has a strong preference for DHAP as the donor substrate, the resulting product must be dephosphorylated to yield the same final product.[108–109]

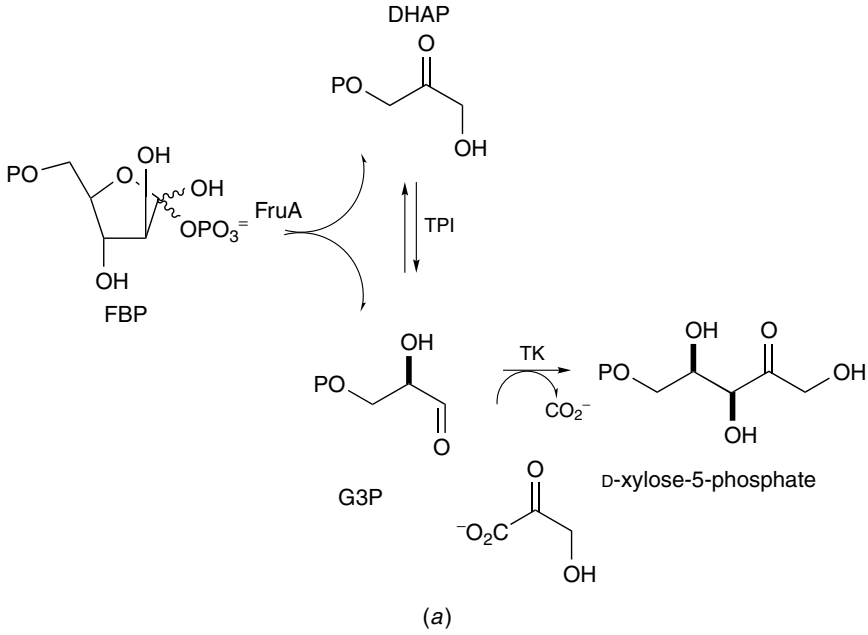

(*a*)

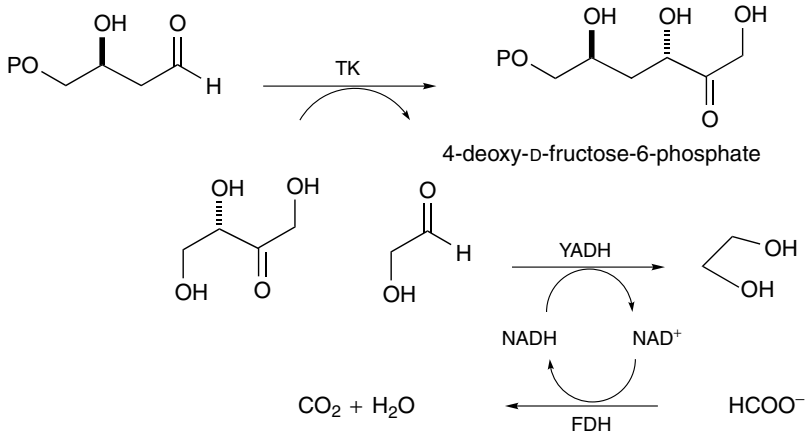

(*b*)

Scheme 5.58. (*a*) TK catalyzed synthesis of D-xylose-5-phosphate from D-fructose-bisphosphate and HPA. (*b*) TK catalyzed synthesis of 4-deoxy-D-fructose-6-phosphate using L-erythrulose as the source of ketol donor. YADH = yeast alcohol dehydrogenase; $P = PO_3^{2-}$.

F. Transaldolase

Like transketolase, transaldolase (TA, E.C. 2.2.1.2) is an enzyme in the oxidative pentose phosphate pathway. TA is a class one lyase that operates through a Schiff-base intermediate and catalyzes the transfer of the C(1)–C(3) aldol unit from D-sedoheptulose 7-phosphate to glyceraldehyde-3-phosphate (G3P) to produce D-Fru 6-P and D-erythrose 4-phosphate (Scheme 5.59). TA from human as well as microbial sources have been cloned.[110–111] The crystal structure of the *E. coli*[14] and human[112] transaldolases have been reported and its similarity to the aldolases is apparent, since it consists of an eight-stranded $(\alpha/\beta)_8$ or TIM barrel domain as is common to the aldolases. As well, the active site lysine residue that forms a Schiff base with the substrate was identified.[14,112] Thus, both structurally and mechanistically it is related to the type I class of aldolases.

Although TA from yeast is commercially available, it has rarely been used in organic synthesis applications, and no detailed study of substrate specificity has yet been performed. This is presumably due to high enzyme cost and also since the reaction equilibrium is near unity, resulting in the formation of a 50 : 50 mixture of products. In addition the stereochemistry accessible by TA catalysis matches that of FruA DHAP-dependent aldolase and the latter is a more convenient system to work with. In one application, TA was used in the synthesis D-fructose from starch.[113] The aldol moiety was transferred from Fru 6-P to D-glyceraldehyde in the final step of this multi-enzyme synthesis of D-fructose (Scheme 5.60). This process was developed because the authors could not identify a phosphatase that was specific for fructose 6-phosphate and TA offered an elegant method to bypass the need for phosphatase treatment.

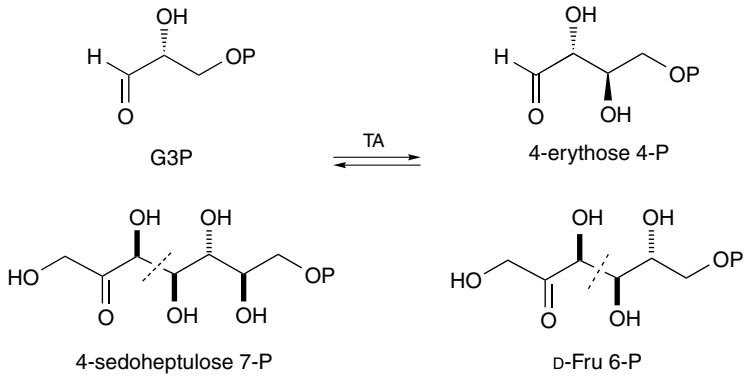

Scheme 5.59. Transaldolase catalyzed the transfer of the C1–C3 aldol unit of D-sedoheptulose-7-phosphate to D-glyceraldehyde-3-phosphate (G3P) generating D-fructose-6-phosphate and D-erythrose 4-phosphate. $P = PO_3^{2-}$.

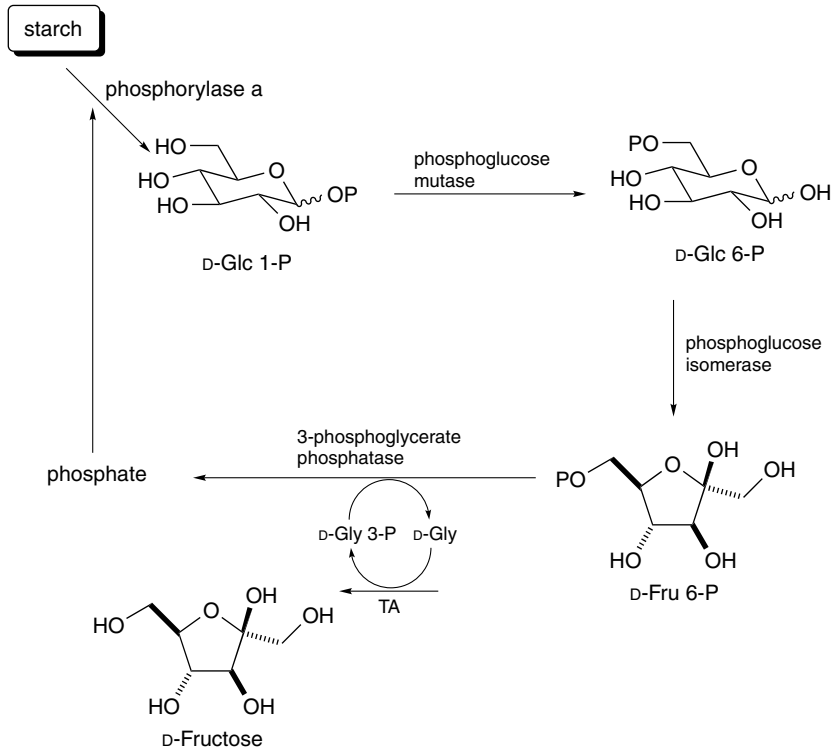

Scheme 5.60. Transaldolase catalyzed synthesis of D-fructose from starch. $P = PO_3^{2-}$.

G. Aldolase Catalytic Antibodies

Since natural enzymes are unable to accept all of the unnatural substrates that they are called upon to accept for organic synthesis applications, alternative biocatalysts with expanded substrate specificity are needed. One approach toward the generation of new biocatalysts is to exploit the molecular diversity of the immune system by recruiting catalytic antibodies as protein catalysts.

The first attempts to generate a catalytic antibody that could effect the aldol condensation reaction exploited the knowledge of the mechanism of type I aldolases. In this regard a library of catalytic antibodies was generated by immunization with a hapten (Scheme 5.61) that incorporated a mimic of the high-energy iminium ion transition state for the first step of the aldol reaction.[114] This transition state analogue consisted of a piperidinium cation bound to the aromatic primary amine cofactor. This hapten was used to elicit the production of antibody Ab72D4, which only in the presence of the designed

cofactor, catalyzed the aldol condensation of acetone and aldehyde acceptors with a rate acceleration of $k_{cat}/k_{uncat} = 100$. However, Ab72D4 is not a very efficient catalyst in absolute terms since $k_{cat} = 3 \times 10^{-6}\,s^{-1}$, $K_M = 1.8$ mM. One contributing factor to its low activity is that the amine in neither activated within the Ab-cofactor complex nor is it covalently linked, and thus preorganization of the complex is entropically unfavorable. The antibody catalyzes stereoselective addition to the *Si*-face of the aldehyde. The resulting product configuration is observed regardless of the absolute configuration of the aldehyde and thus represents a case of reagent controlled stereoselection. When racemic aldehyde is used, aldol products (4*S*, 5*S*) and (4*S*, 5*R*) are formed in a 1 : 2 : 8 ratio.[114–115]

Interestingly, Ab72D4 also catalyzes a (4*S*)-selective retro aldol reaction and a complementary (4*R*)-selective β-elimination reaction (Scheme 5.62). Chemoselectivity in this system appears to be a consequence of the conformational control imposed by the antibody pocket, although the nature of this interaction is not understood.[116]

The same hapten (Scheme 5.61) was employed to elicit antibody Ab78H6, which promotes the intramolecular aldol reaction of a keto-aldehyde yielding a

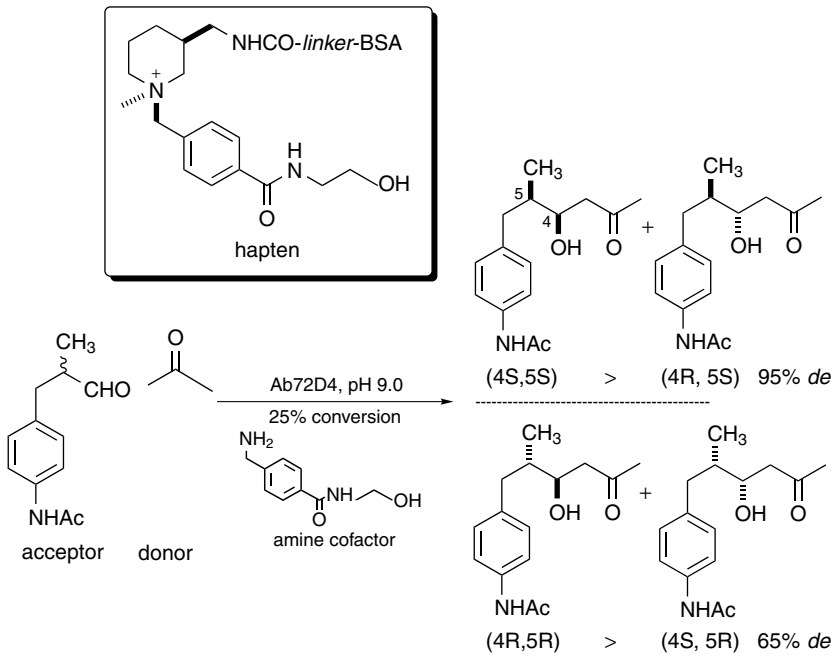

Scheme 5.61. A piperidinium cation containing transition state analogue was used as the hapten to elicit Ab72D4. Aldol reaction catalyzed by Ab72D4. BSA = bovine serum albumin.

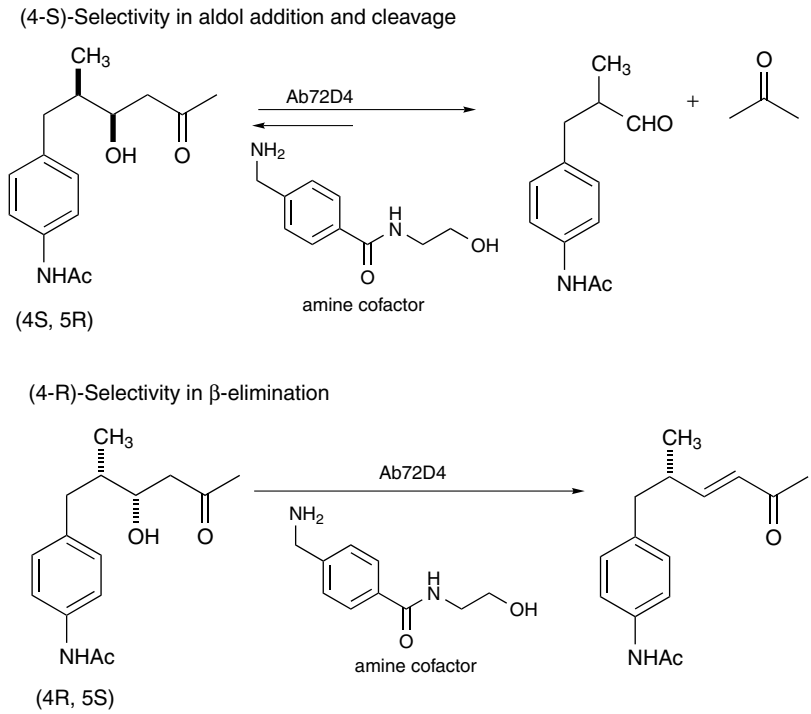

Scheme 5.62. Ab72D4 catalyzes the 4*R*-selective β-elimination reaction and the 4*S*-selective retroaldol reaction.

substituted 2-benzyl-3-hydroxy-cyclohexanone (Scheme 5.63). Ab78H6 functions as a general base catalyst but does not catalyze the carbon–carbon bond forming step. Thus, in the presence of the catalyst all four possible stereoisomers of the aldol product are formed in equal amounts. Ab78H6 also catalyzed the elimination reaction to form a α,β-unsaturated ketone. Interestingly Ab78H6 catalyzes the elimination sequence with complete stereoselectivity for the disfavored *trans*-elimination of the $(2R, 3S)$ enantiomer of the aldol product. However, the system is quite inefficient as demonstrated by the very low specificity constant $k_{\text{cat}}/K_{\text{M}} = 0.0065\ \text{M}^{-1}\,\text{s}^{-1}$.[117]

An alternate complementary approach toward catalytic antibody generation that could overcome the entropic disadvantage of preorganization of the amine cofactor with the Ab catalyst was investigated. A phosphinate (Scheme 5.64) was designed to mimic the expected transition state for the addition of a phenylacetone derived enolate to the carbonyl of benzaldehyde. An Ab raised against this hapten was expected to catalyze the aldol condensation of benzylacetone and benzaldehyde by both proximity and electrostatic effects. However, while

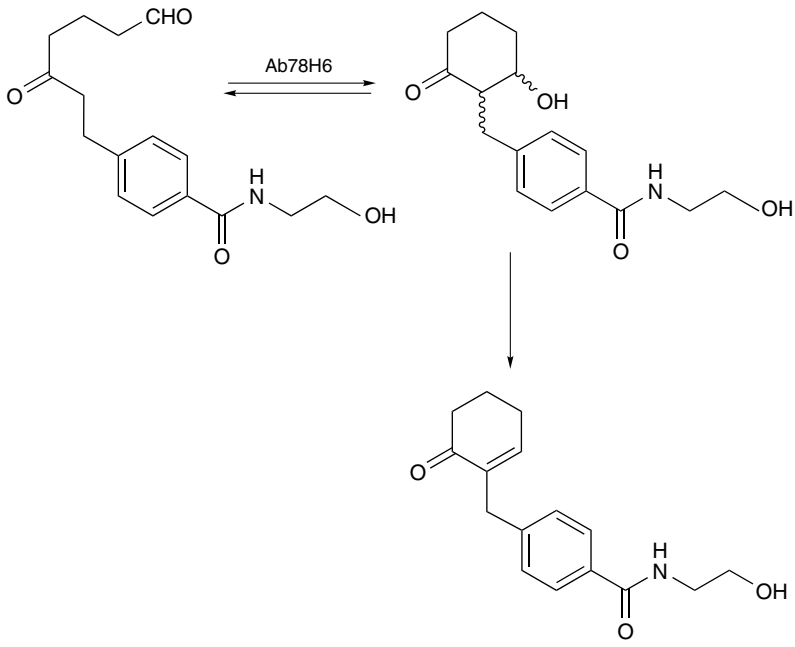

Scheme 5.63. Ab78H6 catalyzed intramolecular aldol reaction to generate 2-benzyl-3-hydroxycyclohexanone.

the Ab isolated did not catalyze this bimolecular aldol reaction for which it was designed, it was found to catalyze the Henry type retro-aldol reaction illustrated.[118]

The development of the concept of reactive immunization yielded more effective antibody aldolases.[119–120] In this new approach, rather than raise antibodies against an unreactive hapten designed to mimic the transition state, the antibodies were raised against a reactive moiety. Specifically, a β-diketone that serves as a chemical trap to imprint a lysine residue in the active site of the Ab (Scheme 5.65) was used.[340] A reactive lysine is a requirement of the type I aldolase mechanism. By this method two aldolase catalytic antibodies, 38C2 and 33F12 were identified.[119]

The aldol reaction catalyzed by Ab33F12 is outlined in Scheme 5.65. Regardless of the stereochemistry at C(2) of the aldehyde substrate shown (Scheme 5.65), its antibody catalyzed reaction with acetone resulted in a diastereoselective addition of acetone to the *Si*-face of the aldehyde. The products were formed with similar yields, and thus kinetic resolution was observed. However, the degree of facial stereochemical control of the reaction is surprising, since no stereochemical information was built into the hapten. For the

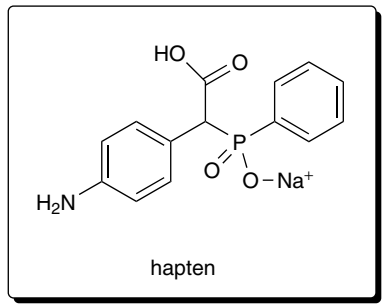

Aldol Reaction:

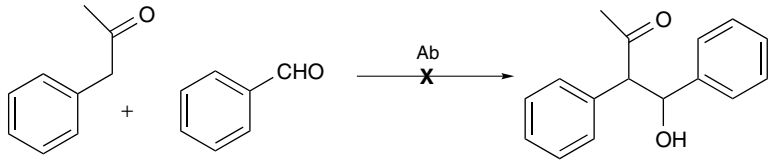

Henry Type Retro-Adol Reaction:

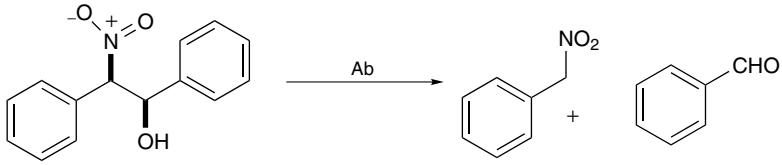

Scheme 5.64. Phosphinate transition-state analogue hapten. Henry type-retro-aldol reaction catalyzed by catalytic antibody.

reaction illustrated in Scheme 5.65, Ab33F12 exhibits $k_{cat} = 1.4 \times 10^{-3}$ s^{-1}; $K_M = 0.125$ mM; $k_{cat}/K_M = 11.2$ $M\,s^{-1}$, which is only about 4000-fold less than the specificity constant exhibited by fructose-1,6-bisphosphate aldolase with its natural substrate. Ab33F12 is three orders of magnitude more efficient than its predecessor Ab78H6, which was generated against the unreactive, antipiperidinium cation.

The presence and unique reactivity of a lysine residue in the active site of AB33F12 was monitored by UV spectroscopy (λ_{max} 316 nm). The formation of a stable vinylogous amide was monitored by UV spectroscopy and was shown to exhibit an apparent pK_a of 5.5. The crystal structure of Ab33F12 revealed the positioning of the reactive lysine Lys^{H93} residue in a predominantly hydrophobic environment consistent with its perturbed pK_a. This reactive lysine accounts for the efficient Schiff-base formation required

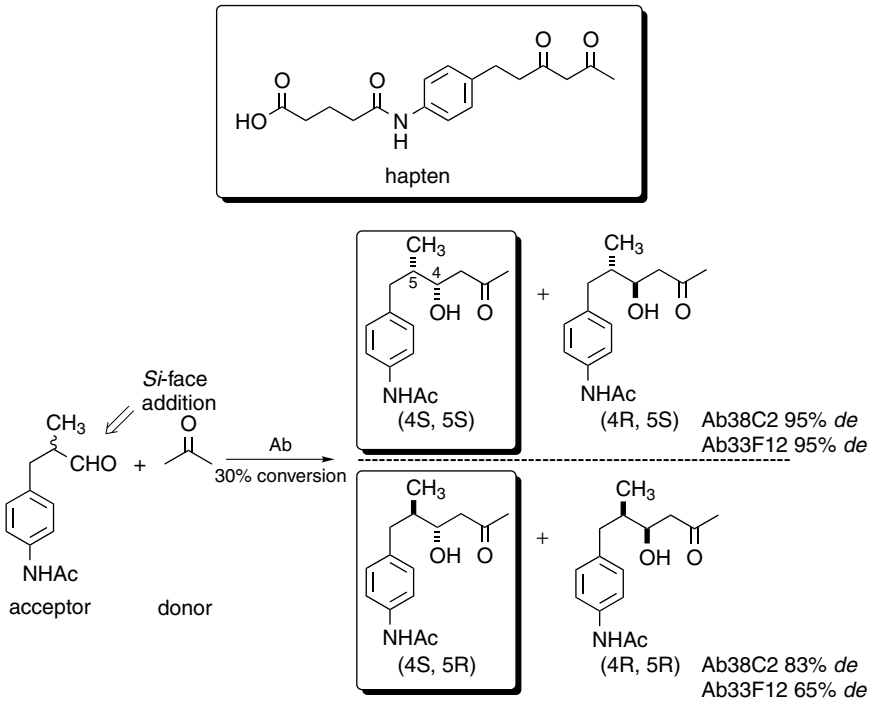

Scheme 5.65. β-diketone chemical trap hapten. Stereospecific aldol reaction catalyzed by the elicited catalytic antibodies Ab38C2 and Ab33F12.

for type I catalysis of the aldol reaction.[121] Further analysis of the substrate specificity of Ab38C2 and Ab33F12 with 23 donors and 16 acceptors revealed promiscuity in both the donor and acceptor substrates accepted by these catalysts. Some representative examples of donor substrates accepted include acetone, cyclopentanone, hydroxyacetone, and fluoroacetone, which exhibited relative rates of 2.5, 6.4, 54.3, and 5.5, respectively, with the 3-(4′-acetamidophenyl) propanol acceptor aldehyde. With cyclopentanone as the donor substrate, the acceptor substrates: *n*-pentanal, 4-acetamidobenzaldehyde, 4-(4′-acetamidophenyl) butyraldehyde, 4-nitrobenzaldehyde, and 4-nitrocinnamaldehyde, exhibited relative rates of 0.4, 142, 82, and 11, respectively.[122] Polyhydroxylated aldehydes, such as glyceraldehyde, glucose, and ribose, were not substrates, presumably due to the hydrophobic nature of the active site. These catalysts exhibited very broad substrate specificity and catalyze aldol reactions with high enantioselectivity. As a rule, high enantioselectivity was observed with acceptors having an sp^2 center in the α-position. Somewhat lower enantioselectivities resulted from acceptors with an sp^3 center in

the α-position. These antibodies have been shown to catalyze intermolecular ketone-ketone, ketone-aldehyde, aldehyde-ketone, and aldehyde-aldehyde aldol additions, and in some cases their subsequent dehydration. The synthetic utility of Ab38C2, which is now commercially available, was illustrated by the antibody catalyzed aldolase route to the brevicomins[123] (Scheme 5.66) and the epothilones[124] (Scheme 5.67).

Since the preparation of enantiomerically pure tertiary aldols remains a challenge, aldolase antibody 38C2 was investigated as a catalyst for the kinetic resolution of racemic tertiary aldols. Ab38C2 was demonstrated to be an efficient catalyst for the retro-aldol reaction of the fluorogenic tertiary aldol *tert*-methodol (Scheme 5.68) and exhibited an E value of $\geq 159 \pm 50$. At 50% conversion, (R)-*tert*-methodol is obtained with an enantiomeric excess of >99% *ee*. Consequently the ability of Ab38C2 to resolve tertiary alcohol was exploited in the enantioselective synthesis of (+)-frontalin (Scheme 5.69).[125]

The originally designed β-diketone hapten (Scheme 5.65) does not address the tetrahedral geometry of the transition state of the C–C bond forming step. Therefore a sulfoxide β-diketone hapten (Scheme 5.70) was designed and used in the search for an antibody with antipodal reactivity. Ab93F3 was identified

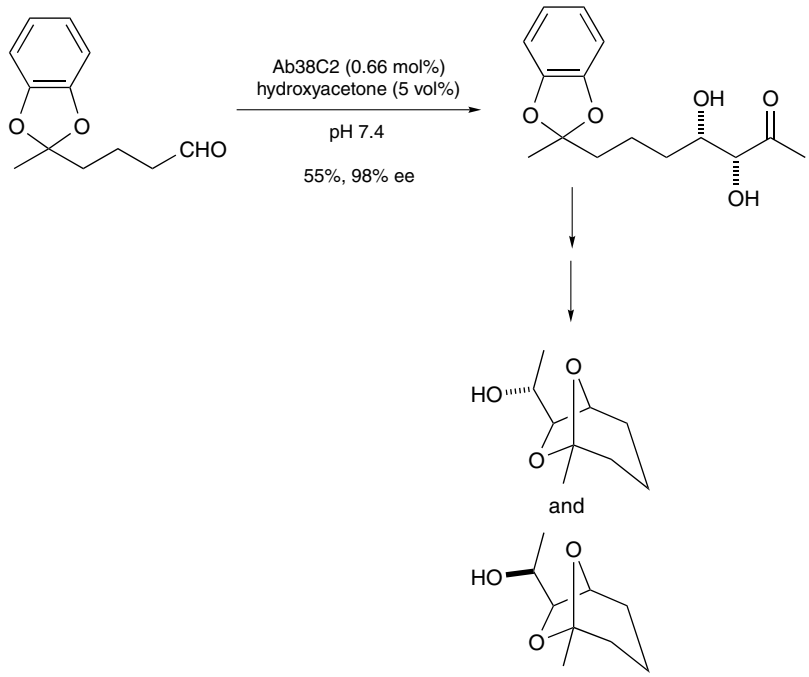

Scheme 5.66. Application of Ab38C2 in the synthesis of the brevicomins.

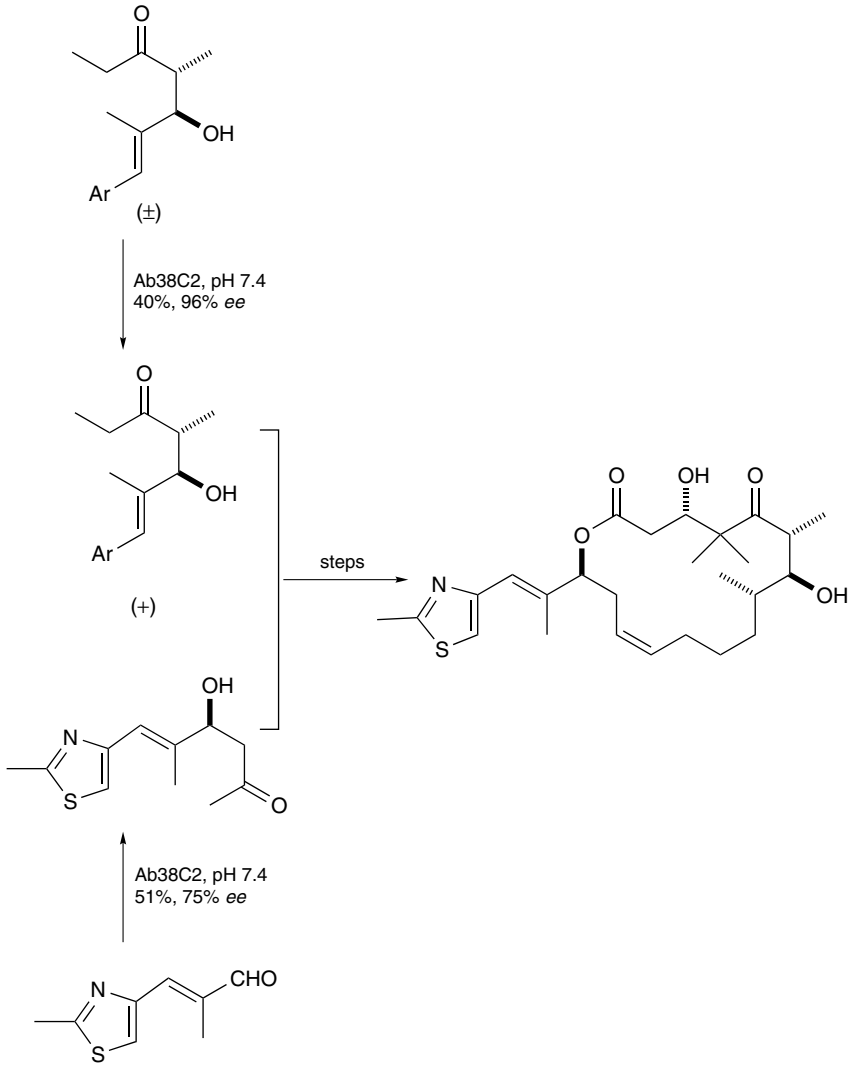

Scheme 5.67. Application of Ab38C2 in the synthesis of epothilone.

and fortuitously was shown to exhibit a complementary enantioselectivity to Ab38C2, thus providing the *S*-aldol with 99% *ee* at 50% conversion by kinetic resolution.[2f] The synthetic utility of this catalyst was demonstrated by its application in the preparation of epothilone E by the antibody-catalyzed resolution of a thiazole aldol (Scheme 5.70).[126]

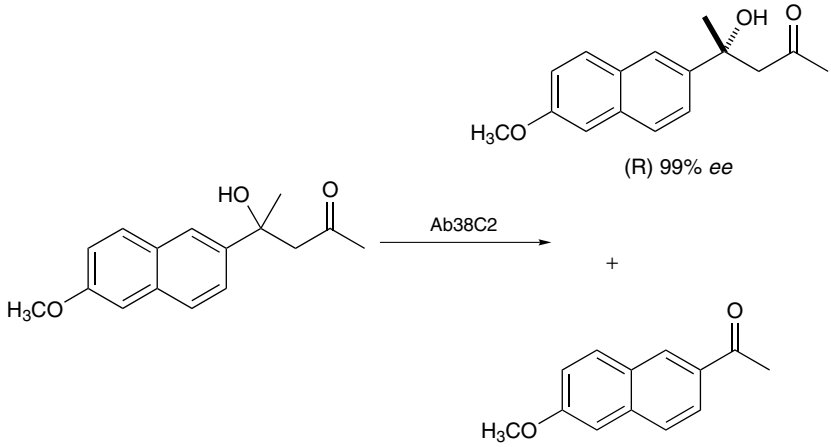

Scheme 5.68. Kinetic resolution of racemic tertiary alcohol by Ab38C2.

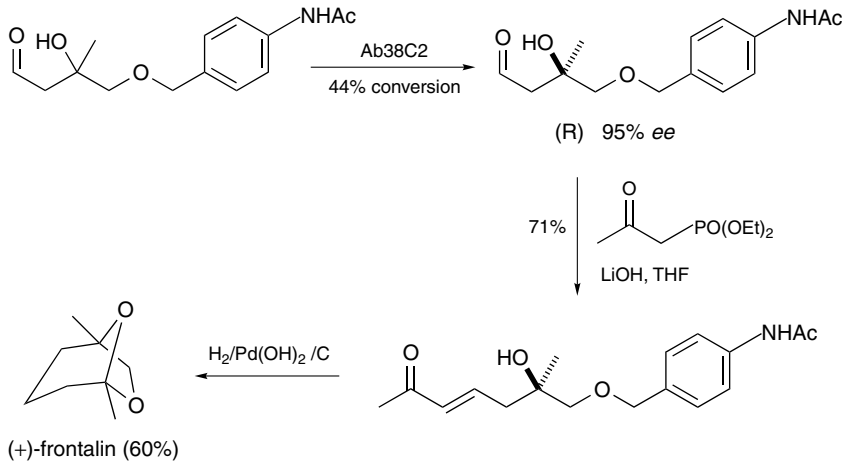

Scheme 5.69. Application of Ab38C2 in the total synthesis of frontalin.

This mechanism-based approach for eliciting catalytic antibodies has demonstrated promising opportunities for biocatalyst generation, and for the first time, it shows the possibility of being competitive with natural enzymes. The application of this second-generation catalytic antibody in the synthesis of several natural products gives credence to their potential applicability and demonstrates their scope.

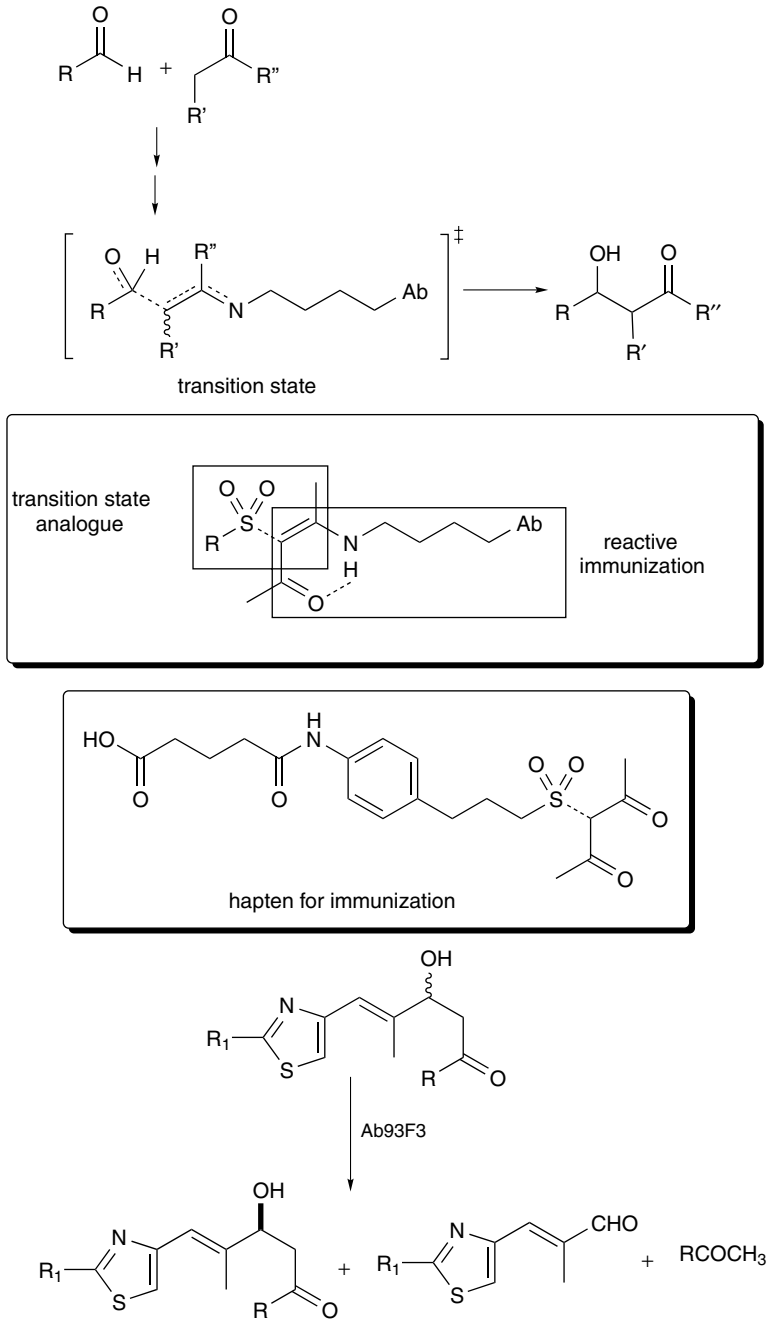

Scheme 5.70. Sulfoxide β-diketone hapten used to elicit Ab93F3. Ab93F3 catalyzed resolution of thiazole precursor of epothilone E.

III. CONCLUDING REMARKS

The aldol reaction is of central importance to synthetic organic chemistry in carbon skeletal elaboration. Furthermore it generates at least one and often two new stereogenic centers. Since an abundance of natural aldolases have now been identified and characterized, interest in the application of aldolases as catalysts in synthetic organic chemistry continues to increase. However, despite the potential synthetic utility of aldolase chemistry, the lyase class of enzymes is still underutilized. In contrast, the oxido-reductase and hydrolase class of enzymes have demonstrated substantial synthetic utility and are the two most utilized class of biocatalysts.

The field of biocatalysis differs substantially from that of traditional chemical asymmetric catalysis. Whereas the range of optimal operational conditions may be broader for the latter case, the issue of substrate specificity of the former is more complex. The practical integration of biological catalysts into synthetic schemes has two main requirements: (1) a suitable biocatalyst able to perform the required transformation must be identified and (2) the ability of the identified biocatalyst to perform the required transformation efficiently on the target substrate on a preparative scale must be assessed and if necessary engineered. Both of these requirements have been recognized and efforts to facilitate the implementation of biocataysts have been studied.[2]

To facilitate the identification of the best available biocatalysts for a specific application, a database of empirically determined substrate specificities should be consulted. The construction of such a database, which contains critical features such as operational parameters for biocatalyst utilization as well as substrate specificity, has recently been addressed.[127] Coupled with a fundamental understanding of the kinetic and thermodynamic factors that affect biocatalyst activity, such databases are indispensable in the identification of a suitable biocatalyst and reasonable reaction conditions.

If a suitable characterized biocatalyst is not available, one may turn to bioprospecting to identify a candidate biocatalyst, since microorganisms are a rich source of hitherto undiscovered biocatalysts.[128] For example, a microbial screen identified the yeast *Candida sorbophila* MY 1833 as a suitable biocatalyst for the asymmetric bioreduction of a ketone to its corresponding *R*-alcohol.[129] Armed with a few acceptable biocatalysts as the starting point, one can then chose to optimize either the biocatalyst itself of alternately exploit techniques such as substrate[130] or solvent[131] engineering and reactor design[132] to improve the efficiency of the overall process.

Recently ways to improve the substrate specificity of biocatalysts or optimization of their operational parameters and stability for particular applications have been extensively investigated. Approach toward the improvement of biocatalysis performance include absorption

on solid support[133] and entrapment in gels[134] or membranes, covalent crosslinking,[135] surface residue modification,[136] rational design by site-directed mutagenesis,[137] and directed evolution by random mutagenesis approaches,[138,63] as well as combining chemical modification and site-directed mutagenesis.[139] All the structurally known type I and type II aldolases (20 or so) have the $(\alpha/\beta)_8$ barrel as the active site for binding and catalysis. Since this structural fold can be engineered to alter substrate specificity while retaining the chemistry of catalysis, and vice versa, the aldolase enzymes represent an interesting class of enzymes for directed evolution with DNA shuffling and error-prone PCR.

The potential environmental and economic advantages that biocatalysts promise certainly warrant the necessary investments required to overcome the energy barriers of reducing biocatalysis to practice in the synthesis of both commodity and fine chemicals. The last quarter-century has brought extensive advancement is the field of biocatalysis and the next quarter-century promises to yield further advances.

REFERENCES

1. (a) Denmark, S. E.; Stavenger, R. A. *Acc. Chem. Res.* **2000**, *33*, 432–440. (b) Mahrwald, R. *Chem. Rev.* **1999**, *99*, 1095–1120. (c) Nelson, S. G. *Tetrahedron: Asymmetry* **1998**, *9*, 357–389. (d) Groger, H.; Vogl, E. M.; Shibasaki, M. *Chem. Eur. J.* **1998**, *4*, 1137–1141. (e) Bach, T. *Angew. Chem. Int. Ed. Engl.* **1994**, *33*, 417–419. (f) Masamune, S.; Choy, W.; Petersen, J. S.; Sita, L. R. *Angew. Chem. Int. Ed. Eng.* **1985**, *24*, 1–31. (g) Evans, D. A.; Nelson, J. V.; Taber, T. R. *Top. Stereochem.* **1982**, *13*, 1–115. (h) Heathcock, C. H. In *Asymmetric Synthesis*, Vol. 3. Morrison, J. D., ed. Academic Press, San Diego, **1984**, pp. 111–212. (i) Mukaiyama, T. *Org. React.* **1982**, *28*, 203–331. (j) Sawamura, M.; Ito, Y. *Chem. Rev.* **1992**, *92* (5), 857–871. (k) Kim, Y.; Singer, R. A.; Carreira, E. M. *Angew. Chem., Int. Ed.* **1998**, *37* (9), 1261–1263. (l) Furuta, K.; Maruyama, T.; Yamamoto, H. *J. Am. Chem. Soc.* **1991**, *113* (3), 1041–1042. (m) Corey, E. J.; Cywin, C. L.; Roper, T. D. *Tetrahedron Lett.* **1992**, *33* (46), 6907–6910. (n) Machajewski, T. D.; Wong, C-H. *Angew. Chem., Int. Ed.* **2000**, *39* (8), 1352–1374.
2. (a) Wong, C.-H.; Whitesides, G. M. *Enzymes in Synthetic Organic Chemistry*. Pergamon, Oxford, **1994**. (b) Drauz, K.; Waldmann, H. *Enzyme Catalysis in Organic Synthesis*. VCH, Weinheim, **1995**. (c) Wyner, N.; Toone, E. J. *Curr. Opin. Chem. Biol.* **2000**, *4*, 110–119. (d) Hendrix, M.; Wong, C.-H. *Bioorganic Chemistry: Carbohydrates*, Oxford University Press, New York **1999**, pp. 198–243, 569–575. (e) Fessner, W.-D.; Gosse, C.; Georg, J.; Oliver, E. *Eur. J. Org. Chem.* **2000**, *1*, 125–132. (f) Zhong, G.; Lerner, R. A.; Barbas, C. F., III *Angew. Chem., Int. Ed. Engl.* **1999**, *38*, 3738–3741. (g) Faber, K.; Patel, R. *Curr. Opin. Biotechnol.* **2000**, *11* (6), 517–519. (h) Roberts, S. M. *Perkin I* **2000**, *5*, 611–633.
3. Meyerhof, O.; Lohmann, K.; Schuster, P. *Biochem. Z.* **1936**, *286*, 301–318, 319–335.
4. Horecker, B. L.; Tsolas, O.; Lai, C.-Y. In *The Enzymes*, vol. 6 Boyer, P. D., ed. Academic Press, New York, **1975**, p. 213. Rutter, W. J. *Federation Proc.* **1964**, *23*, 1248–1257.
5. (a) Sygusch, J.; Beaudry, D.; Allaire, M. *Proc. Natl. Acad. Sci. USA* **1987**, *84*, 7846–7850. (b) Blom, N.; Sygusch, J. *Nat. Struct. Biol.* **1997**, *4*, 36–39.

6. (a) Gamblin, S. J.; Davies, G. J.; Grimes, J. M.; Jackson, R. M.; Littlechild, J. A.; Watson, J. C. *J. Mol. Biol.* **1991**, *219*, 573–576. (b) Dalby, A.; Dauter, Z.; Littlechild, J. A. *Protein Sci.* **1999**, *8*, 291–297.
7. (a) Hester, G.; Brenner-Holzach, O.; Rossi, F. A., Struck-Donatz, M.; Winterhalter, J. H.; Smit, J. D. G.; Piontek, K. *FEBS Lett.* **1991**, *292*, 237–242. (b) Kim, H.; Certa, U.; Dobeli, H.; Jakob, P.; Hol, W. G. J. *Biochem.* **1998**, *37*, 4388–4396.
8. Stura, E. A.; Gosh, S.; Garcia-Junceda, E.; Chen, L.; Wong, C.-H.; Wilson, I. A. *Proteins: Struct. Func. Gene.* **1995**, *22*, 67–72.
9. Mavridis, I. M.; Hatada, M. H.; Tulinsky, A.; Lebioda, L. *J. Mol. Biol.* **1982**, *162*, 419–444.
10. (a) Izard, T.; Lawrence, M. C.; Malby, R.; Lilley, G. G.; Colman, P. M. *Structure* **1994**, *2*, 361–369. (b) Lawrence, M. C.; Barbosa, J. A. R. G.; Smith, B. J.; Hall, N. E.; Pilling, P. A.; Ooi, H. C.; Marcuccio, S. M. *J. Mol. Biol.* **1997**, *266*, 381–399.
11. Hennig, M.; D'Arcy, A.; Hampele, I. C.; Page, M. G. P.; Oefner, C.; Dale, G. E. *Nat. Struct. Biol.* **1998**, *5*, 357–362.
12. Cooper, S. J.; Leonard, G. A.; McSweeney, S. M.; Thompson, A. W.; Naismith, J. H.; Qamar, S.; Plater, A.; Berry, A.; Hunter, W. N. *Structure* **1996**, *4*, 1303–1315.
13. (a) Allard, J.; Grochulski, P.; Sygusch, J. *Proc. Natl. Acad. Sci. USA* **2001**, *98*, 3679–3684. (b) Heine, A.; DeSantis, G.; Luz, J. G.; Mitchell, M.; Wong, C.-H.; Wilson, I. A. *Science* **2001**, *294*, 369–374.
14. (a) Jia, J.; Schorken, U.; Lindqvist, Y.; Sprenger, G.; Schneider, G. *Protein Sci.* **1997**, *6*, 119–124. (b) Jia, J.; Schorken, U.; Sahm, H.; Sprenger, G. A.; Lindqvist, Y.; Schneider, G. *Structure* **1996**, *4*, 715–724.
15. (a) Kobers, R. D.; Simpson, R. T.; Vallee, B. L.; Rutter, W. J. *J. Biochem.* **1969**, *8*, 585–588. (b) Harris, C. E.; Kobers, R. D.; Teller, D. C.; Rutter, J. *J. Biochem.* **1969**, *8*, 2442–2454. (c) Mildvan, A. S.; Kobes, R. D.; Rutter, W. J. *J. Biochem* **1971**, *10*, 1191–1204.
16. (a) Dreyer, M. K.; Schulz, G. E. *J. Mol. Biol.*, **1993**, *231*, 549–553. (b) Dreyer, M. K.; Schulz, G. E. *Acta Crystallogr., Sect. D* **1996**, 1082–1091. (c) Dreyer, M. K.; Schulz, G. E. *J. Mol. Biol.*, **1996**, *259*, 458–466.
17. (a) Joerger, A. C.; Gosse, C.; Fessner, W.-D; Schulz, G. E. *Biochem.* **2000**, *39*, 6033–6041. (b) Fessner, W.-D.; Schneider, A.; Held, H; Sinerius, G.; Walter, C.; Hixon, M.; Schloss, J. V. *Angew. Chem., Int. Ed. Engl.* **1996**, *35*, 2219–2221.
18. (a) Gefflaut, T.; Blonski, C.; Perie, J.; Willson, M. *Prog. Biophys. Mol. Bio.* **1995**, *63*, 301–340. (b) Horecker, B. L.; Tsolas, O.; Lai, C. Y. In *Enzymes*, Vol. 7, 3rd ed. Boyer, P. D., ed. Academic Press, New York, **1972**, pp. 213–258. (c) Branden, C.-I. *Curr. Opin. Struct. Biol.* **1991**, *1*, 978–983.
19. (a) Blom, N.; Tetreault, S.; Coulombe, R.; Sygusch, J. *Nature Struct. Biol.* **1996**, *3*, 856–862. (b) Chevrier, B.; D'Orchymont, H.; Schalk, C.; Tarnus, C.; Moras, D. *Eur. J. Biochem.* **1996**, *237*, 393–398. (c) Kimura, E.; Gotoh, T.; Koike, T.; Shiro, M. *J. Am. Chem. Soc.* **1999**, *121*, 1267–1274.
20. (a) Bednarski, M. D.; Simon, E. S.; Bischofberger, N.; Fessner, W.-D; Kim, J.-J. *J. Am. Chem. Soc.* **1989**, *111*, 627–635. (b) Von der Osten, C. H.; Sinskey, A. J.; Barbas, C. F. III; Pederson, R. L.; Wang, Y.-F.; Wong, C.-H. *J. Am. Chem. Soc.* **1989**, *111*, 3924–3927.
21. (a) Wong, C.-H.; Whitesides, G. M. *J. Org. Chem.* **1983**, *48* (19), 3199–3205. (b) Wong, C.-H.; Halcomb, R. L.; Ichikawa, Y.; Kajimoto, T. *Angew. Chem. Int. Ed. Engl.* **1995**, *34*, 412–432, 521–546. (c) Bednarski, M. D.; Waldmann, J. J.; Whitesides, G. M. *Tetrahedron Lett.* **1986**, *27*, 5807–5810. (d) Sobolov, S. B.; Bartoszko-Malik, A.; Oeschger, T. R.; Montelbano, M. M. *Tetrahedron Lett.* **1994**, *35*, 7751–7754. (e) Qamar, S.; Marshal, K.; Berry, A. *Protein Sci.* **1996**, *5*, 154–161.
22. Choi, K. H.; Mazurkie, A. S.; Morris, A. J.; Utheza, D.; Tolan, D. R.; Allen, K. N. *Biochem.* **1999**, *38*, 12655–12664.
23. Lees, W. J.; Whitesides, G. M. *J. Org. Chem.* **1993**, *58*, 1887–1894.

24. (a) Fessner, W.-D.; Sinerius, G.; Schneider, A.; Dreyer, M.; Schulz, G. E.; Badia, J.; Aguilar, J. *Angew. Chem., Int. Ed. Engl.* **1991**, *30*, 555–558. (b) Garcia-Junceda, E.; Shen, G.-J.; Sugai, T.; Wong, C.-H. *Bioorg. Med. Chem.* **1995**, *3*, 313–320. (c) Fessner, W.-D.; Eyrisch, O. *Angew. Chem., Int. Ed. Engl.* **1992**, *31*, 56–58. (d) Eyrisch, O.; Sinerius, G.; Fessner, W.-D. *Carbohydr. Res.* **1993**, *238*, 287–306.
25. (a) Fessner, W.-D.; Badia, J.; Eyrisch, O.; Schneider, A.; Sinerius, G. *Tetrahedron Lett.* **1992**, *33*, 5231. (b) Durrwachter, J. R.; Wong, C.-H. *J. Org. Chem.* **1988**, *53*, 4175–4181.
26. (a) Bischofberger, N.; Waldmann, H.; Saito, T.; Simon, E. S.; Lees, W. *J. Org. Chem.* **1988**, *53*, 3457–3465. (b) Fessner, W.-D.; Sinerius, G. *Tetrahedron Lett. 33*, 5231–5234. (c) Arth, H.-L.; Fessner, W.-D. *Carbohydrate Res.* **1998**, *305*, 313–321.
27. (a) Colbran, R. L.; Jones, J. K. N.; Matheson, N. K.; Rozema, I. *Carbohydr. Res.* **1967**, *4*, 355–388. (b) Effenberger, F.; Straub, A. *Tetrahedron Lett.* **1987**, *28*, 1641–1644. (c) Pederson, R. L.; Esker, J.; Wong, C.-H. *Tetrahedron Lett.* **1991**, *47*, 2643–2646. (d) Fessner, W.-D.; Walter, C. *Angew. Chem. Int. Ed. Engl.* **1992**, *31*, 614–616. (e) Crans, D. C.; Kazlauskas, R. J.; Hirschbein, B. L.; Wong, C.-H.; Abril, O.; Whitesides, G. M. *Methods Enzymol.* **1987**, *136*, 263–280. (f) Crans, D. C.; Whitesides, G. M. *J. Am. Chem. Soc.* **1985**, *107*, 7019–7027. (g) Wong, C.-H.; Mazenod, F. P.; Whitesides, G. M. *J. Org. Chem.* **1983**, *48*, 3493–3497. (h) Wong, C.-H.; Whitesides, G. M. *J. Org. Chem.* **1994**, *59*, 7182–7184. (i) Fessner, W.-D.; Sinerius, G. *Angew. Chem., Int. Ed. Engl.* **1994**, *106*, 209–212.
28. Jung, S.-H.; Jeong, J.-H.; Miller, P.; Wong, C.-H. *J. Org. Chem.* **1994**, *59*, 7182–7184.
29. Lin, C.-C.; Moris-Varas, F.; Weitz-Schmidt, G.; Wong, C.-H. *Biorg. Med. Chem.* **1999**, *7*, 425–433.
30. Gijsen, H. J. M.; Qiao, L.; Fitz, W.; Wong, C.-H. *Chem. Rev.* **1996**, *96*, 443–473.
31. Pederson, R. L.; Liu, K. K.-C.; Rutan, J. F.; Chen, L.; Wong, C.-H. *J. Org. Chem.* **1990**, *55*, 4897–4901.
32. Henderson, I.; Sharpless, K. B.; Wong, C.-H. *J. Am. Chem. Soc.* **1994**, *116*, 558–561.
33. Alajarin, R.; Garcia-Junceda, E.; Wong, C.-H. *J. Org. Chem.* **1995**, *60*, 4294–4296.
34. Durrwachter, J. R.; Drueckhammer, D. G.; Nozaki, K.; Sweers, H. M.; Wong, C.-H. *J. Am. Chem. Soc.* **1986**, *108*, 7812–7818.
35. Borysenko, G. W.; Spaltenstein, A.; Straub, J. A.; Whitesides, G. M. *J. Am. Chem. Soc.* **1989**, *111*, 9275–9276.
36. Christensen, U.; Tuchsen, E.; Andersen, B. *Acta Chem. Scand. B* **1975**, *29*, 81–87.
37. Petersen, M.; Zannetti, M. T.; Fessner, W.-D. *Top. Curr. Chem.* **1997**, *186*, 87–117.
38. Kim, M.-J.; Lim, I. T.; Kim, H.-J.; Wong, C.-H. *Tetrahedron Asymm.* **1997**, *8*, 1507–1509.
39. (a) Pederson, R. L.; Kim, M.-J.; Wong, C.-H. *Tetrahedron Lett.* **1988**, *29*, 4645–4648. (b) Ziegler, T.; Straub, A.; Effenberger, F. *Angew. Chem.* **1988**, *100*, 737–738.
40. Hung, R. R.; Straub, J. A.; Whitesides, G. M. *J. Org. Chem.* **1991**, *56*, 3849–3855.
41. Takayama, S.; Martin, R.; Wu, J.; Laslo, K.; Siuzdak, G.; Wong, C.-H. *J. Am. Chem. Soc.* **1997**, *119*, 8146–8151.
42. Chou, W.-C.; Chen, L.; Fang, J.-M.; Wong, C.-H. *J. Am. Chem. Soc.* **1994**, *116*, 6191–6194.
43. (a) Chou, W.-C.; Fotsch, C.; Wong, C.-H. *J. Org. Chem.* **1995**, *60*, 2916–2917. (b) Gijsen, H. J. M.; Wong, C.-H. *Tetrahedron Lett.* **1995**, *36*, 7057–7060.
44. Schultz, M.; Waldmann, H.; Vogt, W.; Kunz, H. *Tetrahedron Lett.* **1990**, *31*, 867–868.
45. Shimagaki, M.; Muneshima, H.; Kubota, M.; Oishi, T. *Chem. Pharm. Bull.* **1993**, *41*, 282–286.
46. Chenevert, R.; Lavoie, M.; Dasser, M. *Can. J. Chem.* **1997**, *75*, 68–73.
47. (a) Chenevert, R.; Dasser, M. *J. Org. Chem.* **2000**, *65*, 4529–4531. (b) Romero, A.; Wong C.-H. *J. Org. Chem.* **2000**, *65*, 8264–8268.
48. (a) Comb, D. G.; Roseman, S. *J. Biol. Chem.* **1960**, *235*, 2529. (b) Brunett, P.; Jourdian, G. W.; Roseman, S. *J. Biol. Chem.* **1962**, *237*, 2447. (c) Devries, G. H.; Binkley, S. B. *Arch. Biochem. Biophys.* **1972**, *151*, 234–250. (d) Baumann, W.; Freidenreich, J.; Weisshaar, G.;

Brossmer, R.; Freibolin, H. *Biol. Chem.* **1989**, *370*, 141–149. (e) Deijl, M. M.; Vliegenthart, J. F. G. *Biochem. Biophys. Res. Commun.* **1983**, *111*, 668–674.
49. (a) Uchida, Y.; Tsukada, Y.; Sugimori, T. *Agric. Biol. Chem.* **1985**, *49*, 181–187. (b) Lin, C.-H.; Sugai, T. L.; Halcomb, R. L.; Ichikawa, Y.; Wong, C.-H. *J. Am. Chem. Soc.* **1992**, *114*, 10138–10145.
50. Ichikawa, Y.; Liu, J. L.-C.; Chun, J. L.; Shen, G.-J.; Wong, C.-H. *J. Am. Chem. Soc.* **1991**, *113*, 6300–6302.
51. (a) Uchida, Y.; Tsukada, Y.; Sugimori, T. *J. Biochem.* **1984**, *96*, 507–522. (b) Blacklow, R. S.; Warren, L. *J. Biol. Chem.* **1962**, *237*, 3520–3526. (c) Merker, R. I.; Troy, F. A. *Glycobiology* **1990**, *1*, 93–100. (d) Warren, L.; Blacklow, R. S. *J. Biol. Chem.* **1962**, *237*, 3527–3534.
52. Fitz, W.; Schwark, J.-R.; Wong, C.-H. *J. Org. Chem.* **1995**, *60*, 3663–3670.
53. Smith, B. J.; Lawrence, M. C.; Barbosa, J. A. R. G. *J. Org. Chem.* **1999**, *64*, 945–949.
54. Lin C.-C.; Lin, C.-H.; Wong, C.-H. *Tetrahedron Lett.* **1997**, *38*, 2649–2652.
55. Zhou, P.; Salleh, H. M.; Honek, J. F. *J. Org. Chem.* **1993**, *58*, 264–266.
56. (a) Takayama, S.; Livingston, P. O.; Wong, C.-H. *Tetrahedron Lett.* **1996**, *37*, 9271–9274. (b) Sasaki, K.; Kurata, K.; Kojima, N.; Kurosawa, N.; Ohta, S.; Hanai, N.; Tsuji, S.; Nishi, T. *J. Biol. Chem.* **1994**, *269*, 15950–15956. (c) Liu, J. L.-C.; Shen, G.-J.; Ichikawa, Y.; Rutan, J. F.; Zapata, G.; Vann, W. F.; Wong, C.-H. *J. Am. Chem. Soc.* **1992**, *114*, 3901–3910.
57. Maru, I.; Ohnishi, J.; Yasuhiro, O.; Tsukada, Y. *Carbohydrate Res.* **1998**, *306*, 575–578.
58. (a) Ghalambor, M. A.; Heath, E. C. *J. Biol. Chem.* **1966**, *241*, 3222–3227. (b) Ghalambor, M. A.; Heath, E. C. *Meth. Enzymol.* **1966**, *9*, 534–538. (c) Sugai, T.; Shen, G.-J.; Ichikawa, Y.; Wong, C.-H. *J. Am. Chem. Soc.* **1993**, *115*, 413–421.
59. (a) Raetz, C. R. H.; Dowhan, W. *J. Biol. Chem.* **1990**, *265*, 1235–1238. (b) Schumann, R. R.; Leong, S. R.; Flaggs, G. W.; Gray, P. W.; Wright, S. D.; Mathison, J. C.; Tobias, P. S.; Ulevitch, R. J. *Science* **1990**, *249*, 1429–1431. (c) Andersson, F. O.; Classon, B.; Samuelsson, B. *J. Org. Chem.* **1990**, *55*, 4699–4704.
60. Shelton, M. C.; Cotterill, I. C.; Novak, S. T. A.; Poonawala, R. M.; Sudarshan, S.; Toone, E. J. *J. Am. Chem. Soc.* **1996**, *118*, 2117–2125.
61. Cotterill, I. C.; Shelton, M. C.; Machemer, D. E. W.; Henderson, D. P.; Toone, E. J. *J. Chem. Soc., Perkin Trans.* **1998**, *1*, 1335–1341.
62. Henderson, D. P.; Shelton, M. C.; Cotterill, I. C.; Toone, E. J. *J. Org. Chem.* **1997**, *62*, 7910–7911.
63. Fong, S; Machajewski, T. D.; Mak, C. C.; Wong, C.-H. *Chem. Biol.* **2000**, *7* (11), 873–883.
64. Reimer, L. M.; Conley, D. L.; Pompliano, D. L.; Frost, J. W. *J. Am. Chem. Soc.* **1986**, *108*, 8010–8015.
65. Floyd, N. C.; Liebster, M. H.; Turner, N. J. *J. Chem. Soc., Perkin Trans. I* **1992**, 1085–1086.
66. Auge, C.; Delect, V. *Tetrahedron Asymm.* **1993**, *4*, 1165–1168.
67. (a) McGeown, M. G.; Malpress, F. H. *Nature* **1952**, *170*, 575–576. Hoffee, P. A. *Arch. Biochem. Biophys.* **1968**, *126*, 795–802.
68. (a) Barbas, C. F. III; Wang, Y.-F.; Wong, C.-H. *J. Am. Chem. Soc.* **1990**, *112*, 2013. (b) Chen, L.; Dumas, D. P.; Wong, C.-H. *J. Am. Chem. Soc.* **1992**, *114*, 741–748. (c) Wong, C.-H.; Garcia-Junceda, E.; Chen, L.; Blanco, O.; Gijsen, H. J. M.; Steensma, D. H. *J. Am. Chem. Soc.* **1995**, *117*, 3333–3339.
69. Ouwerkerk, N.; van Boom, J. H.; Lugtenburg, J.; Raap, J. *Eur. J. Org. Chem.* **2000**, 861–866.
70. Kajimoto, T.; Liu, K. K.-C.; Pederson, R. L.; Zhong, Z. Y.; Ichikawa, Y.; Porco, Jr.; J. A., Wong, C.-H. *J. Am. Chem. Soc.* **1991**, *113*, 6187.
71. Gijsen, J. J. M.; Wong, C.-H. *J. Am. Chem. Soc.* **1994**, *116*, 8422–8423.

72. (a) Gijsen, J. J. M.; Wong, C.-H. *J. Am. Chem. Soc.* **1995**, *117*, 7585–7592. (b) Gijsen, J. J. M.; Wong, C.-H. *J. Am. Chem. Soc.* **1995**, *117*, 2947–2948.
73. Machajewski, T. D.; Wong, C.-H. *Synthesis* **1999**, 1469–1472.
74. (a) Schirch, L. *Adv. Enzymol.* **1982**, *53*, 83–112. (b) Stover, P.; Zamora, M.; Shostak, K.; Gautam-Basak, M.; Schirch, V. *J. Biol. Chem.* **1992**, *267*, 17679–17687.
75. (a) Hamilton, B. K.; Hsiao, H. Y.; Swanm, W. E.; Anderson, D. M.; Delente, J. J. *Trends Biotechnol.* **1985**, *3*, 64–68. (b) Hsiao, H. Y.; Wei, T.; Campbell, K. *Biotechnol. Bioeng.* **1986**, *28*, 857–867.
76. Miller, M. J.; Richardson, S. K. J. *Molec. Cat. B: Enzym.* **1996**, *1*, 161–164.
77. (a) Kimura, T.; Vassilev, V. P.; Shen, G.-J.; Wong, C.-H. *J. Am. Chem. Soc.* **1997**, *119*, 11734–11742. (b) Vassilev, V. P.; Uchiyama, T.; Kajimoto, T.; Wong, C.-H. *Tetrahedron Lett.* **1995**, *36*, 5063–5064.
78. (a) Herbert, R. B.; Wilkinson, B.; Ellames, G. J.; Kunec, E. K. *J. Chem. Soc., Chem. Commun.* **1993**, 205–206. (b) Herbert, R. B.; Wilkinson, B.; Ellames, G. J. *Can. J. Chem.* **1994**, *72*, 114–117.
79. (a) Uchiyama, T.; Vassilev, V. P.; Kajimoto, T.; Wong, W.; Huang, H.; Lin, C.-C.; Wong, C.-H. *J. Am. Chem. Soc.* **1995**, *117*, 5395–5396. (b) Wong, C.-H.; Moris-Varas, F.; Hung, S.-C.; Marron, T. G.; Lin, C.-C.; Gong, K. W.; Weitz-Schmidt, G. *J. Am. Chem. Soc.* **1997**, *119*, 8152–8158.
80. Nishide, K.; Shibata, K.; Fujita, T.; Kajimoto, T.; Wong, C.-H.; Node, M. *Heterocycles* **2000**, *52*, 1191–1201.
81. Miura, T.; Fujii, M.; Shingu, K.; Koshimizu, I.; Naganoma, J.; Kajimoto, T.; Ida, Y. *Tetrahedron Lett.* **1998**, *39*, 7313–7316.
82. Thiem, J.; Treder, W. *Angew. Chem. Int. Ed. Engl.* **1986**, *25*, 1096–1097.
83. Schneider, G.; Lindqvist, Y. *Biochim. Biophys. Acta* **1998**, *1385*, 387–398.
84. Schörken, U.; Sprenger, G. A. *Biochim. Biophys, Acta* **1998**, *1385*, 229–243.
85. Sprenger, G.; Pohl, M. *J. Mol. Catal. B: Enzym.* **1999**, *6*, 145–159.
86. Villafranca, J. J.; Axelrod, B. *J. Biol. Chem.* **1971**, *246*, 3126–3131.
87. Dickens, F.; Williamson, D. H. *Nature* **1958**, *181*, 1790.
88. Josephson, B. L.; Fraenkel, D. G. *J. Bacteriol.* **1969**, *100*, 1289–1295.
89. Datta, A. G.; Racker, E. *J. Biol. Chem.* **1961**, *236*, 617–623.
90. Bolte, J.; Demuynck, C.; Samaki, H. *Tetrahedron Lett.* **1987**, *28*, 5525–5528.
91. Kobori, Y.; Myles, D. C.; Whitesides, G. M. *J. Org. Chem.* **1992**, *57*, 5899–5907.
92. Demuynck, C.; Bolte, J.; Hecquet, L.; Dalmas, V. *Tetrahedron Lett.* **1991**, *32*, 5085–5088.
93. Effenberger, F.; Null, V.; Ziegler, T. *Tetrahedron Lett.* **1992**, *33* (36), 5157–5160.
94. Mitra, R. K.; Woodley, J. M.; Lilly, M. D. *Biocatal. Biotransform.* **1999**, *17* (1), 21–36.
95. Effenberger, F.; Straub, A.; Null, V. *Liebigs Ann. Chem.* **1992**, *12*, 1297–1301.
96. Sprenger, G. A. *Biochim. Biophys. Acta* **1993**, *1216*, 307–310.
97. Morris, K. G.; Smith, M. E. B.; Turner, N. J.; Lilly, M. D.; Mitra, R. K.; Woodley, J. M. *Tetrahedron: Asymmetry* **1996**, *7*, 2185–2188.
98. Bongs, J.; Hahn, D. *Biotechnol. Lett.* **1997**, *19*, 213–215.
99. Brocklebank, S.; Woodley J. M.; Lilly, M. D. *J. Mol. Catal. B: Enzym.* **1999**, *7*, 223–231.
100. Chauhan, R. P.; Woodley, J. M.; Powell, L. W. *Ann. NY Acad. Sci.* **1996**, *799* (Enzyme Engineering XIII), 545–554.
101. Myles, D. C.; Andrulis, P. J. III; Whitesides, G. M. *Tetrahedron Lett.* **1991**, *32*, 4835–4838.
102. Hecquet, L.; Lemaire, M.; Bolte, J.; Demuynck, C. *Tetrahedron Lett.* **1994**, *35*, 8791–8784.
103. Effenberger, F.; Null, V. *Liebigs Ann. Chem.* **1992**, *11*, 1211–1212.
104. Humphrey, A. J.; Parsons, S. F.; Smith, M. E. B.; Turner, N. J. *Tetrahedron Lett.* **2000**, *41*, 4481–4485.
105. Hecquet, L.; Bolte, J.; Demuynck, C.; *Tetrahedron*, **1996**, *52*, 8223–8232. 326. Wong, C. H.; Mazenod, F. P.; Whitesides, G. M.; *J. Org. Chem.* **1983**, *48*, 3493–3497.

106. Zimmermann, F. T.; Schneider, A.; Schorken, U.; Sprenger, G. A.; Fessner, N. D. *Tetrahedron: Asymmetry* **1999**, *10*, 1643–1646.
107. Guérard, C.; Alphand, V.; Archelas, A.; Demuynck, C.; Hecquet, L.; Furstoss, R.; Bolte, J. *Eur. J. Org. Chem.* **1999**, 3399–3402.
108. Andre, C.; Guérard, C.; Hecquet, L.; Demuynck, C.; Bolte, J. *J. Mol. Catal. B: Enzym.* **1988**, *5*, 459–466.
109. Andre, C.; Demuynck, C.; Gefflaut, T.; Guérard, C.; Hecquet, L.; Lemaire, M.; Bolte, J. *J. Mol. Catal. B: Enzym.* **1988**, *5*, 1381–1177.
110. Banki, K; Halladay, D.; Perl, A. *J. Biol. Chem.* **1994**, *269*, 2847–2851.
111. Schaaff, I.; Hohmann, S.; Zimmermann, F. K. *Eur. J. Biochem.* **1990**, *188*, 597–603.
112. Thorell, S.; Gergely, P.; Banki, K.; Perl, A.; Schneider, G.; *Febs. Lett.* **2000**, *475* (3), 205–208.
113. Moradian, A.; Benner, S. A. *J. Am. Chem. Soc.* **1992**, *114*, 6980–6987.
114. Reymond, J.-L.; Chen, Y. *Tetrahedron Lett.* **1995**, *36*, 2575–2578
115. Reymond, J.-L.; Chen, Y. *J. Org. Chem.* **1995**, *60*, 6970–6979.
116. Reymond, J.-L. *Angew. Chem., Int. Ed. Engl.* **1995**, *34*, 2285–2287.
117. Koch, T.; Reymond, J.-L.; Lerner, R. A. *J. Am. Chem. Soc.* **1995**, *117* (37), 9383–9387.
118. Flanagan, M. E.; Jacobsen, J. R.; Sweet, E.; Schultz, P. G. *J. Am. Chem. Soc.* **1996**, *118*, 6078–6079.
119. Wagner, J.; Lerner, R. A.; Barbas, C. F. III. *Science* **1995**, *270*, 1797–1800.
120. Wirsching, P.; Ashley, J. A.; Lo, C.-H. L.; Janda, K. D.; Lerner, R. A. *Science* **1995**, *270*, 1775–1782.
121. Barbas, C. F., III; Heine, A.; Zhong, G.; Hoffmann, T.; Gramatikova, S.; Bjornestedt, R.; List, B.; Anderson, J.; Stura, E. A.; Wilson, I. A.; Lerner, R. A. *Science* **1997**, *278* (5346), 2085–2092.
122. Hoffmann, T.; Zhong, G.; List, B.; Shabat, D.; Anderson, J.; Gramatikova, S.; Lerner, R. A.; Barbas, C. F. III. *J. Am. Chem. Soc.* **1998**, *120* (12), 2768–2779.
123. List, B.; Shabat, D.; Barbas, C. F. III; Lerner, R. A. *Chem. Eur. J.* **1998**, *4* (5), 881–885.
124. Sinha, S. C.; Barbas, C. F. III; Lerner, R. A. *Proc. Natl. Acad. Sci. USA* **1998**, *95* (25), 14603–14608.
125. List, B.; Shabat, D.; Zhong, G.; Turner, J. M.; Li, A.; Bui, T.; Anderson, J.; Lerner, R. A.; Barbas, C. F. III. *J. Am. Chem. Soc.* **1999**, *121* (32), 7283–7291.
126. Sinha, S. C.; Sun, J.; Miller, G.; Barbas, C. F. III; Lerner, R. A. *Org. Lett.* **1999**, *1* (10), 1623–1626.
127. Bio*Catalysis*. Available from Synopsys Scientific Systems Leeds, UK: *www.Synopsys.co.uk*.
128. Demirjian, D. C.; Shah, P. C.; Moris-Varas, F *Top. Curr. Chem.* **1999**, *200* (Biocatalysis: From Discovery to Application), 1–29.
129. Chartrain, M.; Roberge, C.; Chung, J.; McNamara, J.; Zhao, D.; Olewinski, R.; Hunt, G.; Salmon, P.; Roush, D.; Yamazaki, S.; Wang, T.; Grabowski, E.; Buckland, B.; Greasham, R. *Enzyme Microb. Technol.* **1999**, *25* (6), 489–496.
130. Berglund, P.; Hedenstrom, E.; Hult, K. *Book of Abstracts, 219th ACS National Meeting*, San Francisco, CA, March 26–30, **2000**.
131. a) Adlercreutz, P. *Appl. Biocatal., 2nd Ed.* **2000**, 295–316. (b) Laane, C. *Biocatalysis* **1987**, *1* (1), 17–22. (c) Catoni, E.; Cernia, E.; Palocci, C. *J. Mol. Catal. A: Chem.* **1996**, *105* (1–2), 79–86.
132. Cabral, J. M. S.; Tramper, J. *Appl. Biocatal., 2nd Ed.* **2000**, 339–378.
133. a) Kermasha, S.; Gaffar, R.; Bisakowski, B. *Process Biochem. (Oxford)* **2000**, *35* (10), 1103–1109. (b) Tischer, W.; Wedekind, F. *Top. Curr. Chem.* **1999**, *200* (Biocatalysis: From Discovery to Application), 95–126.

134. a) Giordano, R. L. C.; Hirano, P. C.; Goncalves, L. R. B.; Netto, W. S. *Appl. Biochem. Biotechnol.* **2000**, 84–86 643–654. (b) Reetz, M. T.; Zonta, A.; Vijayakrishnan, V.; Schimossek, K. *J. Mol. Catal. A: Chem.* **1998**, *134* (1–3), 251–258.
135. a) Peissker, F.; Fischer, L. *Bioorg. Med. Chem.* **1999**, *7* (10), 2231–2237. (b) Govardhan, C. xP. *Curr. Opin. Biotechnol.* **1999**, *10* (4), 331–335.
136. DeSantis, G.; Jones, J. B. *Curr. Opin. Biotechnol.* **1999**, *10* (4), 324–330.
137. (a) Doyle, S. A.; Fung, S.-Y. F.; Koshland, Jr. D. E. *Biochem.* **2000**, *39* (46), 14348–14355. (b) Cedrone, F.; Menez, A.; Quemeneur, E. *Curr. Opin. Struct. Biol.* **2000**, *10* (4), 405–410.
138. (a) Petrounia, I. P.; Arnold, F. H. *Curr. Opin. Biotechnol.* **2000**, *11* (4), 325–330.
139. Berglund, P.; DeSantis, G.; Stabile, M. R.; Shang, X.; Gold, M.; Bott, R. R.; Graycar, T. P.; Lau, T. H.; Mitchinson, C.; Jones, J. B. *J. Am. Chem. Soc.* **1997**, *119* (22), 5265–5266.

SUBJECT INDEX

CUMULATIVE AUTHOR INDEX

Index comprises the names of contributors to Volumes 1–23 of **Topics in Stereochemistry**.

CUMULATIVE TITLE INDEX